ARTICLE IN PRESS Available online http://jopr.mpob.gov.my/category/article-in-press/

Journal of Oil Palm Research

Vol. 35 (2) • June 2023



REVIEW ARTICLE

- Oil Palm Economic Performance in Malaysia and R&D Progress in 2022
- Membrane Technologies in the Oil Industry and the Potential Application for Their Recovery of Phytonutrients from Palm Oil



eISSN 2811-4701

MPOB

JOURNAL OF OIL PALM RESEARCH (formerly known as ELAEIS)

JOURNAL OF OIL PALM RESEARCH, an international refereed journal, carries full-length original research papers, short communications and scientific review papers on various aspects of oil palm and palm oil and other palms. JOURNAL OF OIL PALM RESEARCH is published four times per year, *i.e.* March, June, September and December.

© Malaysian Palm Oil Board, 2023

All rights reserved. No part of this publication may be reproduced in any form or by any means without the written permission of the Malaysian Palm Oil Board.

Impact Factor:
1.594
data from *2021 Journal Citation Report*® Science Edition
– A Clarivate Analytics product.

For more information on advertisement for the JOURNAL OF OIL PALM RESEARCH, please write to:

Editor-in-Chief
Journal of Oil Palm Research
Malaysian Palm Oil Board
6 Persiaran Institusi, Bandar Baru Bangi
43000 Kajang, Selangor, Malaysia

Tel: *603-8769 4400*
E-mail: *pub@mpob.gov.my*
Website: *jopr.mpob.gov.my*

DISCLAIMER
Views of writers expressed in this publication are not necessarily endorsed by or represent the views of the Malaysian Palm Oil Board.

MPOB Press
Malaysian Palm Oil Board
6 Persiaran Institusi, Bandar Baru Bangi
43000 Kajang, Selangor, Malaysia
Tel: +603-8769 4400 | Fax: +603-8925 9446
E-mail: *pub@mpob.gov.my*

JOURNAL OF OIL PALM RESEARCH

Vol. 35 (2) June 2023

CONTENTS

REVIEW ARTICLES

193 Oil Palm Economic Performance in Malaysia and R&D Progress in 2022
Ghulam Kadir Ahmad Parveez; Kalsom Zakaria; Mohd Najib Ahmad; Humaira Mat Taib; Mohd Azwan Mohd Bakri; Sitti Rahma Abdul Hafid; Tn. Noor Maznee Tn. Ismail; Loh Soh Kheang; Meilina Ong-Abdullah; Omar Abd. Rasid and Zainab Idris

217 Membrane Technologies in the Oil Industry and the Potential Application for Their Recovery of Phytonutrients from Palm Oil
Adriana Isabel Rada-Bula; Jesús Alberto García-Nuñez; Carlos Jesús Muvdi-Nova and Consuelo Díaz-Moreno

RESEARCH ARTICLES

236 Effect of Methylene Diphenyl Diisocyanate Index on Physico-Mechanical and Morphological Properties of Palm Olein-based Viscoelastic Polyurethane Foams
Nurul 'Ain Hanzah; Kosheela Devi Poo Palam; Tuan Noor Maznee Tuan Ismail; Srihanum Adnan; Norhayati Mohd Noor; Mohd Norhisham Sattar and Yeong Shoot Kian

247 Effect of Palm Oil Sterilisation Technology on Aqueous Co-products Characteristics
Fatah Yah Abd. Manaf; Rohaya Mohd Halim; Andrew Yap Kian Chung and Yahaya Hawari

256 Effect of Storage Temperature and Duration on Rheological and Thermal Characteristics of Superolein Oleogels
Mei Huey Saw; Wen Huei Lim; Chee Beng Yeoh and Chin Ping Tan

268 Esterification of Free Fatty Acid from Sludge Palm Oil using Zeolite Sulfonated Carbon from Sugar Cane Catalysts
Hasanudin; Wan Ryan Asri; Tri Eltiyah Muthiarani; David Bahrain and Fitri Hadiahia

281 Simulation of Energy Consumption in Sterilisation Process using ASPEN Plus and Response Surface Methodology
Ummi Kalsum Hasanah Mohd Nadzim; Robiah Yunus; Rozita Omar and Mohd Halim Shah Ismail

296 Peculiar Crystallisation Behavior of Palm Oil during Dry Fractionation
Cremer, G; Danthine, S; Blecker, C and Gibon, V

307 Viability of Forage Sorghum Integration in Oil Palm Planting Area for Production of Livestock Fodder
Norkaspi Khasim and Raja Zulkifli Raja Omar

320 A Field Evaluation on Fungicides Application to Control Upper Stem Rot (USR) Disease in Oil Palm Caused by *Ganoderma*
Ramli Nur-Rashyeda; Abu Seman Idris; Shamala Sundram; Nur Hailini Zainol-Hilmi and Su Chong Ming

330 Sustaining Beehive-Fence to Reduce Elephant Encroachment in Oil Palm Plantation
Badrul Amin Abdul Malek; Norasmah Basari; Hisham Hamzah; Wan Nur Amanina Wan Mansor; M. Faizol Shamrie Md Shani; Anis Nazirah Arshad; Wahizatul Afzan Azmi and Mohamed Nor Zalipah

340 Transriptomic and Proteomic Studies to Investigate the Basal Stem Rot Disease in Oil Palm Seedlings
Daim, L D J; Tan, B A; Ithnin, N; Ooi, T E K; Normahnani, M N; Appleton, D R and Harikrishna, K

354 Mixed Planting with Rhizomatous Plants Interfered with *Ganoderma* Disease in Oil Palm
Suwandi Suwandi; Rudi Putra Munandar; Suparman Suparman; Chandra Irsan and A. Muslim

365 Field Efficacy of Anticoagulant Rodenticides against Rat Infestation in Oil Palm Plantation
Ariff Ateed Mohd Noh; Muhammad Syafiq Mohd Zaludin; Wan Mohd Hafezul Wan Abdul Ghani; Abu Hassan Ahmad and Hasber Salim

SHORT COMMUNICATION

376 Cross-validation and Receiver Operating Characteristic Analyses for Oil Palm Leaf Metabolome Dataset Validation
Nur Ain Ishak; Noor Idayu Tahir; Nurul Liyana Rozali; Zain Nurazah; Nur Raihan Abd Rahim; Abrizah Othman and Umi Salamah Ramli

Cover picture:
1. Oil palm economic in Malaysia and R&D progress in 2022
2. Ethanolic transesterification of hybrid crude palm oil as nanofiltration pretreatment.

EDITORIAL BOARD

(1 January 2022 – 31 December 2023)

Datuk Dr. Ahmad Parveez Ghulam Kadir
Malaysia (Editor-in-Chief)

Dr. Carl Traeholt
Malaysia

Prof. Dr. Matthias Finkbenier
Germany

Dr. Julie Flood
United Kingdom

Prof. Dr. Dirk Prufer
Germany

Prof. Dr. Douglas G Hayes
USA

Prof. Fredolin Tangang
Malaysia

Prof. Dr. Norzulani Khalid
Malaysia

Prof. Dr. Ir. Azmi Yahya
Malaysia

PUBLICATION COMMITTEE

CHAIRPERSON
Datuk Dr. Ahmad Parveez Ghulam Kadir

SECRETARY
Anita Taib

COMMITTEE MEMBERS
Dr. Zainab Idris
Dr. Ramle Moslim
Dr. Sivaruby Kanagaratnam
Dr. Astimar Abdul Aziz
Dr. Mohamad Arif Abd Manaf
Dr. Meilina Ong Abdullah
Dr. Aki @ Zaki Aman
Dr. Zafarizal Aldrin Azizul Hasan
Ruba'ah Masri
Johari Minal
Mohd Saufi Awang
Iptisam Abdul Wahab

Journal of Oil Palm Research Vol. 35 (2) June 2023 p. 193-216
DOI: https://doi.org/10.21894/jopr.2023.0028

OIL PALM ECONOMIC PERFORMANCE IN MALAYSIA AND R&D PROGRESS IN 2022

GHULAM KADIR AHMAD PARVEEZ[1]*; OMAR ABD RASID[1]; MOHD NAJIB AHMAD[1]; HUMAIRA MAT TAIB[1]; MOHD AZWAN MOHD BAKRI[1]; SITTI RAHMA ABDUL HAFID[1]; TUAN NOOR MAZNEE TUAN ISMAIL[1]; SOH KHEANG LOH[1]; MEILINA ONG ABDULLAH[1]; KALSOM ZAKARIA[1] and ZAINAB IDRIS[1]

ABSTRACT

The oil palm industry saw a marginal improvement in crude palm oil production in 2022 from 18.12 (2021) to 18.45 million tonnes and overall export volume by 1.8% to 24.72 million tonnes. Export value reached a new record high of RM137.89 billion due to extraordinary hike in palm oil prices. Despite this, upstream efforts remained technologically-driven in maximising oil yield per hectare, managing nutrient cycle, soil fertility, pests and diseases and ecological services. Particularly, planting materials were improved by widening the oil palm gene pool. The unrelenting labour shortage issue intensified adoption of sensor- and vision-based mechanisation technologies for fruit bunches harvesting. In the biomass and bioenergy context, synergistically interfacing supply chains to address logistic issues was key to broader adoption. Integrating engineered nanomaterial, diversely-orientated carbon layering and specialty chemicals from biowastes/byproducts into current palm oil processing not only could ensure that the industry continues to play an important role in the global value chain for food, feed, fibre, fuel and chemicals but also portray multiple industrial symbiosis approaches. Similarly, intensifying businesses and performance of oleo-based industries, such as bio-lubricants, and nutritional research for quality and contamination monitoring, are prioritised in the interest of achieving circular economy.

Keyword: biology, biotechnology, engineering, palm oil, sustainability, value addition.

Received: 26 May 2023**; Accepted:** 24 June 2023**; Published online:** 28 June 2023.

INTRODUCTION

As with most of the economic sectors, the Malaysian oil palm industry started to gain back momentum amid transitioning of COVID-19 pandemic to endemic in April 2022. In particular, the escalation of Russian-Ukraine war and the prolonged labour shortage issue have led to low stock of palm oil and temporary export restriction by Indonesia in the first half of 2022. As a result, palm oil price was pushed to a record high, surpassing RM8000.00 per tonne. Overall, the oil palm industry performed better in 2022 than 2021 in terms of crude palm oil (CPO) production (up by 1.9%), exports (up by 1.8%) and export revenue (up by 27.1%). As the industry experienced an increase in demand, palm oil products fetched higher trading prices globally. Local price of CPO fetched the highest at RM6873.00 t^{-1} in May 2022, up by 15.4% on average. Although fresh fruit bunches (FFB) yield increased only slightly (up by 0.1%), efforts towards addressing FFB harvesting had increased CPO production and palm oil export, thus stabilising CPO price in the second half of 2022.

Challenges facing the oil palm industry continue, demanding effective and yet innovative solutions. Major issues such as sustainability, deforestation, ecosystem degradation and oil quality could make a dent in the industry's performance (Naidu *et al.*, 2022). R&D must therefore associate with the whole palm oil supply chain in order for the industry to maintain and continuously grow. While the upstream initiatives targeting yield improvement through appropriate strategies (such as sustainable agricultural practices, breeding and conservation,

[1] Malaysian Palm Oil Board,
6 Persiaran Institusi, Bandar Baru Bangi,
43000 Kajang, Selangor, Malaysia.

* *Corresponding author e-mail: parveez@mpob.gov.my*

increased use of mechanisation, *etc*.) should be emphasised, the whole of oil palm cultivation should withstand scrutiny in certification for social and environmental integrity, *e.g*., through the mandatory implementation of Malaysian Sustainable Palm Oil (MSPO). Advanced and innovative engineering and bioprocessing technologies adoption for cost-effective palm oil milling and refining, progressive oil quality control programme in preserving natural phytonutrients in palm for human health benefits, projecting by-products' energy sources for livestock feed and dietary essential, advancing bio-wastes valorisations into wealth and value-adding basic oleochemicals into specialty derivatives are among the key elements for applied research consideration and formulation.

Globally, the adoption of the Sustainable Development Goals is increasing in pace for a sustainable future. Areas such as digital revolution, economic decarbonisation and circular economy are of central role in building a low-carbon nation. To this end, the industry's adoption of IR4.0, which is characterised by an increase in automation and smart technologies throughout the whole palm oil supply chain should be seriously planned and executed, with pioneer demonstration put in place to showcase and facilitate mechanisation and automation in reducing heavy labour reliance of the industry. This article reviews the performance of the oil palm industry in 2022 and highlights R&D outcomes and innovations in key areas pertaining to the industry. The deliberation in this review serves as a basis to chart strategies for a sustainable palm oil industry.

PERFORMANCE OF THE MALAYSIAN OIL PALM INDUSTRY

The year 2022 witnessed a global shortage of oil and fat supplies which were mainly attributed to the geopolitical conflict between Russia and Ukraine that disrupted the global supply of sunflower oil. Since soybean oil supply from Argentina was also disrupted by drought, demand for oils and fats has shifted towards Indonesian and Malaysian palm oil and caused prices of all major vegetable oils to rise. The sharp increase in palm oil demand has caused disruption to the local supply of palm oil in Indonesia which then forced Indonesian government to restrict and ban its palm oil for export market. This situation contributed to the high demand for Malaysian palm oil. However, due to improved labour situation in oil palm plantations and low imports of palm oil from other palm oil producing countries, Malaysia managed to increase marginally its palm oil supply to the global market. This situation has caused the prices and export revenue of Malaysian palm oil products to skyrocket to a record high in palm oil history.

Planted Area

Malaysia's overall oil palm planted area declined slightly by 1.1%, from 5.74 million hectares in 2021 to 5.67 million hectares in 2022. The reduction was mainly attributed to the fact that the planted area in Peninsular Malaysia and Sabah has dropped by 2.4% or 2.54 million hectares and 1.0% or 1.50 million hectares, respectively (*Table 1*). The reduction in the planted area was due to the improvement of MPOB renewal licensing procedures for independent smallholders since 2019. This effort was also in line with MSPO implementation.

The nationwide MSPO implementation has resulted in a reduced total oil palm planted area for 2022 as compared to 2021. The organised and independent smallholders own only 11.8% and 14.4% of the total planted area of oil palm, respectively (*Table 2*). The overall planted area from both organised and independent smallholders for 2022 recorded a 3.5% shrinkage as compared to the previous year. The matured oil palm area recorded for 2022 was 5.13 million hectares or 90.4% of the total planted area. In Peninsular Malaysia and Sabah, planted areas decreased by 2.4% and 1.0%, to 2.61 million hectares and 1.50 million hectares, respectively, compared to the previous year. Meanwhile, oil palm cultivation in Sarawak expanded by 1.0% to 16.2 million hectares. In terms of land ownership, oil palm plantations comprised around 4.19 million hectares or 73.8% of the total planted area.

TABLE 1. MALAYSIAN OIL PALM AREA AS IN DECEMBER 2022 AND 2021 (MILLION HECTARES)

	Planted area			Mature area		
	2022	2021	Difference (%)	2022	2021	Difference (%)
Peninsular Malaysia	2.54	2.61	-2.44	2.31	2.36	-2.22
Sabah	1.51	1.52	-1.02	1.33	1.33	-0.38
Sarawak	1.62	1.61	+1.00	1.49	1.45	+2.80
Malaysia	5.67	5.74	(1.10)	5.13	5.14	(0.33)

Source: MPOB (2022).

TABLE 2. OIL PALM PLANTED AREA BY CATEGORY IN 2022 (million hectares)

	2022		2021	
	Hectarage	%	Hectarage	%
Independent Smallholders	0.82	14.4	0.86	15.1
Organised Smallholders	0.67	11.8	0.67	11.7
Private and Government State Agency Estate	4.19	73.8	4.20	73.2
Total	5.67	100	5.73	100

Source: MPOB (2022).

Status of Palm Oil Processing Sector

In 2022, Malaysia had a total of 450 palm oil mills with a combined annual processing capacity of 119.36 million tonnes of FFB. Slightly more than 50.0% of the mills were in Peninsular Malaysia with a capacity to process up to 59.63 million tonnes (*Table* 3). Meanwhile, 28.4% and 18.7% were located in Sabah and Sarawak with a total processing capacity of 34.31 million tonnes and 25.42 million tonnes, respectively. In total, the milling capacity utilisation rate increased by 0.70%, from 77.56% in 2021 to 78.13% due to the higher volume of FFB processed in 2022 as against 2021.

In the refining sector, 52 palm oil refineries with a combined processing capacity of 26.90 million tonnes of CPO and crude palm kernel oil (CPKO) were in operation in 2022. The 34 refineries located in Peninsular Malaysia have a processing capacity of up to 15.05 million tonnes. Meanwhile, 12 and six refineries located in Sabah and Sarawak have processing capacity up to 8.73 million tonnes and 3.12 million tonnes, respectively. The overall refining capacity utilisation rate in Malaysia showed an increase of 1.60% from 56.85% in 2021 to 57.78%, in line with the increasing demand for processed palm oil from export markets.

There were 41 palm kernel crushers operating in Malaysia in 2022, with a total processing capacity of 7.35 million tonnes. During the year, 60.30% of palm kernel crushers operated in Peninsular Malaysia with a total processing capacity of 4.59 million tonnes, while the other 24.40% and 12.20% were located in Sabah and Sarawak with a total capacity of 1.99 million tonnes and 0.76 million tonnes, respectively. The palm kernel crushing capacity utilisation rate declined by 2.00%, from 62.74% in 2021 to 61.48% in 2022, because of lower market demand for palm kernel oil (PKO) from importing countries.

A total of 22 oleochemical and 24 biodiesel plants were in operation in 2022 with processing capacities of 2.69 million tonnes and 2.71 million tonnes, respectively. The majority of these facilities were in Selangor and Johor. There were 10 oleochemical and six biodiesel plants in Selangor and seven oleochemical and nine biodiesel plants in Johor.

CPO Production

Malaysian CPO production in 2022 climbed by 1.9% to 18.45 million tonnes, compared to 18.12 million tonnes in 2021, as a result of a 3.4% increase in FFB processed to 93.65 million tonnes, compared to 90.53 million tonnes in 2021, as well as a 0.1% improvement in FFB yield performance to 15.49 t ha^{-1}. Monthly CPO production had a mixed performance. Comparing the first quarter of 2021, the first quarter of 2022 had higher production. However, CPO production was lower in the second quarter of 2022 and then increased in the third and fourth quarters compared to the same period in 2021. The maximum CPO production in 2022 was 1.81 million tonnes in October, while the lowest was 1.14 million tonnes in February. This normal seasonal trend of Malaysian palm oil production was mainly attributed to the seasonal weather pattern of Malaysia. The fruiting season normally peaks in September to October every year due to seasonal cycles and declines in February due to low fruit formation, short month period and palm oil mill closure due to Chinese New Year celebration (Oettli *et al.*, 2018). On regional comparison, Peninsular Malaysia and Sarawak's CPO production improved by 3.2% to 10.16 million tonnes and 2.5% to 4.01 million tonnes, respectively in 2022, compared to 9.85 million tonnes and 3.85 million tonnes, respectively, in 2021, mainly due to the improvement in FFB yields in both regions. Meanwhile, Sabah's CPO production decreased in 2022, falling 1.7% to 4.29 million tonnes from 4.36 million tonnes (*Table 4*) mainly attributed to the decline in FFB yield.

The FFB yield for 2022 increased by 0.1% (15.49 t ha^{-1}) compared to 2021 (15.47 t ha^{-1}) (*Table* 5) as some estates managed to reduce dependence on foreign workers and adopted mechanisation (The Star, 2022; New Straits Times, 2022; 2023). Compared to 2021, Peninsular Malaysia and Sarawak recorded 1.0% and 1.4% increase in FFB yield to 16.41 t ha^{-1} and 14.13 t ha^{-1} in 2022, respectively, while Sabah declined by 2.4% to 15.39 t ha^{-1}. The decline in FFB yield in Sabah was mainly due to the unfavourable weather condition that affected the FFB production in the state. The highest FFB yield recorded in 2022 was 1.54 t ha^{-1} in October, 5.5% higher than the highest

TABLE 3. NUMBER OF PALM OIL PROCESSING FACILITIES AND THEIR CAPACITIES IN MALAYSIA

Facility	No.	Processing capacity (Million tonnes per year)
Palm oil mill		
Peninsular Malaysia	238	59.63
Sabah	128	34.31
Sarawak	84	25.42
Malaysia	450	119.36
Palm oil refinery		
Peninsular Malaysia	34	15.05
Sabah	12	8.73
Sarawak	6	3.12
Malaysia	52	26.90
Palm kernel crusher		
Peninsular Malaysia	26	4.59
Sabah	10	1.99
Sarawak	5	0.76
Malaysia	41	7.35
Oleochemical plant		
Selangor	10	0.86
Johor	7	0.68
Penang	3	0.79
Others	2	0.37
Malaysia	22	2.69
Biodiesel plant		
Johor	9	1.09
Selangor	6	0.77
Sabah	3	0.40
Others	6	0.45
Malaysia	24	2.71

Source: MPOB (2022).

TABLE 4. MALAYSIAN CRUDE PALM OIL (CPO) PRODUCTION (million tonnes)

	2022	2021	Difference	
			Volume	%
Peninsular Malaysia	10.16	9.85	+0.31	+3.2
Sabah	4.29	4.36	-0.07	-1.7
Sarawak	4.01	3.91	+0.10	+2.5
Malaysia	18.45	18.12	+0.33	+1.9

Source: MPOB (2022).

FFB yield recorded in 2021, which was 1.46 t ha^{-1} in October 2021. Meanwhile, the lowest FFB yield was 0.99 t ha^{-1} in February, up 2.1% from 0.97 t ha^{-1} in February 2021. As mentioned earlier, this trend follows the normal seasonal fruiting of Malaysian oil palms.

The national oil extraction rate (OER) in 2022 was lower by 1.50% to 19.70% compared to 20.01% in 2021 (*Table* 6), mainly attributed to lower ripe FFB processed by palm oil mills (in December 2022, 33.00% of mills reported lower ripe FFB processed compared to 28.00% in December 2021). The monthly OER recorded a lower performance in 2022 as against 2021, except for January 2022 at 19.68% over 19.02% in January 2021, while the performance was the same in April of both years. The highest OER achieved in 2022 was in May at 19.98% due to a higher quantity of ripe FFB input, because of

favourable weather conditions. Meanwhile, the lowest OER performance was recorded in February 2022 at 19.39% due to a lower volume of ripe FFB processed by palm oil mills. Overall, Malaysia recorded lower OER performance in 2022 by 1.30%, 1.50% and 2.10% (*Table 6*) as against the previous year.

Supply and Demand

The overall exports of palm oil and other palm-based products (POPP) in 2022 amounted to 24.72 million tonnes, an increase of 1.8% compared to 2021 (24.28 million tonnes) (*Table* 7). The increase was primarily due to the rise in export of CPO, processed palm oil, processed PKO and finished products. Palm oil accounted for 57.9% of the total exports of POPP. The increase in palm oil exports was attributable to the increased demand from the United Arab Emirates, Saudi Arabia, Japan, Bangladesh, and Egypt, which outweighed the decrease in demand from India, the European Union, and China.

Despite the marginal improvement in export volume, the total export revenue for palm products surged by 27.1% in 2022 to RM137.89 billion from RM108.51 billion in 2021 due to higher export prices for POPP. In 2022, palm oil and PKO export revenues increased by 27.7% and 14.2%, to RM82.49 billion and RM7.62 billion, respectively. In addition, all other palm-based products, such as palm kernel cake (PKC), palm-based oleochemicals, *etc*., also recorded a significant growth between 23.0% and 38.0%.

Imports of Malaysian oil palm products decreased by 8.5% from 1.50 million tonnes in 2021 to 1.38 million tonnes in 2022. Palm oil accounted for 82.8% of the total Malaysian imports of palm oil products in 2022, followed by PKO (14.2%) and palm kernel (3.1%) (*Table 8*). Imports of palm oil decreased by 3.2%, from 1.18 million tonnes in 2021

TABLE 5. AVERAGE FFB YIELD FOR MALAYSIAN OIL PALM ESTATES (t ha^{-1})

	2022	2021	Difference	
			Volume	%
Peninsular Malaysia	16.41	16.24	+0.17	+1.0
Sabah	15.39	15.77	-0.38	-2.4
Sarawak	14.13	13.94	+0.19	+1.4
Malaysia	15.49	14.47	+1.02	+0.1

Source: MPOB (2022).

TABLE 6. MALAYSIAN OIL EXTRACTION RATE (OER) (%)

	2022	2021	Difference	
			Volume	%
Peninsular Malaysia	19.57	19.83	-0.26	-1.3
Sabah	20.25	20.55	-0.30	-1.5
Sarawak	19.47	19.88	-0.41	-2.1
Malaysia	19.70	20.01	-0.31	-1.5

Source: MPOB (2022).

TABLE 7. MALAYSIAN EXPORT OF PALM OIL AND OIL PALM PRODUCTS

	Volume (million tonnes)			Value in RM million (USD million)		
	2022	2021	Difference (%)	2022	2021	Difference (%)
Palm oil	15.72	15.56	+1.0	82.49(18.73)	64.61(15.59)	+27.70(+20.20)
Palm kernel oil	1.04	1.08	-3.6	7.62(1.73)	6.67(1.61)	+14.20(+7.60)
Palm-based oleochemicals	3.04	3.25	-6.5	33.61(7.63)	26.80(6.46)	+25.40(+18.07)
Other palm-based products	2.78	2.09	+0.2	12.46(2.83)	9.04(2.18)	+37.90(+29.80)
Palm kernel cake	2.14	2.30	-6.5	1.71(0.33)	1.39(0.34)	+22.60(+15.80)
Total	24.72	24.28	+1.8	137.89(31.32)	108.52(26.18)	+27.10(+19.60)

Note: Values in parentheses represent prices in US Dollar equivalent.

Source: MPOB (2022); Department of Statistics, Malaysia (2022).

to 1.14 million tonnes in 2022, because of increased CPO production by 1.9%, from 18.12 million tonnes in 2021 to 18.45 million tonnes in 2022. In addition, the decline in palm oil imports in 2022 was also due to the more stringent Indonesian palm oil export policy as the country represented 95.9% of the total Malaysian palm oil imports in 2022.

TABLE 8. MALAYSIAN IMPORT OF OIL PALM PRODUCTS (million tonnes)

	Volume		
	2022	2021	Difference (%)
Palm oil	1.14	1.18	-3.2%
Palm kernel	0.20	0.27	-28.7%
Palm kernel oil	0.04	0.05	-20.2%
Total	1.38	1.50	-8.5%

Source: MPOB (2022).

The 2022 palm oil ending stocks increased by 2.20 million tonnes, or 36.5%, compared to 1.61 million tonnes in December 2021. This was primarily ascribed to higher palm oil opening stocks and higher CPO production by 0.34 million tonnes or 1.9%. In December 2022, all three regions recorded an increase in palm oil stocks, with Sabah recorded the highest stock at 53.3%, followed by Sarawak at 47.1% and Peninsular Malaysia at 27.2% (*Table 9*).

TABLE 9. MALAYSIAN PALM OIL CLOSING STOCKS AS IN DECEMBER 2022 and 2021 (million tonnes)

	2022	2021	Difference	
			Volume	%
Peninsular Malaysia	1.45	1.14	+0.31	+27.2
Sabah	0.46	0.30	+0.16	+53.3
Sarawak	0.25	0.17	+0.08	+47.1
Malaysia	2.19	1.61	+0.55	+34.2

Source: MPOB (2022).

Compared to 2021, all major palm products were extensively traded in 2022 (*Table 10*). In 2022, the local CPO price increased by 15.4%, or RM680.50 t^{-1}, to RM5087.50 t^{-1} compared to RM4407.00 t^{-1} in 2021. The highest CPO price for 2022 was reported in May at RM6873.00 t^{-1}, while the lowest price was in October at RM3682.00 t^{-1}. The increased CPO price during that period was impacted by higher soybean oil prices, firmer Brent crude oil prices, and a weaker Ringgit versus the US Dollar, as well as the Ukraine and Russia war, the restriction on Indonesian palm oil exports, the drought in Argentina, and the reduction of India's import tariff (Medina, 2022; Parveez, 2023; Vasu, 2023).

In 2022, export prices of refined, bleached, and deodorised (RBD) palm oil, RBD palm olein, and RBD palm stearin increased by 7.3%, 8.1%, and 4.9%, respectively, to RM4973.50 t^{-1}, RM5006.00 t^{-1}, and RM4559.50 t^{-1}, while the price of palm fatty acid distillate (PFAD) increased by 1.9% to RM4313.00 t^{-1}.

In the lauric-based market, the palm kernel price improved by 12.4% (RM3118.00 t^{-1}) compared to RM2773.00 t^{-1} in 2021, mainly attributed to higher domestic CPKO prices. The CPKO price in 2022 climbed by 11.5% to RM6327.00 t^{-1} compared to RM5674.50 t^{-1} in the previous year. The highest CPKO price in 2022 was in line with higher PKO price in the global market by USD81 or 5.3% (USD1598 t^{-1}), which coincided with a higher price in coconut oil by USD3 or 0.2% (USD1621 t^{-1}).

FFB price at 1.0% OER in 2022 had grown by 15.3% to RM55.52 from RM48.14 in 2021, corresponding to a significant increase in CPO and palm kernel prices. According to the national OER, the FFB price in 2022 was comparable to RM1094.00 t^{-1}, a 14.6% increase over the RM955.00 t^{-1} reported in 2021.

R&D FOCUS AREAS IN 2022

Enhancement of Sustainable Oil Palm Plantation towards Yield Improvement

While the country has targeted economic revival after COVID-19 pandemic, the upstream oil palm

TABLE 10. MALAYSIAN PRICE OF OIL PALM PRODUCTS (RM t^{-1}/ USD t^{-1})

	2022	2021	Difference	
			Price	%
Crude palm oil	5,087.50(1155.38)	4407.00(1063.05)	+680.50(+92.33)	+15.40(+8.7)
RBD palm oil	4,973.50(1129.49)	4,635.50(1118.17)	+338.00(+11.32)	+7.30(+1.0)
RBD palm olein	5,006.001136.87)	4,632.50(1117.45)	+373.50(+19.42)	+8.10(+1.7)
RBD palm stearin	4,559.50(1038.47)	4,343.00(1047.62)	+216.50(-12.14)	+5.00(-1.2)
Palm fatty acid distillate	4313.00(979.49)	4233.00(1021.08)	+80.00(-41.45)	+1.90(-4.1)
Palm kernel	3,118.00(708.11)	2773.00(668.08)	+345.00(+39.2)	+12.40(+5.9)
Crude palm kernel oil	6,327.00(1436.88)	5674.50(1368.80)	+652.50(+68.08)	+11.50(+5.0)
FFB at 1% OER	55.52(12.61)	48.14(11.61)	+7.38(+1.0)	+15.30(+8.6)

Note: Values in parentheses represent prices in USD equivalent.

Source: MPOB (2022).

sector continued to focus on improving oil palm yield. Climatically, Malaysia has one of the best conditions in ASEAN for optimal oil palm growth. The oil palm yield in Malaysia is about 3.64 t ha^{-1} $year^{-1}$ (Afandi *et al*., 2022), although the estimated average maximum and lowest are about 18.50 t ha^{-1} $year^{-1}$ and 3.00 t ha^{-1} $year^{-1}$, respectively. As there is a lack of spatial and digital data for referencing and decision-making in oil palm plantation management, a digital technology platform, *i.e.*, Oil Palm Resource Information System (OPRIS) using ArcGIS software has been developed to record and store geodatabase inside mobile devices (Nordiana *et al*., 2022). The system contains an administrative boundary, base map, infrastructure layer, water bodies and river networking, soil type, topographic, agricultural climatic information and land use. In Sumatra, Indonesia, in order to find the spatial distinction in yields, the input used and output prices, a designed additive regression model with nonlinear spatial properties called *geosplines* was employed (Kibrom *et al*., 2022).

The variations in ecology and biodiversity during oil palm growth period could help minimise the effects of land conversion (Parveez *et al*., 2022), especially in peat areas cleared and converted into oil palm, pulpwood plants and sago palm (*Metroxylon sagu* Rottb.). Permanently lowering the water table of peatlands through drainage for oil palm growth would risk losing organic carbon stock such as methane (CH_4), compared to uninterrupted peatlands which frequently act as carbon sinks. Maintaining soil moisture content in peatlands cultivated with oil palm is often more difficult and costly than in secondary forests due to drainage and peat compaction (Ngau *et al*., 2022). Based on mapping via geographical information system, such management is essential as soil moisture content is highly correlated with the trunk diameters of oil palm.

While efforts on yield improvement are being intensified, several important sustainability strategies, such as assessing wildlife inhabitants, which are in danger from future habitat damage, are required for proper land-use planning. Combining projections of future deforestation based on endangered areas and logging businesses with species density information is anticipated to address biodiversity declines (Voigt *et al*., 2022). In preserving biodiversity, more environmentally-friendly management strategies, such as the before-after control-impact (BACI) method, are required to support high-level-inside-plantation biodiversity and increase ecosystem service transfer, perhaps increasing oil palm efficiency (Pashkevich *et al*., 2022). One of the species investigated is spider, where abundance and richness in canopy cover and ground differ quite significantly in mature oil palm plantations. Dominant species in the canopy include orb-web builders, cob-web builders and cursorial (running) hunters while those on the ground are cursorial hunters. In addition, the debated human-elephant conflict commonly occurring in the states of Pahang, Sabah and Terengganu can be mitigated by installing beehive-fence. Subsequently, eight months after the fitting, the number of elephant infringements in Ladang Jernih had decreased from 31 to only 16 times (Abdul Malek *et al*., 2022).

As the amount of greenhouse gas (GHG) released from oil palm growing on peats in literature was estimated mainly based on very limited sources, there is a large variation which needs to be rectified (Alcock *et al*., 2022). Estimation of oil palm peat decomposition - CO_2 and N_2O emission factors (EF) - based on process-based modelling has been explored over a 30-year plantation in Central Kalimantan, Indonesia (Swails *et al*., 2022). It was found that the modelled peat onsite CO_2-C EF (7.7 ± 0.4 Mg C ha^{-1} yr^{-1}) in the first ten years was lesser than the IPCC standard (11 Mg C ha^{-1} yr^{-1}) and reduced further to 3.0 ± 0.2 and 1.8 ± 0.3 Mg C ha^{-1} yr^{-1} for the subsequent second and third decades of the rotation, respectively. On the contrary, the modelled N_2O-N EF (3.5 ± 0.3 kg N ha^{-1} yr^{-1}) was more than the standard (1.2 kg N ha^{-1} yr^{-1}), and amplified further to 4.7-4.6 ± 0.5 kg N ha^{-1} yr^{-1} in the next decades. Through re-analysis of systems-wide life cycle GHG emissions estimated amongst various vegetable oils, Alcock *et al*. (2022) concluded that oil palm contributes huge carbon storage opportunities, if more effective sustainability practices are adopted, *e.g.*, proper land use management system and methane capture at mills for energy use. In assessing the performance of each agricultural system, their carbon storage potential should be fairly compared for a better insight into the relative impacts and competitive edge.

The bunch production and oil quality are very much affected by CO_2 enrichment when the oil palm is growing. The rising atmospheric CO_2 implications and impact have been assessed using FACE technique (Amanina *et al*., 2022). On the other hand, the properties of water flow and movement on oil palm have been examined by Pradiko *et al*. (2022). A daily stand transpiration of a 14-year-old oil palm is estimated to be about 0.82-1.66 mm day^{-1}. This information can be used to model water necessities and preservation in oil palm plantations. Besides, the dynamics of soil organic carbon in peatlands are particularly crucial for enhancing soil fertility and accelerating carbon sequestration. The total root respiration and heterotrophic decay of soil organic matter can be quantified as soil CO_2 flux via various methods, but the closed chamber method is the most prevalent (Ching *et al*., 2022) featuring "instantaneous" monitoring. As soil CO_2 fluxes vary between different management zones,

the findings reveal that sustainable crop production can be practiced considerably, by leveraging the associated weaknesses and strengths of current practices.

Oil palm growing and yield depend on passable water supply and consistently disseminated rainfall. Oil palm cultivation in regions with long dry seasons or irregular distribution of rainfall could be effective if an acceptable source of water is obtainable for irrigation. Drip irrigation combined with a fertigation system has been proven as the most effective system to increase oil palm yield because it can efficiently lessen nutrient losses and upsurge nutrient uptake (Afandi *et al*., 2022). Oil palms also require a large quantity of nutrients to withstand high yields. Fertiliser accounts for >30% of the sum charge of palm oil production and approximately 60% of the total maintenance cost of matured planting. Fertiliser contributions, therefore, establish an imperative investment cost. An efficient fertiliser rate at 0.84 N, 0.68 P_2O_5, and 2.40 K_2O was the most appropriate fertiliser proportion to keep ideal palm growth, both vegetative biomass and nutrient status. Mature oil palms supplied with comprehensive NPK fertiliser (N1P1K1 and N2P2K2) amplified 17.3% of FFB yield from 22.9 t ha^{-1} $year^{-1}$ to 27.0 t ha^{-1} in the control plot. The results highlighted the optimistic retort of palm growing and foliar nutrient status with N enriching during this study period (Ariffin *et al*., 2022). Biofertilisers, in combination with consortium microbes, as an alternative to chemical fertilisers help regulate nutrients and microbial activities in soil. Such biofertiliser combined with 30% chemical fertiliser showed better growth at the oil palm nursery stage (Keni *et al*., 2022).

Proper control of pests and diseases could enhance oil palm yield, *e.g*., through satellite imagery (Nuthammachot and Stratoulias, 2022), haplotype network (Badrulisham *et al*., 2022), deep learning neural network (Najib *et al*., 2022), agricultural drone (Masri *et al*., 2022), *etc*. Besides, several anticoagulant rodenticides baits (coumatetralyl, chlorophacinone, flocoumafen and brodifacoum) below 5% threshold level are operative in controlling rat attacks in the infested area (Noh *et al*., 2022). The dominant pest species identified are *Rattus tiomanicus*, *Rattus rattus diardii* and *Rattus argentiventer* (Nasir *et al*., 2022). Besides, disease conquest by fungal control agents has been found equivalent to the chemical counterparts (Muhammad *et al*., 2022; Sundram *et al*., 2022). Fungicides such as hexaconazole are effective in treating upper and basal stem rot *Ganoderma* diseases in oil palm (Nur-Rashyeda *et al*., 2022). The infected palms continue to survive and actively produce fruit bunches. In addition, integrating rhizomatous plants, such as galangal (*A. galanga*), Java turmeric (*C. xanthorrhiza*), or ginger (*Z. officinale*) with oil palms can reduce the disease incidences as well (Suwandi *et al*., 2022). Close monitoring of pathogens in the field is possible with the development of more sensitive real-time PCR assays (Zainol Hilmi *et al*., 2022).

Overall, oil palm yield is the most essential target for sustainable development which can be achieved via proper management of several factors such as environment, climate change, carbon stock, peat ecosystem, pest and disease, nutrient management, *etc*. Adoption of good agricultural practices could ultimately contribute towards oil palm yield increment in relation to the sustainability of the oil palm industry.

Mechanisation and Automation towards Maximising Productivity

Imported labour in the Malaysian oil palm plantations has become scarcer and more rampant in the post-COVID-19 pandemic transition, which has seriously impacted productivity. In order to alleviate the situation, promising technologies in oil palm mechanisation and automation that could improve field productivity and reduce labour requirements must be adopted extensively. In addition, the anticipated technologies should be further revolutionised with advanced digital systems to cope with many complex challenges in the existing agricultural tasks such as FFB harvesting and other field activities.

Agricultural robotics, Internet of Things (IoT), big data, artificial intelligence and cloud computing are of recent interest in finding solutions to overcome labour shortages and field productivity issues (Abbasi *et al*., 2022). The incorporation of these advanced systems enables precision farming and data analytics that could lead to cost-effective field operations (Rejeb *et al*., 2022) and thus, reduction in labour requirements. System advancement is possible because of dynamic improvement associated with sensors, high-end computer processors and algorithms control (Raikwar *et al*., 2022). Besides, the improved system could extend towards safer and greener agriculture processes (Mahroof *et al*., 2021).

An example of improvised system is the land-based agricultural robotics in replacing several tasks carried out by tractors. It takes care of soil compaction effect, gives access to small or narrow areas, reduces operation costs, *etc*. One of the latest trends is applying multiple robots for a specific task (Ju *et al*., 2022), where larger farming areas could be covered in a shorter time during field maintenance like weedicide, chemical application and harvesting. Swarm robotic applications adapted with various sensors and algorithms are an effective method for controlling and navigating the field. However, these technologies are still in

their infancy for commercial adoption (Albiero *et al.*, 2022). Several heterogeneous issues impeding their applications have been identified, which require clear directives catering for multi-mission requirements in agriculture. The robots need to be more equipped with other decision-based systems to support farm analysis. Artificial intelligence and farm digitalisation are key for effective robotics applications in agriculture.

Vision systems with deep learning and big data could revolutionise farming practices. As demonstrated, such technology could provide valuable information for the harvesting process and yield prediction besides others like infection detection and state of health examination (Palacios *et al.*, 2022). A deep learning process that offers multi-layered information for iteration could produce the required solutions. The artificial intelligence system based on vision and deep learning shows better results than the traditional vision inspection system for grain yield estimation (Dhanya *et al.*, 2022). The study by Shiddiq *et al.* (2022) on accommodating vision and artificial intelligent design to detect oil palm FFB ripeness in a controlled environment indicated 80% prediction accuracy. The setup could be replicated for under-canopy fruit detection. The colour spectrum could be easily recognised even with a monocular-based vision system. The vision-based system could be easily made with inexpensive sensors and employed in a real scenario (Bellocchio *et al.*, 2022). The vision system and deep learning process could provide vital information to chart strategies and resource allocation for more cost-effective agricultural practices.

The sensor-based system will be more practical if it can be integrated with IoT as a communication means to enhance farm monitoring capacity and productivity (Subeesh and Mehta, 2021). Farm digitalisation will interrelate sensors, computing processes, machines and monitoring systems. IoT has also been proposed as a digitised-based solution in agriculture for a financially constrained farmer in accessing mechanisation and automation technologies. Thus, a more affordable contractual approach to assist farmers could be realised. Farm support services should also be extended to small- and medium-sized farmers (Gil *et al.*, 2023) for new business opportunities.

Biotechnology Tools for Future Planting Materials

The oil palm sector faces several major issues, including fluctuating prices, labour scarcity, ageing tree populations, and pests and diseases that significantly reduce crop productivity. A practical way to address these issues is to produce new cultivars with improved yield, a variety of high-value traits and more tolerant to changes in climate conditions. Future improvements in commercial yields will partly depend on oil palm breeding programmes that develop higher yielding planting materials with improved water uptake and nutrient usage efficiency. Additionally, palms that are more resistant to diseases as well as have an overall architecture that facilitates harvesting of FFB are also targeted in breeding programmes across the industry.

The current planting materials are based on a narrow genetic base. Recently, a study on advanced oil palm breeding populations was carried out to evaluate the level of genetic variation using amplified fragment length polymorphism (AFLP) markers. Results confirmed the need to incorporate new genetic resources to increase genetic diversity, and with it enhance the crop capacity to withstand environmental challenges (Ithnin *et al.*, 2022). The risk associated with the dependence on a small genetic base and the need to broaden it for effective selection is fully acknowledged by the oil palm industry. New genetic resources were sought through a series of prospection in Africa and South America, leading to the assembly of the world's largest oil palm germplasm collection at MPOB. The richness, in terms of the scale of the genetic variation of these *E. guineensis* and *E. oleifera* germplasm accessions was quantified based on their phenotypic characters and genetic make-up. Using multivariate analyses, most of the important traits in *E. oleifera* and MPOB-Cameroon oil palm germplasms were shown to display a wide range of variation (Tun Mohd Salim *et al.*, 2022; Yaakub *et al.*, 2022). Variables that contribute most to the variation were identified and could be utilised to help determine the population of interest for regeneration and selective breeding for oil palm enhancement programs. In addition to phenotypic data, evaluation of the genetic variation of the accessions was also performed using molecular tools. The phenotypic and molecular-based diversity patterns could subsequently be integrated for systematic formulation of strategies for breeding and conservation. Similarly, genomic characterisation of single nucleotide polymorphisms (SNPs) in *E. oleifera* germplasm assembled in Brazil demonstrated genotypic divergence between populations (Leão *et al.*, 2022). It can be concluded that the germplasm has specialised genetic structures and there is good genetic variability within its populations, as observed within the Malaysian *oleifera* collection.

Potential new genes could be obtained through the exploitation and introgression of germplasm with advanced breeding materials. Generally, these germplasms have a good variability for bunch quality and vegetative traits, thus providing the necessary flexibility to develop new and improved planting materials, some of which can cater for niche markets. This was clearly demonstrated by

the evaluation of several progenies involving the introgressed MPOB germplasms with Algemene Vereniging van Rubberplanters ter Oostkust van Sumatra (AVROS) pisifera (Bakar *et al.*, 2022; Nor Azwani *et al.*, 2020). More specifically, the evaluation of the germplasm introgressed progenies has also led to the identification of potentially *Ganoderma* tolerant materials (Mohd Din *et al.*, 2022). Generally, linking of markers to traits of interest and pilling up favourable alleles in the next generation could improve breeding efficiency. To assist with the use of markers in breeding, Rosli *et al.* (2022) described the establishment of the Oil Palm SSR Resource Database (OPSRI), a highly structured database that can facilitate the development of SSR based molecular markers. Signalling the increase in the repertoire of DNA markers available to the oil palm community, the establishment of intron polymorphism (IP) markers was also reported, in particular for the enhancement of fatty acid composition. A total of 13 fatty acid composition associated IP markers were found within *E. guineensis*, which have potential for improving palm oil composition (Li *et al.*, 2022). Recently, a study identified SNP variation in an expansin gene (*EgExp4*) that was associated with height. This marker may be useful for genetic improvement and selection of semi-dwarf new oil palm varieties (Somyong *et al.*, 2022). The importance of the genetic variability with *E. guineensis* was further demonstrated in an interesting study involving a set of diverse *E. guineensis* progenies. The study indicated that genetic factors determined the foliar contents of K, Mg and Ca, and not by the environment where the progenies were planted, although more research is required to determine if different fertiliser amounts are necessary for optimal production in these progenies (Dassou *et al.*, 2022).

In addition to the DNA-based molecular tools described above, other omics resources are also available to assist in the crop improvement. The integration of various omics technologies has seen tremendous progress in recent years. The development of trustworthy screening techniques and platforms has enabled different omics data sets to be integrated for a better quantification of physiological trait expression in field conditions, which is crucial for the understanding of the inheritance of complex traits (Masura *et al.*, 2017; Ramli *et al.*, 2020; Yang *et al.*, 2021). Using hybrid populations, work to understand the fruit exocarp colour was carried out by detecting expressed sequence tag (EST)-simple sequence repeat (SSR) markers. In widening the use of omics in oil palm research, a number of research articles reported the use of transcriptome data to better understand selected traits. A comparison of immature/mature differentially expressed genes (DEGs) revealed the regulatory role of the anthocyanin biosynthesis pathway (ABP) in nigrescent fruit colour. Additionally, SSR primer motifs that could differentiate the two fruit colour traits, namely nigrescence and virescence, of the Nigerian hybrids were identified (Suraninpong and Nuanlong, 2022). Work to elucidate the function of phytohormone biosynthesis and signalling genes during pollination and fertilisation was also reported. Results showed that energy metabolism and hormone signal transduction related genes were highly expressed during pollination and fertilisation (Yang *et al.*, 2022). The sexual differentiation in oil palm was also studied by characterising miRNAs and differentially expressed genes in male and female inflorescences. A number of genes and miRNA-mRNA target modules that have a developmental regulatory role were identified (Tregear *et al.*, 2022). Furthermore, the transcriptome analysis identified programmed cell death (PCD) and PCD-related genes, predominantly up-regulated in seedless palm tree stigmas and styles compared to *tenera* and *pisifera* fruit forms. PCD may be linked to seedless phenotype formation in oil palm, as it causes pollen tube lethality and double fertilisation failure (Htwe *et al.*, 2022).

Proteomics and metabolomics have also been used in oil palm research with the goal of creating methods for precise tracking of profiles of clonal and transgenic palms and for a range of crucial traits, such as oil quality and yield (Ramli *et al.*, 2020). Tahir *et al.* (2022) used the metabolomics technology to evaluate the effects on clonal palms grown in different environmental conditions. The abundance of primary and secondary metabolites showed the effect of the environment on the palm biosynthetic and metabolism pathways. Similarly, proteomics analysis to investigate bioactive peptides from oil palm mesocarps has led to the identification of peptides with various bioactivities that have potential applications such as plant protection against fungus (Lau *et al.*, 2022). A comparative proteomics study to investigate proteome variation among *Ganoderma* species revealed a number of proteins that are potentially responsible for the variation in pathogenicity between the two studied species (Dzulkafli *et al.*, 2022). Simultaneous evaluation of transcript and protein levels in infected seedlings highlighted the possible defence strategy of the symptomatic seedlings (Daim *et al.*, 2022).

The clustered regularly interspaced short palindromic repeat (CRISPR)-associated protein 9 (Cas9) genome editing system is another biotechnology tool that could complement the oil palm breeding programme. Results so far have shown that an efficient level of gene editing with CRISPR/Cas9 is possible in oil palm by optimising DNA delivery and using efficient gRNAs (Bahariah

et al., 2023; Yeap *et al.*, 2021). Work now is on the way to develop strategy to select more efficient gRNAs for oil palm (Jamaludin *et al.*, 2022).

Sustainable Development for Smallholders

In recent years, a negative attitude towards palm oil has been clearly exhibited especially when the European Union (EU) decided to ban palm oil imports. To address the issue, it is important for the palm oil industry players to introduce sustainable agriculture practice among oil palm smallholders (Abas *et al*., 2021). In Malaysia, through mandatory implementation of MSPO in 2020, the palm oil industry has been enforced to achieve sustainable agriculture practice. As of December 2022, 87.7% of the total independent smallholders have been certified under MSPO, covering 187 215 smallholders with a planted area of 709 088.03 hectares.

The attribute of smallholders, which are self-reliant and manage their own farms individually, has become a major drawback that influences the low participation in MSPO (Parthiban *et al.*, 2021). An empirical study revealed that the majority of smallholders who were already certified have a moderate level of compliance towards MSPO and share a similar non-compliance issue on the clauses related to traceability (Parthiban *et al.*, 2021). This is due to the improper farm record and lack of awareness on the importance of record keeping. The FFB production record is another concern which is one of the important criteria in MSPO. Palm Fruit Dealers (DF) who receive FFB from smallholders were expected to keep the transaction record and share a copy with the smallholders. DF was able to keep a record of the FFB price, weighing ticket number, transportation details and time of transaction. Recent studies revealed that DF is committed to keep a record of the daily FFB transaction of smallholders and submitted to MPOB when requested (Parthiban *et al.*, 2022). An effective traceability system from DF can provide complete traceability of the entire supply chain of oil palm. In such a way, it is crucial for smallholders to reach an understanding of the benefits of getting MSPO certification (Bok *et al*., 2022). Hence, the lack of initiatives taken by the smallholders to comply with the compulsory certification becomes a great challenge, especially to the extension agents.

As food security becomes a major concern globally, smallholders are urged to practice crop integration in their oil palm smallholding. In order to reduce heavy reliance on imported feed products, crop integration is essential and should be encouraged to improve sustainability and efficiency in crop management. By practising crop integration, oil palm growers can generate additional income and optimise their land use, instead of planting oil palm alone. One of the potential crops for integration with oil palm is forage sorghum, which is similar to wheat, maize, and paddy (Norkaspi and Raja Zulkifli, 2022). Sorghum is suitable to be used as animal feed. Thus, by using sorghum as a supplementary element to fodder resources, smallholders can contribute to reducing cost of animal feed. As feed import quantity and value are also expected to increase significantly, introducing new livestock feeds such as sorghum can induce healthy competition in livestock industry. A recent study disclosed that a total of RM1317 ha^{-1} can be generated through integration of forage sorghum with oil palm (Norkaspi and Raja Zulkifli, 2022). In another study, the growth of sago palm in peat soil was evaluated (Zurilawati *et al.*, 2022). Although the applied compound fertiliser did not affect the sago palm growth, proper fertiliser management by smallholders is required for sago to be cultivated in shallow peat land as raw material for potential utilisation in the food and non-food industries, biomass, and poultry industry.

Recovering from the pandemic, smallholders are not only struggling to understand and adhere to the MSPO certification scheme but also need to face the great price increase in agricultural inputs and difficulties in obtaining farm workers. A recent study showed that workers in the palm oil industry possess a higher intention to quit their job since there are a lot of opportunities being offered by other industries such as services, manufacturing, and construction (Amran *et al*., 2021). The motivational factor that influences the workers to turn away from working in the palm oil industry is to look for a better livelihood and achieve their individual needs. Nevertheless, smallholders still show high interest in planting oil palm. They usually hire third parties, namely contractors, DF, or business partners to look after their farm. An empirical study among 375 respondents of the replanting assistance scheme recipients showed that most of them agreed that the increase in FFB selling price have a great influence on their decision to carry out replanting (Mohd Noor Izuddin *et al*., 2022). Family members and preparation for a long-term investment have also affected their choice.

Biomass and Bioenergy Innovations

While an abundance of biomass resources and by-products has been generated by the palm oil industry, many advanced biomass conversion technologies for energy and non-energy applications featuring value addition have been developed. However, most of the development is difficult to be commercialised due to several issues: economics feasibility, quality and market compatibility (Loh *et al.*, 2022; Terry *et al.*, 2022). Key challenges faced

so far are related to high investment, feedstock and supply chain management, which require urgent attention. As such, traditional handling of oil palm biomass should be disruptively transformed into a more appealing digitalised manner that can be cascaded from existing pools for cost-effective integration, to meet more stringent global demand on sustainability.

In doing so, several researchers now look into embracing chemical engineering knowledge for advancing industrial biomass business operations (*e.g.*, bioenergy and biochemicals), from the perspective of (i) reaction, (ii) separation, and (iii) process systems (Terry *et al.*, 2022). These 3 aspects focusing on design, intensification, consolidation, operation, modelling, control, *etc*. are part and parcel of managing an industrial process/plant to maximise outputs. Improvements made at the system level, *i.e.*, industrial symbiosis and process/product modelling are worth exploring for embracing and aligning with future digital interfaces (Ayodele *et al.*, 2022; Terry *et al.*, 2022). The use of digital tools for strengthening biomass business models in terms of techno-economic performance, system prediction and supply chain consolidation could lead to overall sustainable development in pursuit of circular economy (Gilbertson and Vikesland, 2022).

For sustainable palm oil establishment, it is possible to nourish end-of-life resources from the biological or technical cycle, as natural and renewable biomaterial feedstock to foster the inspired nanocircular economy (Gilbertson and Vikesland, 2022). The potential of engineered nanomaterial transforming from biomass is huge as every bit of our life is associated with it, *e.g.*, food, clothing, computer and transportation, *etc*. Harvesting nanocellulose from oil palm biomass through environmental nanotechnology can be one such activity with a huge opportunity, as multiple advanced materials can be created compared with the limited conventional method of disposal and use (Lim *et al.*, 2022). Nevertheless, as mentioned above, its production must withstand extensive scrutiny to create a competitive and feasible industrial symbiosis.

Being versatile with diverse application potential, oil palm biomass has been recently associated with graphene manufacturing. Graphene refers to monolayer of carbon (graphite) with neat hexagonal geometry plus thermal and electrochemical flexibilities, due to its available π-electrons (double bonds). As opposed to graphene, graphite is a stack of a large number of layers of graphene, thus making it inflexible. As graphene is naturally hydrophobic (water repellent), converting it to graphene oxide or reduced graphene oxide could equip it with various oxygen-containing functionalities, making it a hydrophilic (water affinity) alternative to graphene for various applications such as semiconductor, carbon electrode, *etc*.

Oil palm biomass, high in carbon content, could be mined for graphene manufacturing. The many reactive functionalities present in lignin (aromatic-rich compounds) and cellulose are highly required for oxidative/reductive conversion into graphene oxide and its reduced materials. In one example, the composite graphene oxide anodes from lignin of empty fruit bunches (via carbonisation followed by chemical oxidation) are incorporated in a microbial fuel cell to produce electricity and remove heavy metal from the simulated wastewater (Yaqoob *et al.*, 2021). The employed sap of oil palm trunk is also a carbon source for microbial rejuvenation in fuel cell. Lignin and hemicellulose from oil palm biomass are to be separated to unpack cellulose before producing multilayer graphene material (Zhou *et al.*, 2022). High quality graphene (single-crystalline nanoscale product) can be produced with pure lignin due to the anticipated aromaticity (Kumari and Samadder, 2022). In this context, palm kernel shell, which is high in lignin (~50 wt.%, dwb), is pyrolysed and then catalytically ($ZnCl_2$) fabricated via chemical vapour deposition process at 900°C in an inert environment to produce bio-graphene-like structure (Azahar *et al.*, 2022).By manipulating the pyrolysis conditions (temperature and residence time), different proportions of cellulose, hemicellulose and lignin can be decomposed, hence the amount of volatile CH_4 and CO_2 released can be controlled in preparation of biomass precursor, which can then undergo further exfoliation to enhance its functionality, layering and interlayer spacing. Instead of forming monolayer sheets, graphene deriving from biomass shows a much diverse orientation of carbons. As such, alignment through several processes (exfoliation, carbonation or graphitisation) is essential in order to rearrange the biomass molecules into layered (single or multiple) structures (Kumari and Samadder, 2022). These extra processing steps could add cost to graphene production from oil palm biomass.

Biomass or palm-based by-products such as PKC have been much anticipated as a substitute for corn and soy meal in chicken feed as a means to stabilise prices (Azizi *et al*., 2021). Currently, the costs of chicken and chicken feed have drastically increased due to various global issues, including bird flu incidents and Russia-Ukraine confrontation (FAO, 2022; OECD, 2022). Studies have shown that PKC, CPO, and palm oil mill effluent (POME) exhibit substantial nutrients for laying hens and broiler chickens, with no significant impact on performance or egg quality (Herliatika *et al*., 2022). Eggshell thickness was marginally reduced, and the performance of laying hens was unaffected by the addition of lignocellulolytic enzymes to POME in order to increase the nutrient levels and quality

(Herliatika *et al*., 2022; Saminathan *et al*., 2020). The inclusion of 10% PKC in the diet of 40-week-old laying hens is recommended in order to lower feed costs without compromising layer performance (Herliatika *et al*., 2022). Addition of CPO in laying diets increases the absorption of oil-soluble vitamins and provides high caloric levels, while eggs quality can be enhanced with carotenoid-enriched CPO (Longe and Adekoya, 2021; Saminathan *et al*., 2020). Addition of treated or dehydrated POME up to 15% in the diet improved the laying hen's performance and egg production (Saminathan *et al*., 2020). Overall, these palm-based biomass materials are potential energy substitutes in chicken feed in countries producing palm oil (Azizi *et al*., 2021; Hakim *et al*., 2022; Saminathan *et al*., 2022).

Palm Oil Nutrition Research

Palm oil is full of nutritional value as it contains tocotrienols, the most potent vitamin E. Palm tocotrienol is widely used as a health supplement due to its scientifically proven health benefits. It has been found to exhibit anti-cancer properties (Constantinou *et al*., 2020; Fontana *et al*., 2022; Ranasinghe *et al*., 2022,), improve wound healing (Shahrim *et al*., 2022), neuroprotective effects (Zhao, 2022), treat fatty liver patients with/without steatohepatitis (Nawawi *et al*., 2022), increase overall health, reduce cardiovascular disease risk, lower cholesterol levels and has anti-inflammatory mechanisms that help in diverse diseases (Radzun *et al*., 2022; Ranasinghe *et al*., 2022; Zainal *et al*., 2022).

Based on the collective evidence and benefits of tocotrienols over the years, MPOB made a submission to the Ministry of Health to include tocotrienol claims under the Malaysian Food Act 1983. The tocotrienol rich fraction (TRF) can now be claimed as an antioxidant that may help reduce oxidative stress and improve cognitive function (Ministry of Health Malaysia, 2022a). These claims have been approved and are awaiting *gazettement* by the Ministry of Health Malaysia in the Regulation of Food Act 1985 (Ministry of Health Malaysia, 2022a). There must be at least 10 mg of TRF per 100 mL of liquid or solid food to make functional claims on product labels. This will increase consumer awareness and market for palm tocotrienols, as well as raise understanding of their health benefits. At the same time, MPOB has also submitted a new declaration function for *trans* fatty acids under Regulation 18C, Food Regulations 1985 to the Ministry of Health Malaysia that has been approved and gazettement is underway. The independent declaration for free of *trans* fatty acid claim requires edible fat and oil to have a *trans* fatty acids content of not more than 0.5 g per 100 mL, whilst *trans* fatty acids for other food is 0.1 g per 100 mL for both liquid and solid food (Ministry of Health Malaysia, 2022b).

Palm oil is also rich in carotenoids, a pro-vitamin A that is vital as vitamin A supplement. Malnutrition is still quite common among children, especially for those living in rural Malaysia. According to Tan *et al*. (2022), there is a high incidence of malnutrition and vitamin A deficiency among schoolchildren in rural areas and those under 10 years old. Furthermore, it was found that Orang Asli school children had greater rates of malnutrition, vitamin A deficiency, anaemia, iron deficiency, iron deficiency anaemia, and increased inflammation compared to non-Orang Asli children. Furthermore, malnourished children had lower levels of retinol, retinal-binding protein, alpha-carotene, ferritin, and haemoglobin. It was discovered that among children attending Orang Asli schools, stunting was also associated with iron deficiency anaemia (Tan *et al.,* 2022). In order to address malnutrition among Orang Asli school children, a dual intervention involving nutritional supplementation and anthelminthic treatment through a double-blinded and randomised control trial was conducted (Tan *et al.,* 2023). Malnutrition can increase an individual's susceptibility to parasitic infections such as soil-transmitted helminth disease. Red palm oil-enriched biscuits were distributed to the experimental schools. Compared to other studies, the results showed the overall reinfection rate of *A. Lumbricoides* and hookworm at six months were low, and red palm oil may have beneficial effects in conferring protection against reinfection and play an essential role in enhancing immune response.

Other nutritional studies focused on carotenes and water-soluble palm fruit extract (WSPFE). Meganathan *et al.* (2022) showed that natural carotenes with mixed isomers confer protection against oxidative stress induced in age-related macular degeneration (AMD) by modulating the key gene implicated in AMD. These findings indicated that carotenes should be explored further as a nutraceutical supplement for managing AMD. Besides, WSPFE has been found to have potential neuroprotective effects. Leow *et al.* (2021) discussed the great potential of WSPFE for functional application, supplementation and pharmaceutical products since it has inhibitory effects against cholinesterase inhibitors that are responsible for Alzheimer's disease.

Loganathan *et al*. (2022) investigated the chronic effects of diets enriched with palm olein, cocoa butter, or extra virgin olive oil with oleic acid at the *sn*-2 position. The randomised controlled trial found that all three diets resulted in similar lipid profiles and measures of homeostatic model assessment. The study suggested that the healthfulness of a food cannot be predicted solely by its nutrient group but rather by the overall macronutrient composition of the diet. Additionally,

with appropriate carbohydrate intake, there was no evidence of lipogenesis or changes in cardio metabolic risk markers from circulating saturated fatty acids.

Addressing Perceptions on Food Safety and Quality

All vegetable oils are at risk to process contaminants. Since they are mainly used for edible purposes, the presence of contaminants is to be avoided in the oils. Contamination can develop due to the use of pesticides, fertilisers, and unhygienic processing practices during the production of palm oil. Chloropropanols are harmful contaminants found in processed edible oils, and their presence is a major food safety concern. In a recent study by Hammid *et al.* (2022a), the total chloride levels in various refined oils were analysed and these chlorides are the precursor to chloropropanols formation. The total chloride in the refined oils reflects the 3-monochloropropane-1, 2-diol esters (3-MCPDE), which have been considered toxic. Refined oils are extensively used in various frying applications (Tarmizi and Kuntom, 2022; Xin *et al*., 2022). Furthermore, these edible oils may contain some of these processed developed contaminants, including 3-MCPDE and glycidyl esters due to being refined at an excessively high temperature. Analysis of commercially available refined oils revealed a significant range in total chloride level. According to Hammid *et al.* (2022a), the chloride level was below 1 μg mL^{-1} practically for all refined oils from the soft oil cluster. However, peanut oil, olive pomace oil and palm olein showed chloride levels ranging from 1 μg mL^{-1} to 1.5 μg mL^{-1}. The presence of chloride and other contaminants in edible oils can be attributed to the processing methods used during extraction and refining. The removal of some vegetative parts during processing in extra virgin coconut oil resulted in low anticipated chloride content. On the other hand, additional processing of the olive pressed mass revealed a rise in the chloride concentration, analogous to what was shown in the olive pomace oil. To ensure the safety of crude edible oils and eliminate the risk of process-developed contaminants, the industry should implement monitoring and removal of chloride during the production process. Reliable methods have been effectively employed to ascertain the total chloride content in cooking oil sold in commercial markets across Malaysia (Hammid *et al*., 2022a).

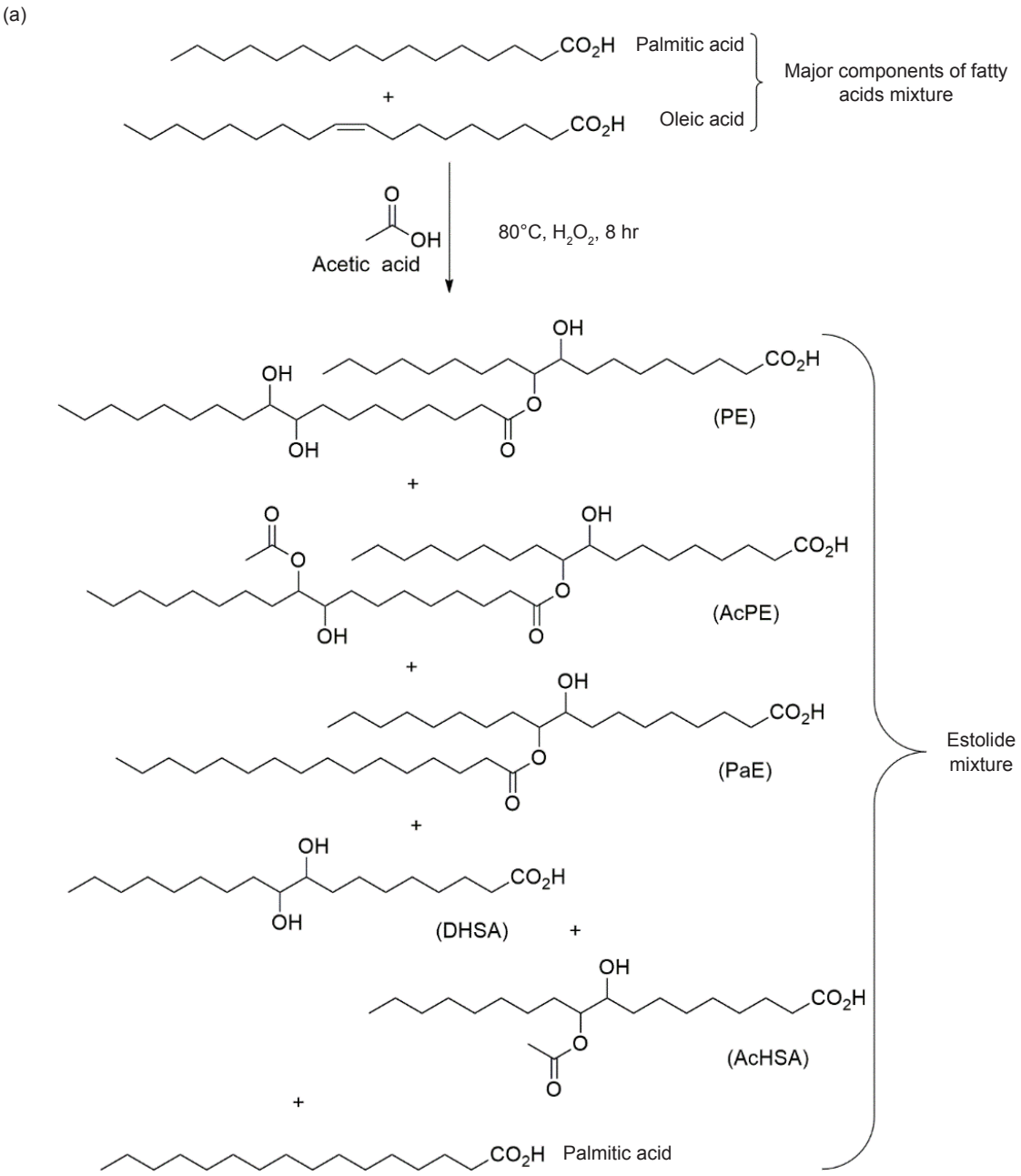
Aflatoxin is another contamination that usually occurs in PKC, which is the by-product of palm oil mainly used in animal feed (Hammid *et al*., 2022b). A significant range in aflatoxin concentration was found among the 24 samples of PKC examined. According to the study, the presence of aflatoxin was detected in 88% of the samples (21 out of 24), with levels varying between 0.70 and 4.65 μg kg^{-1}. Moreover, none of the PKC samples showed aflatoxin contents above the highest tolerance limit of 20 μg kg^{-1} set by the United States Food and Drug Administration (FDA, 2019). The study found that the contamination of aflatoxin in PKC was low *i.e.*, under the allowable limit, but it's still important to take steps in reducing the risks. Mill management should include proper storage techniques, advanced agricultural technologies, good agricultural practices, manufacturing and storage practices. Proper ventilation, uniform loading, reduction of insect infestation, and temperature control can help in reducing aflatoxin contamination (Hammid *et al*., 2022b).

Exploring Value Addition

Palm oil major application is in food at about 90% and about 10% was used for non-food applications (Shahbandeh, 2022). A study by Orjuela and Clark (2020) indicated that about 26% of the world's consumed oils could end up as used cooking oil (UCO), if without proper disposal could lead to many ecological problems. Thus, the potential of UCO as bio-lubricant feedstock was investigated in line with the principles of circular economy and the aim of turning waste into wealth. The estolide esters and amides made from UCO exhibited good cold flow, oxidation stability, and improved viscosity index, making them suitable as a base oil for bio-lubricants. The synthesis of estolide esters and amides involves a three-step reaction as shown in *Figure 1a-c*. The properties of the prepared estolide esters and amides are tabulated in *Table 11*. These base oils obtained are classified as ISO VG 68 and ISO VG 150, respectively (Hoong *et al*., 2022). In addition, a by-product of palm oil refining, PFAD was also used to produce a high purity ester-based bio-lubricant. The feedstock was reacted with 2-ethylhexanol via a non-catalytic esterification reaction. The PFAD ester showed properties comparable to those of the ISO VG 10 lubricant for hydraulic applications (Pauzi *et al*., 2022). These studies are in line with the recent growth in the health and food industries, which reveals a need for using more biodegradable lubricants and less toxic to minimise the risk of contamination by mineral oil saturated hydrocarbon (MOSH) and mineral oil aromatic hydrocarbon (MOAH). As such, attempts should be made to improve the performance of bio-lubricants from edible feedstock (Shah, 2021).

With the increasing demand for bio-based products, R&D of innovative palm-based polyurethane (PU) products continues. Since the formulation of PU is a tedious trial and error process and time-consuming, understanding the structure-property relationship of the reactants,

in this case, polyols and isocyanates, is very crucial in order to reduce the risk of failure. The correlation between the structure of palm olein-based polyols and its solid PUs was evaluated. It was found that the hard segment concentration and crosslink density, which depended on the hydroxyl number of the polyols, had significantly affected the mechanical properties of the solid PUs. On the other hand, the number of carbons of the diols used for epoxide ring-opening during polyol production did not significantly affect the mechanical properties of the solid PUs (Tuan Noor Maznee *et al*., 2022). In viscoelastic PU foam formulation, the incorporation of 25% palm olein-based polyol and an isocyanate index of 80% resulted in the best mechanical properties of the foam, *i.e.*, compression force deflection at 65%, tensile strength and average cell size were improved compared to similar foam formulated with isocyanate indices of 65 and 70% (Nurul 'Ain *et al*., 2022). For rigid PU foams, low-density PU foams made from palm olein-based polyol as a drop-in replacement for petrochemical-based polyol showed potential as insulation for refrigerators, freezers, and piping. The lowest thermal conductivity, k-value, was obtained at 0.0232 W/mk with the incorporation of 10 pph of palm olein-based polyol (Srihanum *et al*., 2022).



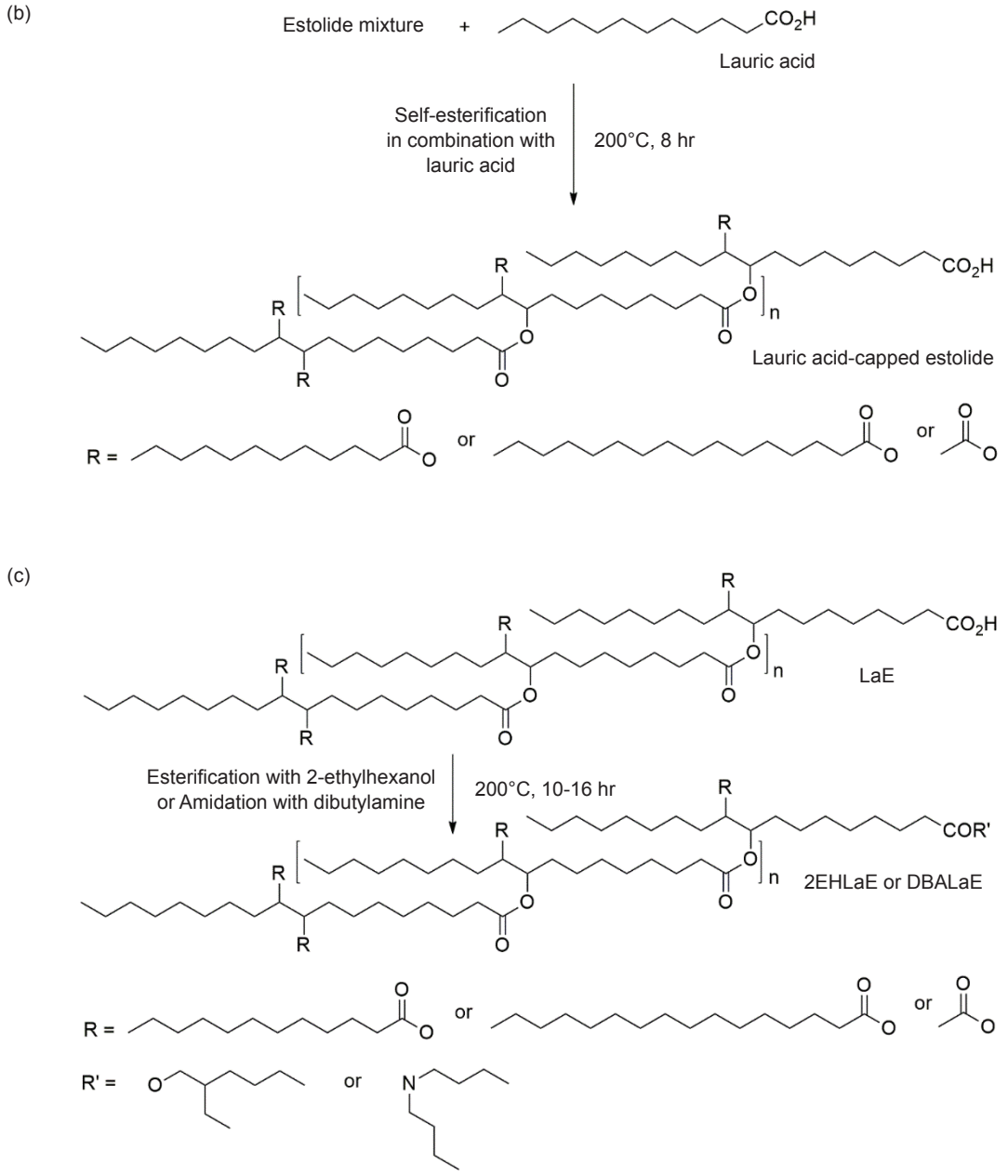


Figure 1. (a) Synthesis of estolide mixture from UCO-based fatty acids mixture, (b) synthesis of lauric acid-capped estolide(LaE), and (c) synthesis of lauric acid-capped estolide ester (2EHLaE) and estolide amide (DBALaE)

TABLE 11. PHYSICOCHEMICAL PROPERTIES OF 2EHLAE, DBALAE, TMPTE, DOPO AND HLP68

Sample	KV		VI	PP (°C)	OOT (°C)	WSD (mm)
	40°C, cSt	100°C, cSt				
2EHLaE	63.1 ± 0.1	11.8 ± 0.1	190	-12 ± 0.0	199.8 ± 0.2	0.58 ± 0.06
DBALaE	136.2 ± 0.2	20.3 ± 0.1	169	-12 ± 0.0	200.3 ± 0.2	0.56 ± 0.05
TMPTE[a]	61.8	14.0	236	9	183	ND
DOPO[b]	417.5	45.4	166	-5	155.8	ND
HLP68[c]	68.2 ± 0.2	8.8 ± 0.1	107	-6 ± 0.0	199.2 ± 0.1	0.60 ± 0.05

Note: 2EHLaE - estolide ester; DBALaE - estolide amide; TMPTE - palm-based trimethylolpropane triesters; DOPO - triglyceride-based estolide; KV - kinematic viscosity; VI - viscosity index; PP - pour point; OOT - oxidation onset temperature; WSD - four-ball wear scar diameter, ND - not determined

Source: [a] Nurazira *et al*. (2019); [b] Derawi and Salimon (2013); [c] Commercial mineral oil-based lubricant.

Phthalates are plasticisers that have been widely used in polymeric materials. They are known to be carcinogenic and toxic, having been shown to disrupt endocrine system and are detrimental to human health (Wang and Qian, 2021). Therefore, a bio-based plasticiser, such as epoxidised oleic acid, offers an alternative to phthalate-based plasticisers. Addition of epoxidised oleic acid into poly(vinylidene fluoride) polymer decreases the degree of crystallisation, melting point and glass transition temperatures of the plasticiser. It was found that 90:10 poly(vinylidene fluoride) and epoxidised oleic acid blend gave the optimum crystallisation, leading to a balanced thermal and mechanical properties of bio-plasticised poly(vinylidene fluoride) (Zulkifli *et al*., 2022).

In developing cosmetic and personal care product, the effect of dihydroxystearic acid (DHSA) as a gelling agent, on crystal morphology, hardness, rheological properties, and stability of various vegetable oils (RBD palm olein, RBD super olein, RBD palm kernel olein, medium chain triglycerides, and soybean oil) was evaluated. It was found that the DHSA organogel prepared with RBD super olein was stable with the lowest critical gel concentration, followed by RBD palm olein, soybean oil, RBD palm kernel olein and medium chain triglycerides. The viscosity and degree of unsaturation of the oils and the resultant crystal network were associated with the strength and elasticity of the DHSA organogels. The developed DHSA organogels have the potential to be formulated as lip care products (Ahmad and Hasan, 2022).

CONCLUSION

Environment, labour and food safety continues to be the pressing issues of the oil palm industry, which warrant effective measures for improvement. Yield stagnation due to continuous shrinkage of planted area and diminishing arable land has further aggravated the issue making it a formidable challenge to the industry. Efforts to produce future planting materials, intensify implementation of good agricultural practices and pest and disease management coupled with the adoption of disruptive mechanisation technologies are continuously pursued offering opportunities in reducing oil palm yield gap for enhancing the sustainability of the industry. Sustainable palm oil production by smallholders is another prevalent issue that requires immediate solutions. An effective and innovative system is needed to ensure complete participation and compliance of smallholders in MSPO certification. Moving downstream, the health benefits of oil palm tocotrienol, carotenes (red palm oil) and WSPFE have been evident. Other than that, PKC, CPO, and POME have shown the potential as cost-effective and nutritious alternatives to corn and soy in reducing imported chicken feed raw materials. Most importantly, contaminant-free processing of palm oil and products is required in order to ensure their safe consumption. The raising interest in the circular economy has also become one of the driving factors for value addition at the downstream, with several successful valorisation of palm-based by-products as mineral-based alternatives. Further works to demonstrate the techno-economic suitability of large scale bio-conversion is necessary in supporting the performance of the whole palm oil supply chain.

ACKNOWLEDGEMENT

The authors are very grateful for all the support and contribution given by all Divisions in preparing this manuscript.

REFERENCES

Abas, A; Er, A C; Tambi, N and Yusoff, N H (2021). A systematic review on sustainable agricultural practices among oil palm farmers. *Outlook Agric., 51(2).* DOI:10.1177/00307270211021875.

Abbasi, R; Martinez, P and Ahmad, R (2022). The digitization of agricultural industry - A systematic literature review on agriculture 4.0. *Smart Agric. Technol.*, 2: 100042. DOI: 10.1016/j.atech.2022.100042.

Abdul Malek, B A; Basari, N; Hamzah, H; Wan Mansor, W N A; Md Shani, F S; Arshad, A N; Azmi, W A and Zalipah, M N (2022). Sustaining beehive-fence to reduce elephant encroachment in oil palm plantation. *J. Oil Palm Res.* DOI: 10.21894/jopr.2022.0050.

Afandi, A M; Zulkifli, H; Nur Zuhaili, H A Z A; Norliyana, Z Z; Hisham, H; Saharul, A M; Dzulhelmi, M N and Vu Thanh, T A (2022). Oil palm water requirement and the need for irrigation in dry Malaysian areas. *J. Oil Palm Res*. DOI: 10.21894/jopr.2022.0052.

Ahmad, N and Hasan, Z A A (2022). Stability and physical properties of dihydroxystearic acid based organogels in different types of vegetable oils. *J. Oil Palm Res*. DOI: 10.21894/jopr.2022.0022.

Albiero, D; Pontin Garcia, A; Kiyoshi Umezu, C and Leme de Paulo, R (2022). Swarm robots in mechanized agricultural operations: A review about

challenges for research. *Computers and Electronics in Agriculture*. Elsevier B.V.

Alcock, T D; Salt, D E, Wilson, P and Ramsden, S J (2022). More sustainable vegetable oil: Balancing productivity with carbon storage opportunities. *Sci. Total Environ.*, *829*: 154539.

Amanina, N S; Linatoc, A C; Haniff, M H and Roslan, M N (2022). Growth and development of oil palm clone P164 exposed to longterm carbon dioxide enrichment in open top chamber. *J. Oil Palm Res.*, *34(1)*: 56-67.

Amran, A; Humaira, M T; Zaki, A and Abdul Rahman, A R (2021). Factors influencing turnover intention among Malaysian unskilled workers in oil palm plantation. *MJSSH, 6(9)*: 374-381. DOI: 10.47405/mjssh.v6i9.1002.

Ariffin, I; Hanafi, M M; Roslan, I; Ubaydah, M U; Karim, A Y; Tui, L C and Hamzah, S (2022). Responses of irrigated oil palm to nitrogen, phosphorus and potassium fertilizers on clayey soil. *Agric. Water Manag., 274*: 107922. DOI: 10.1016/j.agwat.2022.107922.

Ayodele, B V; Mustapa, S I; Kanthasamy, R; Mohammad, N; AlTurki, A and Babu, T S (2022). Performance analysis of support vector machine, Gaussian Process Regression, sequential quadratic programming algorithms in modeling hydrogen-rich syngas production from catalyzed co-gasification of biomass wastes from oil palm. *Int. J. Hydrog. Energy*., *47(98)*: 41432-41443. DOI: 10.1016/j.ijhydene.2022.05.066.

Azahar, A A; Nurhafizah, M D; Omar, M R; Abdullah, N and Ul-Hamid, A (2022). Bio-graphene production from oil palm shell waste valorised through sequential thermal and catalytic means. *Carbon Trends*, *9*: 100225.

Azizi, M N; Loh, T C; Foo, H L and Teik Chung, E L (2021). Is palm kernel cake a suitable alternative feed ingredient for poultry? *Animals (Basel), 11(2)*: 338.

Badrulisham, A S; Kageyama, D; Halim, M; Aman-Zuki, A; Masri, M M M; Ahmad, S N; Md-Zain, B M and Yaakop, S (2022). New insights into the phylogeography of the oil palm pest, *Metisa plana* towards its management control. *J. Oil Palm Res., 34(3)*: 427-438.

Bahariah, B; Masani, M Y A; Fizree, M D P M A A; Rasid, O A and Parveez, G K A (2023). Multiplex CRISPR/Cas9 gene-editing platform in oil palm targeting mutations in *Eg*FAD2 and *Eg*PAT genes. *J. Genet. Eng. Biotechnol*., *21*: 3.

Bakar, N A A; Malike, F A; Amiruddin, M A and Ong-Abdulllah, M (2022). Genetic variability and performance of MPOB-Nigeria *dura* x AVROS *pisifera* planting materials. *Int. J. Oil Palm, 5(1)*: 26-38. DOI:10.35876/ijop.v5i1.76.

Bellocchio, E; Crocetti, F; Costante, G; Fravolini, M L; and Valigi, P (2022). A novel vision-based weakly supervised framework for autonomous yield estimation in agricultural applications. *Eng. Appl. Artif. Intell.*, *109*: 104615.

Bok, C H; Lim, C H; Ngan, S L; How, B S; Ng, W P Q and Lam, H L (2022). Life cycle assessment and life cycle costing for uncertified and Malaysia Sustainable Palm Oil-MSPO-certified independent smallholders. *J. Clean. Prod., 379(1)*: 134646.

Ching, L M; Jantan, N M; Zahari, A H and Tahar, N F (2022). Description of a dynamic closed chamber method for measuring soil respiration: A case study in oil palm plantations on peat. *Oil Palm Bulletin, 84*: 29-35.

Constantinou, C; Charalambous, C and Kanakis, D (2020). Vitamin E and cancer: An update on the emerging role of γ and δ tocotrienols. *Eur J Nutr., 59(3)*: 845-857.

Daim, L D J; Tan, B A; Ithnin, N; Ooi, T E K; Normahnani, M N; Appleton, D R and Harikrishna, K (2022). Transcriptomic and proteomic studies to investigate the basal stem rot disease in oil palm seedlings. *J. Oil Palm Res.* DOI: 10.21894/jopr.2022.0053.

Dassou, O S; Ollivier, J; Vanhove, W; Aholoukpè, H; Impens, R; Bonneau, X; Flori, A; Durand-Gasselin, T; Augustin Sinsin, B; Adjanohoun, A and Van Damme, P (2022). Oil palm (*Elaeis guineensis* Jacq.) genetic differences in mineral nutrition: environmental effects on leaflet mineral concentrations of four oil palm progenies. *OCL, 29*: 23.

Derawi, D and Salimon, J (2013). Palm olein based biolubricant basestocks: synthesis, characterisation, tribological and rheological analysis. *Malaysian J. Anal. Sci.,, 17*: 153-163.

Dhanya, V G; Subeesh, A; Kushwaha, N L; Vishwakarma, D K; Nagesh Kumar, T; Ritika, G and Singh, A N (2022). Deep learning based computer vision approaches for smart agricultural applications. *Artif. Intelli. Agric., 6*: 211-229.

Dzulkafli, S B; Othman, A; Lau, B Y C; Ramli, U S and Karsani, S A (2022). Comparative proteome analysis of mycelial proteins from *G. boninense* vs *G. tornatum*: Identification of proteins potentially involved in the pathogenicity of *G. boninense*. *Physiol. Mol. Plant Pathol., 117*: 101736

FAO (2022). The importance of Ukraine and the Russian Federation for global agricultural markets and the risks associated with the war in Ukraine.

Fontana, F; Anselmi, M and Limonta, P (2022). Exploiting the metabolic consequences of pten loss and akt/hexokinase 2 hyperactivation in prostate cancer: A new role for δ-tocotrienol. *Int. J. of Mol Sci*., *23(9)*: 5269.

Food and Drug Administration (FDA) (2019). CPG Sec. 683.100 Action Levels for Aflatoxins in Animal Food.

Gil, G; Casagrande, D E; Cortés, L P; and Verschae, R (2023). Why the low adoption of robotics in the farms? Challenges for the establishment of commercial agricultural robots. *Smart Agric. Technol*., *3*: 100069.

Gilbertson, L M and Vikesland, P J (2022). Inspiring a nanocircular economy. *Environ. Sci. Nano*, *9*: 839. DOI: 10.1039/d2en90005j

Hakim, A H; Zulkifli, I; Farjam, A S; Awad, E A and Ramiah, S K (2022). Impact of feeding fermented palm kernel cake and high dietary fat on nutrient digestibility, enzyme activity, intestinal morphology and intestinal nutrient transporters mRNA expression in broiler chickens under hot and humid conditions. *Animals (Basel), 12(7)*: 882.

Hammid, A. N; Kuntom, A and Abdul Mutalib, S (2022a). Method for the determination of total chloride content in edible oils. *J. Oil Palm Res.* DOI: 10.2189/jopr.2022.0016.

Hammid, A. N; Kuntom, A and Abdul Mutalib, S (2022b). Prevalence of aflatoxins contamination in palm kernel cake in Malaysia. *Int. J. Enviro. Anal. Chem., 1-13.*

Herliatika, A; Sinurat, A P; Haryati, T and Subeni, I (2022). Effect of palm kernel cake (PKC) inclusion and multi-enzyme supplementation on layer performances. *Adv. Biol. Sci. Res.*, *21*: 55-60.

Hoong, S S; Arniza, M Z; Nik Siti Mariam, N M D; Noor Armylisas, A H; Tang, S W; Tuan Noor Maznee, T I and Yeong, S K (2022). Synthesis and physicochemical properties of estolide ester and amide made from used cooking oil as bio-lubricant. *J. Oil Palm Res.* DOI: 10.21894/jopr.2022.0064.

Htwe, Y M; Shi, P; Zhang, D; Li, Z; Xiao, Y; Yang, Y; Lei, X and Wang, Y (2022). Programmed cell death may be involved in the seedless phenotype formation of oil palm. *Front. Plant Sci.*, *13*:832017. DOI: 10.3389/fpls.2022.832017.

Ithnin, M; Rajanaidu, N; Singh, R and Kushairi, A (2022). An assessment of the Malaysian oil palm breeding populations using AFLP markers. *J. Oil Palm Res.* DOI: 10.21894/jopr.2022.0073.

Jamaludin, N, Bahariah, B, Shaharudin, N A, Ho, C L, Rasid, O A, Parveez, G K A and Masani, M Y A (2022). Designing gRNAs targeting oil palm phytoene desaturase gene and construction of vectors for oil palm CRISPR/Cas9 study. *J. Oil Palm Res.* DOI: 10.21894/jopr.2022.0032.

Ju, C; Kim, J; Seol, J; and Son, H I (2022). A review on multirobot systems in agriculture. *Comput. Electro. Agric.*, *202*: 107336.

Keni, M F; Zainuddin, N and Masri, M M M (2022). Improving the growth performance of oil palm seedlings by mixtures of organic and chemical fertilisers. *J. Oil Palm Res.* DOI: 10.21894/jopr.2022.0033.

Kibrom, T S; Linda, S; Hermanto, S; Matin, Q and Meike, W (2022). Spatial heterogeneity in smallholder oil palm production. *For. Policy Econ., 139*: 102731. DOI: 10.1016/j.forpol.2022.102731.

Kumari, P and Samadder, S R (2022). Valorization of carbonaceous waste into graphene materials and their potential application in water & wastewater treatment: A review. *Mater. Today Chem., 26*: 101192.

Lau, B Y C; Othman, A; Ramli, U S (2022). Antifungal and antioxidant peptides from oil palm mesocarps. *J. Oil Palm Res.*, *34(3)*: 453-464.

Leão, A P; Filho, J A F; Pereira, VM; Alonso Alves, A and Souza Júnior, M T (2022). Genomic characterization of SNPs for genetic differentiation and selection in populations from the American oil palm [*Elaeis oleifera* (Kunth) Cortés] germplasm bank from Brazil. *Diversity, 14*: 270. DOI: 10.3390/d14040270.

Leow, S S; Bakar, S F A and Sambanthamurthi, R (2022). Inhibition of cholinesterases by water-soluble palm fruit extract. *J. Oil Palm Res.*, *34(1)*: 139-151. DOI: 10.21894/jopr.2021.0028.

Li, J; Yang, Y; Sun, X; Liu, R; Xia, W; Shi, P; Zhou, L; Wang, Y; Wu, Y; Lei, X and Xiao, Y (2022). Development of intron polymorphism marker and their association with fatty acid component variation in oil palm. *Front. Plant Sci., 13*: 885418.

Lim, H J; Cheng, W K and Yu, L J (2022). Oil palm-based nanocellulose for a sustainable future: Where are we now?. *J. Environ. Chem. Eng., 10(2)*: 107271.

Loganathan, R; Nagapan, G; Teng, K T; Voon, P T; Yap, S Y; Ng, Y T; Ng, T K W; Choo, Y M; Ong, A S H; Ong, S H and Selvaduray, K R (2022). Diets enriched with palm olein, cocoa butter, and extra virgin olive oil exhibited similar lipid response: a randomized controlled study in young healthy adults. *Nutr. Res., 105*: 113-125.

Loh, S K; Nasrin, A B; Sukiran, M A; Bukhari, N A and Subramaniam, V (2022). Oil palm biomass value chain for biofuel development in Malaysia: part II. *Value-Chain of Biofuels Fundamentals, Technology, and Standardization* (Yusup, Y and Rashidi, N A eds.). Elsevier. p. 505-534.

Longe, O G and Adekoya, O (2021). Response of laying hens to different inclusion levels of palm kernel meal and vegetable oil. *Niger. J. Anim. Prod., 15:* 111-117.

Mahroof, K; Omar, A; Rana, N P; Sivarajah, U;, and Weerakkody, V (2021). Drone as a Service (DaaS) in promoting cleaner agricultural production and circular economy for ethical sustainable supply chain development. *J. Cleaner Prod., 287*: 125522.

Masri, M M M; Kamarudin, N; Ali Napiah, M N R and Keni, M F (2022). Effectiveness of *Bacillus thuringiensis* aerial spraying against the bagworm, *Metisa plana* Walker (Lepidoptera: Psychidae) outbreak in oil palm using drone. *J. Oil Palm Res., 34(2)*: 276-288.

Masura, S S; Tahir, N I; Rasid, O A; Ramli, U S; Othman, A; Masani, M Y A; Parveez, G K A and Kushairi, A (2017). Post-genomic technologies for the advancement of oil palm research. *J. Oil Palm Res., 29(4)*: 469-486.

Medina, A F (2022, 29 April). Indonesia bans the export of palm oil, impacting global food prices. asean briefing. https://www.aseanbriefing.com/news/indonesia-bans-the-export-of-palm-oil-impacting-global-food-prices/, accessed on 13 April 2023.

Meganathan, P; Mai, C; Selvaduray, K R; Zainal, Z and Fu, J (2022). Effect of carotenes against oxidative stress induced age-related macular degeneration in human retinal pigment cells. *ACS Food Science Technol., 2(11)*: 1719-1727.

Ministry of Health Malaysia (2022a). Kelulusan Akuan Fungsi Nutrien Baru Bagi Palm Tocotrienol Rich Fraction (TRF) Di Bawah Peraturan 18F (4) [P.U. (A) 209 Peraturan-Peraturan Makanan (Pindaan) (No.4) 2020], Peraturan-Peraturan Makanan 1985. Retrieved from (Ref. No: KKM.600-1/3/366). Ministry of Health, Malaysia.

Ministry of Health Malaysia (2022b). Kelulusan Akuan Kandungan Baru Bagi Asid Lemak Trans Di Bawah Peraturan 18C, Peraturan-Peraturan Makanan 1985. Retrieved from (Ref. No: KKM.600-1/3/366 (22)). Ministry of Health, Malaysia.

Mohd Din, A; Marhalil, M; Mohd Mustakim, M; Norziha, A; Kushairi, A and Rajanaidu, N (2022). Field evaluation of oil palm genetic materials for partial resistance in *Ganoderma* hotspots of tropical peat soil. *J. Oil Palm Res.* DOI: 10.21894/jopr.2022.0025.

Mohd Noor Izuddin, Z B; Parthiban, K; Rahmahwati, R; Norkaspi, K and Zaki, A (2022) Factors affecting independent oil palm smallholder's decision to participate in government replanting assistance scheme in Malaysia. *MJSSH, 7(9)*: e001744. DOI: 10.47405/mjssh.v7i9.1744.

MPOB (2022). *Malaysian Oil Palm Statistics 2022*. 42nd edition. MPOB, Bangi.

Muhammad, M; Roswanira, A W; Fahrul, H; Rusli, M H**;** Syariffah Nuratiqah, S Y and Teo, H K (2022). An overview of the potential role of microbial metabolites as greener fungicides for future sustainable plant diseases management. *J. Crop Pro., 11*: 1-27.

Naidu, L; Moorthy, R and Mohd Huda, M I (2022). The environmental and health sustainability challenges of Malaysian palm oil in the European Union. *J. Oil Palm Res.* DOI: 10.21894/jopr.2022.0072.

Najib, M A; Izzuddin, M A; Nordiana, A A; Azwan, M M B; Ong, M A and Idris, A S (2022). Addressing functionalities of agricultural robotic (agribots) and automation in the agriculture practices: What's next?. *AAFRJ, 4(1):* DOI: 10.36877/aafrj.a0000298.

Nasir, M H; Mispan, M S; Bhassu, S; Jing, K J; Abu Bakar, S; Azam, M S N I; Ishak, S N; Mohd Taib, S and Omar, H (2022). Spatial distribution of *Rattus* species (Rodentia: Muridae) in oil palm plantations of Peninsular Malaysia with species verification

using Cytochrome Oxidase I (COI) gene. *J. Oil Palm Res., 35(1)*: 58-74. DOI: 10.21894/jopr.2022.0026.

Nawawi, K N M; Wong, Z; Mokhtar, N M and Ali, R A R (2022). Palm tocotrienol-rich fraction significantly improve transaminase levels, hepatic steatosis and inflammation scores in patients with metabolic dysfunction-associated fatty liver disease: an observational real-world study. *Gut* 71: A104-A105.

New Straits Times (2022). KL Kepong likely to achieve better FFB growth, says HLIB Research. https://www.nst.com.my/business/2022/09/832779/kl-kepong-likely-achieve-better-ffb-growth-says-hlib-research%C2%A0, accessed on 10 April 2023.

New Straits Times (2023). FGV Holdings beats HLIB Research, consensus estimates due to better FFB yields. https://www.nst.com.my/business/2023/02/884268/fgv-holdings-beats-hlib-research-consensus-estimates-due-better-ffb-yields, accessed on 10 April 2023.

Ngau, L D; Fong, S S; Khoon, K L; Rumpang, E; Vasander, H; Jauhiainen, J; Yrjala, K and Silvennoinen, H (2022). Mapping peat soil moisture under oil palm plantation and tropical forest in Sarawak. *Mires Peat, 28*: 1-17. DOI: 10.19189/MaP.2022.OMB.StA.2370.

Noh, M A A; Zaludin, M M S; Ghani, W A W M H; Ahmad, A H and Salim, H (2022). Field efficacy of anticoagulant rodenticides against rat infestation in oil palm plantation. *J. Oil Palm Res.* DOI: 10.21894/jopr.2022.0044.

Nor Azwani, A B; Fadila, A M; Mohd Din, A; Rajanaidu, N; Norziha, A; Suzana, M; Marhalil, M; Zulkifli, Y and Kushairi, A (2020). Potential oil palm genetic materials derived from introgression of germplasm (MPOB-Nigeria, MPOB-Zaire and MPOB-Cameroon accessions) to advanced (AVROS) breeding population. *J. Oil Palm Res., 32(4)*: 569-581.

Nordiana, A A; Zulkifli, H; Afandi, A M; Izzuddin, M A; Najib, M A and Idris, A S (2022). Remote sensing and GIS application for sustainability management of oil palm plantation. *Oil Palm Bulletin, 84*: 10-21.

Norkaspi, K and Raja Zulkifli, R O (2022). Viability of forage sorghum integration in oil palm planting area for production of livestock fodder. *J. Oil Palm Res.* DOI: 10.21894/jopr.2022.0031.

Nurazira, M N; Derawi, D and Salimon, J (2019). Esterification and evaluation of palm oil as biolubricant base stock. *Malays. J. Chem., 21*: 28-35.

Nur-Rashyeda, R; Idris, A S; Sundram, S; Zainol-Hilmi, N H and Ming, S C (2022). A field evaluation on fungicides application to control upper stem rot (USR) disease in oil palm caused by *Ganoderma* spp. *J. Oil Palm Res.* DOI: 10.21894/jopr.2022.0000.

Nurul 'Ain, H; Kosheela Devi, P P; Tuan Noor Maznee, T I; Srihanum, A; Norhayati, M N; Mohd Norhisham, S and Yeong, S K (2022). Effect of methylene diphenyl diisocyanate index on physico-mechanical and morphological properties of palm olein-based viscoelastic polyurethane foams. *J. Oil Palm Res*. DOI: 0.21894/jopr.2022.0023.

Nuthammachot, N and Stratoulias, D (2022). Exploring Sentinel-2 satellite imagery-based vegetation indices for classifying healthy and diseased oil palm trees. *J. Oil Palm Res.* DOI: 10.21894/jopr.2022.0000.

OECD (2022). War in Ukraine: Tackling the policy challenges. https://www.oecd.org/ukraine-hub/en/, accessed on 10 April 2023.

Oettli, P, Behera, S K, and Yamagata, T (2018). Climate based predictability of oil palm tree yield in Malaysia. *Sci. Rep., 8(1)*: 1-13.

Orjuela, A and Clark, J (2020). Green chemicals from used cooking oils: Trends, challenges, and opportunities. *Curr. Opin. Green Sustain. Chem., 26*:100369.

Palacios, F; Melo-Pinto, P; Diago, M P and Tardaguila, J (2022). Deep learning and computer vision for assessing the number of actual berries in commercial vineyards. *Biosystems Engineering*, *218*: 175-188.

Parthiban, K; Nurhanani, M; Nazira, K R; Tan, S P and Siti, M M (2021). A review on Malaysian sustainable palm oil certification process amongindependent oil palm smallholders. *J. Oil Palm Res., 33(1)*: 171-180.

Parthiban, K; Tan, S P; Zaki, A; Khairuman, H; Nazirah, C J and Nurul Safinaz, N F. (2022).Effectiveness in reporting of oil palm fresh fruit bunch transactions amongoil palm fruit dealers. *GMJSS, 18(4):* 174-188. DOI:10.17576/geo-2022-1804-13.

Parveez, G K A (2023). The Malaysian palm oil industry performance 2022 & prospects for 2023. Palm Oil Economic Review and Outlook Seminar 2023, Putrajaya, Malaysia.

Parveez, G K A; Kamil, N N; Zawawi, N Z; Abdullah, M O; Rasuddin, R; Loh, S K;

Selvaduray, K R; Hoong S S and Idris, Z (2022). Oil palm economic performance in Malaysia and R&D progress in 2021. *J. Oil Palm Res., 34(2)*: 185-218.

Pashkevich, M D; Spear, D M; Advento, A D; Caliman, J-P; Foster, W A; Luke, S H; Naim, M; Sudharto, Ps; Snaddon, J L and Turner, E C (2022). Spiders in canopy and ground microhabitats are robust to changes in understory vegetation management practices in mature oil palm plantations (Riau, Indonesia). *BAAE, 64*: 120-133. DOI: 10.1016/j.baae.2022.08.004.

Pauzi, N N P N; Ramli, N A S; Chan, C H; Hazmi, A S A; Ikram, R and Jan, B M (2022). Non-catalytic esterification of palm fatty acid distillate with 2-ethylhexanol for high purity production of biolubricant ester. *Biofuel Bioprod. Bioref., 16(6)*: 1583-1598. DOI: 10.1002/bbb.2390.

Pradiko, I; Rahutomo, S; Farrasati, R; Ginting, E N; Hidayati, F and Syarovy, M (2022). Transpiration of oil palm (*Elaeis guineensis* Jacq.) based on sap flow measurement: The relationto soil and climate variables. *J. Oil Palm Res., 35(1)*: 168-184. DOI: 10.21894/jopr.2022.0035.

Radzun, K A; Rusmidi, M H. H; Norisam, I; Iran, N; Pardi, F; Ismail, A; Razak, W R W A and Hafid, S R A (2022). Anti-inflammatory effects of astaxanthin extracted from microalgae *Hematococcus pluvialis* and combinations with palm tocotrienol rich-fraction in RAW 264.7 macrophages. *Pharmacogn. J., 14(1)*: 205-215.

Raikwar, S; Fehrmann, J and Herlitzius, T (2022). Navigation and control development for a four-wheel-steered mobile orchard robot using model-based design. *Comput. Electron. Agric., 202*: 107410. DOI: 10.1016/j.compag.2022.107410.

Ramli, U S; Othman, A; Lau, B Y C; Hassan, H; Mohd Ishak, N; Nurazah, Z; Rozali, N L; Tahir, N I M; Shahwan, S; Dzulkafli, S B; Singh, R; Rasid, O A; Sambanthamurthi, R; Abd Manaf, M A and Parveez, G K A (2020). Omics platform technologies for discovery and understanding the systems biology of oil palm. *J. Oil Palm Res., 34(1)*: 1-25. DOI: 10.21894/jopr.2020.0084.

Ranasinghe, R; Mathai, M and Zulli, A (2022). Revisiting the therapeutic potential of tocotrienol. *BioFactors, 48(4):* 813-856.

Rejeb, A; Abdollahi, A; Rejeb, K and Treiblmaier, H (2022). Drones in agriculture: A review and bibliometric analysis. *Comput. Electron. Agric., 198*: 107017.

Rosli, R; Ab Halim, M A; Ngoot-Chin, T; Modh Zaki, N; Nagapan J; Singh, R; Low, E T L and Mohamed-Hussein, Z (2022). Oil palm SSR resource interface (OPSRI) - Web-based bioinformatics analysis pipeline for SSR Mining. *J. Oil Palm Res., 34(4)*: 643-656. DOI: 10.21894/jopr.2022.0008.

Saminathan, M; Mohamed, W N W; NOH, A; Ibrahim, N A; Fuat, M A; Dian, N L H M and Ramiah, S K (2020). Potential of feeding crude palm oil and co-products of palm oil milling on laying hens' performance and egg quality: A review. *J. Oil Palm Res., 32(4)*: 547-558.

Saminathan, M; Mohamed, W N W; Noh, A M; Ibrahim, N A; Fuat, M A and Ramiah, S K (2022). Effects of dietary palm oil on broiler chicken productive performance and carcass characteristics: a comprehensive review. *Trop. Anim. Health and Prod., 54(1)*: 64.

Shah, R (2021). Bio-based (edible) oils: Feedstock for lubricants of the future. https://www.aocs.org/stay-informed/inform-magazine/featured-articles/bio-based-(edible)-oils/, accessed on 16 November 2022.

Shahbandeh, M (2022). Vegetable oils: Global consumption 2013/2014 to 2021/2022, by oil type. https://www.statista.com/statistic/263937/vegetable -oils-global-consumption/, accessed on 17 November 2022.

Shahrim, Z; Makpol, S; Tan, G C; Muhammad, N A and Hasan, Z A A (2022). Topical application of the palm tocotrienol-rich fraction (TRF) enhances cutaneous wound healing in type 2 diabetic mice. *J. Oil Palm Res., 34(3)*: 546-561. DOI: 10.21894/jopr.2021.0054.

Shiddiq, M; Arief, A A; Defrianto; Dasta V F; Panjaitan, D M and Saputra, D (2022). Counting of oil palm fresh fruit bunches using computer vision. *J. Oil Palm Res.* DOI: 10.21894/jopr.2022.0029.

Somyong, S; Phetchawang, P; Bihi, A K; Sonthirod, C; Kongkachana, W; Sangsrakru, D; Jomchai, N; Pootakham, W and Tangphatsornruang, S (2022). A SNP variation in an expansin (*Eg*Exp4) gene affects height in oil palm. *Peer J., 10*: e13046. DOI 10.7717/*peerj*.13046

Srihanum, A; Tuan Noor Maznee, T I; Kosheela Devi, P P; Hoong, S S; Nurul 'Ain, H; Mohd Norhisham, S; Nik Siti Mariam, N M D and Yeong, S K (2022). Low density rigid polyurethane foam incorporated with renewable polyol as sustainable thermal insulation material. *J. Cell. Plast., 58(3)*: 485-503. DOI: 10.1177/0021955X211062630.

Subeesh, A and Mehta, C R (2021). Automation and digitization of agriculture using artificial intelligence and internet of things. *Artificial Intelligence in Agriculture*. KeAi Communications Co. pp. 278-291. DOI: 10.1016/j.aiia.2021.11.004.

Sundram, S; Naidu, Y; Mohamed-Azni, I N A; Syed Aripin, S M; Nur-Rashyeda, R; Mohamed, M S and Hefni, M R (2022). Fungi in biological management of plant diseases: Current and future perspective. *J. Oil Palm Res.* DOI: 10.21894/jopr.2022.0061.

Suraninpong, P and Nuanlaong, S (2022). Comparative transcriptome profiling and molecular marker development for oil palm fruit color. *Sci. Rep., 12*: 15507. DOI: 10.1038/s41598-022-19890-2.

Suwandi, S; Munandar, R P; Suparman, S; Irsan C and Muslim, A (2022). Mixed planting with rhizomatous plants interferes with *Ganoderma* disease in oil palm. *J. Oil Palm Res.* DOI: 10.21894/jopr.2022.0043.

Swails, E; Hergoualc'h, K; Deng, J; Frolking, S and Novita, N (2022). How can process-based modeling improve peat CO_2 and N_2O emission factors for oil palm plantations?. *Sci. Total Environ., 839:* 156153. DOI: 10.1016/j.scitotenv.2022.156153.

Tahir, N I; Rozali, N L; Rahmah, A R S; Amiruddin, M D; Hwa, L F; Shaari, K; Abas, F; Othman, A; Parveez, G K A and Ramli, U S (2022). Metabolome study of oil palm (*Elaeis guineensis* Jacq.) planted in different environment conditions. *Trop. Plant Biol., 15*: 211-232. DOI: 10.1007/s12042-022-09318-6.

Tan, P Y; Mohd Johari, S N; Teng, K T; Loganathan, R; Lee, S. C; Ngui, R; Selvaduray, K. R and Lim, Y A L (2022). High prevalence of malnutrition and vitamin A deficiency among schoolchildren of rural areas in Malaysia using a multi-school assessment approach. *Br. J. Nutr., 129(3)*: 454-467. DOI:10.1017/S0007114522001398.

Tan, P Y; Loganathan, R; Teng, K T; Lee, S C; Johari, S N M; Selvaduray, K R; Ngui, R and Lim, Y A (2023). Red palm olein-enriched biscuit supplementation lowers *Ascaris lumbricoides* reinfection at 6-month after anthelmintic treatment among schoolchildren with vitamin A deficiency (VAD). *Acta tropica*, *240*: 106860.

Tarmizi, A H A; and Kuntom, A (2022). The occurrence of 3-monochloropropane-1, 2-diol esters and glycidyl esters in vegetable oils during frying. *Crit. Rev. Food Sci. Nutr*., *62(12)*: 3403-3419.

Terry, L M; Loy, A C M; Chew, J J; How, B S; Andiappan, V and Sunarso, J (2022). Chemical engineering and the sustainable oil palm biomass industry - Recent advances and perspectives for the future. *Chem. Eng. Res. Des., 188*: 729-735.

The Star (2022). UMB to prioritise improving FFB yields. https://www.thestar.com.my/business/business-news/2022/06/30/umb-to-prioritise-mproving-ffb-yields, accessed on 10 April 2023.

Tregear, J W; Richaud, F; Collin, M; Esbelin, J; Parrinello, H; Cochard, B; Nodichao, L; Morcillo, F; Adam, H and Jouannic, S (2022). Micro-RNA-regulated *SQUAMOSA-PROMOTER BINDING PROTEIN-LIKE* (*SPL*) gene expression and cytokinin accumulation distinguish early-developing male and female inflorescences in oil palm (*Elaeis guineensis*). *Plants, 11*: 685. DOI: 10.3390/plants11050685

Tuan Noor Maznee, T I, Nor Azowa, I; Kosheela Devi, P P; Hoong, S S; Mohd Azmil, M N; Yeong, S K; Emilia, A M; Sendijarevic, I and Sendijarevic, V (2022). Properties of solid polyurethanes made from palm olein-based polyols prepared with various types of nucleophiles. *J. Oil Palm Res.* DOI: 10.21894/jopr.2022.0015.

Tun Mohd Salim, W N S; Yaakub, Z; Mustafa, S; Abu Bakar, N A; Mohd Nasir, F; Marjuni, M; Amiruddin, M D and Ong Abdullah, M (2022). Genetic variability of MPOB-Cameroon oil palm germplasm based on morphological traits using multivariate analysis. *J. Oil Palm Res.* DOI: 10.21894/jopr.2022.0038.

Vasu, P (2023). Sector of the year: the 'golden crop' shines bright on external factors but ends the year almost unchanged. The Edge Market. https://www.theedgemarkets.com/node/649891, accessed on 13 April 2023.

Voigt, M; Kuhl, H S; Ancrenaz, M; Gaveau, Meijaard, E; Santika, T; Sherman, J; Wich, S A; Wolf, F; Struebig, M J; Pereira, H M and Rosa, I M D (2022). Deforestation projections imply range-wide population decline for critically endangered Bornean orangutan. *PECON, 20*: 240-248.

Wang, Y and Qian, H (2021). Phthalates and their impacts on human health. *Healthcare, 9*: 603. DOI:10.3390/healthcare9050603.

Xin, L; Hu, M; Ma, X; Wu, S; Yoong, J H; Chen, S; Tarmizi, A H A and Zhang, G (2022). Selection of 12 vegetable oils influences the prevalence of polycyclic aromatic hydrocarbons, fatty acids, Tocol homologs and total polar components during deep frying. *J. Food Comp. Anal., 114*: 104840.

Yaakub, Z; Marjuni, M; Mustafa, S; Tun Mohd Salim, W N S; Mohd Nasir, F; Abdullah, Z; Amiruddin, M D; Rajanaidu, N; Kushairi, A and Ong Abdullah, M (2022). Phenotypic variability of *Elaeis oleifera* germplasm revealed by principal component and cluster analyses. *J. Oil Palm Res.* DOI: 10/21894/jopr.2022.0054.

Yang, M; Yarra, R; Zhang, R; Zhou, L; Jin, L; John Martin, J J J and Cao, H (2022). Transcriptome analysis of oil palm pistil during pollination and fertilization to unravel the role of phytohormone biosynthesis and signaling genes. *Funct. Integr. Genomics, 22*: 261-278. DOI: 10.1007/s10142-022-00834-y.

Yang, Y; Saand, M A; Huang, L; Abdelaal, W B; Zhang, J; Wu, Y; Li, J; Sirohi, M H and Wang, F (2021). Applications of multi-omics technologies for crop improvement. *Front. Plant Sci., 12*: 563953. DOI: 10.3389/fpls.2021.563953.

Yaqoob, A A; Serrà, A; Ibrahim, M N M and Yaakop, A S (2021). Self-assembled oil palm biomass-derived modified graphene oxide anode: An efficient medium for energy transportation and bioremediating Cd (II) via microbial fuel cells. *Arab. J. Chem., 14(5)*: 103121.

Yeap, W C; Norkhairunnisa, C M K; Norfadzilah, J; Muad, M R; Appleton, D R and Harikrishna, K (2021). An efficient clustered regularly interspaced short palindromic repeat (CRISPR)/CRISPR-associated protein 9 mutagenesis system for oil palm (*Elaeis guineensis*). *Front. Plant Sci., 12*: 773656. DOI: 10.3389/fpls.2021.773656.

Zainal, Z; Khaza'ai, H; Radhakrishnan, A K and Chang, S K (2022). Therapeutic potential of palm oil vitamin E-derived tocotrienols in inflammation and chronic diseases: Evidence from preclinical and clinical studies. *Food Res. Int., 156*: 111175. DOI: 10.1016/j.foodres.2022.1175.

Zainol Hilmi, N H; Idris, A S; Maizatul-Suriza, M; Madihah, A Z and Nur-Rashyeda, R (2022). Molecular PCR assays for detection of *Ganoderma* pathogenic to oil palm in Malaysia. *Malays. Appl. Biol. 51(1):* 171-182. DOI: 10.55230/mabjournal.v51i1.2201.

Zhao, Y; Jia, M; Chen, W and Liu, Z (2022). The neuroprotective effects of intermittent fasting on brain aging and neurodegenerative diseases via regulating mitochondrial function. *Free Rad. Biol Med., 82*: 206-218. DOI: 10.1016/j.freeradbiomed.2022.02.021.

Zhou, Y; He, J; Chen, R and Li, X (2022). Recent advances in biomass-derived graphene and carbon nanotubes. *Mater. Today Sustain., 18*: 100138.

Zulkifli, W N F W M; Hazmi, A S A and Idris, Z (2022). Incorporation of epoxidised oleic acid plasticiser into poly(vinylidene fluoride). *Green Mater., 11(2)*: 79-86. DOI: 10.1680/jgrma.21.00078.

Zurilawati, Z; Maizan I and Raja Zulkifli, R O (2022). Growth performance of young sago palm (*Metroxylon sago* Rottb.) in peat fertilised using compound fertilisers. *Int. J. Agric. For. Plant., 12(2)*: 1-9.

Journal of Oil Palm Research Vol. 35 (2) June 2023 p. 217-235
DOI: https://doi.org/10.21894/jopr.2022.0069

MEMBRANE TECHNOLOGIES IN THE OIL INDUSTRY AND THEIR POTENTIAL APPLICATION FOR THE RECOVERY OF PHYTONUTRIENTS FROM PALM OIL

ADRIANA ISABEL RADA-BULA[1]*; JESÚS ALBERTO GARCÍA-NUÑEZ[2]; CARLOS JESÚS MUVDI-NOVA[3] and CONSUELO DÍAZ-MORENO[4]

ABSTRACT

Palm oil is one of the most widely commercialised vegetable oils globally. This oil contains important phytonutrients, such as carotenoids (provitamin A), tocopherols and tocotrienols (vitamin E). These phytonutrients are thermally degraded and removed from crude palm oil (CPO) through bleaching techniques in the refinement process. This article focuses on using membrane technology as a green alternative to recover these compounds, specifically, the use of nanofiltration as a potential mechanism for recovering edible oil phytonutrients from palm oil. Furthermore, due to the few studies related to this topic, the review also highlights microfiltration and ultrafiltration uses in other crude oils (CO) for degumming and deacidification refining processes for phospholipids (Pl) and free fatty acids (FFA) removal. Finally, an overview of the biological functions of palm oil phytonutrients in health and their applications in the food industry is presented.

Keywords: microfiltration, nanofiltration, palm oil, phytonutrients, ultrafiltration.

Received: 4 April 2022**; Accepted:** 29 August 2022**; Published online:** 26 October 2022.

INTRODUCTION

Over the years, the food industry has faced new challenges, mainly population growth. According to the United Nations, the world's population is expected to increase by approximately 2.0 billion people to 9.7 billion people by 2050 (United Nations, 2019). This has forced the food industry to research and generate high nutritional content for populations (Cárdenas, 2016). Ways of making this possible include making agro-industrial processes sustainable, better utilising various techniques and recovering nutritional compounds from generated residues and byproducts thereby reducing the environmental impacts of processing while obtaining value-added compounds (Almaraz-Sánchez *et al.*, 2022).

The palm oil industry is one of the most important agro-industrial chains leading to commercial vegetable oil (Cárdenas, 2016; Statista, 2021). From this chain, palm oil is the main product that is obtained from the mesocarp of the fruit via extraction by mechanical pressing. Crude palm oil (CPO) has a characteristic red-orange colour due to compounds that are rarely

[1] Facultad de Ciencias Agrarias,
Universidad Nacional de Colombia,
111321 Bogotá, D.C., Colombia.

[2] Processing Program Coordinator,
Colombian Oil Palm Research Center (Cenipalma),
0906 Bogotá, D.C., Colombia.

[3] Food Science and Technology Research Center (CICTA),
School of Chemical Engineering,
Universidad Industrial de Santander (UIS),
680006 Bucaramanga, Santander, Colombia.

[4] Instituto de Ciencia y Tecnología de Alimentos (ICTA),
Universidad Nacional de Colombia,
111321 Bogotá, D.C., Colombia.

* *Corresponding author e-mail: airadab@unal.edu.co*

present in other foods (Sylvester and Shah, 2004) such as carotenoids, tocopherols, and tocotrienols (Dong *et al.*, 2017). Each compound has nutritional and bioactive functions and must be part of a balanced diet. However, traditional refinement processes (Mosquera *et al.*, 2009) thermally degrade carotenoids and remove tocopherols and tocotrienols (Amado, 2010).

An alternative method for recovering these compounds is by using membrane technologies to separate solutes according to the molecular size by adjusting the pressure conditions, temperature and characteristics of the membrane such as the molecular weight cut-off (MWCO), material and molecule-membrane interactions (Mohammad *et al.*, 2015). This method has multiple advantages over conventional separation techniques such as molecular distillation, supercritical fluid extraction or adsorption, because it does not require the intensive expenditure of energy, conserves selected compounds in the oil (Azmi *et al.*, 2015; Bernardo and Drioli, 2010), is scalable and has a compact design (Kang and Cao, 2014; Mohammad *et al.*, 2019; Otitoju *et al.*, 2016).

Membrane technologies have various applications in the food industry, for example, in the manufacturing processes of dairy products for milk protein recovery (Chamberland *et al.*, 2019; Deshwal *et al.*, 2020; Gavazzi-April *et al.*, 2018; Lauzin *et al.*, 2020; Li and Corredig, 2020; Lobasenko *et al.*, 2019; Renhe and Corredig, 2018; Rodrigues Toledo Renhe *et al.*, 2019; Sánchez-Moya *et al.*, 2020; Schäfer *et al.*, 2019; Shakhno *et al.*, 2019; Sousa *et al.*, 2019; Touhami *et al.*, 2020; Uttamrao *et al.*, 2019; Valencia *et al.*, 2018), the clarification of beverages (Akhtar *et al.*, 2020; Bindes *et al.*, 2020; Destani *et al.*, 2020; Rodrigues *et al.*, 2020), and the recovery of enzymes and metabolites of biotechnological processes (Balti *et al.*, 2018; Díaz-Montes and Castro-Muñoz, 2019; Díaz-Montes *et al.*, 2020; Ter Beek *et al.*, 2019; Todero *et al.*, 2019; Wang *et al.*, 2018; Zhang *et al.*, 2016).

Since 1990, the application of this technological data to the oil industry resulted in a higher academic publication rate in some years than in others. However, there has been an increase in publication rates associated with this topic. According to the Scopus database, these publications have been oriented toward improving the oil refinement processes by membrane technologies using microfiltration, ultrafiltration and nanofiltration for antioxidant separation (Mohammad *et al.*, 2015), degumming (phospholipid removal) (Ariono *et al.*, 2018), deacidification (Azmi *et al.*, 2015; Lai *et al.*, 2016; Purwasasmita *et al.*, 2015), the removal of traces of metals, products of oxidation, and sterols (Iyuke *et al.*, 2004) and decolourisation in relation to carotenoid separation (Ghazali *et al.*, 2022; Manjula and Subramanian, 2007; Reddy *et al.*, 2001). In these articles, there is a particular interest in studying flux, rejection, fouling mechanisms, solute-membrane interactions, membrane material, operative conditions, and feed characteristics due to the high viscosity of oils. This represents a challenge for the use of membrane technology in this agribusiness.

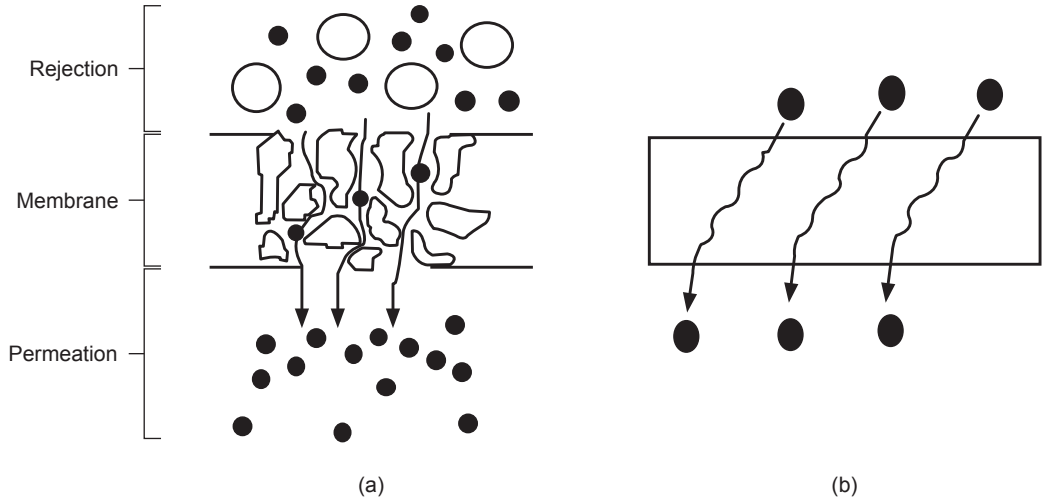
To the best of our knowledge, there are few reviews about applying membrane technologies in CPO for minor components recovery, such as the one published by de Morais Coutinho *et al.* (2009). Chiu *et al.* (2009) and Darnoko and Cheryan (2006a) focused on using membranes for carotenoid concentration. There were few publications from 2009 until 2021 when this topic gained relevant attention again (Ghazali *et al.*, 2022; Lim and Ghazali, 2021; Nabu *et al.*, 2021). For this reason, it is necessary to carry out a new overview of the studies conducted in recent years on membrane technology for the oil refinement process and the recovery and concentration of phytonutrients (specifically from palm oil), which could have applications in the food industry.

The first part of the review corresponds to the separation process principles of membrane technology. Recent applications of this technology in the edible oil industry are then reviewed. Finally, the prospects for palm oil phytonutrients recovered by nanofiltration in functional food formulations are proposed.

MEMBRANE TECHNOLOGY: SEPARATION PROCESS PRINCIPLES

The membrane filtration process involves the application of a driving force on a feed flow with high solute concentration. This driving force enables the separation of molecules or components according to the membrane MWCO and specific pressure ranges: Microfiltration separates particles in the range 0.025-10.000 µm at pressures <0.2 MPa; ultrafiltration separates particles in the range 1000-300 000 Da at pressures >1 MPa; and nanofiltration separates particles in the range 350-1000 Da at pressures of 1-4 MPa (Baker, 2012b; de Morais Coutinho *et al.*, 2009; Solís *et al.*, 2017).

These separation processes are conducted through the membrane by pore flow and solution-diffusion models (Baker, 2012a). According to this, microfiltration and ultrafiltration permeants are transported by the pore flow model, while permeation in nanofiltration can be explained by both models in *Figure 1* (Baker, 2012a).



Source: Baker (2012a).

Figure 1. (a) Pore-flow model and (b) solution-diffusion model.

Within the parameters in the separation process, the retention coefficient or rejection (R) is an important parameter to consider. It is expressed as the rejection rate of the solute in terms of the concentration of the solute in the permeate (C_p) and the concentration of the solute in the retentate (C_R) [Equation (1)]. The flux (J) is expressed as the ratio of the volumetric flow (F_p) of the permeate that is obtained during the process to the area (A) as a function of time [Equation (2)] (Baker, 2004; 2012a; Belfort *et al.*, 1994; Chew *et al.*, 2020; Doran, 2013; de Morais Coutinho *et al.*, 2009).

$$R = (C_R - C_P)/C_R = 1 - C_p/C_R \quad (1)$$

$$J = F_P/A \quad (2)$$

The flux can also be determined using Darcy's law for cases in which cake formation has occurred due to a high concentration of solutes on the membrane surface; such a scenario offers additional resistance to the flux:

$$J = (1/A)(dV/dt) = \Delta\rho/\eta_o\,(R_m + R_c) \quad (3)$$

where (J) denotes the flux, V is the total volume of the permeate, A is the external area of the membrane, t is the filtration time, $\Delta\rho$ is the pressure drop that is imposed through the membrane and cake, (R_m) is the membrane resistance, and (R_c) is the resistance due to cake formation (Doran, 2013).

The concentration factor (F_c) is another critical parameter and it is the ratio of the mass in the feed flow (M_A) at the beginning of the process and the mass in the retentate (M_R) at the end of the process [Equation (4)]. The membrane permeability (JV) is the ratio of the volume of the permeate (V) to the permeation area of the membrane (A), multiplied by the filtration time (t) and the operating pressure (P) [Equation (5)] (Doran, 2013).

$$F_C = M_A/M_R \quad (4)$$

$$JV = V/A\,t\,p \quad (5)$$

The transmembrane pressure ($\Delta\rho$) is the main driving force that directs the filtration process through the membrane. It corresponds to the differential pressure between the feed flow pressure (P_F) and the permeation pressure (P_p) [Equation (6)] (Doran, 2013). However, the driving force can be affected by the osmotic pressure of solutes present in the feed [Equation (7)]. The π_F and π_p values correspond to the feed osmotic pressure and permeation osmotic pressure, respectively. For this case, both can be calculated by the Van´t Hoff equation, where C is the molar concentration of the solute, R is the ideal gas constant, T is the absolute temperature, and i is the number of ions that form as the molecule dissociates [Equation (8)] (Chew *et al.*, 2020; Doran, 2013).

$$\Delta p = p_F - p_P \quad (6)$$

$$\Delta\, p = (p_F - p_p) - (\pi_F - \pi_p) \quad (7)$$

$$\pi = iCRT \quad (8)$$

Regardless of which membrane technique is employed, challenges are encountered during the filtration process, which can be summarised as: Gel layer formation, fouling, pore plugging, adsorption,

and concentration polarisation. The latter occurs when there is an accumulation of particles in the feed near the membrane, which can be estimated by the parameter Ψ [Equation (9)], where C_0 corresponds to the concentration of solutes in the feed stream, C_w is this concentration after the dead-end filtration and R is the retention coefficient. In this case, the flux is expressed by Equation (10), where C_p corresponds to the solute concentration in the permeate and k is the mass transfer constant in cm s^{-1} (Chew *et al.*, 2020).

$$\Psi = C_w/C_0 - 1 = 1/(1 - R) \quad (9)$$

$$J = k\ ln\ (C_w - C_p)/(C_0 - C_p) \quad (10)$$

In contrast, fouling during the filtration process occurs due to the interaction between solutes that are suspended in the feed flow and the membrane, where factors such as the size of the suspended solutes, hydrophobicity, isoelectric point, Brownian motion, van der Waals forces, electrostatic charge, and Lewis acid-base interactions affect the process (Mohammad *et al.*, 2015; Pérez and Labanda, 2013). In addition, other characteristics of the operating system such as the flow regime (laminar or turbulent), affect its formation (Kilduff *et al.*, 2002); these characteristics also include the feed flow and type of filtration (dead-end or crossflow). In addition, to describe the fouling behaviour during filtration, the selectivity of the membrane, the capacity (which refers to the permeation flux per unit area and the phenomenon of mass transfer), and the momentum in the process must be considered (Chew *et al.*, 2020). In general, fouling can be developed through four mechanisms: Cake formation, pore constriction, intermediate blocking (n=1) and complete blocking (n=2) (*Figure 2*) (Chew *et al.*, 2020; Wenten *et al.*, 2019). For each case, the Hermia model can be applied, which describes the behaviour of the permeate flux in relation to time, as expressed in Equation (11), where denotes the filtration time, V the volume of the permeate, and the index or fouling type, which can be selected according to the pore blocking category (*Figure 2*) (Aryanti *et al.*, 2017; Chew *et al.*, 2020; Wenten *et al.*, 2019).

$$d^2t/dV^2 = k\ (dt/dV)^n \quad (11)$$

For each case, a distinct model has been established, according to Ariono *et al.* (2018):

Complete blocking (n=2) $lnJ = lnJ_0 - k_c t$ (12)

Intermediate blocking (n=1) $1/J = 1/J_0 + k_i t$ (13)

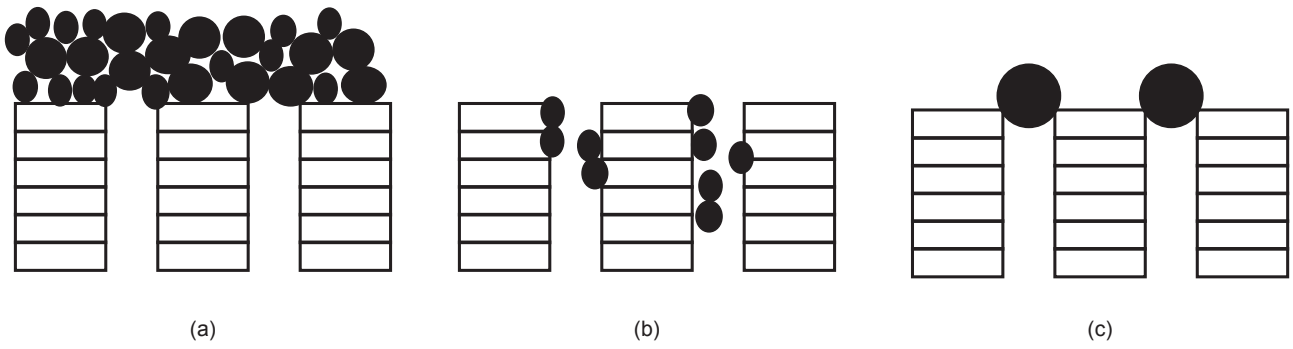
Pore constriction (n=1.5) $1/\sqrt{J} = 1/\sqrt{J_0} + k_s t$ (14)

Cake formation (n=0) $1/J^2 = 1/J_0^2 + k_{cf} t$ (15)

where k_c, k_i, k_s, and k_{cf} denote the respective constants for each case of membrane fouling.

In addition to these models, Chew *et al.* (2020) revisited the research by Kilduff *et al.* (2002), and summarised classic models of flux behaviour according to the type of fouling and classic models when cross- or dead-end filtration was used. In addition, new models have been proposed for cases in which classical models do not fully explain the fouling behaviour.

To describe a real flux behaviour, the resistance in the series model considers the viscosity (μ), pressure drop (ΔP), resistance offered by the



Source: Wenten *et al*. (2019); Aryanti *et al*. (2017) and Chew *et al*. (2020).

Figure 2. (a) Cake formation (n=0), (b) pore constriction (n=1,5) and (c) intermediate blocking (n=1) - complete blocking (n=2).

membrane (R_m), the resistance provided by fouling (R_f), and additional resistance due to concentration polarisation (R_c) [Equation (16)]. However, other aspects must be considered that are not included in the model, such as experimentation with the techniques of characterisation of the cake in real time to understand the molecular mechanism that occurs during the filtration process and its dependence on time (Chew *et al.*, 2020).

$$J = \Delta P/\mu(R_m + R_f + R_c) \quad (16)$$

As an alternative to the resistance in the series model, the concentration polarisation can be measured in terms of mass transfer theory or the hydrodynamic effect of the boundary layer, as devised in film theory (Ghazali *et al.*, 2022). However, by maintaining turbulent flow conditions, the solute concentration can be kept constant (C_B). When this does not occur, the highest concentration of solutes is found close to the membrane wall (C_w). Additionally, during this process, the thickness of the concentration in the boundary layer, δ, which depends on the concentration gradient of these solutes to and from the membrane, must be considered (Ariono *et al.*, 2018; Chew *et al.*, 2020; Othman *et al.*, 2021). If a static state is considered, this behaviour is expressed by Equation (17), where the rate of transport of solutes on the surface of the membrane is related to the rate of transport of solutes to the permeate minus the diffusivity rate in the higher concentration of solutes in the boundary layer, according to Fick's law (Chew *et al.*, 2020; Doran, 2013).

$$JC - JC_p - Ð\,(dC/dy) = 0 \quad (17)$$

In this equation, C is the concentration in the boundary layer, C_p is the concentration in the permeate, Ð is the diffusion coefficient, and dC/dy is the solute concentration gradient with respect to the distance (y). Integrating this expression yields Equation (18), where Ð/δ corresponds to the mass transfer coefficient, which is expressed as Equation (19). When the process pressure rises, the concentration in the membrane wall (C_w) could reach a limit value C_G that corresponds to the formation of a polarisation gel on the surface of the membrane, and this corresponds to the expression in Equation (20) (Chew *et al.*, 2020; Doran, 2013).

$$J = Ð/\delta\, ln\, (C_w - C_p)/(C_B - C_p) \quad (18)$$

$$J = k\, ln\, (C_w - C_p)/(C_B - C_p) \quad (19)$$

$$J = k\, ln\, (C_G/C_B) \quad (20)$$

RECENT APPLICATIONS OF MEMBRANE TECHNOLOGY IN THE EDIBLE OIL INDUSTRY

Microfiltration

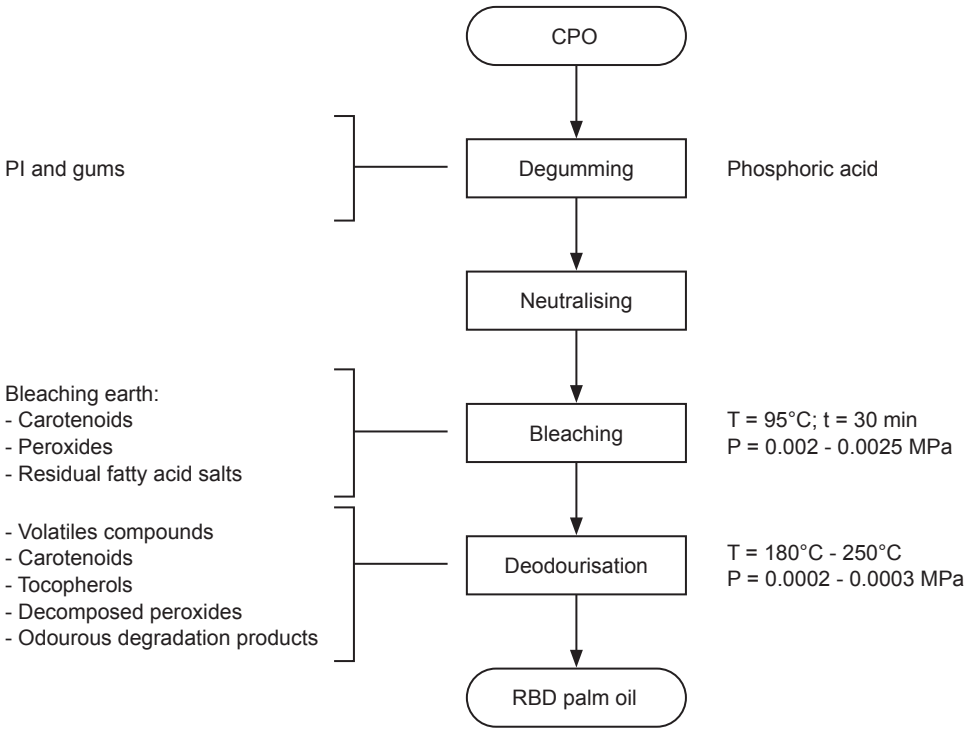
Degumming. Studies of the microfiltration process for Pl removal in CPO are few, although other edible oils, have been studied (Bassam *et al.*, 2001; 2004; 2009; 2011; Hafidi *et al.*, 2005; Hou *et al.*, 2020). Edible oil refinement involves degumming, neutralisation/deacidification, bleaching, and deodourisation to remove FFA, Pl, pigments and other compounds that affect the physicochemical quality, appearance, taste, functionality, and shelf life (*Figure 3*) (Doshi and Shah, 2018).

The degumming process is one of the first steps in refining edible oils and consists of removing Pl and waxes from CO (Corley and Tinker, 2016). However, Pl can form emulsions with the water from clarification, and separation becomes more complicated, resulting in deterioration and low oil quality (Doshi and Shah, 2018).

Likewise, in soybean oil extraction, organic solvents such as hexane increase the probability of reverse micelle formation due to the surfactant nature of Pl (Hou *et al.*, 2020). These micelles can reach MW of 20 000 Da or more (Boynueğri *et al.*, 2017), which simplifies the separation process by membrane technology.

Under traditional refining conditions, these micelles are removed by centrifugation (Hou *et al.*, 2020) but due to the high energy consumption of this process, membrane technologies have become an alternative method for removing these molecules (Doshi and Shah, 2018; Hou *et al.*, 2020). Microfiltration is an excellent option because it performs solid-liquid separation (Baker, 2012a). The membrane performance can vary according to the transmembrane pressure, flow rate, feed temperature, membrane MWCO, and solid concentration in the feed stream (Bernardo and Drioli, 2017). Under these conditions, microfiltration removes large molecules such as phosphatides that are traditionally removed during oil refinement. According to databases, the application of membrane technologies for degumming processes has been maintained over time and is considered an effective method for these processes. Another microfiltration application is FFA and peroxide removal (Hou *et al.*, 2020).

Membrane materials that are used in the degumming process. In the late 1990s, there was a demand to use membrane processes in this phase. As a result, patents were generated, such as those reported by Bassam *et al.* (2001), who proposed a polyacrylonitrile (PAN) polymer membrane with a 0.3 μm MWCO for removing Pl from soybean oil micelles. In 2004, 2009, and 2011, the same authors



Note: RBD - refined, bleached and deodourised oil.

Source: Corley and Tinker (2016).

Figure 3. Traditional palm oil refining process.

patented the use of PAN microfiltration membranes to separate and purify compounds as soy lecithin products as a result of this process (Bassam *et al.*, 2004; 2009; 2011). In recent years, the use of synthetic membranes has increased, and these include polyethersulfone (PES) (Ariono *et al.*, 2018), polyamide (PA), polysulfone (PS), polyvinylidene fluoride (PVDF), polyimide (PI), PAN, and zirconium dioxide-ZnO_2 (ceramic). However, these membranes have primarily been used in microfiltration processes (Hou *et al.*, 2020; Mestre *et al.*, 2019; Roy *et al.*, 2014). Synthetic membranes outperform organic membranes because difficulties are encountered with organic membranes under operating conditions, especially the prolonged use of organic solvents, which reduces the stability and, therefore, mechanical resistance (Hou *et al.*, 2020).

Ceramic materials have shown various advantages because of their resistance to high pressures and temperatures. By comparing the performances of membranes according to their capacity for removing Pl from oils using microfiltration and ultrafiltration, ceramic membranes present a higher flux during filtration than other materials, which is close to 50 L h^{-1} m^{-2} at 0.25 MPa, under similar operating conditions (Hou *et al.*, 2020). In the case of ultrafiltration for degumming processes, this value is higher than those registered in PVDF (MWCO: 6000 Da) and PES (MWCO: 22 000 Da) (Ochoa *et al.*, 2001), thereby demonstrating the advantages of using membranes with larger pore sizes and ceramic materials for this purpose.

Membrane performance - Fouling. Membrane fouling can decline due to the influence of the membrane MWCO. This behaviour can be represented by four precise models (*Figure 1*) in which membranes with smaller pore sizes could lead to a decline in flux in a shorter time than membranes with a higher MWCO, as Hou *et al.* (2020) determined in their research. Hou *et al.* (2020) studied Pl removal from crude rapeseed oil. In this study, the cake model realised the best fit for a hydrophilic ceramic membrane of 0.05 µ MWCO, followed by the intermediate model. In contrast, the intermediate model realised the best fit for the same sample using a ceramic membrane of 0.20 µ MWCO, followed by the cake model. It was also found that a combination of these two models better fit the explained fouling behaviour. Hence, the phenomenon can be explained through these two mechanisms. This finding also demonstrates the incidence of MWCO on membrane fouling

TABLE 1. APPLICATION OF MICROFILTRATION MEMBRANES IN PHOSPHOLIPID REMOVAL FROM DIFFERENT EDIBLE OILS

Crude oil	Phospholipid initial content (mg kg^{-1} oil)	Membrane material	MWCO (µm)	Filtration	T (°C)	Transmembrane pressure (MPa)	Phospholipids rejection (%)	Phospholipid final content (mg kg^{-1} oil)	Authors
Rapeseed	5 851.75	Ceramic membrane: ZrO_2 Support material: α-Al_2O_3	0.2	Crossflow	55	0.15	99.9	1.4	Hou *et al.* (2020)
Rapeseed	5 851.70	Ceramic membrane: ZrO_2 Support material: α-Al_2O_3	0.2	Crossflow	42	0.10	99.9	1.3	
Soybean	545.00	PAN	0.3	-	-	1.00	96.1	21.0	Bassam *et al.* (2011)
Corn oil	1 783.00	PAN	0.3	-	-	1.00	97.6	41.2	
Canola oil	505.00	PAN	0.3	-	-	1.00	95.1	24.4	
Sunflower previous neutralised 20% NaOH	43.00	Cellulose	2.5	Dead end	25	0.20	98.1	-	Hafidi *et al.* (2005)
Sunflower previous neutralised 40% NaOH	43.00	Cellulose	2.5	Dead end	25	0.20	83.7	-	

and Pl micelle rejection. In addition, the authors suggested that it is also affected by the increase in transmembrane pressure, which causes the pores to block and consequently, decrease the flux. Another interesting finding from this research was the increase in fouling with temperature because temperature affects the micelle diameter. However, a temperature increase promotes inverse diffusion of the micelles from the membrane surface to the oil, thereby decreasing the mass transfer coefficient.

Deacidification. Specifically in CPO, Azmi *et al.* (2015) evaluated polyvinyl alcohol (PVA) and PVDF microfiltration membranes for FFA removal. In this research, the hydrophobic membrane significantly facilitates the removal process due to its characteristics, while PVA membranes with low hydrophobicities limit the phospholipid separation process. Thus, materials such as PVDF (with higher hydrophobicity) could have a valuable role in the process (Azmi *et al.*, 2015).

However, the application of microfiltration is not limited to the removal of FFA from oil. Over the years, advances in this topic have been extensive, and new membrane materials have been developed. This opens the possibility for further exploration. The affinity between the compounds to be removed or preserved and the membrane is an essential factor to be considered. Azmi *et al.* (2015) also evaluated the performance of PVA crosslinked PVDF for FFA removal from CPO due to this affinity. FFA corresponds to a derived carboxyl that shows affinity and selectivity for hydroxyl groups. PVA is a material that has abundant hydroxyl groups; hence, it is expected to have a high concentration of FFA in rejection. However, in this research, a high concentration of PVA on the surface of the membrane had adverse effects on the fatty acid removal process since a high fixation of the material could block the surface, thereby suggesting that having just a thin layer of this material on the membrane surface probably has the desired effect on FFA removal.

Other applications of microfiltration membranes are in the separation of oil/water emulsions to remove only the oil phase to purify the water; in this case, the membrane surface can be modified by introducing hydrophilicity. Materials such as PS can be modified with a layer of polydopamine. Membranes with this modification show better separation performance than membranes that have not been modified (Bernardo and Drioli, 2017).

Ultrafiltration

Ultrafiltration enables the separation of colloids and microparticles with particle sizes close to 1000-300 000 Da (Baker, 2012b; Solís *et al.*, 2017). Similar to microfiltration membranes, these membranes have been applied in the oil industry for processes such

as deacidification (Azmi *et al*., 2015; Gonçalves *et al*., 2016), degumming (Ariono *et al*., 2018; Aryanti *et al*., 2017) and solvent removal from micelles (Saravanan *et al*., 2006).

Ultrafiltration has been used in the edible oils industry to remove Pl and FFA, and the complex effects of these compounds on fouling formation have been studied (Aryanti *et al*., 2017). However, micelles also impact fouling during the ultrafiltration process. According to Ariono *et al.* (2018), micelles have an affinity for other polar components, even impurities, which bind and contribute to the formation of fouling. In addition, because Pl molecules are amphiphilic, they can be absorbed by the membrane and contribute to fouling formation. Pl are compounds that form micelles when dispersed in water (Aryanti *et al*., 2018).

Degumming. Studies in CPO have removed Pl with high rejection, above 87.3%. These results are comparable with residual phosphorus in traditional refined palm oil, not above 2 ppm (Othman *et al*., 2021). These results were achieved by adding an inorganic adsorbent in a mixed matrix PVDF membrane, where increasing magnesium silicate, from 3.0% to 8.0% in the matrix, increased the phospholipids rejection.

In addition to the materials, temperature and pressure significantly affect CPO Pl rejection. For example, PES membranes with MWCO close to 100 000 Da were tested. The results showed that as the pressure and temperature increased, the flux permeation increased while Pl were retained. The high flux permeation can be explained because the pressure deforms and enlarges the pores while temperature reduces the feed viscosity promoting the process (Razi *et al*., 2021).

Several reports have analysed the effect of material membranes for degumming CO from various vegetable lipid sources. For example, Doshi and Shah (2018), analysed modifications of PVDF hollow fibre membranes (MWCO 570 000 Da - 600 000 Da) to identify better treatment for separating micelles from crude peanut oil. In this study, the membrane composition of 15% PVDF, 75% N-methyl-2-pyrrolidinone and 10% ethylene glycol showed excellent performance with satisfactory flux (47.5 L h^{-1} m^{-2}) and 94% micelle rejection.

Boynueğri *et al*. (2017) studied the tubular PVDF membrane performance with an MWCO of 20 000 Da for degumming crude soybean oil using a reverse osmosis/ultrafiltration module. According to the results, it was possible to reject 86.11% of phospholipids, and an average flux of 17.04 L h^{-1} m^{-2} at 40°C and 2 MPa pressure was realised. To improve molecular rejection in various membrane materials, Onal-ulusoy (2015) tested PVDF and PES flat sheet membranes (MWCO 30 000 Da) that were modified with hexamethyldisiloxane HMDSO (hydrophobic monomer). This modification was conducted using radiofrequency plasma polymerisation treatment, which improved characteristics such as permeability, polarity, and selectivity of polymeric membrane surfaces, as shown by the studies conducted by Onal-ulusoy *et al.* (2014) and; Tur *et al.* (2011) in which various glow discharge powers and radiofrequencies were tested. These studies evidenced that changes in chemical and physical properties on the membrane surface were due to sequential oxidation and crosslinking reactions once the polymers were deposited in the plasma. In the same study, an exciting change was observed at large values of the contact angle (γS_w): A weak interaction occurred between the water and the membrane surface, which resulted in a hydrophobic membrane. This increase in the modified membrane surface hydrophobicity increased the percentage of rejection of each material by 6.3% and 16.8% for PES and PVDF, respectively.

Ultrafiltration membranes are also used in degumming processes in the study of colloid-enhanced ultrafiltration, or polyelectrictrolyte ultrafiltration (PEUF), and micellar-enhanced ultrafiltration (MEUF) (Danis and Aydiner, 2009; Niazmand *et al*., 2015). These processes involve using a surfactant that adsorbs undesirable components electrostatically or through the hydrophobic feed effect, thereby resulting in the formation of complex aggregates (micelles of the surfactant) that cannot pass through the membrane. Therefore, these aggregates are concentrated in the rejection stream. In this case, the surfactant consists of Pl, which is hydrated to form micelles, which facilitate the separation of these compounds from the oil (Danis and Aydiner, 2009; Niazmand *et al*., 2015).

Niazmand *et al.* (2015) studied micelle formation due to the presence of chelating agents such as ethylenediaminetetraacetic acid (EDTA) which improved the heritability of phosphorus and, in the presence of water, they observed that polyelectrolytes (with magnesium or calcium ions) can form micelles that precipitate, thereby enhancing the separation process. Niazmand *et al.* (2015) reported high efficiency in process of removing phospholipids from crude canola oil.

Deacidification. Aryanti *et al.* (2018), Azmi *et al.* (2015) and Purwasasmita *et al.* (2015) studied the application of various ultrafiltration membranes to CPO and CPO diluted with organic solvents as presented in *Table 2*, where the membrane characteristics and operating conditions are described.

On the other hand, modifications in PVDF membranes by additions of inorganic adsorbents such as magnesium silicate have been studied for

TABLE 2. USES AND MATERIALS OF ULTRAFILTRATION MEMBRANE FOR DEGUMMING, DEACIDIFICATION AND BLEACHING* PROCESSES IN CPO AND DERIVATIVES

Molecule to remove	Vegetable oil	Membrane material	Membrane characteristic	Membrane affinity	T (°C)	P (MPa)	Rejection*** (%)	Authors
Oil/water separation	CPO**	Polypropylene (PP)	Hollow fibre	Superhydrophobic	40	0.2	99	Wenten *et al.* (2019)
Pl FFA	CPO**	Polyethersulfone	Flat sheet	Hydrophilic	30	0.1	99 16	Aryanti *et al.* (2018)
Pl	A mixture of refining palm oil with isopropanol and lecithin (as a representation of CPO)	Polyethersulfone	-	-	24-25	0.1	79	Aryanti *et al.* (2017)
FFA	CPO**	Polyethersulfone	Hollow fibre	Hydrophilic	70	-	97	Purwasasmita *et al.* (2015)
FFA	CPO**	Polyvinyl alcohol (PVA) crosslinked poly-vinylidene (PVDF)	Hollow fibre	Hydrophilic	65	0.2	5.93	Azmi *et al.* (2015)
Pl Carotenoids Tocopherols Tocotrienols	CPO** and crude palm olein	Nonporous composite polymeric membrane with silicon as active layer and PI as support	Flat sheet - - -	Hydrophobic	40	4	95-100 - - -	Arora *et al.* (2006)
Phospholipids Carotenoids Free fatty acids Volatile material	CPO**	Polyethersulfone	Tubular	-	63	2.6	96.4 15.8 0 0	Ong *et al.* (1999)

Note: *Bleaching - refining oil process where pigment is removed, mainly carotenoids; **CPO - crude palm oil; *** - The maximum rejection reported during each experiment.

FFA removal from CPO, obtaining rejections close to 16.51%, with simultaneous Pl rejection (Othman *et al.*, 2021). In this study, although FFA rejection was not as expected, there was a percentage retained due to the increasing pressure and temperature in the experiments. Similar results were obtained by Aryanti *et al.* (2018) using PES. However, in both cases, not only factors such as membrane, material and operation conditions affect the affinity and FFA rejection but MWCO also significantly affected these results.

Oil/water separation. Superhydrophobic membranes are additional membranes used for oil/water separation in CPO. The material repels water on the membrane surface due to a high-water angle (WCA) of above 150° and a low contact angle of hysteresis and a sliding angle of below 10°. This characteristic is helpful in the oil refinement process once the oil has been extracted and hot water or steam is added for hydrolysing gums and resins in CO. Traditionally, to remove this water, centrifugation is performed to clarify the oil, but an alternative is to replace this step with the use of membranes (Wenten *et al.*, 2019). In this case, a superhydrophobic membrane enables the successful removal of the water that is present in the oil.

In CPO, Wenten *et al.* (2019) used a polypropylene (PP) superhydrophilic membrane with a MWCO of 0.05 μm, to remove water from palm oil. According to the reported results, at 40°C and 0.2 MPa, it was possible to remove substantial water content and maintain a high flux and 99% rejection. The transmembrane pressure and the temperature directly impact the oil viscosity; thus, an increase in temperature decreases the oil viscosity, thereby facilitating the permeate flux. Additionally, an increase in TMP influences the flux; in this case, linear behaviour was evaluated at each temperature point.

Nanofiltration

Nanofiltration in the edible oil industry. The application of nanofiltration in the oil industry has shown a rising trend recently. In palm oil, most research is focused on water treatment after oil extraction. However, according to the Scopus database, studies related to the recovery of carotenoids or decolourisation can be an alternative option for maintaining the interest of the academic community. Despite the low number of publications, this area represents a research opportunity in this field. Although technological data were collected in the 1990s and insipient research on nanofiltration in palm oil was conducted between 2006 and 2009, few results have been published until now, with recent publications in the last three years.

Opportunity for phytonutrient recovery in CPO processing. During bleaching, in the traditional refinement process, carotenoids, chlorophylls, and other compounds, such as metals, soaps, polyaromatic compounds, Pl and a fraction of tocopherols and sterols, are removed (González-Tovar *et al.*, 2005) by using clays and bleaching earth (diatoms) at a temperature of 95°C for 30 min under vacuum conditions at 0.15-0.18 Pa (Corley and Tinker, 2016).

During this process, an adsorption mechanism occurs in the bleaching earth. Due to atmospheric factors or induced temperature and oxygen factors, the many cases of non-saturation in α- and β-carotenes produce a tendency for oxidation and isomerisation (from the E configuration to the Z configuration) (Nagarajan *et al.*, 2017). After this, the bleaching earth and these molecules are eliminated as waste, which generates an environmental impact due to aldehydes, ketones, and other compounds that are derived from the process and adsorbed by the material (Haro *et al.*, 2014). Thus, molecules with high nutritional value, such as carotenoids, tocopherols and sterols, are removed during the process. Only a small amount remains in the olein fraction (refined oil) (Loganathan *et al.*, 2020a). For this reason, nanofiltration is an alternative to the bleaching phase. This separation process consists of filtration, where hydraulic pressure is physically applied as a driving force for the transport of mass (Chiu *et al.*, 2009), in this case, palm oil is applied through a membrane. As a result of this operation, there will be a retentate stream where solutes are concentrated (Doran, 2013). In this case, the recovered compounds are carotenoids, tocopherols, and tocotrienols, which can be applied in various industries, such as food additives, functional food formulation, pharmaceutical, nutraceutical and nutricosmetic industries (Mohd-Nasir and Mohd-Setapar, 2018; Taeymans *et al.*, 2014).

Nanofiltration explicitly involves a series of hydrodynamic and interfacial microevents on the membrane surfaces and in their nanopores (Mohammad *et al.*, 2015). A combination of steric, Donnan, dielectric, and transport effects interfere with the process (Mohammad *et al.*, 2015). Solute transport is performed through a steric mechanism (size-based exclusion). According to Pérez and Labanda (2013), the nanofiltration process can also be considered 'low-pressure reverse osmosis' because it combines characteristics of reverse osmosis, where the separation mechanism is based on a solution-diffusion and ultrafiltration and operates based on pore-flow model (*Figure 1*). The interaction between the membrane and the solute charge also plays an important role.

Palm oil is a vegetable source with a high phytonutrients content (Choo, 1994; Saini *et al.*,

2015). It is estimated that palm oil can provide 15 times more retinol equivalent (provitamin A) than carrots and approximately 300 times more than tomatoes (Loganathan *et al.*, 2017; Sundram *et al.*, 2003). According to Mba *et al.* (2015) and Rincón and Martinez (2009), this content can vary between 500-700 ppm or even reach 1000 ppm for the oil of hybrid palm (Interspecific cross: *E. oleifera* x *E. guineensis* - OxG) (Chaves *et al.*, 2018), where 90% corresponds to α- and β-carotene, which are mainly in the all-*trans* state (Yaakob and Chin-Ping, 2003). These variations depend on the genotype (variety/cultivar), geography, season, agronomic management, maturation, and postharvest management conditions (Yaakob and Chin-Ping, 2003). Moreover, the content can also vary among fruits in the same bunch or bunches of the same palm (Corley and Tinker, 2016), although the synthesised retinol equivalent is simultaneously consumed in the lipid of the fruit synthesis as they mature (Prada *et al.*, 2011).

The tocopherol and tocotrienol contents are estimated to be between 600 and 1000 ppm (*Table 3*) (Chaves *et al.*, 2018; Rincón and Martinez, 2009), which corresponds to 70%-80% and consists mostly of tocotrienols (Mba *et al.*, 2015). Seppanen *et al.* (2010) and Kamal-Eldin and Budilarto (2015) used tocopherols and tocotrienols to extend the shelf life of food. These studies showed that α-tocopherols and tocotrienols generally show higher antioxidant activity than γ-tocopherols in fats and oils (Saini and Keum, 2016; Seppanen *et al.*, 2010). Studies have demonstrated that these compounds are antiatherogenic (Kirmizis and Chatzidimitriou, 2009), allergic dermatitis suppressive (Tsuduki *et al.*, 2013), hypolipidemic (Minhajuddin *et al.*, 2005), nephroprotective (Siddiqui *et al.*, 2013), anti-inflammatory (Mocchegiani *et al.*, 2014) and neuroprotective (Rashid Khan *et al.*, 2015) agents.

The molecular weights of these carotenoids, tocopherols and tocotrienols are between 396 to 536 Da. Hence, the use of nanofiltration membranes is suggested with suitable operating conditions for the recovery process (*Table 4*).

State-of-the art nanofiltration membranes that are applied in the palm oil industry. Few studies have been conducted on nanofiltration in the edible oil refinement process because this technology is considered an emerging technology that has not yet been widely exploited (Peeva *et al.*, 2010). It has been reported since 2006 and 2009 that nanofiltration membranes can be used for complete carotenoid recovery or concentration (Chiu *et al.*, 2009; Darnoko and Cheryan, 2006b). Chiu *et al.* (2009) achieved a rejection of 75% of these compounds in palm oil, which mainly included α- and β-carotene,

TABLE 3. CAROTENOID, TOCOPHEROL AND TOCOTRIENOL CONTENT IN O×G AND *E. guineensis* CPO

Compounds	Hybrid OxG (ppm)*	*E. guineensis* (ppm)**
	Chaves *et al.* (2018)	Rincón and Martinez (2009)
α-carotene	447.9-577.7	185.0-209.0
β-carotene	724.0-911.8	401.0-413.0
Total carotene	1 172.1-1449.6	586.0-622.0
δ-tocotrienol	45.6	103.0-115.0
β+ϒ-tocotrienol	666.0	640.0-665.0
α-tocotrienol	199.3	310.0-336.0
β+ϒ-tocopherol	-	-
α -tocopherol	26.8	161.0-162.0
Total tocotrienols and tocopherols	937.6	1 215.0-1 277.0

Note: * - Hybrid of two palm oil species: *E. oleifera* Coarí x *E. guineensis* La Mé; ** - *E. guineensis,* is the oil palm species with a large cultivation area. The values presented correspond to the species sampled in Western Colombia.

TABLE 4. EXAMPLES OF MOLECULES PRESENT IN PALM OIL THAT CAN SEPARATED THROUGH MEMBRANE TECHNOLOGIES

Operative pressure	Filtration	Molecular weight	Examples
< 0.2 MPa	Microfiltration	0.025 - 10 μm	Phospholipids
> 1.0 MPa	Ultrafiltration	1 000-300 000 Da	FFA
1.0 - 4.0 MPa	Nanofiltration	350-1 000 Da	Carotenoids, tocopherols, tocotrienols

Source: Baker (2012), de Morais Coutinho *et al.* (2009) and Doran (2013).

at a temperature of 40°C and a pressure of 2.5 MPa. Similar results were obtained by Darnoko and Cheryan (2006b) when testing membranes with various hydrophobicity properties. Their results demonstrated that both hydrophilic and hydrophobic membranes performed excellently in retaining carotenoid molecules. However, the hydrophobic membrane showed the best flux performance in the process, which demonstrates the value of this characteristic which is deficient in filtration process with hydrophilic membranes. The recovery of nonpolar solvents using nanofiltration membranes has also been studied, especially in oilseeds that require solvents for the oil extraction process, such as soybean. In this case, hydrophobic membranes are recommended (Darvishmanesh *et al.*, 2011).

Challenges for CPO minor components separation using nanofiltration. Another topic that is relevant and considered as a challenge for carotenoids and other minor components separation is the high viscosity of the CPO and the molecular weight of each compound. This situation has led to sample preparation with methanolic transesterification evaluated in previous studies as a good option (Chiu *et al.*, 2009; Darnoko and Cheryan, 2000). Nevertheless, in the last three years, two articles about this topic have been published. Ghazali *et al.* (2022) studied CPO diluted in different organic solvents: Acetone, ethyl acetate and n-hexane, where CPO with hexane, showed higher triglyceride rejection and low carotenoids rejections. In this case, the membrane material, MWCO and pression had an important influence in this separation. Ghazali *et al.* (2022) also determined that P84® PI membrane with 280 Da MWCO had the best performance and low pressure (1 MPa) allowed increased carotenoids rejection.

On the other hand, Lim and Ghazali (2019) analysed the combination of CPO with Organic Solvent Nanofiltration (OSN) membranes. Results indicated high triglycerides rejection as the stirring increased and at the same time, the CPO concentration in dilution with organic solvent decreased. This can be explained because the concentration polarisation that affects separation efficiency (Lim and Ghazali, 2021).

PROSPECTS FOR PALM OIL PHYTONUTRIENTS THAT ARE RECOVERED BY NANOFILTRATION TECHNOLOGY IN FUNCTIONAL FOOD FORMULATIONS

Currently, palm oil is one of the most widely commercialised vegetable oils in the world (Ariono *et al.*, 2018; Hariyadi, 2020) and palm oil and its byproducts are used as ingredients for multiple food formulations, such as frying processes, ice creams, kinds of margarine and ready-to-eat foods (Hariyadi, 2020), due to their thermal stability and functionality (Loganathan *et al.*, 2020b; Mba *et al.*, 2015).

In recent years, interest in using palm oil varieties such as red palm oil (RPO) in the food industry has been increasing, which is mainly because these compounds contain molecules with high health and nutritional values. Both α- and β-carotenes are recognised as provitamin A, with β-carotene having a stronger biological effect, and tocopherols and tocotrienols are recognised as vitamin E and have antioxidant effects. These compounds have been studied separately in intervention studies with controlled clinical trials. These studies have reported that RPO application in food formulations demonstrated a positive effect on health, namely, it increased vitamin A levels, which were measured as serum retinol concentrations, in children and maternals (Loganathan *et al.*, 2020a). RPO is produced by refining traditional palm oil via deacidification and deodourisation processes using molecular distillation to maintain 80% of the pigments and vitamins in the oil (Loganathan *et al.*, 2017).

This demonstrates the interest in examining methods for recovering phytonutrients from CPO and the potential of these phytonutrients as natural ingredients with multiple applications in the development of functional foods. In this case, nanofiltration could play an essential role because it may concentrate phytonutrients in a determinate amount of oil, even at a higher content than is typical for RPO. This opportunity gives the possibility to formulate functional food with barely perceptible changes in rheological and sensory properties.

RPO in Clinical Trials

Intervention studies have employed RPO as a vitamin A supplement. Some of these studies have demonstrated the thermal stability of this compound in high-temperature processing (180°C for 20 min), such as Loganathan *et al.* (2020a). In this research, Loganathan *et al.* (2020a) developed cupcakes with RPO and palm olein addition. The results showed that the cupcakes that were formulated with RPO and the cupcakes that were formulated with palm oil did not differ significantly in terms of stability and both had an acceptable range of rancidity (peroxide value of 7.5 mEq kg^{-1}). Additionally, there was 100% retention of phytonutrients (α- and β-carotene) in the cupcake that was formulated with RPO, in compliance with the vitamin A recommended dietary allowance (RDA).

In intervention studies, the addition of RPO yielded significant improvements in antioxidant

concentrations in red blood cells and the liver (Loganathan *et al.*, 2017). In studies that were conducted by Ojeda *et al.* (2017), RPO was provided to patients during an interventional period in meals at lunch and dinner. Although the primary purpose of this study was to evaluate the functional effect of the oleic acid content in the oil on a population, the study demonstrated that the antioxidant capacity of the oil was comparable to that of virgin olive oil, which was mainly due to the presence of tocopherols and tocotrienols. This provides an opportunity to look for alternatives for the recovery and concentration of these compounds for application as ingredients of natural origin in the development of functional foods.

To promote RPO consumption, studies that were conducted by Stuijvenberg *et al.* (2001) used RPO as an ingredient in the development of cookies for fortification programs to obtain functional cookies that were good sources of provitamin A carotenoids. All these studies have something in common: They demonstrate the nutraceutical effect of RPO on health. However, it is necessary to continue investigating the associated mechanisms for the delivery of these compounds and to protect these compounds in foods to extend their shelf lives by considering the conditions to which the foods are exposed during their manufacture. For this, microcapsules (with a range of 1 to 1000 μm) are an efficient option. They protect the compounds of interest from environmental conditions such as heat, moisture, air, and light (Comunian *et al.*, 2021) while guaranteeing regular interactions between the external and internal parts of the microcapsule and avoiding the loss of biological activity of the compounds (Thakur *et al.*, 2017). For β-carotene from various sources, microcapsules with guar gum, cassava starch, kappa carrageenan, carboxymethyl cellulose, isolated whey protein, casein alginate (Thakur *et al.*, 2017), maltodextrin, chitosan, and arabic gum (Bonilla-Ahumada *et al.*, 2018) have been explored.

CONCLUSION

Microfiltration and ultrafiltration processes have been used as low-energy alternatives within oil refinement processes (degumming, deacidification, and oil/water separation), and rarely, nanofiltrations have been explored for this purpose. This article shows the versatility of nanofiltration as an alternative for recovering phytonutrients with important biological activities, especially from CPO, which constitutes one of the essential phytonutrient vegetable sources of carotenoids, tocopherols, and tocotrienols. These compounds can be recuperated, concentrated, and used in various applications, *e.g.,* as natural ingredients for food formulations such as functional food formulations, as natural pigments in the food industry, in pharmacological, nutraceutical and cosmetics applications. Hence, this topic should be explored further to find new applications of this technology in agroindustrial chains to help generate added value.

ACKNOWLEDGEMENT

Authors would like to acknowledge the support from Colombian Oil Palm Research Center (Cenipalma), Bogotá D.C. Colombia, Universidad Nacional de Colombia, Bogotá, D.C., Colombia and Universidad Industrial de Santander (UIS), Bucaramanga, Colombia for their help in formatting the manuscript. This article was supported by Palm Oil Promotion Fund (FFP), Fedepalma and UN Innova: *Convocatoria de Proyectos para el Fortalecimiento de la Innovación en la Universidad Nacional de Colombia a partir del Desarrollo de Prototipos y Experiencias Piloto* 2019-2021 *(segunda cohorte).*

REFERENCES

Akhtar, A; Subbiah, S; Mohanty, K; Sundar, R; Unnikrishnan, R and Hareesh, U S (2020). Sugarcane juice clarification by lanthanum phosphate nanofibril coated ceramic ultrafiltration membrane: PPO removal in absence of lime pre-treatment, fouling and cleaning studies. *Sep. Purif. Technol.*, *249*: 1-10.

Almaraz-Sánchez, I; Amaro-Reyes, A; Acosta-Gallegos, J A and Mendoza-Sánchez, M (2022). Processing agroindustry by-products for obtaining value-added products and reducing environmental impact. *J. Chem.*, *2022*. 13 pp.

Amado, M A (2010). *Seguimiento a las pérdidas de fitonutrientes durante el proceso de refinación del aceite de palma.* Universidad Nacional de Colombia.

Ariono, D; Wardani, A K; Widodo, S; Aryanti, P T P and Wenten, I G (2018). Fouling mechanism in ultrafiltration of vegetable oil. *Mater. Res. Express*, *5(3)*: 0-8.

Arora, S; Manjula, S; Gopala Krishna, A G and Subramanian, R (2006). Membrane processing of crude palm oil. *Desalination*, *191*: 454-466.

Aryanti, N; Wardhani, D H; Maulana, Z S and Roberto, D (2017). Evaluation of ultrafiltration performance for phospholipid separation. *J. Phys. Conf. Ser.*, *909(1)*.

Aryanti, N; Wardhani, D H and Nafiunisa, A (2018). Ultrafiltration membrane for degumming of crude palm oil-isopropanol mixture. *Chem. Biochem. Eng. Q., 32(3)*: 325-334.

Azmi, R A; Goh, P S; Ismail, A F; Lau, W J; Ng, B C; Othman, N H; Noor, A M and Yusoff, M S A (2015). Deacidification of crude palm oil using PVA-crosslinked PVDF membrane. *J. Food Eng., 166*: 165-173.

Baker, R W (2004). *Membrane Technology and Applications*. John Wiley and Sons, New Jersey, USA. 538 pp.

Baker, R W (2012a). *Membrane Technology and Applications*. 3rd edition. John Wiley and Sons, New Jersey, USA. 589 pp.

Baker, R W (2012b). Ultrafiltration. *Membrane Technology and Applications*. 3rd edition. John Wiley and Sons, New Jersey, USA. p. 253-302.

Balti, R; Le Balc'h, R; Brodu, N; Gilbert, M; Le Gouic, B; Le Gall, S; Sinquin, C and Massé, A (2018). Concentration and purification of *Porphyridium cruentum* exopolysaccharides by membrane filtration at various cross-flow velocities. *Process Biochem., 74*: 175-184.

Bassam, J; Harapanahalli, S and Otten, D (2001). Method for removing phospholipids from vegetable oil micella, method for conditioning a polymeric microfiltration, and membrane. United State Patent.

Bassam, J; Harapanahalli, S and Otten, D (2004). Methods and apparatus for processing vegetable oil miscella method for conditioning membrane, membrane and lecithin product. United State Patent.

Bassam, J; Harapanahalli, S and Otten, D (2009). Method and apparatus for processing vegetable oil miscella, method for conditioning a polymeric microfiltration membrane, membrane, and lecithin product. United State Patent.

Bassam, J; Harapanahalli, S and Otten, D (2011). Method and apparatus for processing vegetable oil miscella, method for conditioning a polymeric microfiltration membrane, membrane, and lecithin product. United State Patent.

Ter Beek, O; Pavlenko, D; Suck, M; Helfrich, S; Bolhuis-Versteeg, L; Snisarenko, D; Causserand, C; Bacchin, P; Aimar, P and van Oerle, R (2019). New membranes based on polyethersulfone - SlipSkin™ polymer blends with low fouling and high blood compatibility. *Sep. Purif. Technol., 225(April)*: 60-73.

Belfort, G; Davis, R and Zydney, A (1994). The behavior of suspensions and macromolecular solutions in crossflow microfiltration. *J. Membr. Sci., 96*: 1-58.

Bernardo, P and Drioli, E (2010). Membrane technology: Latest applications in the refinery and petrochemical field. *Comprehensive Membrane Science and Engineering, 4*: 211-239.

Bernardo, P and Drioli, E (2017). Membrane technology in the refinery and petrochemical field: Research trends and recent progresses. *Comprehensive Membrane Science and Engineering*. p. 164-188.

Bindes, M M M; Terra, N M; Patience, G S; Boffitoorcid, D C; Cardoso, V L and Reis, M H M (2020). Asymmetric Al_2O_3 and PES/Al_2O_3 hollow fibre membranes for green tea extract clarification. *J. Food Eng., 277*: 1-44.

Bonilla-Ahumada, F de J; Khandual, S and Lugo-Cervantes, E del C (2018). Microencapsulation of algal biomass (*Tetraselmis chuii*) by spray-drying using different encapsulation materials for better preservation of beta-carotene and antioxidant compounds. *Algal Res., 36(April)*: 229-238.

Boynueğri, P; Yemişçioğlu, F and Gümüşkesen, A S (2017). Effect of membrane degumming conditions on permeate flux and phospholipids rejection. *GIDA. J. Food, 42(5)*: 597-602.

Cárdenas, A G (2016). Oil palm agro-industry in America. *Revista Palmas, 37*: 21-228.

Chamberland, J; Messier, T; Dugat-Bony, E; Lessard, M H; Labrie, S; Doyen, A and Pouliot, Y (2019). Influence of feed temperature to biofouling of ultrafiltration membrane during skim milk processing. *Int. Dairy J., 93*: 99-105.

Chaves, G; Ligarreto-Moreno, G A and Cayon-Salinas, D G (2018). Physicochemical characterization of bunches from American oil palm (*Elaeis oleifera* H.B.K. *Cortes*) and their hybrids with African oil palm (*Elaeis guineensis* Jacq.). *Acta Agron., 67(1)*: 168-176.

Chew, J W; Kilduff, J and Belfort, G (2020). The behaviour of suspensions and macromolecular solutions in crossflow microfiltration: An update. *J. Membr. Sci., 601(January)*: 117865.

Chiu, M C; de Morais Coutinho, C and Gonçalves, L A G (2009). Carotenoids concentration of palm oil

using membrane technology. *Desalination*, *245(1-3)*: 783-786.

Choo, M Y (1994). Palm oil carotenoids. *Food Nutr. Bull.*, *15(2)*: 1-8.

Comunian, T A; Silva, M P and Souza, C J F (2021). The use of food by-products as a novel for functional foods: Their use as ingredients and for the encapsulation process. *Trends Food Sci. Technol.*, *108(January)*: 269-280.

Corley, R H V and Tinker, P B (2016). *The Oil Palm*. 5th edition. Wiley Blackwell, New Jersey, USA. 680 pp.

Danis, U and Aydiner, C (2009). Investigation of process performance and fouling mechanisms in micellar-enhanced ultrafiltration of nickel-contaminated waters. *J. Hazard. Mater.*, *162*: 577-587.

Darnoko, D and Cheryan, M (2000). Kinetics of palm oil transesterification in a batch reactor. *JAOCS, 77(12)*: 1263-1267.

Darnoko, D and Cheryan, M (2006a). Carotenoids from red palm methyl esters by nanofiltration. *J. Am. Oil Chem. Soc.*, *83(4)*: 365-370.

Darnoko, D and Cheryan, M (2006b). Carotenoids from red palm methyl esters by nanofiltration. *J. Am. Oil Chem. Soc.*, *83(4)*: 365-370.

Darvishmanesh, S; Robberecht, T; Luis, P; Degrève, J and Van Der Bruggen, B (2011). Performance of nanofiltration membranes for solvent purification in the oil industry. *JAOCS, 88(8)*: 1255-1261.

Deshwal, G K; Ameta, R; Sharma, H; Singh, A K; Panjagari, N R and Baria, B (2020). Effect of ultrafiltration and fat content on chemical, functional, textural and sensory characteristics of goat milk-based Halloumi type cheese. *LWT-Food Sci. Technol.*, *126*: 1-9.

Destani, F; Naccarato, A; Tagarelli, A and Cassano, A (2020). Recovery of aromatics from orange juice evaporator condensate streams by reverse osmosis. *Membranes (Basel)*, *10*: 1-12.

Díaz-Montes, E and Castro-Muñoz, R (2019). Metabolites recovery from fermentation broths via pressure-driven membrane processes. *Asia-Pac. J. Chem. Eng.*, *14*: 1-22.

Díaz-Montes, E; Yáñez-Fernández, J and Castro-Muñoz, R (2020). Microfiltration-mediated extraction of dextran produced by *Leuconostoc mesenteroides* SF3. *Food Bioprod. Process.*, *119*: 317-328.

Dong, S; Xia, H; Wang, F and Sun, G (2017). The effect of red palm oil on vitamin A deficiency: A meta-analysis of randomized controlled trials. *Nutrients*, *9(1281)*: 1-15.

Doran, P M (2013). *Bioprocess Engineering Principles*. Academic Press, Cambridge, USA. 919 pp.

Doshi, K and Shah, S R (2018). Removal of phospholipids from crude edible oil by PVDF membrane. *IJARIIT*, *4(2)*: 2524-2529.

Fine, F; Brochet, C; Gaud, M; Carre, P; Simon, N; Ramli, F and Joffre, F (2016). Micronutrients in vegetable oils: The impact of crushing and refining processes on vitamins and antioxidants in sunflower, rapeseed, and soybean oils. *Eur. J. Lipid Sci. Technol.*, *118(5)*: 680-697.

Gavazzi-April, C; Benoit, S; Doyen, A; Britten, M and Pouliot, Y (2018). Preparation of milk protein concentrates by ultrafiltration and continuous diafiltration: Effect of process design on overall efficiency. *J. Dairy Sci.*, *101(11)*: 9670-9679.

Ghazali, N F; Md Hanim, K; Pahlawi, Q A and Lim, K M (2022). Enrichment of carotene from palm oil by organic solvent nanofiltration. *JAOCS*, *99(3)*: 189-202.

Gonçalves, C B; Rodrigues, C E C; Marcon, E C and Meirelles, A J A (2016). Deacidification of palm oil by solvent extraction. *Sep. Purif. Technol*, *160*: 106-111.

González-Tovar, L A; Noriega-Rodríguez, J A; Ortega-García, J; Gámez-Meza, N and Medina-Juárez, L A (2005). *Cinética de adsorción de pigmentos, peróxidos y tocoferoles durante el proceso de blanqueo del aceite de soja. Grasas y Aceites*, *56(4)*: 324-327.

Hafidi, A; Pioch, D and Ajana, H (2005). Membrane-based simultaneous degumming and deacidification of vegetable oils. *Innov. Food Sci. Emerg. Technol.*, *6(2)*: 203-212.

Hariyadi, P (2020). Food safety and nutrition issues: Challenges and opportunities for Indonesian palm oil. *IOP Conference Series: Earth and Environmental Science*, *418(1)*.

Haro, C; De La Torre, E; Aragón, C and Guevara, A (2014). *Regeneración de arcillas de blanqueo empleadas en la decoloración de aceites vegetales comestibles*. *Revista EPN*, *34(1)*: 1-8.

Hou, Z; Cao, X; Cao, L; Ling, G; Yu, Z and Pang, M (2020). The removal of phospholipid from crude rapeseed oil by enzyme-membrane binding. *J. Food Eng.*, *280 (September 2019)*: 1-16.

Iyuke, S E; Ahmadun, F R and Majid, R A (2004). Process intensification of membrane system for crude palm oil pretreatment. *J. Food Process Eng*., *27*: 476-496.

Kamal - Eldin, A and Budilarto, E (2015). Tocopherols and tocotrienols as antioxidants for food preservation. *Handbook of Antioxidants for Food Preservation*. 1st edition. Elsevier Ltd., Amsterdam, Netherlands. 141 pp.

Kang, G and Cao, Y (2014). Application and modification of poly (vinylidene fluoride) (PVDF) membranes - A review. *J. Membr. Sci.*, *463*: 145-165.

Kilduff, J E; Mattaraj, S; Sensibaugh, J; Pieracci, J P; Yuan, Y and Belfort, G (2002). Modeling flux decline during nanofiltration of NOM with poly(arylsulfone) membranes modified using UV-assisted graft polymerization. *Environ. Eng. Sci.*, *19(6)*: 477-495.

Kirmizis, D and Chatzidimitriou, D (2009). Antiatherogenic effects of vitamin E: The search for the Holy Grail. *Vasc. Health Risk Manag.*, *5*: 767-774.

Lai, S O; Heng, S L; Chong, K C and Lau, W J (2016). Deacidification of palm oil using solvent extraction integrated with membrane technology. *Jurnal Teknologi*, *78(12)*: 69-74.

Lauzin, A; Pouliot, Y and Britten, M (2020). Understanding the differences in cheese-making properties between reverse osmosis and ultrafiltration concentrates. *J. Dairy Sci.*, *103(1)*: 201-209.

Li, Y and Corredig, M (2020). Acid induced gelation behavior of skim milk concentrated by membrane filtration. *J. Texture Stud.*, *51(1)*: 101-110.

Lim, K M and Ghazali, N F (2021). Nanofiltration of binary palm oil/solvent mixtures: Experimental and modeling. *Materials Today: Proceedings*. Elsevier Ltd., Amsterdam, Netherlands. p. 1010-1014.

Lobasenko, B A; Kotlyarov, R v. and Sazonova, E K (2019). Automation of the production of cottage cheese using the ultrafiltration method. *2019 International Science and Technology Conference "EastConf", EastConf 2019*. *IEEE*. p. 1-5.

Loganathan, R; Subramaniam, K M; Radhakrishnan, A K; Choo, Y M and Teng, K T (2017). Health-promoting effects of red palm oil: Evidence from animal and human studies. *Nutr. Rev.*, *75(2)*: 98-113.

Loganathan, R; Ahmad, A; Ratna, S and Kim, T (2020a). Thermal stability and sensory acceptance of cupcakes containing red palm olein. *J. Oleo Sci., (June)*: 1-6.

Loganathan, R; Tarmizi, A H A; Vethakkan, S R and Teng, K T (2020b). Storage stability assessment of red palm olein in comparison to palm olein. *J. Oleo Sci.*, *69(10)*: 1163-1179.

Manjula, S and Subramanian, R (2007). Membrane technology in degumming, dewaxing, deacidifying, and decolorizing edible oils. *Crit. Rev. Food Sci. Nutr.*, *7*: 569-592.

Mba, O I; Dumont, M J and Ngadi, M (2015). Palm oil: Processing, characterization and utilization in the food industry - A review. *Food Biosci.*, *10*: 26-41.

Mestre, S; Gozalbo, A; Lorente-ayza, M M and Sánchez, E (2019). Low-cost ceramic membranes: A research opportunity for industrial application. *J. Eur. Ceram. Soc.*, *39(12)*: 3392-3407.

Minhajuddin, M; Beg, Z H and Iqbal, J (2005). Hypolipidemic and antioxidant properties of tocotrienol rich fraction isolated from rice bran oil in experimentally induced hyper- lipidemic rats. *Food Chem. Toxicol.*, *43(5)*: 747-753.

Mocchegiani, E; Costarelli, L; Giacconi, R; Malavolta, M; Basso, A; Piacenza, F; Ostan, R; Cevenini, E; Gonos, E; Franceschi, C and Monti, D (2014). Vitamin E-gene interactions in aging and inflammatory age-related diseases: Implications for treatment. A systematic review. *Ageing Res. Rev.*, *14*: 81-101.

Mohammad, A W; Teow, Y H; Ang, W L; Chung, Y T; Oatley-Radcliffe, D L and Hilal, N (2015). Nanofiltration membranes review: Recent advances and future prospects. *Desalination*, *356*: 226-254.

Mohammad, A W; Teow, Y H; Ho, K C and Rosnan, N A (2019). Recent developments in nanofiltration for food applications. *Micro and Nano Technologies*. Elsevier Ltd., Amsterdam, Netherlands. p. 101-120.

Mohd-Nasir, H and Mohd-Setapar, S (2018). Natural ingredients in cosmetics from Malaysian plants: A review. *Sains Malays.*, *47(5)*: 951-959.

de Morais Coutinho, C; Chiu, M C; Basso, R C; Ribeiro, A P B; Gonçalves, L A G and Viotto, L A (2009). State of art of the application of membrane technology to vegetable oils: A review. *Food Res. Int.*, *42(5-6)*: 536-550.

Mosquera, M; Bernal, P and Silva, A (2009). *Agenda prospectiva de investigación y desarrollo tecnológico para la cadena de oleaginosas, grasas y aceites en Colombia con énfasis en oleína roja*. 184.

Nabu, E B P; Sulaswatty, A and Kartohardjono, S (2021). Palm carotene production technologies - A membrane perspective. *IOP Conference Series: Materials Science and Engineering, 1053(1)*: 012136.

Nagarajan, J; Ramanan, R N; Raghunandan, M E; Galanakis, C M and Krishnamurthy, N P (2017). Chapter 8: Carotenoids. *Nutraceutical and Functional Food Components: Effects of Innovative Processing Techniques*. Elsevier Inc. p. 259-296.

Niazmand, R; Mohammad, S; Razavi, A L I and Farhoosh, R (2015). Colloid-enhanced ultrafiltration of canola oil: Effect of process conditions and MWCO on flux, fouling and rejections. *J. Food Process. Preserv.*, *39*: 292-300.

Ochoa, N; Pagliero, C; Marchese, J and Mattea, M (2001). Ultrafiltration of vegetable oils: Degumming by polymeric membranes. *Sep. Purif. Technol.*, *22-23*: 417-422.

Ojeda, M; Borrero, M; Sequeda, G; Diez, O; Castro, V; García, Á; Ruiz, Á; Pacetti, D; Frega, N; Gagliardi, R and Lucci, P (2017). Hybrid palm oil (*Elaeis oleifera* × *Elaeis guineensis*) supplementation improves plasma antioxidant capacity in humans. *Eur. J. Lipid Sci. Technol.*, *119(2)*: 1-8.

Onal-ulusoy, B (2015). Effects of plasma-modified polyvinylidenefluoride and polyethersulfone ultrafiltration (UF) membrane treatments on quality of soybean oil. *J. Food Qual.*, *38*: 285-296.

Onal-ulusoy, B; Tur, E; Akdog, E and Mutlu, M (2014). Plasma polymerization modified polyvinylidene fluoride (PVDF) membrane development and characterization for degumming of soybean oil. *J. Am. Oil Chem. Soc.*, *91*: 1813-1822.

Ong, K K; Fakhru'l-Razi, A; Baharin, B S and Hassan, M A (1999). Degumming of crude palm oil by membrane filtration. *Artif. Cells Blood Substit. Immobil. Biotechnol.*, *27(5-6)*: 381-385.

Othman, N H; Latip, R A; Noor, A M; Lau, W J; Goh, P S and Ismail, A F (2021). Simultaneous degumming and deacidification of crude palm oil using mixed matrix PVDF membrane. *IOP Conference Series: Materials Science and Engineering*, *1195(1)*: 012030.

Otitoju, T A; Ahmad, A L and Ooi, B S (2016). Polyvinylidene fluoride (PVDF) membrane for oil rejection from oily wastewater: A performance review. *J. Water Process Eng.*, *14*: 41-59.

Peeva, L G; Marchetti, P and Livingston, A G (2010). Nanofiltration operations in nonaqueous systems. *Comprehensive Membrane Science and Engineering*. 2nd edition. Elsevier Ltd., Amsterdam, Netherlands. p. 91-111.

Pérez, R and Labanda, J (2013). Estudio preliminar de la permeación de biomoléculas en membranas de nanofiltración. *Revista Iberoamericana de Polímeros.*, *14(7)*: 44-54.

Prada, F; Ayala, I; Delgado, W; Ruiz-Romero, R and Romero, H (2011). Effect of fruit ripening on content and chemical composition of oil from three oil palm cultivars (*Elaeis guineensis* Jacq.) grown in Colombia. *J. Agric. Food Chem.*, *59*: 10136-10142.

Purwasasmita, M; Nabu, E B P; Khoiruddin and Wenten, I G (2015). Non dispersive chemical deacidification of crude palm oil in hollow fibre membrane contactor. *J. Eng. Technol. Sci.*, *47(4)*: 426-446.

Rashid Khan, M; Ahsan, H; Siddiqui, S and Siddiqui, W A (2015). Tocotrienols have a nephroprotective action against lipid-induced chronic renal dysfunction in rats. *Ren. Fail.*, *37(1)*: 136-143.

Razi, F; Yulia, M; Erfiza, N M and Asnawi, A (2021). Study on the separation of phospholipids from crude palm oil using a polyethersulfone ultrafiltration membrane. *IOP Conference Series: Earth and Environmental Scienc*e, *922*: 012068.

Reddy, K; Subramanian, R; Kawakatsu, T and Nakajima, M (2001). Decolorization of vegetable oils by membrane processing. *Eur. Food Res. Technol.*, *213*: 212-218.

Renhe, I R T and Corredig, M (2018). Effect of partial whey protein depletion during membrane filtration on thermal stability of milk concentrates. *J. Dairy Sci.*, *101(10)*: 1-10.

Rincón, S and Martinez, D (2009). Análisis de las propiedades del aceite de palma en el desarrollo de su industria. *Revista Palmas, 30(2)*: 11-24.

Rodrigues, L M; Romanini, E B; Silva, E; Pilau, E J; da Costa, S C and Madrona, G S (2020). Camu-camu bioactive compounds extraction by ecofriendly sequential processes (ultrasound assisted extraction and reverse osmosis). *Ultrason. Sonochem.*, *64*: 105017.

Rodrigues Toledo Renhe, I; Zhao, Z and Corredig, M (2019). A comparison of the heat stability of fresh milk protein concentrates obtained by microfiltration, ultrafiltration and diafiltration. *J. Dairy Res.*, *86*: 1-7.

Roy, B; Dey, S; Sahoo, G C; Roy, S N and Bandyopadhyay, S (2014). Degumming, dewaxing and deacidification of rice bran oil-hexane miscella using ceramic membrane: Pilot plant study. *J. Am. Oil Chem. Soc.*, *91(8):* 1453-1460.

Saini, R K and Keum, Y S (2016). Tocopherols and tocotrienols in plants and their products: A review on methods of extraction, chromatographic separation, and detection. *Food Res. Int.*, *82*: 59-70.

Saini, R K; Nile, S H and Park, S W (2015). Carotenoids from fruits and vegetables: Chemistry, analysis, occurrence, bioavailability and biological activities. *Food Res. Int.*, *76*: 735-750.

Sánchez-Moya, T; Hidalgo, A M; Ros-Berruezo, G and López-Nicolás, R (2020). Screening ultrafiltration membranes to separate lactose and protein from sheep whey: Application of simplified model. *J. Food Sci. Technol.*, 1-8.

Saravanan, M; Bhosle, B M and Subramanian, R (2006). Processing hexane-oil miscella using a nonporous polymeric composite membrane. *J. Food Eng.*, *74(4)*: 529-535.

Schäfer, J; Schubert, T and Atamer, Z (2019). Pilot-scale β-casein depletion from micellar casein via cold microfiltration in the diafiltration mode. *Int. Dairy J.*, *97*: 222-229.

Seppanen, C M; Song, Q and Csallany, A S (2010). The antioxidant functions of tocopherol and tocotrienol homologues in oils, fats and food systems. *J. Am. Oil Chem. Soc.*, *87(5)*: 469-481.

Shakhno, N; Botvynko, A; Ečer, J and Čurda, L (2019). Electrodialysis application of the ultrafiltration permeate of milk before and after reverse osmosis. *Chem. Eng. Technol.*, *42(4)*: 1-8.

Siddiqui, S; Ahsan, H; Khan, M R and Siddiqui, W A (2013). Protective effects of tocotrienols against lipid-induced nephropathy in experimental type-2 diabetic rats by modulation in TGF-β expression. *Toxicol. Appl. Pharmacol.*, *273*: 314-324.

Solís, C A; Velez, S A and Ramirez-Navas, J S (2017). Tecnología de membranas: ultrafltración. *Entre Ciencia e Ingeniería, (22)*: 26-36.

Sousa, Y R F; Araújo, D F S; Pulido, J O; Pintado, M M E; Martínez-Férez, A and Queiroga, R C R E (2019). Composition and isolation of goat cheese whey oligosaccharides by membrane technology. *Int. J. Biol.Macromol.*, *139*: 57-62.

Statista (2021). Consumption of vegetable oils worldwide from 2013/14 to 2020/2021, by oil type. https://www.statista.com/statistics/263937/vegetable-oils-global-consumption/, accessed on 21 March 2022.

Stuijvenberg, M E V; Dhansay, M A; Lombard, C J; Faber, M and Benade, A J S (2001). The effect of a biscuit with red palm oil as a source of β-carotene on the vitamin A status of primary school children: A comparison with β-carotene from a synthetic source in a randomised controlled trial. *Eur. J. Clin. Nutr.*, *55*: 657-662.

Sundram, K; Sambanthamurthi, R and Tan, Y (2003). Palm fruit chemistry and nutrition. *Asia Pac. J. Clin. Nutr.*, *12(3)*: 355-362.

Sylvester, P W and Shah, S (2004). Potential health benefits of palm tocotrienols in the prevention and treatment of breast cancer. *Palmas*, *25*: 233-244.

Taeymans, J; Clarys, P and Bare, A O (2014). Use of food supplements as nutricosmetics in health and fitness. *Handbook of Cosmetic Science and Technology*. p. 583-596.

Thakur, D; Jain, A; Ghoshal, G; Shivhare, U S and Katare, O P (2017). Microencapsulation of β-carotene cased on casein/guar gum blend using zeta potential-yield stress phenomenon: An approach to enhance photo-stability and retention of functionality. *AAPS PharmSciTech*, *18(5)*: 1447-1459.

Todero, I; Confortin, T C; Soares, J F; Brun, T; Luft, L; Rabuske, J E; Kuhn, R C; Tres, M V; Zabot, G L and Mazutti, M A (2019). Concentration of metabolites from *Phoma* sp. using microfiltration membrane for increasing bioherbicidal activity. *Environ. Technol.*, *40(18)*: 2364-2372.

Touhami, S; Chamberland, J; Perreault, V; Suwal, S; Marciniak, A; Pouliot, Y and Doyen, A (2020). Coupling high hydrostatic pressure and ultrafiltration for fractionation of alpha-lactalbumin from skim milk. *Sep. Sci. Technol.*, *56(6)*: 1-11.

Tsuduki, T; Kuriyama, K; Nakagawa, K and Miyazawa, T (2013). Tocotrienol (unsaturated vitamin E) suppresses degranulation of mast cells and reduces allergic dermatitis in mice. *J. Oleo Sci.*, *60(10)*: 825-834.

Tur, E; Onal-ulusoy, B; Akdogan, E and Mutlu, M (2011). Surface modification of polyethersulfone membrane to improve its hydrophobic characteristics for waste frying oil filtration: Radio frequency plasma treatment. *J. Appl. Polym. Sci.*, *123*: 3402-3411.

United Nations (2019). Growing at a slower pace, world population is expected to reach 9.7 billion in 2050 and could peak at nearly 11 billion around 2100. *Department of Economic and Social Affairs*, *1*.

Uttamrao, H J; Meena, G S; Borad, S G; Punjaram, S A; Khetra, Y; Upadhyay, N and Singh, A K (2019). Effect of disodium phosphate and homogenization on physico-chemical and rheological properties of buffalo skim milk based ultrafiltered retentate. *J. Food Sci. Technol.*, *56(5)*: 2426-2435.

Valencia, A P; Doyen, A; Benoit, S; Margni, M and Pouliot, Y (2018). Effect of ultrafiltration of milk prior to fermentation on mass balance and process efficiency in Greek-style yogurt manufacture. *Foods*, *7*: 1-10.

Wang, H J; Dai, K; Wang, Y Q; Wang, H F; Zhang, F and Zeng, R J (2018). Mixed culture fermentation of synthesis gas in the microfiltration and ultrafiltration hollow-fibre membrane biofilm reactors. *Bioresour. Technol.*, *267(July)*: 650-656.

Wenten, I G; Victoria, A V; Tanukusuma, G; Khoiruddin, K and Zunita, M (2019). Simultaneous clarification and dehydration of crude palm oil using superhydrophobic polypropylene membrane. *J. Food Eng.*, *248 (November 2018)*: 23-27.

Yaakob, C M and Chin-Ping, T (2003). Carotenoids. *Lipids for Functional Foods and Nutraceuticals* (F D Gunstone, ed.). Woodhead Publishingg Ltd., Swaston, UK. p. 25-52.

Zhang, J; Sheng, Y; Yuan, D; Alici, G; Nguyen, N-T and Li, W (2016). High throughput cell-free extraction of plasma by an integrated microfuidic device combining iertia microfluidics and membrane. *Proceedings of the ASME 2016 5th International Conference on Micro/Nanoscale Heat and Mass Tranfer MNHMT 2016*. p. 1-6.

Journal of Oil Palm Research Vol. 35 (2) June 2023 p. 236-246
DOI: https://doi.org/10.21894/jopr.2022.0023

EFFECT OF METHYLENE DIPHENYL DIISOCYANATE INDEX ON PHYSICO-MECHANICAL AND MORPHOLOGICAL PROPERTIES OF PALM OLEIN-BASED VISCOELASTIC POLYURETHANE FOAMS

NURUL 'AIN HANZAH[1]*; KOSHEELA DEVI POO PALAM[1]; TUAN NOOR MAZNEE TUAN ISMAIL[1]; SRIHANUM ADNAN[1]; NORHAYATI MOHD NOOR[1]; MOHD NORHISHAM SATTAR[1] and YEONG SHOOT KIAN[1]

ABSTRACT

This study revealed the behaviour of the effect of varying the methylene diphenyl diisocyanate (MDI) index on foaming reactivity, physico-mechanical and morphological properties of palm olein-based viscoelastic polyurethane (VE-PU) foams. The palm olein-based polyol, E-135 NOP was used from 15% to 25% (w/w) in the VE-PU foam formulations. Our study revealed that by varying the isocyanate indices, no significant changes in cream and gelling times were observed, but the rise time was slightly decreased, indicating that the rate of reaction had increased. The compression force deflection (CFD) and tensile strength with palm olein-based VE-PU foam with 25% of E-135 NOP were significantly increased as the isocyanate indices increased. However, it was observed that other mechanical properties, i.e.*, density and resiliency of palm olein-based VE-PU foam decreased as the isocyanate indices increased. In terms of morphology, the average cell size determined by scanning electron microscope (SEM) also increased as the isocyanate indices increased. The finding of this study could have practical significance in the selection of the optimal isocyanate index to formulate VE-PU products.*

Keywords: bio-based polyol, isocyanate index, viscoelastic polyurethane foam.

Received: 14 October 2021; **Accepted:** 2 March 2022; **Published online:** 9 May 2022.

INTRODUCTION

Polyurethane (PU) foams are one of the most versatile polymeric materials. The chemical nature of these materials allows them to be easily tailor-made to solve challenging problems and to enhance industrial consumer products by adding comfort, warmth and convenience to our lives. PU foams are classified into three major classes, *i.e.*, flexible, rigid and semi-rigid PU foams. Globally, PU rigid foams are the most widely used in terms of application; while PU flexible foams are the fastest in terms of growing demand (Markets and Markets, 2014). Flexible PU foams are mainly used in cushioning applications, *e.g.*, automotive (seats, headrest and armrest) and furniture (pillow and mattresses) (Ionescu, 2005).

Viscoelastic (VE) PU foam is another term for memory PU foam, which constitutes a significant portion of the flexible PU foams market, and they are used primarily for high quality mattress segment and sound absorption applications (Singh *et al.*, 2003). Unlike conventional flexible PU foams, VE-PU foams are characterised by their

[1] Malaysian Palm Oil Board,
6 Persiaran Institusi, Bandar Baru Bangi,
43000 Kajang, Selangor, Malaysia.

* *Corresponding author e-mail: nurulain@mpob.gov.my*

slow response after compression and low resilience (below 20%, ball rebound test) (Polyurethane Foam Association, 2016). In general, parameters involved in formulating and processing VE-PU foams are more restrictive than conventional flexible PU foams. The main challenge is to obtain VE-PU foams that have open cell structure and to avoid shrinkage at a high level of foams softness (compliance) (Rajan *et al.*, 2011).

In recent years, green and bio-polyols (G&B) are becoming more popular due to consumer preference for sustainable and renewable resources. Polyols using natural oils (such as vegetable oil including soybean, castor, palm) as raw materials are known as bio-based polyols. On the other hand, polyols that are recycled from PU via glycolysis or acidolysis process and other sources are known as green polyols or recycled polyols (Markets and Markets, 2014; Sendijarevic *et al.*, 2005). Malaysia is one of the largest palm oil exporters, accounting for 18.3% (17.37 million tonnes) of the world's total vegetable oil trade and 34.3% of the total palm oil trade (Parveez *et al.*, 2021). Palm oil contains molecules with double bonds, *e.g.*, oleic acid, linoleic acid, which can be transformed into epoxy group through epoxidation and then the epoxy undergoes alcoholysis to form hydroxyl (Mohd Zan *et al.*, 2015).

The incorporation of palm oil-based polyol in PU formulation improves the microstructure and mechanical properties of flexible PU foam (Zhang and Chen, 2019). In this study, an introduction of palm oil-based polyol showed a higher closed pore ratio and increased air-flow resistivity, which enhanced the sound absorption coefficient and transmission loss of flexible PU foam. In another similar study, Prociak *et al.* (2018) formulated flexible PU foams using palm oil-based polyols with different hydroxyl numbers. They found that by introducing more than 25% (w/w) of palm oil-based polyols in the flexible PU foam formulation, the hardness, hysteresis, and support factor values of the PU foams produced increased. They also observed that addition of palm oil-based polyols up to 25% had reduced the resiliency of the flexible PU foams. A study by Nurul `Ain *et al.* (2016) discovered that having multiple polyols with different molecular weights in a formulation helped to break the molecular symmetry, which produced PU foams with low resilience. Besides an increase in the palm olein-based polyols (E-135 NOP) concentration in the VE-PU foams formulation does not influence the rate of foaming reactivity. It was also found that the foam cell size was increased and the open cell structure of VE foams was maintained.

PU foams are traditionally produced by a chemical reaction between diisocyanate and polyol. The most commonly used isocyanate (NCO) in PU foam production are aromatic NCO, namely toluene diisocyanate (TDI) and methylene diphenyl diisocyanate (MDI), representing about 90% of the total diisocyanate consumption (Gama *et al.*, 2018). The amount of NCO used in relation to the theoretical equivalent amount is known as the NCO index calculated using Equation (1) (Herrington and Hock, 1997):

$$\text{Isocyanate index} = \frac{\text{Actual amount of isocyanate used}}{\text{Theoretical amount of isocyanate required}} \times 100\% \quad (1)$$

The NCO index value can have a significant impact on the properties of the PU foams. Variation of the NCO index in foam has a pronounced effect on the hardness of the final foam. The increase in hardness is directly related to increased covalent cross-linking resulting from complete consumption of NCO reactive sites caused by the presence of NCO groups (Rojek and Prociak, 2012; Sung and Byung, 2008). In the production of flexible slabstock foams, the NCO index normally ranges from 105 to 115. Within this range, the hardness of the foam can be readily and safely controlled. However, in the commercial process, foam hardness may require adjustment from mould to mould to compensate for changes in the shape of various cushions and the NCO indices in the range of 85 to 110 are common practice (Herrington and Hock, 1997).

The effect of the NCO index on the properties of palm-based flexible PU made with TDI has been previously conducted (Lee *et al.*, 2007). In this research, palm-based flexible PU foams were prepared by using a blend of polyester and petroleum-based polyols with a molecular weight of 5000 g mol^{-1} at a ratio of 1:1 (w/w) and the NCO index was varied from 90% to 110%. It was observed that at 100% NCO index, the palm-based flexible PU foam had the highest density value and lowest hysteresis, *i.e.*, 60.6 kg m^{-3} and 23.80%, respectively. Gama *et al.* (2018) reported that due to health issues, TDI has been the subject of intensive research, in terms of both human and animal toxicological studies. One important reason is that TDI may cause asthma in sensitive individuals even at extremely low concentrations. This led to the prohibition of TDI usage which is a setback to some PU producers. Recently, many studies were conducted by employing less toxic MDI as NCO instead of TDI in flexible PU foam production (Norin *et al.*, 2006).

As far as the authors are aware, only a few published studies have evaluated the performance of MDI NCO indices on palm oil-based PU foams. Thus, this study extensively investigated the effect of variation MDI NCO indices on foaming reactivity,

physico-mechanical and cell morphological properties of VE-PU foams made from palm olein-based polyol (E-135 NOP). As mentioned before, the mechanical properties of VE-PU foams are greatly influenced by NCO indices. Therefore, there is a need to conduct a study on the effect of the NCO index on VE-PU foam since studies on palm oil-based VE-PU foams are limited. The NCO indices used in this study were varied at 65%, 70% and 80% because VE-PU foams are low resilience flexible foams and low NCO index are preferable (Rajan *et al*., 2011).

MATERIALS AND METHOD

Materials

The palm oil-based polyol, E-135 NOP used in this study was obtained from the pilot plant of the Malaysian Palm Oil Board (MPOB) in Malaysia. The palm oil-based polyol was synthesised via epoxidation and alcoholysis routes as described in detail by Tuan Ismail *et al*. (2018). The E-135 NOP polyol had a hydroxyl value of 134.0 mg KOH g^{-1}, moisture content of 0.04%, acid value of 0.70 mg KOH g^{-1}, iodine value of 6.7 g I_2 100 g^{-1}, the viscosity of 4400 mPa.s at 25°C, number average molecular weight (M_n) of 2537 Da and weight average molecular weight (M_w) of 5798 Da.

Three commercial petroleum-based polyols were supplied by Monument Chemicals, Texas, USA, *i.e.*, (i) Poly-G® 76-120 (ethylene oxide capped polyether triol) with hydroxyl value: 121 mg KOH g^{-1}, moisture content: 0.08%, viscosity at 25°C: 290 mPa.s, M_w: ~1400 g mol^{-1}, equivalent weight [calculated using Equation (2)]: 463.64, (ii) Poly-G® 30-240 (oxypropylated polyether triol) with hydroxyl value: 230 mg KOH g^{-1}, moisture content: 0.05%, viscosity at 25°C; 250 mPa.s, M_w: ~700 g mol^{-1}, equivalent weight: 243.91), and (iii) Poly-G® 85-34 (ethylene oxide capped polyether triol) with hydroxyl value: 35 mg KOH g^{-1}, moisture content: 0.03%, viscosity at 25°C: 1150 mPa.s, M_w: ~6000 g mol^{-1}, equivalent weight: 1602. Lumulse POE 26 (ethoxylated glycerine) with a hydroxyl value of 29.5 mg KOH g^{-1} and the equivalent weight of 1902 were supplied by Lambent Technologies Inc., Illinois, USA. Tegostab B 8871 surfactant was purchased from Behn Meyer, Selangor, Malaysia. Diethylene glycol (DEG) was purchased from Sigma-Aldrich, Missouri, USA. Two types of amine catalysts, Dabco 33LV (A33) (triethylenediamine in dipropylene glycol) and Niax A-1 (A-1) bis(2-dimethylaminoethyl) ether in dipropylene glycol, were obtained from Air Products, Pennsylvania, USA and Momentive, New York, USA, respectively. Distilled water was used as a blowing agent. All chemicals were used as received without any modification. The equivalent weight of the polyol was calculated by using Equation (2):

$$\text{Equivalent weight of polyol} = \frac{56.1 \times 1000}{\text{OH number}} \quad (2)$$

where 56.1 is the atomic weight of potassium hydroxide and 1000 is the number of milligrams in one gram of sample.

Two types of MDI NCO were used for this study, *i.e.*, Lupranate MI (MDI with a high content of 2,4-isomer, NCO content: 33.5%, equivalent weight: 125.37) was purchased from BASF, New Jersey, USA and Rubinate M (polymeric MDI, NCO content: 31.3%, equivalent weight: 134.19) was purchased from Huntsman, Michigan, USA. The equivalent weight of an NCO is the weight of an NCO compound per NCO site and calculated using Equation (3):

$$\text{Equivalent weight of isocyanate} = \frac{42 \times 100}{\%\ \text{NCO}} \quad (3)$$

where 42 is the atomic weight of the NCO group.

Methods

Preparation of blends isocyanates. In this study, the NCO component of the PU system was prepared by mixing NCO Lupranate MI and NCO Rubinate M at a ratio of 1:1 (w/w) in a 1 L glass jar at 1800 rpm for 20 min. Prior to preparation, the MDI NCO blend was purged with nitrogen and the glass jar containing the MDI NCO blend was sealed. The viscosity was measured at 25°C and the calculated equivalent weight of this blend are 102.5 mPa.s and 129.78, respectively. The equivalent weight of an NCO blend of different NCOs, the net equivalent weight of the blend was calculated by using Equation (4):

$$\text{Equivalent weight blend} = \frac{100}{\frac{\text{Weight \% of Luranate MI}}{\text{Equivalent of Luranate MI}} + \frac{\text{Weight \% of Rubinate M}}{\text{Equivalent weight of Rubinate M}}} \quad (4)$$

Preparation of VE-PU foam. The free-rise VE-PU foams were prepared by mixing the polyol component (polyols, DEG, surfactant and catalysts) and NCO component with a homogeniser mixer equipped with a 3" diameter mixing blade at 3100 rpm for 10 s. The amount of polyols and isocyanates components are listed in the VE-PU foam formulation (*Table 1*). The mixture was poured into a 34 × 20 × 12 cm polyethylene container and

transferred into an air-circulating oven preheated at 70°C for 60 min to complete the polymerisation process. All the VE-PU foams prepared were aged in ambient conditions for a minimum of one week before testing, according to ASTM D3574-08; Standard Test Method for Flexible Cellular Materials-Slab, Bonded, and Molded Urethane Foams.

Foaming profiles were determined for all VE-PU foams, which included the determination of cream time, gel time, and rise time. The foaming profiles were measured using the start of mixing as time zero. Cream time is an indication of the beginning of the foaming process and at this point, the liquid mixture becomes cloudy and begins to expand. Gel time is measured as the time of string formation, at which point the mixture changes from a liquid to a soft rubbery state, indicating an onset of a cross-linked PU network. Rise time is defined as the time at which the foam rise has been completed (Kattiyaboot and Thongpin, 2016; La *et al.*, 2013).

The control VE-PUs were prepared by using a blend of three commercial petroleum-based polyols, *i.e.*, Poly-G® 30-240, Poly-G® 76-120, Poly-G® 85-34, and Lumulse POE 26. The palm olein-based VE foams containing 15%, 20% and 25% of E-135 NOP (based on the weight of total polyols) as a proportionate replacement for three petroleum-based polyols (Poly-G® 30-240, Poly-G® 76-120, Poly-G® 85-34) were prepared without any adjustment in the catalyst system. The NCO index used in this study was varied at 65%, 70% and 80%.

Characterisation of VE-PU foam. Mechanical properties of VE-PU foams were evaluated on the samples prepared with a total amount of 300 g of polyols. All the properties of VE-PU foams were determined according to ASTM D 3574-08: Foam density (Test A), resilience via ball rebound test (Test H), tensile strength and elongation at break (Test E, load cell speed: 508 mm min^{-1}), compression force deflection (CFD), (in-house modified Test C, load cell speed: 50 mm min^{-1}), hysteresis (Procedure B – CFD hysteresis loss, load cell speed: 50 mm min^{-1}). The VE-PU foam density was measured in kilograms per cubic metre as in Equation (5):

$$\text{Density} = \frac{\text{Mass of samples, g}}{\text{Volume of the samples, mm}^3} \times 10^6 \qquad (5)$$

Tear strength was measured according to ASTM D 624–00 (Test Die C) at 500 mm min^{-1} tear speed. Tensile strength, elongation at break, CFD, and hysteresis were determined using Instron Tester Model 1122 with a 500 N load cell. For each test, three to five pieces of VE-PU foam samples were used. Support factor, or the SAG-index (from the verb sag) was measured by dividing the force needed to indent the foam 65% of its original height by the force needed to indent the foam 25% of its original height. The Fourier transform infrared (FTIR) spectra of palm olein-based VE-PU foams were recorded on a Perkin Elmer FTIR Spectrum 100 MILD DTIR equipped with Universal ATR Attachment in the 650-4000 cm^{-1} wavenumber range with 64 scans using a resolution of 6 cm^{-1} for each spectrum. The cell morphology of VE-PU foam was also captured using scanning electron microscopy (SEM) (JSM-IT 100, InTouch Scope™ SEM, Tokyo, Japan) at an acceleration voltage of 10 kV. A thin foam slab was gold-coated by a sputter-coating (SCD 005) with evaporated gold (20 nm thickness), then the morphology of VE-PU foams was captured at 25x and 100x magnifications. The average cell size of the VE-PU foams was also evaluated via SEM.

TABLE 1. FORMULATION OF VE-PU FOAM

Polyol component of PU system	Amount (g)											
E-135 NOP	0.0	15.0	20.0	25.0	0.0	15.0	20.0	25.0	0.0	15.0	20.0	25.0
Poly-G® 30-240	21.0	16.0	14.3	12.7	21.0	16.0	14.3	12.7	21.0	16.0	14.3	12.7
Poly-G® 76-120	21.0	16.0	14.3	12.7	21.0	16.0	14.3	12.7	21.0	16.0	14.3	12.7
Poly-G® 85-34	18.0	13.0	11.3	9.6	18.0	13.0	11.3	9.6	18.0	13.0	11.3	9.6
Lumulse POE 26	40.0				40.0				40.0			
DEG	2.25				2.25				2.25			
Water	2.3				2.3				2.3			
Tegostab B 8871	1.5				1.5				1.5			
A33	0.1				0.1				0.1			
A-1	0.2				0.2				0.2			
Isocyanate (NCO) index (%)	65				70				80			
MDI NCO component of PU System (Lupranate MI/Rubinate) (1:1 w/w) (g)	45.76	45.88	45.90	45.67	49.56	49.61	49.61	49.76	56.64	56.69	56.69	56.76

RESULTS AND DISCUSSION

In this study, the NCO index was varied at 65%, 70% and 80%, and the E-135 NOP added into VE-PU foam formulation was varied at 15%, 20% and 25%. Based on our previous study, incorporation of E-135 NOP higher than 25% reduced the mechanical properties, *i.e.,* tensile, tear strengths of VE-PU foam and increased the size of the PU foam cells structure compared to petroleum-based VE-PU foams cell structure (Nurul `Ain *et al.*, 2016; Prociak *et al.*, 2018). Therefore, the effect of incorporating E-135 NOP at 25% and below was investigated.

Effect of NCO Index on Foaming Reactivity of Palm Olein-based VE-PU Foam

The impact of three NCO indices (65%, 70% and 80%) of palm olein-based VE-PU foams containing 15%, 20% and 25% E-135 NOP was evaluated on the foaming kinetics through the determination of cream time, gel time, and rise time. *Figure 1* demonstrates the rise time decreased, indicating that the reaction rate had increased as the NCO index increased up to 80%. This could probably be due to increased reaction between NCO and water, which resulted in a greater volume of carbon dioxide (CO_2) gas generated in a short period (Prociak *et al.*, 2016; Rojek and Prociak, 2012). The rise time of the palm olein-based VE-PU foams reached a faster rate with an increase in the E-135 NOP content which is in accordance with the studies conducted previously by La *et al.* (2013) and Lee *et al.* (2007). However, no significant changes in cream and gelling time were observed when the NCO indices were increased for all three percentages of E-135 NOP incorporated.

The changes in functional group of the different NCO index. FTIR analysis of VE-PU foams was conducted to determine functional groups that impact the properties of palm olein-based VE-PU foams with 25% E135 NOP as a result of varying the NCO index (*Figure 2*). The NCO group at the wavelength range of 2250 cm^{-1} to 2255 cm^{-1} in the palm olein-based VE-PU foam spectrum was not present as the MDI and polyol reacted to form the urethane group. It was confirmed with the presence of the N-H stretching band at a wavelength of 3299 cm^{-1} to 3334 cm^{-1} and the N-H bending at the wavelength of 1598 cm^{-1} for all palm olein-based VE-PU foams regardless of the NCO index. Increasing the NCO index from 65% to 80% reduced the unreacted -OH groups as can be seen at the absorption of -OH at 3541 cm^{-1} was shifted to 3546 cm^{-1}. The absorption bands at 1690 cm^{-1} to 1735 cm^{-1} were also of interest. It was reported that the carbonyl groups (-C=O) of urethane are divided into four types based on the degree of hydrogen bonding; 1730 cm^{-1} -free carbonyl groups from the soft domain, 1716 cm^{-1} -disordered hydrogen bonded carbonyl groups, 1704 cm^{-1} -ordered hydrogen bonded carbonyl group from hard domain and 1690 cm^{-1} -ordered hydrogen bonded carbonyl groups from crystalline phase (Liu *et al.*, 2020). In our study, the FTIR spectra of the palm olein-based VE-PU foams with 25% E-135 NOP showed the absorption bands at about 1705 cm^{-1} to 1708 cm^{-1}, depending on the NCO index used, indicating the formation of ordered hydrogen bonded carbonyl group of urethane and free carbonyl groups of urethanes, respectively. It was also observed that the intensity of the absorption band of ordered hydrogen bonded carbonyl groups of urethanes at wavelengths of 1705 cm^{-1} to 1708 cm^{-1} increased with an increase in the NCO index. The presence of ordered hydrogen bonded carbonyl groups of urethanes has been reported to improve the mechanical properties of PU (Tereshatov *et al.*, 2015). It was in agreement with the mechanical properties of VE foams in which higher mechanical properties were observed in palm olein-based VE-PU foam prepared at NCO index of 80% compared to palm olein-based VE-PU foams prepared at NCO indices of 65% and 70% (*Table 2*). The VE-PU foam evaluated in this study only contain urethane bonds and no urea bonds. Thus, the ratio of non-bonded and bonded urethane is a good indicator of the hard and soft segments separation. The extent of reaction of urethane with the increased reaction between NCO groups resulted in the formation of allophanates, biurets, and isocyanurates (Ivdre *et al.*, 2020). An isocyanurate band appears at a wavelength of 1413 cm^{-1}. The absorption band at 2923 cm^{-1} to 2927 cm^{-1} and 2859 cm^{-1} to 2869 cm^{-1} are attributed to stretching vibration of polyol soft segment (Norhayati *et al.*, 2018).

Mechanical properties of VE-PU foams. The effect of varying the NCO indices from 65%, 70% and 80% on the mechanical properties of palm olein-based VE-PU foams containing only 25% of E-135 NOP were further discussed and illustrated in *Figure 3* and *Table 2*. It was observed that the density of palm olein-based VE-PU with 25% E-135 NOP foams was in the range of 52 kg m^{-3} to 58 kg m^{-3} (*Figure 3*). However, the density of palm olein-based VE-PU foam prepared using NCO index of 70% was slightly reduced because of the combined effects of mixture mobility and additional blowing agent (other than physical blowing). These phenomena were likely promoted by increased production of CO_2 from the condensation reaction between NCO groups and water (Sung and Byung 2008). The highest hysteresis was observed at palm olein-based VE-PU foams with 25% E-135 NOP using isocyanate of 80%. This could be due to increased NCO content in the formulation indeed increased the crosslinking

density because the formulation gets closer to the stoichiometric ratio (Chognan *et al.*, 2013). In addition, a high index value provides cell walls with great elasticity by allophanate crosslinks, and the walls are less vulnerable to deformation (Sung and Byung, 2008).

Effect of NCO index at 65%, 70% and 80% on other mechanical properties of palm olein-based VE-PU foam was tabulated in *Table 2*. PU foam with a higher NCO index had high hysteresis, thus, has a greater ability to absorb and dissipate energy as reflected by the increase in the resiliency of the VE-PU foam from 2.0 ± 0.7% to 7.1 ± 0.6%. Resiliency is an indicator of the surface elasticity or 'springiness' of foams. It can be explained in such a way that the hard segment content (contributed by –NCO group) in the VE-PU foams is associated with a higher NCO index (Prociak *et al.*, 2016). Therefore, the VE-PU foams with a higher NCO index had lower elasticity. However, in this study, even at the 80% NCO index, the VE-PU foams had resiliencies below 10%; ball rebound of less than 20%, which are typical characteristics desired for VE-PU foams (Singh *et al.*, 2003).

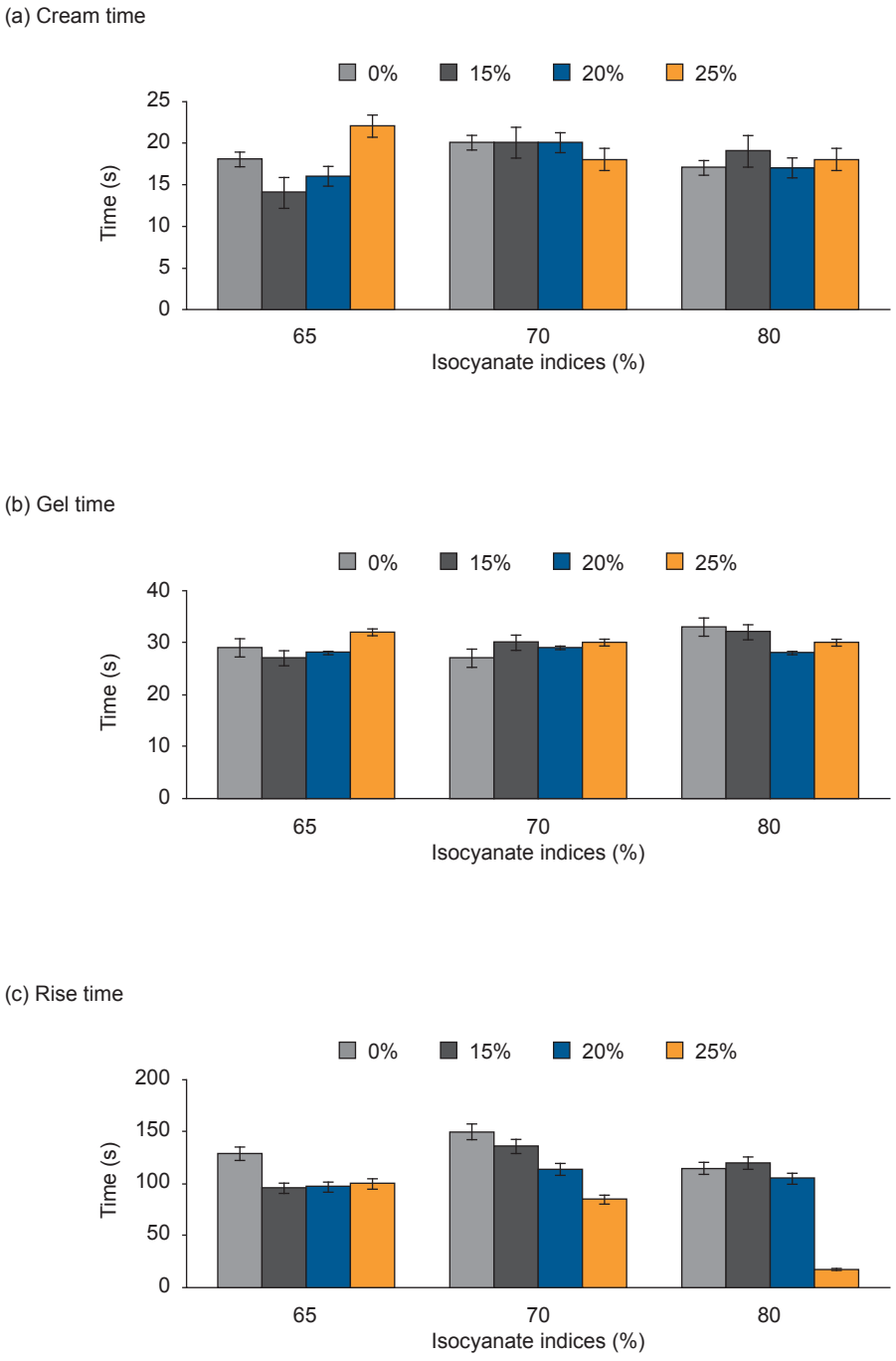


Figure 1. Reaction profiles, i.e., *(a) cream time, (b) gel time and (c) rise time of palm olein-based VE-PU foams prepared with 15% to 25% E-135 NOP at three different NCO indices.*

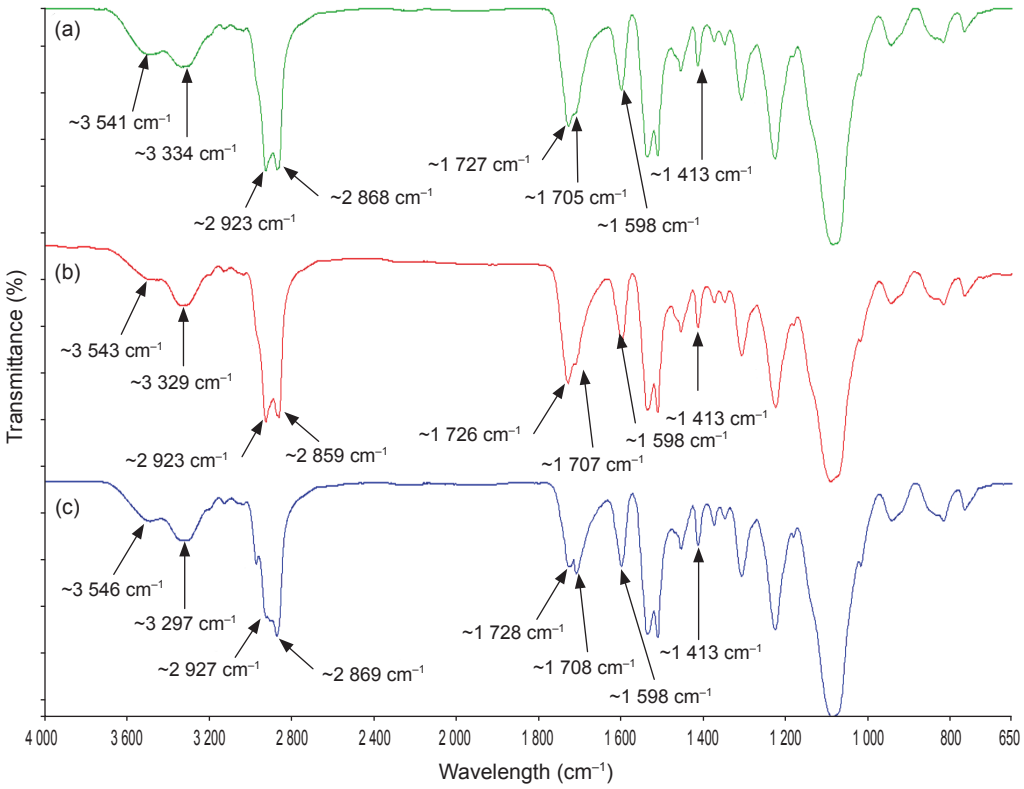


Figure 2. FTIR spectra of palm olein-based VE-PU foam with 25% E-135 NOP at three different NCO indices, i.e., *(a) NCO index at 65%, (b) NCO index at 70%, and (c) NCO index at 80%.*

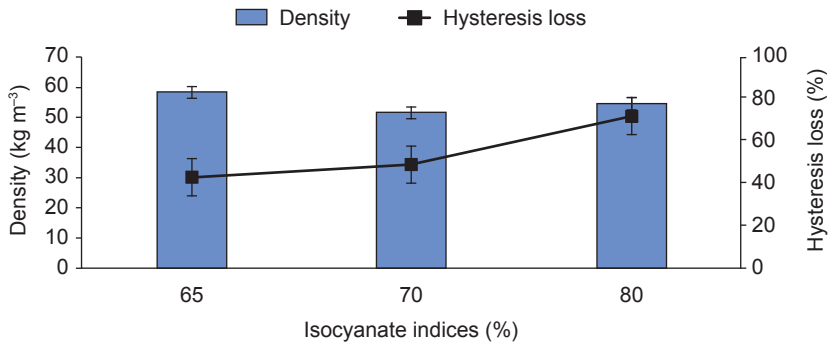


Figure 3. Effect of NCO indices on palm olein-based VE-PU foam density and hysteresis loss with 25% of E-135 NOP at three different NCO indices.

TABLE 2. MECHANICAL PROPERTIES OF VE-PU FOAMS PREPARED WITH 25% OF E-135 NOP AT THREE DIFFERENT NCO INDICES (normalised to 58 kg m^{-3})

Isocyanate indices (%)	65	70	80
Resilience (%)	2.0 ± 0.7	3.3 ± 0.7	7.1 ± 0.6
Compression force deflection (CFD) at 25% (kPa)	0.69 ± 0.09	0.76 ± 0.14	1.77 ± 0.14
Compression force deflection (CFD) at 65% (kPa)	1.59 ± 0.07	1.51 ± 0.07	4.19 ± 0.14
Tensile strength (kPa)	26.61 ± 8.12	36.40 ± 5.63	81.14 ± 7.52
Tear strength (N cm^{-1})	2.10 ± 4.20	2.75 ± 1.50	5.13 ± 3.70
Elongation at break (%)	242 ± 140	177 ± 28	95 ± 10
Support factor (CFD at 65% / CFD at 25%)	2.30 ± 0.78	1.99 ± 0.50	2.36 ± 1.00

Mechanical properties such as CFD and tensile strength values in *Table 2* were normalised to a randomly chosen density of 58 kg m^{-3} of VE-PU foam at 65% NCO index. A normalised value to the density is a must for properties that are dependent on density as it plays an important role in controlling the properties in the flexible PU foam production (Genova *et al.*, 2008). *Table 2* shows that resiliency increased with a higher NCO index, hence an increase in CFD (technically refers to 'hardness') at both deflections, *i.e.*, 25% and 65%. The increase in NCO indices of VE-PU foam has pronounced effect on the hardness of the final foam. Increasing the NCO content in the formulation indeed increased the crosslinking density because the formulation gets closer to the stoichiometric ratio. There are fewer unreacted -OH groups (-OH groups are incorporated in excess to all the VE-PU foam formulations in this work (Chagnon *et al.*, 2013).

Increasing the NCO indices significantly affects the strength of palm olein-based VE-PU foams. It was observed that tensile and tear strengths proportionately increased with the increase of NCO indices from 65% to 80% (*Table 2*). Palm olein-based VE-PU foams with the highest NCO index (80%) produced the highest tensile strength (81.14 kPa) but the lowest elongation at break (95%). Based on the observation above, increasing the NCO index could increase the crosslink density and cohesive strength through the hydrogen bonding, thus, introducing restrictions in the mobility of the soft segment as reflected in lower elongation at break values.

The mechanical properties of VE-PU foams prepared with 25% of E-135 NOP at three different NCO indices in *Table 2* revealed that the support factor of VE-PU foams was highest, *i.e.*, 2.36 ± 1.00 at an isocyanate index of 80%. The SAG index reflects how well the foam envelops the body contours; the better envelopment, the lower the SAG index and *vice versa*. Furthermore, higher SAG index values reflect the foam's ability to support the body and to prevent bottoming out (Soppi *et al.*, 2015). In this study, it was observed that high hysteresis loss and high SAG index which are proportional to the percent of high energy absorption, contributed to better load bearing properties. Higher load bearing properties is desirable in flexible PU foam production (Shan *et al.*, 2013).

The effect of NCO indices on the morphological properties of VE-PU foams. *Figure 4* shows the SEM morphology of the palm olein-based VE-PU with 25% E135 NOP foam cell structure at three different isocyanate indices (65%, 70% and 80%). The VE-PU foam samples were taken randomly in the centre of the foam and parallel to the foam rise. In general, it was observed that all palm olein-based VE-PU foams prepared consisted of spherical and polyhedral shapes. The SEM images also showed voids in cell windows, indicating cell windows were ruptured during the foaming reactions in palm olein-based VE-PU foams (*Figure 4*). Nevertheless, having open cell structures and ruptured windows are desirable properties of VE-PU foams, indicating that the palm olein-based VE-PU foams are fully compressible (Prociak *et al.*, 2021; Rajan *et al.*, 2011).

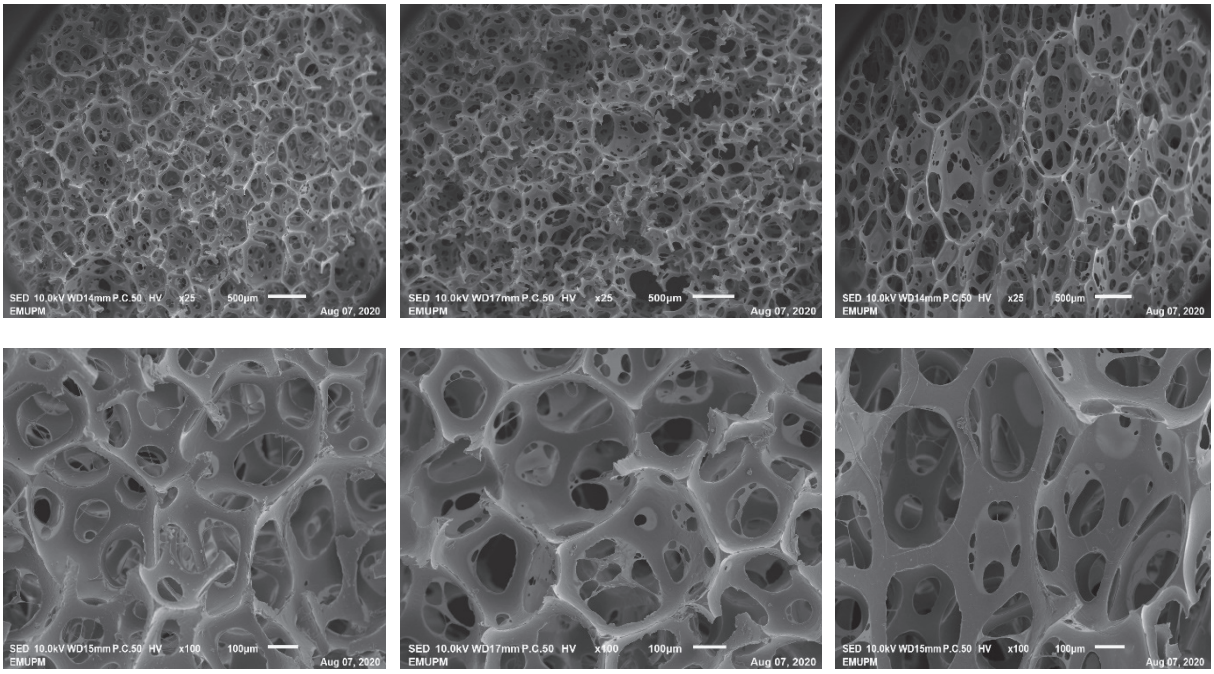


Figure 4. SEM images of palm olein-based VE-PU foam with 25% E-135 NOP at three different NCO indices. PU foams at 25x magnification top row and 100x magnification bottom row. From left to right 65%, 70% and 80% NCO indices.

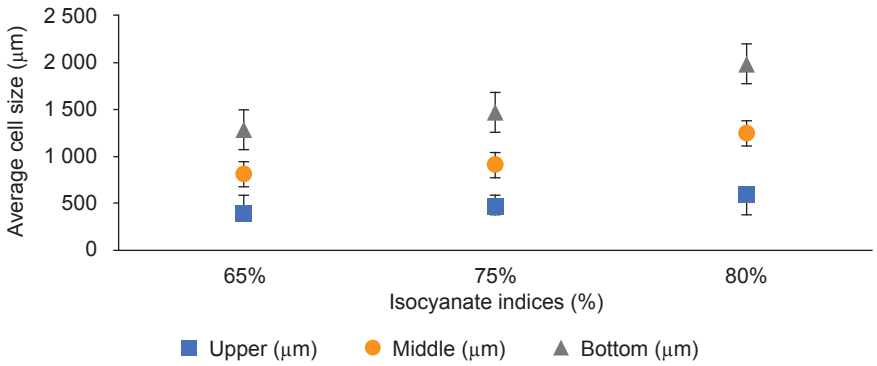


Figure 5. The average cell size of palm-based VE-PU with 25% E-135 NOP three different isocyanate indices.

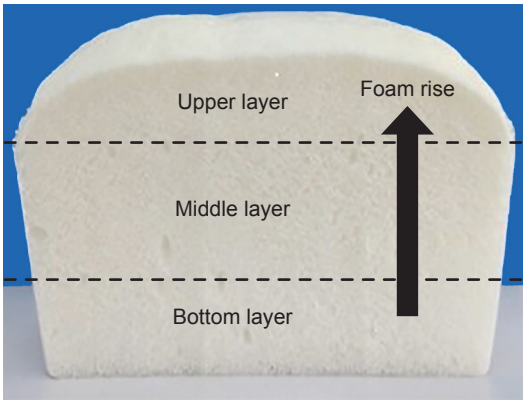


Figure 6. Photograph of a cross-section of palm olein-based VE-PU foam.

These observations were in accordance with the average cell size of palm olein-based VE-PU foam with 25% E-135 NOP at different NCO indices (*Figure 5*). The average cell size was found to increase with the NCO index increment. It was observed the average cell size of VE-PU foams increased with NCO indices from 65% (428.30 µm) to 80% (662.57 µm) at a different layer of the VE-PU foams (*Figure 6*). It is also evident from the SEM morphology of VE foams, where at a higher NCO index of 80% the cell windows of VE-PU foams are more open compared to the cell window of palm olein-based VE-PU foams prepared at NCO indices of 65% and 70%.

CONCLUSION

The effect of varying the MDI NCO indices (65%, 70% and 80%) on foaming reactivity of palm olein-based VE-PU foams containing 15% to 25% (w/w) of E-135 NOP were evaluated. This study shows that no significant changes in cream and gelling times were observed, but the rise time was slightly decreased, indicating the rate of reaction had increased as the NCO index increased up to 80%. Variation of the NCO indices affected physico-mechanical and morphological properties of palm olein-based VE-PU foams with 25% of E-135 NOP. The properties of VE-PU foams such as CFD at 65% deflection, tensile strength and average cell size increased when the NCO index increased from 65% to 80%. However, it was observed that the density and resiliency of palm olein-based VE-PU foam were slightly decreased as the NCO indices increased from 65% to 80%. Overall, it can be concluded that the NCO index of 80% gave the best mechanical properties for VE-PU foam application in comparison to other NCO indices.

ACKNOWLEDGEMENT

The authors would like to thank the Director-General of MPOB for permission to publish this article. Special thanks to Dr. Vahid Sendijarevic from Troy Polymers, Inc. (TPI), USA for his guidance in this research. The authors would also like to thank Mr. Zailan Abu Bakar and the team from Process Engineering and Design (PED) Unit for

providing polyol samples for this project, research officers and supporting staff from Polymer and Composite Group, especially Asura Abd. Rahman and Zuhairi Zainuddin at Advanced Oleochemical Technology Division (AOTD), as well as members of TPI for their invaluable contributions to this work.

REFERENCES

Chognan, L; Arnold, G; Giljean, S and Brogly, M (2013). Elastic recovery and creep properties of water borne two-component polyurethanes investigated by micro-indentation. *Prog. Org. Coat.*, *76*: 1337-1345.

Gama, N V; Ferreira, A and Barros-Timmons, A (2018). Polyurethane foams: Past, present and future. *Materials*, *11(10)*: 1841. DOI: 10.3390/ma11101841.

Genova, R D; Malsam, J; Zlatanic, A and Wazirzada, Y (2008). Bio-based polyols for the flexible slabstock foam industry. *J. Oil Palm Res. Special Issue (October 2008)*: 53-60.

Herrington, R and Hock, K (1997). *Flexible Polyurethane Foams* (Dow Plastics ed). 2nd edition. The Dow Chemical Company. p. 23.

Ionescu, M (2005). *Chemistry and Technology of Polyols for Polyurethanes*. Shawbury, England. Rapra Technol Ltd. p. 11-18.

Ivdre, A; Abolis, A; Sevastyanova, I; Kirpluks, M; Cabulis, U and Merijs-Meri, R (2020). Rigid polyurethane foams with various isocyanate indices based on polyols from rapeseed oil and waste PET. *Polymers*, *12*: 738. DOI: 10.3390/polym12040738.

Kattiyaboot, T and Thongpin, C (2016). Effect of natural oil-based polyols on the properties of flexible polyurethane foams blown by distilled water. *Energy Procedia*, *89*: 177-185.

Kim, S H; Kim, B K and Lim, H (2008). Effect of isocyanate index on the properties of rigid polyurethane foams blown by HFC. *Macromol. Res.*, *16(5)*: 467-472. DOI: 10.1007/BF03218546.

La, I; Nurdjannah; Andi, A; Zakir, S and Kamaruzzaman, J (2013). Identification of urethane linkage, soft segment polyol and hard segment polyurea in polyurethane from palm oil-based polyol. *World Appl. Sci. J.*, *26*: 50-54. DOI: 10.5829/idosi.wasj.2013.26.nrrdsi.26009.

Lee, C S; Ooi, T L, Chuah, C H and Salmiah, A (2007). Effect of isocyanate index on physical properties of flexible polyurethane foams. *Malaysian J. Sci.*, *26*: 91-98.

Liu, Y; Liu, L and Liang, Y (2020). Relationship between structure and dynamic mechanical properties of polyurethane elastomer containing bi-soft segment. *J. Appl. Polym. Sci.*, 37(45). DOI: 10.1002/app.49414.

Markets and Markets (2014). Green polyol and bio polyol market by type (polyester and polyether), application (rigid/flexible PU foam, coating, adhesive and sealant), end-user (construction, transportation, packaging, furniture and carpet) and geography - Global trends and forecasts 2018.

Mohd Zan, A; Seng, S H; Zainab, I; Hazimah, A H; Ahmad, K D and Yuen, M C (2015). Synthesis of transesterified palm olein-based polyol and rigid polyurethanes from this polyol. *J. Am. Oil Chem. Soc.*, *92(2)*: 243-255.

Norhayati, M N; Honng, S S; Tuan Noor Maznee, T I; Nurul `Ain, H; Yeong, S K and Zainab, I (2018). Performance of recycle K10 montmorillonite catalyst in the alcoholysis of epoxidised palm olein. *J. Oil Palm Res.*, *30(2)*: 326-337. DOI: 10.21894/jopr.2018.0026.

Norin Zamiah, K S; Ooi, T L and Salmiah, A (2006). Production of moulded palm-based flexible polyurethane foams. *J. Oil Palm Res.*, *18*: 198-203.

Nurul 'Ain, H; Tuan Noor Maznee, T I; Norhayati, M N; Mohd Azmil, M N; Srihanum, A; Kosheela Devi, P P; Mohd Norhisham, S; Yeong, S K; Hazimah, A H; Campara, I; Sendijarevic, V and Sendijarevic, I (2016). Natural palm olein polyol as replacement for polyether polyols in viscoelastic polyurethane foam. *J. Am. Oil Chem. Soc.*, *93(7)*: 983-993. DOI: 10.1007/s11746-016-2832-7.

Parveez, G K A; Azmil, H A T; Shamala, S; Soh, K L; Meilina, O A; Kosheela, D P P; Kamalrudin, M S; Sheilyza, M I and Zainab, I (2021). Oil palm economic performance in Malaysia and R&D progress in 2020. *J. Oil Palm Res.*, *33(2)*: 181-129. DOI: 10.21894/jopr.2021.0026.

Polyurethane Foam Association (2016). Viscoelastic (Memory) Foam. https://www.pfa.org/wp-content/uploads/2019/02/InTouch_v11.1.pdf, accessed on 15 March 2021.

Prociak, A; Malewska, E and Bak, S (2016). Influence of isocyanate index on selected properties of flexible polyurethane foams modified with various bio-components. *J. Renew. Mater.*, *4(1)*: 78-85. DOI: 10.7569/JRM.2015.634129.

Prociak, A; Malewska, E; Kurańska, M; Bąk, S and Budny, P (2018). Flexible polyurethane foams synthesized with palm oil-based bio-polyols obtained with the use of different oxirane ring opener. *Ind. Crops Prod.*, *115*: 69-77. DOI: 10.1016/j.indcrop.2018.02.008.

Prociak, A; Malewska, E; Uram, K and Wójtowicz, M (2021). Bio-polyurethane foams modified with a mixture of bio-polyols of different chemical structure. *Polymers*, *13*: 2469. DOI: 10.3390/polym13152469.

Rajan, K P; Dhilipraj, B D; Manikandan, R and Veena, N R (2011). Preparation of moulded viscoelastic polyurethane foam for pillow application. *Cell. Polym.*, *30(1)*: 13-21.

Rojek, A and Prociak, A (2012). Effect of different rapeseed oil-based polyols on mechanical properties of flexible polyurethane foams. *J. Appl. Polym. Sci.*, *125(4)*: 2936-2945.

Sendijarevic, V; Sendijarevic, I; Winslow, G R; Duranceau, C M; Simon, N L and Wheeler, C S (2005). Chemical recycling of mixed polyurethane foam stream recovered from shredder residue into polyurethane polyols. *SAE Technical Paper Series.* DOI: 10.4271/2005-01-0850.

Shan, W S; Gazali, M I and Idris, M I (2013). Improved vibration characteristics of flexible polyurethane foam via composite formation. *Int. J. Automot. Mech. Eng.*, *7*: 1031-1042. DOI: 10.15282/ijame.7.2012.19.0084.

Singh, R; Davies, P and Bajaj, K (2003). Identification of nonlinear and viscoelastic properties of flexible polyurethane foam. *Nonlinear Dynamics*, *34*: 319-346.

Soppi, E T; Lehtiö, J and Saarinen, H (2015). An overview of polyurethane foams in higher specification foam mattresses. *Ostomy Wound Manage.*, *61(2)*: 38-46.

Tereshatov, V V; Makarova, M A; Senichev, V Y; Volkova, E R; Vnutskikh, Z A and Slobodinyuk, A I (2015). The role of the soft phase in the hardening effect and the rate dependence of the ultimate physico-mechanical properties of urethane-containing segmented elastomers. *Colloid Polym. Sci.*, *293*: 153-164. DOI: 10.1007/s00396-014-3395-5.

Tuan Ismail, T N M; Mohd Noor, M A; Hoong, S S; Poo Palam, K D; Yeong, S K and Idris, Z (2018). Oligomeric composition of palm olein-based polyols: The effect of nucleophiles. *Eur. J. Lipid Sci. Technol.*, *120(4)*. DOI: 10.1002/ejlt.201700354.

Zhang, D and Chen, S (2019). The study of palm-oil-based bio-polyol on the morphology, acoustic and mechanical properties of flexible polyurethane foams. *Polym. Int.*, *69*: 257-264. DOI: 10.103/pi.5941.

Journal of Oil Palm Research Vol. 35 (2) June 2023 p. 247-255
DOI: https://doi.org/10.21894/jopr.2022.0028

EFFECT OF PALM OIL STERILISATION TECHNOLOGY ON AQUEOUS CO-PRODUCTS CHARACTERISTICS

FATAH YAH ABD. MANAF[1]*; ROHAYA MOHD HALIM[1]; ANDREW YAP KIAN CHUNG[1] and YAHAYA HAWARI[1]

ABSTRACT

With the recent development and new technologies adopted at palm oil mills, the characteristic of aqueous co-products should be updated besides exploring their potential applications. This study was conducted to characterise the aqueous co-products generated from steriliser condensate and sludge separator involving four types of sterilisers (horizontal, continuous, vertical and tilting sterilisers) and empty fruit bunch (EFB) press. The biochemical oxygen demand (BOD) and chemical oxygen demand (COD) concentrations of the overall aqueous co-product were 23 400-36 000 mg L^{-1} and 53 000-80 000 mg L^{-1}, respectively. The concentration of suspended solids (SS) and oil and grease (O&G) were 21 000-45 000 mg L^{-1} and 2800-10 200 mg L^{-1}, respectively. Total nitrogen (TN) concentration was 940-1600 mg L^{-1}, while the ammonium nitrogen (AN) concentration was 37-174 mg L^{-1}, with pH ranging from 4.5-5.8. This study indicated that all processing types yield aqueous co-products which were within the range compared to previous studies. The powder generated from the aqueous co-product contained 10.0% oil, 11.7% protein, 5.1% moisture and 13.1% ash. Other minerals such as phosphorous (P), magnesium (Mg), calcium (Ca), zinc (Zn), manganese (Mn) and potassium (K) were also present in the aqueous co-products.

Keywords: aqueous co-products, characteristics, palm oil steriliser.

Received: 28 November 2021; **Accepted:** 29 March 2022; **Published online:** 27 May 2022.

INTRODUCTION

Palm oil production consists of several stages, namely sterilisation, stripping or threshing, digestion and extraction. A large amount of water is required to extract crude palm oil (CPO) from fresh fruit bunches (FFB). Consequently, this process generates great volume of aqueous co-products, most of which are discharged into the pond as palm oil mill effluent (POME). Approximately, 0.50-0.75 t of aqueous co-products are produced for each tonnes of FFB processed (Sahad *et al.*, 2014; Som and Wahab, 2018; Yacob *et al.*, 2005). Raw POME or known as aqueous co-product is a non-toxic thick brownish acidic slurry with pH 3.4-5.2, containing about 95.0% water, 0.6% oil and 4.0% total solids including 2.0% SS (Hassan and Abd-Aziz, 2012; Mohammad *et al.*, 2021) that are mainly debris from palm fruits. Typically, aqueous co-product is accumulated from three different sources, namely steriliser condensate, clarification wastewater and hydro-cyclone wastewater (Wu *et al.*, 2010). Sterilisation is the first contributor to the accumulation of aqueous co-product stemming from steam condensation. Steriliser condensate originates from the condensation of water vapour either from steam injected into the steriliser or evaporation of moisture in FFB due to temperature differences. The condensate consists of oil, water, fibrous material and sand. In addition, the major source of aqueous co-product is from the clarification station. In the clarification process, the crude oil is separated into pure oil and sludge water.

[1] Malaysian Palm Oil Board,
6 Persiaran Institusi, Bandar Baru Bangi,
43000 Kajang, Selangor, Malaysia.

* *Corresponding author e-mail: fatahyah@mpob.gov.my*

Conventionally, the palm oil mill sterilisation process is carried out in cylindrical pressure vessels at a horizontal or vertical position as a batch process (Sivasothy, 2000). For a well-controlled conventional palm oil mill, about 0.9 m^3, 1.5 m^3 and 0.1 m^3 of steriliser condensate, clarifier sludge and hydro-cyclone wastes are generated, respectively, from each tonnes of CPO produced (Borja and Banks, 1996; Ma, 2000; Madaki and Lau, 2013). Aqueous co-products exist in the forms of high solid, oil, and grease which include biochemical oxygen demand (BOD) and chemical oxygen demand (COD) richness. These are major concerns in environmental pollutants due to their adverse effects on many forms of life (Aziz and Hanafiah, 2017; Ho *et al.*, 2021; Kamyab *et al.*, 2018; Poh *et al.*, 2020). Characteristics of aqueous co-products contain large amounts of total solids (TS) (40 500-75 000 mg L^{-1}), and oil and grease (O&G) (2000-8300 mg L^{-1}). The total nitrogen (TN) is in the range of 400-800 mg L^{-1} and suspended solids (SS) contents are in the range of 5000-54 000 mg L^{-1} (Basiron and Darus, 1995; Ma *et al.*, 1999). The most common value for BOD is 25 000 mg L^{-1} as reported by Ma (2000). The BOD and COD of raw POME can reach up to 50 000 mg L^{-1} and 100 000 mg L^{-1}, respectively.

In line with the increasing demand for palm oil, the processing system is also seen to evolve through the development of sterilisation technology. *Table 1* shows the types of sterilisers that have been used in palm oil mills in Malaysia. The most critical stage of the palm oil mill process is sterilisation. During the sterilisation process, heat penetrates into the pericarp of fruitlets and causes certain physico-chemical changes such as inactivation of lipase enzymes, thus, preventing the accumulation of free fatty acids (FFAs) within the fruits (Junaidah *et al.*, 2015; Omar *et al.*, 2018). FFAs are formed after hydrolysis of triacylglycerols in the presence of heat and water (Nanssou Kouteu *et al.*, 2016). The steam sterilisation technique efficiently removes lipase producing microorganisms from oil palm fruits, but it consumes a large amount of water consequently producing huge volumes of effluent. For every 1 t of FFB sterilised, 0.32 t of steam are required, and generates 0.27 t of aqueous co-products (Chin *et al.*, 2013). Sterilisation process also facilitates the stripping of fruits from bunches and extraction of oil and kernel. The high heat disrupts the cells in the mesocarp to release oil more readily and allows the detachment of the mesocarp from fruit nuts (Saturday *et al.*, 2017). Inefficient sterilisation in the mill contributed to oil losses and might result in secondary oxidation, leading to the discolouration of palm kernel and decreased deterioration of bleachability index (DOBI) (Wae-hayee *et al.*, 2022).

TABLE 1. TYPES OF STERILISERS USED IN MALAYSIAN PALM OIL MILL

Type of steriliser	Percentage adopted (%)
Conventional	63.5
Continuous	9.7
Vertical	13.1
Tilting	6.0
Indexer	5.5
Spherical	2.1

Source: Siti Mashani Ahmad (2020).

The conventional steriliser has evolved in recent years into continuous, vertical, tilting, indexer and spherical, with the purpose of improving palm oil production. The consumption of steam for the sterilisation process varies from 110-400 kg t^{-1} FFB, depending on the type of steriliser technology employed (Energywise, 2013), 140 kg t^{-1} FFB for a single-peak and 224 kg t^{-1} FFB for triple-peaks (Abdullah and Sulaiman, 2013). Recently, novel waterless sterilisation methods have been developed using microwave heating (Sukaribina and Khalid, 2009) or extraction with supercritical carbon dioxide (Omar *et al.*, 2018). However, some of these alternatives have a high specific energy consumption that prevents scale-up.

The benefits and advantages of various sterilisation systems are shown in *Table 2* (Parveez *et al.*, 2019). In previous years, millers have not fully discovered the useful purpose for aqueous co-products, which were often considered as waste and burden to the palm oil industry. Nevertheless, numerous attempts had been made in recent years to convert aqueous co-products into profitable value-added products. Fresh POME can be converted into potential feedstuff through fermentation (anaerobic, thermophilic and acidophilic). Previous studies demonstrated the possibility of recovering and concentrating the bio-resources available in POME using ultrafiltration to be more effectively used as fermentation media, fertilisers and animal feed (Suwandi, 1991; Wu, 2006).

With the development and new technologies adopted at palm oil mills, the characteristics of aqueous co-product need to be updated besides exploring their potential applications. Unfortunately, there is yet any study on the characteristics of aqueous co-products produced by different processing systems. Information on the physical/chemical characteristics of these aqueous co-products has not been updated since 1990. Therefore, this study aimed to characterise and analyse the aqueous co-products produced from the different types of processing systems (steriliser and EFB press). Results from the study will provide beneficial information to the palm oil industry to preserve the environment while exploring the economic potential of the aqueous co-products.

TABLE 2. THE BENEFITS AND ADVANTAGES OF VARIOUS STERILISATION SYSTEMS

Type of steriliser	Advantages
Horizontal (conventional)	Less investment cost is needed due to simple design. Lower oil losses in condensate compared to other types of sterilisers.
Vertical	High throughput due to no cages. Enable 'one way traffic' FFB handling. System which moves away completely from the conventional cages. Good sterilisation efficiency. Low maintenance cost and minimum downtime due to less moving parts. Low steam consumption and closed batch process. Facilitate automation.
Continuous	Reduce labour dependency significantly. Smaller footprint (conveyer concept) and less machinery. Oil extraction rate (OER) of mills improves significantly. Low pressure vessel for better safety. Efficient use of energy. Facilitate automation.
Tilting	High throughput due to no cages. Lower operation and maintenance costs compared to horizontal steriliser. High sterilisation efficiency due to closed and compacted chamber. Facilitate automation.

MATERIALS AND METHODS

Materials

Aqueous co-products which include a mixture of steriliser condensate, separator sludge wastewater and hydro cyclone wastewater was collected from two sampling points, steriliser condensate and clarification station (sludge separator) (*Figure 1*). Sterilisation systems consisting of horizontal, vertical, continuous and tilting sterilisers, and EFB press were examined for their effects on aqueous co-products. Ten palm oil mills were involved in this study and categorised as follows:

i) Mills A1 and A2 - horizontal steriliser
ii) Mills B1 and B2 - vertical steriliser
iii) Mills C1 and C2 - continuous steriliser
iv) Mills D1 and D2 - tilting steriliser
v) Mills E1 and E2 - EFB press

Samples were collected hourly over two days using polyethylene containers and divided into

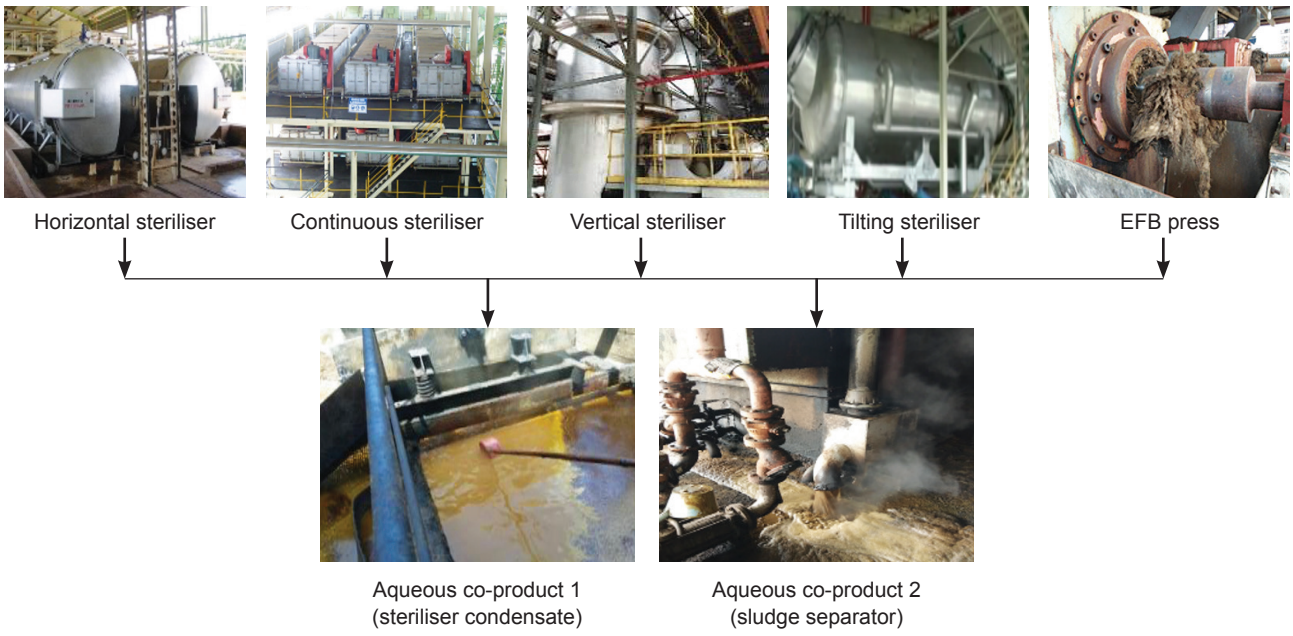


Figure 1. Samples of aqueous co-products from different processing systems.

two batches. Analysis of variance (ANOVA) was employed to study the significant differences between technology employed at the mills and aqueous co-products generated.

Determination of Aqueous Co-product Characteristics

The collected samples were analysed for BOD, COD, SS, TS, O&G, pH and AN according to Standard Methods for the Examination of Water and Waste Water, 21st Edition, American Public Health Association (APHA, 2005).

Production of Dried Aqueous Co-products

Samples of the aqueous co-products were dried using LabPlant SD-06 (OF301) laboratory spray dryer (*Figure* 2) into powder form. The dried aqueous co-products were analysed for proximate (moisture, protein, oil, ash and caloric value), nutrient content (N, P, K, Mg) and heavy metal (Mn, Ni, Zn, Fe, Cd and Cr). Oils extracted from the dry powder were then analysed for FFA, peroxide value (PV), DOBI and its fatty acid composition (FAC) using gas chromatography.



Figure 2. LabPlant SD-06 (OF301) laboratory spray dryer.

RESULTS AND DISCUSSION

Characteristics of Aqueous Co-products from Different Types of Sterilisation Systems

Steriliser condensate. *Table 3* shows the characterisation results of aqueous co-products from steriliser condensate generated from different types of processing systems. Mills A1 and A2 produced aqueous co-products with BOD concentrations of 23 425 mg L^{-1} and 24 871 mg L^{-1}, respectively. The BOD concentrations for Mills B1, B2, C1, C2, D1 and D2 were 28 696 mg L^{-1}, 25 533 mg L^{-1}, 26 212 mg L^{-1}, 25 650 mg L^{-1}, 27 900 mg L^{-1} and 26 300 mg L^{-1}, respectively. Overall, the BOD concentrations of horizontal sterilisers were slightly lower than those of new sterilisation systems. Vertical steriliser contributed to higher BOD concentrations as the FFB were immersed in the condensate during the sterilisation process. On the contrary, aqueous co-products produced by continuous steriliser had high BOD as the palm bunches were crushed prior to sterilisation, thus, leaching out oil during the process. In the case of tilting steriliser, the fruit bunches were dropped from the top of the inlet end at a substantial height to the inside of the vessel. Since most sterilisation vessels measured more than 6 m in length, the falling impact is imparted to the oil palm bunches and their fruits. However, the aqueous co-products from the tilting steriliser should have low BOD as the process was similar to the horizontal steriliser.

Statistical results showed that the BOD concentrations in the condensates of all sterilisers were significantly different ($p<0.05$) and were within the range (10 250-43 750 mg L^{-1}) as reported by Mohammad *et al.* (2021). On the other hand, the COD concentrations of steriliser condensates of all mills were high, ranging from 62 000 to 74 000 mg L^{-1}. Previous study reported that the COD concentrations of steriliser condensate could reach up to 100 000 mg L^{-1} (Ma *et al.*, 1999).

TABLE 3. CHARACTERISTICS OF STERILISER CONDENSATE AQUEOUS CO-PRODUCT FROM DIFFERENT STERILISER SYSTEMS

Types of steriliser/mills		BOD	COD	SS	O&G	TN	AN	pH
Horizontal	A1	23 425	64 300	25 640	3 282	955	40	5.36
	A2	24 871	71 200	22 950	2 818	978	37	5.41
Vertical	B1	28 696	53 000	23 320	5 127	962	85	5.79
	B2	25 533	59 900	21 580	5 683	944	119	5.57
Continuous	C1	26 212	62 200	24 040	5 127	1 270	75	5.59
	C2	25 650	73 700	23 610	3 319	1 034	70	5.63
Tilting	D1	27 900	69 200	28 480	4 492	1 149	45	4.90
	D2	26 300	72 175	26 490	5 769	1 439	93	4.64

Note: BOD - biochemical oxygen demand; COD - chemical oxygen demand; SS - suspended solids; O&G - oil and grease; TN - total nitrogen; AN - ammonium nitrogen. All parameters are in units of mg L^{-1} except pH.

The O&G contents in aqueous co-products from Mills A1 and A2 were 3282 mg L^{-1} and 2818 mg L^{-1}, respectively. In addition, the O&G contents in steriliser condensate for mills using vertical (5127 mg L^{-1} and 5683 mg L^{-1}), continuous (5127 mg L^{-1} and 3319 mg L^{-1}) and tilting (4492 mg L^{-1} and 5769 mg L^{-1}) sterilisation systems were higher compared to mills using the horizontal system. High O&G content in new steriliser systems could be due to additional pre-treatment prior to sterilisation process. On the other hand, the TN concentrations of steriliser condensate for vertical, continuous and tilting sterilisers were in the range of 900-1500 mg L^{-1}. The normal value of TN is 750 mg L^{-1} (Ahmad, 2003; Basiron and Darus, 1995; Ma and Ong, 1985). The highest TN value was found in mills using tilting system (1100-1500 mg L^{-1}). Meanwhile, AN and pH produced from all types of mills processing systems were found to be in the range of 37-120 mg L^{-1} and 4.6-5.8, respectively.

Sludge separator. *Table 4* shows the characterisation results of aqueous co-products from the sludge separator. The BOD concentrations in the aqueous co-products obtained from Mills B1 (30 217 mg L^{-1}), B2 (35 901 mg L^{-1}), C1 (30 065 mg L^{-1}), C2 (33 750 mg L^{-1}), D1 (33 800 mg L^{-1}) and D2 (34 050 mg L^{-1}) were slightly higher than conventional mills, namely Mills A1 (26 475 mg L^{-1}) and A2 (30 028 mg L^{-1}). The O&G contents were also slightly higher than that of the conventional mill. High COD concentrations ranging from 68 800-77 800 mg L^{-1} was recorded for sludge separator aqueous co-product from the clarification station of all mills.

SS is the amount of solids that can be filtered in aqueous. The SS content of aqueous co-products reported by Ma *et al.* (1999) was 18 000 mg L^{-1}, while the SS range reported by Basiron and Darus (1995) was 8000-54 000 mg L^{-1}. Residual O&G are generally trapped in the SS. Removal of SS will remove the O&G as well as some portions of insoluble matter (Ropandi *et al.*, 2010). Statistical analysis of SS data showed that there was no significant difference (p>0.05) in sludge separator aqueous co-products from all mills. In comparison to steriliser condensate, the SS values of the sludge separator were higher. TN concentrations of aqueous co-products from sludge separator for all mills showed no significant difference (p>0.05) as well. The TN values ranged from 1000 mg L^{-1} to 1600 mg L^{-1}. The pH values of sludge separator aqueous co-products for all mills ranged from 4.5 to 5.8.

The BOD concentrations in aqueous co-products contributed by all types of sterilisers both for condensate and sludge separators were in the range reported by a previous study (Mohamad *et al.*, 2021). Mills using horizontal steriliser had the lowest O&G content in steriliser condensate and sludge separator. The ANOVA showed a significant difference (p<0.05) for O&G content in mills with different steriliser technologies. Normally, palm oil mills using new steriliser systems experienced higher oil loss in steriliser condensate compared to conventional steriliser. In the conventional milling process, FFB are loaded into cages and pushed into sterilisers for sterilisation. Therefore, FFB did not experience stress and bruising before the sterilisation process. Thus, the oil loss in conventional steriliser condensate was the lowest among other types of sterilisers.

Nevertheless, the quality of oil in the condensate, such as FFA and DOBI, from new steriliser technology is still good (Parveez *et al.*, 2019). Excess O&G is extracted from the oil recovery pit using an oil skimmer.

The results showed that there were significant differences in the COD concentrations of aqueous co-products from sludge separators for all types of sterilisers. It was also found that there was a significant difference (p<0.05) in the COD, both in aqueous co-products from sterilisation condensate and sludge separator for all types of sterilisers.

TABLE 4. CHARACTERISTICS OF SLUDGE SEPARATOR AQUEOUS CO-PRODUCT FROM DIFFERENT STERILISER SYSTEMS

Types of steriliser/mills		BOD	COD	SS	O&G	TN	AN	pH
Horizontal	A1	26 475	77 800	44 980	4 901	1 542	174	4.66
	A2	30 028	77 600	23 600	3 899	1 074	55	4.70
Vertical	B1	30 217	75 400	29 920	6 468	1 230	47	5.56
	B2	35 901	69 800	29 860	6 493	1 030	144	5.53
Continuous	C1	30 065	74 400	43 140	10 177	1 256	97	5.78
	C2	33 750	68 800	32 610	8 776	1 437	65	5.82
Tilting	D1	33 800	71 900	43 200	5 648	1 537	52	4.59
	D2	34 050	77 250	40 880	7 992	1 591	134	4.56

Note: BOD - biochemical oxygen demand; COD - chemical oxygen demand; SS - suspended solids; O&G - oil and grease; TN - total nitrogen; AN - ammonium nitrogen. All parameters are in units of mg L^{-1} except pH.

Characteristics of Aqueous Co-products from Mills Using EFB Press

Table 5 shows the characteristics of aqueous co-products in steriliser condensate and sludge separator from mills using EFB press. The BOD, COD, O&G, SS, TN and AN concentrations were in the range of 26 000-31 203 mg L^{-1}, 67 750-79 800 mg L^{-1}, 3065-6607 mg L^{-1}, 24 270-40 160 mg L^{-1}, 440-1147 mg L^{-1} and 85-155 mg L^{-1}, respectively. Both Mill E1 and E2 use conventional horizontal sterilisers. Results showed that aqueous co-products from mills using EFB press had higher concentrations in terms of the characters studied than that of the conventional mill.

Characteristics of Dry Aqueous Co-product Powder

Table 6 summarises the compositions of dry aqueous co-products powder. The dry powder contained 4.5% moisture and oil content in the range of 11.0%-13.0%. There are more than 59 million tonnes of aqueous co-products produced annually in Malaysia which can be converted into 2.5 million tonnes of powder. Assuming that the dry powder has 10.0% oil content and the oil can be extracted, nearly 0.3 million tonnes of oil can be recovered based on 5.0% solid in aqueous co-products.

Figure 3 depicts the composition of the aqueous co-product powder and the oil extracted from them. The quality of the oil extracted from the dry powder

TABLE 5. CHARACTERISTICS OF AQUEOUS CO-PRODUCTS FROM MILL USING EFB PRESS

Analysis	Steriliser condensate		Sludge separator	
	Mill E1	Mill E2	Mill E1	Mill E2
BOD	28 751	26 009	31 203	29 355
COD	67 750	68 000	78 700	79 800
SS	24 270	27 480	34 290	40 160
O&G	3 065	3 115	6 607	5 948
TN	1 061	440	1 147	958
AN	85	123	85	155
pH	5.51	5.63	5.33	5.57

Note: BOD - biochemical oxygen demand; COD - chemical oxygen demand; SS - suspended solids; O&G - oil and grease; TN - total nitrogen; AN - ammonium nitrogen. All parameters are in units of mg L^{-1} except pH.

TABLE 6. COMPOSITION OF DRY AQUEOUS CO-PRODUCT POWDER

Element	Composition (%w/w)
Moisture	5.10
Ash	13.10
Protein	11.70
Oil	13.00
Nitrogen (N)	1.650
Phosphorus (P_2O_5)	0.520
Potassium oxide (K_2O)	3.150
Magnesium oxide (MgO)	1.070
Calcium oxide (CaO)	1.230
Manganese (Mn)	0.010
Copper (Cu)	0.010
Zinc (Zn)	0.010
Molybdenum (Mo)	0.002
Selenium (Se)	0.003
Calorific value (kg kg^{-1})	17 700

was not as good as CPO, with high FFA (15.56%) and PV (59.00 mEq kg^{-1}) content and very low DOBI (0.13) and carotene content (30.87 ppm). The oil extracted from the aqueous co-product can be used as an energy source in animal feed.

Figure 4 shows the FAC in the oil extracted from the dry aqueous co-product powder. Results showed that the FAC were similar to that of CPO. Palmitic acid (C:16) and stearic acid (C:8:1) in the oil extracted from the aqueous co-product powder were 44.4% and 40.4%, respectively. Meanwhile, the total protein content of the aqueous co-product powder was in the range of 10.0%-12.0%. Protein can be isolated from the powder to be used as animal feed. Further studies can be performed to seek a more cost-effective method of isolating protein from the aqueous co-product powder. In addition, the calorific value of the powdered aqueous co-product was about 17 742 kg kg^{-1}, indicating an interesting potential as animal feed. According to Wu *et al.* (2009), fresh POME as dietary substitute for aquaculture organisms has become increasingly important.

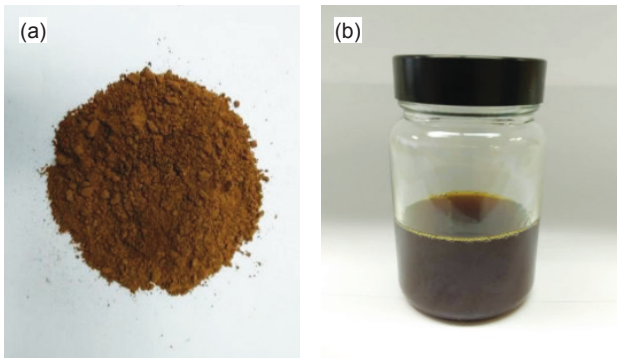
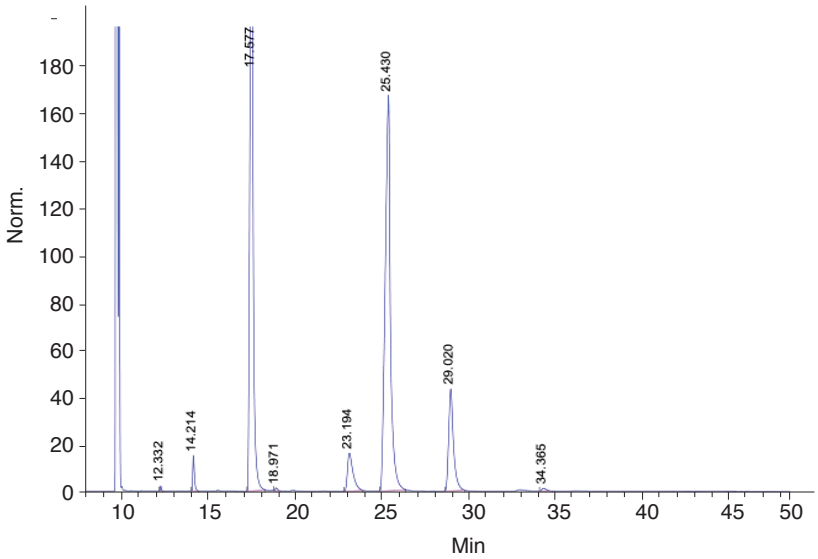


Figure 3. (a) Aqueous co-product powder, (b) oil extracted from aqueous co-product powder.

Apart from organic composition, the aqueous co-product powder was also rich in minerals, containing an appreciable amount of N (1.85%), P (0.62%), K (3.55%) and Mg (1.17%), which are vital elements for plant growth. The potential use of aqueous co-products as inexpensive organic fertilisers may offer an alternative to the excessive application of chemical fertilisers (Wu *et al.*, 2009). Due to its non-toxic nature and fertilising properties, aqueous co-product powder can be used as fertiliser or animal feed to provide sufficient mineral requirements.

Aqueous co-products of condensate steriliser and clarification station wastewater contained highly degradable organic matter which can be converted into value-added products and chemicals. The aqueous co-products are non-toxic and considered a good source of organic nutrients that can be utilised as renewable energy sources. Previous studies have pointed out the possibility of recovering and concentrating the available bio-resources in raw POME by ultrafiltration to reuse concentrated bio-resources more effectively as fermentation media, fertilisers and animal feeds (Suwandi, 1991; Wu, 2006). According to Habib (1997) and Hwang *et al.* (1978), the possibility of reusing raw POME as fermentation media is largely due to the high concentration of carbohydrate, protein, nitrogen compounds, lipids and minerals contained therein. Wu *et al.* (2009) found that raw POME can be used as a dietary substitute for pigs, poultry and small ruminants, as well as aquaculture organisms. Minerals present in raw POME, such as Fe, Zn, P, Mg, Ca and K, are also suitable for microalgae growth. This is supported by previous studies which reported that the nutrients contained in aqueous co-products (fresh POME) are N, P, K, Mg and Ca (Habib, 1997; Muhrizal *et al.*, 2006).



#	Time	Area%	FA
1	12.332	0.1	C 12:0
2	14.214	1.1	C 14:0
3	17.577	44.4	C 16:0
4	18.971	0.1	C 16:1
5	23.194	4.1	C 18:0
6	25.430	40.4	C 18:1
7	29.020	9.5	C 18:2
8	34.365	0.3	C 18:3

Figure 4. Fatty acid (FA) compositions of oil extracted from dry aqueous co-product powder.

CONCLUSION

The characteristics of aqueous co-product may vary considerably between batches, days and mills, depending on the processing techniques and the age or type of fruits as well as the discharge limit of the mill, climate and conditions of palm oil processing. Analysis results of aqueous co-products indicated that mills using horizontal (conventional) steriliser recorded lower BOD and O&G compared to mills using new technologies. The new system designs induced high oil losses via steriliser condensate and sludge separator. Analysis of variance showed that mills with different steriliser technologies had significant differences (p<0.05) in producing aqueous co-products depending on various factors, such as harvesting season and efficiency of palm oil extraction process and technology. Aqueous co-products should be considered as a valuable resource, and their recovery for other applications is a preferred alternative to conserve the environment than to current practice of treatment and disposal.

ACKNOWLEDGEMENT

The researchers would like to thank the Director-General specifically and the management of MPOB generally for the support in conducting this research.

REFERENCES

Abdullah, N and Sulaiman, F (2013). The oil palm wastes in Malaysia. *Biomass Now - Sustainable Growth and Use* (Matovic, M D ed.). www.intechopen.com/chapters/44387.

Ahmad, A L (2003). Water recycling from palm oil mill effluent (POME) using membrane technology. *Desalination, 157*: 87-95.

APHA (2005). Standard Methods for the Examination of Water and Wastewater. 21st edition. American Public Health Association/American Water Works Association/Water Environment Federation. Washington, USA.

Aziz, N and Hanafiah, M M (2017). The potential of palm oil mill effluent (POME) as a renewable energy source. *Acta Scientific Malaysia 1(2)*: 9-11.

Basiron, Y and Darus, A (1995). The oil palm industry-from pollution to zero waste. *The Planter, 72*: 141-165.

Borja, R and Banks, C J (1994). Anaerobic digestion of palm oil mill effluent using an up-flow anaerobic sludge blanket reactor. *Biomass Bioenergy, 6*: 381-389.

Chin, M J; Poh, P E; Tey, B T; Chan, E S and Chin, K L (2013). Biogas from palm oil mill effluent (POME): Opportunities and challenges from Malaysia's perspective. *Renew. Sust. Energ. Rev., 26*: 717-726.

Energywise (2013). Selection of steriliser technology for energy efficient operation of palm oil mills. http://rank.com.my/energywise/?p=310#sthash.zKX8vOvB.UvErIU6o.dpbs, accessed on 12 September 2021.

Habib, M A B (1997). Nutritional values of chironomid larvae grown in palm oil mill effluent and algal culture. *Aquaculture, 158*: 95-105.

Hassan, M A and Abd-Aziz, S (2012). Waste and environmental management in the Malaysian palm oil industry. *Palm Oil - Production, Processing, Characterization and Uses*. DOI: 10.1016/C2015-0-0241.

Ho, K C; Teoh Y X; Teow, Y H and Mohammad, A W (2021). Life cycle assessment (LCA) of electrically-enhanced POME filtration: Environmental impacts of conductive-membrane formulation and process operating parameters. *J. Environ. Manage., 277*: 111434. DOI: 10.1016/j.jenvman.2020.111434.

Hwang, S M; Ong, C C and Seow, H K (1978). Chemical composition of palm oil mill effluents. *Planter, 54*: 749-756.

Junaidah, M J; Norizzah, A R; Zaliha, O and Mohamad, S (2015). Optimisation of sterilisation process for oil palm fresh fruit bunch at different ripeness. *Int. Food Res. J., 1*: 275-282.

Kamyab, H; Chelliapan, S; Md Din, M F; Rezania, S; Khademi, T and Nadda, A (2018). Palm oil mill effluent as an environmental pollutant. *IntechOpen*. London, UK. p. 13-28.

Ma, A N and Ong, A S H (1985). Pollution control in palm oil mills in Malaysia. *J. Amer. Oil Chem. Soc., 62*: 261-266.

Ma, A N; Cheah, S C and Salmiah, A (1999). A status report of research on the treatment of POME. *PORIM Report*.

Ma, A N (2000). Environmental management for the oil palm industry. *Palm Oil Developments, 30*: 1-10.

Madaki, Y S and Lau, S (2013). Palm oil mill effluent (POME) from Malaysia palm oil mills: Waste or resource. *Int. J. Sci. Environ. Technol., 6*: 1138-1155.

Mohammad, S; Baidurah, S; Kobayashi, T; Ismail, N and Leh, C P (2021). Palm oil mill effluent treatment processes - A review. *Processes, 9(5)*: 739. DOI: 10.3390/pr9050739.

Muhrizal, S; Shamshuddin, J; Fauziah, I and Husni, M A H (2006). Changes in iron-poor acid sulfate soil upon submergence. *Geoderma, 131*: 110-122.

Nanssou Kouteu, P A; Baréa, B; Barouh, N E; Blin, J and Villeneuv, P (2016). Lipase activity of tropical oilseed plants for ethyl biodiesel synthesis and their typo-and regioselectivity. *J. Agric. Food Chem., 46*: 8838-8847.

Omar, A K; Tengku Norsalwani, T L; Asmah, M S; Badrulhisham, Z Y; Easa, A M; Omar, F M; Hossain, Md S; Zuknik, M H and Nik Norulaini, N A (2018). Implementation of the supercritical carbon dioxide technology in oil palm fresh fruits bunch sterilisation: A review. *J. CO_2 Utilization, 25*: 205-215.

Parveez, G K A; Azmil Haizam, A T; Hasliyanti, A and Kushairi, A (2019). Palm oil sterilisation technologies and their implication on oil loss, quality and food safety. *International Planters Conference*. Royale Chulan, Kuala Lumpur. p. 96-108.

Poh, P E; Wu, T Y; Lam, W H; Poon, W C and Lim, C S (2020). Waste management in the palm oil industry: Plantation and milling processes. *Springer Nature, 1*: 5-20.

Sivasothy, K (2000). Palm oil milling technology. *Adv. Palm Oil Res., 1*: 745-775.

Ropandi, M; Astimar, A A and Rohaya, M H (2010). Waste minimization from palm oil mills: A case study. *Palm Oil Engineering Bulletin, 122*. http://palmoilis.mpob.gov.my/publications/POEB/poeb122-ropandi.pdf.

Sahad, N; Som, A M; Baharuddin, A S; Mokhtar, N; Busu, Z and Sulaiman, A (2014). Physicochemical characterization of oil palm decanter cake (OPDC) for residual oil recovery. *BioResource, 4*: 6361-6372.

Saturday, A; Peter, O O; Ojo, O I; Odomagah, E S and Amos, A O (2017). Design and development of a continues palm nuts digesting machine. *Spec. J. Eng. Appl. Sci., 3*: 1-19.

Siti Mashani Ahmad (2020). Unpublished data. Economy Techno Research Unit, Economy and Industrial Development Division, MPOB, Wisma Sawit.

Som, A M and Wahab, A F A (2018). Performance study of dragon fruit foliage as a plant-based coagulant for treatment of palm oil mill effluent from three-phase decanters. *BioResources, 13*: 4290-4300.

Sukaribin, N and Khalid, K (2009). Effectiveness of sterilisation of oil palm bunch using microwave technology. *Ind. Crops Prod., 30*: 179-183.

Suwandi, M S (1991). POME, from waste to antibiotic and bio insecticide. *Jurutera Kimia Malaysia, 1*: 79-99.

Wae-hayee, M; Pakdeechot, S; Hanifarianty, S and Suksuwan, W (2022). Minimizing water consumption in oil palm sterilisation using direct steaming: Effects of sterilisation pressure and time. *J. Food Eng*. DOI: 10.1016/j.jfoodeng.2021.110804.

Wu, T Y (2006). Treatment of palm oil mill effluent (POME) using ultrafiltration membrane and sustainable reuse of recovered products as fermentation substrate. *4th Seminar on Water Management (JSPSVCC)*. Johor, Malaysia. p. 128-135.

Wu, T Y; Mohammad, A W; Jahim, J M and Anuar, N (2009). A holistic approach to managing palm oil mill effluent (POME): Biotechnological advances in the sustainable reuse of POME. *Biotechnol. Adv., 27*: 40-52.

Wu, T Y; Mohammad, A W; Jahim, J M and Anuar, N (2010). Pollution control technologies for the treatment of palm oil mill effluent (POME) through end-of-pipe processes. *J. Environ. Manag., 91*: 1467-1490.

Yacob, S; Hassan, M A; Shirai, Y; Wakisaka, M and Subash, S (2005). Baseline study of methane emission from open digesting tanks of palm oil mill effluent treatment. *Chemosphere, 59*: 1575-1581.

Journal of Oil Palm Research Vol. 35 (2) June 2023 p. 256-267
DOI: https://doi.org/10.21894/jopr.2022.0024

EFFECT OF STORAGE TEMPERATURE AND DURATION ON RHEOLOGICAL AND THERMAL CHARACTERISTICS OF SUPEROLEIN OLEOGELS

MEI HUEY SAW[1, 2]; WEN HUEI LIM[1]; CHEE BENG YEOH[1] and CHIN PING TAN[2]*

ABSTRACT

The study was conducted to investigate the effects of storage temperature and duration on the rheological and thermal characteristics of superolein oleogels derived from 3% w/w of polyglycerol behenic acid ester (PBA), 3% w/w of sunflower wax (SFW) and 8% w/w of fully hydrogenated palm-based monoacylglycerols (MGHO). The results indicated that the storage modulus (G'), loss modulus (G") and critical stress values were much higher for all the oleogels when stored at 5°C. At 15°C, the rheological parameters for SFW and MGHO oleogels were gradually increased during storage. From the thermal analysis, the peak intensity at approximately 20°C also gradually increased during storage, demonstrating the marked increase in the rheological parameters were due to the crystallisation of the triacylglycerol (TAG) in the superolein during the three-day storage. This effect was not observed for PBA oleogels, showing that the PBA inhibited or delayed crystallisation of the superolein molecules at 15°C. However, an extended storage study revealed that the PBA actually delayed and did not inhibit the crystallisation of the superolein. At 25°C, all the oleogels were highly unstable with poor thermal and rheological properties. The results suggested that 15°C was a more suitable temperature for the storage of superolein oleogels.

Keywords: monoacylglycerol, oleogels, palm superolein, polyglycerol behenic acid ester, sunflower wax.

Received: 17 August 2021; **Accepted:** 2 March 2022; **Published online:** 9 May 2022.

INTRODUCTION

Oils and fats consist of molecules known as triacylglycerols (TAG), which are made up of three fatty acids attached to a glycerol backbone. Their physical properties are mainly dependent on the chemical structure and polymorphic behaviour of the TAGs (Birker and Padley, 1987), as well as the constituent fatty acids attached to the glycerol backbone. Oils and fats are important for various edible purposes and the applications rely on their physical, rheological and polymorphism properties. For edible purposes, solid fat is desirable. Over the decades, lipid scientists attempted to modify fatty acid and TAG composition to make it more marketable as it possessed the desired properties for formulating various food applications (Gunstone, 2011). One of these popular modification processes is hydrogenation. This process is mainly used to prepare shortenings and margarine from soft vegetable oils such as sunflower oil and rapeseed oil. It causes the production of fat products with high levels of saturated content and monounsaturated fatty acids with *trans* configuration. Numerous clinical researches have suggested that intake of *trans* fatty acid decreases the serum high density lipoprotein (HDL or 'good' cholesterol) in combination with an increase in serum low density lipoprotein (LDL or 'bad' cholesterol) (Marangoni

[1] Malaysian Palm Oil Board,
6 Persiaran Institusi, Bandar Baru Bangi,
43000 Kajang, Selangor, Malaysia.

[2] Department of Food Technology,
Faculty of Food Science and Technology,
Universiti Putra Malaysia, 43400 Serdang,
Selangor, Malaysia.

* *Corresponding author e-mail: tancp@upm.edu.my*

and Garti, 2011), whereas saturated fats induce an increase in serum LDL levels that have a negative effect on cardiovascular health (Flöter *et al.*, 2021; Zetzl and Marangoni, 2011). Therefore, a new strategy for structuring edible oils is required to reduce the use of high saturated fatty acids as well as to eliminate the use of *trans* fats in fat products.

In the food industry, there have been many attempts to find alternative components that can provide the desired features of texture, structuring, stability, and taste that are normally found in animal and vegetable fats or hydrogenated oils (Marangoni and Garti, 2011). One of the alternatives – oleogel, have been recognised for their potential for use to reduce oil migration in multi component foods and to act as an alternative to butter or margarine (Marangoni and Garti, 2011). A study conducted by Hwang *et al.* (2013) investigated the making of margarine from oleogels of plant wax and soybean oil. The literature shows that making of margarine is possible using oleogels from rice bran wax and sunflower wax (SFW), whereby SFW showed the greatest firmness of margarine and higher melting points compared to the commercial margarine and spreads (Hwang *et al.*, 2013).

This non-traditional structuring technique – organogelation has become the current trend of producing solid fat products to reduce the amounts of saturated components and increase the unsaturated components used in the solid products. Most of the research on oleogel preparations involved the use of soft vegetable oils such as sunflower oil, soybean oil, safflower oil, olive oil, canola oil and rice bran oil (Doan *et al.*, 2015; Jang *et al.*, 2015; Öğütcü and Yilmaz, 2014; Toro-Vazquez *et al.*, 2007). There are limited literatures that evaluated the use of palm-based products such as palm olein, superolein or top olein for the preparation of oleogels. According to Co and Marangoni (2012), organogel formation is highly dependent on the type of solvent/ liquid oil that is gelled. Unlike many other vegetable oils, palm superolein contains more saturated components such as POP, this high melting component may also involve the oleogelation and strengthen the oleogels. Therefore, it would be interesting to study the use of palm liquid oils in the formation of oleogels.

The objective of this research work is to investigate the possibility of using palm superolein for the preparation of oleogels using different types of organogelators and the effect of superolein on oleogel formation. In this study, a food-grade polyglycerol ester comprises a mixture of long chain acid esters such as stearic and behenic acid; a food-grade SFW and a palm-based fully hydrogenated monoacylglycerol were chosen for the preparation of superolein oleogels. The stability, physical and rheological characteristics of the oleogels were studied at three temperatures of 5°C, 15°C and 25°C for three days. The effect of temperatures and preparation duration on the oleogel characteristics were discussed.

MATERIALS AND METHODS

Materials

Refined, bleached and deodourised superolein of IV 64 and soybean oil were obtained from PGEO Sdn. Bhd. (Johor, Malaysia). The gelator – polyglycerol behenic acid ester (PBA) was obtained from Sakamoto Yakuhin Kogyo Co., Ltd. (Osaka, Japan), food grade SFW was obtained from Shri Balaji Driers (Karnataka, India), with a melting point of 77°C. Fully hydrogenated palm-based monoacylglycerol (MGHO), was obtained from a local manufacturer in Klang Valley, Malaysia.

Acylglycerol Composition

Acylglycerol composition analysis of palm superolein was performed using high-performance liquid chromatography (U-HPLC) (ACQUITY UPLC H-Class System, Waters Cop., Milford, Massachusetts, USA) according to the AOCS Official Methods Ce 5c-89 and Ce 5c-93 (AOCS, 2017a; 2017b). The instrument was equipped with a refractive index detector (Waters Cop., Milford, Massachusetts, USA) set at 35°C, and an ACQUITY UPLC® BEH C18 column (Waters Cop., Milford, Massachusetts, Column specifications: particle size of 1.7 µm, id. 2.1 mm x 150 mm length). The oil samples were solubilised in acetone to form a 5% w/v solution. About 1 µL of the solution was injected through the column which was maintained at 30°C. The mobile phase consisted of a mixture of acetone (TEDIA Company, Inc., Fairfield, Ohio, USA) and acetonitrile (Merck KGaA, Darmstadt, Germany) in a volume-to-volume ratio of 63.5:36.5 and at a fixed flow rate of 0.25 mL/min. TAG peaks were identified based on the retention times of TAG standards and from the earlier published literature (Ghazali *et al.*, 1995; Haryati *et al.*, 1998; Sulaiman *et al.*, 1997). The TAGs were quantified using the peak area normalisation method. All TAGs concentrations were normalised based on the total TAG present in the sample. Isomers of TAGs are unable to separate using this method. Analyses were carried out in duplicate.

Fatty Acid Composition

Preparations of fatty acid methyl ester (FAME) for the liquid oil and the gelators were conducted using the boron trifluoride method according to ISO 12966-2:2011 (ISO, 2011). FAME was investigated

by using 430-GC gas chromatography (Bruker, Germany). 1 µL of the sample was injected into the SGE BPX70 column with a dimension of 60 m × 0.25 µm × 0.25 µm. The instrument was fitted with a flame ionisation detector (FID). The carrier gases used were hydrogen with a ratio of 1:100 with air and a flow rate of 0.8 mL/min. Detector and injector temperature were both set at 240°C. The separation of FAME was performed under the isothermal condition with a temperature of 185°C. The standard material used for the fatty acid identification was RM6 FAME mix purchased from Supelco.

Preparation of Oleogels

Oleogel sample was prepared by adding 3% w/w of PBA gelator into 200 g of palm superolein of IV 64. The mixture was heated in an oven for an hour at 90°C for the melting of the gelator materials. The mixture was then homogenised by manually stirring using a glass rod until fully dissolved and after which the heating was extended for an additional 15 min. The oleogel mixtures were transferred to three plastic containers, each container being filled with 40 g of the oil mixture. The samples were transferred and incubated at three different temperatures (5°C, 15°C and 25°C) for three days (day 0 denoted as the day of sample preparation) to obtain the oleogels. The same preparation method was conducted using 3% w/w SFW and 8% w/w MGHO gelators. The selection of gelator dosages was based on the indication from the previous study (Saw *et al.*, 2020). The preparation was conducted in duplicate for each oleogel. The oleogels were analysed for their melting properties and rheology properties.

Rheology

The rheological analysis of the oleogel was conducted using Haake Rheostress 600 equipped with a compressor, a water circulator and a universal temperature controller, and a 35 mm parallel-plate geometry. The mixture of the appropriate gelator with palm superolein was melted and homogenised in a 90°C oven. Approximately 100 g of the mixture was placed into a polypropylene plastic container. The samples were left at room temperature for an hour before transferring into incubators set at temperatures of 5°C, 15°C and 25°C. The measurements were conducted from day 1 to day 3. The plate was pre-conditioned to the storage temperature before performing the test. All samples were handled gently to avoid structural damage during the transfer from the incubators. The sample was removed from the incubator and immediately loaded on the temperature-controlled plate geometer at the storage temperature using a stainless-steel spatula. Oscillatory stress sweep was performed at 0 to 1000 Pa with 1 mm gap and 1 Hz frequency to determine the storage modulus (G′) and loss modulus (G″) [method modified from Doan *et al.* (2017) and Patel *et al.* (2015)]. For each type of gelator dosage and palm superolein combination, two experimental replicates were performed, while measurement was done in duplicate. The G'_{LVR} and G''_{LVR} values were determined from the G'_{LVR} and G''_{LVR} curves in the linear viscoelastic region (LVR). It is the constant value obtained from the curves at the LVR. The critical stress value was determined from the G'_{LVR}. It is the point at which the G′ curve starts to deviate. After running the oscillatory sweep experiments at the storage temperature, the most suitable strain amplitude was selected and used for the frequency sweep experiments. The frequency sweep experiments were measured between 1 to 100 Hz and the G′ and G″ were obtained. The data for the analysis was collected using RheoWin software. The jobs required for analysis were selected using Job Manager.

Thermal Properties by Differential Scanning Calorimetry (DSC)

The thermal properties of the gelators in the bulk stage were measured using a Perkin-Elmer DSC (DSC 8000) equipped with an autosampler. The instrument was calibrated using indium by a temperature ramp of 120°C to 180°C at a rate of 5°C/min. Volatile sample pans made of aluminium were used. The sample weights used were from 5-10 mg with an empty sample pan as the reference. The sample was heated from 15°C to 120°C at a heating rate of 10°C/min to determine the melting properties of the gelator. The sample was held at 120°C for 5 min to destroy the entire crystal structure. The sample was then cooled to 0°C at a cooling rate of 10°C/min for the recording of the cooling thermogram. For determination of the melting properties of the oleogels, 5-10 mg of molten oleogels samples were weighed in volatile aluminium sample pans. The sample was then kept in incubators with storage temperatures (T_s) set at 5°C, 15°C and 25°C and stored for 1-3 days for analysis. Each sample was held at T_s for 2 min. The sample was then heated from T_s to 120°C at a rate of 10°C/min. Each analysis was conducted in duplicate.

A storage extension study was conducted for PBA oleogels for verification of the inhibitory effects on the crystallisation of the superolein when stored at 15°C for 14 days. The 3% w/w PBA oleogels were prepared in the DSC sample pans and kept in a 15°C incubator. The melting properties of the oleogels during the storage (day 1 to day 14) were determined by melting the samples from 15°C to 120°C at a heating rate of 10°C/min. The enthalpy of melting for the samples was calculated using Pyris software (Perkin Elmer).

Statistical Analysis

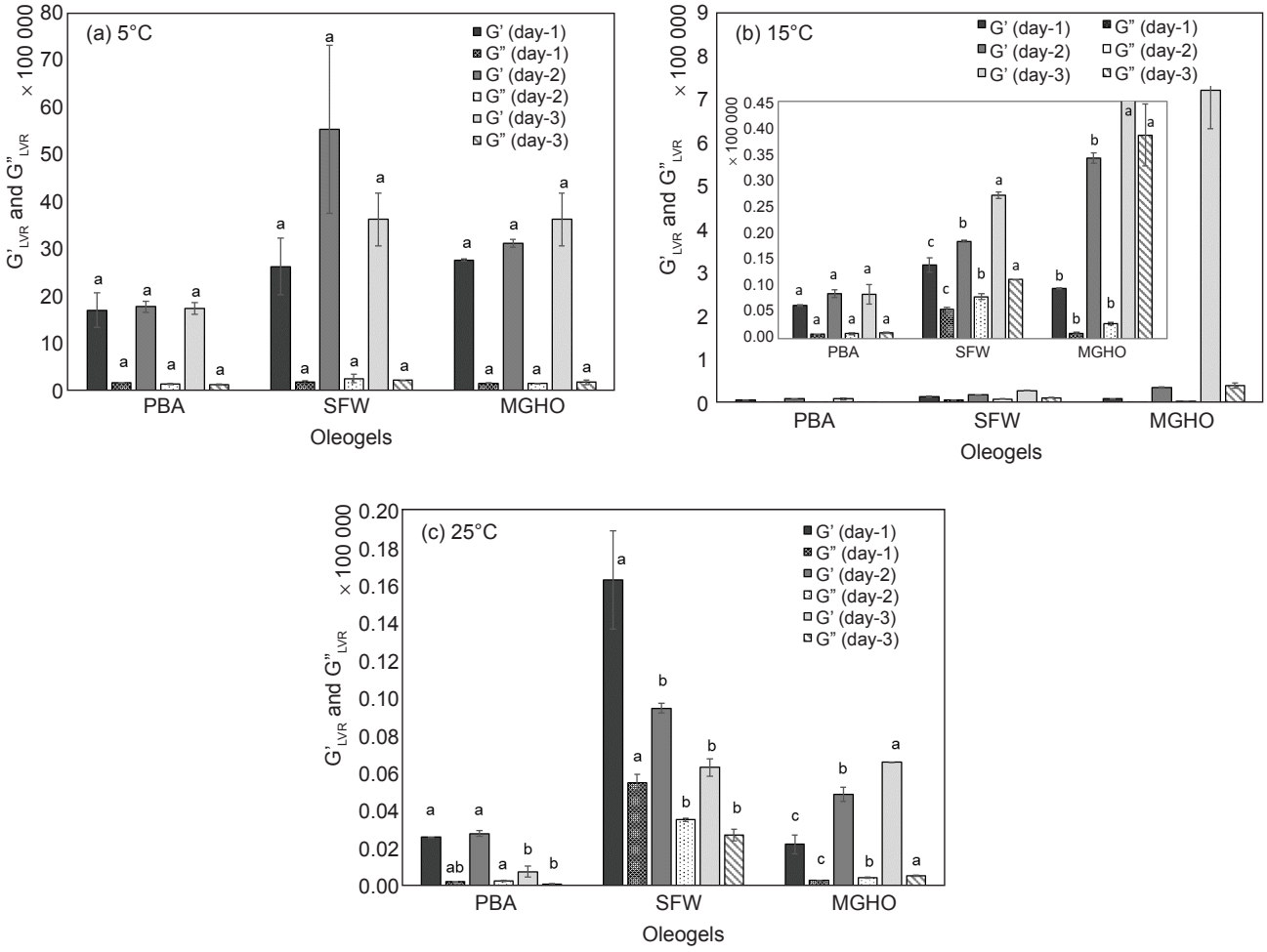
The data were analysed using the one-way analysis of variance (ANOVA) to determine the significance of the day of preparation on the enthalpy of melting and the rheological properties of the palm superolein oleogels. The software used was Minitab 16.2.

RESULTS AND DISCUSSION

Effect of Storage Conditions on Rheology of Superolein Oleogels

The effect of preparation conditions on the oscillatory rheological behaviour of the superolein oleogels was obtained via the stress sweep test at a frequency of 1.0 Hz at 5°C, 15°C and 25°C. The LVR of 3% w/w PBA, 3% w/w SFW and 8% w/w MGHO on day 1 to day 3 is shown in *Figure 1*.

The G′ indicates solid-like behaviour, whereas G″ indicates the liquid-like behaviour of the oleogel system (Doan *et al.*, 2015). The G′ values were higher than G″ for all samples, indicating that all the samples exhibited a gel-like property (Doan *et al.*, 2015; Wang *et al.*, 2019). The G'_{LVR} and G''_{LVR} values of superolein oleogels increased with lower storage temperature. This is because the superolein oil in the gel structure easily crystallised at 5°C. The high values for the rheological properties were the result of both the superolein crystallisation and the gel structure. Although a slight increase in G′ was observed in the SFW and MGHO oleogels, the changes were insignificant ($p>0.05$). The oscillatory rheological behaviour of all the oleogels was not significantly different in the first three days after preparation ($p<0.05$) (*Figure 1a*). This is because, at 5°C, the major factor that gave rise to the high values of G'_{LVR} and G''_{LVR} was the crystallisation of the superolein. In contrast, the effect of organogelation was less significant at this temperature. Only a



Note: Significance testing was conducted to assess the oleogels over time. Different letters indicate significant differences at $p<0.05$ according to the Tukey test.

Figure 1. G'_{LVR} and G''_{LVR} on day 1 and day 3 of superolein oleogels prepared with 3% w/w PBA, 3% w/w SFW and 8% w/w MGHO at (a) 5°C, (b) 15°C and (c) 25°C.

mild effect of organogelation on the rheological properties was observed, causing the PBA oleogels to have lower G'_{LVR} and G''_{LVR} values than other oleogels. This was probably due to the inhibitory effect of the PBA gelator that prevents the crystallisation of superolein molecules.

Solid fat content results from Saw *et al.* (2014) showed that palm superolein was fully melted at 20°C and a minimal solid fat was observed at 15°C, indicating that superolein could be slowly crystallised during storage at 15°C. Therefore, it was believed that superolein began to crystallise slowly into a semi-solid fat at 15°C. At this temperature, two events might have taken place simultaneously, *i.e.*, organogelation and superolein crystallisation. *Figure 1b* shows a significant increase of the G'_{LVR} and G''_{LVR} values during the three days of storage for the SFW and MGHO oleogels. This could be due to the increase of gel strength with increasing time after the preparation. The G'_{LVR} and G''_{LVR} values increased linearly in the SFW gels, from 14 000 Pa to 27 000 Pa, from day 1 to day 3.

The most obvious change observed was the dramatic increase of G′ and G″ in the MGHO oleogels, in which G′ was increased from 9500 Pa to 35 000 Pa on day 2 and further increased to 700 000 Pa on day 3 after preparation. Doan *et al.* (2015) reported that a higher G′ indicated a stronger gel. In this case, the increase of G′ and G″ was probably due to the slow crystallisation behaviour of the superolein liquid oil at 15°C. On day 1, the G′ and G″ were relatively low, indicating PBA oleogels had the lowest G′ (6000 Pa), followed by MGHO (9500 Pa) and SFW (14 000). These rheological properties were believed to be contributed by organogelation, as the superolein remained as a liquid on day 1. The organogelation is generally affected by both the type of gelator and the liquid oils, therefore each oleogels showed different trends in its rheological properties. The G′ and G″ values of the PBA oleogels in the LVR did not vary significantly during the first three days after preparation ($p>0.05$), which was similar to the observations for the 5°C storage. This again shows that the PBA gelator may inhibit the crystallisation of superolein within the gel network structure.

At 25°C, superolein appeared as a liquid, indicating the rheological property of the gels was contributed only by the microstructural development of the gelator. The G'_{LVR} of PBA oleogel was significantly reduced on day 3, indicating the occurrence of the reduction in gel strength due to the rupture of the gel structure. Therefore, the PBA oleogel was not stable at 25°C. Similar to PBA oleogels, significant reductions of G'_{LVR} and G''_{LVR} were observed for the SFW oleogels due to the decrease in gel strength. Interestingly, a significant increase of G'_{LVR} and G''_{LVR} was observed for the MGHO oleogel during the third day of storage, which indicates a possible increase of gel strength or the formation of more crystals. The increase in G'_{LVR} and G''_{LVR} could be due to the agglomeration of the MGHO crystals and the high saturation component in the superolein during prolonged storage at room temperature. Saw *et al.* (2017) and Smith *et al.* (2011) mentioned that compounds with identical acyl groups to the crystallising species can join the crystal matrix by acting at the growth site and altering the morphology of the crystals. Similar to our system, the major component in MGHO is monoacylglycerol with a fatty acid chain lengths of C16 and C18, which are very similar to the fatty acid of the superolein. Therefore, these acylglycerols could agglomerate into larger crystals during storage, thus, increasing the G'_{LVR} and G''_{LVR}.

The critical value stress was determined from the oscillatory stress sweep from LVR. It is the point at which the G′ curve starts to deviate. At stresses below critical stress value, G′ and G″ curves displayed a plateau trend due to zero-permanent deformation (Doan *et al.*, 2015). Above this critical point, the oleogels underwent irreversible or permanent deformation, causing a decrease in G′ and G″ (Doan *et al.*, 2015). According to Bot and Agterof (2006), the critical stress value tells the stability of gels during stress sweeps and the range of stress for oleogels to have linear viscoelastic behaviour during processing. The critical stress value for all oleogels is summarised in *Figure 2*.

Similar to the previous G'_{LVR} and G''_{LVR} results shown in *Figure 1*, the critical stress value was also dependent on the type of gelator, storage temperature and duration of storage. For oleogels stored at 5°C, the oleogels showed similar patterns according to the type of gelator, except for the SFW oleogel, where a slight increase in the critical stress value was observed with longer storage time. The slight increase could be caused by an increase in the gel strength during the third day of storage.

At 15°C, the critical stress values increased over the storage time for the SFW and MGHO oleogels, shown in *Figure 2b*. This finding revealed that the critical stress values were proportional to their G'_{LVR} and G''_{LVR} values. This was not the case for SFW stored at 25°C, as the reduced G'_{LVR} and G''_{LVR} values during storage did not result in the decrease in critical stress values but remained constant throughout the storage. In other words, the reduction of the G'_{LVR} and G''_{LVR} values in the SFW oleogels did not affect the stability of the gels, as deformation can only occur when stress beyond the critical stress value is applied (Bot and Agterof, 2006).

Frequency sweeps were conducted to evaluate the time-dependent deformation behaviour of the oleogels at a stress value within their LVR (Doan *et al.*, 2015). Based on the previous results, the oleogels formed at 15°C showed interesting

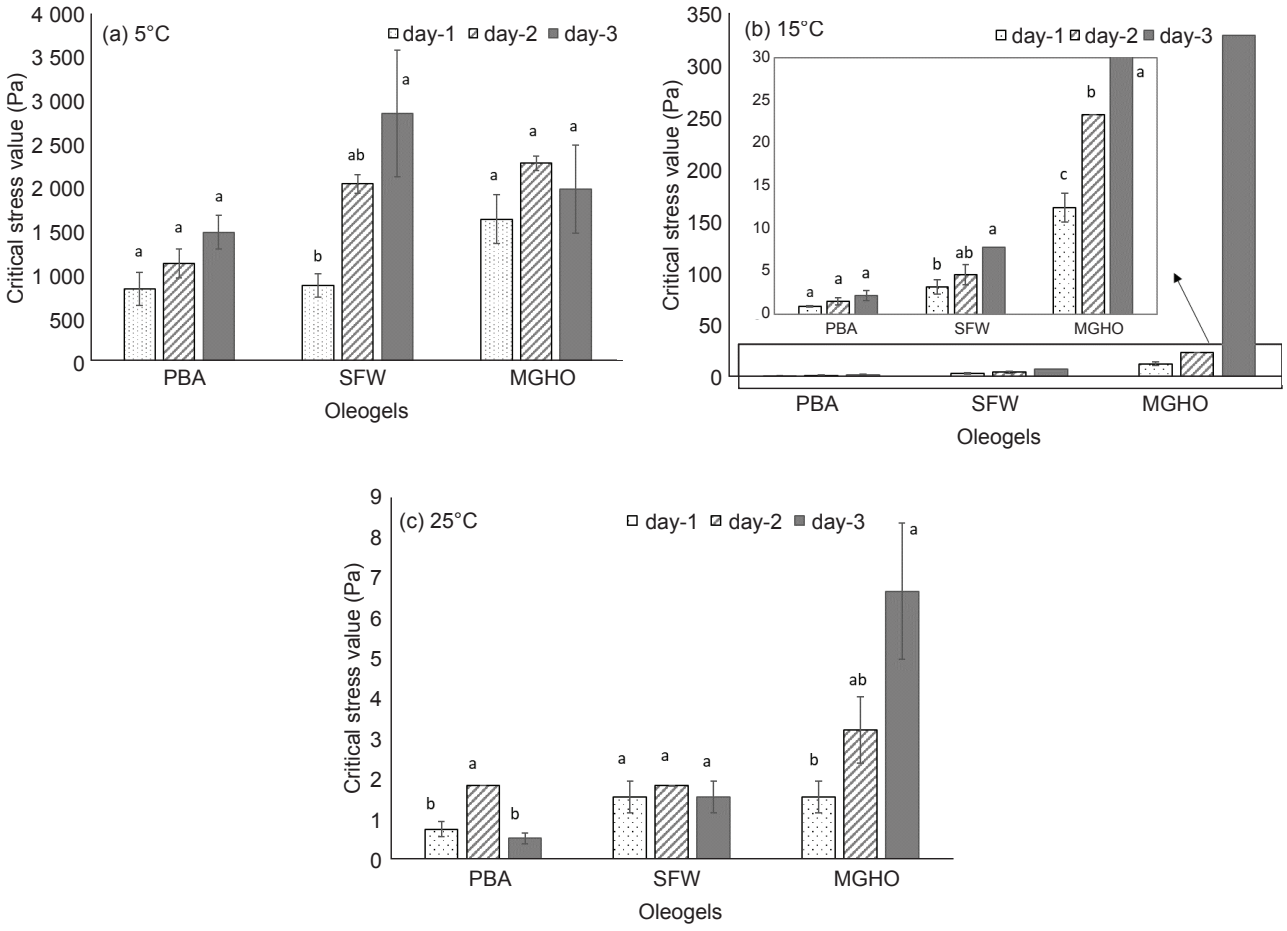
rheological behaviours in which the G'_{LVR}, G''_{LVR} and the critical stress values increased drastically with longer times after preparation; the frequency sweep curves for the oleogels are discussed below and shown in *Figure 3*.

As expected, the trend of moduli values of the G′ and G″ curves in the frequency sweeps were consistent with their G'_{LVR}, G''_{LVR} and critical stress values shown in *Figures 1* and *2*. An increase in the G′ and G″ moduli values was observed for the SFW and MGHO oleogels, and this was probably due to the slow crystallisation of superolein at 15°C. For all oleogels, the G′ and G″ curves were almost linear, with G′ being higher than G″. This indicated that the oleogels were in good tolerance with the rate of deformation within the tested time frame (Doan *et al.*, 2015). As the angular frequency increases, the PBA and SFW oleogels showed a slight upward trend in the G′ and G″ curves, indicating weak gel characteristics (Bin Sintang *et al.*, 2017; Doan *et al.*, 2015; Trappe and Weitz, 2000).

Towards the end of the test at a high angular frequency of nearly 100 Hz, an increase of G′ was observed for the SFW oleogel on day 3; this was thought to be due to the deformation in the gel structure. On the other hand, the MGHO oleogels analysed on day 1 and day 2 showed the least frequency dependence, as constant moduli values were observed during the frequency sweep, implying that MGHO formed a stronger gel compared to the others (Patel *et al.*, 2015). However, a slight increase in the gradient of elastic moduli for MGHO oleogel was observed on day 3, which indicates an increase of frequency dependency or a reduced gel strength with longer storage times.

Effect of Preparation Conditions on Melting Behaviour of Superolein Oleogels

The thermal behaviour of superolein oleogels was conducted to study the effect of storage temperature and duration on the melting



Note: Significance testing was conducted to assess the gels over time. Different letters indicate significant differences at $p<0.05$ according to the Tukey test.

Figure 2. Critical stress value on day 1 to day 3 of superolein oleogels prepared with 3% w/w PBA, 3% w/w SFW and 8% w/w MGHO at (a) 5°C, (b) 15°C and (c) 25°C.

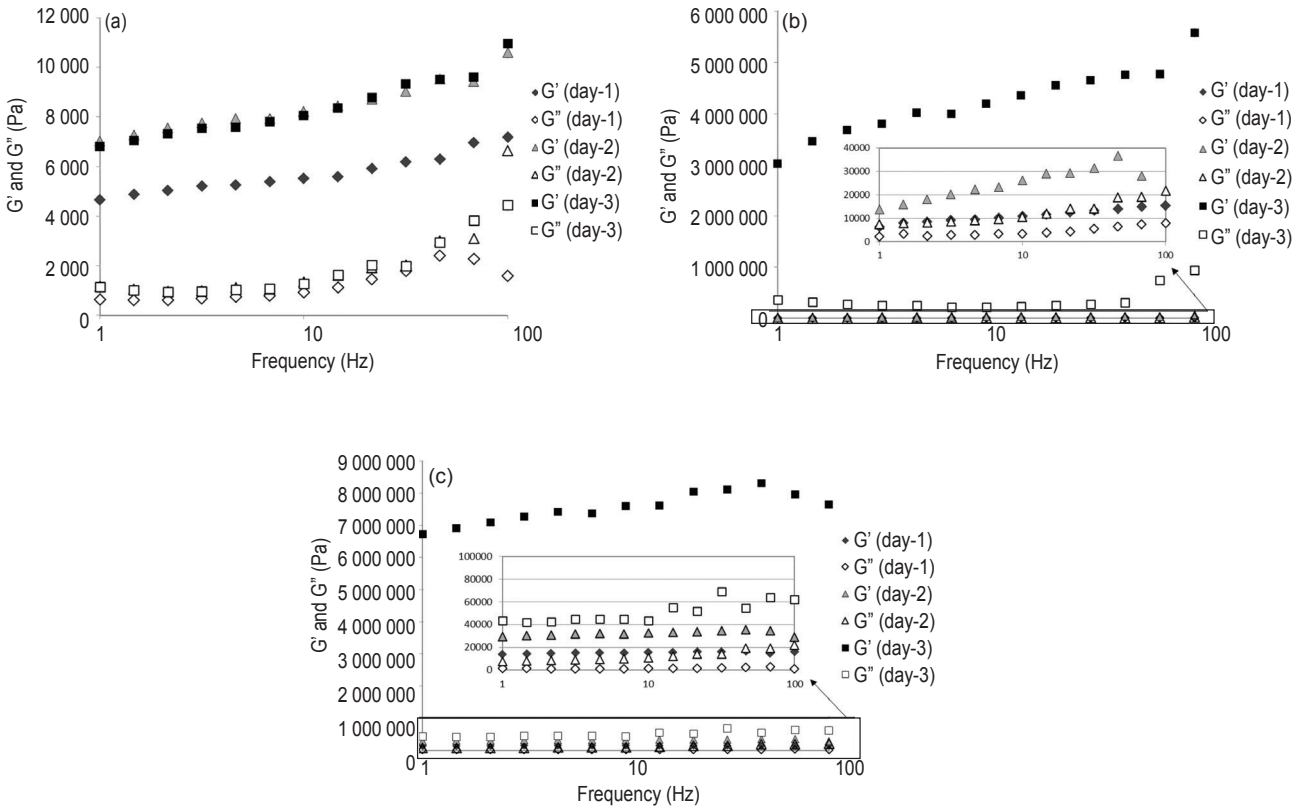


Figure 3. Frequency sweep on day 1 to day 3 of superolein oleogels prepared with (a) 3% w/w PBA, (b) 3% w/w SFW and (c) 8% w/w MGHO at 15°C.

behaviour of superolein oleogels produced with a different type of gelators. The chemical nature and molecular composition of gelators are very important to understand thermodynamic results in the oleogel systems (Blake *et al.*, 2014). *Figure 4* shows the melting profiles of superolein oleogels from PBA, SFW and MGHO melted from their respective T_s from day 1 to day 3. The results show that the short storage duration did not affect the melting properties of PBA oleogels when storing at 15°C and 25°C. Besides, an almost identical melting peak profile was observed consistently at 44°C for all PBA oleogels stored at different temperatures, representing the melting of the gel structure or the deformation of the gel structure upon application of heat *Figure 4a*. This indicates that all the gel networks present in the PBA oleogels were identical even when they were stored at different temperatures.

At 5°C storage, a sharp peak was observed at 16°C for PBA oleogels analysed on day 2 and day 3. This can be associated with the melting of palm superolein TAG that crystallised during prolonged storage at low temperatures. This sharp peak was absent on day 1, which indicates that the liquid component was not crystallised on day 1. Interestingly, the melting of liquid oil did not affect the gel structure as the sample continued to melt at the same melting profile as other PBA oleogels stored at higher temperatures.

Similar to the PBA oleogels, an endotherm with a peak at approximately 57°C was observed for all SFW oleogels. This indicates that T_s did not affect the melting of the gel structure. However, unlike the PBA oleogels, the storage duration seemed to affect the melting profiles of the SFW oleogels when stored at 5°C and 15°C. The peak intensity at 24°C increased when the gel was stored at 15°C because more crystals were formed with longer storage duration, and therefore more heat was required to melt the liquid oil crystals. This result is consistent with the rheological behaviour of the SFW oleogels, as shown in *Figure 1* and 2. The DSC thermogram proved that a drastic increase in G'_{LVR}, G''_{LVR} and critical stress values was due to the slow crystallisation of some TAG components in the superolein within the gel structure. The impact of the crystallisation of superolein was more pronounced in SFW and MGHO oleogels as both of the gel structures were formed by crystalline networking. *Table 1* shows the acylglycerol composition of the superolein used in the preparation of the oleogels

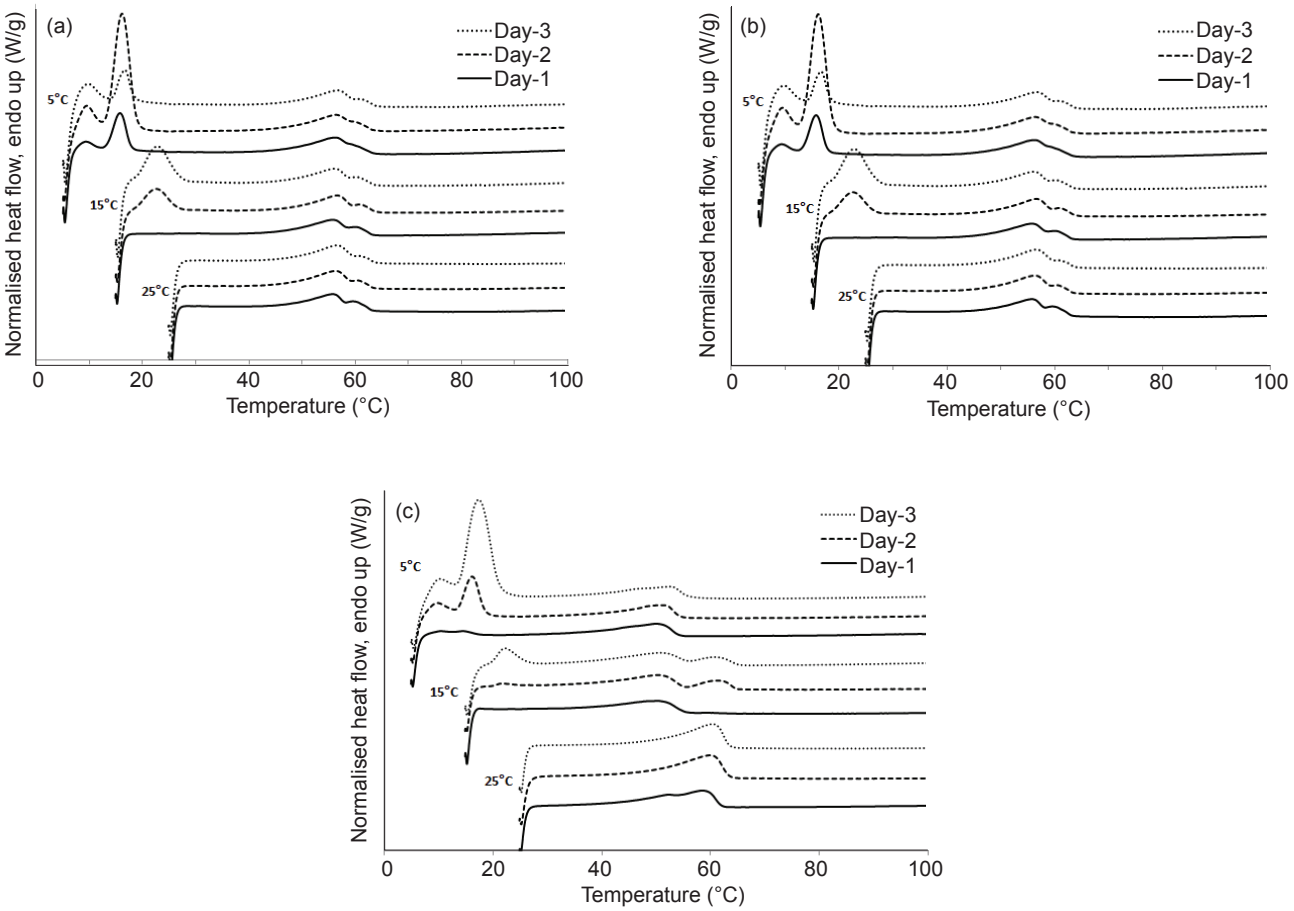


Figure 4. Melting thermograms on day 1 to day 3 of superolein oleogels prepared with (a) 3% w/w PBA (b) 3% w/w SFW and (c) 8% w/w MGHO at 5°C, 15°C and 25°C.

for this study. Superolein, which contained 19.11% of POP and 36.60% of POO, were easily crystallised at 5°C. A sharp peak at 17°C for SFW oleogels stored at 5°C was also detected due to the crystallisation of these superolein TAGs.

TABLE 1. NORMALISED TAG COMPOSITION (AREA %) OF PALM SUPEROLEIN IV 64 (POoIV64)

Triacyglcyerol	Palm superolein (area %)
OLL	0.67 ± 0.01
PLL	2.97 ± 0.05
MLP	0.57 ± 0.05
OLO	2.32 ± 0.03
PLO	12.81 ± 0.10
PLP	11.73 ± 0.01
OOO	6.38 ± 0.04
POO	36.59 ± 0.02
POP	19.11 ± 0.12
SOO	3.81 ± 0.06
POS	2.73 ± 0.06
SOS	0.31 ± 0.03

Note: O - oleic acid; L - linoleic acid; P - palmitic acid; S - stearic acid.

The peak intensity did not show an upward trend like those samples stored at 15°C because the crystals formed were highly unstable and easily melted during transferring from the incubator to perform the analysis. Unlike the other oleogels, MGHO oleogels were shown to have very different melting profiles when they are kept at different temperatures. At 25°C, only a broad endotherm with a peak of 59°C was detected on day 1. The peak intensity slightly increased and shifted to a higher temperature when stored for an additional 1 or 2 days. This could be due to the rearrangement of crystals during storage strengthening the gel network, which required additional energy to melt the oleogel. This observation was also consistent with the rheological behaviour, where a small increase in the G'_{LVR} and critical stress values was observed.

Interestingly, the melting profiles of the MGHO oleogels were very different over the third day of storage at 15°C. On day 1, only a single endothermic peak was observed at approximately 51°C. An additional peak at 62°C started to appear from day 2 onwards while another peak in the low-temperature region of 23°C was observed on day 3. These findings

indicate that rearrangement of the crystal structure could have occurred during the third day storage period. Alternatively, this change could also be due to the polymorphic transition of the MGHO crystals from β'-polymorph to a more stable β polymorph. These two possibilities were also reported by Bin Sintang *et al.* (2017), in which the sunflower oil oleogels formed with hybrid gelators of phytosterol-monoglycerides showed a significant increase in the melting temperature during isothermal storage at 5°C. Interestingly, their study showed that the single component monoglyceride oleogel produced with sunflower oil showed insignificant change in the melting point upon storage, which was different from our finding. This indicated that the change observed in our study could be due to the use of superolein. On day 1, the MGHO gelator formed an entanglement of large crystal network structures that entrapped the superolein. According to *Table 2*, the MGHO and liquid oils contained fatty acids with a similar fatty acid chain length of C16 and C18, in which the palmitic acid (C16:0) for POoIV64 and MGHO were detected at 36.7% and 40.9%, respectively. This similarity has resulted in the high solubility of the gelator in superolein affecting its gelling ability (Doan *et al.*, 2015).

TABLE 2. FATTY ACID COMPOSITION (AREA %) OF THE PALM SUPEROLEIN AND THE GELATORS

Acyglcyerol	POoIV64	MGHO	PBA
12:0	0.4 ± 0.0	0.2 ± 0.0	0.7 ± 0.0
14:0	0.9 ± 0.0	0.9 ± 0.0	0.1 ± 0.0
16:0	36.7 ± 0.1	40.9 ± 0.1	1.6 ± 0.0
16:1	0.3 ± 0.0	-	-
18:0	3.5 ± 0.0	56.8 ± 0.1	32.6 ± 0.1
18:1	45.2 ± 0.1	0.2 ± 0.0	22.8 ± 0.1
18:2	12.4 ± 0.0	0.2 ± 0.0	3.5 ± 0.1
18:3	0.3 ± 0.0	-	-
20:0	0.2 ± 0.0	0.6 ± 0.0	9.8 ± 0.0
20:1	-	-	0.1 ± 0.0
22:0	-	0.1 ± 0.0	26.8 ± 0.0
24:0	-	-	1.8 ± 0.0

Note: POoIV64 - palm superolein; MGHO - fully hydrogenated palm monoacylglycerols; PBA - polyglycerol behenic acid ester.

Storage at 15°C has caused some of the saturated components in the superolein such as POP and some diacylglycerols to have tendency to interact with the MGHO crystals, which mostly consist of C16:0 and C18:0 fatty acids. The original crystal structure was then rearranged and aggregated into larger crystals that melted at higher temperatures. This explains why the additional peak appeared in the melting curves on day 2 and day 3. On day 3, the lower melting TAGs in the superolein started to crystallise within the large crystal network. The formation of these crystals did not affect the crystalline structure that entrapped the liquid oil, as these crystals were first melted at 23°C. The gel crystalline structure was then melted from 45°C to 68°C. Such behaviour is the same as those oleogels kept for two days. This explanation can be correlated with the rheological behaviour data, in which the G'_{LVR}, G''_{LVR} and critical stress values drastically increased from day 1 to day 3 of storage, as shown in *Figure 1b* and *2b*.

Overall, the MGHO oleogels melted at the highest temperature, followed by SFW and PBA oleogels at the T_s. This could be due to the presence of the high amount of MGHO gelator used (8% w/w) in the oleogel formulation, which led to a high saturation content in the gel that rendered it the most thermally stable among the tested oleogels. Nevertheless, the melting peak for the SFW oleogels was approximately 57°C, which was much higher than that of the PBA oleogels, which melted at approximately 45°C. Therefore, these findings show that SFW oleogels have better thermal stability than PBA oleogels.

Verification of the Crystallisation Inhibitory Effect of PBA Oleogels

The DSC analysis again showed that PBA may have an inhibitory effect on the crystallisation of superolein, especially when stored at 15°C (*Figure 4a*). A storage extension for 14 days was conducted to verify this hypothesis. The DSC melting curves of PBA oleogels are shown in *Figure 5*. The melting profiles remained the same until day 8 and a very obscure broad endothermic peak was observed from day 1 to day 8. There were small but noticeable differences between the melting curves. One-way ANOVA revealed that the increase in enthalpy on day 8 was significant. However, the melting curves returned to their initial profiles between day 9 and day 12, showing that the enthalpy of melting (ΔH_m) was not significantly different from the oleogel on day 1. This indicates that the increase of ΔH_m on day 8 could be an outlier due to experimental error. As mentioned earlier, the melting curves remained stable until day 13, enabling the detection of a broad peak from 22°C to 35°C, followed by a steady melting of the sample at a peak of 44°C, as in those samples analysed from day 1 to day 12.

The curves were analysed and ΔH_m was determined and plotted in a bar chart (*Figure 6*). This analysis was able to quantify the total heat required to melt the oleogels during the 14-days storage period. The intensity of this broad peak has further increased on day 14, causing the melting profile to skew slightly to 42°C suggesting a change in the gel structure occurred on day 13. The appearance of the broad peak from 22°C to 35°C could be caused by the crystallisation of superolein, causing breakage of the gel structure.

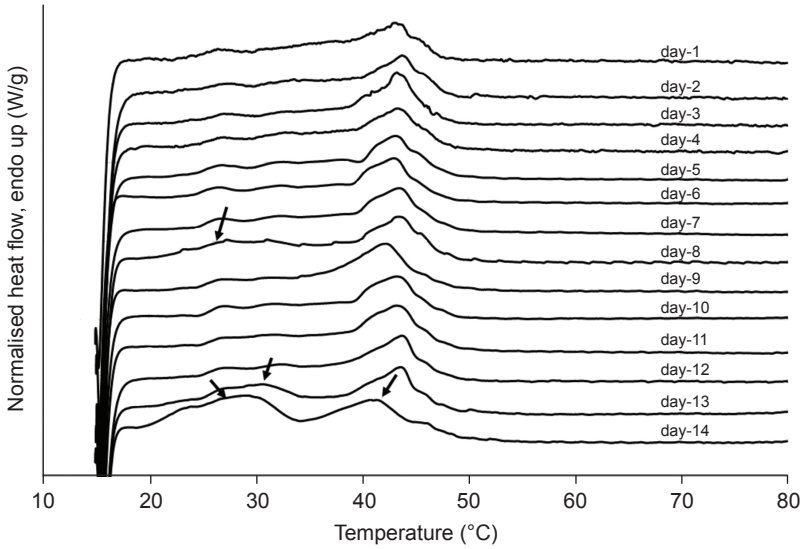


Figure 5. DSC melting curves for 3% w/w PBA superolein oleogels stored at 15°C for 14 days.

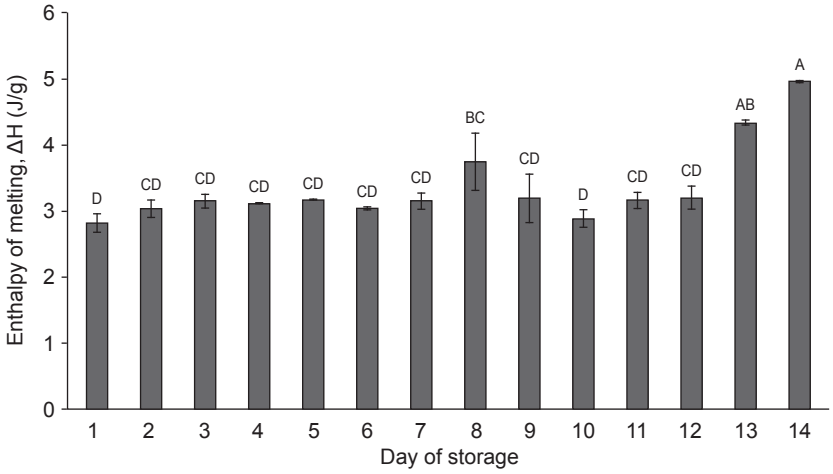


Figure 6. Enthalpy of melting for 3% w/w PBA superolein oleogels stored at 15°C for 14 days.

This observation was different from SFW and MGHO oleogels as the formation of more crystals increased the rheological properties of the SFW and MGHO oleogels. This is because the type of oleogelation in PBA oleogels was different from that of SFW and MGHO oleogels. The PBA oleogels is a self-assembly type of oleogels. Thus, the formation of more crystals did not further strengthen the gel structure but break the self-assembly structure formed by the PBA gelator. The rupture of the gel structure resulted in lower gel strength, as the peak of melting was shifted to a slightly lower temperature on day 14. This proves that PBA did not completely inhibit the crystallisation of superolein, but only caused a delay in the crystallisation process.

CONCLUSION

The investigation of the effect of storage temperature and duration revealed that both factors affect the rheological and melting properties of oleogels. In conclusion, the oleogelation of superolein oleogels happened when enough supercooling was provided. The temperature of 25°C was insufficient to supercool the oleogelators to form stable oleogels. Therefore, the produced oleogels demonstrated poor rheological and melting properties. During storage at 15°C, some high melting components in superolein showed the tendency to slowly crystallise, leading to gradually elevated rheology parameters and enthalpy of melting in SFW and MGHO oleogels. This effect

was not observed for PBA oleogels, which indicates that the PBA prevented or delayed crystallisation of the superolein molecules at 15°C. An extended storage study revealed that PBA delays rather than inhibit the crystallisation of superolein. At 5°C, high-melting components in superolein tended to crystallise and resulted in much higher G'_{LVR}, G''_{LVR} and critical stress values. As expected, the use of palm superolein in oleogels formation showed different characteristics compared to the oleogels produced from other soft vegetable oils. This is because the high melting components in the superolein may take part in the oleogelation via crystallisation at low storage temperature, which resulted in a unique characteristic of oleogels.

ACKNOWLEDGEMENT

The authors thank Mr. Kuriyama Juhei from Sakamoto Yakuhin Kogyo Co. Ltd. for sponsoring the polyglycerol behenic acid esters for this study. The authors also would like to acknowledge the Malaysian Palm Oil Board (MPOB) for the financial support to conduct this research. Lastly, the authors would like to thank the Director-General of MPOB for permission to publish this article.

REFERENCES

AOCS (2017a). AOCS Official Method Ce 5b-89: Triglycerides in Vegetable Oils by HPLC. AOCS Revised 2017.

AOCS (2017b). AOCS Official Method Ce 5c-93: Individual Triglycerides in Oils and Fats by HPLC. AOCS Reapproved 2017.

Bin Sintang, M D; Danthine, S; Patel, A R; Rimaux, T; Van De Walle, D and Dewettinck, K (2017). Mixed surfactant systems of sucrose esters and lecithin as a synergistic approach for oil structuring. *J. Colloid Interface Sci.*, *504*: 387-396.

Birker, P J M W L and Padley, F B (1987). Physical properties of fats and oils. *Recent Advances in Chemistry and Technology of Fats and Oils* (Bhati, R J H ed.). Elsevier. New York. p. 1-11.

Blake, A I; Co, E D and Marangoni, A G (2014). Structure and physical properties of plant wax crystal networks and their relationship to oil binding capacity. *J. Am. Oil Chem. Soc.*, *91(6)*: 885-903.

Bot, A and Agterof, W G M (2006). Structuring of edible oils by mixtures of γ-oryzanol with β-sitosterol or related phytosterols. *J. Am. Oil Chem. Soc.*, *83(6)*: 513-521.

Co, E D and Marangoni, A G (2012). Organogels: An alternative edible oil-structuring method. *J. Am. Oil Chem. Soc.*, *89*: 749-780.

Doan, C D; To, C M; Vrieze, M D; Lynen, F; Danthine, S; Brown, A; Dewettinck, K and Patel, A R (2017). Chemical profiling of the major components in natural waxes to elucidate their role in liquid oil structuring. *Food Chem.*, *214*: 717-725.

Doan, C D; Van de Walle, D; Dewettinck, K and Patel, A R (2015). Evaluating the oil-gelling properties of natural waxes in rice bran oil: Rheological, thermal, and microstructural study. *J. Am. Oil Chem. Soc.*, *92(6)*: 801-811.

Flöter, E; Wettlaufer, T; Conty, V and Scharfe, M (2021). Oleogels – Their applicability and methods of characterization. *Molecules*, *26*: 1673-1691.

Ghazali, H M; Hamidah, S and Che Man, Y B (1995). Enzymatic transesterification of palm olein with nonspecific and 1,3-specific lipases. *J. Am. Oil Chem. Soc.*, *72(6)*: 633-639.

Gunstone, F D (2011). Production and trade of vegetable oils. *Vegetable Oils in Food Technology. Composition, Properties and Uses* (Frank, D G ed.). 2nd edition. Wiley-Blackwell. West Sussex. p. 1-24.

Haryati, T; Che Man, Y B; Ghazali, H M; Asbi, B A and Buana, L (1998). Determination of iodine value of palm oil based on triglyceride composition. *J. Am. Oil Chem. Soc.*, *75(7)*: 789-792.

Hwang, H-S; Singh, M; Bakota, E L; Winkler-Moser, J K; Kim, S and Liu, S X (2013). Margarine from organogels of plant wax and soybean oil. *J. Am. Oil Chem. Soc.*, *90(11)*: 1705-1712.

ISO (2011). ISO 12966-2:2011. Animal and vegetable fats and oils – Gas chromatography of fatty acid methyl esters – Part 2: Preparation of methyl esters of fatty acids.

Jang, A; Bae, W; Hwang, H-S; Lee, H G and Lee, S (2015). Evaluation of canola oil oleogels with candelilla wax as an alternative to shortening in baked goods. *Food Chem.*, *187*: 525-529.

Marangoni, A G and Garti, N (2011). An overview of the past, present, and future of organogels. *Edible Oleogels: Structure and Health Implications* (Alejandro, G M and Nissim G eds.). AOCS Press. Urbana. p. 1-18.

Öğütcü, M and Yilmaz, E (2014). Oleogels of virgin olive oil with carnauba wax and monoglyceride as spreadable products. *Grasas Aceites*, *63(3)*: e040.

Patel, A R; Babaahmadi, M; Lesaffer, A and Dewettinck, K (2015). Rheological profiling of organogels prepared at critical gelling concentrations of natural waxes in a triacylglycerol solvent. *J. Agric. Food Chem.*, *63(19)*: 4862-4869.

Saw, M H and Siew, W L (2014). The effectiveness of immobilized lipase *Thermomyces lanuginosa* in catalyzing interesterification of palm olein in batch reaction. *J. Oleo Sci.*, *63(3)*: 295-302.

Saw, M H; Hishammudin E; Chong, C L; Yeoh, C B and Lim, W H (2017). Effect of polyglycerol esters additive on palm oil crystallization using focused beam reflectance measurement and differential scanning calorimetry. *Food Chem.*, *214*: 277-284.

Saw, M H; Lim, W H; Yeoh, C B; Baharin, B S and Tan, C P (2020). Screening of organogelators for structuring palm superolein. *J. Oil Palm Res.*, *32(1)*: 152-158.

Smith, K W; Bhaggan, K; Talbot, G and van Malssen, K F (2011). Crystallization of fats: Influence of minor components and additives. *J. Am. Oil Chem. Soc.*, *88*: 1085–1101.

Sulaiman, M Z; Sulaiman, N M and Kanagaratnam, S (1997). Triacylglycerols responsible for the onset of nucleation during clouding of palm olein. *J. Am. Oil Chem. Soc.*, *74(12)*: 1553-1558.

Toro-Vazquez, J F; Morales-Rueda, J A; Dibildox-Alvarado, E; Charó-Alonso, M; Alonzo-Macias, M and González-Chávez, M M (2007). Thermal and textural properties of organogels developed by candelilla wax in safflower Oil. *J. Am. Oil Chem. Soc.*, *84(11)*: 989-1000.

Trappe, V and Weitz, D A (2000). Scaling of the viscoelasticity of weakly attractive particles. *Phys. Rev. Lett.*, *85(2)*: 449-452.

Wang, Y; Eastwood, B; Yang, Z; Campo, L; Knott, R; Prosser, C; Carpenter, E and Hemar, Y (2019). Rheological and structural characterization of acidified skim milks and infant formulae made from cow and goat milk. *Food Hydrocoll.*, *96*: 161-170.

Zetzl, A K and Marangoni, A G (2011). Novel strategies for nanostructuring liquid oils into functional fats. *Edible Oleogels: Structure and Health Implications* (Alejandro, G M and Nissim, G eds.). AOCS Press. Urbana. p. 19-47.

Journal of Oil Palm Research Vol. 35 (2) June 2023 p. 268-280
DOI: https://doi.org/10.21894/jopr.2022.0051

ESTERIFICATION OF FREE FATTY ACID FROM SLUDGE PALM OIL USING ZEOLITE-SULFONATED CARBON FROM SUGAR CANE CATALYSTS

HASANUDIN[1,2]*; WAN RYAN ASRI[1,2]; TRI ELTIYAH MUTHIARANI[1,2]; DAVID BAHRAIN[3] and FITRI HADIAH[3]

ABSTRACT

In this research, the zeolite-sulfonated carbon from sugar cane catalyst has been employed for the free fatty acid (FFA) esterification in sludge palm oil (SPO) optimised by response surface methodology and central composite design. The effect of the catalyst weight ratio of zeolite to sulfonated carbon was evaluated. The result showed that the catalyst with a weight ratio of zeolite to sulfonated carbon of 1:3 (% w/w) had the highest acidic value of 10.80 mmol g^{-1} and was used for further esterification optimisation. FTIR and EDX analysis affirmed the existence of a sulfonated group of the composite catalysts. The ^{13}C NMR analysis showed that the esterification successfully produced an ester compound. The optimum conditions for FFA conversion were acquired at a reaction temperature of 78.98°C, a reaction time of 119.97 min, a catalyst weight of 2.97 g, with 94.19% FFA conversion, and followed by a statistically significant model. The catalyst reusability study revealed that the catalyst had a slight decrease in catalyst performance and could generate up to 80.00% conversion after the fourth cycle. This study could bring forth early information about the potential of zeolite-sulfonated carbon from sugar cane catalyst for FFA conversion from SPO into high-value ester products.

Keywords: esterification, free fatty acid, sludge palm oil, zeolite-sulfonated carbon catalyst.

Received: 26 January 2022; **Accepted:** 14 July 2022; **Published online:** 23 August 2022.

INTRODUCTION

Crude palm oil (CPO) is an essential resource in Indonesia and has grown as one of the world's biggest producers, with Indonesia accounting for more than half of global CPO production. In recent decades, CPO production in Indonesia has surged from 0.84 million tonnes in 2001 to about 27.00 million tonnes in 2017 (Nasution *et al*., 2018a; Rahman *et al*., 2021). CPO production tends to increase every year by 1.50%-10.96%, resulting in a significant accumulation of by-products. Besides empty fruit bunches (EFB), shells, and fibres as palm oil by-products (Nasution *et al*., 2018b), liquid waste palm oil mill effluent (POME) is reported as the most considerable waste fraction of the palm oil sector, wherein sludge palm oil (SPO) is the major oil residue observed in the top layer of POME (Tang *et al*., 2020). Extraction of free fatty acids (FFA) from SPO has been carried out to increase the value of waste (Goh *et al*., 2019). SPO is also reported to have been used as a feedstock for the production of biogas (Garritano *et al*., 2018). On the other hand, it has a relatively high content of FFA (>20%) and is low-cost (USD1 t^{-1}); hence it has the potential to be utilised as biodiesel feedstocks (Abdullah *et al*., 2017; Liu *et al*., 2021; Muanruksa and Kaewkannetra, 2020).

[1] Department of Chemistry,
Faculty of Mathematics and Natural Science,
Universitas Sriwijaya, Indralaya,
30662 South Sumatra, Indonesia.

[2] Biofuel Research Group,
Faculty of Mathematics and Natural Science,
Universitas Sriwijaya, Indralaya,
30662 South Sumatra, Indonesia.

[3] Department of Chemical Engineering,
Faculty of Engineering,
Universitas Sriwijaya, Indralaya,
30662 South Sumatra, Indonesia.

* *Corresponding author e-mail: hasanudin@mipa.unsri.ac.id*

Biodiesel can be generated through transesterification using a homogeneous alkaline catalyst such as KOH (Abdullah *et al.*, 2017) and NaOH (Aslan and Eryilmaz, 2020). However, the high FFA content in SPO makes homogeneous alkaline catalysts to produce soap, prompting a drastic decline in conversion and biodiesel yield and complicating the separation process (dos Santos *et al.*, 2019). Esterification pretreatment can reduce the FFA content in SPO using homogeneous acid catalysts. Nevertheless, the catalyst is corrosive, produces water that reduces biodiesel products, and requires high biodiesel purifying costs (Anguebes-Franseschi *et al.*, 2018; Quah *et al.*, 2019). Heterogeneous acid catalysts based on oxides such as niobium oxide, heteropoly acids, resins, and carbon can substitute homogeneous acid catalysts. These catalysts are more economical in product separation and have good recyclability, but they require a longer reaction time, high catalyst loading, and low activity (Arumugamurthy *et al.*, 2019; Junior *et al.*, 2020). Heterogeneous carbon-based acid catalysts have fascinated much recognition due to the characteristics of a significant raw material source, have large surface functional groups, and exhibit high esterification catalytic activity (Zhang *et al.*, 2021).

One of the sources of a carbon-based catalyst that could behave as a catalyst in the esterification reaction is sugar cane. Studies show that the carbonisation of sugar cane produces amorphous carbon that can be easily functionalised (Balan *et al.*, 2021). Carbonised sugar cane is then sulfonated to increase stability and higher compactness of active sites (Tang *et al.*, 2018). Amorphous carbon with sulfonate groups (-SO_3H) on the surface provides excellent acidity (Fonseca *et al.*, 2020). Many studies report that sulfonated carbon catalysts from various feedstocks provide outstanding catalytic activity and properties (Farabi *et al.*, 2019; Ibrahim *et al.*, 2020; Ngaosuwan *et al.*, 2016; Tao *et al.*, 2015) sulfonated carbon-based catalysts are promising, economical, environment friendly, and can potentially replace sulfuric acid catalysts for industrial-scale esterification.

Supporting material with a large specific surface area and adequate catalytic activity is required to increase the ability of a sulfonated carbon catalyst, which could have a synergic effect in esterification. Zeolites are crystalline, porous, have Lewis and Brønsted acid sites, suitable as supporting materials (Ketzer *et al.*, 2020; Lawan *et al.*, 2020; Sun *et al.*, 2015). According to the literature review, composite zeolite-sulfonated carbon from sugar cane catalyst has not been reported yet for esterification of FFA from SPO. This catalyst was chosen for the study because the combination of sulfonated carbon with zeolite, where both materials have a high active catalytic site and good physicochemical properties, could exhibit the synergic effect and promote high FFA conversion into esters. Therefore, this study would be focused on optimising FFA conversion derived from SPO utilising a zeolite-sulfonated carbon composite from a sugar cane catalyst using RSM-CCD. The advantages of the RSM-CCD result are high precision, good optimisation and can minimise experimental trials (Guo *et al.*, 2020; Kenawy *et al.*, 2019). The effect of the weight ratio of zeolite to sugar cane was also evaluated and the catalyst was characterised using FTIR, SEM-EDX, as well as acidity using the titration method. The input variables observed were the catalyst weight, reaction time and temperature, and the output variable observed was the FFA conversion into esters. The SPO and esterification products were analysed using ^{13}C-NMR.

MATERIALS AND METHODS

Materials

The materials utilised in this study were SPO waste (PT. Agro Indralaya Mandiri, Ogan Ilir, South Sumatra, Indonesia) and the fatty acid composition of SPO was assessed using gas chromatography (GC) (Shimadzu; using an HP-5 capillary column equipped with a flame ionisation detector and a flow rate of 3 mL min^{-1}), natural zeolite (Lampung), distilled water, sodium hydroxide, oxalic acid, phenolphthalein, methanol, sulfuric acid, hydrochloric acid, glacial acetate acid and anhydrous calcium dichloride. All chemicals were of analytical grade from Merck, New Jersey, USA.

Effect of Ratio of Zeolite to Sugar Cane

Natural zeolite was sieved with a 200-mesh, cleaned with distilled water, and then dried at 120°C in the oven for one day. Zeolite-sugar cane composites with a weight ratio of zeolite to sugar cane of 1:3, 1:2, 1:1, 2:1 and 3:1 (% w/w) were set out, and the solution subsequently was stirred using a magnetic stirrer at 300 rpm, temperature of 80°C for 1 hr. Zeolite-sugar cane composites were carbonised at 400°C using a furnace for 15 hr to produce zeolite-carbon composite.

Sulfonation of Zeolite-carbon Composite

A total of 20 g of the zeolite-carbon composite was mixed with 0.1 L of concentrated H_2SO_4. The solution was refluxed at 175°C for 15 hr and then washed with distilled water to neutral pH. The catalyst was dried at 120°C for one day. This result was then called a zeolite-sulfonated carbon composite.

Sludge Palm Oil (SPO) Esterification

The esterification was conducted using a batch reactor. Prior to esterification, the SPO was liquified in the oven at 80°C (Hayyan *et al.*, 2011). Afterwards, 25 g of liquified SPO was added with 75 mL methanol, followed by the zeolite-sulfonated carbon from sugar cane composite. The material was separated by centrifugation. The product was separated by adding distilled water (temperature around 70°C) to the separating funnel with 1:1 (v/v) between the esters and distilled water. The catalyst regeneration was conducted for reusability study by washing with ethanol and subsequently dried in the oven at 100°C. The determination of conversion of the reaction product was determined based on Equation (1) as follows:

$$\text{Conversion } (\%) = \frac{\text{Initial FFA - Final FFA}}{\text{Initial FFA}} \text{ x } 100 \qquad (1)$$

SPO and products were then analysed using ^{13}C-NMR Bruker 300 MHZ with $CDCl_3$ solvent. The FFA content of SPO and products were determined using the titration method according to SNI 01-2901-2006 with the FFA content as palmitic acid.

Characterisation of Catalyst

The catalyst acidity strength was analysed using the titration method. Zeolite-sulfonated carbon composite, 1 g, was shacked with 0.1 L of 0.5 N NaOH for 24 hr. Afterwards, 5 mL of the mixture was taken and titrated with 0.1 N HCl. The amount of acid was defined as a difference between initial and final moles of NaOH divided by the catalyst weight. The functional groups of the as-synthesised catalyst were characterised using FTIR (Shimadzu), and the morphology surface of the catalyst was characterised using SEM-EDX (JEOL JSM-6300 Shimadzu).

Experimental Design using RSM-CCD

RSM is an experimental design-based technique for establishing the relationship between input and output variables. RSM can be used to model, analyse and optimise a process (Manojkumar *et al.*, 2020). The experimental design in this study used three input variables, X_1, X_2 and X_3, which were temperature (°C), catalyst weight (g), as well as reaction time (min), respectively, with the output variable being FFA conversion (Y). For the three variables in the experiment, the total number of experiments for three input variables was 17, including eight factorial and six axial points, as well as three replicates at the centre point. The variables were coded ± 1 referred to the factorial points, 0 for middle points, and ± α (± 1.68) for axial points. The ranges of the studied variables are shown in *Table 1*. Analysis of variance (ANOVA) was assessed to evaluate statistical parameters at the 95% confidence interval. Design Expert 12 software was used for the determination coefficient analysis of the model, plotting 3D response surfaces, as well as contour plots, whereas the coefficient R^2 determined the model's accuracy.

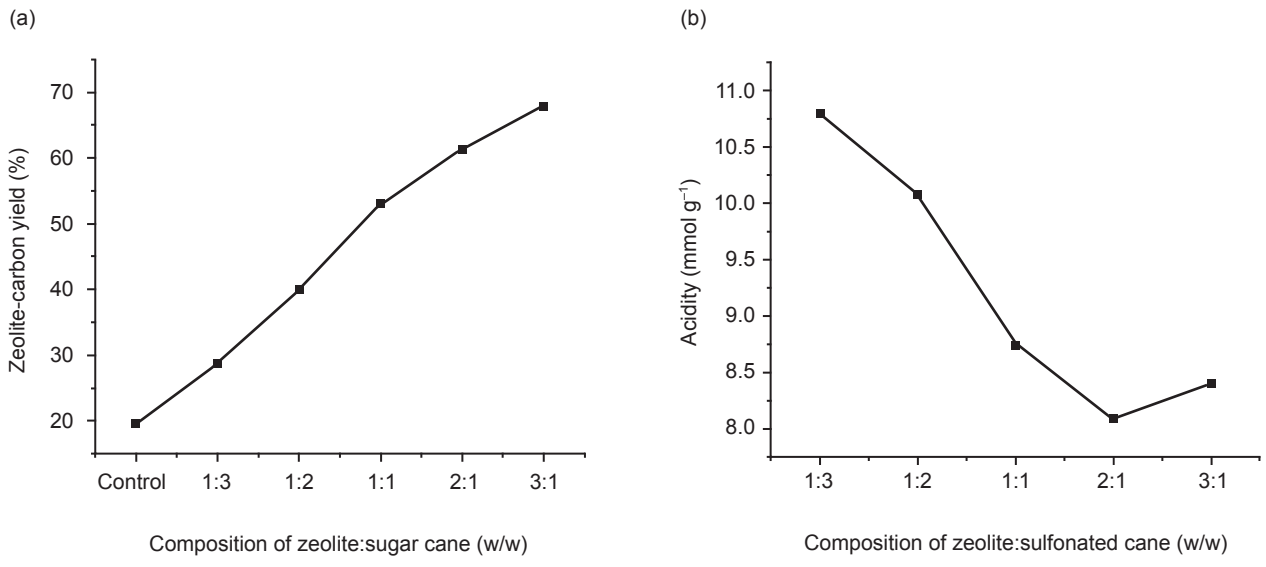


Figure 1. (a) The influence of zeolite weight ratio to sugarcane on zeolite-carbon yield, and (b) the influence of zeolite weight ratio to sulfonated carbon over catalyst acidity.

TABLE 1. CODED EXPERIMENTAL RANGE AND LEVELS OF INDEPENDENT VARIABLES

Variable	Range and levels					
	Code	-1.68	-1	0	1	1.68
Reaction temperature (°C)	X_1	63.18	70	80	90	96.82
Catalyst weight (g)	X_2	0.30	1	2	3	3.68
Reaction time (min)	X_3	69.54	90	120	150	170.46

RESULTS AND DISCUSSION

Effect of Ratio of Zeolite to Sugar Cane

The effect of the weight ratio of zeolite to sugar cane over carbon zeolite catalyst yield and the weight ratio of zeolite to sulfonated carbon over catalyst acidity as well are shown in *Figure 1.*

Figure 1a shows that the weight ratio of zeolite-sugar cane (3:1) resulted in the highest zeolite-carbon yield of 67.78% compared to others, which indicated that the greater the amount of zeolite added, the greater the yield of zeolite-carbon produced. The yield also shows that the water and volatile materials have been evaporated in this process. *Figure 1b* shows that the weight ratio of zeolite-sulfonated carbon (3:1) resulted in the highest zeolite-carbon acidity of 10.80 mmol g^{-1} compared to others. The H^+ ion bound to the sulfonate group acts as the catalyst's active site. The catalyst acidity tends to decrease until it finally increases again. The enormous acidity value indicates that the more polycyclic aromatic hydrocarbons formed, the more ortho polycyclic aromatic hydrocarbons could be attacked by electrophiles (-SO_3H).

Figure 2 shows the FTIR spectra of the zeolite-sulfonated carbon. From *Figure 2a*, FTIR spectra of carbon shows an absorption near 3417.00 cm^{-1}, which suggests the presence of hydroxyl vibrations. Strong absorption was also observed in the area of 1627.92 cm^{-1}, whereby corresponded to the existence of an aromatic ring; this indicated that the carbon only contained an aromatic ring and an OH group, without any functionalised sulfonate group in the sugar cane carbon. Subsequently, zeolite-sulfonated carbon of 1:3, 1:1 and 2:1 in *Figure 2* show that the zeolite-sulfonated carbon composite of each catalyst had a strong absorption of -SO_3H at 1064.71, 1064.70 and 1072.42 cm^{-1}, respectively (Hajamini *et al.*, 2016). Furthermore, the zeolite-sulfonated carbon of 1:3, 1:1 and 2:1 had width absorption bands of 3416.82, 3448.72 and 3417.86 cm^{-1}, respectively, associated with O-H vibrational ranges (Lathiya *et al.*, 2018). The aromatic ring at 1650-1450 cm^{-1} zeolite-sulfonated carbon was observed in the absorption peaks of 1627.92 cm^{-1} as well as 1635.64 cm^{-1}, respectively, in this way inherently demonstrated that the aromatic ring had functionalised by the sulfonated group. This sulfonate group acted as the active site of the zeolite-sulfonated carbon catalyst.

The catalyst's SEM analysis is shown in *Figure 3* with x5000 magnification. The surface morphology of the zeolite-sulfonated carbon catalyst (1:3) shows

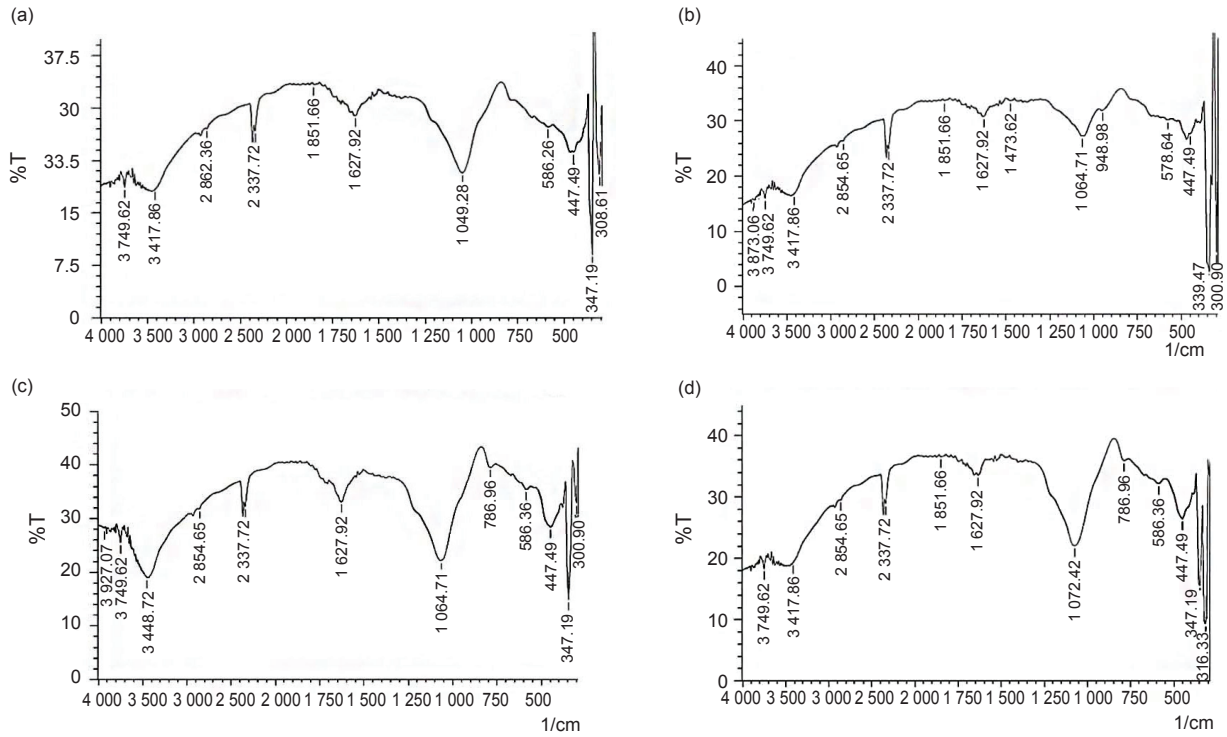


Figure 2. FTIR spectrum of (a) carbon, (b) 1:3, (c) 1:1, and (d) 2:1 zeolite-sulfonated carbon catalyst.

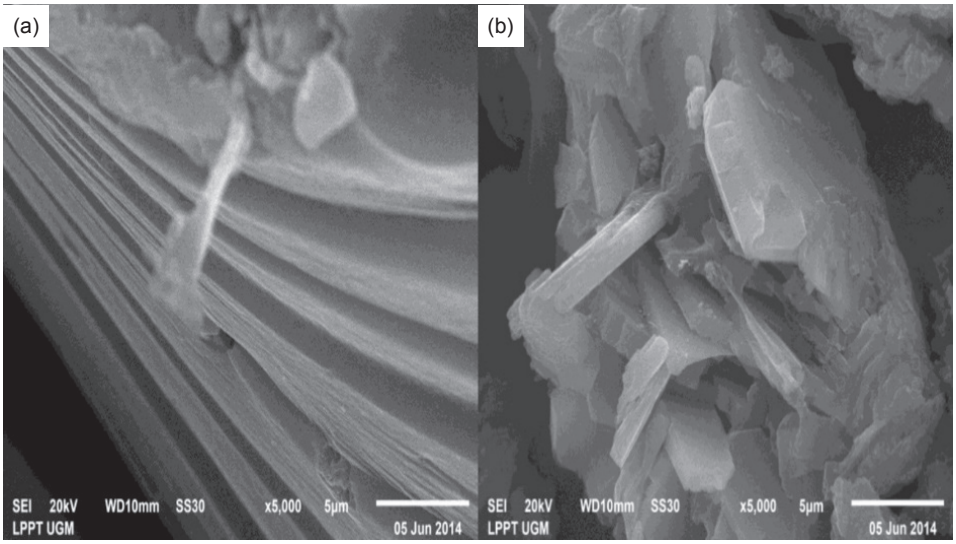


Figure 3. SEM analysis of (a) sulfonated carbon, and (b) zeolite-sulfonated carbon catalyst.

a surface with slightly rough characteristics, and thick and long fibrous granules, whereas, on the carbon sulfonate catalyst, the surface morphology was smooth, dense multi-layered. The zeolite-sulfonated carbon elemental composition was assessed using EDX. The EDX result shows that the zeolite-sulfonated carbon catalyst has elements of C with a mass of 36.47%, Si of 13.22% and S of 0.49%, whereas the sulfonated carbon catalyst has a mass of carbon elements of 61.94%, Si of 0.11% and S of 0.49%. The presence of element S as a sulfonate group attached to the zeolite-carbon indicated that there was a sulfonate group in the catalyst. Based on the results of the study, a zeolite-sulfonated carbon catalyst with the ratio of 1:3 (% w/w) was used for the esterification reaction because it has the greatest acidity value.

Fatty Acid in SPO

Analysis of fatty acids in SPO using GC shows that SPO contained palmitic acid at 60.21% as the highest fatty acid, accompanied by oleic acid at 17.44%. The FFA on SPO obtained an average value of 85.38%; this shows that SPO from PT Agro Indralaya Mandiri could be processed into esters because SPO had free fatty acids that could be reacted with alcohol.

Modelling Results and ANOVA

The reduced cubic model in coded form for the conversion of FFA (Y) was shown in Equation (2) as follow:

$$\text{Conversion (Y)} = 089.67 + 0.1784X_1 + 6.35X_2 + 0.7135X_3 - 1.59X_1X_2 - 3.00X_1X_3 - 0.2187X_2X_3 + 2.44X_1^2 - 2.38X_2^2 - 2.38X_3^2 + 5.74X_1X_2X_3 - 4.03X_1^2X_2 + 0.6502X_1^2X_3 + 5.45X_1X_2^2 \quad (2)$$

The positive sign in Equation (2) shows a synergistic effect on the FFA conversion whereas the negative sign shows the opposite effect.

According to the statistical analysis, the greater F-value and the smaller *p*-value indicated that the coefficient which corresponded to the model was increasingly significant (Behera *et al*., 2018). It shows that the F_{model} was 2887.10, whereas F_{table} = F(13; 16; 0.05) was 2.40. Since $F_{model} > F_{table}$, this designated that the model obtained was statistically significant. The *p*-value also shows that the variable model was significant. The model's importance could be strengthened by looking at the Lack of Fit. F_{model} for Lack of Fit was 1.46, whereas F_{table}= F(1; 16; 0.05) was 4.49. Since $F_{model} < F_{table}$, this implied that the Lack of Fit was insignificant, which indicated that the proposed model was suitable with experimental data and independent variables provided a sizeable effect on the response (Adepoju, 2020).

The signal/noise ratio was calculated with adequate precision, which consists of the predicted response derived from the model and the average prediction error. The ratio of adequacy precision obtained in this experiment was greater than 4; indicating a good adequacy precision ratio for experimental data (Đặng *et al*., 2017). The sufficiency of the proposed model was a major role in checking the model analysis. The normal and studentised residual probability were analysed for the FFA conversion are shown in supplementary data. It can be seen that all response values, random scatter plots, and observed variance were constant, and this indicated that there was no need to transform the response variable (Helmi *et al*., 2021). The calculated absolute error did not exceed 1.00% error, is in the range between 0.05%-0.22%; this indicated that the model met the criteria to be

within the 95.00% confidence interval (Samuel *et al.*, 2020) and proposed an adequate model (Hasanudin *et al.*, 2022a).

The statistical parameters obtained from ANOVA show that the R^2 and adjusted R^2 (R_{adj}) values were obtained at 0.9999 and 0.9996, respectively. The value of R^2 described the extent to which the model could estimate the experimental data points and R_{adj} calculated the sum of variation in the mean value described by the proposed model (Adepoju, 2020). The predicted R^2 for Equation (2) was 0.9924 and precisely to the R^2 value, this revealed that the experimental results for the FFA conversion were in accordance with the model prediction value. The model's standard deviation was 0.1783; indicating a good model that matched the predicted with the actual value for the response (Pascoal *et al.*, 2020).

The Combination Influence of Reaction Temperature, Time and Catalyst Weight on the FFA Conversion

The effect of the factor on the FFA conversion and the three-dimensional (3D) response surface were plotted. The experimental outcome of FFA conversion is as *Table 2*.

TABLE 2. THE EXPERIMENTAL DATA OF FFACONVERSION

No.	Temperature (°C)	Reaction time (min)	Catalyst weight (g)	Y (%)
1	70.00	90.00	1.00	70.50
2	90.00	90.00	1.00	79.83
3	70.00	90.00	3.00	89.46
4	90.00	90.00	3.00	71.03
5	70.00	150.00	1.00	90.37
6	90.00	150.00	1.00	66.29
7	70.00	150.00	3.00	87.05
8	90.00	150.00	3.00	78.02
9	63.18	120.00	2.00	82.54
10	96.82	120.00	2.00	83.14
11	80.00	120.00	0.30	72.31
12	80.00	120.00	3.68	93.68
13	80.00	69.54	2.00	72.31
14	80.00	170.46	2.00	74.71
15	80.00	120.00	2.00	89.76
16	80.00	120.00	2.00	89.75
17	80.00	120.00	2.00	89.47

Figure 4 shows the combined influence of catalyst weight (X_2) and reaction time (X_3) on the conversion of FFA at constant temperature (80°C) and the effect of the combination of reaction temperature (X_1) and time (X_3) on the conversion of FFA at constant catalyst weight (2 g), respectively.

Figure 4a shows that the maximum FFA conversion was achieved at a catalyst weight of 2.00-3.68 g and a reaction time of 100-140 min. This statement was validated with the optimal condition of catalyst weight of 3.68 g along with a reaction time of 120 min resulting in an experimental conversion of 93.68%, and in this condition, it gave an FFA content of 5.39%. This indicated that there was a decrease in FFA on the ester product. The more catalyst used, the more Lewis and Brønsted acid active sites. This acid site lowers the activation energy, which speeds up the esterification reaction rate resulting in a high conversion (Anguebes-Franseschi *et al.*, 2018). Contrastingly, if the reaction time was too short, less than 100 min, the collision between the reactants and the catalyst will be less effective. As a result, conversion was relatively low (Levenspiel, 1964), and if the reaction time was too long, more than 140 min, the resulting conversion will relatively decrease. The reduction in the conversion yield over the longer reaction time was likely due to the formation of by-products or deactivation of the active sites of the catalyst (Chellappan *et al.*, 2019). This condition was consistently reported by Jenie *et al.* (2020) for oleic acid esterification using sulfonated magnetic biochar catalyst. Hidayat and Sutrisno (2017) reported that the ZrO_2/SO_4^{-2} combined rice husk catalyst provided up to 83.10% FFA conversion derived from SPO using 10%wt catalyst and 60°C, whereas Abdullah *et al.* (2017) used alum as a catalyst and generated up to 90.00% FFA. Furthermore, Hayyan *et al.* (2010) showed that the 0.75%wt of toluene-4-sulfonic monohydrate acid (PTSA) catalyst exhibited FFA conversion up to 80.00%.

Figure 4b shows that the maximum FFA conversion was attained at a reaction temperature of 70°C-90°C and 100-140 min reaction. Generally, an increase in reaction temperature esterification reaction will give higher conversion due to an increase in reaction rate. As the temperature increases, the viscosity of the solution diminishes and makes mixing better (Ong *et al.*, 2014). However, a reaction temperature that was too high will have a negative influence on the conversion, this was probably due to the reduction of methanol from the liquid phase to the gas phase, thereby minimising the esterification reaction process and making the conversion relatively low (Qu *et al.*, 2020). In addition, too low a reaction temperature did not significantly increase the conversion rate. The reaction at low temperature will take more time to complete than at high temperature (Marwaha *et al.*, 2019). Ibrahim

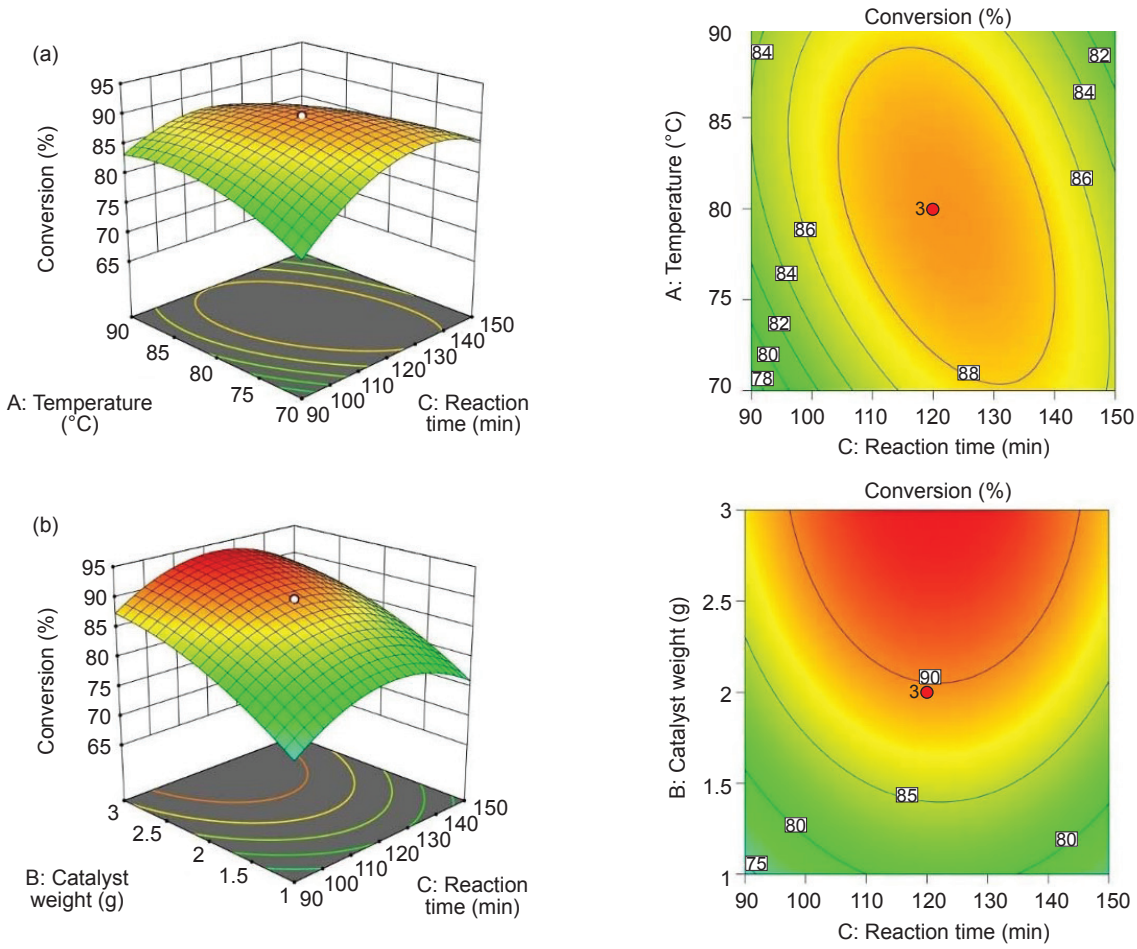


Figure 4. (a) Effect of combination of catalyst weight and reaction time, (b) effect of the combination of temperature and reaction time on FFA conversion.

et al. (2020) used sulfonated carbon from corncob waste for FFA esterification from PFAD and showed that the increment of reaction temperature from 65°C to 70°C promotes FFA conversion up to 92.00%. Nevertheless, if the reaction temperature was too high, it caused a decrement in FFA conversion up to 90.00%. The study also reported that 2 hr of esterification exhibited a high conversion of 92.00%. Hayyan *et al.* (2010) showed that a high conversion of FFA derived from SPO was achieved up to 90.93% when a temperature at 60°C and 60 min reaction using PTSA catalyst.

Optimisation and Validation

The FFA conversion optimisation was executed by the numerical method (Pascoal *et al*., 2020) and the maximum option was selected as the main factor *i.e*., catalyst weight, reaction temperature and reaction time. According to the optimisation process, variables in optimum conditions for conversion were accomplished at a reaction temperature of 78.98°C, a reaction time of 119.97 min, catalyst weight of 2.97 g and an FFA conversion of 94.19%. Additional experiments were performed and showed that the experimental result was close to the predicted response by the model. It could be concluded that the mathematical model obtained in the RSM-CCD can accurately predict the conversion to obtain optimum conditions.

Esterification Products Analysis using ^{13}C-NMR

The analysis of SPO and products at optimum conditions using ^{13}C-NMR spectroscopy is shown in *Figure 5*.

The results of the identification of esterification products showed that there was a typical C=O signal of ester at a chemical shift around 176.00 ppm, and at 180.31 ppm, there was no signal indicating that esterification occurred which the carboxyl group as FFA turned into ester products (Tariq *et al*., 2011). The ester products are also identified by the presence of the C-methoxy signal, which is a representative carbon in the ester with a chemical shift of 51.44 ppm (Munir *et al*., 2021). Apart from C=O ester and methoxy, the spectrum shows a high peak at the chemical shift of 49.74 ppm, indicating there was still methanol leftover from the esterification reaction.

The proposed mechanism of esterification reaction using zeolite-sulfonated carbon is

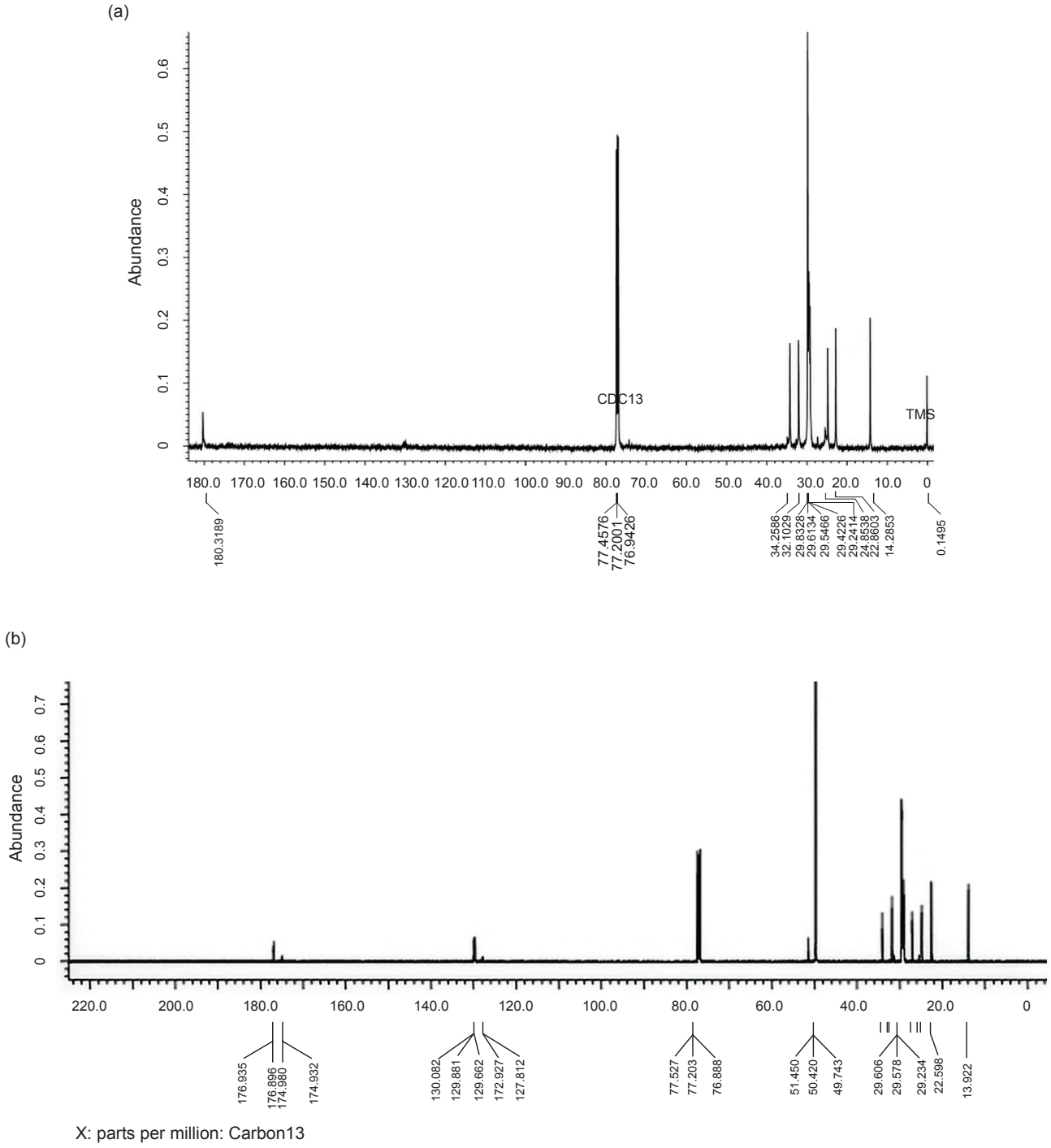
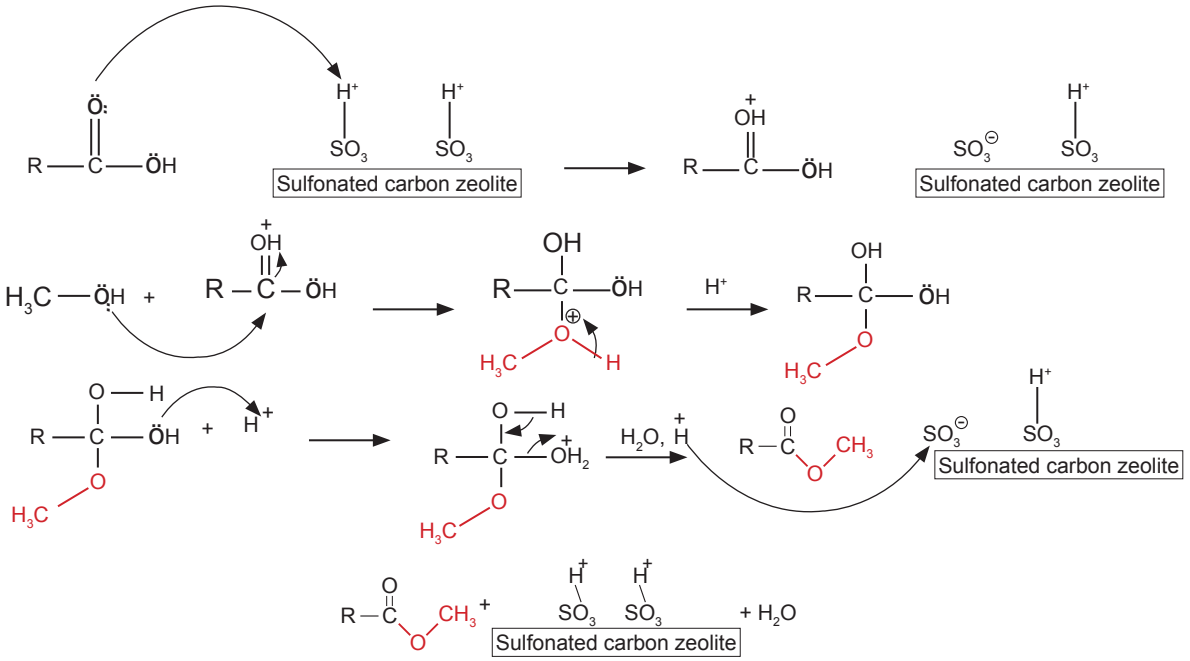


Figure 5. The ^{13}C-NMR spectrum of (a) SPO and (b) esterification product.

shown in *Figure 6* (Hasanudin *et al.*, 2022b). The formation of esters using a zeolite-sulfonated carbon composite catalyst went through a two-step process; that was the attack of unprotected phi (π) electrons in the ethanol double bond, which would attract electrophiles (H^+) on the catalyst; hence a carbocation was produced at C_1 ethanol compounds. Subsequently, the carbocation was attacked by the nucleophile (CH_3COOH^-), resulting in an ester product.

Catalyst Reusability

The study of catalyst reusability was conducted on the optimum condition employed by RSM-CCD using zeolite-sulfonated carbon from sugar cane catalyst. The catalyst was washed with methanol and then reused after drying. *Figure 7* shows the reusability accession of FFA conversion derived from SPO up to four times reused.



Source: Hasanudin *et al.* (2022b).

Figure 6. Proposed mechanism of esterification reaction using zeolite-sulfonated carbon.

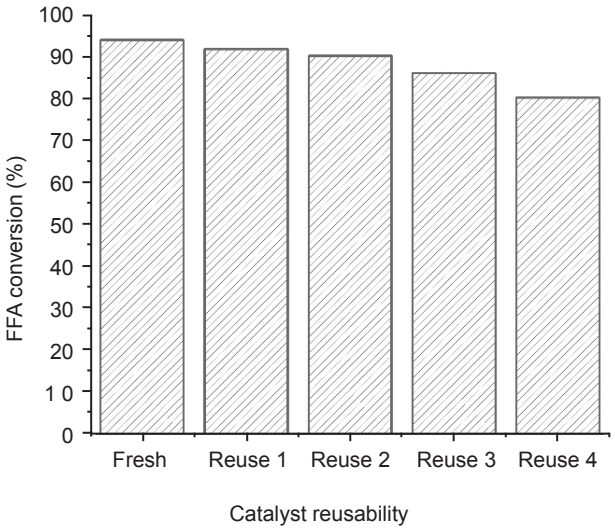


Figure 7. Reusability of catalyst.

It can be noticed that the FFA conversion decreased with the incrementing catalyst reuse cycle. Previous studies also reported a similar finding using various sulfonated carbon-based catalysts (Balan *et al.*, 2021; Ballotin *et al.*, 2020; Peng *et al.*, 2010). *Figure 7* appears that FFA conversion decreased from 94.20% to 92.03%, indicating that the catalyst performance decreased by 7.51%. The second and third cycles generated 90.44% and 86.23% conversions, with a drop in catalyst performance of 9.01% and 12.97%, respectively. Furthermore, the reaction with the fourth cycle was only able to produce a conversion of 80.42%, with a lower catalyst performance decreased by 18.44%. The decrease in catalytic activity might be due to the leaching of the -SO_3H active (Tang and Niu, 2019). Methanol could dissolve fatty acid interaction with the catalyst. However, methanol washing causes a decrease in catalytic performance by forming methyl sulfonate from the reaction of methanol with sulfonate groups. Thus, the active functional groups of the catalyst are reduced and lead to lower catalytic activity (Dawodu *et al.*, 2014).

In this research, the zeolite-sulfonated carbon derived from sugar cane catalyst composite has been employed for the esterification of FFA from SPO and optimised by RSM-CCD. The study suggested that the catalyst could be potentially upgraded up to mass-produce for the practical application as an FFA esterification catalyst, as indicated by relatively good catalyst reusability and high FFA conversion. The high FFA content of SPO also provided a primary option as a FAME feedstock as well as leading to the valorisation of SPO waste into value-added oil. However, since this study conducted reaction in the batch system, it is necessary to conduct future studies using the continuous system. This system would provide better economic feasibility and improve the reaction process. Further study regarding the kinetic parameters also needed to be evaluated to understand the esterification process comprehensively.

CONCLUSION

The RSM-CCD was applied to optimise the conversion of free fatty acids into biodiesel from SPO using a zeolite-sulfonated carbon composite catalyst. SPO had a high content of FFA which had potential as a feedstock for biodiesel production. The zeolite-sulfonated carbon composite catalyst (1:3) (% w/w) was chosen as the best catalyst as it revealed the highest acidity compared to other catalyst weight ratios. FTIR analysis of zeolite-sulfonated carbon (1:3) catalyst showed the presence of sulfonate group absorption which was confirmed by SEM-EDX analysis. The ^{13}C-NMR analysis of the products showed a chemical shift of 176 ppm for C=O ester, 51.45 ppm and 50.42 ppm for C-methoxy. The optimum condition for the conversion was acquired at a reaction temperature of 78.98°C, a reaction time of 119.97 min, catalyst weight of 2.97 g, with an FFA conversion of 94.19%. The reduced cubic mathematical model was successful in predicting the response with a minimal percentage of error. The catalyst reusability analysis demonstrated that the catalyst had a minor decline in catalyst performance and could generate up to 80.00% FFA conversion after the fourth cycle.

ACKNOWLEDGEMENT

The author wishes to express gratitude to all members of the Biofuel Research Group, Laboratory of Physical Chemistry, Department of Chemistry, Universitas Sriwijaya who contributed to this research.

REFERENCES

Abdullah; Sianipar, R R N; Ariyani, D and Nata, I F (2017). Conversion of palm oil sludge to biodiesel using alum and KOH as catalysts. *Sustain. Environ. Res.*, *27(6)*: 291-295. DOI: 10.1016/j.serj.2017.07.002.

Adepoju, T F (2020). Optimization processes of biodiesel production from pig and neem (*Azadirachta Indica* A. Juss) seeds blend oil using alternative catalysts from waste biomass. *Ind. Crops Prod.*, *149*: 112334. DOI: 10.1016/j.indcrop.2020.112334.

Anguebes-Franseschi, F; Abatal, M; Bassam, A; Soberanis, M A E; Tzuc, O M; Bucio-Galindo, L; Quiroz, A V C; Ucan, C A A and Ramirez-Elias, M A (2018). Esterification optimization of crude African palm olein using response surface methodology and heterogeneous acid catalysis. *Energies*, *11(1)*: 157. DOI: 10.1016/j.wasman.2019.09.030.

Arumugamurthy, S S; Sivanandi, P; Pandian, S; Choksi, H and Subramanian, D (2019). Conversion of a low value industrial waste into biodiesel using a catalyst derived from brewery waste: An activation and deactivation kinetic study. *Waste Manag.*, *100*: 318-326. DOI: 10.1016/j.wasman.2019.09.030.

Aslan, V and Eryilmaz, T (2020). Polynomial regression method for optimization of biodiesel production from black mustard (*Brassica nigra* L.) seed oil using methanol, ethanol, NaOH, and KOH. *Energy*, *209*: 118386. DOI: 10.1016/j.energy.2020.118386.

Balan, W S; Janaun, J; Chung, C H; Semilin, V; Zhu, Z; Haywood, S K; Touhami, D; Chong, K P; Yaser, A Z; Lee, P C and Zein, S H (2021). Esterification of residual palm oil using solid acid catalyst derived from rice husk. *J. Hazard. Mater.*, *404*: 124092. DOI: 10.1016/j.jhazmat.2020.124092.

Ballotin, F C; Da Silva, M J; Lago, R M and Teixeira, A P D C (2020). Solid acid catalysts based on sulfonated carbon nanostructures embedded in an amorphous matrix produced from bio-oil: Esterification of oleic acid with methanol. *J. Environ. Chem. Eng.*, *8(2)*: 103674. DOI: 10.1016/j.jece.2020.103674.

Behera, S K; Meena, H; Chakraborty, S and Meikap, B C (2018). Application of response surface methodology (RSM) for optimization of leaching parameters for ash reduction from low-grade coal. *Int. J. Min. Sci. Technol.*, *28(4)*: 621-629. DOI: 10.1016/j.ijmst.2018.04.014.

Chellappan, S; Aparna, K; Chingakham, C; Sajith, V and Nair, V (2019). Microwave assisted biodiesel production using a novel Brønsted acid catalyst based on nanomagnetic biocomposite. *Fuel*, *246*: 268-276. DOI: 10.1016/j.fuel.2019.02.104.

Đặng, T H; Chen, B H and Lee, D J (2017). Optimization of biodiesel production from transesterification of triolein using zeolite LTA catalysts synthesized from kaolin clay. *J. Taiwan Inst. Chem. Eng.*, *79*: 14-22. DOI: 10.1016/j.jtice.2017.03.009.

Dawodu, F A; Ayodele, O; Xin, J; Zhang, S and Yan, D (2014). Effective conversion of non-edible oil with high free fatty acid into biodiesel by sulphonated carbon catalyst. *Appl. Energy*, *114*: 819-826. DOI: 10.1016/j.apenergy.2013.10.004.

Farabi, M S A; Ibrahim, M L; Rashid, U and Taufiq-Yap, Y H (2019). Esterification of palm fatty acid

distillate using sulfonated carbon-based catalyst derived from palm kernel shell and bamboo. *Energy Convers. Manag*., *181*: 562-570. DOI: 10.1016/j.enconman.2018.12.033.

Fonseca, J M; Spessato, L; Cazetta, A L; Bedin, K C; Melo, S A R; Souza, F L and Almeida, V C (2020). Optimization of sulfonation process for the development of carbon-based catalyst from crambe meal via response surface methodology. *Energy Convers. Manag*., *217*: 112975. DOI: 10.1016/j.enconman.2020.112975.

Garritano, A N; Faber, M de O; De Sà, L R V and Ferreira-Leitão, V S (2018). Palm oil mill effluent (POME) as raw material for biohydrogen and methane production via dark fermentation. *Renew. Sustain. Energy Rev*., *92*: 676-684. DOI: 10.1016/j.rser.2018.04.031.

Goh, C L; Sethupathi, S; Bashir, M J and Ahmed, W (2019). Adsorptive behaviour of palm oil mill sludge biochar pyrolyzed at low temperature for copper and cadmium removal. *J. Environ. Manage*., *237*: 281-288. DOI: 10.1016/j.jenvman.2018.12.103.

Guo, Z; Wu, J; Zhang, Y; Cao, K; Feng, Y; Liu, J and JIan, L (2020). Briquetting optimization method for the lignite powder using response surface analysis. *Fuel*, *267*: 117260. DOI: 10.1016/j.fuel.2020.117260.

Hajamini, Z; Sobati, M A; Shahhosseini, S and Ghobadian, B (2016). Waste fish oil (WFO) esterification catalyzed by sulfonated activated carbon under ultrasound irradiation. *Appl. Therm. Eng*., *94*: 1-10. DOI: 10.1016/j.applthermaleng.2015.10.101.

Hasanudin, H; Asri, W R; Said, M; Hidayati, P T; Purwaningrum, W; Novia, N and Wijaya, K (2022a). Hydrocracking optimization of palm oil to bio-gasoline and bio-aviation fuels using molybdenum nitride-bentonite catalyst. *RSC Adv.*, *12(26)*: 16431-16443.

Hasanudin, H; Putri, Q U; Agustina, T E and Hadiah, F (2022b). Esterification of free fatty acid in palm oil mill effluent using sulfated carbon-zeolite composite catalyst. *Pertanika J. Sci. Technol*., *30(1)*: 377-395. DOI: 10.47836/pjst.30.1.21.

Hayyan, A; Alam, M Z; Mirghani, M E S; Kabbashi, N A; Hakimi, N I N M; Siran, Y M and Tahiruddin, S (2011). Reduction of high content of free fatty acid in sludge palm oil via acid catalyst for biodiesel production. *Fuel Process. Technol*., *92(5)*: 920-924. DOI: 10.1016/j.fuproc.2010.12.011.

Hayyan, A; Alam, M Z; Mirghani, M E S; Kabbashi, N A; Hakimi, N I N M; Siran, Y M and Tahiruddin, S (2010). Sludge palm oil as a renewable raw material for biodiesel production by two-step processes. *Bioresour. Technol*., *101(20)*: 7804-7811. DOI: 10.1016/j.biortech.2010.05.045.

Helmi, M; Tahvildari, K; Hemmati, A and Aberoomand, P (2021). Phosphomolybdic acid/graphene oxide as novel green catalyst using for biodiesel production from waste cooking oil via electrolysis method: Optimization using with response surface methodology (RSM). *Fuel*, *287*: 119528. DOI: 10.1016/j.fuel.2020.119528.

Hidayat, A and Sutrisno, B (2017). Esterification free fatty acid in sludge palm oil using ZrO_2/SO_4^{2-}-Rice husk ash catalyst. *AIP Conf. Proc*., *1840(1)*: 050001. DOI: 10.1063/1.4982275.

Ibrahim, S F; Asikin-Mijan, N; Ibrahim, M L; Abdulkareem-Alsultan, G; Izham, S M and Taufiq-Yap, Y H (2020). Sulfonated functionalization of carbon derived corncob residue via hydrothermal synthesis route for esterification of palm fatty acid distillate. *Energy Convers. Manag*., *210*: 112698. DOI: 10.1016/j.enconman.2020.112698.

Jenie, S N A; Kristiani, A; Sudiyarmanto; Khaerudini, D S and Takeishi, K (2020). Sulfonated magnetic nanobiochar as heterogeneous acid catalyst for esterification reaction. *J. Environ. Chem. Eng*., *8(4)*: 103912. DOI: 10.1016/j.jece.2020.103912.

Junior, W A G P; Takeno, M L; Nobre, F X; Barros, S de S; Sá, I S C; Silva, E P; Manzato, L; Iglauer, S and de Freitas, F A (2020). Application of water treatment sludge as a low-cost and eco-friendly catalyst in the biodiesel production via fatty acids esterification: Process optimization. *Energy*, *213*: 118824. DOI: 10.1016/j.energy.2020.118824.

Kenawy, I M M; Eldefrawy, M M; Eltabey, R M and Zaki, E G (2019). Melamine grafted chitosan-montmorillonite nanocomposite for ferric ions adsorption: Central composite design optimization study. *J. Clean. Prod*., *241*: 118189. DOI: 10.1016/j.jclepro.2019.118189.

Ketzer, F; Celante, D and de Castilhos, F (2020). Catalytic performance and ultrasonic-assisted impregnation effects on WO3/USY zeolites in esterification of oleic acid with methyl acetate. *Microporous Mesoporous Mater*., *291*: 109704. DOI: 10.1016/j.micromeso.2019.109704.

Lathiya, D R; Bhatt, D V and Maheria, K C (2018). Synthesis of sulfonated carbon catalyst from waste orange peel for cost effective biodiesel production.

Bioresour. Technol. Reports, *2*: 69-76. DOI: 10.1016/j.biteb.2018.04.007.

Lawan, I; Garba, Z N; Zhou, W; Zhang, M and Yuan, Z (2020). Synergies between the microwave reactor and CaO/Zeolite catalyst in waste lard biodiesel production. *Renew. Energy*, *145*: 2550-2560. DOI: 10.1016/j.renene.2019.08.008.

Levenspiel, O (1964). *Chemical Reaction Engineering*. 3rd edition. Wiley. New York. 671 pp.

Liu, X; Zhu, F; Zhang, R; Zhao, L and Qi, J (2021). Recent progress on biodiesel production from municipal sewage sludge. *Renew. Sustain. Energy Rev.*, *135*: 110260. DOI: 10.1016/j.rser.2020.110260.

Manojkumar, N; Muthukumaran, C and Sharmila, G A (2020). Comprehensive review on the application of response surface methodology for optimization of biodiesel production using different oil sources. *J. King Saud Univ. - Eng. Sci.*, *34(3)*: 198-208. DOI: 10.1016/j.jksues.2020.09.012.

Marwaha, A; Rosha, P; Mohapatra, S K; Mahla, S K and Dhir, A (2019). Biodiesel production from *Terminalia bellerica* using eggshell-based green catalyst: An optimization study with response surface methodology. *Energy Reports*, *5*: 1580-1588. DOI: 10.1016/j.egyr.2019.10.022.

Muanruksa, P and Kaewkannetra, P (2020). Combination of fatty acids extraction and enzymatic esterification for biodiesel production using sludge palm oil as a low-cost substrate. *Renew. Energy*, *146*: 901-906. DOI: 10.1016/j.renene.2019.07.027.

Munir, M; Ahmad, M; Mubashir, M; Asif, S; Waseem, A; Mukhtar, A; Saqib, S; Munawaroh, H S H; Lam, M K; Khoo, K S; Bokhari, A and Show, P L (2021). A practical approach for synthesis of biodiesel via non-edible seeds oils using trimetallic based montmorillonite nano-catalyst. *Bioresour. Technol.*, *328*: 124859. DOI: 10.1016/j.biortech.2021.124859.

Nasution, M A; Wibawa, D S; Ahamed, T and Noguchic, R (2018a). Comparative environmental impact evaluation of palm oil mill effluent treatment using a life cycle assessment approach: A case study based on composting and a combination for biogas technologies in North Sumatera of Indonesia. *J. Clean. Prod.*, *184*: 1028-1040. DOI: 10.1016/j.jclepro.2018.02.299.

Nasution, M A; Wibawa, D S; Ahamed, T and Noguchi, R (2018b). Selection of palm oil mill effluen treatment for biogas generation or compost production using an analytic hierarchy process. *J. Mater. Cycles Waste Manag.*, *20(2)*: 787-799. DOI: 10.1007/s10163-017-0638-9.

Ngaosuwan, K; Goodwin, J G and Prasertdham, P (2016). A green sulfonated carbon-based catalyst derived from coffee residue for esterification. *Renew. Energy*, *86*: 262-269. DOI: 10.1016/j.renene.2015.08.010.

Ong, H C; Masjuki, H H; Mahlia, T M I; Silitonga, A S; Chong, W T and Leong, K Y (2014). Optimization of biodiesel production and engine performance from high free fatty acid *Calophyllum inophyllum* oil in CI diesel engine. *Energy Convers. Manag.*, *81*: 30-40. DOI: 10.1016/j.enconman.2014.01.065.

Pascoal, C V P; Oliveira, A L L; Figueiredo, D D and Assunção, J C C (2020). Optimization and kinetic study of ultrasonic-mediated *in situ* transesterification for biodiesel production from the almonds of *Syagrus cearensis*. *Renew. Energy*, *147*: 1815-1824. DOI: 10.1016/j.renene.2019.09.122.

Peng, L; Philippaerts, A; Ke, X; Van Noyen, J; De Clippel, F; Van Tendeloo, G; Jacobs, P A and Sels, B F (2010). Preparation of sulfonated ordered mesoporous carbon and its use for the esterification of fatty acids. *Catal. Today*, *150(1-2)*: 140-146. DOI: /10.1016/j.cattod.2009.07.066.

Qu, T; Niu, S; Gong, Z; Han, K; Wang, Y and Lu, C (2020). Wollastonite decorated with calcium oxide as heterogeneous transesterification catalyst for biodiesel production: Optimized by response surface methodology. *Renew. Energy*, *159*: 873-884. DOI: 10.1016/j.renene.2020.06.009.

Quah, R V; Tan, Y H; Mubarak, N M; Khalid, M; Abdullah, E C and Nolasco-Hipolito, C (2019). An overview of biodiesel production using recyclable biomass and non-biomass derived magnetic catalysts. *J. Environ. Chem. Eng.*, *7(4)*: 103219. DOI: 10.1016/j.jece.2019.103219.

Rahman, N; Giller, K E; de Neergaard, A; Magid, J; van de Ven, G and Bruun, T B (2021). The effects of management practices on soil organic carbon stocks of oil palm plantations in Sumatra, Indonesia. *J. Environ. Manage.*, *278*: 111446. DOI: 10.1016/j.jenvman.2020.111446.

Samuel, O D; Okwu, M O; Oyejide, O J; Taghinezhad, E; Afzal, A and Kaveh, M (2020). Optimizing biodiesel production from abundant waste oils through empirical method and grey wolf optimizer. *Fuel*, *281*: 118701. DOI: 10.1016/j.fuel.2020.118701.

dos Santos, L K; Hatanaka, R R; de Oliveira, J E and Flumignan, D L (2019). Production of biodiesel

from crude palm oil by a sequential hydrolysis/esterification process using subcritical water. *Renew. Energy*, *130*: 633-640. DOI: 10.1016/j.renene.2018.06.102.

Sun, K; Lu, J; Ma, L; Han, Y; Fu, Z and Ding, J (2015). A comparative study on the catalytic performance of different types of zeolites for biodiesel production. *Fuel*, *158*: 848-854. DOI: 10.1016/j.fuel.2015.06.048.

Tang, P L; Hong, W L; Yue, C S and Harun, S (2020). Palm oil mill effluent as the pretreatment solvent of oil palm empty fruit bunch fiber for fermentable sugars production. *Bioresour. Technol*., *314*: 123723. DOI: 10.1016/j.biortech.2020.123723.

Tang, Z E; Lim, S; Pang, Y L; Ong, H C and Lee, K T (2018). Synthesis of biomass as heterogeneous catalyst for application in biodiesel production: State of the art and fundamental review. *Renew. Sustain. Energy Rev*., *92*: 235-253. DOI: 10.1016/j.rser.2018.04.056.

Tang, X and Niu, S (2019). Preparation of carbon-based solid acid with large surface area to catalyze esterification for biodiesel production. *J. Ind. Eng. Chem.*, *69*: 187-195. DOI: 10.1016/j.jiec.2018.09.016.

Tao, M L; Guan, H Y; Wang, X H; Liu, Y C and Louh, R F (2015). Fabrication of sulfonated carbon catalyst from biomass waste and its use for glycerol esterification. *Fuel Process. Technol*., *138*: 355-360. DOI: 10.1016/j.fuproc.2015.06.021.

Tariq, M; Ali, S; Ahmad, F; Ahmad, M; Zafar, M; Khalid, N and Khan, M A (2011). Identification, FT-IR, NMR (1H and 13C) and GC/MS studies of fatty acid methyl esters in biodiesel from rocket seed oil. *Fuel Process. Technol*., *92(3)*: 336-341. DOI: 10.1016/j.fuproc.2010.09.025.

Zhang, B; Gao, M; Geng, J; Cheng, Y; Wang, X; Wu, C; Wang, Q; Liu, S and Cheung, S M (2021). Catalytic performance and deactivation mechanism of a one-step sulfonated carbon-based solid-acid catalyst in an esterification reaction. *Renew. Energy*, *164*: 824-832. DOI: 10.1016/j.renene.2020.09.076.

Journal of Oil Palm Research Vol. 35 (2) June 2023 p. 281-295
DOI: https://doi.org/10.21894/jopr.2022.0059

SIMULATION OF ENERGY CONSUMPTION IN STERILISATION PROCESS USING ASPEN PLUS AND RESPONSE SURFACE METHODOLOGY

UMMI KALSUM HASANAH MOHD NADZIM[1]; ROBIAH YUNUS[2,3]*; ROZITA OMAR[3] and MOHD HALIM SHAH ISMAIL[3]

ABSTRACT

*Improving energy consumption in the palm oil milling process is regarded as one of the sustainable palm oil elements. Thus, this study highlights the use of ASPEN Plus-response surface methodology (RSM) approach to simulate and optimise the energy consumption of sterilisation process based on exergy analysis (*i.e. *exergy destroyed) and chemical reaction. ASPEN Plus V8.6 was employed to simulate the sterilisation process and then optimised using RSM. The validation of simulation results with experimental results demonstrating error values of less than 5.0%. Comparison of outlet stream simulation results with mill's data also showed deviation values less than 10.0%. These indicated that the actual values were in good agreement with model prediction. For optimisation, three variables were considered, namely pressure, steam mass flow and sterilisation time. For conventional steriliser operated at 2.8 bar, 90 min and 14 580 kg/hr steam mass flow, the exergy destroyed was 5259.3 MJ/hr. Under optimised conditions at 5 bar pressure, 70 min and 17 550 kg/hr steam mass flow, the exergy destroyed was 3493.9 MJ/hr. In comparison to conventional conditions, the heat loss was reduced by 33.6%. This approach is considered sustainable as it could predict the performance of industrial process without impacting processing time, cost and resources consumption.*

Keywords: ASPEN Plus, exergy analysis, optimisation, simulation, sterilisation.

Received: 24 August 2021; **Accepted:** 29 July 2022; **Published online:** 22 September 2022.

INTRODUCTION

In palm oil milling process, the fresh fruit bunches (FFB) sterilisation process uses the highest amount of steam (Aziz *et al*., 2015), thereby becoming a major contributor to high energy consumption. According to Kong *et al.* (2018), vegetable oil production is an energy-intensive process. In recent years, palm oil research has been directed towards sustainable development across the oil palm supply chain (Parveez *et al*., 2021). Hence, the issue of energy consumption in the crude palm oil (CPO) production process in Malaysia should be given attention so as not to compromise its sustainability.

Fundamentally, FFB sterilisation efficiency is often evaluated based on the ability of the fruits to detach from the bunch. Higher percentage of fruit detachment can be achieved via higher degradation rate of lignocellulosic fibres to sugars (Thang *et al*., 2021). It is vital to ensure that all fruits are detached from the bunch to successfully implement subsequent operations, which means more oil can be extracted from the fruits. Inefficient sterilisation may result in unstripped bunches (USB) which contribute to oil loss (Nadzim *et al.,* 2020; Thang *et al.,* 2021). This is due to poor heat distribution to the FFB which impairs carbohydrate degradation, and is also usually influenced by the operating conditions (*e.g.* pressure, temperature, time) during FFB sterilisation. Consequently, the sterilisation operating conditions should be improved.

However, it is a question of whether using different operating conditions such as high/low pressure, longer/shorter sterilisation period and

[1] Institute of Advanced Technology, Universiti Putra Malaysia, 43400 UPM Serdang, Selangor, Malaysia.

[2] Institute of Plantation Studies, Universiti Putra Malaysia, 43400 UPM Serdang, Selangor, Malaysia.

[3] Department of Chemical and Environmental Engineering, Universiti Putra Malaysia, 43400 UPM Serdang, Selangor, Malaysia.

* *Corresponding author e-mail: robiah@upm.edu.my*

decrease/increase steam amount is efficient in terms of energy consumption. Therefore, this concern should be addressed through the exergy analysis concept based on the ideal requirement. Exergy analysis is the maximum obtainable work that brings a system into equilibrium with its surroundings and helps identify the energy degradation in a process (Gharagheizi *et al.,* 2018; Martínez *et al.,* 2016). Exergy analysis is primarily used in industry to measure the amount of usable energy and calculate how efficiently the process uses the available energy.

Nevertheless, any improvement made to complex industrial processes will incur additional costs, and consume considerable resources and energy. This is where simulation software could be used to replicate complex processes such as palm oil milling process. In a previous study, Kamarden *et al.* (2018) successfully simulated and integrated palm oil milling, refinery and oleo-chemical processing using ASPEN Plus version 8.6. The use of materials and energy from one process unit to another and the sharing of energy supply from a centralised utility system were integrated to minimise waste and emission generation. The study demonstrated the applicability of simulation software in making the best possible decision for process improvement. To embark advancement in industrial processes, ASPEN Plus combined with response surface methodology (RSM) is expected to serve the purpose. RSM could be used to identify variables that could potentially affect the desired outputs. The integration of ASPEN Plus into RSM to combine both experimental and simulated data is seen as a powerful tool for process assessment and improvement (Cifuentes *et al.,* 2017). Several previous studies have employed this approach for energy studies in various fields, such as refinery operations (Braimah *et al.,* 2016), catalytic steam reforming of ethanol (Cifuentes *et al.,* 2017), acetic acid production (Feyzi and Beheshti, 2017) and gas-to-liquid (GTL) condensation (Hosseini and Iranshahi, 2017).

However, no recent studies have been reported on the application of ASPEN Plus-RSM on palm oil milling process focusing on energy consumption. Exergy analysis also has received little attention in palm oil milling, particularly the sterilisation process. This approach has not been adopted in palm oil mills due to a lack of relevant expertise and information. Moreover, previous studies have yet to examine extensively the role of carbohydrate degradation in sterilisation process, which is the most important stage for oil productivity as it reflects the ability of fruits to detach from the bunch. Thus, this study employed ASPEN Plus-RSM to simulate and identified significant variables which affected the energy consumption in FFB sterilisation based on exergy analysis and carbohydrate degradation. All simulated results were validated and compared with experimental results and mill data. This article will provide beneficial information to palm oil millers to improve the current processes and promote opportunities to learn more about palm oil milling.

MATERIALS AND METHODS

Steady-state Simulation in ASPEN Plus

Input specification for simulation. The steady-state simulation of the FFB sterilisation process was performed for conventional horizontal steriliser using ASPEN Plus V8.6. The operating conditions of the simulated sterilisation process were 2.8 bar pressure (130°C temperature) and 90 min sterilisation time in accordance with the conditions used in selected palm oil mill located in Selangor, Malaysia. Other inputs included in the simulation were the compositions of main components in FFB and steam estimated from Ariffin (1984), Keshvadi *et al.* (2012) and Simarani *et al.* (2009) as presented in *Table 1*.

In addition, chemical reactions of carbohydrate and triglycerides (*Table 2*) were also included as simulation inputs together with reaction kinetics estimated from previous studies.

Model selection. The simulation model of the sterilisation process was represented by a continuous-stirred tank reactor (RCSTR) and a flash block. *Figure 1* exhibits the schematic diagram of a typical sterilisation process in a palm oil mill and flowsheet diagram in ASPEN Plus.

After inserting all the inputs in the simulator, the thermodynamic model was selected. This study

TABLE 1. INPUTS OF STEAM AND FFB USED IN SIMULATION

	Fresh fruit bunches (FFB)	Steam
Condition		
Temperature (°C)	32	131
Pressure (bar)	1.0	2.8
Total mass flow (kg/h)	54 000	14 580
Component mass fraction		
Tripalmitin	0.1480	-
Triolein	0.1480	-
Glucan	0.2540	-
Xylan	0.1490	-
Water	0.3000	1.0
Palmitic acid	0.0045	-
Oleic acid	0.0045	-

TABLE 2. KINETIC PARAMETERS USED IN SIMULATION OF STERILISATION PROCESS

Reactions	Temperature (K)	Rate constant, k (s^{-1})	Activation energy, E (kJ/mol)	Reference
Tripalmitin + water → Palmitic acid + Glycerol	404	9.974	232.90	Anozie and Dzobo (2006)
Triolein + water → Oleic acid + Glycerol	404	9.974	232.90	Anozie and Dzobo (2006)
Glucan + water → Glucose	404	0.011	106.58	Husin (2016)
Xylan + water → Xylose	404	0.010	56.04	Husin (2016)

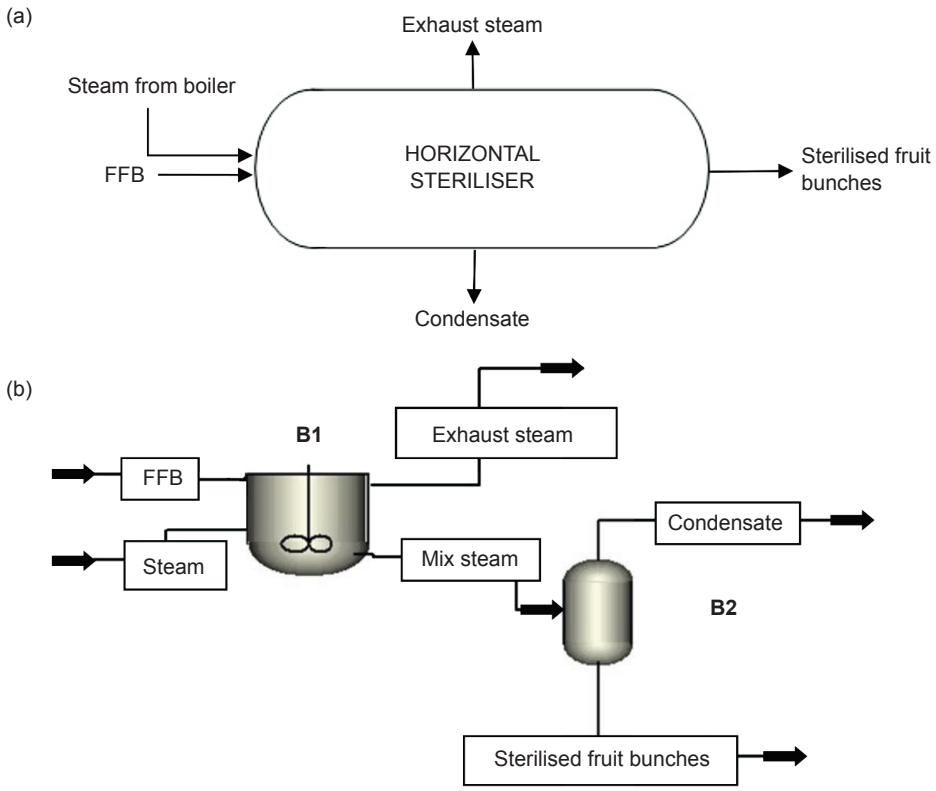


Figure 1. Sterilisation process; (a) schematic diagram and (b) flowsheet diagram in ASPEN Plus.

used non-random two-liquid (NRTL) for immiscible components (oil and water) and steam table (STEAM-TA) for saturated steam.

Model Validation and Comparison

The simulation results of the sterilisation process were validated in terms of component composition in streams, namely oil, glucan, xylan and moisture content. The streams involved for validation were condensate and sterilised fruit bunches. The oil contents in the sterilised fruits and condensate were determined using the Soxhlet extraction method according to MPOB Test Method (2005), while glucan and xylan contents were measured via proximate analysis. The moisture contents of the samples from sterilised fruits and condensate were determined using the oven drying method in accordance with MPOB Test Method (2005). The differences between simulation and actual results were expressed as absolute error (Equation 1). Moreover, the mass balance of the simulated sterilisation process was compared with the data obtained from the palm oil mill. Absolute relative deviation in Equation (2) was used to determine the differences between the simulation and mill's data.

$$\text{Absolute error (AE)} = \text{Simulation value} - \text{Actual value} \quad (1)$$

$$\text{Absolute relative deviation (ARD)} = \frac{\text{Simulation} - \text{Actual}}{\text{Actual}} \times 100 \quad (2)$$

Exergy Analysis

This study adopted the method from Hinderink *et al.* (1996) for exergy analysis calculation as it

was developed appropriately for application in flowsheeting simulators such as ASPEN Plus. The total exergy of a stream is presented in Equation (3).

$$Ex = Ex_{chem} + Ex_{phys} + \Delta_{mix}Ex \quad (3)$$

where Ex is total exergy of a stream; Ex_{chem} is total chemical exergy of a stream; Ex_{phys} is total physical exergy of a stream; and $\Delta_{mix}Ex$ denotes the exergy change of mixing. The unit is expressed in Watts (W) or Joules (J). Each term has to be calculated separately and systematically.

Chemical exergy is defined as a minimum work needed to synthesise a pure chemical compound at an environmental reference state from its constituent elements at the same state (Gharagheizi *et al.*, 2018). In this study, the chemical exergy was calculated using Equation (4) adopted from Gharagheizi *et al.* (2018) with a slight adjustment on the symbol used to represent chemical exergy.

$$Ex^{o}_{chem,i} = \Delta_f G^{o}_i - \sum \eta_j Ex^{o}_{chem,j} \quad (4)$$

where $Ex^{o}_{chem,i}$ denotes standard chemical exergy of any species i, $\Delta_f G^{o}_i$ denotes Gibbs energy of formation of species i, $Ex^{o}_{chem,j}$ denotes standard chemical exergy of the element j in species i, and η_j denotes the number of atoms of elements j in species i. To evaluate consistent results of standard chemical exergy, the thermodynamic values ($\Delta_f G^{o}_i$) were retrieved from the internal database of ASPEN Plus.

Since standard chemical exergy is phase-dependent, the phase at which a species component is present at a reference state should be considered when dealing with mixtures (Hinderink *et al.*, 1996). Therefore, Equation (5) was used to determine the standard chemical exergy of species i expressed in phase α from the value in phase β.

$$Ex^{o\alpha}_{chem,i} = Ex^{o\beta}_{chem,i} + \Delta_{\beta\rightarrow\alpha} G^{o}_i \quad (5)$$

in which

$$\Delta_{\beta\rightarrow\alpha} G^{o}_i = \Delta_f G^{o\alpha}_i - \Delta_f G^{o\beta}_i \quad (6)$$

The Gibbs energy formation of species i in its unstable phase at reference state was retrieved from the ASPEN Plus database. Hence, the chemical exergy of a multi-component stream is given by Equation (7) at the reference state (T_o and P_o).

$$Ex_{chem} = L_o \sum_{i=1}^{n} x_{o,i} Ex^{ol}_{chem,i} + V_o \sum_{i=1}^{n} y_{o,i} Ex^{ov}_{chem,i}[T_o, P_o] \quad (7)$$

Physical exergy is defined by Equation (8) which can be obtained from ASPEN Plus simulation for each stream as EXERGYFL (exergy flow rate). It is calculated as a function of enthalpy and entropy difference.

$$Ex_{phys} = (H - H_o) - T_o (S - S_o) \quad (8)$$

Calculation of exergy change of mixing from enthalpy and entropy of mixture and pure components is shown in Equation (9), while Equation (10) denotes total exergy flow rate of a material stream at actual conditions (Hinderink *et al.*, 1996).

$$\Delta_{mix} Ex = \Delta_{mix}H - T_0 \Delta_{mix}S \qquad [T,P] \quad (9)$$

$$Ex_{tot} = F (Ex_{chem} + Ex_{phys} + \Delta_{mix} Ex) \quad (10)$$

The main focus of this study was to obtain the exergy destroyed by the process. Exergy destroyed, known as irreversibility, shows how much exergy is lost through the process unit as shown in Equation (11).

$$Ex_{destroyed} = \sum Ex_{in} - \sum Ex_{out} \quad (11)$$

Sensitivity Analysis

Sensitivity analysis is useful to study the sensitivity of process performance to modification in process feeds and operating variables prior to optimisation. In this study, sensitivity analysis was conducted to study the effect of reactor pressure (3-7 bar), sterilisation time (20-120 min) and steam mass flow (10 800-24 300 kg/hr) on the degradation of glucan and xylan to produce glucose and xylose, respectively, which later on would be used in RSM as variables. The purpose was to determine whether the selected variable ranges have significant effect on degradation. The selection of variables were made based on that reported by Ariffin (2011) where temperature/pressure, water equilibrium and period of reaction are three predominant factors that can influence the efficiency of degradation. Ranges of the operating variables of sterilisation process used for sensitivity analysis are given in *Table 3*.

Optimisation

Using similar ranges of operating variables as presented in *Table 3*, the energy use in sterilisation process was optimised using central composite design (CCD) through response surface methodology (RSM) in Design Expert software version 11. About 16 sets of experimental designs were established and run in ASPEN Plus to obtain the responses.

TABLE 3. RANGES OF OPERATING VARIABLES USED FOR SENSITIVITY ANALYSIS

Parameter	Lower range	Upper range	Points
Pressure (bar)	3	7	5
Steam flow rate (kg/hr)	10 800	24 300	5
Reaction time (min)	20	120	5

RESULTS AND DISCUSSION

Simulation and Model Validation

Simulation. The sterilisation process is of utmost importance in the palm oil milling process, typically performed in a horizontal pressure vessel as a batch process with steam supplied from the boiler. The FFB sterilisation uses pressurised steam in an enclosed vessel at a steam pressure between 40-45 psig (equivalent to 2.8-3.1 bar) and at a sterilisation time of around 1.0-1.5 hr (Wondi *et al.*, 2021). Sterilisation is imperative for fruit detachment from the bunch, softening fruit structures, and inhibiting lipase enzyme (Wondi *et al.*, 2021) to prevent free fatty acids (FFA) formation. The process generates sterilised fruit bunches, condensate as liquid discharge and exhaust steam to evacuate air from the vessel.

To ensure simulation is possible, several simplifications were made to overcome the constraints inherent in the simulation. This study used simple triglycerides (tripalmitin and triolein) to represent complex mixed triglycerides (carbon chains between C46 to C58) due to the absence of mixed triglycerides in the ASPEN Plus component database. This was followed by selecting palmitic and oleic acids to represent FFA. Hemicellulose was represented by xylan in the simulation as the component was also absent in the database, and its properties were estimated by ASPEN Properties. Similar to cellulose, it was represented by glucan. Due to model limitation in ASPEN Plus, the steriliser was represented by two blocks, namely continuous-stirred tank reactor (B1) and flash block (B2) (*Figure 1b*). The reactor works based on the kinetic reaction of a process, while the flash block runs based on the separation of a single vapour phase and a single liquid phase. To connect B1 and B2, an additional stream was included in the simulation. Conventionally, the sterilisation process is operated mostly in a triple-peak pressure pattern for uniform steam heat distribution to the FFB, but this was excluded in the simulation to reduce convergence constraints.

The results obtained from the steady-state simulation of the sterilisation process using ASPEN Plus are shown in *Table 4*. The simulation results showed that the sterilised fruit bunches stream was mainly composed of oil, water, glucan and xylan with a small amount of glucose, xylose, palmitic acid and oleic acid. The degradation of glucan and xylan to simple sugars, namely glucose and xylose, respectively, was evidenced after sterilisation as observed in the sterilised fruit bunches stream (*Table 4*). Moreover, the simulation results showed that the amount of xylose (0.03 kg/hr) produced in sterilised fruit bunches stream was higher than glucose ($1.5x10^{-8}$ kg/hr). This was because glucan (represented cellulose) has a more stable structure which was challenging to degrade at low sterilisation temperature (130ºC). Unlike xylan (represented hemicellulose), its unstable structure easily degraded under such conditions.

Generally, palm fruit is majorly composed of fleshy mesocarp fibre and kernel. Mesocarp fibre contains mainly oil, carbohydrate and water. The primary constituents of carbohydrate are hemicellulose, cellulose and lignin, which contribute to the structure of the fruits and bunch stalk. Hemicellulose, for instance, holds the oil cells in the fruits together and attaches the fruits to the bunch stalk by the abscission layer. *Figure 2* illustrates the components in the FFB. During sterilisation at high temperatures, hydrolysis in palm fruit will degrade the semi-stable hemicellulose (Nadzim *et al.*, 2020). The deformation properties of both the abscission and mesocarp layers of the fruits are significantly affected by the thermal softening process (Thang *et al.*, 2021) via sterilisation. Therefore, the presence of glucose in the sterilised fruit bunches stream, as indicated in *Table 4*, was more likely due to glucan degradation, whose molecular structure was shorter and less stable than cellulose. The chemical breakdown of cellulosic materials, particularly hemicellulose during sterilisation process will result in the fruits being detached from the spikelets of the bunch stalk.

Moreover, the simulation results obtained for the sterilised fruit bunches stream showed that the oil content of 15 187.8 kg/hr (represented by tripalmitin and triolein) was similar to that of the FFB stream. This proved that oil was not degraded at the given conditions. The oil breakdown process requires a higher temperature (~250ºC) and pressure around 3000-5000 kN/m^2 (30-50 bar) (Siew, 2011). The actual sterilisation process inactivates oil-splitting enzymes and prevents the formation of FFA (Shehu *et al.*, 2019). However, small amounts of palmitic acid and oleic acid representing FFA found in the sterilised fruit bunches stream were not caused by oil degradation but due to the initial simulation input. This study assumed that the initial condition of fruits in the bunches received at the palm oil mill might contain FFA slightly. This was justified by Ariffin (1984) that oil palm fruit mesocarp considered intact and undamaged has an FFA of 0.025%.

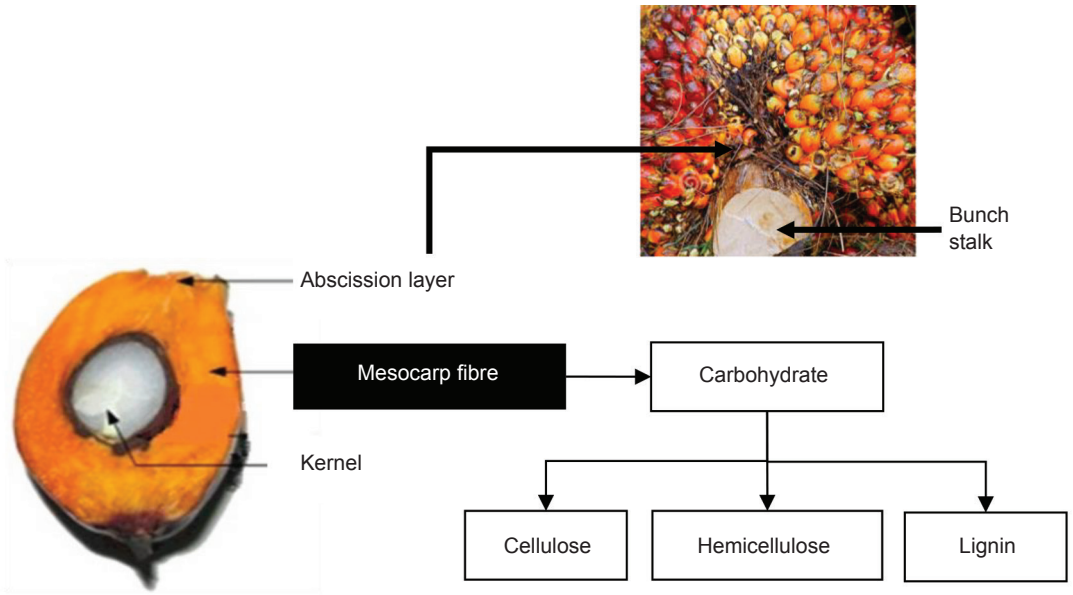


Figure 2. Illustration of components in fresh fruit bunches.

TABLE 4. SIMULATION RESULTS OF STERILISATION PROCESS

Components	Stream mass flow (kg/hr)					
	Steam	FFB	Mix stream	Exhaust steam	Sterilised fruit bunches	Condensate
Tripalmitin	-	7 593.90	7 593.90	$7.2x10^{-8}$	7 593.90	$1.9x10^{-7}$
Triolein	-	7 593.90	7 593.90	0.00	7 593.90	0.00
Glucan	-	13 032.80	13 031.00	1.90	13 025.20	5.80
Xylan	-	7 645.20	7 645.10	0.10	7 645.00	0.20
Water	14 580.00	15 393.10	20 761.20	9 211.90	10 229.00	10 532.20
Glucose	-	-	$1.5x10^{-8}$	$1.5x10^{-15}$	$1.5x10^{-8}$	$4.0x10^{-15}$
Xylose	-	-	0.03	$7.1x10^{-8}$	0.03	$1.8x10^{-7}$
Palmitic acid	-	20.50	19.60	1.00	19.00	0.50
Oleic acid	-	20.50	19.80	0.70	19.50	0.30
Glycerol	-	-	0.00	0.00	0.00	0.00
Trash	-	2 700.00	0.00	0.00	0.00	0.00
Total flow rate (kg/hr)	14 580.00	54 000.00	48 368.30	9 215.50	46 125.60	10 539.00

In comparison with the initial composition of FFB as shown in *Table 1*, it was found that the composition of oil in the sterilised fruit bunches stream indicated in *Table 4* increased from 29.6% to 32.9% and water decreased from 30.0% (15 393.1 kg/hr) to 22.2% (10 229.0 kg/hr). Although the mass flow rate of oil in both streams was similar, their compositions differed due to the reduced total mass flow rate of each stream. The reduction of water content in sterilised fruit bunches stream was influenced by water dehydration of FFB during sterilisation, which increased the composition of oil. In the real process, loss of moisture in FFB occurs when the steam is blown off during sterilisation (Ropandi *et al.*, 2017).

Meanwhile, condensate and exhaust steam streams (*Table 4*) have water as their main component. Condensate is generated from the condensation of water vapour from the steam or evaporated moisture in FFB due to the temperature effect, consisting of oil, water, fibrous material and sand (Ropandi *et al.*, 2017). From *Table 4*, the loss of oil in the condensate was insignificant at only $1.8x10^{-7}$ kg/hr, almost no oil loss. This was probably affected by the kinetic parameters of oil estimated from the literature used in the simulation. As the estimated value was small (*Table 2*), thus simulation predicted slight oil loss in the condensate. According to Garcia *et al.* (2017), the selection of kinetic parameters used in ASPEN Plus will significantly influence the model prediction.

On the other hand, the total amount of condensate produced from the simulation of sterilisation was 19.5%. This value was close to the reported values by Menon (2016), which is 20.0%/ FFB.

Model validation and comparison. After obtaining the simulation results, the sterilised fruit bunches and condensate streams were then validated with the experimental results in terms of oil, moisture (water), glucan and xylan content, as exhibited in *Table 5*. The errors obtained for condensate and sterilised fruit bunches between simulation and actual results were in the range of 1.1%-3.8%, signifying that the experimental results were in good agreement with model prediction. From previous studies, the reported oil content in condensate is 0.07%-0.64% per FFB (Corley and Tinker, 2016) and the moisture content of sterilised fruits is nearly 28.00% of total fruit composition (Wondi *et al.*, 2021). According to Thang *et al.* (2021), the compositions of the mesocarp of the sterilised fruit are as follows: 56.68% total oil content, 2.89% soluble sugars, 8.27% glucan and 4.52% xylan. These values differ from those obtained in this study as they depend on the type of fruit, sterilisation techniques and conditions.

Based on the simulation results, the oil content in condensate was insignificant, contradicting with the experimental results. As mentioned above, the simulation of the sterilisation process employed kinetic parameters of triglyceride estimated from literature, which most likely influenced the oil content present in the condensate. In the actual process, oil in the condensate is very significant, which commonly stems from the sterilisation of overripe and bruised fruits. Oil from the bruised fruits will be released to the steam and floated through steam condensation (Oi-Ming *et al.*, 2012). Furthermore, *Table 6* presents the total mass flow for outlet streams of the sterilisation process compared with the palm oil mill data. The deviation values between the simulated and actual results were below 10%, signifying that the actual results were in good agreement with model prediction. As exhaust steam stream is immeasurable in the real process, thus, it was excluded from this validation study.

Sensitivity Analysis

Effect of reactor pressure. *Figure 3* displays the effect of varying pressure on the degradation of glucan and xylan into glucose and xylose in sterilised fruit bunches, respectively. It showed that as the pressure increased from 3 to 7 bar, the glucose and xylose production increased as well. According to Ariffin (2012), the hydrolysis rate is proportional to temperature. For saturated steam, temperature is corresponding to pressure. Moreover, Yulianto and Panji (2012) revealed that the higher the temperature, the hemicellulose residues in fibres are most likely to decrease. This means that sugar production increases as the temperature increases. Production of high sugar in fruits after sterilisation could reflect the possibility of high fruit detachment from the bunch. According to Menon (2013), the detachment of fruits from bunches and oil extraction are closely related. If fruit detachment is not efficient, thus, it will result in low oil extraction and high USB. In addition, Thang *et al.* (2021) emphasized that the composition of sugars in sterilised fruits or condensate could be used as an indicator to optimise the sterilisation parameters to achieve full detachment of fruits without USB.

TABLE 5. VALIDATION OF SIMULATION AND EXPERIMENTAL RESULTS

Parameter	Sterilised fruit bunches		AE (%)	Condensate		AE (%)
	Actual	Simulation		Actual	Simulation	
Oil content (%)	34.0	32.9	1.1	1.9	$1.8x10^{-7}$	1.9
Moisture content (%)	23.8	22.2	1.6	96.1	99.9	3.8
Glucancontent (%)	26.2	28.2	2.0	N/A	N/A	-
Xylan content (%)	15.2	16.6	1.4	N/A	N/A	-

Note: AE - Absolute error; N/A - Not available.

TABLE 6. COMPARISON OF TOTAL MASS FLOW RATE OF STREAMS BETWEEN SIMULATION AND MILL'S DATA

Stream name	Simulation (kg/hr)	Mill (kg/hr)	*ARD (%)
Sterilised fruit bunches	46 125.6	47 055.6	2.0
Condensate	10 539.0	11 577.6	9.0

Note: *ARD - Absolute relative deviation.

Effect of sterilisation time. The effect of sterilisation time on glucose and xylose production is shown in *Figure 4*. It can be observed that glucose and xylose productions increased as the sterilisation time increased from 20 min (0.3 hr) to 120 min (2 hr). According to Hadi *et al.* (2012), sufficient sterilisation time is crucial for efficient degradation process or detachment of fruits to take place to

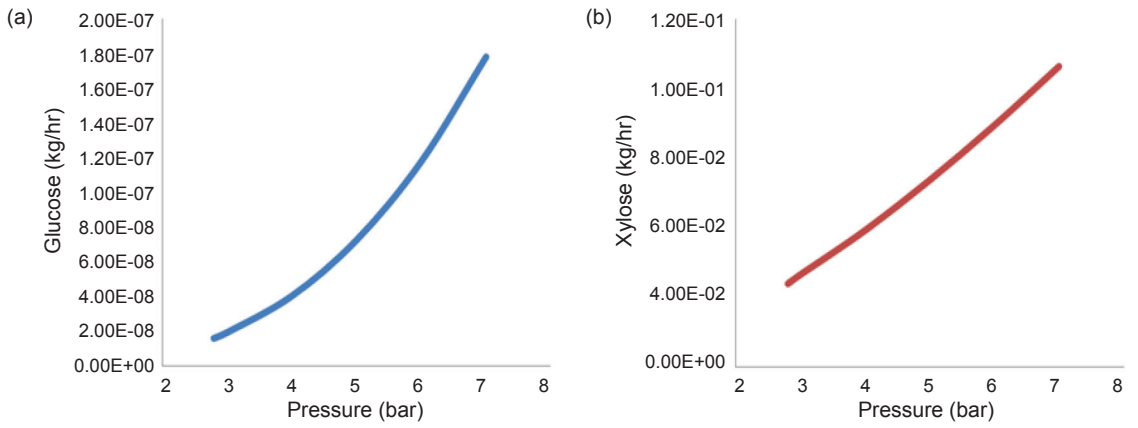


Figure 3. Effect of pressure on production of (a) glucose and (b) xylose in sterilised fruit bunches.

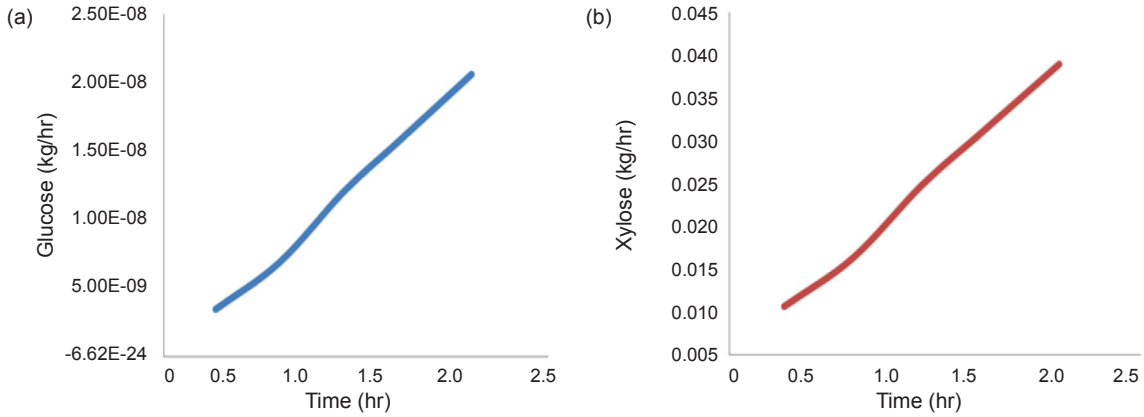


Figure 4. Effect of sterilisation time on production of (a) glucose and (b) xylose in sterilised fruit bunches.

ensure every fruit on the bunch is detached. High temperature/pressure sterilisation reduces the period for complete detachment of fruit in one sterilisation consignment.

Effect of steam mass flow. Another crucial variable involved in the degradation of glucan and xylan to produce glucose and xylose is the amount of water present in the sterilised fruit bunches. Hadi *et al.* (2012) mentioned in their study that prolonged steaming period and large quantity of steam are compulsory to ensure complete heating up till the inner layers of the bulky FFB. Unlike previous variables, increment of steam mass flow into the steriliser exhibited declining trend of glucose and xylose production in sterilised fruit bunches (*Figure 5*). Apparently, the degradation of glucan and xylan to produce glucose and xylose, respectively, was not proportional to the increase of water (steam) to the bunch. This is because glucose and xylose production increased in condensate stream as the amount of steam increased during sterilisation as exhibited in *Figure 6*. Glucose and xylose are soluble in water, thus more sugar dissolved in condensate as the amount of steam increased. This is supported by Yan *et al.* (2014) revealing that more glucose dissolves with presence of high amount of water.

Optimisation of Operating Conditions and Exergy Destroyed

Owing to the engineering and operational considerations, various constraints were also considered to obtain optimum results for this study. In the actual process, the applied pressure for sterilisation process should not be more than 5 bar and longer sterilisation time is not favourable as the minor components in palm oil, namely carotene, will deteriorate as well as affect the conditioning of palm nuts, thereby affecting the palm kernel oil production.

Prior to optimisation, the exergy destroyed of sterilisation process at conventional operating conditions of 2.8 bar pressure, 90 min sterilisation time and 14 500 kg/hr steam mass flow were determined based on Equations (3)-(11). The use of ASPEN Plus simulator can help evaluate and

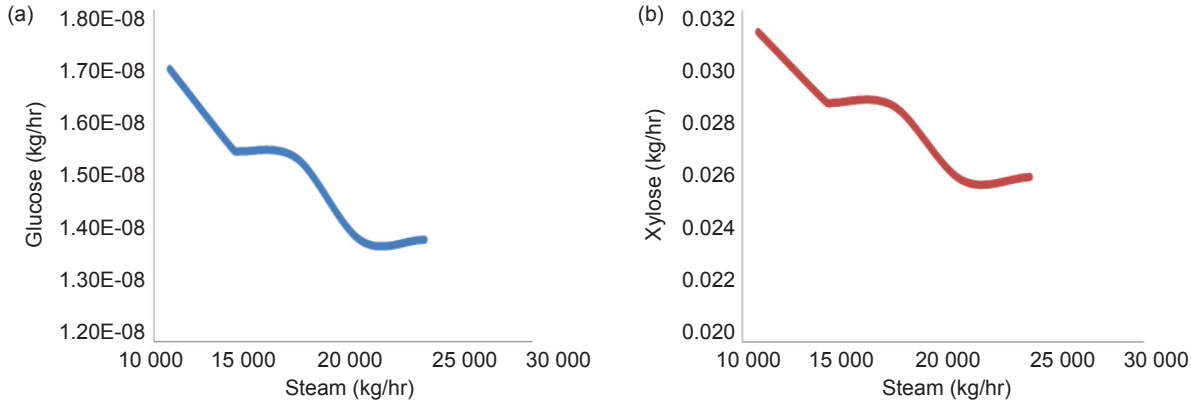


Figure 5. Effect of steam flow rate on production of (a) glucose and (b) xylose in sterilised fruit bunches.

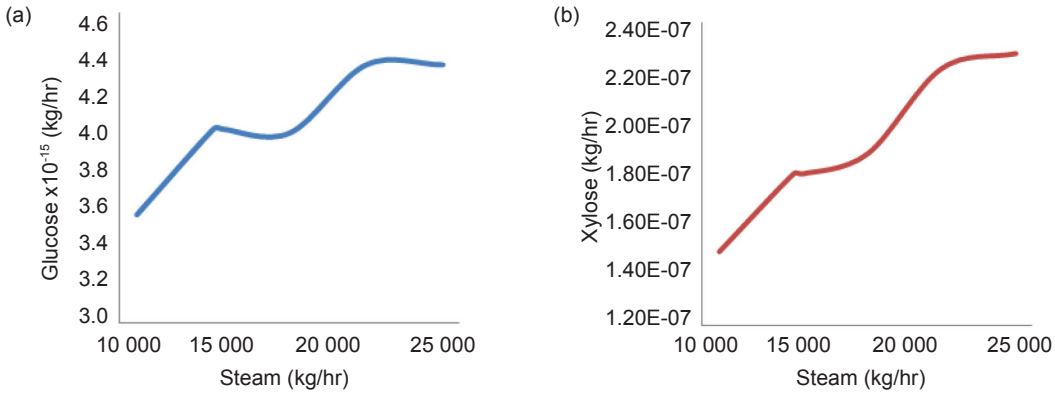


Figure 6. Effect of steam flow rate on production of (a) glucose and (b) xylose in condensate.

identify energy inefficiency by providing crucial parameters for exergy analysis, namely enthalpy, entropy and Gibbs free energy. It also provides thermo-physical properties of process stream flows and validates mass and energy balances which are essential for exergy analysis (Dogbe *et al.*, 2018). Using these data, the software computes the chemical and physical exergy of process streams (Ruiz-de la Cruz *et al.*, 2015). *Table 7* summarises the exergy analysis for the sterilisation process.

From Equation (11), it was found that 5259.3 MJ/hr of exergy was destroyed or energy was wasted during the conventional sterilisation process, indicating an opportunity for improvement. The factors that contributed to high exergy destroyed could be large steam consumption and high heat losses to the environment during the blow-down step. In addition, steriliser produces a large amount of condensate as liquid waste, which becomes the main water contributor for palm oil mill effluent. Generally, the sterilisation process consumes about 30%-60% of total process steam, which depends on the technology used and sterilisation pattern (single-peak, double-peak and triple-peak cycles utilised) (Reese, 2009). Therefore, it is essential to predict the possibility of conducting sterilisation process of FFB at optimum operating conditions with minimum energy consumption at the mill.

In this study, the effects of varying operating conditions of steriliser were evaluated in terms of hydrolysis of carbohydrate and exergy destroyed through optimisation via response surface methodology (RSM). According to Montgomery (2001), RSM is one of the statistical methods that can model and analyse the response of interest influenced by several variables. RSM selects the optimum operating conditions among a group of variables by efficient quantitative methods and provides a better understanding of the process, effect of control variables and interactions between all variables (Braimah *et al.*, 2016). The results obtained from RSM are presented in *Table 8*.

The proposed mathematical models from RSM for the glucose and xylose production in a steriliser, as well as exergy destroyed, are given by Equations (12)-(14).

Glucose =

+5.74076E-08		
+6.13520E-08	Pressure	
-1.37400E-09	Steam mass flow	
+5.24720E-08	Sterilisation time	
-1.15750E-09	Pressure * Steam mass flow	
+4.50475E-08	Pressure * Sterilisation time	
-1.05750E-09	Steam mass flow * Sterilisation time	
+2.03386E-08	Pressure^2	
-1.11379E-10	Steam mass flow^2	
-2.56138E-09	Sterilisation time^2	
-8.42500E-10	Pressure * Steam mass flow * Sterilisation time	(12)

Xylose =

+0.051372		
+0.027779	Pressure	
-0.000521	Steam mass flow	
+0.037817	Sterilisation time	
-0.000280	Pressure * Steam mass flow	
+0.020365	Pressure * Sterilisation time	
-0.000385	Steam mass flow * Sterilisation time	
+0.002416	Pressure^2	
+0.000036	Steam mass flow^2	
-0.002134	Sterilisation time^2	(13)

Exergy destroyed =

+8010.68621		
+503.38000	Pressure	
+4868.56000	Steam mass flow	
-9.01812E-13	Sterilisation time	
+320.17500	Pressure * Steam mass flow	
-1.08370E-12	Pressure * Sterilisation time	
-1.01137E-12	Steam mass flow * Sterilisation time	
-207.57931	Pressure^2	
+153.42069	Steam mass flow^2	
-109.47931	Sterilisation time^2	(14)

The values of coefficient of determination (R^2) for these models were close to 1, indicating the high accuracy of the developed model. Analysis of variances (ANOVA) was used to evaluate the adequacy of the developed model and to examine the interaction of each operating variable which exhibited a significant effect on the production of glucose and xylose as well as exergy destroyed as responses. The ANOVA results are summarised in *Table 9*. The significance of each variable or interaction between variables was indicated by *p*-values and *f*-values. The corresponding variables are considered more significant if the magnitude of the *f*-value is greater and *p*-value is smaller (less than 0.05) (Feyzi and Beheshti, 2017). Based on the ANOVA results, it can be inferred that the production of glucose and xylose in sterilised fruit bunches during sterilisation was mostly affected by pressure and sterilisation time. In contrast, exergy destroyed was affected significantly by pressure and steam mass flow. *Figure 7* shows the interactions between operating variables and responses.

From the results predicted by ASPEN Plus, the production of glucose and xylose in the sterilised fruit bunches during sterilisation was affected mainly by pressure and sterilisation time, whereas exergy destroyed was affected by pressure and steam mass flow. Pressure (or temperature) and time are among the main contributing factors for hydrolysis efficiency (Ariffin, 2012), which can be associated with water evaporation from the fruit and steam condensation on the bunch due to differences in temperature inside and outside. According to Ariffin (2012), both evaporation and condensation activities will stop if the temperature within the bunch and surrounding is the same, achieving an equilibrium state. Thus, the remained water in the fruits will be used to degrade the unstable carbohydrate. Ariffin (2012) also explained that the hydrolysis process takes time to ensure that each fruit on the bunch is detached. At low pressure (<40 psi), the required sterilisation time is 90 min, but the period will be shortened at high sterilisation pressure.

On the other hand, exergy destroyed refers to the irreversibilities in the process, of which the potential of a system to produce work that is not used (Martínez *et al.*, 2016). In other words, exergy destroyed indicates the loss of heat to the environment. As calculated, the conventional sterilisation process had 5259.3 MJ/hr of exergy destroyed, signifying that the conventional operating conditions contributed to high heat loss to the environment. Minimising heat loss is crucial for high-temperature industrial processes. For the palm oil milling process, steam consumption for the heating process has the greatest implication on energy utilisation at the mill (Energywise, 2013). Steam supplies heat for FFB sterilisation as a heating medium in a pressure vessel, either horizontal or vertical. Pressure is the key player for ensuring the process feasibility owing to fruits detachment and enzyme inactivation. The contributing factor to high exergy destroyed or heat loss could also be attributed to the blow-down step, which evacuates air from the steriliser to facilitate uniform heat distribution to the FFB consignment.

Considering the process constraints mentioned earlier, it can be deduced that the degradation process is the best in terms of glucan and xylan degradation at 5 bar, 17 550 kg/hr of steam and 70 min with minimum exergy destroyed of 3493.9 MJ/hr. The optimised conditions reduced the exergy destroyed by 33.6%. In other words, the predicted heat loss to

TABLE 7. PHYSICAL, CHEMICAL AND MIXING EXERGY OF STREAMS FOR STERILISATION PROCESS

Stream no.	Stream name	Physical exergy (ASPEN Plus) (MJ/hr)	Chemical exergy and mixing exergy (calculated) (MJ/hr)	Total exergy (MJ/hr)
1	Fresh fruit bunches	0.0	1 002 292.6	1 002 292.6
2	Steam (steriliser)	8 926.0	7 669.1	16 595.1
4	Exhaust steam	553.7	5 645.1	6 198.8
5	Sterilised fruit bunches	1 298.7	999 008.1	1 000 306.8
6	Condensate	6 461.1	661.6	7 122.7

TABLE 8. EFFECT OF PRESSURE, STEAM MASS FLOW AND STERILISATION TIME ON GLUCOSE AND XYLOSE PRODUCTION IN STERILISER

Run	Factors			Responses		
	Pressure (bar)	Steam mass flow (kg/hr)	Sterilisation time (min)	Glucose mass flow (kg/hr)	Xylose mass flow (kg/hr)	Exergy destroyed (MJ/hr)
1	3	10 800	20	$3.76x10^{-9}$	0.00636	2 745.7
2	3	24 300	20	$3.62x10^{-9}$	0.00623	11 923.4
3	7	10 800	120	$2.41x10^{-7}$	0.13920	3 112.1
4	5	17 550	20	$1.46x10^{-8}$	0.01299	7 937.7
5	5	17 550	70	$5.72x10^{-8}$	0.05132	7 937.7
6	7	24 300	120	$2.32x10^{-7}$	0.13641	13 570.5
7	7	17 550	70	$1.41x10^{-7}$	0.08250	8 343.0
8	3	10 800	120	$2.51x10^{-8}$	0.04239	2 745.7
9	3	24 300	120	$2.41x10^{-8}$	0.04155	11 923.4
10	3	17 550	70	$1.47x10^{-8}$	0.02513	7 336.2
11	7	10 800	20	$3.61x10^{-8}$	0.02088	3 112.1
12	5	17 550	120	$9.53x10^{-8}$	0.08554	7 937.7
13	5	10 800	70	$5.85x10^{-8}$	0.05195	3 493.9
14	7	24 300	20	$3.47x10^{-8}$	0.02046	13 570.5
15	5	24 300	70	$5.63x10^{-8}$	0.05092	12 907.2
16	5	17 550	70	$5.72x10^{-8}$	0.05132	7 937.7

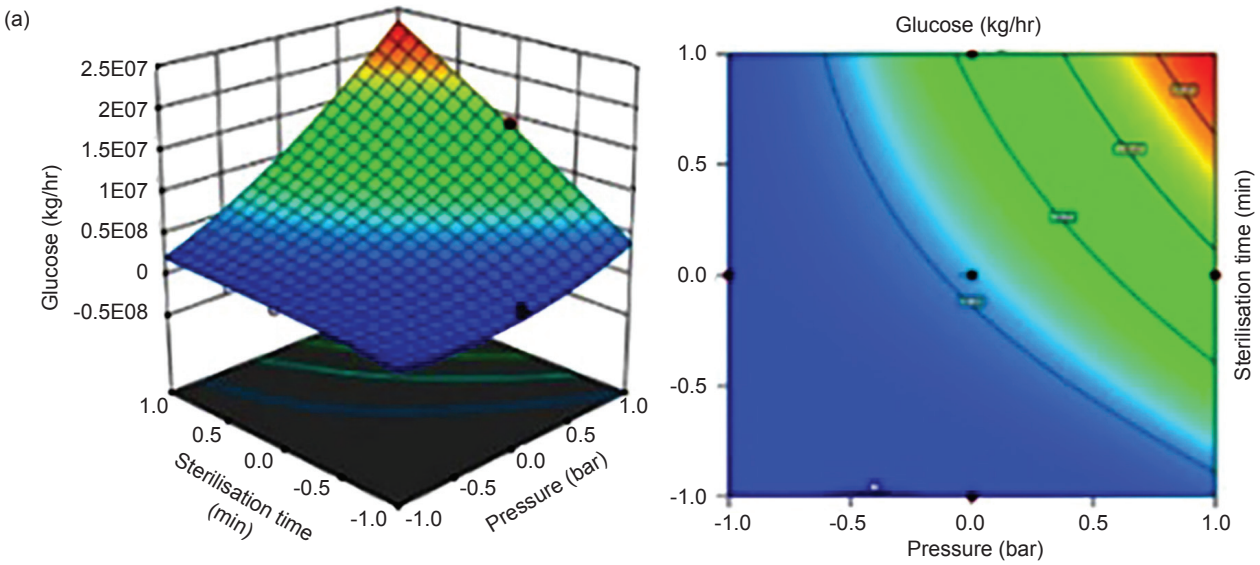
the environment is minimum when the steriliser vessel is operated at 5 bar pressure and 70 min with 17 550 kg/hr steam supplied to the vessel. The use of high-pressure sterilisation may create uniform heat distribution of steam to the inner part of the bunch, facilitating the fruits to easily detach from the bunches due to the high carbohydrate degradation rate, which possibly reduces the occurrence of USB during threshing. Importantly, efficient energy use at palm oil mills is the predominant factor that may reduce the carbon footprint and impact global warming trends (Energywise, 2013), thus creating a sustainable palm oil production operation.

CONCLUSION

Steady-state simulation of the FFB sterilisation process was successfully conducted using ASPEN Plus V8.6, where the deviation values between the simulation and experimental results were less than 5%. The comparison of mass balance between simulation and mill also showed deviation values of less than 10%. Overall, the actual values were in good agreement with the model predictions. Based on the exergy calculated for conventional sterilisation, 5259.3 MJ/hr of energy was estimated to be wasted when operated at 2.8 bar and 1.5 hr (90 min). However, based on the RSM results, the energy loss to the environment was reduced to 3493.9 MJ/hr when the FFB was sterilised at 5 bar (pressure), 70 min (sterilisation time) and 17 550 kg/hr (steam mass flow), 33.6% lower than the conventional conditions. Thus, the RSM-ASPEN Plus approach can assist industry players in minimising energy consumption for palm oil milling process. Future research should extend this study at palm oil mills using actual data so that process improvements do not affect the use of mill resources.

TABLE 9. ANOVA RESULTS OF THE DEVELOPED MODELS FROM RSM

Source	*f*-value	*p*-value
Glucose		
Quadratic	144.7600	<0.0001
A-Pressure	592.0500	<0.0001
B-Steam mass flow	0.2969	0.6055
C-Sterilisation time	433.0700	<0.0001
AB	0.1686	0.6956
AC	255.3500	<0.0001
BC	0.1407	0.7205
A^2	17.1500	0.0061
B^2	0.0005	0.9826
C^2	0.2721	0.6206
R^2 = 0.9954, R^2 (adj) = 0.9885, R^2 (pred) = 0.9603		
Xylose		
Quadratic	2 024.6200	<0.0001
A-Pressure	5 544.2900	<0.0001
B-Steam mass flow	1.9500	0.2120
C-Sterilisation time	10 275.1200	<0.0001
AB	0.4506	0.5270
AC	2 383.8100	<0.0001
BC	0.8520	0.3916
A^2	11.0600	0.0159
B^2	0.0025	0.9617
C^2	8.6200	0.0261
R^2 = 0.9997, R^2 (adj) = 0.9992, R^2 (pred) = 0.9970		
Exergy destroyed		
Quadratic	1 891.2500	<0.0001
A-Pressure	179.2700	<0.0001
B-Steam mass flow	16 769.5200	<0.0001
C-Sterilisation time	0.0000	1.0000
AB	58.0200	0.0003
AC	0.0000	1.0000
BC	0.0000	1.0000
A^2	8.0400	0.0298
B^2	4.3900	0.0810
C^2	2.2400	0.1855
R^2 = 0.9996, R^2 (adj) = 0.9991, R^2 (pred) = 0.9974		



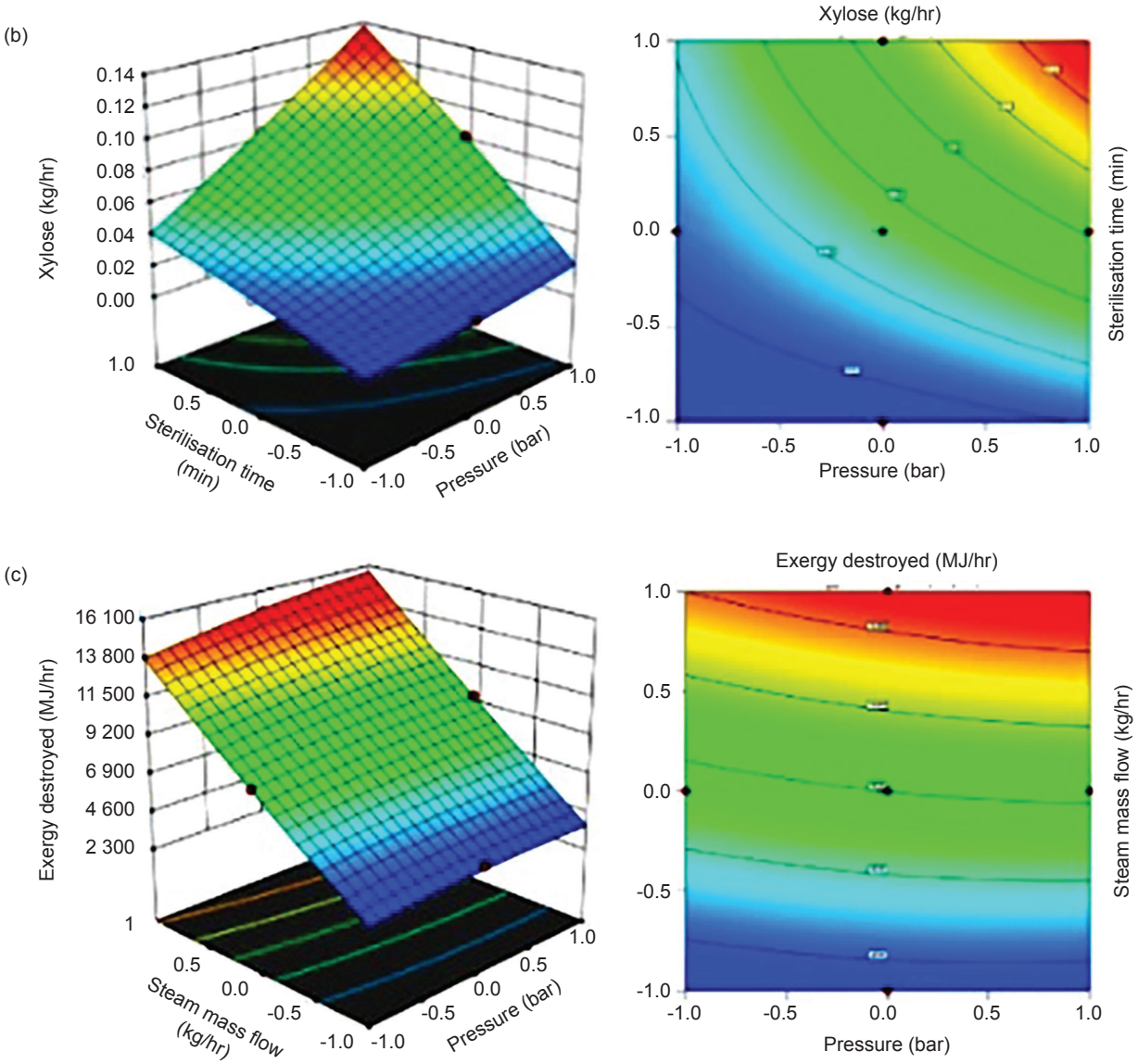


Figure 7. Interactions of (a) sterilisation time against pressure on glucose production, (b) sterilisation time against pressure on xylose production and (c) steam mass flow against pressure on exergy destroyed

ACKNOWLEDGEMENT

The authors would like to express their gratitude to Malaysia Ministry of Higher Education (MOHE) for funding this research through LRGS grant (Vot. No: 5526101). We would also like to acknowledge Universiti Putra Malaysia for providing the facility and supporting our research.

REFERENCES

Anozie, A N and Dzobo, J M (2006). Kinetics of the hydrolysis of palm oil and palm kernel oil. *Ind. Eng. Chem. Res., 45(5)*: 1604-1612.

Ariffin, A A (1984). The biochemical aspects of ripeness standards. *Proc. of the Symposium on Impact of the Pollinating Weevil on the Malaysian Oil Palm Industry*. Kuala Lumpur, Malaysia. p. 165-176.

Ariffin, A A (2011). Ripeness standards and palm fruit maturity affecting oil extraction rate (OER). *International Conference and Exhibition of Palm Oil (ICEPO 2011)*. Jakarta, Indonesia.

Ariffin, A A (2012). High pressure equilibrated sterilisation of fresh fruit bunches (FFB) for zero USB (unstripped fruit bunches) and 5% max. oil to pressed fiber (ODM). *XVII International Oil Palm Conference*. Cartagena, Colombia.

Aziz, M; Oda, T and Kashiwagi, T (2015). Design and analysis of energy efficient integrated crude palm oil and palm kernel processes. *J. Jpn. Inst. Energy, 94*: 143-150.

Braimah, M N; Anozie, A N and Odejobi, O J (2016). Utilisation of response surface methodology (RSM) in the optimisation of crude oil refinery process, New Port-Harcourt Refinery, Nigeria. *JMEST, 3(3)*: 4361-4369.

Cifuentes, B; Figueredo, M and Cobo, M (2017). Response surface methodology and Aspen Plus integration for the simulation of the catalytic steam reforming of ethanol. *Catalysts, 7(1)*: 15.

Corley, R H V and Tinker, P B (2016). *The Oil Palm*. 5th edition. Wiley Blackwell, New Jersey. 680 pp.

Dogbe, E S; Mandegari, M A and Gorgens, J F (2018). Exergetic diagnosis and performance analysis of a typical sugar mill based on ASPEN Plus simulation of the process. *Energy, 145*: 614-625.

Energywise (2013). Selection of steriliser technology for energy efficient operation of palm oil mills. http://rank.com.my/energywise/#sthash.4dvD0T1E.GGrQ0oHc.dpbs, accessed on 28 August 2019.

Feyzi, V and Beheshti, M (2017). Exergy analysis and optimisation of reactive distillation column in acetic acid production process. *Chem. Eng. Process, 120*: 161-172.

Garcia, M; Knuutila, H K and Gu, S (2017). ASPEN PLUS simulation model for CO_2 removal with MRA: Validation of desorption model with experimental data. *J. Environ. Chem. Eng., 5(5)*: 4693-4701.

Gharagheizi, F; Ilani-Kashkouli, P and Hedden, R C (2018). Standard molar chemical exergy: A new accurate model. *Energy, 158*: 924-935.

Hadi, N A; Ng, M H; Choo, Y M and Ma, A N (2012). Dry heating of palm fruits: Effect on selected parameters. *Am. J. Eng. Appl. Sci., 5(2)*: 128-131.

Hinderink, A P; Kerkhof, F P J M; Lie, A B K; De Swaan Arons, J and Van der Kooi, H J (1996). Exergy analysis with a flowsheeting simulator-I. Theory; calculating exergies of material streams. *Chem. Eng. Sci., 51(20)*: 4693-4700.

Hosseini, K and Iranshahi, D (2017). Simulating and optimising the separation process of the gas-to-liquid condensation products by the use of exergy technology. *IJCSNS, 17(11)*: 203-206.

Husin, U N H (2016). *Sugar production from oil palm empty fruit bunch fiber using ultrasonic-assisted two-stage dilute-acid hydrolysis*. MSc thesis, Universiti Putra Malaysia.

Kamarden, H; Kidam, K; Hashim, H; Hassim, M H; Shahlam, S S; Ngadi, N; Johari, A; Kamaruddin, M J and Ten, J Y (2018). Process simulation of integrated palm oil mill, refinery and oleochemical processes. *IOP Conf. Ser. Mater. Sci. Eng., 458*: 012062.

Keshvadi, A; Endan, J; Harun, M H and Taip, F S (2012). The reflection of moisture content on palm oil development during the ripening process of fresh fruits. *J. Food Agric. Environ., 10(1)*: 203-209.

Kong, W; Baeyens, J; Qin, P; Zhang, H and Tan, T (2018). Towards an energy-friendly and cleaner solvent-extraction of vegetable oil. *J. Environ. Manage., 217*: 196-206.

Martínez, D; Puerta, A; Mestre, R; Peralta-Ruiz, Y and Delgado, A G (2016). Exergy-based evaluation of crude palm oil production in North-Colombia. *Aust. J. Basic Appl. Sci., 10(18)*: 82-88.

Menon, N R (2013). Process review: Part 1. *Palm Oil Engineering Bulletin, 108*: 21-24.

Menon, N R (2016). Datasheet-material balance for processing 100 t fresh fruit bunches. *Palm Oil Engineering Bulletin, 121*: 55.

Montgomery, D C (2001). *Design and Analysis of Experiments*. 5th Edition. John Wiley and Sons, New York, USA. 696 pp.

MPOB (2005). *MPOB Test Method*. MPOB, Bangi.

Nadzim, U K H M; Yunus, R; Omar, R and Lim, B Y (2020). Factors contributing to oil losses in crude palm oil production process in Malaysia: A review. *IJBR, 9(1)*: 10-24.

Oi-Ming, L; Chin-Ping, T and Casimir, C A (2012). *Palm Oil: Production, Processing, Characterisation and Uses*. AOCS Press, Urbana. 852 pp.

Parveez, G K A; Tarmizi, A H A; Sundram, S; Loh, S K; Ong-Abdullah, M; Palam, K D P; Salleh, K M; Ishak, S M and Idris, Z (2021). Oil palm economic performance in Malaysia and R&D progress in 2020. *J. Oil Palm Res., 33(2)*: 181-214.

Reese, C D (2009). *Industrial Safety and Health for Infrastructure Services*. CRC Press, Boca Raton. 560 pp.

Ropandi, M; Astimar, A A and Rohaya, M H (2017). Waste minimisation for palm oil mills: A case study. *Palm Oil Engineering Bulletin, 122*: 29-30.

Ruiz-de la Cruz, I; Orozco-Munoz, A; Bonilla-Correa, D and Peralta-Ruiz, Y (2015). Exergy evaluation of biodiesel production from *Eurphobia Lathyris*. *Chem. Eng. Trans.*, *43*: 535-540.

Shehu, U E; Mokhtar, M N; Mohd Nor, M Z; Baharuddin, A S and Nawi, N M (2019). A study on the use of water as a medium for the thermal inactivation of endogeneous lipase in oil of palm fruit. *Energies, 12*: 3981.

Siew, W L (2011). Edible oil processing - production: Palm oil milling process. http://lipidlibrary.aocs.org, accessed on 28 August 2019.

Simarani, K; Hassan, M A; Abd-Aziz, S; Wakisaka, M and Shirai, Y (2009). Effect of palm oil mill sterilisation process on the physicochemical characteristics and enzymatic hydrolysis of empty fruit bunch. *Asian J. Biotechnol., 1*: 57-66.

Thang, Y M; Yunus, R; Mokhtar, M N; Appleton, D R; Asis, A J; Kong, P S; The, H F and Ariffin, A A (2021). Roles and principles of sterilisation process in palm oil mills. *Pertanika J. Sci. & Technol., 29(4)*: 2705-2722.

Wondi, M H; Shamsudin, R; Yunus, R; Baharudin, M S; Aman, M Z and Rahman, A F A (2021). Physical and mechanical properties of sterilized oil palm fruits at different component. AMA - *Agr. Mech. Asia, 52(3)*: 3985-3997.

Yan, L; Zhang, L and Yang, B (2014). Enhancement of total sugar and lignin yields through dissolution of poplar wood by hot water and dilute acid flow through pretreatment. *Biotechnol. Biofuels, 7(76)*.

Yulianto, W A and Panji, D M K (2012). The effect of temperature and time on hydrolisis of palm oil empty fruit bunch and its enzymatically biodegradation for xylose production. *Agroindustrial J., 1(1)*: 15-20.

Journal of Oil Palm Research Vol. 35 (2) June 2023 p. 296-306
DOI: https://doi.org/10.21894/jopr.2022.0066

PECULIAR CRYSTALLISATION BEHAVIOUR OF PALM OIL DURING DRY FRACTIONATION

CREMER, G[1]; DANTHINE, S[1]; BLECKER, C[1] and GIBON, V[2]*

ABSTRACT

Multi-step dry fractionation of palm oil generates fractions with specific physicochemical properties suitable for many food formulations. The present study addresses the pilot scale production of palm olein iodine value 56 starting from palm oil. The aim was to investigate the influence of the tri-saturated triacylglycerol content (StStSt) in palm oil on its crystallisation behaviour. Four StStSt contents were investigated: 7.0%, 7.6%, 8.2% and 9.8%, and the palm oil crystallisation was examined during a period of 240 min. Oil temperatures were recorded, and crystallisation kinetics were monitored by p-NMR; crystal morphology and polymorphic forms were characterised by optical microscopy and powder X-ray diffraction. One of the compositions (StStSt: 7.6%) was crystallising faster. All the crystallised matrices were filtered at 25°C with a membrane press filter; the olein yields, iodine values, cloud points and triacylglycerol compositions were analysed. The olein from the matrix crystallising faster showed a yield, an iodine value and a cloud point higher than expected. A more detailed HPLC analysis of this olein indicated unusual enrichment in OPP and depletion in OPO, which led to the conclusion of an unusual crystallisation behaviour at this specific composition.

Keywords: dry fractionation, palm oil, palm olein, peculiar crystallisation behaviour, tri-saturated triacylglycerols.

Received: 10 February 2022; **Accepted:** 3 August 2022; **Published online:** 19 October 2022.

INTRODUCTION

Edible oils are made up of a wide variety of triacylglycerols (TAGs) with diverse fatty acid (FA) compositions, leading to complex physicochemical behaviour. TAGs can be classified according to their saturation: The tri-saturated (StStSt), the di-saturated (St_2U), the di-unsaturated (StU_2) and the tri-unsaturated (UUU). In palm oil (PO), tripalmitin (PPP), oleo-dipalmitin (P_2O), palmito-diolein (PO_2) and trilolein (OOO) are the most abundant of each class. PO crystallisation behaviour has important implications in the manufacture of many edible fatty products like margarine, spreads or shortenings.

Crystallisation operates in two steps: Nucleation followed by crystal growth. The driving force for nucleation is determined by the degree of supersaturation of the liquid. PO crystallisation has been extensively reviewed by Omar *et al.* (2015). The authors described the effect of chemical composition, crystallisation conditions and the presence of additives. They also focussed on crystallisation kinetics, thermal properties, polymorphism and recrystallisation aspects. Braipson-Danthine and Gibon (2007) reported a relationship between melting properties, polymorphism and TAG composition of PO and fractions. De Oliveira *et al.* (2014), Saberi *et al.* (2011) and Siew and Ng (1999) studied the effect of diacylglycerol (DAG) content on PO nucleation and crystal growth. Basso *et al.* (2010) and Verstringe *et al.* (2013; 2014) characterised the effects of PPP and monoglycerides (MAG) on crystal formation. Fredrick *et al.* (2008) studied the influence of MAG on the crystallisation behaviour of PO. Saadi *et al.* (2012) reported that 1,2-dipalmitoyl-3-oleoyl glycerol/1,3-dipalmitoyl-2-oleoyl glycerol (PPO/POP) were the major components of the primary nucleus developed during the crystallisation of PO and palm stearin (PS) blend systems. The influence of sorbitan esters and soya lecithin in PO blends were studied by Kwamura (1980) and Miskandar *et al.* (2006; 2007). The effects of polyglycerol behenic acid esters on PO crystallisation were described by Sakamoto *et al.* (2003) and of polyglycerol ester additives by Saw *et al.* (2017), using focused beam reflectance (FBRM)

[1] Food Science and Formulation, Gembloux Agro-Bio Tech, ULiège, Gembloux Belgium.

[2] Desmet Ballestra Group, R&D Center, Zaventem, Belgium.

* *Corresponding author e-mail: VGibon@desmetballestra.com*

and differential scanning calorimetry (DSC). The influence of high-intensity ultrasound (HIU) on PO crystallisation was investigated by Fangfang *et al.* (2013) and Yubin *et al.* (2015). Hubbes *et al.* (2018) studied the crystallisation of PO-PS blends to obtain fats with higher PPP contents and PPP/OOO ratios; they showed that the global rate constant of the enriched PO increased with the addition of PPP. PO is a good candidate for dry fractionation, which was extensively reviewed by Deffense (1985), Gibon and Tirtiaux (2002), Gibon (2006; 2012), Gibon *et al.* (2009; 2020), Kellens *et al.* (2007), Mei Huey *et al.* (2015), Tong *et al.* (2021) and Zaliha *et al.* (2004).

Multi-step dry fractionation generates a large number of solid and liquid fractions with specific physico-chemical properties; it shows three steps, and three different routes that can be followed (*Figure 1*); the solid route (for PPP enrichment), the hard palm mid fraction (HPMF) route (for P_2O enrichment) and the liquid route (for PO_2/OOO enrichments). In dry fractionation, crystallisation is followed by crystal separation typically using membrane press filters. Chong *et al.* (2014a; 2014b; 2015) described technology for higher olein yield using a special cooling programme and additional steps mid-way. Deffense (2009) proposed an ultrasound seeding technique for improved crystallisation. Kuriyama *et al.* (2011) showed that the addition of polyglycerol ester additives enhances the olein yield and alters the fractions characteristics. Tong *et al.* (2021) reviewed the fractionation conditions that affect the yield and quality of the oil produced and published updates on the influence of seeding agents (DAG, hard fats, *etc.*) used in fractionation.

In industrial practice, a quantity of StStSt is classically added to palm olein, to ensure an efficient and reproducible crystal initiation for superolein production (Calliauw *et al.*, 2007a; 2007b; 2010). On the contrary, the naturally existing StStSt content of PO permits crystal initiation. In this work, the influence of the StStSt content on PO crystallisation is explored. PO was blended with PS and matrices containing variable contents of StStSt were considered. Crystallisation kinetics were established, operation yields were quantified and the quality of the olein fractions was analysed. The aim of this paper is to highlight and explain a particular crystallisation behaviour observed unexpectedly while studying the effect of StStSt on the crystallisation of PO during dry fractionation.

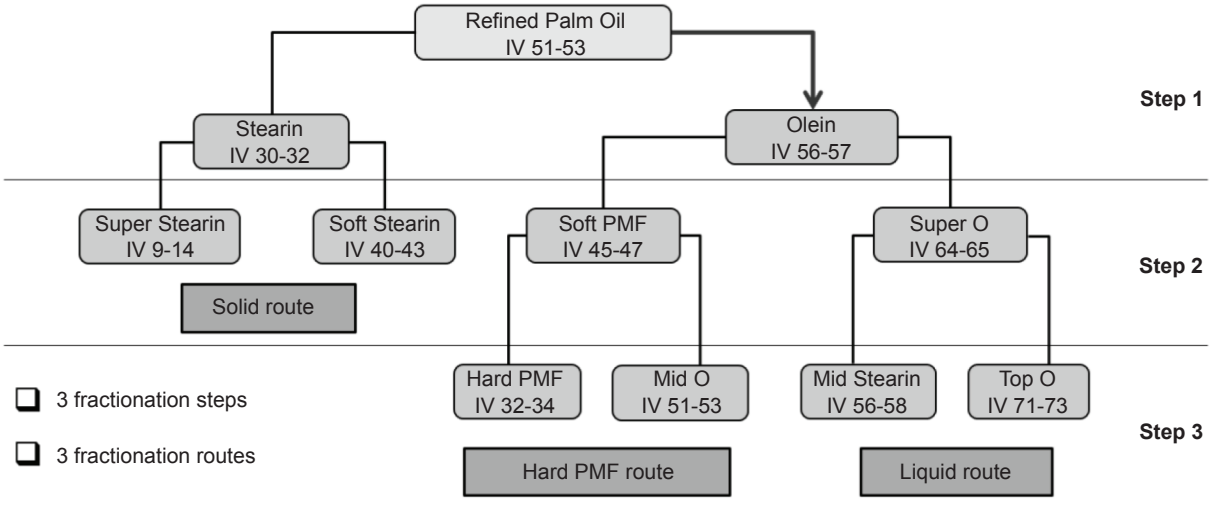
MATERIALS AND METHODS

Materials

PO was supplied by Fuji Oil Europe (Ghent, Belgium); refined PS was provided by Desmet Ballestra Group (Zaventem, Belgium). Increasing amounts of PS were added to PO in order to reach StStSt TAGs contents of 7.0%, 7.6%, 8.2% and 9.7% in matrices named M1, M2, M3 and M4 respectively (= internal seeding). To this end, PS was first placed in an oven at 80°C to ensure a complete melting before being mixed with PO. The appropriate quantity was weighed into a preheated glass beaker and then added as liquid in the melted PO in the crystalliser.

Crystallisation

Crystallisation was performed in a 30 kg capacity pilot-scale crystalliser having an exchange surface of approximately 15 m^2/T; all the tests were carried out with a total oil quantity of 20 kg. The crystalliser was a cylindrical stainless-steel double-jacketed



Source: Gibon and Danthine (2020).

Figure 1. Multi-step dry fractionation of palm oil.

tank connected to an external programmable water bath for controlling the temperature. The agitation was conducted by a double-bladed rotor. The oil temperature was measured by a Pt100 probe which was dipped into the oil. Cooling programmes controlling water temperature, oil temperature, and Δ oil/water temperature were applied using the Citect SCADA RunTime application (Citect, Australia). The cooling programme (13 parameters) was first optimised for each system to ensure minimal oil temperature increase during the crystal growth. The oil melting temperature was 75°C, the time allocated for crystal initiation and growth (main crystallisation) was 240 min, and the final temperature was set at 25°C (*Figure 2*). The crystallisation tests were conducted in triplicate.

Vacuum and Membrane Press Filtrations

The separation of the crystals from the liquid was done by vacuum filtrations (Büchner) and by membrane press filtrations (lab press filter). Vacuum filtrations were performed at regular intervals (every 30 min) during the main crystallisation and press filtrations were only done at the final cooling temperature (25°C).

Vacuum filtrations. Approximately 100 mL of oil were sampled from the crystalliser and immediately filtered over a Büchner (55 mm diameter) covered with filter cloth (500 L $min^{-1}.dm^{-2}$ at 196 Pa) and connected to a vacuum by means of an MZ 2C NT vacuum pump (Vacuubrand, Germany). The filtrations were stopped based on visual observation of cake dryness.

Membrane press filtrations. Press filtrations were performed with a single chamber lab-scale membrane press filter (Choquenet S.A.S., France) covered with the same filter cloth as for vacuum filtrations. The diameter of the chamber was 5.6 cm and the width was 20 mm. The filter was filled with a volume of approximately 200 mL of oil sampled in the crystalliser (at 25°C). Air pressure, which gradually increased by 0.5 bar min^{-1} to 3 bar, was used for filling; it was then held at this value for 15 min. Afterwards, additional pressure was applied to squeeze the cake by gradually increasing the air pressure by 1 bar every 2 min to 6 bar. The squeezing pressure was held at this value for 10 min. The olein was collected in vessels and the stearin cake was recovered after opening the filter. The operation yield was derived from weighing the recovered fractions.

Monitoring of the Crystallisation by Pulsed Nuclear Magnetic Resonance (pNMR)

The kinetics of crystallisation was established by measuring the solid fat content (SFC) of the crystallising oil as a function of the time using p-NMR (Minispec-mq20, Germany). Daily calibrations were performed with three standards containing 0.0%, 31.1% and 74.8% of solids, respectively. NMR tubes were filled with crystal slurry directly from the crystalliser using a glass tube with a tight-fitting plunger (Danthine *et al.*, 2003 and Danthine, 2012) and the SFC was immediately measured.

Microstructure by Optical Microscopy

For each sampling, crystal microstructure was observed by optical microscopy (OM) using a microscope coupled to a camera transmitting live images to a computer. The crystals were observed using an Eclipse E400 microscope (Nikon, Japan) equipped with a DS-Fi2 camera (Nikon, Japan).

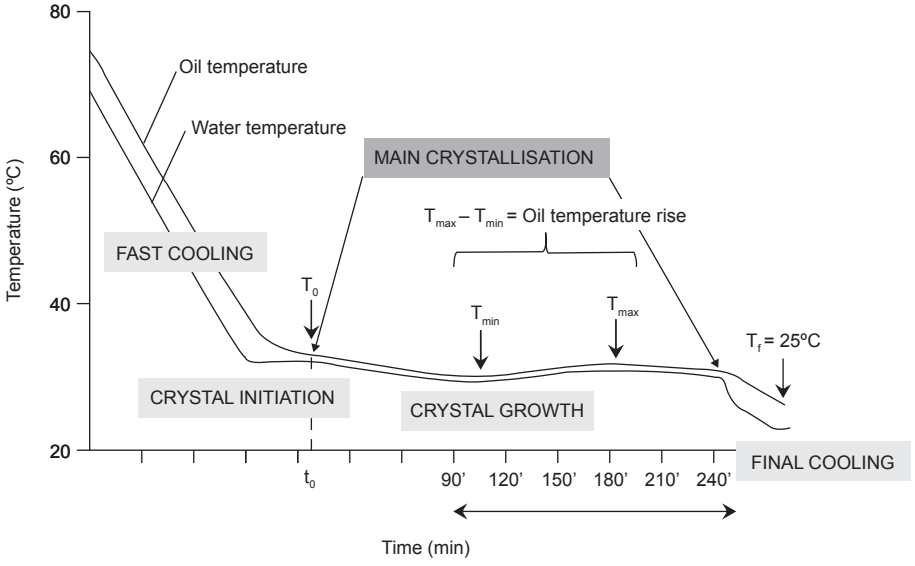


Figure 2. Schematic cooling curve with fast cooling, crystal initiation, crystal growth and final cooling steps.

The pictures were processed using NIS-elements 4.30 software (Nikon, Japan). A magnification of 20x was selected to analyse the pictures. One droplet of crystal slurry was randomly sampled from the NMR tube with a glass Pasteur pipette; it was then put on a microscope slide. A cover slip was carefully placed and centred over the drop of the sample to ensure homogeneity of the sample thickness. For each sampling, images of crystal microstructures were taken in triplicate.

Polymorphism by Powder X-ray Diffraction (XRD)

The polymorphic forms of the crystals were determined by XRD using a Bruker D8-Advance Diffractometer and a Lynx-eye detector (Bruker, Germany) (λ Cu= 1.5406, 40kV, 30mA). Calibration was performed using corundum, silver behenate, and tristearin standards. The X-ray diffraction patterns were analysed using DIFFRAC.EVA V4.2.2 software (Bruker, Germany). Crystals were placed on a sample holder directly after the vacuum filtration and immediately analysed. Small-angle X-ray diffraction patterns (long spacings) were investigated from $2\theta = 1°$ to 10° with 452 steps and a time per step of 0.2 s. Wide-angle X-ray diffraction patterns (short spacings) were investigated from $2\theta = 15°$ to 27° with 603 steps and at 0.5 s per step. The total duration of a run was approximately 7 min.

Composition by Reversed-Phase High-performance Liquid Chromatography (RP-HPLC)

The DAG content and the TAG composition were analysed by RP-HLPC based on the official AOCS Ce 5b-89 method (AOCS, 2017), which does not distinguish between positional isomers. Analyses were performed with a Waters e2695 HPLC system (Waters, USA), equipped with two stainless steel Nova-Pak C18 columns (4 μm, 3.9 × 150 mm). The mobile phase was an isocratic solvent [mixture of acetone and acetonitrile (62.5/37.5 v/v)] with a flow rate of 1.2 mL min^{-1}; the injection volume was 20 μL. The samples were dissolved in methanol/chloroform (1/1 v/v) and a differential refractometer was used for the detection. The assignment was confirmed by comparing retention times with those of some standards. Peaks were integrated with Empower Pro "Apex Track" algorithm (Waters, USA); peak areas below 4000 area counts (equivalent to approximately 0.04% of the total peak area) were not considered. The mean of two independent measurements is reported.

Iodine Value (IV) by Titration

The IV was determined by titration based on the official method AOCS Cd 1d-92 (Wijs method) (AOCS, 2017). The mean of two measurements is reported.

Cloud Point (CP) by Differential Scanning Calorimetry (DSC)

DSC analyses were carried out using a Q-2000 DSC (TA Instruments, USA) coupled with a refrigerated cooling system (TA Instruments, USA), using aluminium hermetic pans. Calibration was made with indium (melting point 156.6°C; $\Delta H = 28.7$ J g^{-1}) and eicosane (melting point 36.8°C; $\Delta H = 247.4$ J g^{-1}) standards. Nitrogen was used as a purge gas to prevent condensation in the cells. Samples (8-10 mg) were hermetically sealed in aluminium pans; an empty pan was used as a reference.

The crystallisation onset temperatures of the four matrices (M1, M2, M3 and M4) were determined as the intersection of the baseline with the absolute highest tangent of the first crystallisation exotherm. The following time-temperature program was applied: (1) heating to 80°C at 15°C min^{-1} and holding for 10 min to erase the thermal memory, (2) cooling at -0.5°C min^{-1} to -60°C. This cooling rate of 0.5°C min^{-1} was used to mimic the slow cooling conditions used during fractionation.

The CP of the different olein obtained after filtration was determined as the intersection of the baseline with the absolute highest tangent of the first crystallisation exotherm, according to the following time-temperature program: (1) heating to 80°C at 15°C min^{-1} and holding for 10 min at 80°C to erase the thermal memory, (2) cooling to 30°C at -25°C min^{-1}, holding this temperature for 2 min and finally cooling down to -25°C at a rate of -3°C min^{-1}. All DSC measurements were done in triplicate.

Positional Isomerism by Silver Ion High-performance Liquid Chromatography - Mass spectroscopy (Ag-HPLC-MS)

The positional isomerism of some TAGs from selected olein was determined by Ag-HPLC-MS, as described by Santoro *et al.* (2018). This separation technique uses columns where silver ions are bound to the stationary phase and rely on the ability of the π electrons of unsaturated fatty acids to react with silver ions to form polar complexes. The separation system was an HPLC Ultimate 3000 (Thermo Fisher Scientific, Italy) interfaced through an APCI ionisation source to a linear ion trap coupled to a high-resolution mass analyser (LTQ-Orbitrap Thermo Fisher Scientific, Italy). The ionisation source was heated at 450°C and used in positive ions mode. The instrument was equipped with a silver-modified cation exchange column (Luna SCX, Phenomenex, 150 × 2.0 mm, 5 μm, 100 Å). A gradient separation made up of two isocratic steps at different mobile phase compositions (*n*-heptane:ethylacetate 93:7 and 90:10) was used. The flow rate was 0.300 mL min^{-1}, and the injection volume was 10.0 μL. The mean of two measurements is reported.

Statistical Analyses

Data were statistically analysed using Minitab 19 software (Minitab LLC, USA). All assays were conducted in triplicate unless otherwise specified. Means and standard deviations were calculated and differences between means were determined with a significance level of α=0.05.

RESULTS AND DISCUSSION

Compositional properties by HPLC, IVs by titration and crystallisation onsets by DSC of the 4 matrices are listed in *Table 1*. The major StStSt TAG was PPP, followed by P_2S (S: stearic acid); the StStSt content increased gradually from 7.0% in M1 to 9.8% in M4. On the contrary, the DAG content was slightly reduced from 9.3% to 8.9% due to the lower DAG content in the stearin. The IV decreased from 52.1 to 49.9. The crystallisation onset shifted towards higher temperatures; this shift could only be attributed to the nucleation effect of higher amounts of StStSt in the matrices.

The crystallisation behaviour of PO was investigated during pilot scale dry fractionation. A water-cooling program was applied, and the oil temperature response was recorded. The crystallised oil was sampled at regular intervals and the SFC was immediately measured by p-NMR; this gave an insight into the rate of crystallisation in the different matrices. At the same time, a microstructural analysis was performed by optical microscopy. Vacuum filtrations were carried out to recover the olein, the composition of which was determined by HPLC, and the polymorphism of the crystals by powder X-ray diffraction. *Figure 2* represents the cooling curves, with water and oil temperatures plotted as a function of time. After fast cooling, the oil was brought into supercooling conditions for crystal initiation and the crystal growth was examined for 240 min. This period was called "main crystallisation". T_0 was the oil temperature at the beginning of the main crystallisation step. Due to crystallisation exothermicity, some heat was released during the crystal growth. When this heat released by crystallisation exceeded the heat of dissipation capacity of the crystalliser, a rise in oil temperature was observed. T_{max} and T_{min} corresponded to the minimum and maximum oil temperatures observed during the crystal growth respectively. After 240 min of main crystallisation, the oil was cooled down to 25°C (T_f) before proceeding to membrane press filtration.

Figure 3a shows the oil temperature rise (T_{max} - T_{min}) during the main crystallisation for the four matrices. This temperature rise was particularly important for M3 and M4 having the highest StStSt contents. A sharp increase was observed between M2 and M3 and the highest value was detected for M4 (≈1.8°C). *Figure 3b* illustrates the minimum oil temperature achieved during the main crystallisation before the rise (T_{min}); this temperature increased with the StStSt content, sharply from M1 to M2, and then gradually from M2 to M4. The ΔT_{min} between M1 and M4 was ~5°C. The time before the oil temperature rise was also determined (*Figure 3c*); it was significantly shorter for M2, M3 and M4 compared to M1 (*p*-values <0.05), and M2 had the highest reduction (40 min). In all cases, the crystallisation exothermicity caused a rise in oil temperature during the crystal growth. This rise was more important and occurred at higher temperatures in the matrices with higher StStSt content. It led to partial crystal melting, affecting the crystal slurry quality, especially for M3 and M4. The time before the temperature rise was shorter for higher StStSt contents but surprisingly, M2 showed the shortest time tending to indicate a faster crystal initiation.

Figure 4a presents the SFC of the crystallising oils determined by p-NMR as a function of time during the main crystallisation where M3 and

TABLE 1. TRI-SATURATED TRIACYLGLYCEROL AND DIACYLGLYCEROL CONTENTS, IODINE VALUES (WIJS) AND CRYSTALLISATION TEMPERATURE ONSETS FOR M1, M2, M3 AND M4

	M1	M2	M3	M4
TAG (% HPLC)				
MP_2	0.5	0.5	0.5	0.5
PPP	5.1 (+/- 0.1)	5.6 (+/- 0.0)	6.1 (+/- 0.0)	7.5 (+/- 0.1)
P_2S	1.2 (+/- 0.1)	1.2 (+/- 0.1)	1.3 (+/- 0.1)	1.5 (+/- 0.1)
PS_2	0.1	0.2	0.2	0.2
SSS	0.1	0.1	0.1	0.1
Total StStSt	7.0 (+/- 0.1)	7.6 (+/-0.0)	8.2 (+/- 0.0)	9.8 (+/- 0.1)
DAG (% HPLC)	9.3 (+/- 0.1)	9.2 (+/- 0.1)	9.1 (+/- 0.0)	8.9 (+/- 0.1)
IV (Wijs)	52.1 (+/ -0.2)	51.6 (+/- 0.2)	51.2 (+/- 0.2)	49.9 (+/- 0.2)
Crystallisation temperature onset (°C by DSC)	22.3 (+/- 0.1)	25.1 (+/- 0.1)	26.0 (+/- 0.1)	27.7 (+/- 0.1)

Note: DAG - diacylglycerol; TAG - triacylglycerol; M - myristic acid; P - palmitic acid; S - stearic acid; St - saturated fatty acids.

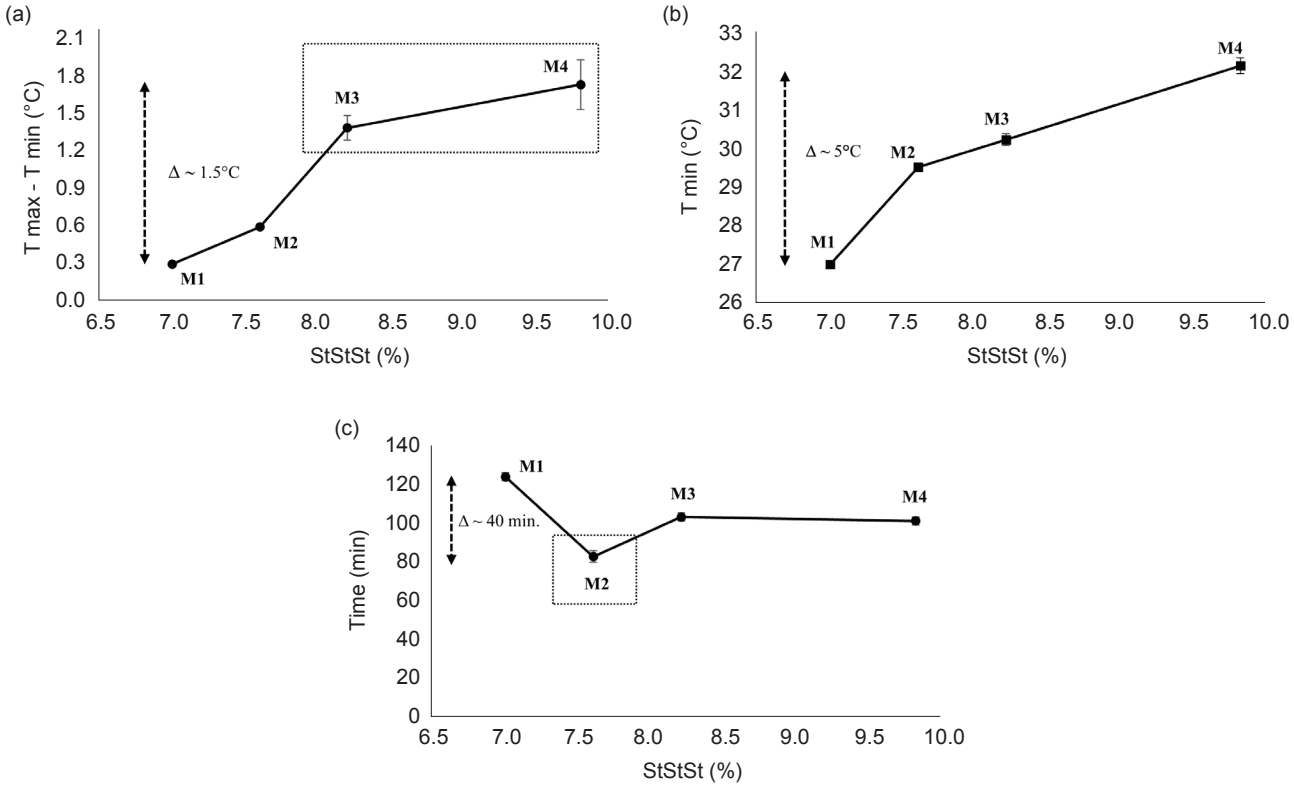


Figure 3. (a) Oil temperature rise ($T_{max} - T_{min}$), (b) minimal oil temperature and (c) time before oil temperature rise during the main crystallisation for the four matrices.

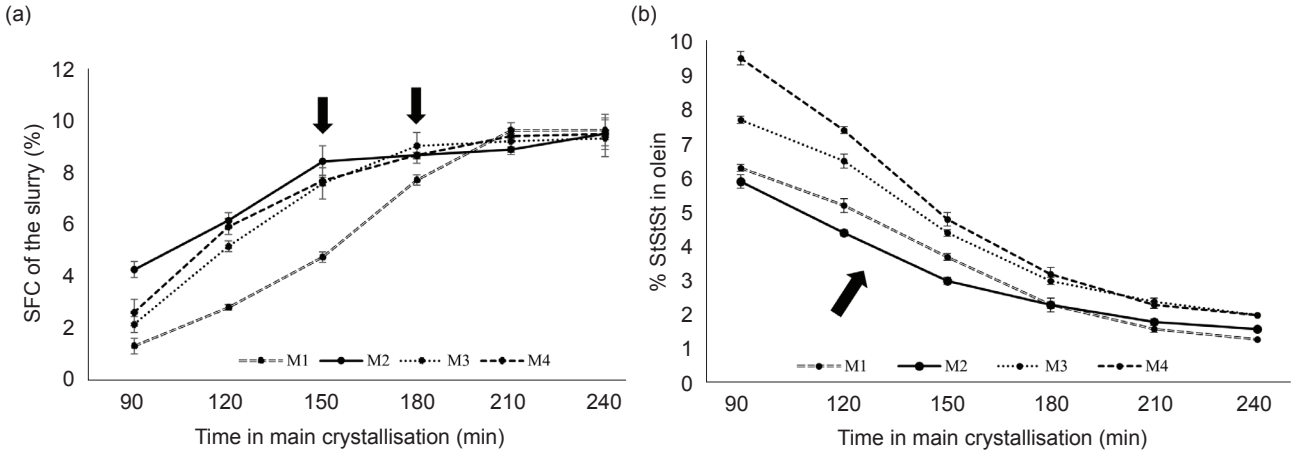


Figure 4. (a) SFC of the crystallising oils by p-NMR and (b) StStSt content of the olein by RP- HPLC as function of the time during the main crystallisation of the four matrices.

M4 crystallised faster than M1. However, their crystallisation kinetics slowed down starting at 180 min. Interestingly, M2 presented the highest SFC from 90 min, reaching a plateau after 150 min. The final SFC after 240 min was similar (~ 9%) for all the matrices. The crystallising oil was filtered under vacuum every 30 min, and the composition of the collected olein was evaluated by RP- HPLC. The residual StStSt content in the olein is shown in *Figure 4b*. This content was higher in M3 and M4 oleins, in relation to the higher content in the initial matrices. However, the residual content in M2 olein was lower than in M1 olein after 90 min.

Polymorphism of the crystals was evaluated every 30 min during the main crystallisation. M1 and M2 showed β' polymorphism during the main crystallisation time, with WAXD peaks at 4.3 Å, 4.2 Å, 4.0 Å and 3.8 Å (*Figure 5*). In both cases, a double-chain length packing was observed (β'-2L). M3 started to crystallise in β'-2L as well but a β form was observed after 210 min, with WAXD peaks at 3.9 Å and 4.6 Å. The β form also corresponded to

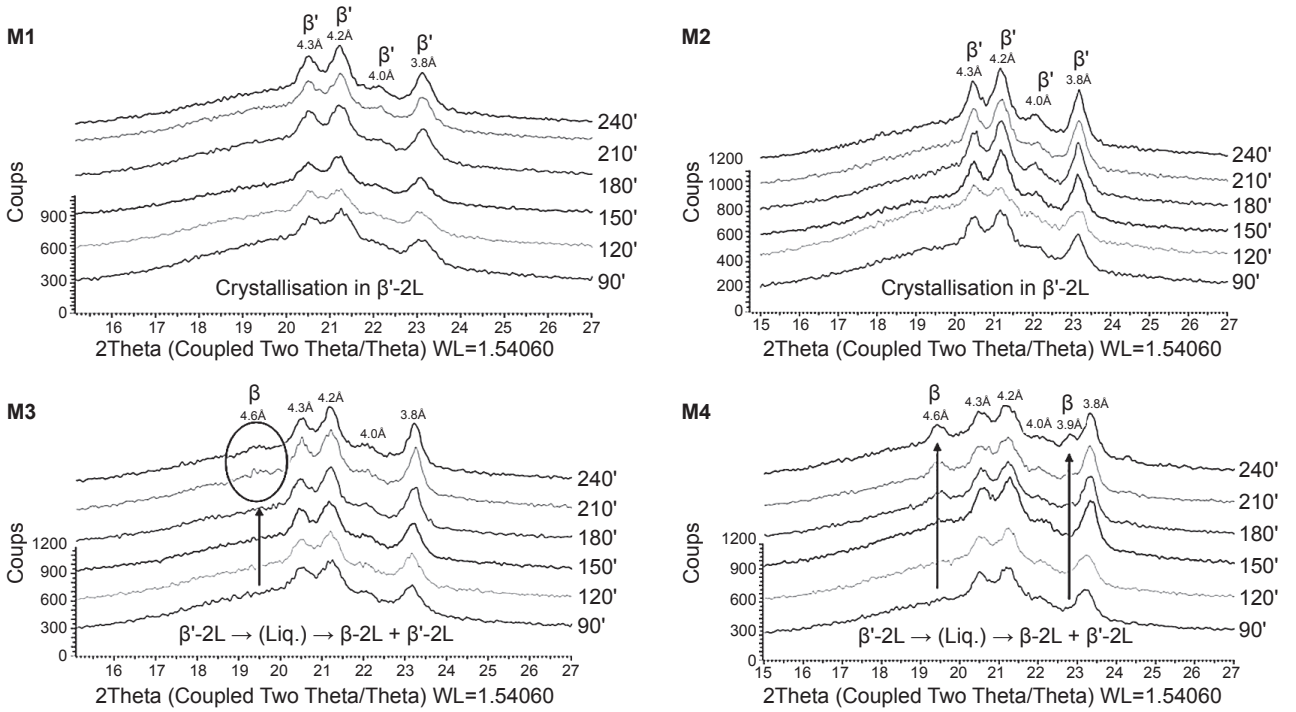


Figure 5. Powder X-ray diffraction patterns of M1, M2, M3 and M4 crystals as function of time during the main crystallisation.

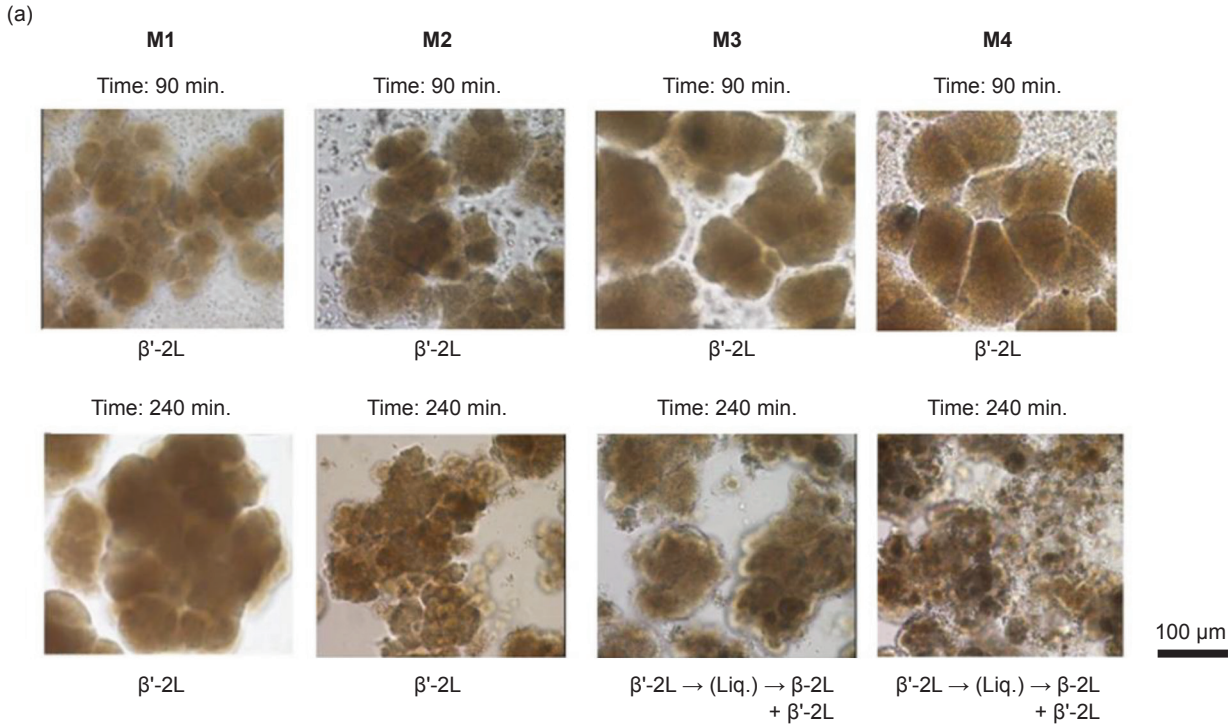
double chain length packing. The appearance of this β-2 form was accompanied by a slight decrease in the intensity of the β'-2L peaks. The same was seen for M4 with the β-2 peaks appearing already after 180 min. This β form most probably resulted from re-crystallisation of partially melted β'-2L crystals.

Crystal morphology was observed by optical microscopy, and the differences observed are illustrated in *Figure 6a*. After 90 min of crystallisation, bigger crystals were formed in M3 and M4, which are the matrices with higher StStSt content (≈ 150-250 μm, compared to 50-150 μm for M1 and M2). M1 showed aggregates with cauliflower-like morphology, growing from 90 to 240 min. After 240 min, M2 presented a particular morphology with aggregates made of small round-shaped structures and well-defined smaller urchin-like shaped crystals (≈ 25-50 μm) growing on the external surface (see arrows in *Figure 6b*). Very small crystals were also visible in the bulk. M3 and especially M4 crystals were more dislocated in consequence of the partial crystal melting as previously mentioned. Crystal size of M3 did not change over time (150-250 μm). However, a less dense layer was observed on crystal surface, due to re-crystallisation of the liquid phase in β-2L arising from partial melting of β'-2L crystals. A much more disaggregated structure was observed for M4, but still with this less dense layer on the crystal surface (β crystals on the surface of the β' ones).

Membrane press filtrations were carried out at 25°C (final cooling temperature). The olein yields were calculated based on the collected stearin and olein fractions. Results are presented in *Figure 7a*. The increase in StStSt content is associated with a decrease in olein yield; a Δyield of ≈ -12% is observed between M1 and M4. M3 (73.0 ± 1.6%) and M4 (64.2 ± 0.9%) matrices have significantly lower olein yield compared to M1 (76.1 ± 0.5%) (*p*-value = 0.0304, and 0.0001 respectively). The same is expected for M2 but this is not the case; the olein yield is even slightly higher in M2, highlighting again the unexpected behaviour of this matrix. The IVs by Wijs and cloud point by DSC of the oleins are presented in *Figures 7b* and *7c*. Oleins from M3 and M4 had higher IV which correlated to lower yield. The IV of M2 olein was the highest and was significantly higher compared to M1 olein (*p*-value=0.0017). In general, oleins with a higher IV are characterised by a lower CP. This is not the case for M2 olein, which has the highest CP while having a higher IV.

The olein compositions were analysed by RP-HPLC; the StStSt, St2U, StU2, UUU and DAG contents are presented in *Table 2*. The StStSt and DAG contents decreased from M1 to M4, whereas the unsaturated (UUU) and di-unsaturated (StU2) contents increased. However, the St2U content was weakly modified. Both DAG contents and TAG compositions were in line with normal variations of the IV and the cloud point.

M2 olein has an unusual behaviour. It combines a yield higher than expected with a higher IV and a higher CP. The RP-HPLC profiles did not show any peculiar composition associated with M2 olein. However, this technique does not allow the



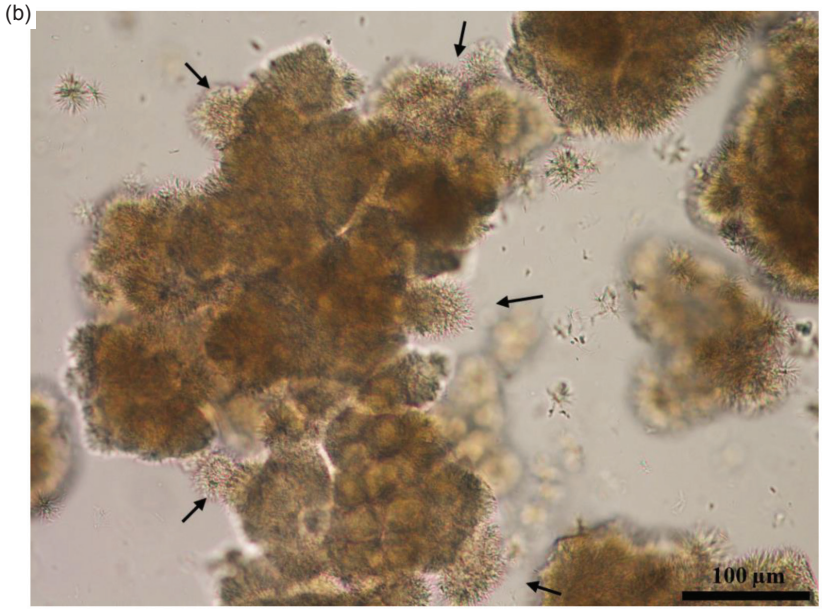


Figure 6. (a) Morphology of M1, M2, M3 and M4 crystals as function of time during the main crystallisation and (b) morphology of M2 crystals after 240 min of main crystallisation.

TABLE 2. TRI-SATURATED, DI-SATURATED, DI-UNSATURATED AND TRI-UNSATURATED TAG CONTENTS IN THE OLEIN FROM M1, M2, M3 AND M4 AFTER PRESS FILTRATION AT 25°C

	Olein from M1	Olein from M2	Olein from M3	Olein from M4
TAG (% HPLC)				
StStSt	1.2 (+/- 0.0)	1.1 (+/- 0.1)	1.0 (+/- 0.0)	0.8 (+/- 0.0)
St_2U	44.3 (+/- 0.0)	44.7 (+/- 0.1)	44.8 (+/- 0.1)	44.8 (+/- 0.1)
StU_2	38.0 (+/- 0.3)	38.4 (+/- 0.1)	38.6 (+/- 0.0)	38.9 (+/- 0.1)
UUU	5.9 (+/- 0.1)	6.0 (+/- 0.0)	6.0 (+/- 0.1)	6.1 (+/- 0.0)
DAG (% HPLC)	10.6 (+/- 0.1)	9.7 (+/- 0.1)	9.5 (+/- 0.0)	9.4 (+/- 0.0)

Note: DAG - diacylglycerol; TAG - triacylglycerol; St - saturated fatty acids; U - unsaturated fatty acids.

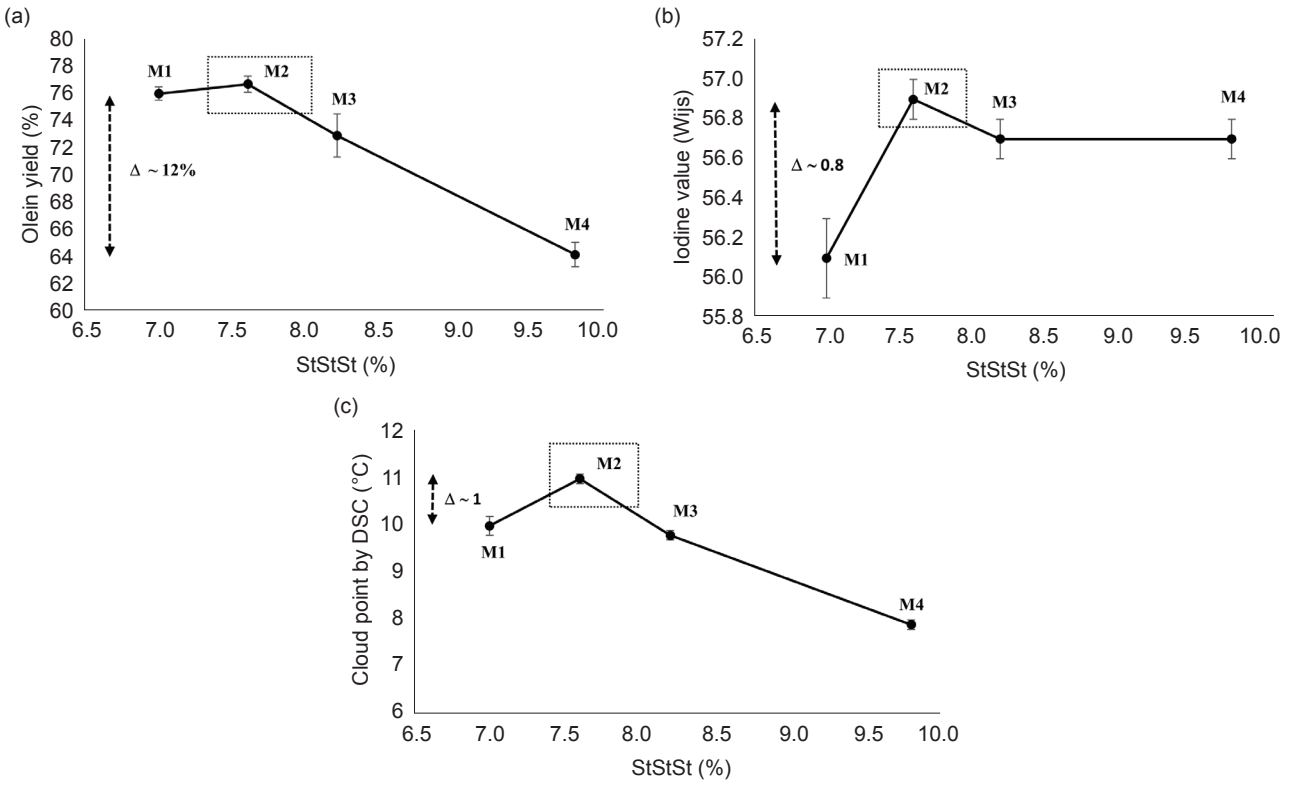


Figure 7. (a) Olein yield, (b) iodine value and (c) cloud point by DSC of the olein collected after membrane press filtrations at 25°C of the four matrices.

differentiation of positional isomers. In order to identify the reasons for the peculiar behaviour of M2 olein, oleins from M1, M2, M3 and M4 were analysed by Ag-HPLC. This technique is the most reliable for the regioisomeric separation of TAG. P_2O and PO_2, the most abundant TAGs, were highlighted and the corresponding 1,3-dipalmitoyl-2-oleoyl glycerol/1-oleoyl-2,3-dipalmitoyl glycerol (POP/OPP) and 1,2-oleoyl-3-palmitoyl glycerol/1,3-dioleoyl-2-dipalmitoyl glycerol (POO/OPO) contents were calculated as reported in *Figures 8a* and *8b*. The relative percentage of OPP was higher and the one of OPO lower in the olein from M2 compared to the other matrices. These differences are highly significant (p-values=0.0009 and 0.0002 for OPP and OPO respectively), thus confirming our hypothesis that the atypical behaviour of M2 olein arises from differences in positional isomers.

CONCLUSION

This study showed that the StStSt content in palm oil has a significant impact on crystal initiation and crystal growth. Control of the oil temperature increase was more difficult for high StStSt contents (matrices M3 and M4), inducing a partial melting of the initially formed β′-2L crystals. The resulting

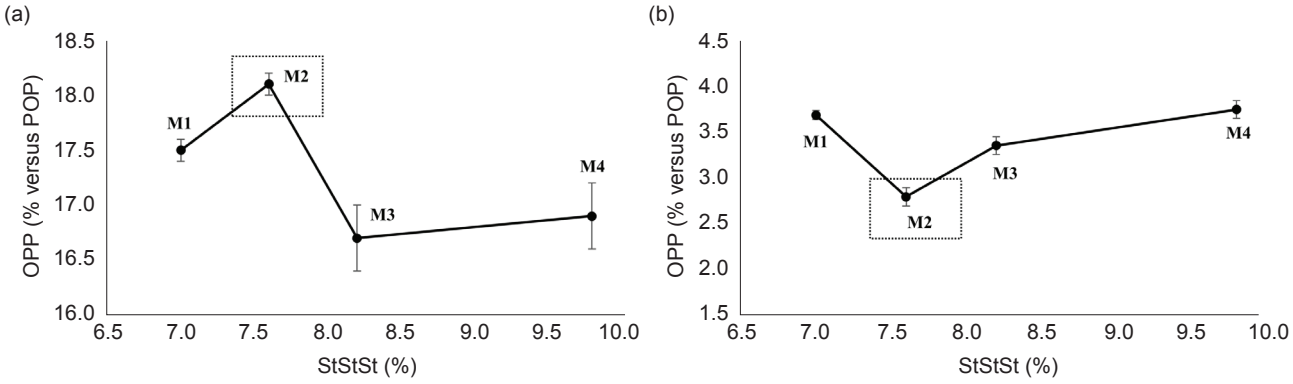


Figure 8. Percentage of (a) OPP vs. *POP and (b) OPO* vs. *POO (by Silver ion HPLC-MS) in olein after press filtration at 25°C.*

liquid is then further recrystallised in β-2L, leading to a mix of β′ and β polymorphic forms. Although crystallising both in β′ form, M1 and M2 had different crystal morphology. The time before temperature rise was the shortest for M2; M2 also crystallised faster than the other matrices and its StStSt content was more efficiently removed in the olein during vacuum filtrations. The highest IV and the highest cloud point as well as a higher yield than expected were observed for M2 olein after press filtration at 25°C, which is atypical behaviour. RP-HPLC could not explain this unusual behaviour; however, Ag-HPLC showed significantly more POP and less OPO in the M2 olein. A particular $PPP/P_2O/PO_2$ co-crystallisation behaviour at M2 composition explains the atypical behaviour of the M2 matrix during crystallisation to produce olein IV 56.

ACKNOWLEDGEMENT

The authors would like to thank Dr. E. Forte, R&D Manager, Soremartec Italy srl Ferrero Group, Italy and the department of molecular biotechnology and health sciences, University of Turin Italy for the silver ion HPLC analyses.

REFERENCES

AOCS (2017). Official Methods and Recommended Practices of the American Oil Chemist's Society. 7th edition. Champaign, AOCS Press.

Basso, R C; Ribeiro, A P B; Masuchi, M H; Gioielli, L A; Goncalvez, L A G; Dos Santos, A O; Cardoso, L P and Grimaldi, R (2010). Tripalmitin and monoacylglycerols as modifiers in the crystallization of palm oil. *Food Chem., 122(4)*: 1185-1192.

Braipson-Danthine, S and Gibon, V (2007). Comparative analysis of melting properties, polymorphic behavior and triacylglycerol composition of palm oil and fractions. *Eur. J. Lipid Sci. Technol., 109(4)*: 359-372.

Calliauw, G; Gibon, V; De Greyt, W; Plees, L; Foubert, I and Dewettinck, K (2007a). Phase composition during palm olein fractionation and its effect on soft PMF and superolein quality. *J. Am. Oil Chem. Soc., 84*: 885-891.

Calliauw, G; Gibon, V and De Greyt, W (2007b). Principles of palm olein fractionation: A bit of science behind the technology. *Lipid Technol., 19(7)*: 152-155.

Calliauw, G; Fredrick, E; Gibon, V; De Greyt, W; Wouters, J; Foubert, I and Dewettinck, K (2010). On the fractional crystallization of palm olein: Solid solutions and eutectic solidification. *Food Res. Int., 43(4)*: 972-981.

Chong, C L and Yeoh, C B (2014a). Process for fractionating refined triglyceride oil. *US Patent*, US8791283B1.

Chong, C L and Yeoh, C B (2014b). Process for fractionating crude triglyceride oil. *US Patent*, US8962874B2.

Chong, C L and Yeoh, C B (2015). Offer for technology adoption of MPOB modified fractionation programme for increased olein yield. *Palm Oil Development, 60*: 24-27.

Danthine, S and Deroanne, C (2003). Physical and textural characteristics of hydrogenated low-erucic acid rapeseed oil and low-erucic acid rapeseed oil blends. *J. Am. Oil Chem. Soc., 80(2)*: 109-114.

Danthine, S (2012). Physicochemical and structural properties of compound dairy fat blends. *Food Res. Int., 48(1)*: 187-195.

Deffense, E (1985). Fractionation of palm oil. *J. Am. Oil Chem. Soc., 62(2)*: 376-385.

Deffense, E (2009). Method for continuous crystallisation with seeding for body fat. *European Patent*, EP 2166072 A1.

De Oliveira, I F; Grimaldi, R and Gonsalves, L A G (2014). Effect of diacylglycerols on crystallization of palm oil (*Elaeis guineensis*). *Eur. J. Lipid Sci. Technol., 116(7)*: 904-909.

Fangfang, C; Zhang, H; Xiaoyang, S; Xingguo, W and Xuebing, X (2013). Effects of ultrasonic parameters on the crystallization behavior of palm oil. *J. Am. Oil Chem. Soc., 90*: 941-949.

Fredrick, E; Foubert, I; Van De Sype, J and Dewettinck, K (2008). Influence of monoglycerides on the crystallization behavior of palm oil. *Cryst. Growth Des., 8(6)*: 1833-1839.

Gibon, V and Tirtiaux, A (2002). Latest trends in dry fractionation. *Lipid Technol., 14(3)*: 33-36.

Gibon, V (2006). Fractionation of lipids for use in food. *Modifying Lipids for Use in Food* (Gunstone, F ed.). Woodhead Publishing Ltd, Sawston. p. 201-233.

Gibon, V; Ayala, J; Dijckmans, P; Maes, J and De Greyt, W (2009). Future prospects for palm oil refining and modifications. *OCL, 16(4)*: 193-200.

Gibon, V (2012). Palm oil and palm kernel oil refining and fractionation technology. *Palm Oil: Production, Processing, Characterization and Uses*. Elsevier Inc., Netherlands. p. 329-375.

Gibon, V and Danthine, S (2020). Systematic investigation of co-crystallization properties in binary and ternary mixtures of triacylglycerols containing palmitic and oleic acids in relation with palm oil dry fractionation. *Foods*, *9(12)*: 1891.

Hubbes, S S; Danzl, W and Foerst, P (2018). Crystallization kinetics of palm oil of different geographic origins and blends thereof by the application of the Avrami model. *LWT*, *93*: 189-196.

Kellens, M; Gibon, V; Hendrix, M and De Greyt, W (2007). Dry fractionation of palm oil. *Eur. J. Lipid Sci. Technol.*, *109(4)*: 336-349.

Kuriyama, J; Miyaji, Y; Tamura, K; Zaliha, O and Chong, C L (2011). Improved sustainable fractionation of palm oil using polyglycerol fatty acid esters. *J. Oil Palm Res.*, *23*: 1141-1145.

Kwamura, K (1980). The DSC thermal analysis of crystallization behaviour of palm oil. *J. Am. Oil Chem. Soc.*, *56(8)*: 48-52.

Mei Huey, S; Chiew Let, C and Chee Beng Yeoh (2015). New developments in palm oil fractionation. *Palm Oil Developments*, *62*: 1-7.

Miskandar, M S; Che Man, Y B; Yusoff, M S A and Abdul, R R (2006). Effect of emulsifiers on crystallization properties of low melting blends of palm oil and olein. *J. Food Lipids*, *13(1)*: 57-72.

Miskandar, M S; Che Man, Y B; Yusoff, M S A and Abdul, R R (2007). Effect of emulsifiers on crystal behaviour of palm oil blends on slow crystallization. *J. Food Lipids*, *14(1)*: 1-18.

Omar, Z; Hishamuddin, E; Sahri, M M; Fauzi, S H; Habi Mat Dian, N L; Ramli, M R and Rashid, N A (2015). Palm oil crystallization: A review. *J. Oil Palm Res.*, *27(2)*: 97-106.

Saadi, S; Ariffin, A A; Mohd Ghazali, H; Miskandar, M H; Boo, H C and Abdul Karim, S M (2012). Application of differential scanning calorimetry (DSC), HPLC and pNMR for interpretation of primary crystallization caused by combined low and high melting TAG. *Food Chem.*, *132(1)*: 603-612.

Saberi, A H; Lai, O M and Toro-Vazquez, J F (2011). Crystallization kinetics of palm oil in blends with palm-based diacylglycerols. *Food Res. Int.*, *44(1)*: 425-435.

Sakamoto, M; Maruo, K; Kuryama, J; Kouno, M; Ueno, S and Sato, K (2003). Effects of adding polyglycerol behenic acid esters on the crystallization of palm oil. *J. Oleo. Sci.*, *52(12)*: 639-645.

Santoro, V; Dal Bello, F; Aigotti, R; Gastaldi, D; Romaniello, F; Forte, E; Magni, M; Baiocchi, C and Medana, C (2018). Characterization and determination of interesterification markers (Triacylglycerol Regioisomers) in confectionery oils by liquid chromatography-mass spectrometry. *Foods, 7(2)*: 23.

Saw, M H; Hishamuddin, E; Chong, C L; Yeoh, C B and Lim, W H (2017). Effect of polyglycerol esters additive on palm oil crystallization using focused beam reflectance measurement and differential scanning calorimetry. *Food Chem.*, *214*: 277-284.

Siew and Ng (1999). Influence of diglycerides on crystallization of palm oil. *J. Sci. Food Agric.*, *79(5)*: 722-726.

Tong, S C; Tang, T K and Lee, Y Y (2021). A review on the fundamentals of palm oil fractionation: Processing conditions and seeding agents. *Eur. J. Lipid Sci. Technol.*, *123(12)*: 2100132.

Verstringe, S; Danthine, S; Blecker, C; Depypere, F and Dewettinck, K (2013). Influence of monopalmitin in the isothermal crystallization mechanism of palm oil. *Food Res. Int.*, *51(1)*: 344-353.

Verstringe, S; Danthine, S; Blecker, C and Dewettinck, K (2014). Influence of commercial monoacylglycerols on the crystallization mechanism of palm oil as compared to its pure constituants. *Food Res. Int.*, *62*: 694-700.

Yubin, Y and Martini, S (2015). Application of high-intensity ultrasound to palm oil in a continuous system. *J. Agric. Food Chem., 63(1)*: 319-327.

Zaliha, O; Chong, C L; Cheow, C S; Norizzah, A R and Kellens, M J (2004). Crystallization properties of palm oil by dry fractionation. *Food Chem., 86(2)*: 245-250.

Journal of Oil Palm Research Vol. 35 (2) June 2023 p. 307-319
DOI: https://doi.org/10.21894/jopr.2022.0031

VIABILITY OF FORAGE SORGHUM INTEGRATION IN OIL PALM PLANTING AREA FOR PRODUCTION OF LIVESTOCK FODDER

NORKASPI KHASIM[1]* and RAJA ZULKIFLI RAJA OMAR[1]

ABSTRACT

Forage sorghum has great potential to be integrated with oil palm as a fodder source for ruminant livestock. However, there was no study conducted on the suitability of forage sorghum cultivation in oil palm agriculture. Hence, the primary goals of this study were to investigate the suitability of several forage sorghum varieties integrated into the oil palm planting area and how they affect the oil palm yield. Five varieties of forage sorghum, i.e., *Superdan, Jumbo, Pacific BMR, Sugargraze and BMR Revolution obtained from Australia were used in this study. The field trials were carried out at five locations,* i.e., *Malaysian Palm Oil Board (MPOB) Kluang Research Station, MPOB Keratong Research Station, MPOB Teluk Intan Research Station, MPOB Lahad Datu Research Station and Ladang MAAH KLIA. The trials were laid down in a randomised complete block design (RCBD). Each plot was 7 m × 4 m (28 m^2) in size with four replicates (20 plots). Seeds were manually dibbled into 70 cm × 20 cm bands. One planting season of forage sorghum took almost six months to complete with four harvesting rounds. Two rounds of planting can be carried out in one year depending on the climatic condition. Results of the study indicated that forage sorghum grew well in the double avenue oil palm planting area. Sugargraze variety produced the highest fresh and dry fodder weight at all trial locations except MPOB/MAAH plantation. It was followed by BMR Revolution as the second highest fodder producer. The highest estimated dry fodder yield was 18.23 t ha^{-1} season^{-1} for Sugargraze variety and 12.97 t ha^{-1} season^{-1} for BMR Revolution. In terms of nutritional values, total digestible nutrient (TDN) values ranged from 57.00%-63.93% for all five varieties. This study also revealed that forage sorghum planting in the double avenue oil palm planting area did not affect the oil palm yield. The gross and net revenue of fresh fodder production were RM18 840 ha^{-1} and RM7680 ha^{-1}, respectively. A total monthly income of RM1317 ha^{-1} can be generated by forage sorghum and oil palm integration. Thus, the integration of forage sorghum in the double avenue oil palm planting area is technically and economically viable for adoption to optimise land use, diversify the income stream of oil palm growers and lend support to ensure the sustainability of Malaysia's livestock industry.*

Keywords: double-avenue, forage sorghum, oil palm crop integration.

Received: 30 April 2021; **Accepted:** 11 March 2022; **Published online:** 3 June 2022.

INTRODUCTION

Sorghum, *Sorghum vulgare* originated from East Central Africa, in Ethiopia and Sudan. It was introduced into Malaysia in 1969 and has been cultivated at the Agriculture Station, Sungai Udang, Melaka, Malaysia during the paddy off-season. It belongs to the family *Poaceae* similar to wheat, rice and maize. It can grow up to 0.5 to 4.0 m high. Sorghum grows well in a warm climate with temperatures ranging from 26°C to 37°C. It can be grown at as high as 1200 m above sea level. It can tolerate high temperatures, drought conditions and intermittent waterlogging.

[1] Malaysian Palm Oil Board,
6 Persiaran Institusi, Bandar Baru Bangi,
43000 Kajang, Selangor, Malaysia.

* *Corresponding author e-mail: kaspi@mpob.gov.my*

Sorghum has shown great potential to supplement fodder resources in India (Reddy, 2017). It was extensively cultivated in the Americas and Australia primarily for animal feed (Taylor, 2019). It is a fast-growing, tasty, and nutritious fodder that may be used as silage and hay in addition to fresh feeding (Singh *et al.*, 2016). Forage sorghum performs best on heavier soils due to its greater moisture holding capacity and natural fertility. Although forage sorghum has good drought tolerance and can be sown on lighter soils, productivity may be reduced unless adequate fertilising is carried out and suitable varieties are being used. It has a reputation for producing fast and large quantities of livestock feed. It can be grazed or turned into silage or hay. Under the average condition, it can produce 4 t ha^{-1} of DM within 50 days of planting. An irrigated study in New Mexico discovered that Brown Mid Rib (BMR) forage sorghum produced 21.1 t ha^{-1} of DM when harvested at the soft dough stage (Lyons *et al.*, 2019). It has great potential to be integrated with oil palm as a fodder source because of its wide adaptation, rapid growth, high green, and dry fodder yields.

Annually, Malaysia is importing feed for livestock and ruminant worth about RM3 billion. Feed import quantity and value are expected to increase significantly in the future due to an increase in demand and price. Thus, it is crucial to minimise dependencies on imported fodder by introducing new livestock feeds which are competitive for the livestock industry in Malaysia. Forage sorghum integration with oil palm has the potential to be the alternative feed for livestock production. Three years of observation on the forage sorghum planting indicated that it adapted well to Malaysian soil and climatic conditions. In line with that, it has a great potential to be planted large-scale under an integration system with oil palm specifically for forage production for the livestock industry. Therefore, there is an urgent need to adopt and conduct a thorough study that includes comprehensive data, especially on the suitability of forage sorghum integration with oil palm for forage production.

MATERIALS AND METHODS

Study Sites

Trials on forage sorghum integration with oil palm were carried out at five MPOB research plots. They were Ladang Malaysian Agriculture and Horticulture (MAAH) KLIA, Selangor (2°46′44″ N 101°40″26″ E); MPOB Research Station in Kluang, Johor (1°57′23″ N 103°22′19″ E); MPOB Research Station in Keratong, Pahang (2°46′42″ N 103°55′18″ E); MPOB Research Station in Lahad Datu, Sabah (5°01′46″ N 118°25′01″ E) and MPOB Research Station in Teluk Intan, Perak (3°49′05″ N 118°58′58″ E). This experiment was carried out for five years.

Oil Palm Planting System

Oil palm was planted following the double avenue oil palm planting system. The average age of the oil palms at the start of this study was six years old. The palms were planted at 6.1 m within the same row and 9.1 m between the rows, while the vacant space between the two oil palm rows was 15.2 m (*Figure 1*). The palm density was 136 palms ha^{-1}, similar to the conventional triangular oil palm planting system with a planting distance of 9.1 m × 9.1 m × 9.1 m. The 15.2 m vacant area of double avenue oil palm planting was cleared of bushes and debris from the previous crop. This area was used for trials on forage sorghum planting.

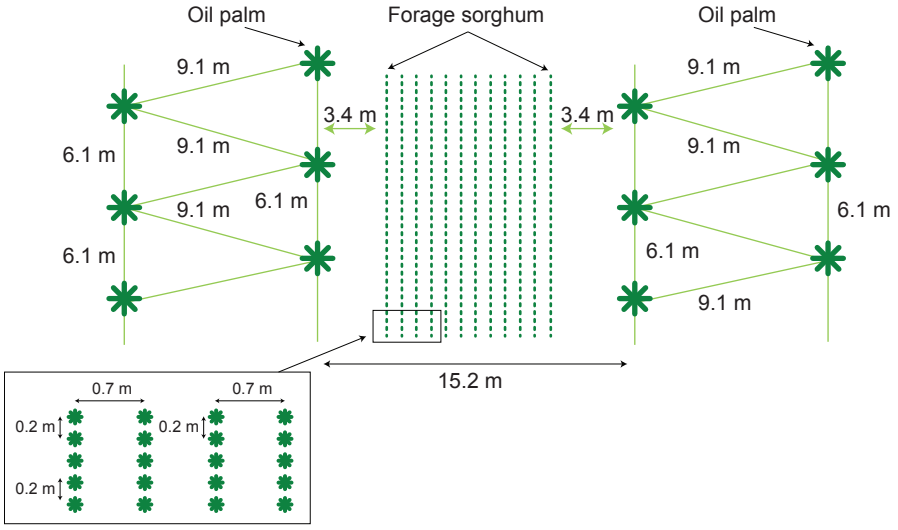


Figure 1. Layout of forage sorghum integration in double-avenue oil palm planting area.

Experimental Plot and Design

Field trials were conducted to compare the performance of several forage sorghum varieties integrated into the oil palm planting area. The forage sorghum seeds used in this study were obtained from two companies in Australia, *i.e.*, Pacific Seeds Pty. Ltd. and Heritage Seeds Pty. Ltd. In this study, five varieties of forage sorghum were tested in the field using a randomised complete block design (RCBD) with four replications. The plot size was 7 m × 4 m (28 m^2) with a total of 20 plots. The treatments were assigned at random to the experimental units or plots (*Table 1*). All agricultural practices were the same at five different locations of the study.

Land preparation. The experimental plots were subjected to three rounds of ploughing, *i.e.*, two rounds of disc ploughing and one round of rotor tilling. Ground Magnesium Limestone (GML) was applied to each plot at the rate of 1 t ha^{-1}, three weeks before seeds planting.

Seed planting. The seeds were manually dibbled into a 70 cm × 20 cm band. The seeds can also be planted using a seeder machine. The Alachlor herbicide was sprayed at 2.0 kg ha^{-1} after seeds sowing to control pre-emergence weeds in the plots. Manual weeding was carried out a month after planting. Three rounds of the weeding programme were conducted for one planting season. It was conducted at an interval of 10-14 days after each harvesting programme. Generally, four rounds of harvesting can be conducted for one planting season.

Fertiliser application. The types of fertiliser and rates used are shown in *Table 2*. The fertilisers were hand broadcasted and raked evenly into related plots as basal dressing before seed planting. Basal fertilisers were broadcasted in the plots before the final rotor tilling to ensure that fertilisers were evenly incorporated into the soil. Row dressing was applied as the top dressing after every harvest or cutting to promote forage sorghum re-growth from its stubble or stump. The top dressing was conducted on day three after the first, second and third harvesting programmes.

Pest and disease control. Generally, there are no major or severe pests and diseases reported for forage sorghum cultivation. Pest control was conducted based on incidence by applying insecticides such as dimethoate, carbaryl, trichlorphon and deltamethrin. The rat problem was controlled by using rat baits containing flocoumafen 0.005% w/w which were placed in the Ecorat (plastic container). The incidence of diseases was controlled by spraying fungicides such as Benomyl and Thiram.

Vegetative Measurement

Vegetative measurements of forage sorghum such as the plant height and the number of leaves were collected at each harvesting round and were carried out 40 to 45 days after each harvesting programme. Data were collected from the first to fourth harvesting programmes.

Dry Matter (DM) Estimation

DM is referred to as the portion of forage material that remained after its moisture is extracted. All animal feed requirements are calculated on a dry matter basis. DM content is measured by drying the samples in an oven at 100°C and is expressed as a percentage. The plants were sampled using the quadrant square (1 m × 1 m) and they were collected from all the treatments. Each sample was made-up of five plants. The plant parts were separated into leaflets and stem before they were dried in the oven. The above-ground sorghum's biomass (wet and dry) was estimated by multiplying the average wet and dry weight of sampled plants with the total number of sorghum plants per hectare (71 428 plants).

Forage Sorghum Nutritional Values

The nutritional value of forage is defined as its ability to support a certain level of animal performance. The nutrient or chemical composition

TABLE 1. ARRANGEMENT OF THE TREATMENTS IN THE FIELD

Replicate 1	Replicate 2	Replicate 3	Replicate 4
Superdan	Pacific BMR	BMR Revolution	Jumbo
Jumbo	BMR Revolution	Jumbo	BMR Revolution
Pacific BMR	Superdan	Sugargraze	Superdan
Sugargraze	Jumbo	Pacific BMR	Pacific BMR
BMR Revolution	Sugargraze	Superdan	Sugargraze

Note: BMR - Brown Mid Rib.

TABLE 2. FERTILISER PROGRAMME FOR FORAGE SORGHUM INTEGRATION IN OIL PALM PLANTING AREA

Types of fertiliser	Basal dressing (kg ha^{-1})	Top dressing (kg ha^{-1})
Nitrophoska 15:15:15	500	
Triple super phosphate	98	
Muriate of potash	75	
Urea		163

of forage largely determines its quality. The quality of the forage is determined by plant characteristics, harvesting and storage methods. Three plants were randomly sampled from each treatment plot. The plants were weighed and then dried in an oven at a temperature of 60°C for 24 hr. The samples were sent to the Department of Veterinary and Services for nutritional analysis. The analysis was carried out for DM, crude protein (CP), metabolisable energy (ME), total digestible nutrient (TDN), crude fibre (CF), neutral detergent fibre (NDF) and acid detergent fibre (ADF). The analysis was carried out using Malaysian Standard Methods of Test for Animal Feedstuffs, First Revision, 1982, (Goering and Soest, 1970; Menke *et al.*, 1975).

Fresh Fruit Bunch (FFB) Yield Recording at Ladang MAAH, KLIA

The FFB yield of 16 recording palms in all trial plots at Ladang MAAH, KLIA were recorded at every harvesting round of two weeks interval. The data was recorded for five years harvests.

Statistical Analysis

The effects of various treatments on forage sorghum growths, nutrients uptake, and physiological parameters were subjected to analysis of variance (ANOVA) and the means were compared using Duncan Multiple Range Test (DMRT) by SAS version 9.3. Unless otherwise stated, statistical significance refers to the 0.05 probability level (Steel and Torrie, 1980).

RESULTS AND DISCUSSION

Data of the field trials on five forage sorghum varieties integration in oil palm planting areas conducted at Ladang MAAH, KLIA and four MPOB Research Stations were analysed using Statistical Analysis System, SAS version 9.3. Results of the data analysis are as shown in *Tables 3-12*. The results are an average of four harvests from the main crop and three ratoon crops for each location of the trial except for the MPOB Research Station in Keratong, Pahang. In Keratong, the data were recorded for three harvests only due to a severe drought season during the experiment.

Vegetative Growth and Yield Production

MPOB Research Station in Keratong, Pahang. ANOVA for vegetative growth and fodder yield of forage sorghum planting at MPOB Research Station in Keratong, Pahang is presented in *Table 3*. The results indicated that the means of treatment were not significantly different at $p<0.05$. *Table 4* shows the treatments that were not significantly different at $p<0.05$. The results showed that the Jumbo variety had the highest number of leaves (mean=7.8) and plant height (mean=97.9 cm) but were not significantly different compared to other varieties.

Jumbo variety produced higher fresh fodder weight (mean=36.53 g plant^{-1}) and dry fodder weight (mean=9.74 g plant^{-1}) compared to other varieties. The results indicated that the Jumbo variety produced the highest fodder yield

TABLE 3. ANOVA FOR VEGETATIVE GROWTH AND FODDER YIELD AT MPOB RESEARCH STATION IN KERATONG

Source	df	Number of leaves	Height (cm)	Fresh weight of leaves (g plant^{-1})	Dry weight of leaves (g plant^{-1})	Fresh weight of stem (g plant^{-1})	Dry weight of stem (g plant^{-1})	Total fresh weight (g plant^{-1})	Total dry weight (g plant^{-1})
Replicate	3	14.70 **	1 395.23 ^{ns}	15 865.37 ^{ns}	19.15 ^{ns}	1 485.09 **	122.74 **	2 973.33 **	232.10 **
Treatment	4	10.12 ^{ns}	1 697.15 ^{ns}	13 236.01 ^{ns}	11.74 ^{ns}	141.24 ^{ns}	19.54 ^{ns}	411.24 ^{ns}	52.01 ^{ns}

Note: Figure are means of treatment; ns - not significant; ** - significant at 5% level (Duncan Multiple Range Test).

TABLE 4. EFFECT OF TREATMENTS ON VEGETATIVE GROWTH AND FODDER YIELD AT MPOB RESEARCH STATION IN KERATONG

Treatment	Number of leaves	Height (cm)	Fresh weight of leaves (g plant^{-1})	Dry weight of leaves (g plant^{-1})	Fresh weight of stem (g plant^{-1})	Dry weight of stem (g plant^{-1})	Total fresh weight (g plant^{-1})	Total dry weight (g plant^{-1})
Superdan	7.26 ^{b}	89.43 ^{a}	11.78 ^{a}	3.30 ^{a}	17.96 ^{a}	3.83 ^{a}	29.83 ^{a}	7.13 ^{a}
Jumbo	7.83 ^{ab}	97.95 ^{a}	15.48 ^{a}	4.41 ^{a}	21.55 ^{a}	5.33 ^{a}	36.53 ^{a}	9.74 ^{a}
Pacific BMR	8.21 ^{a}	94.33 ^{a}	13.69 ^{a}	3.72 ^{a}	18.51 ^{a}	4.67 ^{a}	32.20 ^{a}	8.40 ^{a}
Sugargraze	7.15 ^{b}	86.43 ^{a}	12.55 ^{a}	3.34 ^{a}	18.19 ^{a}	4.98 ^{a}	30.91 ^{a}	8.33 ^{a}
BMR Revolution	7.42 ^{ab}	98.29 ^{a}	13.85 ^{a}	3.73 ^{a}	19.51 ^{a}	4.48 ^{a}	33.37 ^{a}	8.21 ^{a}
Coefficient of variation (%)	27.97	34.84	81.03	75.08	113.88	138.60	98.17	107.28

Note: Mean in the same column with similar alphabet are not significantly different at $p<0.05$ (Duncan Multiple Range Test).

(*Figure 2*). Jumbo produced the highest total dry weight compared to other varieties, *i.e.*, Superdan (by 26.7%), BMR Revolution (by 15.8%), Sugargraze (by 14.5%) and Pacific BMR (by 13.8%). Jumbo variety showed the highest in vegetative growth and plant DM production but not significantly different compared to other forage sorghum varieties.

Ladang MAAH, KLIA. ANOVA in *Table 5* indicates that the means of totally fresh and DM weight were significantly different at $p<0.05$ for forage sorghum planting at Ladang MAAH, KLIA. Results in *Table 6* show that the Pacific BMR variety had the highest number of leaves (mean=12.5) and the Jumbo variety had the highest plant height (mean=97.9 cm) but not significantly different compared to other varieties except for Pacific BMR.

BMR Revolution variety produced significantly higher fresh fodder weight (mean=168.12 g plant^{-1}) and total dry fodder weight (mean=28.886 g plant^{-1}) compared to other varieties except for Jumbo, Pacific BMR and Sugargraze. The results indicated that the BMR revolution produced the highest total dry weight compared to other varieties, *i.e.*, Superdan (by 21.3%), Pacific BMR (by 15.9%), Jumbo (by 12.9%) and Sugargraze (by 4.3%). BMR Revolution variety (*Figure 3*) showed the highest in vegetative growth and plant DM production but not significantly different compared to other forage sorghum varieties.

MPOB Research Station in Kluang, Johor. ANOVA in *Table 7* indicates that the means of several treatments were significantly different at $p<0.05$. Results in *Table 8* indicated no significant difference in the number of leaves for all tested varieties. However, the Jumbo variety recorded significantly higher plant height (mean=151.7 cm) compared to other varieties except for Superdan and BMR Revolution.

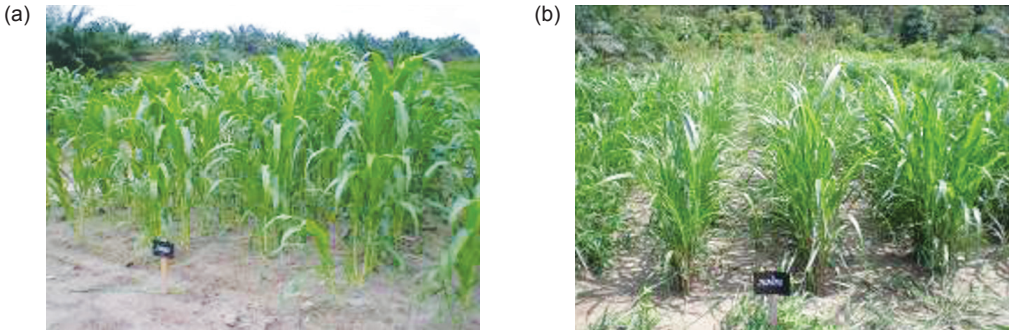


Figure 2. Jumbo variety at (a) 25 days after planting and (b) 20 days after the second harvest at MPOB Research Station in Keratong, Pahang.

TABLE 5. ANOVA FOR VEGETATIVE GROWTH AND FODDER YIELD AT LADANG MAAH, KLIA

Source	df	Number of leaves	Height (cm)	Fresh weight of leaves (g plant^{-1})	Dry weight of leaves (g plant^{-1})	Fresh weight of stem (g plant^{-1})	Dry weight of stem (g plant^{-1})	Total fresh weight (g plant^{-1})	Total dry weight (g plant^{-1})
Replicate	3	176.58 **	25 597.51 ***	568.23 ^{ns}	15.68 ^{ns}	24 355.34 **	656.75 **	32 313.74 ***	844.81 **
Treatment	4	43.43 **	7 146.09 **	1 820.59 **	69.74 **	7 321.40 ^{ns}	467.83 **	6 767.38 ^{ns}	243.23 ^{ns}

Note: Figure is means of treatment; ns - not significant; ** - significant at 5% level (Duncan Multiple Range Test).

TABLE 6. EFFECT OF TREATMENTS ON VEGETATIVE GROWTH AND FODDER YIELD AT LADANG MAAH, KLIA

Treatment	Number of leaves	Height (cm)	Fresh weight of leaves (g plant^{-1})	Dry weight of leaves (g plant^{-1})	Fresh weight of stem (g plant^{-1})	Dry weight of stem (g plant^{-1})	Total fresh weight (g plant^{-1})	Total dry weight (g plant^{-1})
Superdan	11.54 ^{ab}	103.63 ^{a}	57.95 ^{ab}	11.02 ^{a}	89.98 ^{b}	11.87 ^{c}	147.93 ^{a}	22.73 ^{b}
Jumbo	12.31 ^{ab}	115.16 ^{a}	59.12 ^{a}	11.04 ^{a}	94.96 ^{b}	14.33 ^{bc}	154.09 ^{a}	25.17 ^{ab}
Pacific BMR	12.58 ^{a}	92.77 b	53.98 ^{ab}	10.49 ^{ab}	91.29 ^{b}	15.94 ^{bc}	142.24 ^{a}	24.28 ^{ab}
Sugargraze	10.38 ^{b}	113.82 ^{a}	56.97 ^{ab}	10.70 ^{a}	106.97 ^{ab}	18.13 ^{ab}	162.16 ^{a}	27.63 ^{a}
BMR Revolution	11.94 ^{ab}	110.42 ^{a}	48.59 ^{b}	8.78 ^{b}	119.54 ^{a}	22.48 ^{a}	168.12 ^{a}	28.89 ^{a}
Coefficient of variation (%)	48.5097	29.04	49.20	49.32	56.37	62.46	48.46	50.48

Note: Mean in the same column with similar alphabet are not significantly different at $p<0.05$ (Duncan Multiple Range Test).

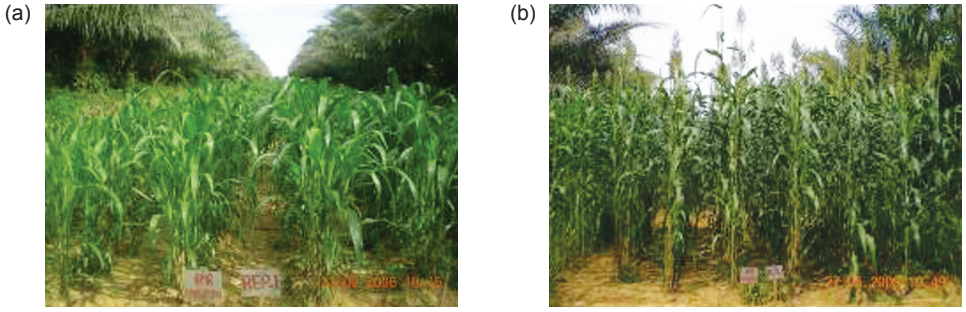


Figure 3. BMR Revolution variety at (a) 25 days and (b) 60 days after planting at Ladang MAAH, KLIA.

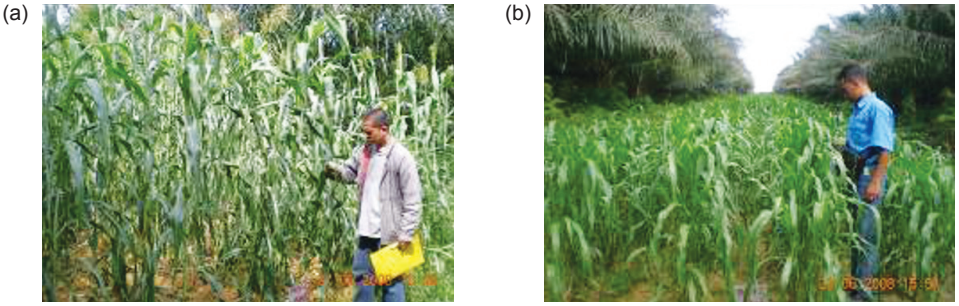


Figure 4. Pacific BMR variety at (a) 60 days after planting and (b) 25 days after the first harvest at Ladang MAAH, KLIA.

The BMR Revolution variety produced a significantly higher fresh weight of leaves (mean=53.7 g plant^{-1}) and dry weight of leaves (mean=11.7 g plant^{-1}) compared to other varieties except for Sugargraze. However, Sugargraze variety recorded significantly higher fresh weight of stem (mean=174.1 g plant^{-1}), dry weight of stem (mean=27.9 g plant^{-1}) and total dry weight (mean=38.9 g plant^{-1}) (*Table 8*). The results indicated that Sugargraze variety produced the highest total dry weight compared to other varieties, *i.e.*, BMR Revolution (by 24.3%), Pacific BMR (by 34.7%), Jumbo (by 35.9%) and Superdan (by 43.2%). The results showed that Sugargraze (*Figure 5*) was the best forage sorghum variety in terms of vegetative growth and plant DM production and followed by BMR Revolution and Pacific BMR and Jumbo.

TABLE 7. ANOVA FOR VEGETATIVE GROWTH AND FODDER YIELD AT MPOB RESEARCH STATION IN KLUANG, JOHOR

Source	df	Number of leaves	Height (cm)	Fresh weight of leaves (g plant^{-1})	Dry weight of leaves (g plant^{-1})	Fresh weight of stem (g plant^{-1})	Dry weight of stem (g plant^{-1})	Total fresh weight (g plant^{-1})	Total dry weight (g plant^{-1})
Replicate	3	4.75 **	2 901.94 **	1 514.05 **	24.56 **	7 989.48 **	30.04 ^{ns}	1 024 165.48 ^{ns}	54.95 ^{ns}
Treatment	4	0.94 ^{ns}	434.47 **	2 010.38 **	91.89 **	67 151.49 **	2 317.95 **	1 148 168.99 ^{ns}	2878.81 **

Note: Figure is means of treatment; ns - not significant; ** - significant at 5% level (Duncan's Multiple Range Test).

TABLE 8. EFFECT OF TREATMENTS ON VEGETATIVE GROWTH AND FODDER YIELD AT MPOB RESEARCH STATION IN KLUANG, JOHOR

Treatment	Number of leaves	Height (cm)	Fresh weight of leaves (g plant^{-1})	Dry weight of leaves (g plant^{-1})	Fresh weight of stem (g plant^{-1})	Dry weight of stem (g plant^{-1})	Total fresh weight (g plant^{-1})	Total dry weight (g plant^{-1})
Superdan	9.55 ^{a}	147.98 ^{ab}	41.34 ^{c}	9.20 ^{b}	95.37 ^{c}	17.81 ^{b}	136.82 ^{c}	22.15 ^{d}
Jumbo	9.41 ^{a}	151.79 ^{a}	41.78 ^{c}	9.18 ^{b}	105.01 ^{bc}	15.80 ^{b}	147.12 ^{c}	24.98 ^{c}
Pacific BMR	9.38 ^{a}	145.93 ^{b}	46.74 ^{b}	9.89 ^{b}	103.25 ^{bc}	15.54 ^{b}	149.97 ^{c}	25.44 ^{c}
Sugargraze	9.41 ^{a}	147.53 ^{b}	48.73 ^{b}	11.03 ^{a}	174.13 ^{a}	27.96 ^{a}	222.85 ^{a}	38.99 ^{a}
BMR Revolution	9.33 ^{a}	149.18 ^{ab}	53.72 ^{a}	11.71 ^{a}	113.85 ^{b}	17.81 ^{b}	167.88 ^{b}	29.52 ^{b}
Coefficient of variation (%)	10.44	8.37	32.63	25.68	35.34	39.41	39.41	31.64

Note: Mean in the same column with similar alphabet are not significantly different at $p<0.05$ (Duncan's Multiple Range Test).

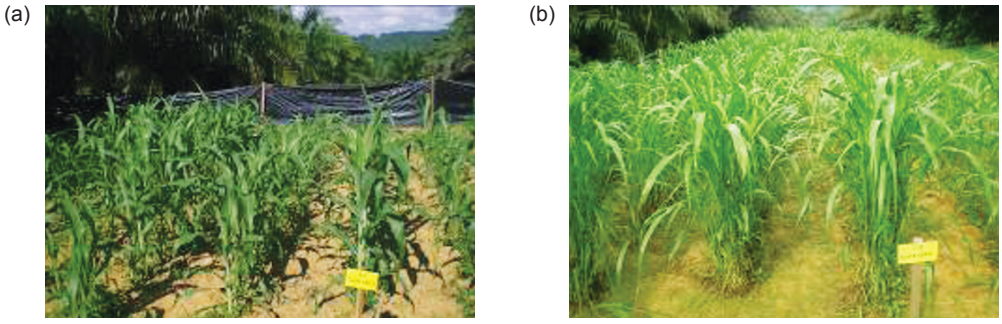


Figure 5. Sugargraze variety at (a) 20 days after planting and (b) 25 days after the second harvest at MPOB Research Station in Kluang, Johor.

MPOB Research Station in Lahad Datu, Sabah. ANOVA in *Table 9* indicates that the means of treatment were significantly different at $p<0.05$ except for the fresh weight of leaves. *Table 10* indicates that the Pacific BMR variety recorded a significantly higher number of leaves (mean=10.8) compared to other varieties. Meanwhile, the Jumbo variety recorded significantly higher plant height (mean=214.7 cm) compared to other varieties except for Sugargraze.

The results indicated no significant difference in the fresh weight of leaves for all tested sorghum varieties. Sugargraze produced a significantly higher dry weight of leaves (mean=12.2 g plant^{-1}), fresh weight of stem (mean=297.5 g plant^{-1}), dry weight of stem (mean=51.5 g plant^{-1}), total fresh weight (mean=353.3 g plant^{-1}) and total dry weight (mean=63.7 g plant^{-1}) (*Table 10*). The results indicated that Sugargraze variety produced the highest total dry weight compared to other varieties, *i.e.*, BMR Revolution (by 28.9%), Pacific BMR (by 32.9%), Jumbo (by 36.0%) and Superdan (by 52.4%). The results showed that Sugargraze (*Figure 6*) is the best forage sorghum variety in terms of vegetative growth and plant DM production and followed by BMR Revolution and Pacific BMR and Jumbo.

MPOB Research Station in Teluk Intan, Perak. ANOVA in *Table 11* indicates that the means of treatment were significantly different at $p<0.05$. *Table 12* indicates that the Pacific BMR variety recorded a significantly higher number of leaves (mean=7.8) compared to other varieties except for BMR Revolution and Jumbo. Meanwhile, the Jumbo variety recorded significantly higher plant height (mean=145.8 cm) compared to other varieties.

The results indicated that Sugargraze produced a significantly higher fresh weight of leaves (mean=54.9 g plant^{-1}), dry weight of leaves (mean=9.8 g plant^{-1}), fresh weight of stem (mean=164.3 g plant^{-1}), dry weight of stem

TABLE 9. ANOVA FOR VEGETATIVE GROWTH AND FODDER YIELD AT MPOB RESEARCH STATION IN LAHAD DATU, SABAH

Source	df	Number of leaves	Height (cm)	Fresh weight of leaves (g plant^{-1})	Dry weight of leaves (g plant^{-1})	Fresh weight of stem (g plant^{-1})	Dry weight of stem (g plant^{-1})	Total fresh weight (g plant^{-1})	Total dry weight (g plant^{-1})
Replicate	3	2.61 ^{ns}	6 423.82 **	43 791.67 ^{ns}	33.89 ^{ns}	21 393.27 ^{ns}	306.31 ^{ns}	49 681.06 ^{ns}	500.94 ^{ns}
Treatment	4	318.14 **	53 188.134 **	51 260.067 ^{ns}	979.94 **	1 247 193.57 **	42 405.34 **	15 646.21 ***	55 729.79 **

Note: Figure is means of treatment; ns - not significant; ** - significant at 5% level (Duncan Multiple Range Test).

TABLE 10. EFFECT OF TREATMENTS ON VEGETATIVE GROWTH AND FODDER YIELD AT MPOB RESEARCH STATION IN LAHAD DATU, SABAH

Treatment	Number of leaves	Height (cm)	Fresh weight of leaves (g plant^{-1})	Dry weight of leaves (g plant^{-1})	Fresh weight of stem (g plant^{-1})	Dry weight of stem (g plant^{-1})	Total fresh weight (g plant^{-1})	Total dry weight (g plant^{-1})
Superdan	9.656 ^{c}	192.61 ^{c}	34.63 ^{d}	7.94 ^{d}	145.21 ^{c}	22.746 ^{d}	179.84 ^{c}	30.38 ^{d}
Jumbo	10.12 ^{b}	214.78 ^{a}	42.75 ^{c}	9.49 ^{c}	192.28 ^{b}	31.19 ^{c}	257.72 ^{b}	40.83 ^{c}
Pacific BMR	10.80 ^{a}	187.57 ^{d}	46.09 ^{b}	10.03 ^{bc}	191.47 ^{b}	32.73 ^{bc}	236.86 ^{b}	42.76 ^{bc}
Sugargraze	8.33 ^{d}	211.73 ^{a}	55.79 ^{a}	12.29 ^{a}	297.59 ^{a}	51.54 ^{a}	353.38 ^{a}	63.79 ^{a}
BMR Revolution	9.48 ^{c}	201.84 ^{b}	46.83 ^{b}	10.65 ^{b}	181.78 ^{b}	34.73 ^{b}	228.48 ^{b}	45.39 ^{b}
Coefficient of variation (%)	32.27	16.91	45.06	46.04	63.45	51.29	97.31	46.04

Note: Mean in the same column with similar alphabet are not significantly different at $p<0.05$ (Duncan Multiple Range Test).

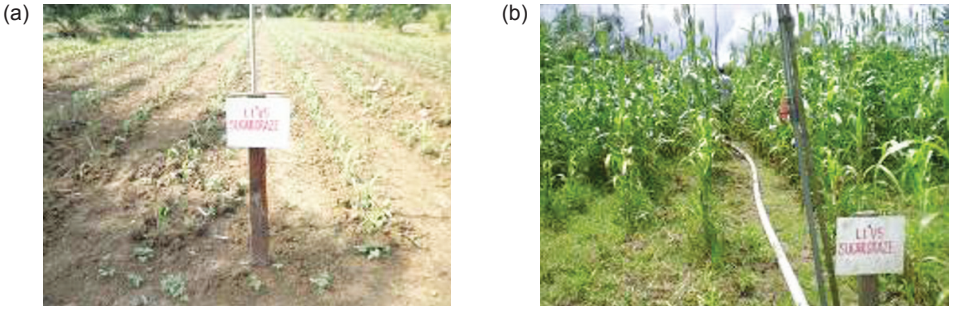


Figure 6. Sugargraze variety at (a) 7 days and (b) 60 days after planting at MPOB Research Station in Lahad Datu, Sabah.

(mean=16.3 g plant^{-1}), total fresh weight (mean=219.3 g plant^{-1}) and total dry weight (mean=26.2 g plant^{-1}) (*Table 12*). The results indicated that Sugargraze variety produced the highest total dry weight compared to other varieties, *i.e.*, BMR Revolution (by 28.6%), Jumbo (by 29.0%), Pacific BMR (by 38.6%) and Superdan (by 54.4%). The results showed that Sugargraze (*Figure 7*) is the best forage sorghum variety in terms of vegetative growth and plant DM production and followed by BMR Revolution and Jumbo and Pacific BMR.

Estimation of Forage Sorghum Production

Table 13 shows the estimated fresh and DM weight of forage sorghum production for one

TABLE 11. ANALYSIS OF VARIAN FOR VEGETATIVE GROWTH AND FODDER YIELD AT MPOB RESEARCH STATION IN TELUK INTAN, PERAK

Source	df	Number of leaves	Height (cm)	Fresh weight of leaves (g plant^{-1})	Dry weight of leaves (g plant^{-1})	Fresh weight of stem (g plant^{-1})	Dry weight of stem (g plant^{-1})	Total fresh weight (g plant^{-1})	Total dry weight (g plant^{-1})
Replicate	3	18.12 **	25 641.44 **	683.7270 **	23.6527 **	27 612.75 **	323.343 **	35 396.527 **	509.79 **
Treatment	4	15.86 **	11 202.41 **	7 424.67**	245.00 **	121 842.97 **	1 022.72 **	182 729.20 **	2 193.74 **

Note: Figure is means of treatment; ns - not significant; ** - significant at 5% level (Duncan Multiple Range Test).

TABLE 12. EFFECT OF TREATMENTS ON VEGETATIVE GROWTH AND FODDER YIELD AT MPOB RESEARCH STATION IN TELUK INTAN, PERAK

Treatment	Number of leaves	Height (cm)	Fresh weight of leaves (g plant^{-1})	Dry weight of leaves (g plant^{-1})	Fresh weight of stem (g plant^{-1})	Dry weight of stem (g plant^{-1})	Total fresh weight (g plant^{-1})	Total dry weight (g plant^{-1})
Superdan	6.91 ^{b}	122.05 ^{c}	28.94 ^{c}	5.09 ^{d}	64.77 ^{d}	6.89 ^{d}	93.71 ^{c}	11.98 ^{d}
Jumbo	7.68 ^{a}	145.89 ^{a}	37.67 ^{b}	7.19 ^{c}	93.79 ^{b}	11.43 ^{b}	131.46 ^{b}	18.62 ^{b}
Pacific BMR	7.85 ^{a}	115.21 ^{c}	41.79 ^{b}	7.25 ^{c}	77.75 ^{cd}	8.85 ^{c}	119.54 ^{b}	16.10 ^{c}
Sugargraze	7.03 ^{b}	135.41 ^{b}	54.99 ^{a}	9.84 ^{a}	164.39 ^{a}	16.39 ^{a}	219.38 ^{a}	26.23 ^{a}
BMR Revolution	7.73 ^{a}	130.537 ^{b}	42.76 ^{b}	8.09 ^{b}	87.32 ^{bc}	10.63 ^{b}	130.08 ^{b}	18.72 ^{b}
Coefficient of variation (%)	15.36	18.83	37.81	35.05	45.28	46.68	40.87	39.21

Note: Mean in the same column with similar alphabet are not significantly different at p<0.05 (Duncan Multiple Range Test).

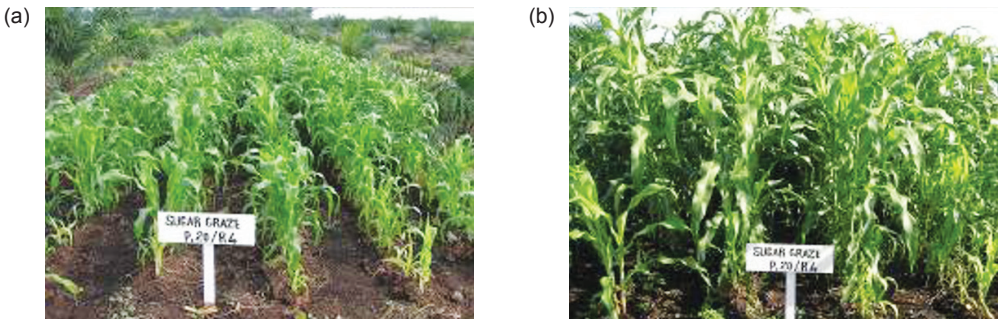


Figure 7. Sugargraze variety at (a) 20 days and (b) 50 days after planting at MPOB Research Station in Teluk Intan, Perak.

planting season. Results of this study indicated that one planting season took almost six months to complete with four harvesting rounds. Generally, two rounds of planting can be conducted in one year depending on the climatic condition. Results of this study showed that Sugargraze variety produced the highest fresh and DM weight in four MPOB Research Stations, *i.e.*, Keratong, Pahang (8.83 t ha^{-1} and 2.38 t ha^{-1}), Kluang, Johor (63.69 t ha^{-1} and 11.14 t ha^{-1}), Lahad Datu, Sabah (100.96 t ha^{-1} and 18.23 t ha^{-1}) and Teluk Intan, Perak (62.68 t ha^{-1} and 7.49 t ha^{-1}) except for BMR Revolution variety which recorded higher at Ladang MAAH, KLIA (48.03 t ha^{-1} and 8.26 t ha^{-1}). Results of the study in Lahad Datu indicated that higher DM yield of forage sorghum compared to other locations. The DM of fodder yield was a little bit higher than reported by Meena *et al.* (2020) and Gnanagobal and Sinniah (2018). Meena *et al.* (2020) reported that Sugargraze produced fresh and DM yields of 56.37 t ha^{-1} and 15.13 t ha^{-1}, respectively. However, Gnanagobal and Sinniah (2018) recorded an average DM yield of 14.1 t ha^{-1} for Sugargraze. Bhat (2019) reported that forage sorghum has more biomass production potential in limited moisture regimes and forage quality comparable to that of forage maize. It has a good source of roughage for the livestock in the warm seasons and the tropics.

The study indicated that Sugargraze variety performed well in four MPOB's Stations except BMR Revolution performed better in Ladang MAAH, KLIA. Both of these forage sorghum varieties had better DM percentages compared to the rest of the tested varieties that contributed to the higher dry fodder yield per hectare.

Forage Sorghum Nutritional Values

All the different sorghum varieties were analysed to determine their nutritional values for livestock feed. The forages were analysed for DM, CP, fibre (acid detergent or neutral detergent) and

TABLE 13. ESTIMATED FRESH AND DRY WEIGHT OF FORAGE SORGHUM YIELD*

MPOB Research Station	Variety	Total fresh weight (t ha^{-1} season^{-1}*)	Total dry weight (t ha^{-1} season^{-1}*)	Dry matter percentage (%)
Keratong, Pahang	Superdan	8.52	2.04	23.94
	Jumbo	10.43	2.78	26.65
	Pacific BMR	9.20	2.40	26.08
	Sugargraze	8.83	2.38	26.95
	BMR Revolution	9.53	2.35	24.65
Ladang MAAH, KLIA, Sepang, Selangor	Superdan	42.27	6.49	15.35
	Jumbo	44.03	7.19	16.33
	Pacific BMR	40.64	6.93	17.05
	Sugargraze	46.32	7.89	17.03
	BMR Revolution	48.03	8.25	17.17
Kluang, Johor	Superdan	39.09	6.33	16.19
	Jumbo	42.03	7.13	16.96
	Pacific BMR	42.85	7.27	16.97
	Sugargraze	63.69	11.14	17.49
	BMR Revolution	47.96	8.43	17.58
Lahad Datu, Sabah	Superdan	51.38	8.68	16.89
	Jumbo	73.65	11.67	15.84
	Pacific BMR	67.67	12.22	18.06
	Sugargraze	100.96	18.23	18.06
	BMR Revolution	65.28	12.97	19.86
Teluk Intan, Perak	Superdan	26.77	3.42	12.78
	Jumbo	37.56	5.32	14.16
	Pacific BMR	34.15	4.60	13.46
	Sugargraze	62.68	7.49	11.95
	BMR Revolution	37.17	5.35	14.39

Note: * Six months per season and four harvests.

available energy (Weiss *et al.*, 1999). The nutrient information of the forages such as mineral content is needed to balance the diets. Forage quality affects feed intake and the amount of concentrate needed to balance the diet. Digestibility of a diet has a major influence on feed intake by livestock. Fibre is generally less digestible than non-fibre components; therefore, high-fibre feeds such as forages are less digestible than low-fibre feeds such as grains. High quality forages such as corn silage and vegetative grasses are usually digestible enough that feed intake is not restricted significantly.

Generally, CP content is positively correlated with quality. Normally, high-protein forages generally are high-quality forages. The CP content is positively correlated to the energy content of forages. High protein forages generally are more digestible and provide more energy per kilogram than low-protein forages. *Table 14* shows the average nutritional values for five forage sorghum varieties that were integrated with oil palm at MPOB/MAAH Plantation in KLIA, Sepang. The results showed that the CP values were almost comparable for all varieties except for Sugargraze, which was slightly lower.

Plant fibre is composed largely of cellulose and hemicellulose. The amount of cellulose is relatively constant among forage, but the amount of hemicellulose differs greatly between grasses and legumes. Cellulose is the primary constituent of ADF, but NDF contains both cellulose and hemicellulose. Therefore, grasses and legumes may have similar ADF values, but NDF values will almost always be substantially higher for grasses. High quality forages will contain 55% to 70% NDF (30% to 40% ADF). Low quality forages contain 70% to 80% ADF. The results in *Table 14* showed that all the forage sorghum varieties were in the category of high-quality forage because the value was in the ranges value of ADF and NDF.

TDN is calculated by estimating the difference between the amount of nutrient ingested minus the amount of nutrient excreted in the faeces, expressed as a percentage of the nutrient ingested. It could also be estimated through ADF content. For instance, if the ADF content is 30%, the estimated TDN content of feed could be 61.85% in the legume or 66.84% in corn silage (Deanne and Kevin, 1990). The study results showed that the TDN values of all the five sorghum varieties were within the ranges of 57.10% to 63.93%.

The ME value of a feed is a measure of the energy available to an animal after accounting for the energy losses in faeces, urine, and methane. ME values are expressed as megajoules per kilogram of DM (MJ kg^{-1}). It is closely related to the digestibility of the feed. When digestibility is high, the ME will be high (Stuart, 2002). The results in *Table 14* showed that ME values were almost similar for all forage sorghum varieties.

Pests and Diseases

The yield of forage sorghum was determined by the variety and application of good agricultural practices (GAP) in its management. Several agricultural practices such as good land preparation, fertilisation programme, pest and disease control and harvesting programme must be carried out according to GAP to ensure the integrated forage sorghum produced a higher yield.

Generally, pests and diseases are not the major problems in cultivating forage sorghum for livestock. Similarly, Khalin *et al.* (2020) reported that Romania had significantly expanded the planted area with sorghum in 2007-2017 owing to its advantages: Strong adaptation to diverse soil types, tolerance to high temperatures and low rainfalls, resistance to diseases and pests, inexpensive inputs, and production cost. During the study, we had

TABLE 14. NUTRITIONAL VALUE OF FORAGE SORGHUM INTEGRATED WITH OIL PALM AT DIFFERENT HARVESTING CYCLE

Nutrition	Superdan	Jumbo	Pacific BMR	Sugargraze	BMR Revolution
Crude protein (%)	16.80	17.10	17.10	14.90	16.20
Crude fat (%)	3.20	2.90	3.40	2.80	3.30
Crude fibre (%)	40.90	36.10	27.60	32.80	33.60
Ash (%)	8.00	8.40	9.50	8.90	8.00
Calcium (%)	0.42	0.39	0.39	0.32	0.33
Phosphorus (%)	0.28	0.26	0.28	0.28	0.29
Neutral detergent fibre (%)	64.90	68.00	64.40	61.70	63.90
Acid detergent fibre (%)	37.70	39.60	36.90	35.30	35.50
Hemicellulose (%)	27.30	28.40	27.50	26.40	28.30
Total digestible nutrient (%)	57.90	57.10	63.90	57.10	61.00
Metabolisable energy (MJ/kg)	8.65	8.50	9.63	8.51	9.16

found that grasshopper, *Valanga* sp. attacked forage sorghum at MPOB Research Station in Kluang, Johor (*Figure 8*). Nutrient disorder in the form of the red tip was detected on forage sorghum at MPOB Research Station in Teluk Intan, Perak (*Figure 9*) and both incidents were not serious. These incidents happened during the dry season. The cause of the red tip was not fully understood but it was believed to be due to deficiencies of nitrogen (N), phosphorus (P), magnesium (Mg) and zinc (Zn). This disorder was controlled by the application of nitrogen fertiliser and sorghum rotation with legume crops.

Effect of Forage Sorghum Integration on Oil Palm Yield

Table 15 compares the average FFB weight for the double avenue oil palm integrated with forage sorghum to the control oil palm plot without forage sorghum integration at Ladang MAAH KLIA. The data was collected for the first five years of harvesting. The results showed that the FFB yield of double avenue oil palm and sorghum integration plots were not significantly different to the control oil palm plots except for the third year FFB yield. These results showed that integrating sorghum with a double avenue oil palm planting system did not reduce oil palm yield. Integration of other crops in double avenue oil palm planting will not result in a negative impact on FFB production if done systematically (Raja Zulkifli *et al.*, 2009).



Figure 8. Valanga *sp. attacks on the leaf of forage sorghum.*

Cost and Return Analysis

Economic analysis was conducted on the oil palm-forage sorghum integration. Total production cost for integrating forage sorghum in the double avenue oil palm planting area was RM5580/ha/season (*Table 16*).

Table 17 shows the cost analysis for fresh fodder production at an average yield of 157 t ha^{-1} yr^{-1} and the price of fresh fodder at RM120 t^{-1}. Based on that assumption, the gross revenue and net revenue per hectare were RM18 840 and RM7680, respectively. The monthly income per hectare from forage sorghum was RM640. The oil palm revenue was calculated based on the FFB yield of the trial plots and the average FFB price of RM540 t^{-1}. Based on this FFB price and FFB yield of 25.40 t ha^{-1} yr^{-1}, the gross and net revenue per hectare was RM13 716 and RM8128, respectively. The monthly income from oil palm was RM677. The total monthly income from the integration of forage sorghum with oil palm was RM1317.

However, the oil palm double avenue-forage sorghum integrated plot produced a slightly lower FFB yield compared to the conventional triangular oil palm control (N148). The difference in FFB yield was 2.45 t ha^{-1} yr^{-1}. But the difference in FFB yield was only 0.80 t ha^{-1} yr^{-1} between the oil palm double avenue-forage sorghum integrated plot compared to the conventional triangular oil palm control (N136). Higher FFB yield in the conventional triangular oil palm control (N148) was due to

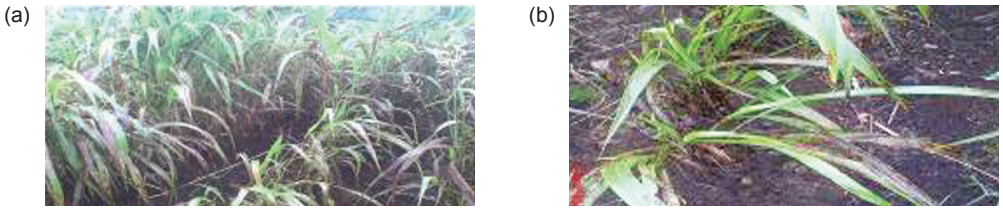


Figure 9. Red tip symptom on (a) whole sorghum plants and (b) leaves.

TABLE 15. AVERAGE FFB YIELD AT LADANG MAAH, KLIA (t ha^{-1} yr^{-1})

Oil palm planting system	Year 1	Year 2	Year 3	Year 4*	Year 5	Average	+/-
Double avenue oil palm integrated with sorghum	3.74 ^{a}	10.30 ^{a}	23.46 ^{bc}	23.13 ^{abcd}	24.62 ^{abcd}	17.05	-
Double avenue oil palm control	4.92 ^{a}	9.77 ^{a}	23.93 ^{bc}	20.63 ^{d}	21.35 ^{d}	16.12	-0.93
Conventional triangular oil palm control (N136)	3.52 ^{a}	9.04 ^{a}	24.66 ^{abc}	26.31 ^{ab}	25.71 ^{abc}	17.85	+0.80
Conventional triangular oil palm control (N148)	4.29 ^{a}	11.42 ^{a}	28.22 ^{a}	26.64 ^{a}	26.92 ^{ab}	19.50	+2.45

Note: * The FFB yield in Year 4 decreased due to severe infestation of bagworm.

an extra number of 12 palms in the plot. But, the conventional triangular oil palm control (N136) that has similar palm density per hectare with the oil palm double avenue-forage sorghum integration plot produced similar FFB yields. However, the loss of return from FFB reduction by adopting a double avenue oil planting system can be compensated by forage sorghum integration.

CONCLUSION

Forage sorghum is technically and economically viable for planting in the double avenue oil palm planting area. In this study, the Sugargraze variety is the most suitable forage sorghum variety for commercial cultivation as an integration crop for fodder production in the oil palm planting area. This was followed by BMR Revolution, Pacific BMR, Jumbo and Superdan varieties. This integration of forage sorghum will optimise the oil palm land use and maximise income per unit land area in order to generate additional income for oil palm growers. To ensure that the integrated forage sorghum produces the highest fodder yield, good agricultural practices for forage sorghum cultivation must be practised by the growers.

ACKNOWLEDGEMENT

The authors wish to thank the Director-General of MPOB for his permission to publish this article. The authors also acknowledge all staff of the Crop and Livestock Integration Unit for their contribution to this project.

REFERENCES

Bhat, B V (2019). Breeding forage sorghum. *Breeding Sorghum for Diverse End Uses* (Aruna, C; Visaraola, K B R S; Venkatesh - Bhat, B and Tonapi, V A eds.). Woodhead Publishing, Sawston, United Kingdom. p. 175-191.

Deanne, M and Kevin, S (1990). Know your forage. Extension Dairy Specialist. North Dakota State University Agriculture and University Extension. http://www.sg.ndsu.edu/pubs/ansci/dairy/as991w.htm, accessed on 10 January 2022.

Gnanagobal, H and Sinniah, J (2018). Evaluation of growth parameters and forage yield of Sugargraze and Jumbo Plus sorghum hybrids under three different spacings during the *maha* season in the

TABLE 16. PRODUCTION COST OF FORAGE SORGHUM INTEGRATION WITH OIL PALM (RM/ha/season*)

Input/activities	Input cost/contract (RM)	Labour		Total (RM)
		Man-day	Cost (RM)	
Seed	400.00	-	-	400.00
Land preparation	850.00	-	-	850.00
Planting	-	10	300.00	300.00
Liming and fertiliser	2 180.00	13	390.00	2 570.00
Weeding	80.00	9	270.00	350.00
Pest and disease control	150.00	2	60.00	210.00
Harvesting	-	30	900.00	900.00
Total cost	**3 660.00**	**64**	**1 920.00**	**5 580.00**

Note: * Six months per season and four harvest cycles.

TABLE 17. ESTIMATED REVENUE FROM FORAGE SORGHUM INTEGRATION WITH OIL PALM (RM ha^{-1} yr^{-1})

Item	Forage sorghum	Oil palm	Total (RM)
	Price: RM120 t^{-1}	Price: RM540 t^{-1}	
Fresh yield (t ha^{-1} yr^{-1})	157.00	25.40	-
Gross return (RM ha^{-1})	18 840.00	13 716.00	32 556.00
Total cost (RM ha^{-1})	11 160.00	5 588.00	16 748.00
Net return (RM ha^{-1})	7 680.00	8 128.00	15 808.00
Monthly income (RM)	640.00	677.00	1 317.00

dry zone of Sri Lanka. *Trop. Grassl.-Forrajes Trop., 6(1)*: 34-41.

Goering, H K and Soest, V (1970). Forage fibre analyses (apparatus, reagents, procedures and some applications) (No. 379). US Agricultural Research Service.

Khalin, S; Koliada, V; Nazarok, P; Koliada, L; Koliada, O and Chuhaiev, S (2020). Perspectives of hay-making production on slopes with south and north orientation on example of Chernozem Podzolized in Ukraine. *Scientific Papers: Management, Economic Engineering in Agriculture and Rural Development, 20(3)*: 311-316.

Lyons, S E; Ketterings, Q M; Godwin, G S; Cherney, D J; Cherney, J H; Van Amburgh, M E; Meisinger, J J and Kilcer, T F (2019). Optimal harvest timing for brown midrib forage sorghum yield, nutritive value and ration performance. *J. Dairy Sci., 102(8)*: 7134-7149.

Malaysian Standard (1982). Method of test for animal feedstuffs (First revision).

Meena, H; Singh, P; Meena, S N; Yadav, D L and Meena, N L (2020). Performance of hybrid fodder sorghum (Sugargraze). *Int. J. Curr. Microbiol. Appl. Sci., 9(5)*: 1601-1606.

Menke, K H; Raab, L; Salewski, A; Steinggas, H; Fritz, D and Schneider, W (1975). The estimation of the digestibility and metabolizable energy content of ruminant feeding stuffs from the gas production when they are incubated with rumen liquor *in vitro*. *J. Agric. Sci., 93*: 217-222.

Raja Zulkifli, R O; Wahid, O; Suboh, I and Norkaspi, K (2009). Performance of crop integrated with oil palm using double avenue system. *Proc. of the PIPOC 2009 International Palm Oil Congress*. p. 365.

Reddy, P S (2017). Sorghum, *Sorghum bicolor* (L.) Moench. *Millets and Sorghum: Biology and Genetic Improvement* (Patil, J V ed.). Wiley Blackwell, West Sussex, United Kingdom. p. 1-32.

Singh, K P; Chaplot, P C; Sumeriya, H K and Choudhary, G L (2016). Performance of single cut forage sorghum genotypes to different fertility levels. *Forage Res., 42(2)*: 184-188.

Steel, R G D and Torrie, J H (1980). *Principles and Procedures of Statistics*. 2nd edition. McGraw Hill, New York. p. 50-60.

Stuart, P (2002). A comprehensive guide to forage management. *The Forage Book*. 2nd edition. Pacific Seeds Pty Ltd. Toowoomba, Australia. p. 8.

Taylor, J R (2019). Sorghum and millets: Taxonomy, history, distribution and production. *Sorghum and Millets* (Taylor, J R N and Duodu, K G eds.). 2nd edition. AACC International Press. Sawston, United Kingdom. p. 1-21.

Weiss, W P; Eastridge, M L and Underwood, J F (1999). Forage for dairy cattle. Ohio State University Fact Sheet. *Animal Sciences*. http://ohioline.osu.edu/as-fact/0002.html, accessed on 14 January 2022.

Journal of Oil Palm Research Vol. 35 (2) June 2023 p. 320-329
DOI: https://doi.org/10.21894/jopr.2022.0037

A FIELD EVALUATION ON FUNGICIDES APPLICATION TO CONTROL UPPER STEM ROT (USR) DISEASE IN OIL PALM CAUSED BY *Ganoderma* spp.

RAMLI NUR-RASHYEDA[1]*; ABU SEMAN IDRIS[1]; SHAMALA SUNDRAM[1]; NUR HAILINI ZAINOL-HILMI[1] and SU CHONG MING[2]

ABSTRACT

Ganoderma *spp. causes basal stem rot (BSR) and upper stem rot (USR) diseases in oil palm. In recent years, there has been an increasing report of USR disease in oil palm, which prompted investigation on fungicides application. This study aimed to evaluate the ability of fungicides to control USR-infected palms. The study was conducted on standing oil palm, selected based on the disease severity index (DSI) in the categories of DSI 1 (early infection) and DSI 2 (moderate infection). Two trials were conducted at two different locations in Sarawak (Miri and Sessang), Malaysia. The fungicides, hexaconazole (4.5 g a.i - 90 mL) and tetraconazole (7.5 g a.i. - 60 mL) were dissolved in 3 L of water; applied using a trunk injector three times at six months interval and followed up with disease assessments conducted at six-monthly intervals. The investigation found that more palms succumbed to USR infection in the control treatment than in the treated USR-infected palms. After 60-months post-treatment, the USR-infected palms treated with hexaconazole gave a lower percentage of dead palms at 33.33% (Miri) and 50.00% (Sessang) compared with USR-infected palms treated with tetraconazole at 66.70% (Miri) and 100.00% (Sessang) and untreated USR-infected palms at 100.00%. The hexaconazole-treated USR-infected palms continued surviving and actively producing fruit bunches. In conclusion, hexaconazole was found to be more effective than tetraconazole. It gave a higher survival rate by ceasing the progress of disease development, resulting in lengthening the productive lifespan of USR-infected palms.*

Keywords: fungicide, *Ganoderma boninense*, hexaconazole, tetraconazole, upper stem rot.

Received: 28 November 2021**; Accepted:** 10 May 2022**; Published online:** 6 July 2022.

INTRODUCTION

The oil palm (*Elaeis guineensis* Jacq.) is an important perennial crop in Malaysia and plays an essential role in the agricultural and economic development of the country (Kushairi *et al.*, 2019; Parveez *et al.*, 2021). Palm oil production in Malaysia has increased over the years, from 4.1 million tonnes in 1985 to 6.1 million tonnes in 1990, and up to 19.86 million tonnes in 2019 (Parveez *et al.*, 2020). However, one of the main constraints faced by the oil palm industry is diseases caused by plant pathogens. Basal stem rot (BSR) is the biggest threat to oil palm production and has been documented to cause huge damage to the oil palm industry in Malaysia. Although BSR is the most prominent disease affecting the oil palm industry, the upper stem rot (USR) disease in oil palm in recent years has seen a sharp rise in incidences, reported mostly in Sabah, Malaysia (Gassner *et al.*, 2005), Sarawak, Malaysia (Rakib *et al.*, 2017) and Indonesia (Hari *et al.*, 2011). A number of *Ganoderma* spp., including *Ganoderma boninense* are known to cause BSR and USR. In USR-infected palm, the infection of *Ganoderma* was found to be on

[1] Malaysian Palm Oil Board,
6 Persiaran Institusi, Bandar Baru Bangi,
43000 Kajang, Selangor, Malaysia.

[2] Sarawak Oil Palms Berhad (SOPB),
124-126, Jalan Bendahara, P. O. Box 547,
98007 Miri, Sarawak, Malaysia.

* *Corresponding author e-mail: shyeda@mpob.gov.my*



Figure 1. Upper stem rot (USR) symptoms; formation of the fruiting body and stem rotting appear at one meter from ground level.

the upper portion of the stem or trunk, appearing at 1 m above ground (*Figure 1*) as opposed to the BSR symptoms which appear at the base of an infected palm (Rakib *et al.*, 2014).

USR disease is generally accepted to be less common than BSR disease, and its occurrence is very estate-specific (Gassner *et al.*, 2005). Research has proven that BSR disease spreads through root-to-root contact and from one palm to the adjacent palm. It was suggested that USR disease spread is associated with the airborne-basidiospores or insect-transmitted, although the disease initiation remains unknown (Hushiarian *et al.*, 2013). The role of *Ganoderma* basidiospores in disease infection remains unclear. Despite the fact that large numbers of basidiospores are released from basidiomata in oil palm fields, most oil palms are not infected, indicating that the basidiospores are less effective to cause infection, possibly requiring more specific conditions to succeed (Ho and Nawawi, 1986). However, a study conducted by Pilotti *et al.* (2018) revealed that multiple isolates of *G. boninense* were found in seedlings growing near infected palms in the oil palm field, indicating that colonisation of roots by basidiospores and dikaryons, resulting from mating between basidiospores occurred in oil palm plantations.

There are several methods to control *Ganoderma* in BSR, such as cultural practices, including deboling and sanitation, soil mounding and the application of biological control agents (Idris *et al.*, 2016). As a short-term control measure, fungicide application as a curative treatment remains crucial for managing the disease in the fields. Various fungicides have been investigated to control this disease, and systemic fungicides such as drazoxolone, cycloheximide, triadimefon, carbonix, benomyl, hexaconazole, penconazol and tetraconazole were found to be effective based on *in vitro* studies (Arifurrahman and Idris, 2008). Hexaconazole and tetraconazole are classified under the triazole group, a broad-spectrum systemic fungicide. These triazole fungicides were previously reported as a foliar treatment to control apple scab caused by *Venturia inaequalis* (Shahinasi *et al.*, 2017) and powdery mildew in wheat caused by *Blumeria graminis* f. sp. *tritici* (Basandrai *et al.*, 2013). These pathogens are fungi and were successfully controlled by fungicide applications. Yaduman *et al.* (2018) observed that a combination of fungicides, carbendazim and propiconazol as a foliar spray and seed treatment was most effective for sheath blight of rice caused by *Rhizoctonia solani*, a soil-borne plant pathogenic basidiomycete. More recently, a new triazole fungicide, mefentrifluconazole, is available for the disease management of *Septoria tritici* blotch disease in wheat, with promising results obtained via *in vitro* assessment (Klink *et al.*, 2021).

A study by Idris *et al.* (2009) assessed the effectiveness of these triazole groups, namely hexaconazole and tetraconazole, in prolonging the productive life of BSR-infected palms. Their findings showed promising results where these fungicides could halt disease progression in infected palms, hence, prolonging the productive life of the palms. It was reported that 74.4% of the palms treated with hexaconazole remained productive by continuously producing fruit bunches for more than five years, while none of the untreated palms survived (Idris *et al.*, 2010). The increased number of USR diseases in existing oil palm requires immediate short-term control measures. Given the success of the fungicides in controlling BSR disease, this study aimed to assess the potential of hexaconazole and tetraconazole in controlling USR-infected palms through trunk injection.

MATERIALS AND METHODS

Study Sites

The study was conducted at two oil palm plantations in Miri, Sarawak (Site 1) and Sessang, Sarawak (Site 2). The palms, 12 years old (first generation) *Dura* x *Pisifera* (DxP) were planted on peat soil in Miri, Sarawak, covering approximately 32.0 ha. Meanwhile, in Sessang, Sarawak, the palms (DxP) selected for the study were 11 years old (first generation), planted on peat soil covering approximately 40.0 ha.

Treatments

Thirty-six USR-infected palms that were still producing fruit bunches in categories DSI 1 and DSI 2 (*Table 1*) were selected, and the trial was laid down in a completely randomised design (CRD). Twelve healthy oil palms were also included in the study as the negative control. Four treatments were applied, whereby each treatment consisted of 12 oil palms (*Table 2*). Both fungicides, hexaconazole (4.5 g a.i. - 90 mL) and tetraconazole (7.5 g a.i. - 60 mL) were dissolved in 3 L of water and applied three times at six-month intervals (Idris *et al.*, 2010).

TABLE 1. DISEASE SEVERITY INDEX (DSI) CORRESPONDING WITH LEVELS OF SEVERITY IN MATURE PALM

Disease class	Signs and symptoms of infection
0	Healthy palm. Absence of fruiting body, foliar symptom or stem rotting at the base. Early detection tests (*e.g.*, GSM or PCR-DNA) are negative for the presence of *Ganoderma*.
1	Early infection or mildly infected palm. Presence of white mycelium or fruiting body (*e.g.*, small white button) or no foliar symptoms with mild or no stem rotting (<10%) at trunk/stem. Early detection methods (*e.g.*, GSM or PCR-DNA) show positive *Ganoderma* detection.
2	Moderately infected palm. Presence of white mycelium or fruiting body (*e.g.*, small white button or bracket shape). Palm showing foliar symptoms: yellowing and collapsed fronds (<50%) and stem rotting (<30%) at the trunk. Confirmed presence of *Ganoderma* fungus using early detection methods (*e.g.*, GSM or PCR-DNA).
3	Severely infected palm. Presence of white mycelium or fruiting body (*e.g.*, small white button or bracket shaped form). Palm showing severe foliar symptoms (>50%) and stem rotting (>30%) at the trunk. Confirmed presence of *Ganoderma* fungus using early detection methods (*e.g.*, GSM or PCR-DNA).
4	Dead palm. Presence of white mycelium or fruiting body (*e.g.*, small white button or bracket shaped form). Collapsed/dead palm with severe foliar symptoms and stem rotting at the trunk. Confirmed presence of *Ganoderma* fungus using early detection methods (*e.g.*, GSM or PCR-DNA).

Note: GSM - *Ganoderma* selective medium; PCR-DNA - polymerase chain reaction-deoxyribonucleic acid.
Source: Idris *et al.* (2016).

TABLE 2. TREATMENTS OF FUNGICIDES APPLIED TO UPPER STEM ROT (USR) - INFECTED PALMS

Treatments	Description	No. of palms
T1	USR-infected palm treated with hexaconazole - 4.5 g a.i. (90 mL) + 3 L water	12
T2	USR-infected palm treated with tetraconazole - 7.5 g a.i. (60 mL) + 3 L water	12
T3	Positive Control – Untreated USR-infected palm	12
T4	Negative Control – Untreated healthy palm	12

Trunk injection was carried out using a hand knock injector attached to the motorised knapsack sprayers to pressure-inject the fungicide solution into a hole made on the trunk (2 L/hole) at one-meter height from the ground level. The remaining 1 L of the fungicide solution was sprayed directly onto the USR-infected trunk (*Figure 2*).

Disease Assessments

The presence of *Ganoderma* in the trunk tissue was confirmed by culturing the collected sample on *Ganoderma* selective medium (GSM), prepared according to Idris *et al.* (2016). The palms status in each of the treatments was assessed at six-monthly intervals over five years by recording the presence or absence of USR symptoms, including external symptoms (*e.g.*, foliar symptoms and appearance of *Ganoderma* fructification) and decay of the trunk. Oil palms were scored according to disease class, ranging from 0-4 (*Table 3*). Disease severity of foliar index (DSFI) was calculated based on the symptoms appearing on the foliage (external), according to Liu *et al.* (1995) [Equation (1)].

$$\text{DSFI}\ (\%) = \frac{\sum (\text{Number of palms in the scale} \times \text{Severity rating})}{\text{Total number of palms assessed} \times \text{Highest rating}} \times 100 \qquad (1)$$

The extent of disease developed over time for each treatment was further expressed as the area under the disease progress curve (AUDPC), calculated based on a Equation (2) as described by Campbell and Madden (1990):

$$\text{AUDPC} = \sum_{i}^{n-1} [(y_i + y_{i+1})/2]\ (t_{i+1} + t_i) \qquad (2)$$

where n is the number of assessments, y is the measurement of disease (DSFI) and t is the time of observation. Disease reduction (DR) was calculated based on the value of AUDPC by the following Equation (3):

$$\text{DR}\ (\%) = \frac{(\text{AUDPC control} - \text{AUDPC treatment})}{\text{AUDPC control}} \times 100 \qquad (3)$$

The assessment was also carried out based on the quantitative assessment measured by inspection of the dead palms. All data in percentage were arcsine transformed (Gomez and Gomez, 1984) and subjected to analysis of variance (ANOVA) with the means compared by LSD at $p \leq 0.05$ using Statistical Analysis System (SAS® Software) (SAS Institute Inc).



Figure 2. Application of fungicides on the upper stem rot (USR)-infected palm (a) selection of USR infected-palm with disease severity index (DSI) 1 and 2 and still producing fruit bunches, (b) removal of the old frond and fruiting bodies from the USR-infected stem/trunk tissues using a chisel, (c) drilling of one hole on the stem/trunk at 1-m height above ground level using motorised engine drill attached with a drill bit (45 cm long, 11 mm diameter), (d) injecting a total of 2 L/palm of fungicide solution using hand knock injector attached to the motorised knapsack sprayers and (e) spraying remaining 1-L fungicide solution onto the USR stem/trunk infected tissues.

TABLE 3. SIGNS AND SYMPTOMS OF DISEASE SEVERITY FOLIAR INDEX (DSFI) SCORED ON A SCALE OF 0-4

Disease class	Signs and symptoms of infection
0	Healthy palms with green leaves and without the appearance of fungal mycelium on any part of the plant.
1	Presence of white mycelium or fruiting body on any part of the plant without necrosis or chlorosis of leaves.
2	Presence of white mycelium or fruiting body on any part of the plant with necrosis or chlorosis of leaves (<25%).
3	Presence of white mycelium or fruiting body on any part of the plant with necrosis or chlorosis of leaves (<75%).
4	Presence of white mycelium or fruiting body on any part of the plant with necrosis or chlorosis of leaves (>75%) or the palm is dead.

Source: Izzati and Abdullah (2008).

RESULTS AND DISCUSSION

The current field study was conducted between 2014 and 2020 to evaluate the response of *Ganoderma*-USR infected palms upon the application of hexaconazole and tetraconazole. Isolates of *Ganoderma* were isolated from the USR infected trunk tissues on GSM (*Figure 3*). The formation of a brown halo on the GSM media confirmed the presence of basidiomycete fungi including *Ganoderma* (Naidu *et al.*, 2018). The data was presented annually for five years, although the census was carried out at six-monthly intervals. The symptoms of USR infection were observed with the appearance of white mycelium, which later developed into the white button and fruiting body along the stem or trunk. Before the application of the fungicides, the DSFI of each palm within each treatment was found to be similar, with no significant differences recorded (*Figure 4*). Twelve months after application (MAA), all the treated palms in both study sites significantly showed lower DSFI with hexaconazole, T1 (10.8% -17.2%) and tetraconazole, T2 (14.6%-18.9%) compared to the untreated palms in T3 (18.6%-37.7%). In Site 1 (Miri), the difference between the DSFI percentage of T1 and T2 became bigger at 48 MAA where it was observed that 100.0% of DSFI was recorded in all palms in T2. On the contrary, palms of T2 in Site 2 (Sessang), showed a significantly lower infection symptom than the untreated palms (T3). It was observed that after 48 months, untreated palms (T3) showed DSFI significantly higher at 70.0% and 100.0% for both study sites, as compared to DSFI of only 36.3%-42.1% in the palms treated with hexaconazole, T1. At 60 MAA, the palms in T1 showed the lowest DSFI percentage ranging from 41.7%-48.1%, highlighting the potentials of hexaconazole in suppressing the disease. Meanwhile, no fruiting bodies, white buttons or mycelia were observed on the control palms in T4 (healthy).

DSFI data was further evaluated by AUDPC (*Table 4*). The AUDPC values suggest the amount of disease development in each treatment whereas the treatment with the lowest AUDPC value indicate the effectiveness of the treatment in reducing the disease. The treated palms in T1 exhibited significantly lowest AUDPC of 132.96 unit^2 and 108.02 unit^2 in Site 1 and Site 2, respectively. This was followed by T2 with AUDPC values of 284.98 unit^2 and 148.35 unit^2, respectively. It was then followed by T3 with significantly the highest AUDPC values of 316.35 unit^2 and 210.80 unit^2. The highest DR for both sites were indicated by T1 treatment with 48.76% and 57.97% reduction compared to the control.

The disease assessment data in *Figure 5* represents the percentage of dead palms due to *Ganoderma* infection observed until 60 MAA. In both study sites, there were no dead palms recorded on palms treated with hexaconazole and tetraconazole at the beginning. Twelve months post-application, it was recorded that the percentage of dead palms was

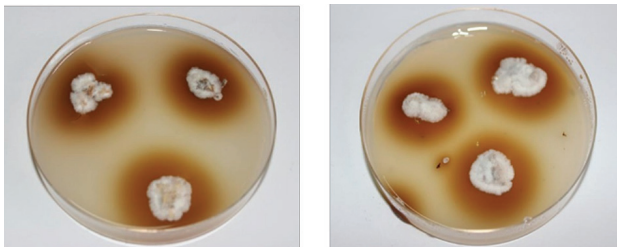
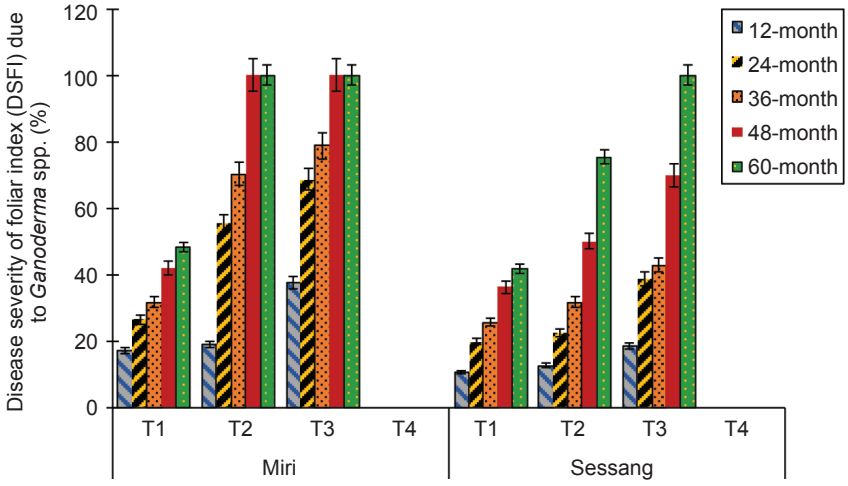


Figure 3. Infected tissues from USR-infected palms cultured on Ganoderma *Selective Medium (GSM).*



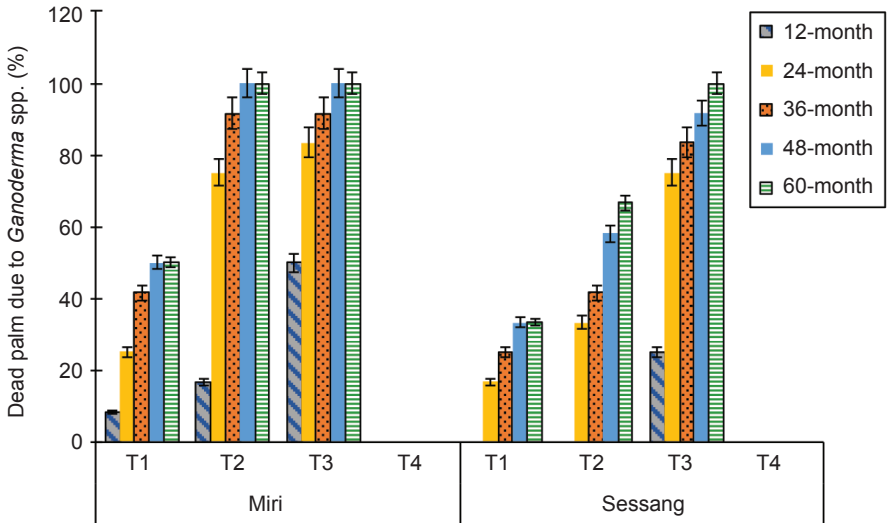
Note: Values are represented by the mean (n=12), with vertical bars representing standard error. T1 is the USR-infected palms treated with hexaconazole at 4.5 g a.i. (90 mL) + 3 L water; T2 is the USR- infected palms treated with tetraconazole at 7.5 g a.i. (60 mL) + 3 L water; T3 is the control (untreated USR-infected palms); T4 is the control (untreated healthy palms).

Figure 4. Percentage of disease severity of foliar index (DSFI) due to upper stem rot (USR) disease at the study sites, Miri and Sessang.

TABLE 4. AREA UNDER THE DISEASE PROGRESS CURVE (AUDPC) AND DISEASE REDUCTION (DR) DUE TO UPPER STEM ROT (USR) DISEASE IN OIL PALM AFTER FUNGICIDE TREATMENT

Treatments	Site 1 (Miri)		Site 2 (Sessang)	
	The area under the disease progress curve (AUDPC) (unit²)	Disease reduction (DR) (%)	The area under the disease progress curve (AUDPC) (unit²)	Disease reduction (DR) (%)
T1	132.96 ± 30.50a	57.97	108.02 ± 12.77a	48.76
T2	284.98 ± 41.20b	9.92	148.35 ± 21.10b	29.63
T3	316.35 ± 22.50c		210.8 ± 32.70c	
T4	0	-	0	-

Note: Means followed by the same letter within a column are significantly not different ($p \leq 0.05$) (n=12). T1 is the USR-infected palms treated with hexaconazole at 4.5 g a.i. (90 mL) + 3 L water; T2 is the USR- infected palms treated with tetraconazole at 7.5 g a.i. (60 mL) + 3 L water; T3 is the control (untreated USR-infected palms); T4 is the control (untreated healthy palms).



Note: Values are represented by the mean (n=12), with vertical bars representing standard error. T1 is the USR-infected palms treated with hexaconazole at 4.5 g a.i. (90 mL) + 3 L water; T2 is the USR- infected palms treated with tetraconazole at 7.5 g a.i. (60 mL) + 3 L water; T3 is the control (untreated USR-infected palms); T4 is the control (untreated healthy palms).

Figure 5. Percentage of dead palms due to upper stem rot (USR) disease at the study sites, Miri and Sessang.

lower in both treated palms of T1 (hexaconazole) and T2 (tetraconazole) in Site 1 (Miri) while there was no dead palm recorded in Site 2 (Sessang). Interestingly, the dead palms recorded in T2 were three times higher compared to dead palms in T1 after 24 MAA at Site 1, and this value continued to increase to 100.0% after 48 MAA. A similar situation was also observed in Site 2, as the percentage of dead palms in T2 was significantly higher compared to T1. On the other hand, untreated palms (T3) showed significantly the highest percentage of dead palms over the years. Based on this study, the percentage of dead palms was significantly lowest at $p<0.05$ in palms treated with hexaconazole (T1) (33.3%-50.0%) after 60 MAA.

This study presents the first report on USR disease control in oil palm through fungicides application. One common characteristic between USR-infected and BSR-infected palms is that both diseases are caused by a similar pathogen, *Ganoderma* spp. The pathogen can cause a significant increase of incidences in the affected area. The difference between USR and BSR is that the former infects the palm approximately 1 m above the stem base, while the latter occurs at the stem base of the oil palm (Rakib *et al.*, 2014). Generally, in the initial stage of USR infected palm, the yellowing of leaves will be accompanied by the formation of sporophores at the oil palm trunk. In the final stage of infection, severe desiccation of leaves and the production of fruiting bodies at the mid-section of the trunk will be observed.

The field trial was conducted on USR-infected palms with early symptoms of infection with continuous production of fruit bunches. Visual-based disease observation is still the only method to identify the USR disease in the field (Idris, 2011; Rakib *et al.*, 2015). Most fungicides need to be applied before

the onset of disease or at the first appearance of the disease symptoms for effective control (Poole and Arnaudin, 2014). For instance, research on managing northern corn leaf blight (NCLB) suggested that the appropriate time for trifloxystrobin and epoxiconazole fungicides application in reducing NCLB was at the onset of disease (severity below 2%) (Carpane *et al.*, 2020). In the current study, the use of fungicides was shown to prolong the economic lifespan of the diseased palms as it suppressed the spread of *Ganoderma* infection within the infected area of standing palms in category of DSI 1 and DSI 2. Although *Ganoderma* infection cannot be eliminated, the economic life of infected palms was prolonged with continuous production of fresh fruit bunches (FFB) due to the effective chemical control. Having said this, another setback in most fungicides' is the fact that the effect is temporary. More applications and higher dosages are likely to improve the disease control; however, the number of applications and dosage must be optimised to achieve efficient disease control with a prolonged effective lifespan of the plant (Van den Berg *et al.*, 2016). This study suggested that repeated application of the fungicide is necessary in the event of a relapse of infection within the oil palms. Therefore, infection of adjacent healthy tissues by the fungus would be halted with repeated applications of systemic fungicide over a period of time. This method was successfully demonstrated by Thangeswari *et al.* (2019), who found that repeated fungicides application was effective in the management of BSR disease in coconut. The application of hexaconazole (5.0% EC) and tetraconazole (3.8% EC) as root feeding at a quarterly interval in BSR-infected coconut palm recorded lower disease incidence at 3.28% and 4.86% when compared to 17.40% in control.

Fungicides application contributes significant importance to crop protection (Oliver and Hewitt, 2014). Hexaconazole, a systemic fungicide, is used to control a broad spectrum of diseases and is more productive and cost-effective than other triazole fungicides. The fungicide, which is a potent inhibitor of ergosterol biosynthesis (Huang *et al.*, 2012), is active mainly against basidiomycetes and ascomycetes. The triazole fungicides can inhibit a specific enzyme, C14-demethylase, which plays an important role in sterol production (Yan *et al.*, 2016). Sterols, such as ergosterol, are required for membrane structure and function, making them essential for developing functional cell walls in fungi. The sterols are extremely crucial that their deficiency results in abnormal fungal growth and eventually death in fungi (Alcazar-Fuoli and Mellado, 2013). In the present work, disease manifestation through DSFI was lower in USR-infected palms treated with hexaconazole (T1) compared to the percentage recorded in USR-infected palms treated with tetraconazole (T2) and untreated control (T3). This finding showed that hexaconazole application prolonged the lifespan of the treated palms and significantly reduced the number of dead palms. Similar findings were reported in rice, whereby Kumar *et al.* (2013) found that the application of hexaconazole at 75% WG@50 g a.i./ha, gave effective control of sheath blight with increased yield when compared to the untreated plot. Recently, a new chitosan nanoparticles formulation containing the active ingredient of hexaconazole was successfully developed and showed promising results with a significant percentage reduction of disease in oil palm seedlings infected with *G. boninense* (Maluin *et al.*, 2020). This observation suggested that *Ganoderma* infection in treated oil palms was slowed down, particularly in palms treated with hexaconazole, hence, delaying the appearance of foliar symptoms.

Previous studies have also indicated that hexaconazole was able to treat BSR disease in oil palms (Idris, 2011; Maluin *et al.*, 2019). Similarly, tetraconazole was reported to reduce the BSR incidence in oil palm (unpublished data) and coconut (Thangeswari *et al.*, 2019). However, the use of tetraconazole in the present study was ineffective against USR-infected palms. This was evident with the application of tetraconazole in Site 1 (Miri) which failed to reduce the disease severity in infected palms giving a higher number of dead palms. The possible reasons for these findings remain unclear, but the failure of tetraconazole to control the disease has been found in this study. Additionally, this result is in line with that of Arabiat (2015), who evaluated tetraconazole for the management of *Aphanomyces cochlioides* in sugarbeet. The study concluded that this fungicide was ineffective at controlling *A. cochlioides* in the *in vivo* assessment. However, it was capable of reducing the disease based on the *in vitro* study. Different fungicide products may have different levels of biological efficacy against the same pathogen. Ramdial *et al.* (2016; 2017) highlighted several reasons that might be associated with fungicide failure and resistance due to multiple interacting factors. Among these were repetitive use and exceeding dose rate, and inaccuracy in the application interval. The application of tetraconazole in USR-infected palms did not improve the level of disease control provided by trunk injection applications. It may require a higher dosage, but this remains to be investigated in the future. In some cases, some products can be effective for the control of a specific disease but differ in their effectiveness. A study on fruit anthracnose disease of the chili plant was conducted using two fungicides, namely tebuconazole and hexaconazole. The study results gave varying control efficacy, with hexaconazole being superior at 83.3% disease control (Anand *et al.*, 2020). This study should be explored further to confirm the consistency of the results and possibly with the mixture application of two different

fungicides or a higher dosage with a varied interval of applications.

CONCLUSION

Hexaconazole can be recommended to control USR disease in oil palms. This is shown by the significant reduction of dead oil palms, and lower DSFI observed after hexaconazole treatment compared to the non-treated control oil palms. The recommended rate is 4.5 g a.i. (90 mL) + 3 L water per palm, combining the trunk injection and spray application at the infected trunk, repeated three times at six-monthly intervals. The application of hexaconazole on USR-infected palms demonstrates that it could control the progress of USR disease development hence, prolonging the life of diseased palms.

ACKNOWLEDGEMENT

The authors would like to thank MPOB for funding this study. A heartful thanks to Sarawak Oil Palms Berhad for providing field area and manpower to conduct the trials. A special thanks to all staff of Plant Pathology and Biosecurity Unit, MPOB for their technical assistance throughout the study.

REFERENCES

Alcazar-Fuoli, L and Mellado, E (2013). Ergosterol biosynthesis in *Aspergillus fumigatus*: Its relevance as an antifungal target and role in antifungal drug resistance. *Front. Microbiol., 3*: 439.

Anand, A; Guptha, H B and Chourasia, H K (2020). Management of anthracnose of red chilli caused by *Colletotrichum capsici. Ann. Plant Soil Res., 22(4)*: 390-395.

Arabiat, S I (2015). Sensitivity of *Rhizoctonia solani* and *Aphanomyces cochlioides* to fungicides, and fitness of tetraconazole-resistant isolates of *Cercospora beticola* after exposure to different temperature regimes. North Dakota State University.

Arifurrahman, R and Idris, A S (2008). *In vitro* evaluation of an effective fungicide against *Ganoderma boninense*, the causal agent of basal stem rot (BSR) in oil palm. *7th International Conference on Plant Protection in the Tropic-Update on GAP in IPM*. Kuala Lumpur. p. 1-4.

Basandrai, A K; Sharma, B K and Basandrai, D (2013). Efficacy of triazole fungicides for the integrated management of yellow rust, leaf rust and powdery mildew of wheat. *Plant Dis. Res., 28(2)*: 135-139.

Campbell, C L and Madden, L V (1990). *Introduction to Plant Disease Epidemiology*. New York, USA, John Wiley and Sons.

Carpane, P D; Peper, A M and Kohn, F (2020). Management of Northern corn leaf blight using Nativo (trifloxistrobin+ tebuconazole) fungicide applications. *Crop Prot., 127*: 104982.

Flood, J; Hasan, Y and Foster, H (2002). *Ganoderma* diseases of oil palm - An interpretation from Bah Lias research station. *Planter, 78(921)*: 689-710.

Gassner, A; Wong, W C; Hong, H W and Kuil, S (2005). Assessment of the spatial and temporal proliferation of upper stem rot in oil palm plantation (*Elaeis guineensis*) in the Kudat Region, Sabah. *Proc. of the PIPOC 2005 International Palm Oil Congress - Agriculture, Biotechnology and Sustainability Conference*. MPOB, Bangi. p. 1-4.

Gomez, K A and Gomez, A A (1984). Statistical procedures for agricultural research. John Wiley and Sons. New York. 680 pp.

Hari, P; Susanto, A and Surianto (2011). Physical barrier on the oil palm trunk: An approach to prevent upper stem rot disease caused by *Ganoderma boninense*. *Proc. of the PIPOC 2011 International Palm Oil Congress - Agriculture, Biotechnology and Sustainability Conference*. MPOB, Bangi. p. 79-83.

Ho, Y W and Nawawi, A (1986). Germination studies of *Ganoderma boninense* spores from oil palms in Malaysia. *Pertanika, 9(2)*: 151-154.

Huang, L; Lu, D; Zhang, P; Diao, J and Zhou, Z (2012). Enantioselective toxic effects of hexaconazole enantiomers against *Scenedesmus obliquus. Chirality, 24(8)*: 610-614.

Hushiarian, R; Yusof, N A and Dutse, S W (2013). Detection and control of *Ganoderma boninense*: Strategies and perspectives. *SpringerPlus, 2(555)*: 1-12.

Idris, A S (2011). Biology, detection and control of *Ganoderma* in oil palm. *Further Advances in Oil Palm Research* (2000-2010) (Basri, M W eds.). MPOB, Bangi. p. 485-521.

Idris, A S; Arifurrahman, R and Kushairi, A (2009). An evaluation of hexaconazole for controlling *Ganoderma* basal stem rot of oil palm in the field as a preventive treatment. *Proc. of the PIPOC 2009 International Palm Oil Congress - Agriculture, Biotechnology and Sustainability Conference*. MPOB, Bangi. p. 1292-1300.

Idris, A S; Arifurrahman, R and Kushairi, A (2010). Hexaconazole as a preventive treatment for managing *Ganoderma* in oil palm. *MPOB Information Series, 533*. p. 1-4.

Idris, A S; Ramli, N R; Rusli, M H; Sundram, S and Norman, K (2016). *The Standard Operating Procedure (SOP) Guidelines for Managing* Ganoderma *Disease in Oil Palm.* MPOB, Bangi. p. 1-41.

Izzati, M Z N A and Abdullah, F (2008). Disease suppression in *Ganoderma*-infected oil palm seedlings treated with *Trichoderma harzianum. Plant Prot. Sci., 44(3)*: 101-107.

Klink, H; Verreet, J-A; Hasler, M and Birr, T (2021). Will triazoles still be of importance in disease control of *Zymoseptoria tritici* in the future? *Agronomy, 11(5)*: 933.

Kumar, M K P; Gowda, D K S; Moudgal, R; Kumar, N K; Gowda, K T P and Vishwanath, K (2013). Impact of fungicides on rice production in India. *Fungicides-showcases of Integrated Plant Disease Management from around the World, U.K*. IntechOpen. p. 76-99.

Kushairi, A; Ong-Abdullah, M; Nambiappan, B; Hishamuddin, E; Zanal Bidin, M N I; Ghazali, R; Subramanian, V; Sundram, S and Parveez, G K A (2019). Oil palm economic performance in Malaysia and R&D progress in 2018. *J. Oil Palm Res., 31(2)*: 165-194.

Liu, L; Kloepper, J W and Tuzun, S (1995). Induction of systemic resistance in cucumber against *Fusarium* wilt by plant growth-promoting rhizobacteria. *Phytopathology, 85(6)*: 695-698.

Maluin, F N; Hussein, M Z; Yusof, N A; Fakurazi, S; Idris, A S; Zainol Hilmi, N H and Jeffery Daim, L D (2019). Preparation of chitosan–hexaconazole nanoparticles as fungicide nanodelivery system for combating *Ganoderma* disease in oil palm. *Molecules, 24(13)*: 2498.

Maluin, F N; Hussein, M Z; Azah Yusof, N; Fakurazi, S; Idris, A S; Zainol Hilmi, N H and Jeffery Daim, L D (2020). Chitosan-based agronanofungicides as a sustainable alternative in the basal stem rot disease management. *J. Agric. Food Chem., 68(15)*: 4305-4314.

Naidu, Y; Siddiqui, Y; Rafii, M Y; Saud, H M and Idris, A S (2018). Inoculation of oil palm seedlings in Malaysia with white-rot hymenomycetes: Assessment of pathogenicity and vegetative growth. *Crop Prot., 110*: 146-154.

Oliver, R P and Hewitt, H G (2014). *Fungicides in Crop Protection*. CABI, United Kingdom. 200 pp.

Parveez, G K A; Elina, H; Loh, S K; Ong-Abdullah, M; Kamalrudin, M S; Zanal Bidin, M N I; Sundram, S; Zafarizal, A A H and Zainab, I (2020). Oil palm economic performance in Malaysia and R&D progress in 2019. *J. Oil Palm Res., 32(2)*: 159-190.

Parveez, G K A; Tarmizi, A H A; Sundram, S; Loh, S K; Ong-Abdullah, M; Palam, K D P; Salleh, K M; Ishak, S M and Idris, Z (2021). Oil palm economic performance in Malaysia and R&D progress in 2020. *J. Oil Palm Res., 33(2)*: 181-214.

Pilotti, C A; Gorea, E A and Bonneau, L (2018). Basidiospores as sources of inoculum in the spread of *Ganoderma boninense* in oil palm plantations in Papua New Guinea. *Plant Pathol., 67(9)*: 1841-1849.

Poole, N F and Arnaudin, M E (2014). The role of fungicides for effective disease management in cereal crops. *Can. J. Plant Pathol., 36(1)*: 1-11.

Rakib, M; Bong, C; Khairulmazmi, A; Idris, A S; Jalloh, M B and Wahida, N H (2017). *Ganoderma* species of basal and upper stem rots in oil palm (*Elaeis guineensis*) in Sarawak, Malaysia. *J. Acad., 5(1)*: 27-35.

Rakib, M R M; Bong, C-F J; Khairulmazmi, A and Idris, A S (2014). Occurrence and spatial distribution of *Ganoderma* species causing upper and basal stem rot in oil palm. *J. Food. Agric. Environ., 12(2)*: 360-364.

Rakib, M R M; Bong, C F J; Khairulmazmi, A and Idris, A S (2015). Aggressiveness of *Ganoderma boninense* and *G. zonatum* isolated from upper and basal stem rot of oil palm (*Elaeis guineensis*) in Malaysia. *J. Oil Palm Res., 27(3)*: 229-240.

Ramdial, H; Hosein, F N and Rampersad, S N (2016). Detection and molecular characterization of benzimidazole resistance among *Colletotrichum truncatum* isolates infecting bell pepper in Trinidad. *Plant Dis., 100(6)*: 1146-1152.

Ramdial, H; De Abreu, K and Rampersad, S N (2017). Fungicide sensitivity among isolates of *Colletotrichum truncatum* and *Fusarium incarnatum-equiseti* species complex infecting bell pepper in Trinidad. *Plant Pathol. J., 33(2)*: 118.

Shahinasi, E; Brahushi, F; Devolli, A and Kodra, M (2017). The ecotoxicology of pesticides group of triazole and their use to control apple scab (*Venturia inaequalis*). *J. Hyg. Eng. Des., 634(11)*: 36-42.

Thangeswari, S; Karthikeyan, A and Maheswarappa, H P (2019). Management of basal stem rot disease in coconut through fungicides. *J. Plant. Crop., 47(3)*: 207-210.

Van den Berg, F; Paveley, N D and Van den Bosch, F (2016). Dose and number of applications that maximize fungicide effective life exemplified by *Zymoseptoria tritici* on wheat - A model analysis. *Plant Pathol., 65(8)*: 1380-1389.

Yaduman, R; Lal, A A; Singh, S and Simon, S (2018). Management of sheath blight disease (*Rhizoctonia solani* L.) of rice. *Ann. Plant Prot. Sci., 26(1)*: 150-152.

Yan, B; Li, H-Y; Gao, J; Wang, A-M; Ren, G-Y; Li, Y-J and Ma, H-X (2016). Thermodynamic properties of diniconazole and hexaconazole. *J. Chem. Thermodyn., 99*: 82-85.

Journal of Oil Palm Research Vol. 35 (2) June 2023 p. 330-339
DOI: https://doi.org/10.21894/jopr.2022.0050

SUSTAINING BEEHIVE-FENCE TO REDUCE ELEPHANT ENCROACHMENT IN OIL PALM PLANTATION

BADRUL AMIN ABDUL MALEK[1]; NORASMAH BASARI[2*]; HISHAM HAMZAH[1]; WAN NUR AMANINA WAN MANSOR[2]; M. FAIZOL SHAMRIE MD SHANI[2]; ANIS NAZIRAH ARSHAD[2]; WAHIZATUL AFZAN AZMI[2] and MOHAMED NOR ZALIPAH[2]

ABSTRACT

Human-elephant conflict is among the important issues debated since the oil palm industry was established in Malaysia. Various mitigation methods have been implemented to reduce economic loss due to crop raiding by the elephants, but none seems to be highly effective. Hence, the beehive-fence (BHF) was implemented as an alternative control method in Ladang Jernih Oil Palm Plantation in Terengganu, Malaysia. However, data from previous BHF studies showed that the number of bee colonies had reduced over time due to various reasons. In this article, we present the challenges of sustaining the Asian honeybee, Apis cerana*, colonies used for the BHF project in Ladang Jernih. We collected data on pests and predators, bee activity levels, food sources and the number of elephant encroachment incidents. Although the number of elephant encroachment incidents in Ladang Jernih was reduced, we found that the beehives faced a significantly high number of pest infestations. The activity levels of the bee colonies were also found to be passive due to limited food sources. We therefore conclude that the BHF may become another sustainable mitigation method to reduce elephant encroachment, but more attention must be given to the bee colonies to ensure the success of this eco-friendly mitigation effort.*

Keywords: *Apis cerana*, beehive-fence, human-wildlife conflict, Malaysia, oil palm.

Received: 23 August 2021**; Accepted:** 4 July 2022**; Published online:** 23 August 2022.

INTRODUCTION

Human-wildlife conflict is a common issue when it comes to industrial, development, and agriculture practices. Certain activities of land development require deforestation which led to the loss of wildlife habitats, foraging sites and hunting areas. As such, the affected wildlife will enter farms or house perimeters during foraging. In the Malaysian oil palm industry, planters are required to follow the New Planting Procedures (NPP) under the Roundtable on Sustainable Palm Oil (RSPO) standards, in which the primary forest, high conservation value (HCV) areas, high carbon stock (HCS) forests, peatland, fragile and marginal soils, as well as local people's lands should not be developed into oil palm planting area. Oil palm planting areas are either through the utilisation of idle land or conversion from other crops, primarily rubber and cocoa. Nevertheless, human-elephant conflict (HEC) is among the important issues that have been debated since the early days when the industry was first started (Ahmad Zafir and Magintan, 2016). This is perhaps unavoidable since most of the agricultural lands were adjacent to the forest areas where wildlife is abundant. Wild elephant encroachment and crop raiding commonly occur especially in the states of Sabah, Terengganu and Pahang.

[1] TDM Berhad, Jalan Masjid Abidin, 20100 Kuala Terengganu, Terengganu, Malaysia.

[2] Fakulti Sains dan Sekitaran Marin, Universiti Malaysia Terengganu, 21030 Kuala Nerus, Terengganu, Malaysia.

* *Corresponding author e-mail: norasmah@umt.edu.my*

Various mitigation methods were implemented in Malaysia to minimise elephant encroachments such as digging trenches, electric fencing, elephant translocation, throwing firecrackers, night patrolling to chase the elephants, and even culling if deemed necessary (Ahmad Zafir and Magintan, 2016). However, none of the methods was found to be effective in the long-term. Another mitigation method like chilli-tobacco rope was found to be effective in preventing elephants from entering the farm but only works significantly better in the low-rainfall regions compared to medium and high-rainfall regions (Chelliah *et al.*, 2010).

Over time, elephants have become habituated to the methods and they constantly find ways to overcome them. In 2007, a new practice using honeybees as a natural deterrent to prevent wild elephant encroachment was introduced (King *et al.*, 2007). The project was originally performed in Kenya, Africa and further studies were conducted in other countries until today. The study yielded positive results where the number of wild elephant encroachments was reduced (King *et al.*, 2007; 2009; 2011; 2017). Wild elephants avoided contact with the beehive boxes, including the empty ones, which indicated that the elephants have already 'memorised' the previous bee attack experiences. The study was replicated and tested in other countries including Thailand (Dror *et al.*, 2020; van de Water *et al.*, 2020) and India (Nair and Jayson, 2016).

However, a model study has not been tested on large scale, particularly in the oil palm plantation areas. According to the Department of Wildlife and National Parks Peninsular Malaysia (PERHILITAN), in Malaysia, and HEC ranks second in the number of recorded cases. In Kemaman district in the state of Terengganu, HEC ranks seventh in the number of reported cases from 2006 to 2015 (Othman, 2016). Ladang Jernih in Kemaman, which is under Terengganu Development and Management Berhad (TDM), experienced significant economic loss due to serial elephant encroachments which caused severe damage, mostly to the young oil palms. Typical mitigation methods such as electric fences and trenches were not fully effective in preventing elephant encroachments. Hence, the beehive fencing method using the native honeybee species, *Apis cerana*, was introduced into Ladang Jernih as an alternative mitigation plan to deter crop raiding elephants. The method introduced by King *et al.* (2009) was modified to suit the local environment and the large-scale oil palm plantations. This new mitigation approach was chosen as it could be the best biological control method to reduce elephant encroachment incidents (Choong and Dayang Norwana, 2005). This is important since Malaysian oil palm planters are required to comply with the best practices of oil palm management and care for the endangered species, as listed under the Malaysian Sustainable Palm Oil (MSPO) standard as well as to meet the RSPO standards.

A study by King *et al.* (2011) in northern Kenya using honeybees, *A. mellifera*, to deter elephants gave promising results in reducing elephant damage to plantation fields, which has indirectly guided a new non-lethal way to minimise human-wildlife conflict. The bees are likely effective to deter elephants due to their quick response to any disturbance, which in this case is the elephant (Collins *et al.*, 1980).

However, data from previous studies showed that not all beehives used in the beehive-fences (BHF) studies can be sustained (King *et al.*, 2011; Ngama *et al.*, 2016). Some of the colonies emigrated or abandoned their hives after a while due to a lack of food resources, predation by pests and diseases (Ruttner, 1988). Moreover, since this study was conducted in an oil palm plantation area which is adjacent to the forest reserve, we believed that the BHF containing *A. cerana* colonies installed in this area is prone to be infested and invaded by pests and predators which originated from the surrounding oil palm plantations and nearby forest reserve areas.

Predators of *A. cerana* are attracted to all parts of the bee colony, including larvae, pollen, honey and wax. Predators that usually invade bee colonies are wasps, hornets, ants and also vertebrates such as toads, frogs, lizards, geckos, rats, Asian bears, birds, as well as humans (Oldroyd and Wongsiri, 2006). Numerous types of pests can be found around the oil palm plantation area, such as the greater wax moth, *Galleria mellonella*, and the lesser wax moth, *Achroia grisella*. In addition, most of the flying honeybees are foragers and hence, they are more prone to predation by the Asian hornet, *Vespa velutina*, due to their pollen or nectar loads which can represent up to 40% extra body mass, thus, reducing their flying maneuverability to escape predators (Feuerbacher *et al.*, 2003). Moreover, to work efficiently, the beehive colony must be healthy and show high activity levels as stated by Woyke (1992). A colony's defence mechanism correlates with its beehive activity levels, which means that when they are highly active, the bees' reaction to attack any predator is also likely higher, as they possess stronger defence ability.

In this article, we present data on the challenges of sustaining beehives in oil palm plantation areas associated with the BHF project conducted in Ladang Jernih, Kemaman, Terengganu. This is the first BHF project, to our knowledge, performed in large agricultural areas. We conducted this study to determine the type of pests and predators that could be enemies to the bee colonies and the bee's activity levels after BHF installation in the oil palm plantation area. We also looked at the types of pollen collected by the bees to determine the food sources of the bees in the oil palm plantation areas. This study is vital to gain information on how to sustain

bee colonies in the agricultural field, especially in oil palm plantation areas that are usually located near the forest reserve. Finally, we also compared the number of elephant encroachment incidents in Ladang Jernih before and during this study was conducted, including the association between elephant encroachment with the bee activity levels. We believe that these findings are important for the future of the oil palm industry, especially to companies and smallholders who wish to use BHF as an alternative method to reduce HEC.

MATERIALS AND METHODS

Study Site

This study was conducted in Ladang Jernih, Kemaman, Terengganu, Malaysia (4° 25′ 29.53″ N, 103° 12′ 51.78″ E). This oil palm plantation area is under the management of TDM Berhad. Ladang Jernih comprises 2207.53 ha of mature oil palm areas and 405.40 ha of immature oil palm areas. The oil palm plantation area is adjacent to the protected forest reserve, Hutan Sungai Nipah and other neighbouring oil palm plantation areas which are also owned by TDM Berhad. Elephant encroachments occurred along the forest reserve borderline, marked as Point 1 to Point 5 (*Figure 1*).

Experimental Set-up

Due to the very large plantation areas, it is uneconomical to build a BHF along the plantation perimeter. Hence, we only identified the active entry points by the elephants and build the BHF along 60 m to cover this entrance. In total, there were five active entry points, and each point was marked as Point 1 to Point 5 (*Figure 1*). However, in this study, only Point 1, 2, 3 and 4 were installed with the BHF.

Apis cerana (Asian honeybees) was used in this study because this is a native bee species proven to be effective to deter elephants based on the study conducted in Kerala, India (Nair and Jayson 2016). Six hives containing colonies of *A. cerana* were hung 1 m above ground at each point, with a 10 m distance between hives as suggested by Nair and Jayson (2016). Each hive was labelled as Hive 1 to Hive 6 and all were connected with a rope following the method suggested by King *et al.* (2011) as shown in *Figure 2*. Varieties of flowers such as *Turnera subulata*, *Antigonon leptopus*, *Combretum indicum* and *Ixora coccinea* were planted surrounding the beehive areas. For integrated pest management purposes, these flowering plants were originally planted throughout the plantation area, to act as a biological control for oil palm pests such as bagworms. In total, 27 hives containing colonies of *A. cerana* (24 hives and three reinstallation hives at Point 1) were installed in Ladang Jernih throughout this study. The three additional hives installed at Point 1 in November were to replace the collapsed hives.

Four types of data collection were performed: a) pests and predators of *A. cerana*; b) bee activity levels; c) melissopalynology, and d) the number of elephant encroachment incidents. The data collections were conducted for eight months from August 2018 until March 2019.

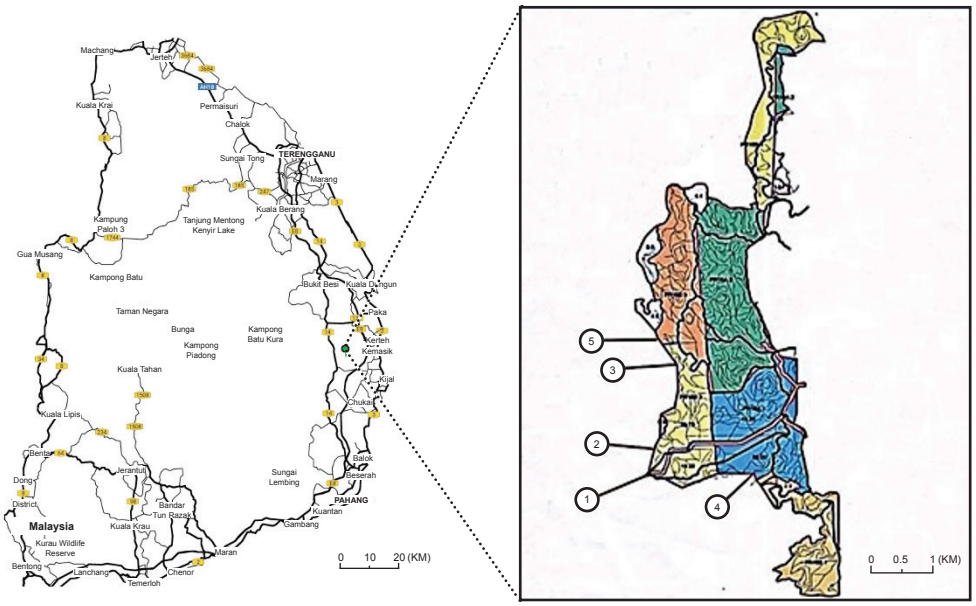


Figure 1. A map of Ladang Jernih in Kemaman, Terengganu (4.444° N, 103.257° E). Numbers shown in the circle indicate the active elephant encroachment points.



Figure 2. The beehive boxes installed as beehive-fence in the oil palm plantation at the four elephant entry points in Ladang Jernih. Each point was installed with six beehives and connected by a rope.

***Collection and observation of pests and predators of* A. cerana**. Pest samples were collected to evaluate their effects on the sustainability of bee colonies throughout this project. Pest observation and collection were done from three sources: Outside the beehives, inside the beehive boxes and from the trail cameras. The trail cameras were used to gather digital proofs (photos and videos) of predators that disturbed the BHF, especially at night.

Each beehive was inspected and observed monthly for the presence of any pests. Pictures of pests present outside the beehives were captured and recorded. To inspect pests inside the beehives, the lids of the beehive boxes were carefully opened. Frames (four to five frames per hive) were lifted one after another to inspect the presence of any pest. Pictures of pests present were captured for record purposes and the samples were collected for identification. All pests found in the hives were collected using a pair of forceps and were put into a killing jar before being brought back to the laboratory for further identification. Meanwhile, any pest's larvae found inside the hives were reared in the laboratory until the adult stage to ease the identification process. After all, pests were collected, hives were cleaned using brushes and the frames were placed in their original positions inside the hive before they were closed. It is impossible to count the individual number of certain species of the pests such as ants. Hence, any beehive that was infested by ants were counted as one, for each ant species.

Any larvae found within the honeycomb and beehive box were collected along with the whole bee comb as their food source. Based on the rearing method by Steyskal *et al.* (1986) and Basari *et al.* (2019), the larvae were reared in a 2 L jar and sealed with a muslin cloth. Then, the specimens were left in the laboratory at room temperature (27°C ± 0.05) and observed regularly until they emerged into adult forms. Once they have entered the adult stage, the insects were put into a killing jar and pinned at their thorax for further identification. The number of the wax moth found in the beehive was based on the number of larvae found during the data collection.

To determine the predators of the beehives at night, two wildlife trail cameras (Toguard, 14 MP 1080P) were installed at strategic spots at each point. The night vision cameras were set up at chest height to ensure a wide range of observations over the six colony-containing hives installed at each point. The cameras were programmed to capture videos for 10 min, with 1 s intervals between each video. All evidence captured was observed and analysed for the existence of pests and predators during the day and night.

Bee activity levels. For each beehive, the inbound and outbound movements of the beehives were recorded for 10 min using a camera (Nikon Coolpix L340). Data were recorded from 1000 hr when they were active (Koetz, 2013). The camera was pointed towards the hive entrance. The bee's activity level was then calculated based on the number of inbound and outbound individuals. Bee activity levels were calculated using the method put forward by Ngama *et al.* (2016), by estimating the number of bee movements per minute (b.mvt min^{-1}). The classification was done using the natural breakpoint of 70 b.mvt min^{-1}. If the movement is less than 70 b.mvt min^{-1}, it will be classified as a "low" activity level, whereas movement of more than 70 b.mvt min^{-1} will be classified as a "high" activity level.

Melissopalynology analysis. The bee activity level (*i.e.*, active or weak) could be due to many reasons and one of the reasons is the availability of food sources. Bee colonies might emigrate to new nesting sites or become less active if the food sources in the area are scarce. Hence, melissopalynology analysis was also conducted in this study to determine the relationship between the bee activity levels and food availability in the oil palm area. Samples of pollens were collected monthly from August 2018 until January 2019. Three hives were selected randomly on each sampling for their pollen load. The pollens were acquired directly from the forager bees, by using insect nets inside the hive and from pollen combs or beebread, by using forceps. Pollen samples were collected using sterilised forceps and were stored in individual glass vials of 5 mL capacity with 70% alcohol. Three to five samples were taken from each hive. Altogether, 30 samples were collected.

The reference samples of dominant vegetation in the study area were collected using the sampling methods by Azmi *et al.* (2015). Flower buds of

dominant species found in the apiary were plucked cautiously and were preserved in labelled vials containing 70% ethanol. The ethanol was used to ensure that the flower buds collected were maintained in good condition. The preserved pollens were then transferred using a micropipette onto haemocytometer slides. Five replicates of slides were prepared for each vial, to provide descriptive coverage of pollens collected by each honeybee.

Number of elephant encroachment incidents. Each elephant entry point was monitored visually, and camera traps were also checked daily to determine any sign of elephant encroachment. The elephant encroachment incidents at each entry point were recorded daily. The number of elephant encroachment incidents eight months before the beehive installation (August 2017 - March 2018) *vs*. the number of elephant encroachment incidents after the commencement of the BHF project (August 2018 - March 2019) were then compared. Finally, the number of elephant encroachments against the pest occurrences and sustained beehives were plotted.

Data Analysis

A Chi-Square test for relatedness was conducted to determine the relationship between pest occurrences and sustained hives towards the number of elephant encroachment. Chi-Square goodness of fit test was also conducted to analyse the number of elephant encroachment incidents before and after the BHF installation and the frequency of pest occurrence and the number of pollen loads between months. All analyses were conducted using SPSS v. 24 (IBM® software).

RESULTS AND DISCUSSION

Pest and Predators of *A. cerana*

Overall, 17 species of pests and predators were observed invading *A. cerana* hives in Ladang Jernih (*Table 1*). All these pests were found either living inside the beehives or preying on the bees outside the hives. *Rattus tiomanicus* and many species of ants were found inhabiting abandoned beehives.

The bee colonies suffer from the attack of various types of insects and vertebrates. For instance, the results showed that wasps, geckos, frogs, ants and wax moths were present in a vast number and very commonly encountered. This was most likely due to the location of the oil palm areas which are adjacent to Hutan Simpan Sungai Nipah, Kemaman, Terengganu. Hence, many predators such as predatory insects, geckos, rats and frogs took advantage to invade and prey upon the bee colonies in the beehives installed in Ladang Jernih. The number of pests recorded was the highest in September, in which ants and cockroaches especially in Point 2 and Point 3 were abundant followed by geckos in Point 1 and Point 4. The sustained colonies were declining each month, causing it necessary to reinstall three new colonies in Point 1. Besides, the sustained hives seem to have a declining pattern throughout the project period (August 2018 - January 2019). We believed that this was caused mainly by the pests and predators that disturbed the bee colonies. Wax moths were the most frequent pests recorded in this project and they could be the greatest contributors to the emigration of the bee colonies as also suggested previously by Kwadha *et al.* (2017), likely causing most of the colonies installed in this study to become less active and finally collapse.

TABLE 1. PESTS AND PREDATORS FOUND INSIDE AND OUTSIDE BEEHIVES IN LADANG JERNIH OIL PALM PLANTATION AREA

Location	Pests (Order/ Common name)
Inside hive	*Periplaneta americana* (Blattodea/ American cockroach) *Galleria mellonella* (Lepidoptera/ Greater wax moth) *Achroia grisella* (Lepidoptera/ Lesser wax moth) *Rattus tiomanicus* (Rodentia/Malaysian wood rat)
Inside and outside hive	*Myrmica* sp. (Hymenoptera/ Ant) *Paratrechina longicornis* (Hymenoptera/ Black crazy ant) *Tetramorium* sp. (Hymenoptera/ Ant) *Solenopsis geminata* (Hymenoptera/ Fire ant) *Oecophylla smaragdina* (Hymenoptera/ Weaver ant) *Monomorium floricola* (Hymenoptera/ Ant) *Monomorium pharaonis* (Hymenoptera/ Pharaoh ant) *Camponotus* sp. (Hymenoptera/ Ant) *Anoplolepis gracilipes* (Hymenoptera/ Yellow crazy ant) *Hemidactylus frenatus* (Squamata/ Common house lizard) *Hylarana* sp. (Anura/ Frog)
Hive perimeter/ outside	*Vespa tropica* (Hymenoptera/ Tropical wasp) *Gekko* sp. (Squamata/ Lizard)
Video trail camera	*Sus scrofa* (Artiodactyla/ Wild boar)

We also found that *G. mellonella* (Greater wax moths) appears to be more abundant compared to *A. grisella* (Lesser wax moths). The two species of wax moths can be easily identified by examining the presence of four stemmata on the larvae of *G. mellonella* (Ellis *et al*., 2013). A study by Oldroyd and Wongsiri (2006) also yielded a similar result, with the discovery of ants, cockroaches, geckos, frogs, wasps and rats as pests of *A. cerana*. Rats infestation might seem to be rare or unusual for *A. cerana* colonies. However, the occurrence of this pest in this study is expected, since the study site is located within the oil palm plantation areas. Previous studies in several localities in Malaysia had reported *R. tiomanicus* as the most common Murids rodent caught in oil palm plantations, other than *R. argentiventer* and *R. rattus* (Hafidzi and Saayon, 2001; Mohd-Azlan *et al*., 2019; Puan *et al*., 2011). *R. tiomanicus* is well adapted in various agricultural habitats and is said to have good adaptation in the oil palm plantation areas due to its arboreal habits (Hafidzi and Saayon, 2001). We believe that the rats' infestation upon *A. cerana* hives in the present study occurred because they required shelter and protection for their young. In general, the number of pests correlated with the number of sustained hives. Based on the results shown in *Figure 3*, the increment in the number of pests disturbing the colonies had led to the declining pattern of sustained hives. In short, it can be concluded that the number of sustained beehives decreased when the number of pests increased.

Number of Pests *vs.* Sustained Hives and Number of Elephant Encroachment Incidents in Each Sampling Point

As shown in *Figure 3*, it can be seen that when the number of pests and predators increased, the number of sustained beehives decreased. There was a significant difference in the number of pests infesting beehives between months [$\chi^2(18) = 32.90$, p=0.02]. Moreover, when the number of pests was high and sustained hives decreased, the number of elephant encroachment incidents also increased [$\chi^2(1, N=65) = 20.53$, $p<0.001$].

Eight months after the BHF installation, the number of elephant encroachment events in Ladang Jernih had reduced from 31 times to only 16 times. Even though elephant encroachment incidents were recorded almost every month before and after the BHF installation, the encroachment events were clearly shown to decrease significantly after the BHFs were installed [$\chi^2(63) = 15.254$, $p<0.001$]; *Table 2*.

Oil palm plantations serve as a place for elephants to find food resources, which are the palm seedlings. The availability of palm seedlings has caused the elephants to intrude into oil palm areas and damage the crops (Blake, 2002). The common control methods that are still being used such as electric fences and trenches are considered harmful as they tend to cause injuries to the elephants. These mitigation methods also demand a high cost of maintenance and are

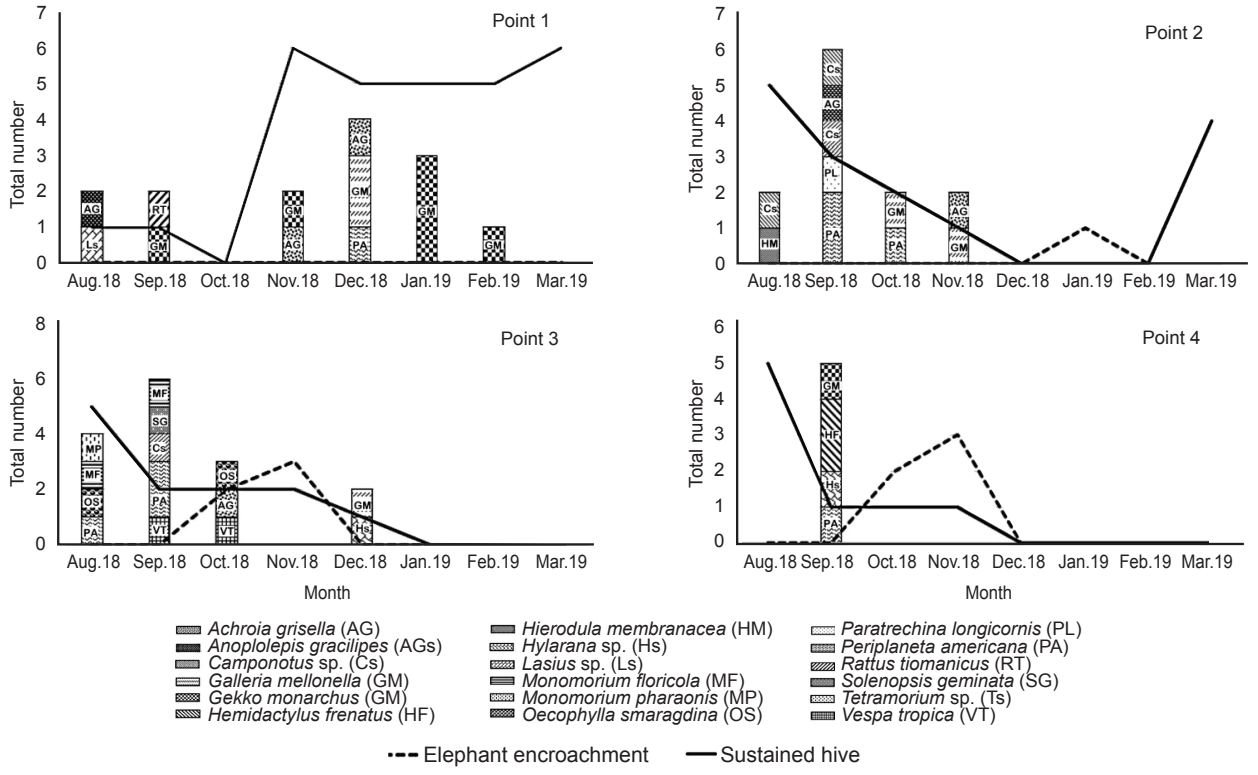


Figure 3. The number of pests which infested the beehives in each month vs. *the number of sustained beehives and elephant encroachment in Ladang Jernih. The existence of ants in the beehives was counted as one pest per species. The common name of each species can be referred to* Table 1.

therefore considered uneconomical to be practised over a long time.

The results shown in *Figure 3* also indicated that the number of elephant encroachment incidents varies between months, with the highest frequency occurring in October and November 2018. Digital proofs in the form of photos and videos indicated that encroachment had occurred several times throughout this project, in which elephants (a group usually consisting of two to seven individuals) most frequently intrude, followed by wild boars. This could be one of the reasons for bee colonies to be unsustainable in the study area. The bees tend to emigrate after the disturbance following these encroachments, as well as the occurrence of pests and predators in their hives. However, many other factors could also contribute to the emigration of the bees such as food availability, which will be discussed below.

The Mean Activity Level of *A. cerana* in Ladang Jernih

Table 3 showed the mean activity level of bee colonies placed at each sampling point. The activity levels of the bee colonies were less than 70 b.mvt min^{-1}, considered low activity. This indicates that the colonies became less active in foraging after they were placed in Ladang Jernih.

Our results also showed that most of the honeybee colonies showed less than 70 b.mvt min^{-1}, which indicates that most of the hives were classified as having low activity levels. Although it is known that *A. cerana* migrated more often (Olydrod *et al*., 2006) when compared to *A. mellifera*, we believe that pest infestation was one of the factors that lead to the decreasing value of *A. cerana* activity. For example, research by Hyatt (2011) found that, after being attacked by ants and disturbed by the local people, *A. cerana* colonies then deserted their hives within a short time. *A. cerana* was more stressed by the predation pressure compared to the temperate honeybee species, *A. mellifera* (Koetz, 2013). The study by Koetz (2013) showed that honeybees tend to be stressed by ant infestation. Based on our data, many species of ants were found infesting the beehives in Ladang Jernih, especially predatory ants such as the weaver ant (*O. smaragdina*) and the yellow crazy ant (*A. gracilipes*). Honeybees also have many other predators such as wasps and hornets, that often attack the bee foragers. These predators often attack almost all parts of the colony such as adult

TABLE 2. THE NUMBER OF ELEPHANT ENCROACHMENT INCIDENTS IN EIGHT MONTHS BEFORE AND AFTER BHF INSTALLATION IN LADANG JERNIH, KEMAMAN, TERENGGANU

Before BHF		After BHF	
Months	**Encroachment No.**	**Months**	**Encroachment No.**
Aug. 2017	0	Aug. 2018	0
Sept. 2017	8	Sept. 2018	0
Oct. 2017	9	Oct. 2018	4
Nov. 2017	8	Nov. 2018	9
Dec. 2017	9	Dec. 2018	1
Jan. 2018	9	Jan. 2018	1
Feb. 2018	3	Feb. 2018	0
Mar. 2018	1	Mar. 2018	1
Total	47		16

TABLE 3. THE MEAN ACTIVITY LEVEL OF *A. cerana* CALCULATED IN BEE MOVEMENTS PER MINUTE (b.mvt min^{-1}) FOR EACH SAMPLING POINT (PT) IN EACH MONTH IN LADANG JERNIH

Month	Pt. 1	Pt. 2	Pt. 3	Pt. 4
Aug. 2018	14.70*	3.18 ± 2.69	3.24 ± 1.82	0.00**
Sept. 2018	0.27 ± 0.27	4.58 ± 1.92	13.67 ± 12	0.00**
Oct. 2018	0.0**	2.83 ± 2.01	1.370 ± 1.11	0.00**
Nov. 2018	41.89 ± 5.21	0.35*	0.67 ± 0.54	0.97*
Dec. 2018	20.70 ± 7.68	0.00**	0.16*	0.00**
Jan. 2019	13.87 ± 9.42	0.00**		
Feb. 2019	0.92 ± 0.31	0.00**		
Mar. 2019	28.95 ± 14.4	1.12 ± 1.01		

Note: Colonies at Pt. 3 and 4 had sustained until December 2018 only.
*Only one colony showed inbound and outbound activity.
**Colonies were too weak with no inbound and outbound activity recorded.

honeybees, larvae and pupae, and the food sources of the honeybees which is pollen and honey (Fuchs and Tautz, 2011). The pressure from these pest infestations gives a bad impact on *A. cerana* because it influences the bee's decision to choose a nesting site, the size of the population itself and it can also alter the behaviour of the workers (Seeley *et al*., 1982). For example, a study conducted by Visscher and Seeley *et al*. (1982) in Northeast Thailand found that 10% of the observed honeybee colonies had to migrate due to pressure from predators.

Floral Diversity of Pollens Collected by *A. cerana* in Ladang Jernih

Based on the pollen analysis, there were 12 types of pollen and five unidentified pollens attached to the bees' corbiculae (*Figure 4*). The most dominant pollens (more than 45% of pollen grains counted) collected from the bees' corbiculae came from *Mimosa pudica*, *T. subulat*a and *Melastoma malabatrichum*, but no oil palm pollen was collected from the bees. A number of pollens for different species of flowers collected from the forager bees were significantly different ($\chi^2(16) = 3573.03$, $p \leq 0.01$).

Apis cerana colonies in Ladang Jernih also faced other problems such as a lack of pollen and nectar sources for their food production. According to Partap (2011), *A. cerana* is an active crop pollinator and this species can forage through diverse species of vegetable and fruit crops. However, because most of the flowering plants were newly planted in the study area, the production of nectar and pollen from the plants may not have been enough to support the number of food sources needed by the *A. cerana* colonies. Furthermore, most of the oil palm trees in our study area were also newly planted and did not produce flowers. Although the bees can forage from the wildflowers within the neighbouring forest area, the foraging distance of *A. cerana* which is only about 200-900 m from their hives (Corlett, 2011) may limit their options. *A. cerana* is known to forage in a short distance as compared to the western honeybee, *A. mellifera* and is likely to abscond its colony under unfavourable conditions such as lack of food sources (Gratzer *et al*. 2019). Hence, the bees chose to emigrate to a new location that could give them more benefits in terms of food supply and colony sustainability. For honeybees, migration factors are related to lacking food resources and the surrounding environmental conditions of that area (Koetz, 2013). This situation is supported by *A. cerana* themselves because they are usually not prepared for untoward conditions, making them not had enough food sources when the condition is unfavourable to them (Nanork *et al*., 2006). Research by Chen *et al*. (1995) also stated that *A. cerana* is likely to abscond their hives influenced by the flower blooming season. The bee colonies tend to migrate when the number of pollen-carrying workers drops, and the honey, eggs and pollen stores decrease rapidly (Pokhrel *et al*., 2006).

CONCLUSION

Our results showed that the number of elephant encroachment incidents had significantly reduced at each entry point after the BHFs were installed. We believe that the presence of the beehives at the elephant entry points had likely contributed to the reduction in elephant encroachments at Ladang Jernih. However, due to the pest infestations and lack of food, many bee colonies struggled to persist

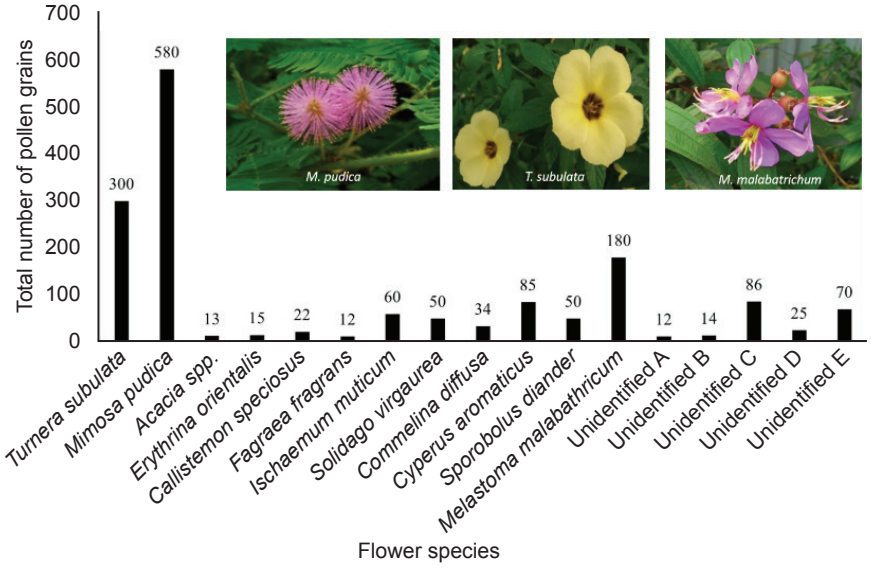


Figure 4. Total number of pollen grains based on plant species foraged by A. cerana *at Ladang Jernih from August 2018 until January 2019.*

in the area. When the number of active bee colonies reduced, the number of elephant encroachment incidents also started to increase. Hence, having a full-time caretaker(s) is crucial to ensure the persistence of the bee colonies in the oil palm areas. The bee colonies need to be delicately maintained, particularly during the initial phase of the beehives instalment, since disturbance from other animals as well as lack of food sources might hinder the establishment of the introduced colonies. We are aware that more research needs to be done in the future to support our findings, particularly to look at the effects of the BHF on elephant encroachments over a long time. Nevertheless, we hope that this study could help future planning in developing eco-friendlier pest management in oil palm plantation areas.

ACKNOWLEDGEMENT

We sincerely thank TDM Berhad for funding this project through the University-Industry grant project (Vote number 53300). We thank University Malaysia Terengganu and TDMP field staff in Ladang Jernih for providing all the facilities needed for data collection and analysis. We also thank our colleagues who were involved in the early planning of this project namely, Mr. Jalaini Che Kar (TDM Berhad), Mr. Mohamad Ashraf Idrus (TDM Berhad), Mr. Mohd. Shariff Daim, Prof. Dato' Dr. Mohd. Tajuddin Abdullah, Associate Prof. Dr. Faridah Mohamad and Mr. Nor Ehsan Abd Rahman. Last but not least, we would also like to thank our colleagues from Phuluang Wildlife Research Station, Department of National Park, Wildlife and Plant Conservation of Thailand, Mrs. Rachaya Arkajak and her team for their advice based on an example of the BHF project conducted in Thailand.

REFERENCES

Ahmad Zafir, A W and Magintan, D (2016). Historical review of human-elephant conflict in Peninsular Malaysia. *J. Wildlife and National Parks*, *3*: 1-19.

Azmi, W A; Zulqurnain, N S and Ghazi, R (2015). Melissopalynology and foraging activity of stingless bees, *Lepidotrigona terminata* (Hymenoptera: Apidae) from an apiary in Besut, Terengganu. *J. Sustain. Sci. Manag., 10(1)*: 27-35.

Basari, N; Nurul Salsabila, M; Nur Elya Nabila, Y and Wei-Yean, C (2019). The effect of temperature on the development of *Trilocha varians* (Lepidoptera: Bombycidae) and control of the ficus plant pest. *J. Trop. Life Sci., 30(1)*: 23-31.

Blake, S (2002). *The Ecology of Forest Elephant Distribution and Its Implications for Conservation.* PhD thesis, University of Edinburgh, United Kingdom. 307 pp.

Chen, S N (1995). Absconding in *Apis cerana. Honeybees of Asia* (Hepburn, H R and Radloff, S E eds.). SpringerVerlag, Berlin. p. 133-158.

Chelliah, K; Kannan, G; Kundu, S; Nair, A; Baskaran, N; Sukumar, R and Madhusudan, A (2010). Testing the efficacy of a chilli–tobacco rope fence as a deterrent against crop-raiding elephants. *Commun. Res.*, *99(9)*: 1239-1243.

Choong, D K F and Dayang Norwana, A A B (2005). *Guidelines On The Better Management Practices for the Mitigation and Management of Human-Elephant Conflict in and Around Oil-Palm Plantations in Indonesia and Malaysia.* Version 1. WWF Malaysia, Petaling Jaya. 36 pp.

Collins, A M; Rinderer, T E; Tucker, K W; Sylvester, H A and Lackett, J J (1980). A model of honeybee defensive behavior. *J. Apic. Res.*, *19*: 224-231.

Corlett, R T (2011). Honeybees in natural ecosystems. *Honeybees of Asia*. Springer, Berlin, Heidelberg. 215-225 pp.

Dror, S; Harich, F; Duangphakdee, O; Savini, T; Pogány, Á; Roberts, J; Geheran, J and Treydte, A C (2020). Are Asian elephants afraid of honeybees? Experimental studies in Northern Thailand. *Mamm. Biol.*, *100*: 355-363.

Ellis, J D; Graham, J R and Mortensen, A (2013). Standard methods for wax moth research. *J. Apic. Res., 52(1)*: *1-17*. DOI: 10.3896/IBRA.1.52.1.10.

Feuerbacher, E; Fewell, J H; Roberts, S P; Smith, E F and Harrison, J F (2003). Effects of load type (pollen or nectar) and load mass on hovering metabolic rate and mechanical power output in the honey bee *Apis mellifera*. *J. Exp. Biol.*, *206*: 1855-1865.

Fuchs, S and Tautz, J (2011). Colony defense and natural enemies. *Honeybees of Asia*. Springer, Berlin, Heidelberg. p. 369-395.

Gratzer, K; Susilo, F; Purnomo, D; Fiedler, S and Brodschneider, R (2019). Challenges for beekeeping in Indonesia with autochthonous and introduced bees. *Bee World. 96(2)*: 40-44. DOI: 10.1080/0005772X.2019.1571211.

Hafidzi, M N and Saayon, M K (2001). Status of rat infestation and recent control strategies in oil

palm plantations in Peninsular Malaysia. *Pertanika J. Trop. Agric. Sci.*, 24(2): 109-114.

Hyatt, S (2011). Asian honeybee (*Apis cerana javana*) in Cairns, Far North Queensland: Foraging, nesting and swarming behaviour. *BQCC Report*. Cairns, Queensland, Australia. 22 pp.

King, L E (2011). Beehive fence construction manual. A step by step guide to building a protective beehive fence to deter crop-raiding elephants from small scale farm land. *The Elephants and Bees Project Save the Elephants*. Nairobi, Kenya. 40 pp.

King, L E; Douglas-Hamilton, I and Vollrath, F (2007). African elephants run from the sound of disturbed bees. *Curr. Biol.*, *17(19)*: R832-R833.

King, L E; Lala, F; Nzumu, H; Mwambingu, E and Douglas-Hamilton, I (2017). Beehive fence as a multidimensional conflict-mitigation tool for farmers coexisting with elephants. *Conserv. Biol.*, *31*: 743-752.

King, L E; Lawrence, A; Douglas-Hamilton, I and Vollrath, F (2009). Beehive fence deters crop-raiding elephants. *Afr. J. Ecol.*, *47(2)*: 131-137.

Koetz, A H (2013). Ecology, behaviour and control of *Apis cerana* with a focus on relevance to the Australian incursion. *Insects*, *4(4)*: 558-592.

Kwadha, C A; Ong'amo, G O; Ndegwa, P N; Raina, S K and Fombong, A T (2017). The biology and control of the greater wax moth, *Galleria mellonella*. *Insects*, *8(2)*: 61. DOI: 10.3390/insects8020061.

Mohd-Azlan, J; Kaicheen, S S; Lok, L and Lawes, M J (2019). The role of forest fragments in small mammal conservation in an oil palm plantation in northern Sarawak, Borneo. *J. Oil Palm Res.*, *31(3)*: 422-436.

Nair, R P and Jayson, E A (2016). Effectiveness of beehive fences to deter crop raiding elephants in Kerala, India. *IRJNAS*, *3(1)*: 14-19.

Nanork, P; Wongsiri, S and Oldroyd, B P (2006). The reproductive dilemmas of queenless red dwarf honeybee (*Apis florea*) workers. *Behav. Ecol. Sociobiol.*, *61(1)*: 91.

Ngama, S; Korte, L; Bindelle, J; Vermeulen, C and Poulsen, J R (2016). How bees deter elephants: Beehive trials with forest elephants (*Loxodonta africana cyclotis*) in Gabon. *Public Library of Science*, *11(5)*: 1-12.

Oldroyd, B P and Wongsiri, S (2006). *Asian honey bees: Biology, conservation, and human interactions*. Harvard University Press. Cambridge, Massachusetts. 360 pp.

Othman, N (2016). Human elephant conflict in Peninsular Malaysia. Jabatan Perlindungan Hidupan Liar dan Taman Negara (PERHILITAN) Semenanjung Malaysia. *Biodiversity Forum 2016*. Awana Genting Resort. 23-24 May 2016.

Partap, U (2011). The pollination role of honeybees. *Honeybees of Asia*. Springer, Berlin, Heidelberg. p. 227-255.

Pokhrel, S; Thapa, R B; Neupane, F P and Shrestha, S M (2006). Absconding behavior and management of *Apis cerana* F. honeybee in Chitwan, Nepal. *J. Inst. of Agric. Anim. Sci.*, *27*: 77-86.

Puan, C L; Goldizen, A W; Zakaria M; Hafidzi, M N and Baxter, G S (2011). Relationships among rat numbers, abundance of oil palm fruit and damage levels to fruit in an oil palm plantation. *Integr. Zool.*, *6*: 130-139.

Ruttner, F (1988). Biogeography and taxonomy of honeybees. Springer-Verlag: Berlin. Heidelberg, Germany. 284 pp.

Sakagami, S F; Matsumura, T and Ito, K (1980). *Apis laboriosa* in Himalaya, the little known world's largest honey bee (Hymenoptera, Apidae). *Insecta Matsumurana*, *19*: 47-78.

Seeley, T D; Seeley, R H and Akratanakul, P (1982). Colony defense strategies of the honeybees in Thailand. *Ecol. Monogr.*, *52(1)*: 43-63.

Steyskal, G C; Murphy, W L and Hoover, E M (1986). *Collecting and Preserving Insects and Mites: Techniques and Tools*. Agric. Res. Washington, DC. 68 pp.

van de Water, A; King, L E; Arkajak, R; Arkajak, J; van Doormaal, N; Ceccarelli, N; Sluiter, L; Doornwaard, S M; Praet, V; Owen, D and Matteson, K (2020). Beehive fences as a sustainable local solution to human-elephant conflict in Thailand. *Conserv. Sci. and Pract.*, *2020*: e260.

Visscher, P K and Seeley, T D (1982). Foraging strategy of honeybee colonies in a temperate deciduous forest. *Ecology*, *63(6)*: 1790-1801.

Woyke, J (1992). Diurnal flight activity of African bees *Apis mellifera adansonii* in different seasons and zones of Ghana. *Apidologie*, *23(2)*: 107-117.

Journal of Oil Palm Research Vol. 35 (2) June 2023 p.340-353
DOI: https://doi.org/10.21894/jopr.2022.0053

TRANSCRIPTOMIC AND PROTEOMIC STUDIES TO INVESTIGATE THE BASAL STEM ROT DISEASE IN OIL PALM SEEDLINGS

DAIM, L D J[1]*; TAN, B A[1]; ITHNIN, N[1]; OOI, T E K[2]; NORMAHNANI, M N[3]; APPLETON, D R[1] and HARIKRISHNA, K[4]

ABSTRACT

When oil palm is exposed to, and infected by Ganoderma boninense*, the initial defence system is launched in the roots to reduce the damage caused by the disease. The present work described the transcript and protein profiles in roots of 18 months old oil palm seedlings that were exposed to the fungal pathogen for 12 months, following artificial inoculation at six months old. Three different phenotypes were observed; control (uninoculated), asymptomatic, and symptomatic (inoculated). It was found that the transcripts from the ubiquitin-mediated proteolysis pathway were common in control and asymptomatic seedlings; while proteins involved in cellular processes, and protein and sugar metabolisms were higher in abundance in asymptomatic seedlings. The transcripts involved in carbon fixation, glycolysis/gluconeogenesis, and pyruvate metabolism together with proteins responsible for stress response were identified in symptomatic seedlings. By integrating these omics data, it was observed that symptomatic seedlings were moving towards generating and storing energy for a possible defence strategy, and at the same time emitting stress signals and responses. This was in contrast with asymptomatic seedlings where regular functions such as cellular processes and carbohydrate metabolisms were found to be active.*

Keywords: asymptomatic, disease tolerance, oil palm, omics technologies, symptomatic.

Received: 24 October 2021**; Accepted:** 5 July 2022**; Published online:** 6 September 2022.

INTRODUCTION

The basal stem rot (BSR) disease, caused by *Ganoderma boninense*, is prevalent in Malaysia's oil palm plantations, especially in the coastal region (Mercière *et al*., 2017). The transmission and control of the disease are still ambiguous, thus making an accurate diagnosis and carrying out suitable treatments difficult (Hushiarian *et al*., 2013). The accepted mode of invasion by *Ganoderma* into the oil palm is through its massive network of roots. The fungal pathogen will attack the root at a point of entry, and slowly reaches the base of the oil palm (Pilotti, 2005; Rees *et al*., 2009).

There have been many unsuccessful attempts to investigate the thorough infection process at the point of entry at the roots and approaching the bole, up towards the effects of the disease by way of foliar symptoms. Most earlier studies had compared diseased and non-diseased (control *vs.* treated) young seedlings, following a short exposure time using a specific technology *e.g.,* transcriptome or genome sequencing, where the data are subsequently analysed using a combination of bioinformatic tools (Ho *et al*., 2019; Qistina Othman *et al*., 2018). Protein studies related to BSR were also conducted on leaf and root tissues (Daim *et al*., 2015a; 2015b).

Other than targeting candidates that are frequently studied in plant root-fungal interaction, plant immunisation is an alternative process for studying the defence system induced by biotic or

[1] Biotechnology and Breeding Department, Sime Darby Plantation Technology Centre Sdn. Bhd., 43400 Serdang, Selangor, Malaysia.

[2] A-16-6, Danau Idaman Condo, Jalan 2/109F, Taman Danau Desa, 58100 Kuala Lumpur, Malaysia.

[3] Crop Protection Unit, Plantation Research and Advisory Department, Sime Darby Plantation Research Sdn. Bhd., 42700 Banting, Selangor, Malaysia.

[4] Sime Darby Plantation Research Sdn. Bhd., 42700 Banting, Selangor, Malaysia.

* *Corresponding author e-mail: leona.daniela.jefferydaim@simedarbyplantation.com*

abiotic stresses. In this case, asymptomatic seedlings, those that do not exhibit foliar symptoms following artificial inoculation with *Ganoderma*, could be considered as 'immunised' against the disease. Other scientists classify an asymptomatic host as 'resistant' to a specific disease, while a symptomatic host as 'susceptible'. Nevertheless, asymptomatic or resistant plants could still host the pathogen as the latter grows as a biotroph (Crone *et al*., 2013).

Omics technologies have long been used in many plant research areas, especially in investigating crop diseases, and understanding how these diseases affect crop health and yield. Previous studies were often conducted using a single method to probe into abiotic or biotic stresses (Bahari *et al*., 2018; Dai *et al*., 2019). The findings revolved around either gene expression/regulatory analysis, protein identification, interaction network, or metabolite profiling in the target tissues. A subset of these findings was then routinely validated through various methods. The major findings of omics experiments are the presence and expressions of these specific candidate genes (genomics), proteins (proteomics), or metabolites (metabolomics) in the target tissues.

The research using a multi-omics approach by combining several omics technologies to investigate disease ecology has allowed detailed representations of plant-disease interactions and plant-disease and environment interactions (Crandall *et al*., 2020; Neik *et al*., 2020). The plant stress response and defence system can be better understood by integrating data from multi-omics experiments. Specific functions that are expressed in a combined network are far more informative as compared to functions that are obtained using individual omics approaches.

The major problem in the estimation of root disease progression is connected to the fact that data are only collected when the oil palm is destructed. Observations on the changes in the site-specific tissues will then be determined. However, once the plant is destructed, it is practically impossible to track any further changes. Therefore, the present work used omics technologies to simultaneously examine the global transcript and protein levels in the roots of asymptomatic and symptomatic seedlings after prolonged exposure to *Ganoderma*.

MATERIALS AND METHODS

Materials

Elaeis guineensis Jacq. germinated seeds from a single cross were obtained from Sime Darby Plantation Research Sdn. Bhd. A subset of these samples was also used for expression analyses in a separate study (Tan *et al*., 2016). The parental cross came from Progeny Trial 59 in Dusun Durian Estate, Banting, Selangor, Malaysia planted in May 1979. The palm showed no signs and symptoms of *G. boninense* infection and was still producing bunches at the time of sampling. A total of 790 seedlings were screened in this trial, where 700 of them were subjected to *G. boninense* inoculation, while the remaining 90 seedlings served as control.

Preparation of Fungal Inoculum

Ganoderma boninense strain PER71 was obtained from the Malaysian Palm Oil Board (MPOB), and maintained at the Crop Protection Unit, Sime Darby Plantation Research Sdn. Bhd. The rubber wood block (RWB) inoculation process using *G. boninense* cultures, Disease Severity Index (DSI) and Disease Severity (Internal) (DI) analyses were conducted by Crop Protection Unit (Breton *et al*., 2006; Sariah and Zakaria, 2000). A customised RWB with a dimension of 6 × 6 × 6 cm was used as a source of inoculum for *G. boninense*. The RWB was sterilised at 80°C overnight, and then autoclaved at 121°C for 1 hr. A plastic bag containing 120 mL of malt extract agar and one RWB was sealed, autoclaved at 121°C for 15 min, and left to solidify overnight at room temperature. A seven-day-old *G. boninense* culture, maintained on a potato dextrose agar plate, was divided into half, where one part was inoculated onto the sterilised RWB. Inoculated RWBs were sealed in individual plastic bags and incubated in the dark at 25°C-28°C for 150 days, for mycelia to fully colonise all six surfaces of the RWB.

Artificial Inoculation

Oil palm germinated seeds (*Dura* × *Dura*) were sowed in 10" × 12" polybags containing topsoil and sand, at a ratio of 2:1. They were maintained in a shaded nursery for six months, in accordance with the Oil Palm Nursery Technique Good Agricultural Practices (Sime Darby Plantation). Two stringent selection processes were done when the seedlings were three and six months old, where those that were abnormal were culled before the infection process using inoculated RWB. Only those that were normal and healthy were subjected to nursery trials. During transplanting, *Ganoderma*-inoculated RWB was placed in the middle of 15" × 18" polybags that were half-filled with soil. The six months old seedlings were then placed in close contact above the RWB, before more soil was used to fill up the polybags. Control seedlings were prepared in a similar manner using sterilised, uninoculated RWB instead of inoculated ones. Each polybag was positioned above a concrete slab to obstruct the geotropic growth of roots into the soil. All seedlings were maintained in a nursery under the artificial shade with a 50% light cut-off. They were monitored until 18 months old (12 months post-inoculation).

TABLE 1. DISEASE PROGRESSION BASED ON THE DISEASE SEVERITY INDEX (DSI)

Class	Symptom
0	Healthy (green, healthy leaves)
1	Presence of white mycelium, with or without chlorotic/necrotic leaves
2	Presence of basidioma initials at the stem base with 1-3 chlorotic/necrotic leaves
3	Formation of basidioma at the stem base with more than 3 chlorotic/necrotic leaves
4	Presence of fruiting body with 50% necrotic leaves; plant is dried/dead

The progression of the disease was also assessed based on DSI (*Table 1*).

Sampling

The boles and roots of three seedlings from three phenotypes were sampled and washed under running water to remove excess soil. These phenotypes were control (uninoculated seedlings), asymptomatic (inoculated seedlings without foliar symptoms), and symptomatic (inoculated seedlings with foliar symptoms). The boles were cut into half, to identify the extent of severity of rotten tissues in inoculated oil palm seedlings (*Table 2*). Roots were dipped in liquid nitrogen and frozen at -80°C. All samples were pulverised using a mortar and pestle, into fine powder under constant liquid nitrogen, and frozen at -80°C until further analysis. The roots of three biological replicates from each phenotype were used for both transcriptomic and proteomic studies.

TABLE 2. THE SEVERITY OF BOLE TISSUES IN INOCULATED OIL PALM SEEDLINGS BASED ON INTERNAL DISEASE SEVERITY

Class	Symptom
0	Healthy (no internal rot)
1	Less than 20% of rotten tissues
2	20%-50% rotten tissues
3	51%-90% rotten tissues
4	More than 90% of rotten tissues

'Omics' Technologies

RNA extraction. The CTAB method was used to extract total RNA from the roots of oil palm seedlings with several modifications (Asemota and Shah, 2004; Tan *et al*., 2016). Briefly, 4 mL of extraction buffer (2% CTAB; 0.1 M Tris-HCl, pH 8; 2 M NaCl; 25 mM EDTA; 2% β-mercaptoethanol; 2% PVPP) was added to 2 g of frozen ground material, and mixed well using a vortex. An equal volume of phenol (pH 4.3): chloroform: isoamyl alcohol was added, and the mixture was centrifuged at 10 000 rpm for 15 min at 4°C. The supernatant was transferred into a new tube and precipitated twice in equal volumes of 2 M LiCl. The mixture was centrifuged at 10 000 rpm for 20 min at 4°C, and the pellet was resuspended in RNase-free water. A total of 0.1 vol of 3 M sodium acetate and 2.5 vol of absolute ethanol was added to the solution, and incubated at -80°C for 3 hr. The tube was centrifuged at 12 000 rpm at 4°C for 20 min. The resulting pellet was then washed in 70% ethanol, and thereafter, DNaseI (Epicentre) was applied before the RNA was precipitated in ethanol. Quantification was achieved using a Nanodrop ND-1000 spectrophotometer, where the 260/280 and 260/230 ratios between 1.8-2.0 were accepted. The RNA was run on 1% agarose gels to check the integrity of 18S and 28S rRNA.

Sequencing library preparation. The cDNA sequencing libraries were prepared using ScriptSeq™ v2 RNA-Seq Library Preparation Kit (Epicentre, Illumina), according to the manufacturer's instructions. The RNA was treated with terminator 5'-phosphate dependant exonuclease (Epicentre, Illumina) to deplete the rRNA.

Bioinformatics analysis. *De novo* assembly of raw counts was performed using Trinity software (Broad Institute, Hebrew University of Jerusalem), and unigenes were generated by CAP3 (Huang and Madan, 1999). The NOIseq analysis was used to determine the differential expression between the samples (Tarazona *et al*., 2011). The RPKM (normalised counts) for each sample was first calculated, and the M value, which is the $\log_2$ fold change, and D value, which is the absolute difference of the comparison, were later determined. With this, the noise distribution was generated for the background, M-D, using the available replicates. The probability value was calculated by comparing the M-D of the gene *vs.* the noise distribution and was set at >0.75.

iTRAQ analysis. The TCA-acetone-phenol method was used to extract the total protein (Daim *et al*., 2015b). The pellets were air-dried prior to labelling using iTRAQ reagents. The samples were then precipitated using acetone, reduced and alkylated, and finally digested using trypsin. A total of 100 µg of protein was then labelled using the iTRAQ reagents (4-plex). All procedures were conducted according

to the manufacturer's instructions (iTRAQ, AB Sciex). Three separate iTRAQ experiments were conducted to analyse all nine biological samples; one sample from each group (control, asymptomatic, and symptomatic) was labelled with a dye, while the fourth dye was labelled with the same control sample.

A pooled sample was prepared by combining all labelled samples. The peptides were desalted using a reversed-phase column (Strata-X 33 μm polymeric, Phenomenex). They were then dissolved in 10 mM KH_2PO_4 (pH 3) containing 10% acetonitrile. The peptides were separated using a strong cation exchange liquid chromatography column (PolySulfoethyl column, 4.6 × 100 mm, 5 μm, 300 A) on an Agilent 1100 HPLC system.

The peptide elution was done with a linear gradient of 0-400 mM KCl. Eight fractions were collected and desalted on Strata-X columns. The fractions were analysed using the 1260 Infinity HPLC system (Agilent) coupled to a 1260 Chipcube Nanospray interface (Agilent) on a QTOF 6540 mass spectrometer (Agilent). The peptides were separated in a ProtID-Chip-150 C_{18} column with a linear gradient of acetonitrile/0.1% formic acid (v/v). The spectral data were analysed against the NCBI Viridiplantae database, and protein identifications were done with ProteinPilot™ 4.5 Software (AB Sciex). The database was downloaded in July 2013 and contained 2 747 034 sequences.

Proteins with a relative abundance of >5 and with a *p*-value <0.05 were selected as statistically significant to ensure up- and downregulation. The protein lists were further analysed by the UniProt database. A global FDR was set at <0.1%.

RESULTS AND DISCUSSION

Phenotypic Evaluation

The trial was conducted on 18 months old seedlings to assess the disease severity of one single cross of interest. These seedlings were selected after a final round of culling right before they were exposed to *Ganoderma*-inoculated RWB at the six months old seedling. Results showed that this cross had an estimated disease severity of 5.32% and 10.12% severity of the bole tissues.

Seedlings were chosen for omics studies based on their DSI and disease severity (internal) (*Figure 1*). They were destructed to confirm the presence of lesions in the boles. Inoculated seedlings that were classified as Class 0 for both DSI and disease severity (internal) were considered asymptomatic, while those that were classified as Class 2 and above for DSI, and Class 1 and above for disease severity (internal) were considered symptomatic. Uninoculated seedlings with Class 0 for both DSI and disease severity (internal) served as control. The roots of three biological replicates that represented the three different phenotypes (control, asymptomatic and symptomatic) were used to construct the libraries for both transcriptomic and proteomic studies.

Destructive sampling was conducted when the seedlings were 18 months old, when there was positive root contact with RWB, in control and treated seedlings (data not shown). This situation (positive root contact with RWB) occurred by using polybags that are suitable for six to nine months old seedlings instead of APM polybags that are bigger in size. Roots of 18 months old seedlings were forced to expand and grow in a confined space within the polybag.

The mode of infection of BSR is through the roots. The progression of the disease is slow and varies for each individual, especially for older seedlings. Once the infection is established in the roots, the disease progresses towards the boles, and the seedlings may or may not show signs of foliar symptoms. Signs and symptoms of infection are prominent and occur early in germinated or younger seedlings. For six months old seedlings, their immune system is more developed than the much younger seedlings. They would have acquired the ability to defend themselves from the same source of fungal infection (the same inoculum source and size).

Asymptomatic seedlings do not show lesions in the boles, but infection is established in the roots (roots that were rotten or starting to rot were visible). DSI and DI data were collected from the foliar and bole, respectively. Control (uninoculated RWB) was put in place to ensure that it was treated in the same manner as inoculated seedlings. In this condition, both control and treated seedlings were treated equally, except for the inoculated RWB in treated (asymptomatic and symptomatic) seedlings. All treated seedlings were exposed to the same fungal pathogen at the same time with the same inoculum size.

The plant's defence system will entirely dictate its susceptibility (or tolerance) to the disease. Furthermore, infection is more often atopic and might have stopped progressing at the time the seedlings were sampled in the present work. In the case of asymptomatic seedlings, the infection has progressed to the roots but not the boles. Hence, they were identified as asymptomatic (fronds were healthy and green with a few roots that were rotten or started to rot). Symptomatic seedlings showed foliar symptoms but did not present lesions in the boles.

Unigenes in Control, Asymptomatic and Symptomatic Seedlings

Comparisons were made between asymptomatic *vs.* control, and symptomatic *vs.* control seedlings

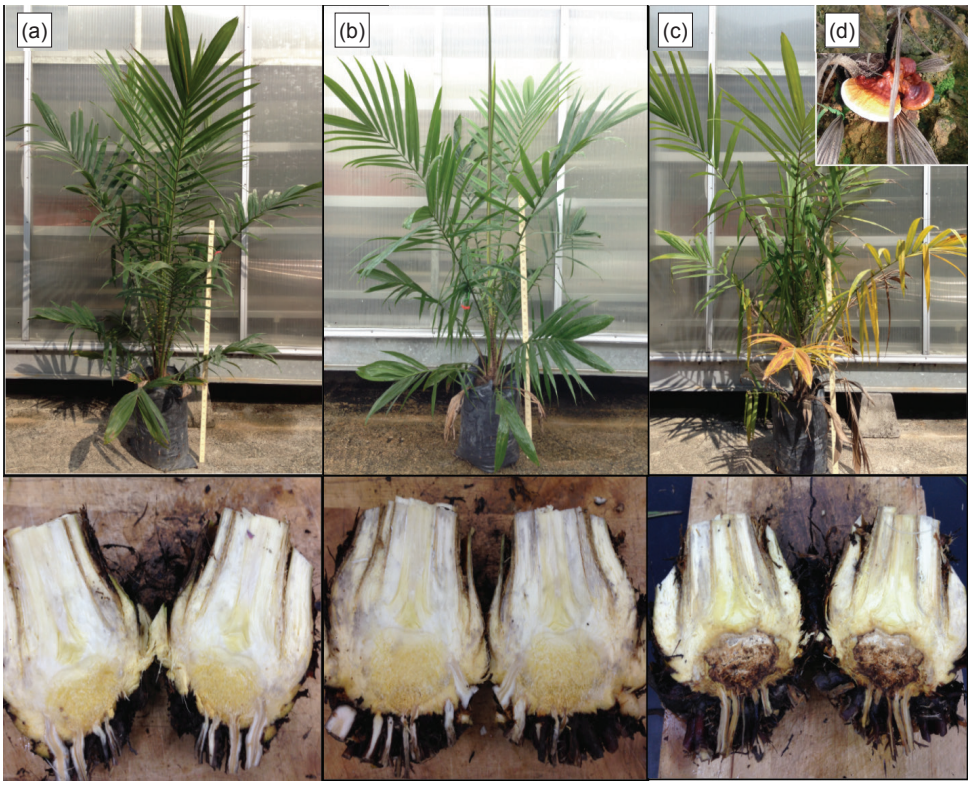


Figure 1. Oil palm seedlings were destructed to observe the severity of rotten tissues in the boles. Seedlings were chosen based on three different categories. (a) control seedling with class 0 DSI, and class 0 DI (internal); (b) asymptomatic seedling with class 0 DSI, and class 0 DI (internal); (c) asymptomatic seedling with class 3 DSI, and class 3 DI (internal), (d) basidiocarp growing at the base of a seedling.

in terms of differential expression of transcripts. The cDNA libraries were constructed from three biological replicates from the three groups (*Table 3*). A total of 464 701 946 paired-end reads with an average read length of 150 nucleotides (nt) were obtained. Annotations were performed by using BLAST against the UniProt database at http://www.uniprot.org/. Unigenes from control, asymptomatic, and symptomatic seedlings were identified and categorised into KEGG pathways via https://www.genome.jp/kegg/pathway.html.

A subset of the expressed genes was validated using both real-time quantitative PCR and NanoString in the same samples (data not shown). A part of the present work was also filed for a patent (WO2017155384A1, 2017).

A Venn diagram analysis was performed to group unigenes that appeared only in control, symptomatic, and asymptomatic seedlings (*Figure 2*). The unigenes were grouped into three different phenotypes based on the KEGG pathways (*Table 4*). Eight pathways from the unigenes appeared in all three phenotypes. Most of the pathways that appeared in either one or two phenotypes were common in cell metabolism, and carboxylic and amino acid metabolisms.

The ubiquitin-mediated proteolysis pathway was detected in the roots of asymptomatic seedlings and control. It made use of receptors that recognised and deciphered the ubiquitin code to regulate most cellular processes, including host-pathogen interactions (Li *et al.*, 2016). Modifications of the genes that are regulated by the ubiquitin system have been shown to manipulate the host defence system. Increased resistance against the root-infecting fungal pathogen *Fusarium oxysporum* has

TABLE 3. SUMMARY OF PRE- AND POST-PROCESSED READS OF RNA-SEQUENCING LIBRARIES

	RNA-Seq libraries		
	Control	**Asymptomatic**	**Symptomatic**
Raw reads	221 907 420	199 546 208	148 818 010
Raw nucleotides	33 286 113 000	29 931 931 200	22 322 701 500
Processed reads	137 203 583	197 032 111	137 203 582
Processed nucleotides	30 148 229 470	26 032 716 787	18 391 549 644
Mapped (%)	52	57	50

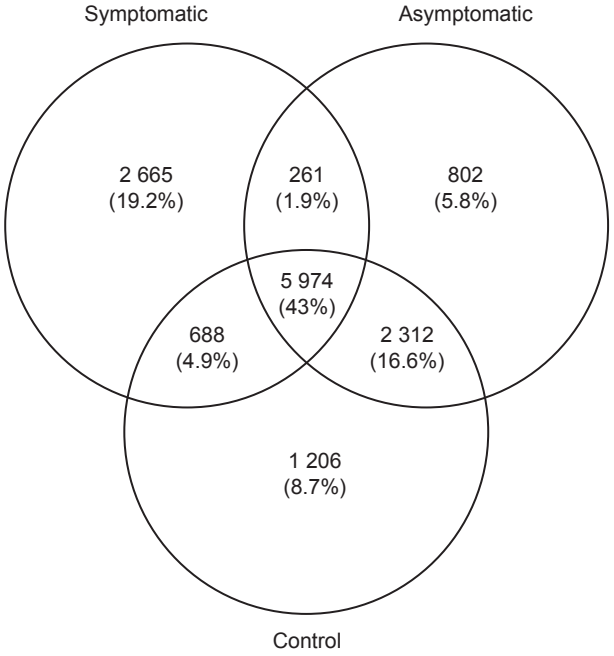


Figure 2. Venn diagram of unigenes from root tissues of oil palm seedlings that displayed three different phenotypes; control, asymptomatic, and symptomatic.

been displayed by the pub22/23/24 triple mutant. This suggested a role in root-mediated defence by PUB22/23/24 against soil-borne pathogens (Chen *et al*., 2013; Zhou and Zeng, 2017).

Transcriptional Expression in Roots of Symptomatic and Asymptomatic Seedlings

Most of the transcripts detected in symptomatic and asymptomatic seedlings were linked to cell walls, transporters, disease resistance, and phytohormone signalling pathways. A total of 20 upregulated and 20 downregulated transcripts were found in symptomatic and asymptomatic seedlings (*Table 5*).

Cell wall-related transcripts were differentially expressed in symptomatic seedlings. Endoglucanase, which is required for secondary cell wall formation in the developing xylem (Glass *et al*., 2015), was found to be downregulated. Glucanases also belong to the pathogenesis-related protein family (PR-2). They were also found to be involved in the infection of rice roots by *Azoarcus* sp. strain BH72. The visible sites of expression of the endoglucanase gene *eglA* were the points where lateral roots and root tips emerged, which are also the primary points of entry into the roots (Reinhold *et al*., 2006).

The ATP-binding cassette (ABC) proteins transport secondary metabolites and plant hormones that regulate the overall development of plants (Hwang *et al*., 2016). The ABCC transporters respond to pathogen-specific biotic stress where particular changes in ABCC transcript levels are found to induce distinct signalling cascades (Wanke and Kolukisaoglu, 2010). The ABCB proteins may serve as basal auxin transporters (Cho and Cho, 2013). The ABCI and ABCF transporters which are found down-regulated in asymptomatic seedlings are not directly involved in the transport process but likely function in ribosome recycling and translational control (Kang *et al*., 2011).

The transcripts of resistance proteins were detected in the roots of inoculated oil palm seedlings. Resistance gene analogues (RGAs) are a large class of potential R-genes (resistance genes) that enable plants to recognise specific races of pathogens and to mount an effective localised defence response (Jones, 1996). Disease resistance and abiotic stress tolerance in *Nicotiana benthamian* were enhanced in the overexpressed pathogen-induced grapevine *VaRGA1* gene (Li *et al*., 2017). In strawberries, the *Phytophthora cactorum* infection in crown rot showed that the gene transcriptional profiles of most RGAs were stronger and quicker in the resistant Bukammen than in the susceptible FDP821 genotype during the early infection stage (Chen *et al*., 2016).

Gene expression is regulated by gibberellins by promoting the degradation of transcriptional regulator proteins (Murase *et al*., 2008). The earliest findings of gibberellic acid (GA) in plant immunity were related to the decreased levels of GA in infected rice caused by Phytoreovirus (Zhu *et al*., 2005). However, exogenous GA was found to lower the resistance to two rice pathogens *Magnaporthe oryzae* and *Xanthomonas oryzae* (Qin *et al*., 2013; Yang *et al*., 2008). The rice GA signalling also appears to promote resistance to necrotrophs, and susceptibility to hemibiotrophs (De Bruyne *et al*., 2014).

Unique Proteins with Different Abundance

The iTRAQ analysis provides a relative quantification and was used for comparing control and diseased roots of oil palm seedlings in the present work. A total of 53 proteins were found to be higher in abundance, while 69 proteins were lower in abundance. The number of proteins that were higher in abundance was found in roots of asymptomatic seedlings, compared to symptomatic seedlings, while proteins that were lower in abundance were found in symptomatic seedlings. The activities of an increased number of proteins could be suppressed in the roots of symptomatic seedlings when the plants are showing signs of disease symptoms. When necrotic tissues in roots of symptomatic seedlings increase with the progression of disease infection, the functions of proteins in healthy tissues will decrease.

These proteins were subsequently grouped based on their functions (*Table 6*). The number of proteins with the following functions is lower in abundance in the roots of symptomatic seedlings;

TABLE 4. CLASSIFICATION OF UNIGENES BASED ON KEGG PATHWAYS

a) Appear in all phenotypes

(KO00520) Amino sugar and nucleotide sugar metabolisms

(KO00190) Oxidative phosphorylation

(KO04075) Plant hormone signal transduction

(KO04626) Plant-pathogen interaction

(KO04141) Protein processing in the endoplasmic reticulum

(KO03010) Ribosome

(KO03013) RNA transport

(KO00230) Purine metabolism

b) Appear in roots of control and asymptomatic seedlings

(KO04120) Ubiquitin-mediated proteolysis

c) Appear in roots of control and symptomatic seedlings

(KO00710) Carbon fixation in photosynthetic organisms

(KO00010) Glycolysis/gluconeogenesis

(KO00620) Pyruvate metabolism

d) Appear in roots of asymptomatic and symptomatic seedlings

Aspartate and glutamate metabolisms

e) Appear in one phenotype only

Control	Asymptomatic	Symptomatic
(KO00330) Arginine and proline metabolisms	(KO00020) Citrate cycle (TCA Cycle)	(KO00250) Alanine
(KO00270) Cysteine and methionine metabolisms	(KO04144) Endocytosis	(KO00720) Carbon fixation pathways in prokaryotes
(KO00051) Fructose and mannose metabolisms	(KO00564) Glycerophospholipid metabolism	(KO00071) Fatty acid metabolism
(KO03015) mRNA surveillance pathway	(KO03015) mRNA surveillance pathway	(KO00680) Methane metabolism
(KO00030) Pentose phosphate pathway	(KO03008) Ribosome biogenesis in eukaryotes	(KO04146) Peroxisome
(KO03050) Proteasome	(KO00072) Synthesis and degradation of ketone bodies	(KO00240) Pyrimidine metabolism
(KO03040) Spliceosome	(KO00900) Terpenoid backbone biosynthesis	(KO03018) RNA degradation
(KO00500) Starch and sucrose metabolisms	(KO00280) Valine	(KO00500) Starch and sucrose metabolisms

carbohydrate metabolism, cellular processes, protein metabolism and sugar metabolism. These main metabolic processes were also identified in soybean root diseases, Chinese cabbage and wheat (Bai *et al*., 2019; Kang *et al*., 2019; Lan *et al*., 2019). Carbohydrate metabolism, cellular processes, energy and protein metabolisms, signalling and stress response were higher in asymptomatic seedlings. The difference in protein abundances and identities in the symptomatic and asymptomatic seedlings indicated that specific protein requirements were needed when these seedlings were under stressed conditions. A proteomic profile of banana roots infected with *F. oxysporum* revealed that differentially regulated proteins involved in different defence pathways are likely associated with different resistant levels of the three banana cultivars (Li *et al*., 2013).

Proteins in Roots of Symptomatic and Asymptomatic Seedlings

Many proteins of lower abundance were detected in the roots of symptomatic seedlings (*Table 7*). Most of these proteins are involved in defence, stress response, and signalling. Unique, 14-3-3 proteins are phosphate-binding proteins

TABLE 5. UPREGULATED AND DOWNREGULATED TRANSCRIPTS FOUND IN ROOTS OF SYMPTOMATIC AND ASYMPTOMATIC SEEDLINGS

Contig	Differential expression (log2)	Uniprot
Downregulated transcripts		
Singleton1	-7.39	ABC transporter C family member 10 OS=*Arabidopsis thaliana*
Singleton2	-6.58	NAC domain-containing protein 68 OS=*Oryza sativa* subsp. *japonica*
Singleton3	-6.07	Adenosine kinase 2 OS=*A. thaliana*
Singleton4	-6.04	BI1-like protein OS=*A. thaliana*
Singleton5	-5.57	DDB1- and CUL4-associated factor homolog 1 OS=*A. thaliana*
Singleton6	-5.49	Pentatricopeptide repeat-containing protein At3g63370 OS=*A. thaliana*
Singleton7	-5.48	COP9 signalosome complex subunit 6a OS=*A. thaliana*
Singleton8	-5.30	Endoglucanase 25 OS=*A. thaliana*
Singleton9	-5.10	Putative lipoxygenase 5 OS=*O. sativa* subsp. *japonica*
Singleton10	-5.04	Cleavage and polyadenylation specificity factor CPSF30 OS=*A. thaliana*
Singleton11	-4.52	Plastidic glucose transporter 4 OS=*A. thaliana*
Singleton12	-4.37	Ammonium transporter 3 member 3 OS=*O. sativa* subsp. *japonica*
Singleton13	-4.28	Chalcone synthase 3 OS=*Ruta graveolens*
Singleton14	-4.25	40S ribosomal protein S4-3 OS=*A. thaliana*
Singleton15	-4.19	Probable serine/threonine-protein kinase CCRP1 OS=*Zea mays*
Singleton16	-4.19	Zinc finger A20 and AN1 domain-containing stress-associated protein 8 OS=*O. sativa* subsp. *japonica*
Singleton17	-4.17	ABC transporter B family member 11 OS=*A. thaliana*
Singleton18	-4.09	Putative late blight resistance protein homolog R1B-17 OS=*Solanum demissum*
Singleton19	-4.02	Proteasome subunit alpha type-6 OS=*Nicotiana tabacum*
Singleton20	-4.00	Phosphoenolpyruvate carboxylase kinase 1 OS=*A. thaliana*
Upregulated transcripts		
Singleton21	9.18	Alpha, alpha-trehalose-phosphate synthase _UDP-forming_1 OS=*A. thaliana*
Singleton22	9.08	Gibberellin receptor GID1 OS=*O. sativa* subsp. *japonica*
Singleton23	9.07	Xyloglucan endotransglucosylase/hydrolase protein 22 OS=*A. thaliana*
Singleton24	9.07	Protein GAST1 OS=*S. lycopersicum*
Singleton25	8.95	Sphingosine-1-phosphate lyase OS=*O. sativa* subsp. *japonica*
Singleton26	8.76	Pentatricopeptide repeat-containing protein At3g02650, mitochondrial OS=*A. thaliana*
Singleton27	8.75	Probable peptide/nitrate transporter At1g33440 OS=*A. thaliana*
Singleton28	8.68	Transcription factor AS1 OS=*A. thaliana*
Singleton29	8.64	Probable receptor-like protein kinase At5g18500 OS=*A. thaliana*
Singleton30	8.60	Long chain acyl-CoA synthetase 4 OS=*A. thaliana*
Singleton31	8.40	Shaggy-related protein kinase beta OS=*A. thaliana*
Singleton32	8.40	Phosphoenolpyruvate carboxylase 1 OS=*A. thaliana*
Singleton33	8.35	Peptide transporter PTR1 OS=*A. thaliana*
Singleton34	8.31	Dehydrin COR410 OS=*Triticum aestivum*
Singleton35	8.21	DNA-directed RNA polymerase D subunit 1 OS=*A. thaliana*
Singleton36	8.18	Malate dehydrogenase, chloroplastic OS=*A. thaliana*
Singleton37	8.18	Regulatory protein NPR1 OS=*A. thaliana*
Singleton38	8.15	Putative disease resistance protein RGA1 OS=*S. bulbocastanum*
Singleton39	8.10	12-oxophytodienoate reductase 3 OS=*A. thaliana*
Singleton40	8.09	Uncharacterised protein At4g10930 OS=*A. thaliana*

TABLE 6. ABUNDANCE OF UNIQUE PROTEINS PERFORMING SPECIFIC FUNCTIONS

Function	Symptomatic		Asymptomatic	
Protein abundance	**Higher**	**Lower**	**Higher**	**Lower**
Carbohydrate metabolism	-	4	2	1
Cell wall-related defence	1	2	-	1
Cellular processes	-	12	9	5
Energy	1	1	5	-
Lipid metabolism	-	-	1	-
PR protein	1	1	1	2
Protein metabolism	2	7	6	1
Signalling	1	1	2	1
Stress response	1	11	2	-
Sugar metabolism	-	6	6	-
Transporter	-	2	2	2

that regulate multiple signalling pathways. These proteins control hormone signalling, cell division, and disease resistance. The 14-3-3 isoform protein family are key targets of bacterial effectors for *Xv3* disease resistance in tomatoes (Dubrow *et al*., 2018). The acireductone dioxygenase-like protein contributes to the production of ethylene, a product of the methionine salvage pathway (Friedman *et al*., 2011). It is important in maintaining the S-adenosylmethionine levels for ethylene production (White and Flashman, 2016). Ethylene is important in the hormonal regulation of plant development, as a virulence factor of fungal and bacterial pathogens, and as a signalling compound in disease resistance (Loon *et al*., 2006).

Beta-1,3-glucanases are abundant in plants; they work either alone or with chitinases and other antifungal proteins to protect plants against fungal pathogens (Balasubramanian *et al*., 2012). Beta-1,3-glucanases inhibit the growth of fungal pathogens when they catalyse the hydrolytic cleavage of beta-1,3-glucans, a major structural component present in the fungal cell wall (Su *et al*., 2016).

Cyclophilins have multiple functions and are highly versatile. Many growth and development processes in plants, particularly hormone signalling and stress responses, are regulated by cyclophilins (Singh *et al*., 2020). In soybean, the *CYP1* transcript level was reduced in response to *Phytophthora sojae* infection (Mainali *et al*., 2017). Since isoflavonoids are involved in plant stress resistance against biotic and abiotic factors, the interaction of *GmCYP1* with the isoflavonoid regulators *GmMYB176* and 14-3-3 protein, suggests its role in the defence system of soybean.

Enolase is essential for the growth and development of plants. Altered ENO2 functions in *Arabidopsis* plants have reduced cell size and defective cell differentiation with restricted lignification (Eremina *et al*., 2015).

The 40S ribosomal protein S18-like protein is highly abundant in asymptomatic seedlings (*Table 8*). Ribosomal proteins are important in maintaining the stability of the ribosomal complex and mediating protein synthesis (Moin *et al*., 2016). Rice infected with *X. oryzae* and *Rhizoctonia solani* have induced the up-regulation of several ribosomal proteins. The transcript levels of *RPS4* are also higher during biotic stresses (Saha *et al*., 2017).

The cellular membrane potential in plants is established by plasma membrane (PM) H^+-ATPases (Elmore and Coaker, 2011). They interact with *RIN4*, a negative regulator of disease resistance, to manage stomatal apertures during *Pseudomonas syringae* invasion of leaf tissues in *Arabidopsis* (Liu *et al*., 2009). Furthermore, PM H^+-ATPase activities have been manipulated by evolving pathogens during infection, and are targeted by pathogens to increase plant susceptibility (Elmore and Coaker, 2011).

Receptor kinases are important in plant immunity, growth and development. They deploy many receptor kinases as pattern recognition receptors that detect microbe- and host-derived molecular patterns as the first layer of inducible defence (Tang *et al*., 2017). The serine/threonine protein phosphatase 2A controls pathogenesis responses in various plant species. It contributes to the regulation of receptor signalling, organellar signalling, gene expression, metabolic pathways, and cell death, all of which essentially impact plant immunity (Durian *et al*., 2016).

CONCLUSION

Research using a combination of omics technologies is useful for providing a universal view of understanding the molecular systems that underlie various functions in oil palm seedlings infected with BSR. The present work explored both the transcripts

TABLE 7. PROTEINS WITH DIFFERENT ABUNDANCE PRESENT IN THE ROOTS OF SYMPTOMATIC OIL PALM SEEDLINGS

Accession	UniProt	Name	Fold change	Unused ProtScore	Total ProtScore	% Coverage	Peptide (95%)
a) Proteins with higher abundance							
gi|310689155	E3V1H6	6-phosphogluconate dehydrogenase [*Pinus sylvestris*]	87.90	2.00	4.42	17.4	7
gi|514814998	K4A649	PREDICTED: 5-methyltetrahydropteroyltriglutamate--homocysteine methyltransferase-like [*Setaria italica*]	87.90	3.01	8.83	18.7	7
gi|192910882	B3TLW8	Beta-1,3-glucanase [*Elaeis guineensis*]	6.14	12.64	12.64	38.1	28
gi|7271955	Q9M511	Cytosolic pyruvate kinase [*Lilium longiflorum*]	6.08	3.16	3.17	8.4	2
gi|192910890	B3TLX2	Early flowering protein 1 [*E. guineensis*]	2.11	16.06	16.06	55.1	17
gi|192911934	B3TLZ4	Temperature-induced lipocalin [*E. guineensis*]	1.29	2.03	2.03	15.4	1
gi|502136998	A5BUU4	PREDICTED: 40S ribosomal protein SA-like [*Cicer arietinum*]	1.19	8.00	8.00	20.9	7
gi|148927382	A6N8F8	Cysteine proteinase [*E. guineensis*]	1.18	4.76	4.76	19.2	7
gi|75259589	Q6I544	RecName: Full=Germin-like protein 5-1; Flags: Precursor	1.14	5.87	5.87	18.6	8
gi|22535406	Q6F2Y7	Heat shock protein 101 [*O. sativa*]	1.06	2.34	2.34	4.6	1
b) Proteins with lower abundance							
gi|164652940	B6RF01	14-3-3d protein [*Gossypium hirsutum*]	90.09	2.00	2.00	6.5	1
gi|192913044	B3TM49	Aci-reductone dioxygenase-like protein [*E. guineensis*]	90.09	2.44	2.44	1.3	1
gi|448872690	M1H922	Alpha-1,4-glucan-protein synthase [*E. guineensis*]	90.09	4.00	4.00	27.8	2
gi|192910882	B3TLW8	Beta-1,3-glucanase [*E. guineensis*]	90.09	2.16	2.16	6.4	2
gi|192910744	B3TLP9	Cyclophilin [*E. guineensis*]	90.09	2.00	2.00	4.0	1
gi|255539693	B9R9N6	Enolase isoform X2, putative [*Ricinus communis*]	89.29	1.57	1.59	10.7	2
gi|255539693	B9R9N6	Enolase isoform X2, putative [*R. communis*]	77.52	3.48	9.68	26.5	7
gi|511537412	R9VV88	FVE protein [*Litchi chinensis*]	42.02	2.22	4.30	23.8	2
gi|508785294	A0A061GRR9	General regulatory factor 7, NU [*Theobroma cacao*]	40.16	2.00	5.13	17.1	3
gi|192910866	B3TLW0	Glutathione S-transferase [*E. guineensis*]	36.36	4.05	4.05	5.2	2
gi|82400215	Q2XQF4	Glyceraldehyde 3-phosphate dehydrogenase [*E. guineensis*]	33.11	15.00	15.00	62.4	12
gi|302805526	D8SMA1	Hypothetical protein SELMODRAFT_156635 [*Selaginella moellendorffii*]	25.84	2.42	2.42	10.8	1
gi|192910730	B3TLP2	Light-inducible protein ATLS1 [*E. guineensis*]	22.08	2.85	7.17	9.3	5
gi|351724907	Q71EW8	Methionine synthase [*Glycine max*]	18.18	4.01	10.91	59.3	9
gi|192910736	B3TLP5	Mitochondrial F0 ATP synthase D chain [*E. guineensis*]	16.00	3.62	3.62	19.8	1
gi|897618	C0HF32	Mitochondrial F-1-ATPase subunit 2 [*Zea mays*]	15.70	5.89	5.89	21.9	3
gi|192910872	B3TLW3	Pathogenesis-related protein [*E. guineensis*]	12.24	11.21	11.21	30.3	9
gi|211906450	D2D2Z8	Phosphoglycerate kinase [*Gossypium hirsutum*]	9.73	4.16	4.16	12.5	2
gi|508712850	A0A061EK37	Phosphoglycerate mutase, 2,3-bisphosphoglycerate-independent isoform 2 [*Theobroma cacao*]	9.63	2.00	2.00	7.2	1
gi|359482944	F6HYG1	PREDICTED: 97 kDa heat shock protein-like [*Vitis vinifera*]	8.47	12.60	12.60	39.1	8
gi|470102123	Q8S9S4	PREDICTED: IAA-amino acid hydrolase ILR1-like 4-like [*Fragaria vesca*]	8.02	4.21	4.21	8.6	3
gi|514779322	K3XJN7	PREDICTED: malate dehydrogenase, mitochondrial-like [*Setaria italica*]	7.45	5.33	5.33	30.7	3
gi|514814448	K4A6V8	PREDICTED: phosphoglucomutase, cytoplasmic 2-like isoform X2 [*S. italica*]	6.92	8.93	8.93	35.3	8
gi|225452974	Q42290	PREDICTED: probable mitochondrial-processing peptidase subunit beta [*V. vinifera*]	5.34	15.75	15.75	36.2	12
gi|514798087	K3YJL3	PREDICTED: proteasome subunit beta type-1-like [*S. italica*]	5.01	4.05	23.44	49.2	28

Note: Unused (ProtScore)- A measure of the protein confidence for a detected protein, calculated from the peptide confidence for peptides from spectra that have not already been completely "used" by higher scoring winning proteins. For 95% confidence, the required Unused ProtScore is 1.3; Total (ProtScore)- A measure of the total amount of evidence for a detected protein; % Coverage- The percentage of matching amino acids from identified peptides divided by the total number of amino acids in the sequence.

TABLE 8. PROTEINS WITH DIFFERENT ABUNDANCE PRESENT IN THE ROOTS OF ASYMPTOMATIC OIL PALM SEEDLINGS

Accession	UniProt	Name	Fold change	Unused ProtScore	Total ProtScore	% Coverage	Peptide (95%)
a) Proteins with higher abundance							
gi|502093390	P34788	PREDICTED: 40S ribosomal protein S18-like [*Arabidopsis thaliana*]	99.1	1.48	1.48	17.8	1
gi|159465541	P55195	Phosphoribosylaminoimidazole carboxylase, eukaryotic-type [*Chlamydomonas reinhardtii*]	87.9	1.35	1.35	3.2	1
gi|46430485	Q75N96	Plasma membrane H+-ATPase [*Daucus carota*]	87.9	2	5.24	7	3
gi|514778521	K3XF69	PREDICTED: probable inactive receptor kinase At2g26730-like [*Setaria italica*]	87.1	2	2	2.5	1
gi|514728147	Q38950	PREDICTED: serine/threonine-protein phosphatase 2A 65 kDa regulatory subunit A beta isoform-like isoform X2 [*S. italica*]	86.3	2.7	2.7	9.1	1
gi|310689155	E3V1H6	6-phosphogluconate dehydrogenase [*Pinus sylvestris*]	77.3	2	4.42	17.4	7
gi|192911934	B3TLZ4	Temperature-induced lipocalin [*Elaeis guineensis*]	6.9	2.03	2.03	15.4	1
gi|374256013	H6TNN9	Putative methionine synthase protein, partial [*E. guineensis*]	5.4	7.68	10.61	28.9	7
gi|192910908	B3TLY1	Fructose-bisphosphate aldolase [*E. guineensis*]	5.1	18.23	18.23	51.4	20
gi|48527431	Q5J1K3	Elongation factor 1-alpha 1 [*E. guineensis*]	5	12.62	12.62	27.3	14
gi|25396545	A9TW09	Alpha tubulin [*Physcomitrium patens*]	4.4	19.07	19.07	36.3	14
gi|47026989	Q677B2	Nucleoside diphosphate kinase [*Hyacinthus orientalis*]	4	6	6	19.5	4
gi|192910730	B3TLP2	Light-inducible protein ATLS1 [*E. guineensis*]	3.9	4.09	4.09	42.6	2
gi|192910882	B3TLW8	Beta-1,3-glucanase [*E. guineensis*]	3.8	16.88	16.88	36	28
gi|4126976	Q9ZWI8	Vacuolar H+-pyrophosphatase [*Chara corallina*]	3.5	1.47	1.47	4.3	1
gi|50251203	Q6EUQ9	Putative vacuolar proton-ATPase [*Oryza sativa*]	3.5	15.45	15.45	26.7	14
gi|192910674	B3TLL4	Triose phosphate isomerase cytosolic isoform [*E. guineensis*]	2.8	4.49	4.54	26	5
gi|81686725	Q6ZI55	NAD-dependent isocitrate dehydrogenase c;2 [*O. sativa*]	2.5	4.03	4.03	16.9	2
gi|357167236	P08926	PREDICTED: ruBisCO large subunit-binding protein subunit alpha, chloroplastic-like [*Brachypodium distachyon*]	2.3	9.85	9.85	19.9	8
gi|192910890	B3TLX2	Early flowering protein 1 [*E. guineensis*]	2	13.68	13.68	56.3	15
gi|502082135	P54774	PREDICTED: cell division cycle protein 48 homolog [*Cicer arietinum*]	1.7	6.77	6.77	13.1	4
gi|225435632	P28723	PREDICTED: formate--tetrahydrofolate ligase-like [*Vitis vinifera*]	1.4	2.79	2.79	4.9	1
gi|77553679	Q2QXR7	Pyruvate kinase family protein expressed [*O. sativa*]	1.4	4	4	12.5	2
gi|470107271	Q6K9N6	PREDICTED: succinyl-CoA ligase [*ADP*-forming] subunit beta, mitochondrial-like [*Fragaria vesca* subsp. *vesca*]	1.2	4.13	4.13	22	4
gi|353441078	G8FGH1	Putative enolase [*E. guineensis*]	1.2	4.01	10.91	59.3	9
gi|192910928	B2CZK7	Plasma membrane intrinsic protein [*E. guineensis*]	1.2	5.07	5.07	22.3	5
gi|508722839	A0A061G0U1	Sugar isomerase (SIS) family protein isoform 2 [*Theobroma cacao*]	1.1	5.12	5.12	9.5	3
gi|192910860	B3TLV7	Adenine phosphoribosyltransferase 1 [*E. guineensis*]	1.1	2.59	2.59	18.8	1
gi|353441104	G8FGJ2	Putative cytosolic malate dehydrogenase [*E. guineensis*]	1.1	1.51	6.32	32	4
gi|225452974	Q42290	PREDICTED: probable mitochondrial-processing peptidase subunit beta [*V. vinifera*]	1.1	4.53	4.53	9.9	2
gi|192912964	B3TM09	Protein disulphide isomerase 2 precursor [*E. guineensis*]	1.1	10.67	10.67	25.7	6
gi|897618	C0HF32	ATP synthase subunit beta [*Zea mays*]	1	38.01	38.01	56.2	42
b) Proteins with lower abundance							
gi|8698725	Q42605	Bifunctional UDP-glucose 4-epimerase and UDP-xylose 4-epimerase 1 [*A. thaliana*]	89.3	1.79	1.79	12	2
gi|192910924	B3TLY9	Annexin P35 [*E. guineensis*]	5.1	4.76	4.76	33.7	6
gi|508774440	A0A061FWS9	P-type H(+)-exporting transporter [*T. cacao*]	4.8	4.88	4.88	6.1	2
gi|192910890	B3TLX2	Early flowering protein 1 [*E. guineensis*]	4.7	15.76	15.76	65.8	23
gi|192912982	B3TM18	Pathogenesis-related protein 10c [*E. guineensis*]	4.5	9.36	11.54	52.2	7
gi|192912964	B3TM09	Protein disulphide isomerase 2 precursor [*E. guineensis*]	4.3	25.16	25.16	41.3	13
gi|502136998	A5BUU4	PREDICTED: 40S ribosomal protein SA-like [*Cicer arietinum*]	4.2	8	8	20.9	7
gi|474160132	M7ZC83	Adenosylhomocysteinase [*Triticum urartu*]	4.1	4.66	4.66	6.9	3
gi|448872668	M1GS77	5′-methylthioadenosine/s-adenosylhomocysteine nucleosidase 1-like protein [*E. guineensis*]	3.4	4.33	4.33	13.1	3
gi|192911934	B3TLZ4	Temperature-induced lipocalin [*E. guineensis*]	3.3	2.59	2.59	42.6	1
gi|508774440	A0A061FWS9	H(+)-transporting ATPase plant/fungi plasma membrane type [*T. cacao*]	2.5	7.38	7.38	4.9	4
gi|192910866	B3TLW0	Glutathione S-transferase [*E. guineensis*]	1.9	5.33	5.33	30.7	3
gi|148872938	A6MZ92	ATP citrate lyase alpha subunit [*Glycyrrhiza uralensis*]	1	6.16	6.16	19.2	4

Note: Unused (ProtScore)- A measure of the protein confidence for a detected protein, calculated from the peptide confidence for peptides from spectra that have not already been completely "used" by higher scoring winning proteins. For 95% confidence, the required Unused ProtScore is 1.3; Total (ProtScore)- A measure of the total amount of evidence for a detected protein; % Coverage- The percentage of matching amino acids from identified peptides divided by the total number of amino acids in the sequence.

and proteins in artificially inoculated seedlings after a 12 months prolonged exposure to *Ganoderma*. The biological functions of asymptomatic seedlings resembled those of healthy, uninoculated ones where cellular processes for regular growth and development were observed. Stress-responsive proteins and transcripts related to carbon fixation, glycolysis and pyruvate metabolism were detected in symptomatic seedlings. The profiles of asymptomatic and symptomatic seedlings can be used to understand the behaviour of host plants towards the mechanisms of disease infection after prolonged exposure. These findings add value to previous publications where seedlings were usually destructed after a three to four months exposure to the disease, and comparisons were made only for control and treated seedlings. Further investigations into the mechanisms of disease tolerance in oil palm could be proposed, where asymptomatic seedlings are thoroughly scrutinised. Integration of transcriptomic and proteomic approaches will also provide a better understanding of host-pathogen interactions, leading to new insights which would not be easy to attain using either the protein or mRNA differential analysis alone.

ACKNOWLEDGEMENT

The authors would like to acknowledge the contribution of Sime Darby Plantation R&D Centre, especially the Oil Palm Breeding Unit, for providing the oil palm germinated seeds, and the Crop Protection Unit, Plantation Research and Advisory Department, for assisting with nursery trials.

REFERENCES

Asemota, O and Shah, F (2004). Detection of mesocarp oleoyl-thioesterase gene of the South American oil palm *Elaeis oleifera* by reverse transcriptase polymerase chain reaction. *Afr. J. Biotechnol.*, *3(11)*: 595-598.

Bahari, M N A; Sakeh, N M; Abdullah, S N A; Ramli, R R and Kadkhodaei, S (2018). Transciptome profiling at early infection of *Elaeis guineensis* by *Ganoderma boninense* provides novel insights on fungal transition from biotrophic to necrotrophic phase. *BMC Plant Biol.*, *18*: 377.

Bai, L; Sun, H B; Liang, R T and Cai, B Y (2019). iTRAQ proteomic analysis of continuously cropped soybean root inoculated with *Funneliformis mosseae*. *Front. Microbiol.*, *10*: 61.

Balasubramanian, V; Vashisht, D; Cletus, J and Sakthivel, N (2012). Plant β-1,3-glucanases: Their biological functions and transgenic expression against phytopathogenic fungi. *Biotechnol. Lett.*, *34*: 1983-1990.

Breton, F; Hasan, Y; Hariadi; Lubis, Z and de Franqueville, H (2006). Characterization of parameters for the development of an early screening test for basal stem rot tolerance in oil palm progenies. *J. Oil Palm Res.*, *Special Issue*: 24-36.

Chen, X R; Brurberg, M B; Elameen, A; Klemsdal, S S and Martinussen, I (2016). Expression of resistance gene analogs in woodland strawberry (*Fragaria vesca*) during infection with *Phytophthora cactorum*. *Mol. Genet. Genomics*, *291*: 1967-1978.

Chen, Y T; Liu, H; Stone, S and Callis, J (2013). ABA and the ubiquitin E3 ligase KEEP ON GOING affect proteolysis of the *Arabidopsis thaliana* transcription factors ABF1 and ABF3. *Plant J.*, *75(6)*: 965-976.

Cho, M and Cho, H T (2013). The function of ABCB transporters in auxin transport. *Plant Signal. Behav.*, *8*: e22990.

Crandall, S G; Gold, K M; Jiménez-Gasco, M D M; Filgueiras, C C and Willett, D S (2020). A multi-omics approach to solving problems in plant disease ecology. *PLoS ONE*, *15*: e0237975.

Crone, M; McComb, J A; O'Brien, P A and Hardy, G E S J (2013). Assessment of Australian native annual/herbaceous perennial plant species as asymptomatic or symptomatic hosts of *Phytophthora cinnamomi* under controlled conditions. *Forest Pathol.*, *43*: 245-251.

Dai, T; Chang, X; Hu, Z; Liang, L; Sun, M; Liu, P and Liu, X (2019). Untargeted metabolomics based on GC-MS and chemometrics: A new tool for the early diagnosis of strawberry anthracnose caused by *Colletotrichum theobromicola*. *Plant Dis.*, *103*: 2541-2547.

Daim, L D J; Ooi, T E K; Yusof, H; Abdul Majid, N and Karsani, S (2015a). Optimization of protein extraction and two-dimensional electrophoresis protocols for oil palm leaf. *Protein J.*, *34*: 304-312.

Daim, L D J; Ooi, T E K; Ithnin, N; Mohd Yusof, H; Kulaveerasingam, H; Abdul Majid, N and Karsani, S A (2015b). Comparative proteomic analysis of oil palm leaves infected with *Ganoderma boninense* revealed changes in proteins involved in photosynthesis, carbohydrate metabolism, and immunity and defense. *Electrophoresis*, *36*: 1699-1710.

De Bruyne, L; Höfte, M and De Vleesschauwer, D (2014). Connecting growth and defense: The

emerging roles of brassinosteroids and gibberellins in plant innate immunity. *Mol. Plant*, *7*: 943-959.

Dubrow, Z; Sunitha, S; Kim, J G; Aakre, C D; Girija, A M; Sobol, G; Teper, D; Chen, Y C; Ozbaki-Yagan, N; Vance, H; Sessa, G and Mudgett, M B (2018). Tomato 14-3-3 proteins are required for Xv3 disease resistance and interact with a subset of *Xanthomonas euvesicatoria* effectors. *Mol. Plant Microbe Interact*., *31*: 1301-1311.

Durian, G; Rahikainen, M; Alegre, S; Brosché, M and Kanagasjärvi, S (2016). Protein phosphatase 2A in the regulatory network underlying biotic stress resistance in plants. *Front. Plant Sci.*, *7*: 812-812.

Elmore, J M and Coaker, G (2011). The role of the plasma membrane H+-ATPase in plant-microbe interactions. *Mol. Plant, 4*: 416-427.

Eremina, M; Rozhon, W; Yang, S and Poppenberger, B (2015). ENO2 activity is required for the development and reproductive success of plants, and is feedback-repressed by *At*MBP-1. *Plant J*., *81*: 895-906.

Friedman, E; Wang, H; Jiang, K; Perovic, I; Deshpande, A; Pochapsky, T; Temple, B; Hicks, S; Harden, T and Jones, A (2011). Acireductone dioxygenase 1 (ARD1) is an effector of the heterotrimeric G protein subunit in *Arabidopsis*. *J. Biol. Chem.*, *286*: 30107-18.

Glass, M; Barkwill, S; Unda, F and Mansfield, S D (2015). Endo-β-1,4-glucanases impact plant cell wall development by influencing cellulose crystallization. *J. Integr. Plant Biol.*, *57*: 396-410.

Ho, C L; Tan, Y C; Yeoh, K A; Lee, W K; Ghazali, A K; Yee, W Y and Hoh, C C (2019). Leaf transcriptome of oil palm (*Elaeis guineensis* Jacq.) infected by *Ganoderma boninense*. *Trees, 33*: 943-950.

Huang, X and Madan, A (1999). CAP3: A DNA sequence assembly program. *Genome Res*., *9*: 868-877.

Hushiarian, R; Yusof, N A and Dutse, S W (2013). Detection and control of *Ganoderma boninense*: Strategies and perspectives. *SpringerPlus, 2*: 555.

Hwang, J U; Song, W Y; Hong, D; Ko, D; Yamaoka, Y; Jang, S; Yim, S; Lee, E; Khare, D; Kim, K; Palmgren, M; Yoon, H S; Martinoia, E and Lee, Y (2016). Plant ABC transporters enable many unique aspects of a terrestrial plant's lifestyle. *Mol. Plant*., *9*: 338-355.

Jones, J D G (1996). Plant disease resistance genes: Structure, function and evolution. *Curr. Opin. Biotechnol.*, *7*: 155-160.

Kang, J; Park, J; Choi, H; Burla, B; Kretzschmar, T; Lee, Y and Martinoia, E (2011). Plant ABC transporters. *Arabidopsis Book*, *9*: e0153.

Kang, X; Wang, L; Guo, Y; Ul Arifeen, M Z; Cai, X; Xue, Y; Bu, Y; Wang, G and Liu, C (2019). A comparative transcriptomic and proteomic analysis of hexaploid wheat's responses to colonization by *Bacillus velezensis* and *Gaeumannomyces graminis*, both separately and combined. *Mol. Plant Microbe Interact., 32*: 1336-1347.

Lan, M; Li, G; Hu, J; Yang, H; Zhang, L; Xu, X; Liu, J; He, J and Sun, R (2019). iTRAQ-based quantitative analysis reveals proteomic changes in Chinese cabbage (*Brassica rapa* L.) in response to *Plasmodiophora brassicae* infection. *Sci. Rep., 9*: 12058-12058.

Li, J; Chai, Q-Y and Liu, C H (2016). The ubiquitin system: A critical regulator of innate immunity and pathogen-host interactions. *Cell Mol. Immunol., 13*: 560-576.

Li, X; Bai, T; Li, Y; Ruan, X and Li, H (2013). Proteomic analysis of *Fusarium oxysporum* f. sp. *cubense* tropical race 4-inoculated response to *Fusarium* wilts in the banana root cells. *Proteome Sci*., *11*: 41.

Li, X; Zhang, Y; Yin, L and Lu, J (2017). Overexpression of pathogen-induced grapevine TIR-NB-LRR gene VaRGA1 enhances disease resistance and drought and salt tolerance in *Nicotiana benthamiana*. *Protoplasma, 254*: 957-969.

Liu, J; Elmore, J M; Fuglsang, A T; Palmgren, M; Staskawicz, B and Coaker, G (2009). RIN4 functions with the plasma membrane H^+-ATPase to regulate stomatal apertures during pathogen attack. *PLoS Biol*., *7(6)*: e1000139.

Loon, L; Geraats, B and Linthorst, H (2006). Ethylene as a modulator of disease resistance in plants. *Trends Plant Sci., 11*: 184-191.

Mainali, H R; Vadivel, A K A; Li, X; Gijzen, M and Dhaubhadel, S (2017). Soybean cyclophilin *Gm*CYP1 interacts with an isoflavonoid regulator *Gm*MYB176. *Sci. Rep*., *7*: 39550.

Mercière, M; Boulord, R; Carasco-Lacombe, C; Klopp, C; Lee, Y P; Tan, J S; Syed Alwee, S S R; Zaremski, A; De Franqueville, H; Breton, F and Camus-Kulandaivelu, L (2017). About *Ganoderma boninense* in oil palm plantations of Sumatra and Peninsular Malaysia: Ancient population expansion, extensive gene flow and large scale dispersion ability. *Fungal Biol., 121*: 529-540.

Moin, M; Bakshi, A; Saha, A; Dutta, M; Madhav, S M and Kirti, P B (2016). Rice ribosomal protein large subunit genes and their spatio-temporal and stress regulation. *Front. Plant Sci.*, *7*: 1284.

Murase, K; Hirano, Y; Sun, T P and Hakoshima, T (2008). Gibberellin-induced DELLA recognition by the gibberellin receptor GID1. *Nature, 456*: 459-463.

Neik, T X; Amas, J; Barbetti, M; Edwards, D and Batley, J (2020). Understanding host-pathogen interactions in *Brassica napus* in the omics era. *Plants, 9*: 1336.

Pilotti, C A (2005). Stem rots of oil palm caused by *Ganoderma boninense*: Pathogen biology and epidemiology. *Mycopathologia, 159*: 129-137.

Qin, X; Liu, J H; Zhao, W S; Chen, X J; Guo, Z J and Peng, Y L (2013). Gibberellin 20-oxidase gene *Os*GA20ox3 regulates plant stature and disease development in rice. *Mol. Plant Microbe Interact., 26*: 227-239.

Qistina Othman, N; Paravamsivam, P; Tan, J S; Lee, Y P; Kwan, Y Y and Syed Alwee, S S R (2018). Validation of differential gene expression of transcriptome assembly via Nanostring® Technologies analysis platform. *J. Oil Palm Res.*, *30(4)*: 36-46.

Rees, R W; Flood, J; Hasan, Y; Potter, U and Cooper, R M (2009). Basal stem rot of oil palm (*Elaeis guineensis*); Mode of root infection and lower stem invasion by *Ganoderma boninense*. *Plant Pathol., 58*: 982-989.

Reinhold, B; Maes, T; Gemmer, S; Van Montagu, M and Hurek, T (2006). An endoglucanase is involved in infection of rice roots by the not-cellulose-metabolizing endophyte *Azoarcus* sp. strain BH72. *Mol. Plant Microbe Interact., 19*: 181-188.

Saha, A; Das, S; Moin, M; Dutta, M; Bakshi, A; Madhav, M S and Kirti, P B (2017). Genome-wide identification and comprehensive expression profiling of ribosomal protein small subunit (RPS) genes and their comparative analysis with the large subunit (RPL) genes in rice. *Front. Plant Sci.*, *8*: 1553.

Sariah, M; Zakaria, H; Flood, J; Bridge, P D and Holderness, M (2000). The use of soil amends for the control of basal stem rot of oil palm seedlings. Ganoderma *Diseases of Perennial Crops*. CABI Publishing, United Kingdom. p. 89-100.

Singh, H; Kaur, K; Singh, M; Kaur, G and Singh, P (2020). Plant cyclophilins: Multifaceted proteins with versatile roles. *Front. Plant Sci.*, *11*: 585121.

Su, Y; Wang, Z; Liu, F; Li, Z; Peng, Q; Guo, J; Xu, L and Que, Y (2016). Isolation and characterization of *Sc*GluD2, a new sugarcane beta-1,3-glucanase D family gene induced by *Sporisorium scitamineum*, ABA, H_2O_2, NaCl, and $CdCl_2$ stresses. *Front. Plant Sci.*, *7*: 1348.

Tan, B A; Daim, L D J; Ithnin, N; Ooi, T E K; Md-Noh, N; Mohamed, M; Mohd-Yusof, H; Appleton, D R and Kulaveerasingam, H (2016). Expression of phenylpropanoid and flavonoid pathway genes in oil palm roots during infection by *Ganoderma boninense*. *Plant Gene, 7*: 11-20.

Tang, D; Wang, G and Zhou, J M (2017). Receptor kinases in plant-pathogen interactions: More than pattern recognition. *Plant Cell*, *29*: 618-637.

Tarazona, S; García-Alcalde, F; Dopazo, J; Ferrer, A and Conesa, A (2011). Differential expression in RNA-seq: A matter of depth. *Genome Res., 21*: 2213-2223.

Wanke, D and Kolukisaoglu, H U (2010). An update on the ABCC transporter family in plants: Many genes, many proteins, but how many functions? *Plant Biol., 12*: 15-25.

White, M D and Flashman, E (2016). Catalytic strategies of the non-heme iron dependent oxygenases and their roles in plant biology. *Curr. Opin. Chem. Biol., 31*: 126-135.

Yang, D L; Li, Q; Deng, Y W; Lou, Y G; Wang, M Y; Zhou, G X; Zhang, Y Y and He, Z H (2008). Altered disease development in the eui mutants and Eui overexpressors indicates that gibberellins negatively regulate rice basal disease resistance. *Mol. Plant, 1*: 528-537.

Zhang, X; Kuivenhoven, J and Groen, A (2015). Forward individualized medicine from personal genomes to interactomes. *Front. Physiol., 6*: 364.

Zhou, B and Zeng, L (2017). Conventional and unconventional ubiquitination in plant immunity. *Mol. Plant Pathol.*, *18*: 1313-1330.

Journal of Oil Palm Research Vol. 35 (2) June 2023 p. 354-364
DOI: https://doi.org/10.21894/jopr.2022.0043

MIXED PLANTING WITH RHIZOMATOUS PLANTS INTERFERES WITH *Ganoderma* DISEASE IN OIL PALM

SUWANDI SUWANDI[1]*; RUDI PUTRA MUNANDAR[1]; SUPARMAN SUPARMAN[1]; CHANDRA IRSAN[1] and A. MUSLIM[1]

ABSTRACT

Basal stem rot (BSR) caused by Ganoderma boninense *remains the most destructive disease in oil palm monoculture plantations. This study investigates the nature of* Ganoderma *infection and survival under mixed planting with rhizomatous plants and its impact on the growth of oil palm. Two mixed plants (oil palm seedling and Java turmeric, galangal, or ginger) and single planting of those plants were inoculated with* Ganoderma boninense*-colonised rubber wood block (RWB). The results showed that* Ganoderma *inoculation in mixed planting caused an infection on both host species (dual-host infection). Under mixed planting for 9 months with Java turmeric and ginger, the disease index of oil palm was reduced by 47%-59% compared to the single planting. Planting oil palm with rhizomatous plants showed a minor effect on the decay of RWB and fungal survival but planting with ginger induced basidiocarp formation. The rhizomatous plants habitually did not exhibit allelopathic inhibition of oil palm growth. Growth of* Ganoderma*-infected seedlings was recovered under mixed planting. This study highlights a novel insight that mixed planting with rhizomatous plants can interfere with and reduce* Ganoderma *disease in oil palm.*

Keywords: *Ganoderma*, intercrop, infection interference, oil palm, rhizomatous plant.

Received: 25 October 2021; **Accepted:** 14 June 2022; **Published online:** 27 July 2022.

INTRODUCTION

Ganoderma spp. are polypore fungi that mainly live saprophytically but can also be pathogenic to most woody plants (Zhou *et al.*, 2015). In Southeast Asia, *Ganoderma* spp. play an important role as pathogens of woody plantation plants such as coconut (Kandan *et al*., 2010; Vinjusha and Kumar, 2022), acacia (Glen *et al*., 2009; Page *et al*., 2020) and oil palm (Ariffin *et al.*, 2000; Siddiqui *et al.*, 2021). *Ganoderma boninense* has been identified as the main pathogen of oil palm that causes basal stem rot (BSR) (Midot *et al.*, 2019; Pilotti, 2005; Purba *et al.*, 2020). BSR disease has become a serious problem in all soil types and oil palm planted areas in Indonesia and Malaysia. In some inland plantations of North Sumatra, BSR killed 31%-67% of oil palm trees during its 25 years of planting (Riyanto *et al*., 2020). In a peatland oil palm plantation in Sumatra, *Ganoderma* infection was reported to cause 30%-54% plant mortality and was estimated to reduce 0.5-0.7 t ha^{-1} yr^{-1} yield in its 14 years of planting (Pujianto *et al*., 2016). Recent disease surveillance of 37 359.81 ha of smallholder's plantations in Malaysia reported that BSR disease had affected 8.72%, 14.00%, 6.08% and 27.70% of oil palm in inland, coastal, peat and lateritic area, respectively (Ibrahim *et al*., 2020). BSR disease can reduce oil palm yields in some severely affected plantings by 68% (Kamu *et al.*, 2021). Inocula of *G. boninense* survive for a long time in infested plant debris left in the soil and therefore infect the next generation of plantings. Infested planting may harbour many infested roots, while a small infected root piece could be an infective inoculum (Rees *et al.*, 2007). The abundance of inoculum sources in a recent planting was considered responsible for the disease increase over several plant generations (Priwiratama *et al.*, 2020). Several control measures, including cultural practices, mechanical, chemical and microbial treatments, were applied to control BSR; however, none has been really able to reduce the spread of the disease (Siddiqui *et al*., 2021).

Oil palm plantations in Indonesia generally apply a standard monoculture cropping procedure with 25-30 years of commercial lifespan. This

[1] Department of Plant Protection, Faculty of Agriculture, Sriwijaya University, Jl. Palembang-Prabumulih Km.32, Palembang 30862, Indonesia.

* *Corresponding author e-mail: suwandi@fp.unsri.ac.id*

perennial tree planting forms a complex habitat of abundant understorey vegetation. This vegetation is dominated by herbaceous weeds (Ashton-Butt *et al.*, 2018; Luke *et al.*, 2019; Rembold *et al.*, 2017). Understorey vegetation in oil palm plantations could benefit both under- and above-ground biodiversity, including improving avian biodiversity (Nájera and Simonetti, 2010; Tohiran *et al.*, 2017), helping above-ground invertebrate communities (Ashraf *et al.*, 2018; Chung *et al.*, 2000; Spear *et al.*, 2018) and improving soil biodiversity and decomposition rates (Ashton-Butt *et al.*, 2018). In contrast to a large-scale plantation, some smallholders intercrop young oil palm with non-permanent food and cash crops, such as rice, maize, soybean, pineapple, cassava, banana, yam and cocoyam, particularly during the preharvest period until five years (Teuscher *et al.*, 2016). Intercropping oil palm with food and cash crops could provide both economic and environmental gains (Khasanah *et al.*, 2020). Boudreau (2013) demonstrated that intercropping practices had reduced rot/wilt diseases in 86% of 14 studies comparing diseases in monocrops and intercrops. The increase in host diversity through mixed cropping can lead either to a decrease in disease pressure (inoculum dilution mechanism) or to induce resistance in neighbouring plants (molecular mechanism) (Zhu and Morel, 2019). Rhizomatous plants from the Zingiberaceae family are among the cash crops adaptable to understorey intercropping with young oil palm or even mature palm (Yusron and Januwati, 2003). In rubber planting, mixed planting with perennial herbaceous plants, including rhizomatous plants, could reduce white root rot disease caused by *Rigidoporus microporous* and improve the decomposition of the infested stump (Silva *et al.*, 2014, Situmorang *et al.*, 2007).

However, it is not known how mixed planting as understorey intercropping with rhizomatous perennial plants influences the infection and survival of *G. boninense* and the growth of oil palm. The present study aimed to determine the effects of mixed planting with rhizomatous plants on the infection, development and survival of *G. boninense* and the growth of oil palm. This study hypothesised that *Ganoderma* infection, survival and development would be negatively interfered by mixed planting. Our findings will have important implications for a new approach to BSR management.

MATERIALS AND METHODS

Plant and Planting System

The rhizomatous plants tested were Java turmeric (*Curcuma xanthorrhiza* D. Dietr.), galangal (*Alpinia galanga* (L.) Willd.), and ginger (*Zingiber officinale* Roscoe). Rhizomes as planting materials were collected from local markets in South Sumatra and allowed to sprout for one month in sand medium to obtain plants of homogenous size. Oil palm material was obtained as germinated *dura* x *pisifera* (D×P) seeds from the Indonesian Oil Palm Research Institute. Seedlings were pregrown in a sand culture for two months until they had two leaves.

Three planting systems with *Ganoderma* inoculation were evaluated in this study: (i) mixed planting between oil palm seedlings and one of three rhizomatous plants, (ii) single planting of oil palm seedlings, and (iii) single planting of rhizomatous plants. Two additional planting systems equal to (i) and (ii) but without pathogen inoculation were also implemented to determine the effect of inoculation and mixed planting on the growth of oil palm. Each planting system comprised 15 plants. The experiment was replicated once. A mixture of field soil and sand (1:1) with a total volume of 5 L was filled within a black polyethylene bag (polybag) and used to grow plants in all planting systems. For mixed planting, plants were spaced 10 cm apart. Polybags were arranged at 90 cm spacing under a 25% paranet. Plants were fertilised every month with 0.5% NPK 16-16-16. Plant inoculation was performed one month after mixed planting (at the three-leaf stage for oil palm).

Inoculum and Inoculation of *G. boninense*

G. boninense isolate GbA from diseased oil palm identified based on morphology and the ITS sequences showed high aggressiveness (Rahmadhani *et al*., 2020) was used throughout the study. Pathogen inoculum was prepared as a two-month-old mycelium colonising a 12×5×5 cm rubber wood block (RWB). Inoculation was performed following Rees *et al.* (2007) by binding a wounded primary root (10 cm in length) with a single RWB using a parafilm. For mixed planting, a single RWB was inoculated onto two mixed plants (dual-host inoculation). Inoculated roots and RWB were buried at a 10 cm depth.

Disease Evaluation

Inoculated plants were uprooted every three, six and nine months post-inoculation (mpi) to examine root necrosis and disease severity. The length of root necrosis, as shown by discoloured and rotted primary roots, was recorded to measure the degree of root infection. Root infection was confirmed by direct plating of rotted roots on the *Ganoderma*-selective medium (GSM) (Ariffin and Seman, 1991). Five roots were examined for the presence or absence of *Ganoderma* infection. Disease severity was recorded following the rating of Breton *et al.* (2006) with an additional root rot rating: (0) healthy,

(1) rotting on primary roots, (2) up to 20% rotting of bole tissues, (3) from 20% to 50% internal rotting, (4) over 50% internal rotting, and (5) total rotting of bole tissues along with total desiccation of the plant.

Pathogen Development and Survival

Basidiocarp formation either on RWB as a source of inoculum or diseased plants was recorded as a variable for fungal development. The number of basidiocarps was counted, and the fresh weight was measured after detaching from its substrates. The decay of RWB and mycelial viability were recorded to measure pathogen survival within RWB in response to the planting system. RWB decay was calculated as the percentage of dry weight loss (Fernanda *et al*., 2021) after inoculation treatment for nine months. The viability of *Ganoderma* mycelia colonising RWB was assessed as the percentage of colonised wood fragments from which the *Ganoderma* mycelia emerged on GSM, out of 20 randomly cut wood fragments for each RWB (Chang, 2003).

Growth of Oil Palm

The leaf area and plant height of oil palm were recorded monthly to assess the growing interference of rhizomatous plants against oil palm seedlings. Leaf area was predicted by 0.55 × length × width of each of the whole plant leaves (Gromikora *et al.*, 2014).

Data Analyses

Data were analysed using R studio Version 1.4.1106 (RStudio PBC, Boston, MA, USA). The data were tested for normal distribution using the Shapiro-Wilk test and for variance homogeneity by Levene's test. Logarithmic transformation was performed to homogenous variance for the length of root necrosis before being subjected to one-way analyses of variance. The mean root necrosis length and disease index were compared using Tukey's honestly significant test (HSD). The mean RWB dry weight loss, percentage of mycelium survival, and fresh weight of basidiocarp were compared to the control treatment of single oil palm inoculation using the Dunnett test. The palm leaf area and height of single planting were compared to those of mixed planting by Student's t-test for equal variance and Welch t-test for unequal variance.

RESULTS AND DISCUSSION

Effects of Mixed Planting on Plant Disease

Ganoderma boninense infection occurred in all plants either under inoculation in a single or mixed planting. Root infection was observed on all inoculated plant species at one month post-inoculation (mpi). Infected roots were rotted and slightly darkened in colour. Oil palm infection (inoculation on a single oil palm) started to cause complete basal stem rot and plant death (mortality 80%) with basidiocarp formation on the dead plant at 6 mpi (*Figure 1*). On rhizomatous plants, root infection was extended towards the rhizome, causing rhizome root rot/rhizome rot (*Figures 2b*, *3b* and *4b*). Root and rhizome infections were confirmed by the recovery of *Ganoderma* mycelium on GSM (*Figures 2d*, *3d* and *4d*). Root and rhizome rot caused by *G. boninense* infection was more severe in galangal with a disease index of 1.8-3.4 at 6 mpi than in Java turmeric and ginger with a disease index of 0.6-0.8 and 1.0-1.4, respectively (*Figure 5*). *Ganoderma* infection caused galangal mortality (20%-60%) with basidiocarp formation (*Figure 2c*) under either single or mixed planting after 6 months of inoculation. In contrast to infection on galangal, root and rhizome rot of infected Java turmeric and ginger did not cause plant mortality even though the basidiocarp was also formed on the infected ginger rhizome at 9 mpi.

Artificial inoculation of *G. boninense* on rhizomatous plants, *viz*. Java turmeric, galangal, and ginger caused infection and rotting in the root and rhizome. Mycelium of *G. boninense* was consistently reisolated from the diseased root and rhizome tissue. This is the first study reporting that *G. boninense* is also pathogenic to rhizomatous plants. It is reported that *Ganoderma* spp. have a wide range of host plants, and all of them are woody plants (Loyd *et al.*, 2018b). Galangal was susceptible to *G. boninense* infection because fungal inoculation resulted in severe disease, plant death, and the formation of basidiocarps on diseased plants. Java turmeric and ginger were more resistant to pathogen infection, as root and rhizome rot developed slowly and did not cause plant mortality. *Ganoderma* spp. are known

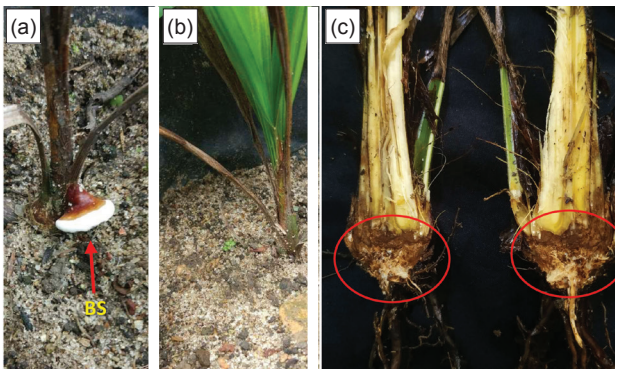


Figure 1. Symptoms of basal stem rot on inoculated oil palm seedlings under single planting at 6 months post-inoculation with Ganoderma boninense*-colonised rubber wood block showing dead palm with the formation of basidiocarp (BS) of* G. boninense *(a) drying of lower leaves without formation of basidiocarp (b) and complete basal stem (bole) and root rotting (red circle) (c).*

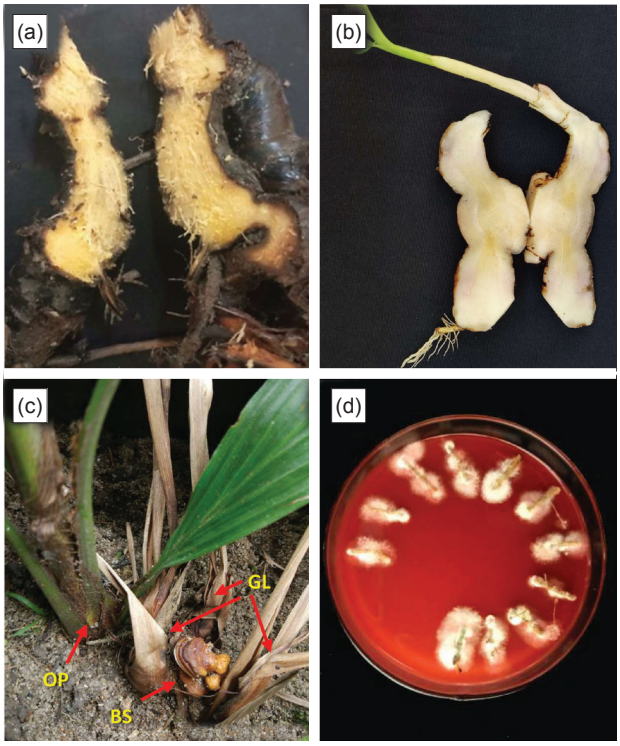


Figure 2. Symptoms of Ganoderma boninense *inoculation on mixed planting of oil palm and galangal at six months post-inoculation (mpi). (a) Complete rotting of infected roots and rhizomes relative to (b) the healthy uninoculated galangal plant. (c) Basidiocarp (BS) emerging from dead, diseased galangal plants (GL) with adjacent root-infected oil palm (OP) (the palm showed leaf symptoms at 9 mpi) and (d) mycelium of* G. boninense *growing out of infected tissues of galangal root and rhizome on GSM.*

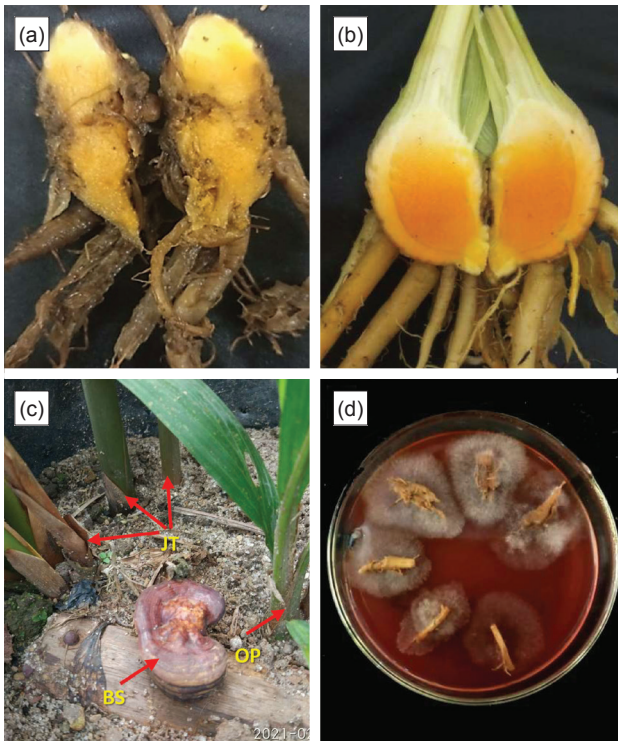


Figure 3. Symptoms of Ganoderma boninense *inoculation on mixed planting of oil palm and Java turmeric at six months post-inoculation (mpi). (a) Complete rotting of infected root dan rhizome relative to (b) the healthy uninoculated turmeric plant. (c) Basidiocarp (BS) emerging from rubber wood block as a source of inoculum with adjacent root infected oil palm (OP) and Java turmeric (JT) and (d) mycelium of* G. boninense *growing out infected tissues of Java turmeric root and rhizome on GSM.*

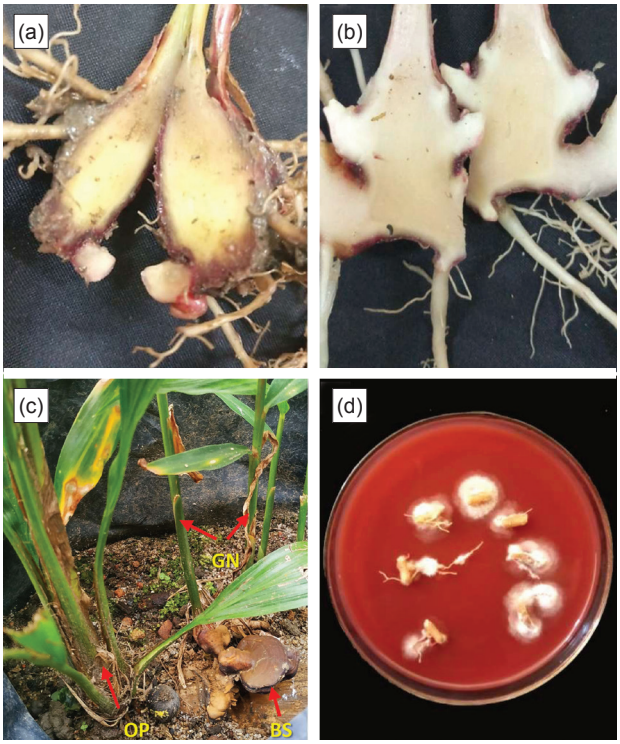


Figure 4. Symptoms of Ganoderma boninense *inoculation on mixed planting of oil palm and ginger at six months post-inoculation (mpi). (a) Partial rotting of infected root dan rhizome relative to (b) the healthy uninoculated ginger plant. (c) Basidiocarp (BS) emerging from rubber wood block as a source of inoculum with adjacent root infected oil palm (OP) and ginger (GN) and (d) mycelium of* G. boninense *growing out of infected tissues of ginger root and rhizome on GSM.*

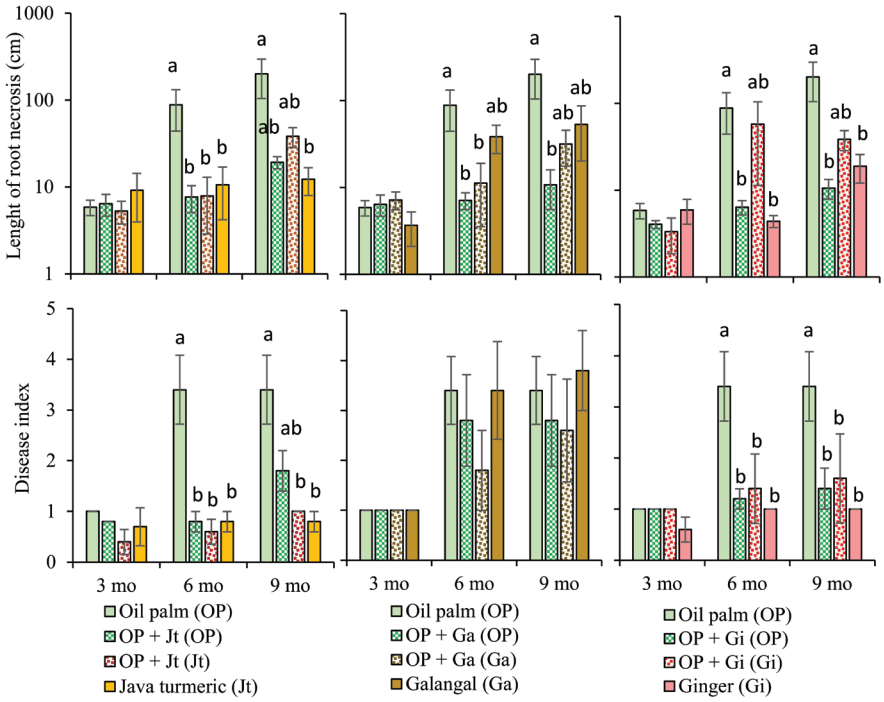


Figure 5. Effects of single or mixed planting of oil palm with rhizomatous plants (Java turmeric, galangal, and ginger) on Ganoderma boninense *infection on single host or dual host plants. Graphic bars with a pattern fill are for plants with mixed planting, and the graphic bar describes the mean for the plant name within the bracket. Error bars denote standard error of means (SEM). For each plant species and month, values followed by different letters are significantly different (HSD test).*

to secrete cell wall-degrading enzymes, which are considered the main infection mode used by wood decay fungi to infect a wide variety of woody plants (Dhillon *et al.*, 2021; Ramzi *et al.*, 2019; Rees *et al.*, 2009). Infection of rhizomatous plants, as described in this study, confirmed the cosmopolitan nature of the pathogen, which can utilise a wide variety of lignins from herbaceous to woody plants.

Dual host plant inoculation by a single mycelium inoculum under mixed planting caused *G. boninense* infection at 1 mpi on all mixed plants. The disease developed in a similar manner until 3 mpi in all planting systems. There was no significant ($p \geq 0.05$) effect of single versus mixed planting on root necrosis or the disease index on either mixed plants at the initial infection stage at 3 mpi. Dual host inoculation started to significantly ($p<0.05$) affect root necrosis at 6 mpi and continued similarly at 9 mpi. Root necrosis of oil palm in dual host inoculation was significantly ($p<0.05$) lower, ranging from 6.4-19.3 cm in length compared to that of single inoculation (88.1-200.8 cm). In contrast to oil palm infection, there was no difference ($p \geq 0.05$) in the length of root necrosis between single and dual inoculation of rhizomatous plants. A reduction of oil palm infection for dual inoculation treatment was significantly ($p<0.05$) described for disease index for mixed planting with Java turmeric and ginger but did not occur ($p \geq 0.05$) for galangal. Under mixed planting for nine months with Java turmeric and ginger, the disease index of oil palm was reduced by 47%-59% compared to the single planting. Infection suppression through mixed planting with Java turmeric and ginger constantly occurred at 6 and 9 mpi (*Figure 5*).

Inoculating a single inoculum of *G. boninense* with two different plant species (dual host inoculation) in mixed planting of oil palm and rhizomatous plants resulted in multiple host infections on all mixed plants. The present study described the evidence of dual or multiple host species infections by a single individual fungal mycelium network under artificial inoculation. Since understorey growth by herbaceous vegetation is common in oil palm fields, multiple host infections by *G. boninense* can also occur in nature. Multiple host species infections have been reported in *Rigidoporus microporus*, in which a single individual mycelium, as revealed by somatic compatibility, infected four woody and two herbaceous plant species, galangal and banana (Suwandi, 2007). In this study, the responses of rhizomatous plants were parallel in severity either in dual hosts (under mixed planting) or in single hosts (under single planting). Galangal was susceptible, whereas Java turmeric and ginger were resistant in both inoculation methods. Conversely, oil palm responded to different severities under single inoculation compared to dual inoculation. A marked reduction in disease index was noticed when mixed planting with a resistant

host, whereas the disease was less affected when inoculated with mixed planting with a susceptible host. However, host resistance was unlikely to be the only contributing factor to the reduced disease of oil palm under mixed planting. In our other experiment, there was no disease suppression of *Ganoderma*-inoculated oil palm in a mixed planting with a resistant rhizomatous plant, arrowroot (*Maranta arundinacea*) (Rahmadhani *et al.,* 2020).

The disease was significantly reduced on oil palm as the primary host, suggesting infection interference by Java turmeric and ginger against *Ganoderma* in a mixed planting. Suppression of fungal growth and disease under mixed planting with rhizomatous plants has been reported against *R. microporus*, a white root rot pathogen of rubber trees, but with different magnitudes of activity. In the present study, planting with ginger resulted in disease suppression on oil palm, whereas ginger did not show a suppressive effect against white root rot caused by *R. microporus* on rubber trees (Silva *et al.,* 2014, Situmorang *et al.,* 2007). In this study, Galangal was susceptible and could not protect oil palm from *Ganoderma* infection. Still, the plant had potent allelopathic inhibition of *R. microporus* either *in vitro* or in soil and even markedly suppressed white root rot in field trials (Silva *et al.,* 2014, Situmorang *et al.,* 2007). In contrast, Java turmeric established a similar suppression activity against either *G. boninense* or *R. microporus.* Planting with Java turmeric decreased white root rot and rubber tree death by 38% and 44%, respectively (Situmorang *et al.,* 2007), and reduced fungal rhizomorph growth by 56% (Yulianti *et al.,* 2017). Rhizomatous plants likely have different magnitude activity in infection interference against root rot pathogens, *Ganoderma* and *Rigidoporus.* Under mixed planting, Java turmeric could interfere with infection of both *Ganoderma* and *Rigidoporus*, whereas ginger showed a more specific interference infection of *Ganoderma* on oil palm as the main host. Galangal did not interfere with *Ganoderma* infection but showed an interference against infection of *Rigidoporus*. Further field studies are needed to assess the host specificity/preference of the rhizomatous plants.

Effect on Pathogen Development and Survival

The development of *G. boninense,* as manifested by basidiocarp formation, was favoured following attachment and burial in the root zone of rhizomatous plants (*Figures 2c*, *3c* and *4c*). Basidiocarp started to produce on RWB after 3 mpi in a single inoculation of rhizomatous plants compared to that produced after 6 mpi of oil palm inoculation. Basidiocarps were more produced on RWB in all planting types (3-9 basidiocarps on RWBs relative to 0-1 basidiocarps on host plants), except for single oil palm planting (4 basidiocarps on RWBs close to 3 basidiocarps on host plant) (*Table 1*). The average fresh weight of basidiocarps developed on all substrates or hosts was much higher ($p<0.05$) on Java turmeric single planting and mixed planting of oil palm and ginger plants (oil palm + ginger) than on those inoculated on single oil palm planting (*Table 1*).

The colonisation of *G. boninense* mycelia on RWB used to artificially inoculate tested plants resulted in dry weight loss at 9 mpi. The present observation confirmed the typical characteristics of *Ganoderma* fungus as a decaying fungus. Single inoculation did not affect RWB decay, as there was no difference ($p\geq0.05$) in the RWB dry weight losses between single plantings of different plants. A reduction in RWB decay was observed when RWB was dual inoculated on oil palm and Java turmeric with 55.7% RWB weight loss. In contrast, dual inoculation on oil palm and galangal significantly ($p<0.05$) increased RWB decay to be 82.4% compared to single inoculation on the palm with 71.8% RWB decay (*Figure 6*).

Mycelia of *G. boninense* colonising the most fragments (>82%) of RWB remained viable after being buried for nine months. Dual host inoculation on oil palm and rhizomatous plants had less effect on the survival of *G. boninense* mycelia colonising RWB. A slightly reduced ($p<0.05$) viability by 14.6% was only observed with dual inoculation of oil palm and ginger (*Figure 6*).

Mixed planting for nine months of oil palm and rhizomatous plants had less effect on the decaying of RWB colonised with *Ganoderma* after nine months. A slight increase in RWB decay was observed in the interaction of two susceptible hosts, galangal and oil palm. Wood decaying fungi will utilise any wood's lignin and polysaccharide components (Loyd *et al.*, 2018a; Naidu *et al.*, 2017; Zabel and Morrell, 2020) in the present case, RWB as nutrient sources. Once the RWB is completely decayed, the fungi will obtain nutrients from the host oil palm/rhizomatous plant as the nutrient-depleted from the RWB. Therefore, infection will occur as a result of the decaying process as manifested by the bole infection and foliar symptoms (Naidu *et al.*, 2017; Rees *et al.*, 2009). The severe infection occurred due to inoculum intensity or other environmental factors conducive to the fungi development (Breton *et al.*, 2006; Rees *et al.*, 2007). A similar higher RWB decay was also noted on other mixed plantings of oil palm with susceptible hosts, taro plants (Alesia *et al.,* 2021) and winged yam (*Dioscorea alata*) (unpublished result). However, planting rhizomatous plants for a longer period (two years) increased the decay of *Rigidoporus*-colonised rubber stumps by 46%-85% (Situmorang *et al.,* 2007).

A minor effect of mixed planting was also shown on the survival of *Ganoderma* mycelia colonising RWB in the 9-mpi study. A slight reduction in mycelial viability was noticed on mixed plantings of oil palm and ginger. Reduced *Ganoderma*

TABLE 1. FORMATION OF *G. boninense* BASIDIOCARPS AFTER INOCULATION ON SINGLE OR TWO MIXED PLANTS FOR NINE MONTHS

Planting type (n=10)	Fresh weight (g) and number (value within brackets) of basidiocarp emerging from			
	Rubber wood block	Oil palm	Rhizomatous plants	All substrates
Oil palm	6.62 (4)	3.63 (3)	NA	5.34 (7)
Oil palm + Java turmeric	7.08 (3)	0.30 (1)	0	5.39 (4)
Java turmeric	19.01 (9)*	NA	0	19.01 (9)*
Oil palm + Galangal	5.51 (5)	0	2.51 (1)	5.01 (6)
Galangal	5.14 (7)	NA	0	5.14 (7)
Oil palm + Ginger	11.40 (9)	0	34.50 (1)	13.71 (10)*
Ginger	8.33 (9)	NA	4.71 (1)	7.97 (10)

Note: NA - not available, * - denotes a significant difference (Dunnett test) from the respective mean values of oil palm single planting (oil palm).

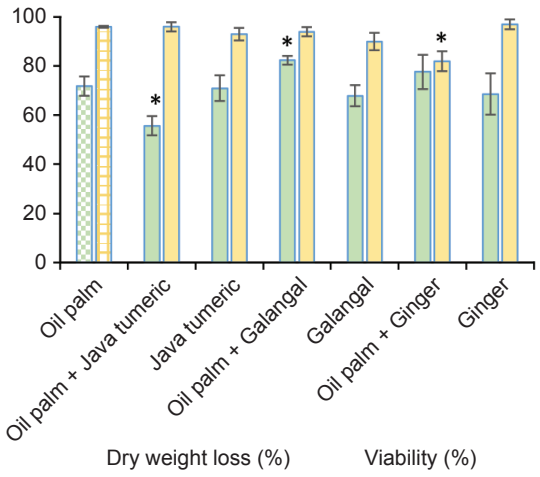


Figure 6. Effects of single or mixed oil palm planting with rhizomatous plants (Java turmeric, galangal, and ginger) on the decay of G. boninense*-colonised rubber wood block and pathogen viability after burial for nine months. For each dry weight loss and viability, * denotes a significant difference (Dunnett test) from the respective mean values of oil palm single planting.*

survival and disease severity under mixed cropping with ginger were possibly associated with allelochemical substances secreted in the rhizome. Ginger has been widely reported to have anti-fungal allelochemicals against numerous fungi. For example, ginger essential oil and gingerol showed anti-fungal activity against *Pestalotiopsis microspora* and suppressed fruit rot caused by the fungus on Chinese olive via a membrane-targeted mechanism with alteration of membrane permeability (Chen *et al.*, 2018). The anti-fungal activity also occurred on Java turmeric essential oil, xanthorrhizol (Akter *et al.*, 2018; Rukayadi *et al.*, 2006). Further study is needed to elaborate on the role of the anti-fungal allelochemical on disease suppression in a mixed planting with these plants. Although both ginger and Java turmeric potentially have allopathic activity against *G. boninense*, both essential oil-producing plants could trigger the basidiocarp formation of *G. boninense*. The induction of basidiocarp formation by the rhizomatous plant can be used further as an indicator plant for monitoring the colonisation of *G. boninense* on wood or palm debris in the field.

Effects on Oil Palm Growth

Mixed planting in a small volume of soil (5 L) between oil palm seedlings and rhizomatous plants for eight months (7 mpi) had less effect on the growth of oil palm as measured by leaf area and plant height. On non-inoculated control plants (-Gb, roots were tied with RWB without *G. boninense*) up to 7 mpi, there were no significant differences recorded in leaf area (*Figure 7a*) or plant height (*Figure 7b*) of oil palm between single and mixed planting. Significant growth inhibition on oil palm in leaf area and plant height was observed at 8 and 9 mpi under mixed planting with Java turmeric and galangal. Among the three rhizomatous plants, ginger showed less negative interference in the growth of oil palm seedlings. Differences between the growth of oil palm under mixed planting with ginger compared with single planting were observed only in the leaf area at 9 mpi. There were no significant differences between the leaf area and plant height of inoculated oil palm under single and mixed planting. The growth of inoculated single planting oil palm was suppressed, whereas oil-palm growth under inoculated mixed planting was less affected (*Figure 7*).

Rhizomatous plants habitually have not exhibited allelopathic inhibition on oil palm growth, as there was no significant difference between leaf area and height for eight months of planting of non-inoculated oil palm between single and mixed planting. Growth inhibition was observed after nine months of planting (8 mpi), which was likely due to limitations of growing space. It has been widely reported that intercropping with rhizomatous plants in an appropriate population is harmless to the growth and yield of the main crop (Chapagain *et al.*, 2018; Kathwal *et al.*, 2019).

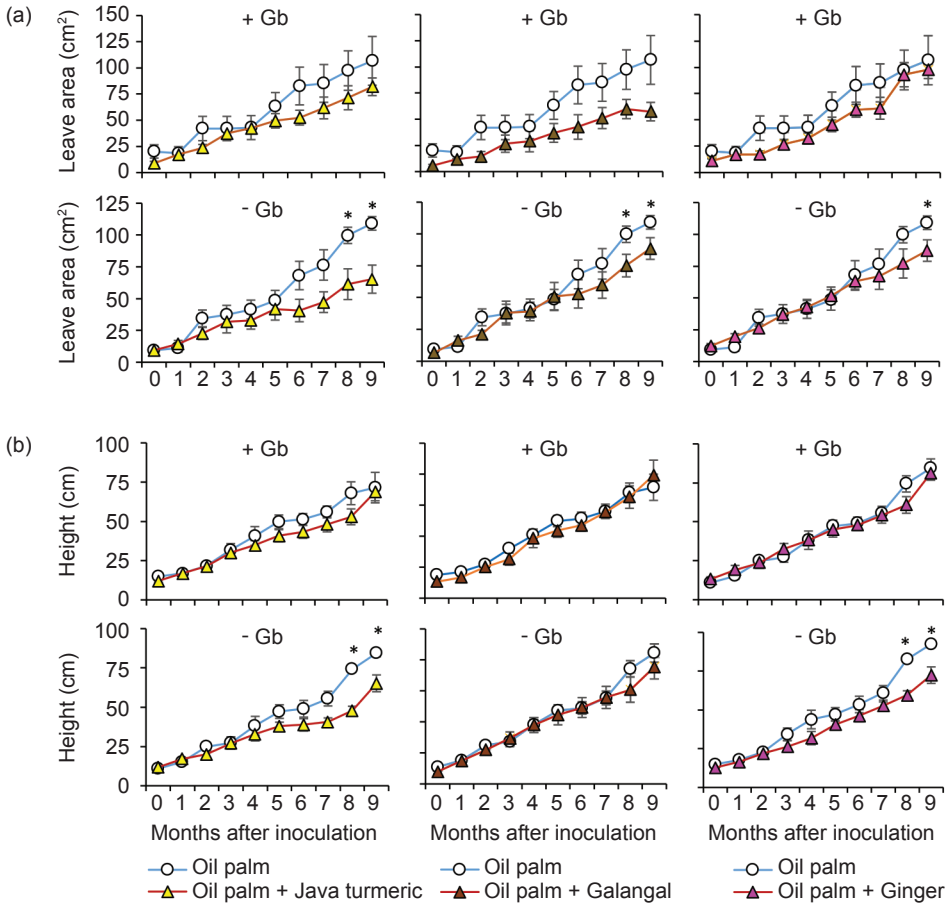


Figure 7. Effects of single or mixed planting with rhizomatous plants (Java turmeric, galangal, and ginger) on (a) leaf area and (b) plant height of Ganoderma boninense*-inoculated oil palm (+ Gb) and non-inoculated oil palm (- Gb). For each plant species and month, * denotes a significant difference (t-test) between the mean values of oil palm in single planting compared to mixed planting.*

The growth of inoculated single planting oil palm was suppressed eight months after inoculation. This growth retardation was not observed in mixed planting, suggesting the growth recovery of infected seedlings. Reduction in disease severity under mixed planting contributed to the growth recovery of infected seedlings. The indirect mechanism through beneficial soil microbial community can also enhance growth under mixed planting and needs further exploration. In the pathosystem of apple replant disease caused by numerous soil-borne fungi such as *Cylindrocarpon*, *Rhizoctonia*, *Phytophthora*, and *Pythium*, enhanced growth of apple seedlings under mixed cropping with *Allium fistulosum*, or *Brassica juncea* had been mediated through modifying the resident fungal community (Zhao *et al.*, 2022). Zeng *et al.* (2020) demonstrated that intercropping turmeric and ginger with patchouli could improve the contents of the active ingredient in the main crop (patchouli) by enhancing the beneficial soil microbial community and modifying soil enzyme activity, soil pH, and soil exchangeable Ca. The results from our study highlight the beneficial use of rhizomatous plants in the management of *Ganoderma* basal stem rot. The rhizomatous plant is potentially applied as an understorey intercrop for young replanted plantations or planted locally in the area of the excavated or chipped diseased palms, and further field study is needed to assess the long-term control efficacy.

CONCLUSION

Ganoderma inoculation on mixed planting of oil palm seedling with rhizomatous plants, *i.e.*, Java turmeric (*C. xanthorrhiza*), galangal (*A. galanga*), or ginger (*Z. officinale*) caused an infection on both host species (dual-host infection). The disease was significantly reduced on oil palm as the main host, suggesting infection interference by Java turmeric and ginger in a mixed planting. The rhizomatous plants habitually did not exhibit allelopathic inhibition of oil palm growth. Growth of *Ganoderma*-infected seedlings was recovered under mixed planting. This study highlights a novel insight that dual-host species infection in a mixed planting with rhizomatous plants can interfere with and reduce *Ganoderma* disease on oil palm as the main host.

ACKNOWLEDGEMENT

This work was supported by a Basic Research Grant (150/SP2H/LT/DRPM/2021) from Directorate for Research and Community Service, Ministry of Research and Technology/National Research and Innovation Agency, the Republic of Indonesia.

REFERENCES

Akter, J; Hossain, Md A; Sano, A; Takara, K; Islam, Md Z and Hou, D X (2018). Antifungal activity of various species and strains of turmeric (*Curcuma* spp.) against *Fusarium solani* sensu Lato. *Pharm. Chem. J., 52*: 320-325. DOI: 10.1007/s11094-018-1815-4.

Alesia, M; Suwandi, S and Suparman, S (2021). Decaying activity of *Ganoderma boninense* wood inoculum on mixed planting of oil palm seedling and taro plants. *Sainmatika, 18*: 108-115. DOI: 10.31851/sainmatika.v17i3.5737.

Ariffin, D and Idris, A S (1991). A selective medium for isolation of *Ganoderma* from diseased tissues. *Proc. of the 1991 International Palm Oil Conference, Progress, Prospects and Challenges towards the 21st Century*. MPOB, Bangi. p. 517-519.

Ariffin, D; Idris, A S and Singh, G (2000). Status of *Ganoderma* in oil palm. *Ganoderma Diseases of Perennial Crops* (Flood, J; Bridge, P D and Holderness, M eds.). CAB International, Wallingford. p. 49-68.

Ashraf, M; Zulkifli, R; Sanusi, R; Tohiran, K A; Terhem, R; Moslim, R; Norhisham, A R; Ashton-Butt, A and Azhar, B (2018). Alley-cropping system can boost arthropod biodiversity and ecosystem functions in oil palm plantations. *Agric. Ecosyst. Environ., 260*: 19-26. DOI: 10.1016/j.agee.2018.03.017.

Ashton-Butt, A; Aryawan, A A K; Hood, A S C; Naim, M; Purnomo, D; Suhardi; Wahyuningsih, R; Willcock, S; Poppy, G M; Caliman, J P; Turner, E C; Foster, W A; Peh, K S H and Snaddon, J L (2018). Understory vegetation in oil palm plantations benefits soil biodiversity and decomposition rates. *Front. For. Glob Change, 1*: 10. DOI: 10.3389/ffgc.2018.00010.

Breton, F; Hasan, Y; Hariadi; Lubis, Z and Franqueville, H D (2006). Characterization of parameters for the development of an early screening test for basal stem rot tolerance in oil palm progenies. *J. Oil Palm Res. Special Issue, 2006*: 24-36.

Boudreau, M A (2013). Diseases in intercropping systems. *Annu. Rev. Phytopathol., 51*: 499-519. DOI: 10.1146/annurev-phyto-082712-102246.

Chang, T T (2003). Effect of soil moisture content on the survival of *Ganoderma* species and other wood-inhabiting fungi. *Plant Dis., 87*: 1201-1204. DOI: 10.1094/PDIS.2003.87.10.1201.

Chapagain, T; Pudasaini, R; Ghimire, B; Gurung, K; Choi, K; Rai, L; Magar, S; Bishnu, B K and Raizada, M N (2018). Intercropping of maize, millet, mustard, wheat and ginger increased land productivity and potential economic returns for smallholder terrace farmers in Nepal. *Field Crop Res., 227*: 91-101. DOI: 10.1016/j.fcr.2018.07.016.

Chen, T; Lu, J; Kang, B; Lin, M; Ding, L; Zhang, L; Chen, G; Chen, S and Lin, H (2018). Antifungal activity and action mechanism of ginger oleoresin against *Pestalotiopsis microspora* isolated from Chinese olive fruits. *Front. Microbiol., 9*: 2583. DOI: 10.3389/fmicb.2018.02583.

Chung, A Y C; Eggleton, P; Speight, M R; Hammond, P M and Chey, V K (2000). The diversity of beetle assemblages in different habitat types in Sabah, Malaysia. *Bull. Entomol. Res., 90*: 475-496. DOI: 10.1017/S0007485300000602.

Dhillon, B; Hamelin, R C and Rollins, J A (2021). Transcriptional profile of oil palm pathogen, *Ganoderma boninense*, reveals activation of lignin degradation machinery and possible evasion of host immune response. *BMC Genom., 22*: 326. DOI: 10.1186/s12864-021-07644-9.

Fernanda, R; Siddiqui, Y; Ganapathy, D; Ahmad, K and Surendran, A (2021). Suppression of *Ganoderma boninense* using benzoic acid: Impact on cellular ultrastructure and anatomical changes in oil palm wood. *Forests, 12*: 1231. DOI: 10.3390/f12091231.

Glen, M; Bougher, N L; Francis, A A; Niqq, S Q; Lee, S S; Irianto, R; Barry, K M; Beadle, C L and Mohammed, C L (2009). *Ganoderma* and *Amauroderma* species associated with root-rot disease of *Acacia mangium* plantation trees in Indonesia and Malaysia. *Australas. Plant Pathol., 38*: 345-356. DOI: 10.1071/AP09008.

Gromikora, N; Yahya, S and Suwarto, S (2014). Growth and production modeling of oil palm at different levels of frond pruning. *J. Agron. Indones., 42*: 228-235.

Ibrahim, M S; Seman, I A; Rusli, M H; Izzuddin, M A; Kamarudin, N; Hasyim, K and Manaf, Z A

(2020). Surveillance of *Ganoderma* disease in oil palm planted by participants of the smallholders replanting incentive scheme in Malaysia. *J. Oil Palm Res., 32*: 237-244. DOI: 10.21894/jopr.2020.0024.

Kamu, A; Phin, C K; Seman, I A; Gabda, D and Mun, H C (2021). Estimating the yield loss of oil palm due to *Ganoderma* basal stem rot disease by using bayesian model averaging. *J. Oil Palm Res., 33*: 46-55. DOI: 10.21894/jopr.2020.0061.

Kandan, A; Bhaskaran, R and Samiyappan, R (2010). *Ganoderma* - a basal stem rot disease of coconut palm in south Asia and Asia pacific regions. *Arch. Phytopathol. Plant Prot., 43*: 1445-1449. DOI: 10.1080/03235400802536527.

Kathwal, R; Mohammed, S and Kumar, A (2019). Studies on intercropping of turmeric and ginger in mango orchard. *Ann. Biol., 35*: 225-228.

Khasanah, N; van Noordwijk, M; Slingerland, M; Sofiyudin, M; Stomph, D; Migeon, A F and Hairiah, K (2020). Oil palm agroforestry can achieve economic and environmental gains as indicated by multifunctional land equivalent ratios. *Front. Sustain. Food Syst., 3*: 122. DOI: 10.3389/fsufs.2019.00122.

Loyd, A L; Held, B W; Linder, E R; Smith, J A and Blanchette, R A (2018a). Elucidating wood decomposition by four species of *Ganoderma* from the United States. *Fungal Biol., 122*: 254-263. DOI: 10.1016/j.funbio.2018.01.006.

Loyd, A L; Linder, E R; Anger, N A; Richter, B S; Blanchette, R A and Smith, J A (2018b). Pathogenicity of *Ganoderma* species on landscape trees in the Southeastern United States. *Plant Dis., 102*: 1944-1949. DOI: 10.1094/PDIS-02-18-0338-RE.

Luke, S H; Purnomo, D; Advento, A D; Aryawan, A A K; Naim, M; Pikstein, R N; Ps, S; Rambe, T D S; Soeprapto; Caliman, J P; Snaddon, J L; Foster, W A and Turner, E C (2019). Effects of understory vegetation management on plant communities in oil palm plantations in Sumatra, Indonesia. *Front. For. Glob. Change, 2*: 33. DOI: 10.3389/ffgc.2019.00033.

Midot, F; Lau, S; Wong, W C; Tung, H J; Yap, M L; Lo, M L; Jee, M S; Dom, S P and Melling, L (2019). Genetic diversity and demographic history of *Ganoderma boninense* in oil palm plantations of Sarawak, Malaysia inferred from ITS regions. *Microorganisms, 7*: 464. DOI: 10.3390/microorganisms7100464.

Naidu, Y; Siddiqui, Y; Rafii, M Y; Saud, H M and Idris, A S (2017). Investigating the effect of white-rot hymenomycetes biodegradation on basal stem rot infected oil palm wood blocks: Biochemical and anatomical characterization. *Ind. Crops Prod., 108*: 872-882. DOI: 10.1016/j.indcrop.2017.08.064.

Nájera, A and Simonetti, J A (2010). Enhancing avifauna in commercial plantations: Research note. *Conserv. Biol., 24*: 319-324. DOI: 10.1111/j.1523-1739.2009.01350.x.

Page, D E; Glen, M; Puspitasari, D; Prihatini, I; Gafur, A and Mohammed, C L (2020). Acacia plantations in Indonesia facilitate clonal spread of the root pathogen *Ganoderma philippii*. *Plant Pathol., 69*: 685-697. DOI: 10.1111/ppa.13153.

Pilotti, C A (2005). Stem rots of oil palm caused by *Ganoderma boninense*: Pathogen biology and epidemiology. *Mycopathologia, 159*: 29-137. DOI: 10.1007/s11046-004-4435-3.

Priwiratama, H; Prasetyo, A E and Susanto, A (2020). Incidence of basal stem rot disease of oil palm in converted planting areas and control treatments. *IOP Conf. Ser.: Earth Environ. Sci., 468*: 012036. DOI: 10.1088/1755-1315/468/1/012036.

Pujianto; Achmad, W S; Dafian, P; Syaiful; Suhardi; Putri, A W and Caliman, J P (2016). Impact of mineral nutrition management on *Ganoderma* incidence in oil palm planted on peat soil. *Proc. of the 15th International Peat Congress*. IPS, Kuching. p. 75-78.

Purba, A; Hayati, R; Putri, L A P; Chalil, D; Afandi, D; Syahputra, I and Basyuni, M (2020). Genetic diversity and structure of *Ganoderma boninense* isolates from oil palm and other plantation crops. *Biodivers. J., 21*: 451-456. DOI: 10.13057/biodiv/d210204.

Rahmadhani, T P; Suwandi, S and Suparman, S (2020). Growth responses of oil palm seedling inoculated with *Ganoderma boninense* under competition with edible herbaceous plants. *J. Sci. Agric., 4*: 45-49. DOI: 10.25081/jsa.2020.v4.6231.

Ramzi, A B; Che Me, M L; Ruslan, U S; Baharum, S N and Nor Muhammad, N A (2019). Insight into plant cell wall degradation and pathogenesis of *Ganoderma boninense* via comparative genome analysis. *PeerJ, 7*: e8065. DOI: 10.7717/peerj.8065.

Rees, R W; Flood, J; Hasan, Y and Cooper, R M (2007). Effects of inoculum potential, shading and soil temperature on root infection of oil palm seedlings by the basal stem rot pathogen *Ganoderma boninense*. *Plant Pathol., 56*: 862-870. DOI: 10.1111/j.1365-3059.2007.01621.x.

Rees, R W; Flood, J; Hasan, Y; Potter, U and Cooper, R M (2009). Basal stem rot of oil palm (*Elaeis*

guineensis); mode of root infection and lower stem invasion by *Ganoderma boninense*. *Plant Pathol., 58*: 982-989. DOI: 10.1111/j.1365-3059.2009.02100.x.

Rembold, K; Mangopo, H; Tjitrosoedirdjo, S S and Kreft, H (2017). Plant diversity, forest dependency, and alien plant invasions in tropical agricultural landscapes in Sumatra. *Biol. Conserv., 213*: 234-242. DOI: 10.1016/j.biocon.2017.07.020.

Riyanto; Sartini and Nasution, J (2020). Oil palm yield in related to plant density and *Ganoderma boninense* infection in Simalungun and Asahan plantations, North Sumatera, Indonesia. *EJBMSR, 8*: 1-7.

Rukayadi, Y; Yong, D and Hwang, J K (2006). *In vitro* anticandidal activity of xanthorrhizol isolated from *Curcuma xanthorrhiza* Roxb. *J. Antimicrob. Chemother., 57*: 1231-1234. DOI: 10.1093/jac/dkl132.

Siddiqui, Y; Surendran, A; Paterson, R; Ali, A and Ahmad, K (2021). Current strategies and perspectives in detection and control of basal stem rot of oil palm. *Saudi J. Biol. Sci., 28*: 2840-2849. DOI: 10.1016/j.sjbs.2021.02.016.

Silva, M K R; Jayasinghe, C K and Tennakoon, B I (2014). Evaluation of the antagonistic effect of different plant species on white root disease causing fungus: *Rigidoporus microporus*. *J. Rubber Research Institute of Sri Lanka, 94*: 25-32. DOI: 10.4038/jrrisl.v94i0.1822.

Situmorang, A; Suryaningtyas, H and Febbianti, T R (2007). The control of white root disease using antagonistic plant on rubber plantation. *Proc. International Workshop on White Root Disease of Hevea Rubber*. IRRDB, Salatiga. p. 82-86.

Spear, D M; Foster, W A; Advento, A D; Naim, M; Caliman, J P; Luke, S H; Snaddon, J L; Ps, S and Turner, E C (2018). Simplifying understory complexity in oil palm plantations is associated with a reduction in the density of a cleptoparasitic spider, *Argyrodes miniaceus* (Araneae: Theridiidae), in host (Araneae: Nephilinae) webs. *Ecol. Evol., 8*: 1595-1603. DOI: 10.1002/ece3.3772.

Suwandi, S (2007). Mode of dispersal and variation in population of white root fungus *Rigidoporus microporus* as revealed by mycelial incompatibility. *Proc. International Workshop on White Root Disease of Hevea Rubber*. IRRDB, Salatiga. p. 68-75.

Teuscher, M; Gérard, A; Brose, U; Buchori, D; Clough, Y; Ehbrecht, M; Hölscher, D; Irawan, B; Sundawati, L; Wollni, M and Kreft, H (2016). Experimental biodiversity enrichment in oil-palm-dominated landscapes in Indonesia. *Front. Plant Sci., 7*: 1538. DOI: 10.3389/fpls.2016.01538.

Tohiran, K A; Nobilly, F; Zulkifli, R; Maxwell, T; Moslim, R and Azhar, B (2017). Targeted cattle grazing as an alternative to herbicides for controlling weeds in bird-friendly oil palm plantations. *Agron. Sustain. Dev., 37*: 62. DOI: 10.1007/s13593-017-0471-5.

Vinjusha, N and Kumar, T K A (2022). Revision of *Ganoderma* species associated with stem rot of coconut palm. *Mycologia, Jan-Feb, 114(1)*: 157-174. DOI: 10.1080/00275514.2021.1974724.

Yulianti, S; Suwandi, S and Nurhayati, N (2017). Suppression ability of herbaceous plants on inoculum potential of *Rigidoporus microporus*. *J. Fitopatol. Indones., 13*: 81-88. DOI: 10.14692/jfi.13.3.81.

Yusron, M and Januwati, M (2003). Intercropping young oil palm with rhizomatous plants. *Proc. Technical Integration of Oil Palm and Cattle Production*. Indonesian Medicinal and Aromatic Crops Research Institute, Bogor. p. 199-210.

Zabel, R A and Morrell, J J (2020). *Wood Microbiology (Second Edition) - Decay and Its Prevention*. Academic Press, London. 576 pp.

Zeng, J; Liu, J; Lu, C; Ou, X; Luo, K; Li, C; He, M; Zhang, H and Yan, H (2020). Intercropping with turmeric or ginger reduce the continuous cropping obstacles that affect *Pogostemon cablin* (patchouli). *Front. Microbiol., 11*: 579719. DOI: 10.3389/fmicb.2020.579719.

Zhao, L; Wang, G; Liu, X; Chen, X; Shen, X; Yin, C and Mao, Z (2022). Control of apple replant disease using mixed cropping with *Brassica juncea* or *Allium fistulosum*. *Agriculture, 12*: 68. DOI: 10.3390/agriculture12010068.

Zhou, L W; Cao, Y; Wu, S H; Vlasák, J; Li, D W; Li, M J and Dai, Y C (2015). Global diversity of the *Ganoderma lucidum* complex (Ganodermataceae, Polyporales) inferred from morphology and multilocus phylogeny. *Phytochem., 114*: 7-15. DOI: 10.1016/j.phytochem.2014.09.023.

Zhu, S and Morel, J B (2019). Molecular mechanisms underlying microbial disease control in intercropping. *Mol. Plant-Microbe Interact., 32*: 20-24. DOI: 10.1094/MPMI-03-18-0058-CR.

Journal of Oil Palm Research Vol. 35 (2) June 2023 p. 365-375
DOI: https://doi.org/10.21894/jopr.2022.0044

FIELD EFFICACY OF ANTICOAGULANT RODENTICIDES AGAINST RAT INFESTATION IN OIL PALM PLANTATION

ARIFF ATEED MOHD NOH[1]; MUHAMMAD SYAFIQ MOHD ZALUDIN[1]; WAN MOHD HAFEZUL WAN ABDUL GHANI[2]; ABU HASSAN AHMAD[1] and HASBER SALIM[1,3]*

ABSTRACT

Field efficacy of anticoagulant rodenticides against rat infestation in oil palm plantation was carried out in a comparative study between five rodenticide baits. They were first-generation anticoagulant rodenticide baits, coumatetralyl, chlorophacinone and warfarin, and second-generation anticoagulant rodenticide baits, flocoumafen and brodifacoum. A control plot was left untreated for comparison purposes. In general, all treatments were effective to reduce the fresh rat damage on oil palm fresh fruit bunch (FFB) below the threshold level (5.0%) except for warfarin bait treatment. In the final round of baiting (5th round), the flocoumafen bait recorded the lowest fresh rat damage on FFB at 1.54 ± 0.14%. Coumatetralyl, chlorophacinone and brodifacoum recorded 2.95 ± 0.73%, 2.42 ± 0.57% and 4.30 ± 0.53% of fresh rat damage on FFB at the end of the study. The least effective was warfarin treatment which recorded 5.40 ± 0.18% in the final round of baiting. Only flocoumafen, coumatetralyl and chlorophacinone baits recorded more than 70.00% of rat damage reduction throughout the study as compared to pre-treatment. The brodifacoum treatment recorded rat damage reduction up to 58.70% and warfarin treatment was in the range of 13.58%-33.62%. All the rodenticide treatments managed to reduce the relative abundance of the estimated rat population in the field at the end of the study, except in the control plot.

Keywords: first generation, rat control, rodent, second generation, wood rat.

Received: 17 November 2021**; Accepted:** 17 June 2022**; Published online:** 5 August 2022.

INTRODUCTION

Rats have been considered an agricultural problem in Malaysia for many years, particularly in relation to oil palm cultivations (Chung, 2012; Turner and Gillbanks, 2003; Wood, 2001). The three main rodent pests in Peninsular Malaysia, namely, Malayan wood rat (*Rattus tiomanicus*), rice-field rat (*Rattus argentiventer*) and Malaysian house rat (*Rattus rattus diardii*) have been reported as important rodent pests in oil palm plantations (Hafidzi and Saayon, 2001). Rat activities in mature oil palm plantations can cause crop damage on palm fruit bunch ranging from 8%-20% (Abidin *et al*., 2021). Damage by rats on oil palm is inflicted throughout the growth of the palm regardless of age, leading to losses of seedlings through the attack in nurseries, damage to inflorescences and both ripe and unripe fruits, causing substantial oil yield losses up to 10% in oil palm plantations (Wood, 2001). Several control measures have been practised for controlling rats such as cultural, mechanical, biological and chemical control with varying degrees of effectiveness (Chung, 2012; Khoo *et al*., 1982).

Chemical control by using anticoagulant rodenticides (ARs) has become the main control

[1] Barn Owls and Rodent Research Group (BORG), School of Biological Sciences, Universiti Sains Malaysia, 11800 Minden, Penang, Malaysia.

[2] Plant Protection Department, Faculty of Agriculture, Universiti Putra Malaysia, 43400 Serdang, Selangor, Malaysia.

[3] Vector Control Research Unit (VCRU), School of Biological Sciences, Universiti Sains Malaysia, 11800 Minden, Penang, Malaysia.

* *Corresponding author e-mail: hasbersalim@usm.my*

measure of rat populations in oil palm plantations as it is effective to reduce pest numbers in such a short time and is also more practical to handle in the field (Chung, 2012; Wood and Chung, 2003). ARs can be grouped into two classes; first-generation anticoagulant rodenticides (FGAR) and second-generation anticoagulant rodenticides (SGAR), based on the number of doses to cause death to target animals (Valchev *et al.*, 2008). SGARs were developed and used following the increasingly widespread development of resistance amongst rodents to FGARs, in particular warfarin (Berny, 2011; Cowan *et al.*, 1995; Erickson and Urban, 2004).

Regardless of their classification, ARs interfere with vitamin K in the production of clotting factors in the liver, disrupt normal blood-clotting mechanisms and induce capillary damage (Rattner *et al.*, 2014; Valchev *et al.*, 2008). Death results from haemorrhage and exposed animals may exhibit increasing weakness prior to death. Rodents typically die five to 10 days after ingesting a lethal dose of ARs (Erickson and Urban, 2004). Both groups of ARs have different levels of toxicity against animals. SGARs are much more acutely toxic than FGARs; SGARs require only a single feeding to reach the lethal dosage to the target animals (Fisher, 2005; Pitt *et al.*, 2010). Meanwhile, FGARs need to be consumed multiple times by animals such as rats to reach the lethal dosage (Fisher, 2005). The most commonly used and registered FGARs in oil palm plantations in Malaysia are warfarin, chlorophacinone and coumatetralyl, while SGARs include brodifacoum and flocoumafen. Depending on the toxicity, the active ingredient for SGARs ranges from 0.005% to 0.050%, and from 0.025% to 0.050% for FGARs (DOA, 2021). Cereal-based baits are the most widely used formulation in oil palm plantations and the baits are available as wax block baits due to their durability in the tropical condition of Malaysian oil palm plantations (Chung, 2012).

Six-monthly baiting campaigns or two campaigns per year routine are commonly practised by oil palm plantations to deal with rat infestation. In each campaign, two to five rounds of baiting are carried out depending on the threshold level (below 5%) of fresh rat damage on oil palm fresh fruit bunch (FFB). FGAR baits are usually replaced at three to four days intervals while SGAR baits, which are more lethal, are replaced at seven to eight days intervals (Sime Darby Plantation, 2010). Nowadays, the application of AR bait is a routine activity in controlling rat populations in oil palm plantations (Chung, 2012; Turner and Gillbanks, 2003). However, the application and continued use of this chemical control for a long period have raised concerns about the development of resistance in rats in oil palm plantations. For commensal rat species such as Norway rat (*Rattus norvegicus*) and Roof rat (*Rattus rattus*) development of warfarin resistance has been well documented and reportedly caused ineffective management of the rat population in the field (Buckle and Smith, 2015). The only available report of the development of resistance in Malaysian oil palm was reported in the 1980s against FGAR, warfarin in three different localities (Klang, Teluk Intan, Renggam, Malaysia) and SGARs such as brodifacoum and flocoumafen, which are more toxic than FGARs, were used and reportedly effective against warfarin-resistant rats (Wood and Chung, 1990). Besides this relatively old report, the field efficacy and resistance status of ARs in oil palm plantations in controlling rat infestation are scarce and have not been well documented. Thus, the main objective of this study is the evaluation of the field efficacy of selected ARs against rat infestation in oil palm plantations through key parameters such as fresh fruit damages and relative abundance of rats to determine the efficacy of different treatments against the target pest.

MATERIALS AND METHODS

Study Sites and Experimental Design

The study was carried out in an oil palm plantation in Besout, Sungkai, Perak, Malaysia from 15 September 2017 until 14 June 2018. The plantation is located at 03.48˚N, 100.17˚E. The total area of the plantation is 1000.10 ha, and the age of the palm ranges from six to 12 years old after planting. A single campaign of rat baiting using FGARs either warfarin, chlorophacinone or coumatetralyl was annually carried out to control rat pest populations at the plantation. The usual baiting campaign was last carried out about one year before the start of this study.

A total of five AR baits were used in this study. The first three treatments were FGAR baits consisting of coumatetralyl, chlorophacinone and warfarin. Two types of SGAR baits, *i.e.*, brodifacoum and flocoumafen were also tested. Field efficacy of each treatment was conducted in 3 ha study areas and was replicated three times in a randomised complete block design (RCBD). A control plot that was not treated with any rodenticide was also included for comparison purposes. The total plot area of the study site for all the treatments in the plantation was 54 ha. The distance between each study plot was at least 2 km apart since the home range of the rodent pest is about 1 km (Buckle *et al.*, 1997; Oyedele *et al.*, 2015; Pryde *et al*, 2005). The sites were sufficiently far apart to prevent rats from migrating across different plots. The experimental layout description of all treatments is summarised in *Figure 1*.

The replacement round baiting technique, which is the standard baiting technique where

replacement of the baits takes place after every round of baiting according to the replacement interval, was adopted as the method of bait application. Replacement of the bait only took place when the bait was missing, spoilt (*e.g.*, fungus, disfigured, attacked by insects, *etc.*) or 50% of the baits were consumed, which was evaluated by the observer. The bait replacement was an important step to maintain the bait quality throughout the study. For FGAR treatments, the bait replacement interval was set at four days while SGAR treatments were at seven days. All the baiting programs were set up for five rounds of baiting. It took 20 days for FGAR and 35 days for SGAR treatments to complete five rounds of baiting. All the rodenticide baits were applied one bait per palm on the ground near the oil palm weeding circle, which is approximately 1 m away from the palm base, as typically practised by plantations. The details of treatments rounds and replacement rounds of rodenticide baits are summarised in *Table 1*.

Rat Damages on Fruit Bunch

Pre-treatment assessment on FFB was carried out in order to determine the rat damage incidence in each plot prior to the baiting program. Post-treatment assessment was carried out following the round and interval of each rodenticide application. The assessment was conducted prior to the routine of harvesting by the plantation operator. A total of 100 palms (10 x 10 rows of fixed palms) were systematically selected in the centre of each plot (a total of 300 palms were selected for each treatment). A fresh rat damage score was used to quantify and compare the severity of damage between plots (Buckle, 2015). The scoring assessment was conducted and calculated at the end of each replacement round, before baiting application of the consequent round commenced. Only fresh damage was included in the quantification while old damages were excluded from the assessment.

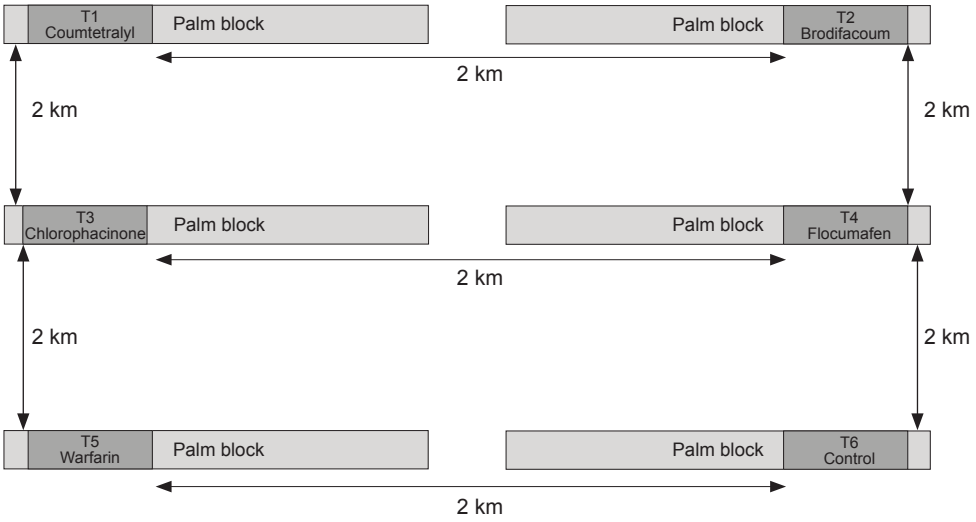


Figure 1. Experimental layout of first replicate for all treatments.

TABLE 1. DETAILS OF ROUND AND REPLACEMENT OF RODENTICIDE TREATMENTS

Treatment ID	Treatments	Bait weight (g)	*Average total bait used (g)	Total replacement round	Replacement interval (day)	Active ingredient (%)
T1	Coumatetralyl	5.0	6 897	5	4	0.0375
T2	Brodifacoum	10.0	14 623	5	7	0.0050
T3	Chlorophacinone	12.5	23 592	5	4	0.0050
T4	Flocoumafen	4.0	8 833	5	7	0.0050
T5	Warfarin	10.0	16 297	5	4	0.0500
T6	Control	-	-	-	-	-

Note: *Average total bait used from pre to final round of baiting per replicate.

Fresh damages were identified by the condition where the wound is moist and has a bright colour while the old damaged wound is dry and discoloured. The severity of the rat damages was determined according to the presence of rat damage on unripe and ripe oil palm fruits on the trees during the sampling. The final fresh damage score was calculated using Buckle (1994) in Equation (1) as follows:

$$\text{Fresh damage score} = \frac{(1xa) + (2xb) + (3xc)}{3\,N} \times 100\% \quad (1)$$

where a = No. of the bunch with light damage (1-3 damaged fruit/bunch)

b = No. of the bunch with medium damage (4-6 damage fruit/bunch)

c = No. of the bunch with heavy damage (>6 damaged fruit/bunch)

N = Total number of bunches assessed

To determine the impact of a particular treatment, the percentage reduction of fresh rat damage after each replacement baiting round was calculated as follows Equation (2):

$$\text{Reduction of fresh damage} = \frac{\text{Pre-treatment fresh damage - Current fresh damage}}{\text{Pre-treatment fresh damage}} \times 100\% \quad (2)$$

Estimated Rat Population (Relative abundance)

Rat populations were estimated in pre- and post-treatment to measure the impact of the treatments on rat populations in each plot. Rat populations were assessed using the relative abundance of the trapping success. A total of 100 standard commercial live traps measuring 28 cm (length) x 13 cm (width) x 13 cm (height) were used. The live traps were set up in each treatment plot at 50 points at 50 selected palms (5 x 10 palms) in the middle of the plots following a grid-based configuration where the distance between each trap point was the same as the distance between palm trees at approximately 9 m (9 x 9 m). Two traps were placed at each point with a loose ripe palm fruit used as bait. Both traps were placed on the weeding circle, and the distance between each trap was approximately 2 m. The trapping program was carried out for four consecutive nights. To maintain the quantity of the baits, the replacement of absent bait in any trap was conducted every day. Meanwhile, to maintain the quality of the bait throughout the four nights of trapping, the old bait in every trap was replaced with fresh bait during the second night of the trapping program. All traps were checked for captures daily from 8.00 am to 10.30 am until the last day of the trapping. Rats caught were recorded, marked, and subsequently released near the trapping point. Identification of caught rats was conducted based on physical features such as the size of the rat's body, size of the hindfoot, colour of fur and belly as stated by Francis (2008); Harrison (1974) and Payne *et al*. (1985). After trapping sessions were completed, the traps were removed from the trapping site. Trapping sessions were conducted twice during the study; once during pre-treatment and once post-treatment. Once trapping sessions were completed for the pre-treatment assessment, there was a lag period of seven days without the interference of any experiment on the trapping site to prevent the development of neophobic behaviour among the rats during the baiting program. The relative abundance or trapping success of rats (Puan *et al*., 2011) before and after the treatment was calculated using the following Equation (3):

$$\text{*Trap success (relative abundance)} = \frac{\text{Number of individual rats captured}}{(2 \times \text{Number of trap points}) \times \text{Number of trap nights}} \quad (3)$$

Statistical Analysis

Prior to analysis, data were tested for normality using the Shapiro-Wilk test. One-way ANOVA was performed to detect any statistical significance in fresh rat damage and the percentage of damage reduction between the treatments at each round of baiting. When there was a statistically significant difference, *post hoc* analysis, the Tukey's test was performed. Additionally, an independent sample t-test was used to analyse for a significant difference in relative abundance of rat population between treatment plots. All statistical analysis was conducted using the statistical package for social sciences (SPSS) for windows version 26.0 (IBM Corp., 2019).

RESULTS

Fresh Rat Damage on FFB

The results of average fresh rat damage per round of baiting on FFB at all treatments are shown in *Figure 2*. All treatments were effective and able to reduce fresh rat damage on oil palm FFB below the threshold level (5%) after three rounds of baiting except for warfarin bait (5.60 ± 0.29%) and control plot (7.42 ± 1.21%). At this stage, the result of all

treatments except warfarin bait and control had fallen below the threshold level in the range of 1% to 4%. Warfarin bait treatment score in fresh rat damages remained above the threshold level even after three rounds of baiting while the control plot scored the highest fresh rat damages at this stage compared to other treatments. According to one-way ANOVA analysis, at this stage, there was a significant difference ($F_{5, 12}$ = 6.91, P = 0.00) between treatments and the control plot. At the final round of baiting (5th round), flocoumafen bait recorded the lowest fresh rat damage compared to other treatments at 1.54 ± 0.14%. Apart from flocoumafen bait, chlorophacinone and coumatetralyl baits recorded close results at 2.42 ± 0.57% and 2.95 ± 0.73%, respectively. Meanwhile, brodifacoum bait recorded fresh rat damage at 4.30 ± 0.53% at the end of the study. There was a significant difference ($F_{5, 12}$= 11.29, P= 0.00) detected in all treatments as compared to warfarin and control. Warfarin bait treatment produced poor control towards fresh rat damage and failed to reduce the fresh rat damage on FFB below the threshold level (5.4 ± 0.18%) even after five rounds of a rodenticide application. Meanwhile, the control plot showed a fluctuating trend of fresh rat damages in the range of 5.05%-7.54% throughout the study. The highest fresh rat damage in the control plot was recorded in the last round of baiting at 7.54 ± 1.17%, which was higher than fresh rat damage recorded in pre-treatment (7.24 ± 1.05%) and this indicated the rat activities increased at the site.

Percentage of Rat Damage Reduction

The results of the percentage reduction of fresh rat damages at pre-application and post-application of rodenticides are shown in *Figure 3*. There was no significant difference ($F_{5, 12}$= 0.99, P = 0.47) indicated by one-way ANOVA of the percentage reduction of fresh rat damage in the first rounds of baiting. There was also no significant difference ($F_{5, 12}$= 1.70, P= 0.21) in the second round of baiting. As early as the third round of baiting, flocoumafen and chlorophacinone baits recorded more than 70% reduction, indicating the high efficacy of both treatments. The flocoumafen bait treatment maintained more than 70% damage reduction at 75.22 ± 2.72% until the last round at 79.00 ± 3.88% reduction from pre-treatment damages while chlorophacinone bait treatment maintained more than 70% reduction from the third (73.73 ± 10.19%) to the fourth round of baiting (73.75 ± 6.06%) and later slightly reduced to 64.46 ± 13.35%. Coumatetralyl bait treatment reached 70% damage reductions in the last round of baiting at 71.08 ± 5.73%. Brodifacoum bait treatment recorded 2.76 ± 15.53% of fresh rat damage reduction throughout the study. At this stage, a significant difference ($F_{5, 12}$ = 20.12, P = 0.00) among all the rodenticide treatments was detected as flocoumafen, chlorophacinone and coumatetralyl baits recorded a significantly higher reduction of fresh rat damages compared to warfarin bait and control plot. Warfarin bait treatment recorded poor results with the reduction ranging from 13.58% to 33.78%. The control recorded fluctuating trend of damage, with reductions up to 28.88 ± 5.17% in the first round of baiting and the reduction dropped to -5.90 ± 12.64% in the last round of baiting, indicating an increase in rat activities since there were no rodenticides applied in the plot. At the final round of baiting, the impact of flocoumafen, coumatetralyl and chlorophacinone baits was also significantly different ($F_{5, 12}$ = 8.39, P = 0.00) compared to control plots.

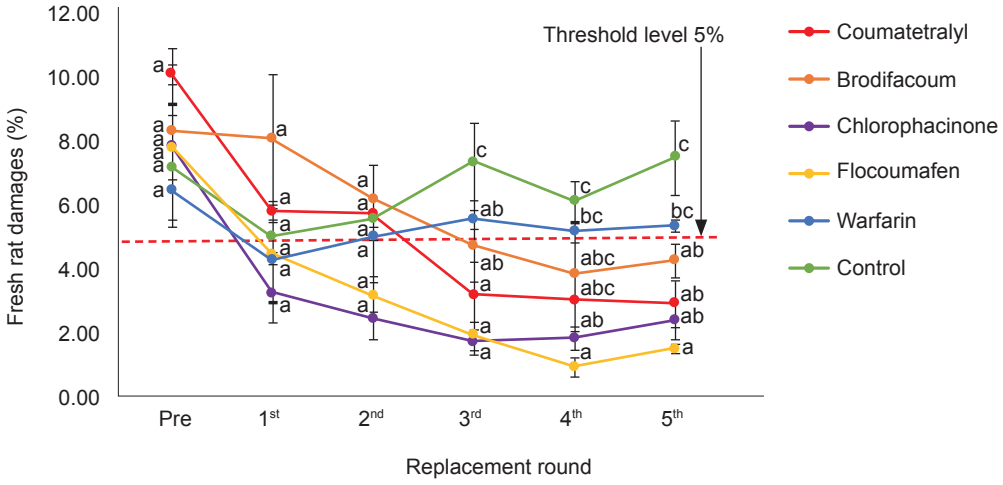


Figure 2. Fresh damages on oil palm fruit bunches in pre- and post-treatments where means in column with different letters are statistically significant different (p<0.05) by Tukey's test.

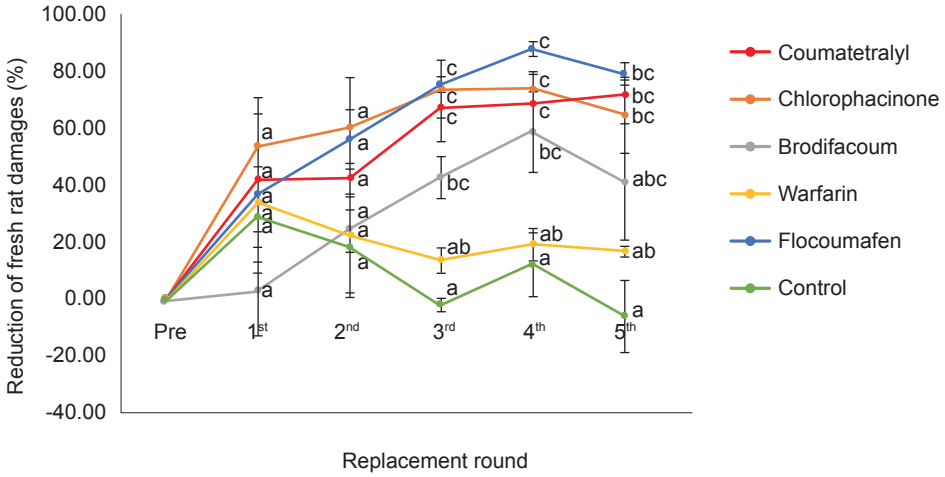


Figure 3. Percentage reduction of fresh rat damage before and after application of rodenticide baits where means in column with different letters are statistically significant different (p<0.05) *by Tukey's test.*

Relative Abundance

The results of the estimated rat abundance in this study are shown in *Figure 4*. Based on the trapping results, all treatments recorded reduced rat populations except for the control plot. The post-trapping results show there was a reduction in the relative abundance of rats captured in the treated plots. The difference in reduction of relative abundance in pre- and post-treatments ranged from 0.02 to 0.05 rats per trapping. Flocoumafen bait recorded the highest relative abundance reduction up to 0.05 rats per trapping. The treatment was able to reduce the relative abundance of rats from 0.07 ± 0.03 (pre-treatment) to 0.02 ± 0.01 rats per trapping (post-treatment). The reduction of relative abundance of rat population by chlorophacinone (reduced from 0.07 ± 0.03 to 0.03 ± 0.01 per trapping) and coumatetralyl (reduced from 0.08 ± 0.03 to 0.04 ± 0.01 per trapping) bait treatments where both treatments recorded a reduction of 0.04 rats per trapping, indicated the high efficacy of both rodenticides to reduce rat population in the study site.

Similarly, warfarin bait scored a similar reduction of relative abundance as chlorophacinone and coumatetralyl treatment baits. The treatment effectively reduced the relative abundance of the rat population by 0.04 rats per trapping, which was a drop in the relative abundances recorded during pre-treatment from 0.14 ± 0.03 rats per trapping to 0.09 ± 0.02 rats per trapping. Brodifacoum bait treatment recorded the least reduction compared to other treatments. The relative abundance of the rat population recorded during pre-treatment in the brodifacoum bait treatment plot was 0.09 ± 0.03 rats per trapping and dropped by 0.02 to score 0.07 relative abundance at the end of the study. The control plots showed no reduction and instead recorded an increment by +0.04 of relative abundance from 0.08 ± 0.03 to 0.12 ± 0.03 rats per trapping, indicating the rat population in the control plot increased. According to independent sample T-test analysis, there was no significant difference (p>0.05) in the relative abundance of rats recorded between pre and post-trapping in all the rodenticide bait and control plots.

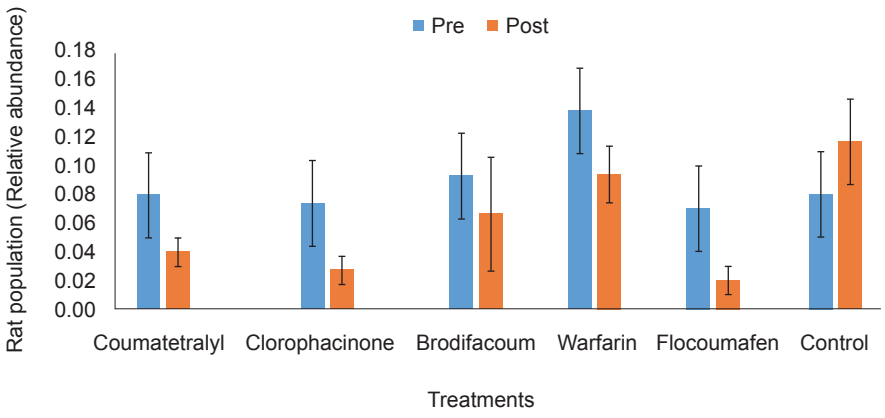


Figure 4. Relative abundance of R. tiomanicus *populations.*

DISCUSSION

In general, all rodenticide baits in this study were effective in reducing the fresh rat damage in the study sites. The high efficacy of flocoumafen bait has generally been reported in several previous research against many species of rat pests. Flocoumafen has recorded almost complete control against mice in the field (European Commission, 2009; Rowe *et al.*, 1985) and Norway rats, *R. norvegicus* (Buckle, 1986; European Commission, 2009) from trials conducted in infested farm buildings. A similar result was reported by Woo (1987), who reported high efficacy of flocoumafen wax block bait in controlling the rat population in oil palm plantations. In a laboratory no-choice feeding trial, Parshad (1988) reported flocoumafen (0.005% a.i) recorded 100% mortality against the Indian bush rat, *Golunda ellioti,* the Indian gerbil, *Tatera indica* and the Soft-furred field rat, *Rattus meltada.* Similarly, Srivinas *et al.* (2019) reported that flocoumafen (0.005% a.i) recorded 100% mortality of Lesser bandicoot rat, *Bandicota bengalensis* in choice and no-choice feeding. Flocoumafen bait also recorded high efficacy on wild warfarin-resistant mice, *Mus domesticus* (Gill, 1992; Johnson, 1988) and wild warfarin-resistant *R. norvegicus* (Gill, 1992).

Brodifacoum is a SGAR and one of the most potent of ARs (Pitt *et al.*, 2010; Prescott *et al.*, 2007). However, in the current study, brodifacoum bait was less effective compared to flocoumafen bait and other FGARs tested in the study. The current result contrasts with previous findings by Chia and Visvalingam (1990) who reported high efficacy of brodifacoum wax block bait against rat population in oil palm plantations. However, to the best of our knowledge, there has been no recent published report on the efficacy of brodifacoum baits against specific rat species in oil palm plantations. Unpalatable and poor bait formulation could be a possible factor for the relatively lower efficacy of brodifacoum bait used in the current study (Whisson, 1996). In contrast, several published data present a high degree of field efficacy of different formulations of brodifacoum baits against commensal rodents, both in susceptible and warfarin resistant populations (Blazic *et al.*, 2018; Buckle *et al.*, 2012). A recent field study by Frankova *et al.* (2019) reported the highly palatable bait of a low dose of brodifacoum (0.0025%) showed 95.7% and 99.8% efficacy against house mice, *Mus musculus* from an agriculture building in Prague, Czech Republic. Unpalatable bait formulation would cause ineffective results due to little or no consumption of the applied bait in the field (Cowan *et al.*, 1995). The repercussion of poor bait formulation would also be a misunderstanding that the treatment might experience resistance issues, as stated by Quy *et al.* (1992) regarding the resistance of brodifacoum in an earlier report by Greaves *et al.* (1982) in Hamsphire, United Kingdom area was premature due to the possibility of poor bait consumption. Naturally, rats prefer high-quality foods and do not favour less attractive food items (Syahputri and Priyambodo, 2020; Whisson, 1996). The result of the poor formulation of bait will lead to poor acceptance by rats in the field. Similarly, Johnson and Collier (2001) stated that in the situation where a more palatable diet is present, the rats tend to choose the more palatable diet and consume less
of the least palatable diet. Rodriguez *et al.* (2006) stated that the reason for the low efficacy of rat control is probably due to the low palatability of bait used and the seasonal availability of rat's normal food in the field which reduce the consumption of bait by the target pest. According to Brown and Singleton (1998), brodifacoum was effective to control the population of *M. domesticus* in Southern Australia. High palatable brodifacoum bait at 1 kg $ha^{-1}$and 2 kg ha^{-1} applied aerially recorded reduction of mice population up to 99% after seven days of treatment application.

In addition, the current study reported the high efficacy of two FGAR baits, namely coumatetralyl and chlorophacinone, to control rat infestation in the field study. Both compounds were able to reduce fresh fruit damage on FFB as early as the first and third rounds of rat baiting. A field study conducted by Ocampo and Lontoc (2016) showed that coumatetralyl bait (0.0375% a.i) was highly effective in reducing *R. tanezumi* activities in rice fields based on the percentage of the damaged tiller of paddy at harvest in the Philippines. A significant reduction in rat activities based on tracking or feeding census was also noted. Coddou *et al.* (2014) reported the baiting program of coumatetralyl bait had a mean efficacy of 76.5% against rat populations in Christmas Island, Australia. A more recent study carried out by Shahwar (2017) reported that coumatetralyl (0.0375% a.i) produced excellent control of up to 82.0% of rodent activity in a poultry farm in Rawalpindi-Islamabad, Pakistan. Laboratory testing by Chopra and Parshad (1985) recorded 100.0% mortality of coumatetralyl treated *B. bengalensis* (n=10) and *R. rattus* (n=10) after single and 10-day feeding testing. Additionally, Kowalski *et al.* (2006) demonstrated high efficacy of chlorophacinone against California ground squirrel (*Spermophilus beecheyi*) up to 94.2%. Similarly, Salmon *et al.* (2007) showed that chlorophacinone effectively controlled California ground squirrel (*S. beecheyi*) by more than 80.0% in cattle-grazed rangeland areas in Sierra Nevada foothills and Monterey County, California. The laboratory study by Marsh *et al.* (1977) reported that 0.005% of chlorophacinone was able to achieve complete control against deer mice, *Peromyscus maniculatus* in four days of free choice

feeding test. A comparative study by Mathur and Prakash (1984) showed high efficacy of up to 90.5% of brodifacoum, 83.2% of chlorophacinone and 81.1% of coumatetralyl against desert rodents near Bikaner, Rajasthan, India.

The poor result of warfarin bait treatment aligned with past literature which reported that the poor efficacy of the compound that contributed to poor control in the field was largely due to resistance (*e.g.*, Wood and Chung, 1990; Wood and Liau, 1977). Warfarin resistance of major rat species of oil palm plantation, *R. tiomanicus* was reported six to seven years after systematic rodent control was introduced in Malaysia (Wood and Liau, 1977). Wood and Chung (1990) reported high resistance of warfarin against *R. tiomanicus* in Kluang, Johor. The authors reported that two baiting campaigns using warfarin conducted in March-May 1983 and November 1984-January 1985 failed to completely control damage even after 13 and 16 rounds of baiting were conducted. The conclusion was also supported by an increase in the number of rats trapped during post trapping sessions in both campaigns. A laboratory study by Lam *et al.* (1982) reported that five out of 14 samples of *R. rattus diardii* that were captured from a cocoa plantation in Kuala Bernam Estate, Teluk Anson (now known as Teluk Intan), Perak showed high tolerance to 0.025% warfarin in six days exposure in a no-choice feeding test. Despite the historically poor performance against the rats, warfarin is still in production as it is still reliable to control the rats in certain plantation areas where barn owl conservation is practised, and also the compound provides additional alternatives to existing FGARs in the market such as chlorophacinone and coumatetralyl.

There are no other reports of warfarin-resistant rats in oil palm, however, there are vast reports on the emergence of warfarin resistance in other species of commensal rats all over the world. The first incidence of warfarin resistance in the commensal rat of house rats, *R. rattus* and Norway rats, *R. norvegicus* was reported in the late 1950s (Lasseur *et al.*, 2005) and later house mice, *M. musculus* (Pelz *et al.*, 2005). The majority of warfarin resistance reports were made in Europe (Buckle, 2013; Kohn *et al.*, 2000), however, the issue was also raised in North America (USA, Canada), Asia (Japan, China) and Australia (Marquez *et al.*, 2019). A field study by Pelz and Klemann (2004) reported warfarin resistance of live-trapped rats up to 89% in dairy cattle and pig fattening farms in North-West Germany through a blood clot resistance (BCR) test. Warfarin resistance of buff-breasted rat, *Rattus flavipectus* was documented in Zhanjiang in Guandong, China by Huang *et al.* (2010). The researchers reported that four of 36 samples of rats fed with 0.005% warfarin in a nine-day no-choice feeding survived. Further mutation screening analysis via DNA sequencing showed that three of four surviving *R. flavicpectus* carried Tyr139Cys mutation, which is a mutation of the VKORC1 gene. The mutation of the gene was reported to be responsible for anticoagulant resistance in many species of rodents across Europe (Pelz *et al.*, 2005; Rost *et al.*, 2005).

CONCLUSION

All ARs used in the study, except warfarin, were effective in controlling rat damage in the study site by reducing damage on oil palm bunches below the threshold level of 5%. All treatments also recorded a reduction in rat abundance at the sites (except for the control plot). The relatively low effectiveness of warfarin bait was suspected to be due to the resistance development of the rat populations towards the compound that has been used for a long period in oil palm plantations. Thus, further studies are needed to confirm the presence of AR-resistant, especially warfarin-resistant, rats in oil palm plantations in Malaysia to ensure more effective and efficient rat management.

ACKNOWLEDGEMENT

The authors would like to thank all members of Barn Owl and Rodent Research Group (BORG), USM for all technical and logistic support. The authors are grateful to the plantations in Besout, Sungkai for their participation and cooperation throughout the study.

REFERENCES

Abidin, C M R Z; Noor, H M; Hamid, N H; Ravindran, S; Puan, C L; Kasim, A and Salim, H (2021). Comparison of effectiveness of introduced barn owls, *Tyto javanica javanica*, and rodenticide treatments on rat control in oil palm plantations. *J. Pest. Sci.*, *95*: 1009-1022. DOI: 10.1007/s10340-021-01423-x.

Berny, P (2011). Challenges of anticoagulant rodenticides: Resistance and ecotoxicology. *Pesticides in the Modern World - Pests Control and Pesticides Exposure and Toxicity Assessment, 20*: 441-468. DOI: 10.5772/19916.

Blazic, T; Jokic, G; Gotz, A; Esther, M; Vuksa, M and Dedovic, S (2018). Brodifacoum as a first choice rodenticide for controlling bromadiolone-resistant *Mus musculus*. *J. Stored Prod. Res.*, *79*: 29-33.

Brown, P R and Singleton, G R (1998). Efficacy of brodifacoum to control house mice, *Mus domesticus*,

in wheat crops in Southern Australia. *Crop. Prot., 17(4)*: 345-352.

Buckle, A P (1986). Field trials of flocoumafen* against warfarin-resistant infestations of the Norway rat (*Rattus norvegicus* Berk.). *J. Hyg., 96*: 467-473.

Buckle, A P (1994). Rodent control methods: Chemical. *Rodent Pests and their Control* (Buckle, A P and Smith, R H eds.). CAB International. Wallingford, Oxon. pp. 127-160.

Buckle, A P; Chia, T H; Fenn, M G P and Visvalingam, M (1997). Ranging behaviour and habitat utilisation of the Malayan wood rat (*Rattus tiomanicus)* in an oil palm plantation in Johore, Malaysia. *Crop. Prot., 16(5)*: 467-473.

Buckle, A P; Klemann, N and Colin, P (2012). Brodifacoum is effective against Norway rats (*Rattus norvegicus*) in tyrosine139cysteine focus of anticoagulant resistance in Westphalia, Germany. *Pest Manag. Sci., 68(12)*: 1579-1585.

Buckle, A (2013). Anticoagulant resistance in the United Kingdom and a new guideline for the management of resistant infestations of Norway rats (*Rattus norvegicus* Berk.). *Pest Manag. Sci., 69(3)*: 334-341.

Buckle, A P (2015). Damage assessment and damage surveys. *Rodent Pests and their Control* (Buckle, A P and Smith, R H eds.). *2nd edition*. CAB International. Wallingford, Oxon. p. 209-230.

Buckle, A P and Smith, R H (2015). *Rodent Pests and Their Control*. 2nd edition. CAB International. Wallingford, Oxon. 432 pp.

Chia, T H and Visvalingam, M (1990). Methods for evaluation of rodenticides in oil palm plantations (Malaysia). *Proc. of 3rd International Conference on Plant Protection in the Tropic: Volume IV.* Malaysian Plant Protection Society. Kuala Lumpur. p. 19-26.

Chung, G F (2012). Rat management in oil palm. *Fourth MPOB-IOPRI International Seminar: Existing and Emerging Pests and Diseases of Oil Palm Advances in Research and Management*. 52 pp.

Chopra, G and Parshad, V R (1985). Evaluation of coumatetralyl against two predominant murid species. *J. Hyg., 94(3)*: 327-330.

Coddou, A; Mills, H; Hamilton, N and Algar, D (2014). Baiting effectiveness for introduced rats (*Rattus* sp.) on Christmas Island. *Raffles Bull. Zool., 30*: 54-59.

Cowan, D P; Dunsford, G; Gill, J E; Jones, A; Kerins, G M; MacNicoll, A D and Quy, R J (1995). The impact of resistance on the use of second-generation anticoagulants against rats on farms in Southern England. *Pestic. Sci., 43*: 83-93.

DOA (2021). List of registered agricultural pesticides in Malaysia. Department of Agriculture Malaysia (DOA). http://www.doa.gov.my/index.php/pages/view/388?mid=235, accessed on 16 May 2022.

Erickson, W and Urban, D (2004). Potential risks of nine rodenticides to birds and nontarget mammals: A comparative approach. Washington, DC, USA, United States Enviromental Protection Agency, Office of Pesticides Programs Environmental Fate and Effects Division. 225 pp.

European Commission (2009). Directive 98/8/EC concerning the placing biocidal products on the market. European Commission Netherland. 83 pp.

Fisher, P (2005). Review of house mouse (*Mus musculus)* susceptibility to anticoagulant poisons. *DOC Science Internal Series, 198*: 19.

Francis, C M (2008). *A Field Guide to the Mammals of South-East Asia.* New Holland Publication. 392 pp.

Frankova, M; Stejskal, V and Auliky, R (2019). Efficacy of rodenticide baits with decreased concentration of brodifacoum: Validation of the impact of the new EU anticoagulant regulation. *Sci. Rep., 9*: 16779.

Gill, J E (1992). Laboratory evaluation of the toxicity of flocoumafen as a single-feed rodenticide to seven rodent species. *Int. Biodeterior. Biodegradation, 30*: 65-76.

Greaves, J H; Shepherd, D S and Quy, R (1982). Field trials of second-generation anticoagulants against difenacoum-resistant Norway rat populations. *J. Hyg., 89*: 295-301.

Hafidzi, M N and Saayon, M K (2001). Status of rat infestation and recent control strategies in oil palm plantations in Peninsular Malaysia. *Pertanika J. Trop. Agric. Sci., 24(2)*: 109-114.

Harrison, J (1974). *An Introduction to the Mammals of Singapore and Malaya.* Malayan Nature Society. 340 pp.

Huang, B H; Feng, Z Y; Yue, L F; Yao, D D; Gao, Z X; Wang, D W and Liu, X H (2010). Warfarin resistance test and polymorphism screening in the VKORC1 gene in *Rattus flavipectus. J. Pest Sci., 84*: 87-92.

IBM Corp. (2019). IBM SPSS Statistics for Windows, Version 26.0. IBM Corp, Armonk, New York.

Johnson, R A (1988). Performance studies with the new anticoagulant rodenticide, flocoumafen, against *Mus domesticus* and *Rattus norvegicus*. *Bulletin OEPP/EPPO Bulletin, 18*: 481-488.

Johnson, D F and Collier, G (2001). Taste, intake rate, and food choice in rats. *Physiol. Behav., 72*: 37-44.

Khoo, K C; Lam, Y M; Teoh, C H; Lim, W H and Mohamad, B M (1982). *Rodent Pests of Agricultural Crops in Malaysia*. Malaysian Plant Protection Society, Kuala Lumpur, Malaysia. 69 pp.

Kohn, M H; Pelz, H J and Wayne, R K (2000). Natural selection mapping of the warfarin-resistance gene. *Proc. Natl. Acad. Sci., 97(14)*: 7911-7915.

Kowalski, V J; Long, R; Sullins, J; Garcia, S and Salmon, T P (2006). *Grower Evaluation of California Ground Squirrel* (Spermophilus beecheyi) *control using Anticoagulant Baits.* (Timm, R M and O'Brien J M eds.). *Proc. 22nd Vertebr. Pest Conf.* University of California, Davis, USA. p. 142-147.

Lam, Y M; Lee, A K; Tan, Y P and Mohan, E (1982). A case of warfarin resistance in *Rattus rattus diardii* (Jentink). *MARDI Res. Bull., 10(3)*: 378-383.

Lasseur, R; Longin-Sawageon, L; Videmann, B; Billeret, M; Berny, P and Benoit, E (2005). Warfarin resistance in a French Strain of rats. *J. Biochem. Mol., 19(6)*: 379-385.

Mathur, R P and Prakash, I (1984). Field trials of brodifacoum, chlorophacinone and coumatetralyl against desert rodents in India. *Trop. Pest Manag., 30(1)*: 59-61.

Marquez, A; Khalil, R A and Fourel, I (2019). Resistance to anticoagulant rodenticides in Martinique could lead to inefficient rodent control in a context of endemic leptospirosis. *Sci. Rep., 9*: 13491. DOI: 10.1038/s41598-019-49661-5.

Marsh, R E; Howard, W E and Cole, R E (1977). The toxicity of chlorophacinone and diphacinone to deer mice. *J. Wildl. Manag., 41(2)*: 298-301.

Ocampo, P O and Lontoc, B M (2016). On-farm pulsed baiting with coumatetralyl paste for the control of rice field rats. *Philipp. Entomol., 20(1)*: 81-93.

Oyedele, D T; Mohd Sah, S A; Kairuddin, L and Ibrahim, M W (2015). Range measurement and a habitat suitability map for the norway rat in a highly developed urban environment. *Trop. Life Sci. Res., 26(2)*: 27-44.

Parshad, V R (1988). Laboratory and field evaluation of flocoumafen for Rodent control. *Int. Biodeterior., 24*: 475-480.

Payne, J; Francis, C M and Phillipps, K (1985). *A Field Guide to the Mammals of Borneo.* Sabah Society, Malaysia. 332 pp.

Pelz, H J; Rost, S; Hunerberg, M; Fregin, A; Heiberg, A C; Baert, K; MacNicoll, A D; Prescott, C V; Walker, A S; Oldenburg, J and Muller, C R (2005). The genetic basis of resistance to anticoagulants in rodents. *Genetics, 170*: 1839-1847. DOI: 10.1534/genetics.104.040360.

Pelz, H J and Klemann, N (2004). Rat control strategies in organic pig and poultry production with special reference to rodenticide resistance and feeding behaviour. *NJAS, 52(2)*: 173-184.

Pitt, W C; Driscoll, L C and Sugihara, R T (2010). Efficacy of rodenticide baits for the control of three invasive rodent species in Hawaii. *Arch. Environ. Contam. Toxicol., 60(3)*: 533-542. DOI: 10.1007/s00244-010-9554-x.

Prescott, C V; Buckle, A P; Hussain, I and Endepols, S (2007). A standardised BCR resistance test for all anticoagulant rodenticides. *Int. J. Pest Manag., 53*: 265-272.

Pryde, M; Dilks, P and Fraser, I (2005). The home range of ship rats (*Rattus rattus*) in beech forest in the Eglinton Valley, Fiordland, New Zealand: A pilot study. *N Z J Zool., 32*: 139-142.

Puan, C L; Goldizen, A W; Zakaria, M; Hafidzi, M N and Baxter, G S (2011). Relationships among rat numbers, abundance of oil palm fruit and damage levels to fruit in an oil palm plantation. *Integr. Zool, 6*: 130-139. DOI: 10.1111/j.1749-4877.2010.00231.x.

Quy, R J; Shepherd, D S and Inglis, I R (1992). Bait avoidance and effectiveness of anticoagulant rodenticides against warfarin and difenacoum-resistant populations of Norway rats (*Rattus norvegicus*). *Crop Prot., 11*: 14-20.

Rattner, B A; Lazarus, R S; Elliott, J E; Shore, R F and van den Brink, N (2014). Adverse outcome pathway and risks of anticoagulant rodenticides to predatory wildlife. *Environ. Sci. Technol., 48*: 8433-8445. DOI: 10.1021/es501740n.

Rodriguez, C; Torres, R and Drummond, H (2006). Eradicating introduced mammals from

a forested tropical island. *Biol. Conserv., 130*: 98-105.

Rost, S; Fregin, A and Hunerberg, M (2005). Site-directed mutagenesis of coumarin-type anticoagulant-sensitive *VKORC*$_1$: Evidence that highly conserved amino acids define structural requirements for enzymatic activity and inhibition by warfarin. *J. Thromb. Haemost., 94(4)*: 780-786.

Rowe, F P; Bradfield, A and Swinney, T (1985). Pen and field trials of a new anticoagulant rodenticide flocoumafen against the house mouse *(Mus musculus* L.). *J. Hyg. Cambridge, 95*: 623-627.

Salmon, T P; Whisson, D A; Berentsen, A R and Gorenzel, W P (2007). Comparison of 0.005% and 0.01% diphacinone and chlorophacinone baits for controlling California ground squirrels (*Spermophilus beecheyi*). *Wildl. Res., 34*: 14-18.

Sime Darby Plantation (2010). Pioneers and innovators of integrated pest management in oil palm. Sime Darby Plantation Sdn. Bhd. Subang Jaya, Selangor.

Shahwar, D E (2017). Review on development of cereal baits and comparative field efficiency of some additives as bait carrier for zinc phosphide and coumatetralyl against rodent pests of poultry farms. *J. Pestic. Biofert*. p. 1-4. DOI: 10.2017/1.10001.

Syahputri, D A A and Priyambodo, S (2020). Flavor ingredients in the rodenticide formulation to improve consumption rate and mortality of house rat (*Rattus tanezumi* L.). *IOP Conf. Ser.: Earth Environ.* IOP Publishing. 468 pp.

Turner, P D and Gillbanks, R A (2003). Oil Palm Cultivation and Management - 2nd edition. The Incorporated Society of Planters, Kuala Lumpur, Malaysia. 915 pp.

Srivinas, R N; Anusha, B; Narasimha Rao, C H V and Tripathi, R S (2019). Evaluation of flocoumafen and difenacoum against lesser bandicoot rat, *Bandicota bengalensis* (gray) in rice. *J. Entomol. Zool. Stud., 7(3)*: 907-910.

Valchev, I; Binev, A R; Yordanova, V; Ordanova, A and Nikolov, Y (2008). Anticoagulant rodenticide intoxication in animals - A review. *Turkish J. Vet. Anim., 32(4)*: 237-243.

Whisson, D (1996). Rodenticides for control of Norway rats, roof rats and house mice. *Poultry Fact Sheet No. 23, Cooperative extension*, 7. Retrieved from http://animalscience.ucdavis.edu/avian/pfs23.htm, accessed on 20 January 2020.

Woo, Y K (1987). Efficacy against oil palm rats in Malaysia. Flocoumafen, a new second generation anticoagulant rodenticide. National Crop Protection Centre Library (The Philippines).

Wood, B J and Liau, S S (1977). Preliminary studies on the toxicity of anticoagulants to rats of oil palms, with special reference to the prospect of resistance. *International Development in Oil Palms* (Earp, D A and Newall, W eds.). Incorporated Society of Planters, Kuala Lumpur.

Wood, B J and Chung, G F (1990). Warfarin resistance of *Rattus tiomanicus* in oil palms in Malaysia and the associated increase of *Rattus diardii*. *Proc. of the 14th Vertebrate Pest Conference 1990*. p. 129-134.

Wood, B J (2001). Rat control in oil palms and rice fields. *Pestic Outlook, 4*: 71-74.

Wood, B J and Chung, G F (2003). A critical review of the development of rat control in Malaysian agriculture since the 1960s. *Crop Prot., 22*: 445-461.

SHORT COMMUNICATION

Journal of Oil Palm Research Vol. 35 (2) June 2023 p. 376-384
DOI: https://doi.org/10.21894/jopr.2022.0046

CROSS-VALIDATION AND RECEIVER OPERATING CHARACTERISTIC ANALYSES FOR OIL PALM LEAF METABOLOME DATASET

NUR AIN ISHAK[1]; NOOR IDAYU TAHIR[1]; NURUL LIYANA ROZALI[1]; ZAIN NURAZAH[1]; NUR RAIHAN ABD RAHIM[2]; ABRIZAH OTHMAN[1] and UMI SALAMAH RAMLI[1]*

ABSTRACT

The advancement of systems biology research has emphasised the capabilities of statistical analysis tools in distinguishing many factors associated with oil palm including genetic vs. *environment (GxE) components from omics data. The availability of an efficient and robust ecometabolomics workflow has a high potential in augmenting oil palm precision agriculture. In this study, we employed cross-validation (CV) and receiver operating characteristic (ROC) methodologies to evaluate the performance of an oil palm metabolome dataset linked to GxE factors for its predictive ability and integrity. The specificity and sensitivity of identified metabolite candidates contributing to the demarcation of the two oil palm groups in the dataset were found to be distinctive and were of discrimination quality. The dataset showed no overfitting and exhibited excellent predictive power. This work provides fundamental information and a guideline for universal metabolome data exploration toward oil palm phenotyping and precision agriculture.*

Keywords: cross-validation, metabolome, oil palm, phenotyping, ROC.

Received: 3 February 2022**; Accepted:** 17 June 2022**; Published online:** 8 August 2022.

INTRODUCTION

The high throughput and big data domain of systems biology provide attractive omics data collection for data mining and further utilisation in precision agriculture (Li and Yan, 2020). Defined as a holistic, eco-efficient and innovative tool to assist crop management sustainably, precision agriculture is viewed as a solution for the increasing human population and managing the implications of climate change (Lee *et al.,* 2021). One of the key areas in the omics studies is metabolomics; the in-depth analysis of a set of metabolites within an organism, cell or tissue under a given set of conditions at a specific time (Goodacre *et al.*, 2004; Reinke and Broadhurst, 2012). It is regarded as an important crop phenotyping tool that revolutionises the traditional assessment of phenotype by observing and measuring an organism's physical characteristics (Razzaq *et al.*, 2019). Crop phenotyping facilitates the selection efficiency of breeding programs, expedites genetic gains and helps automate or mechanise the monitoring of crop vigour status (Chawade *et al.,* 2019).

In plants, especially oil palm, the use of metabolomics is aimed at shedding light on several significant biological traits and responses to biotic and abiotic stimuli in numerous environmental conditions affecting plants' phenotypic performance, *e.g.,* yield, oil quality and disease resistance. Various metabolomics investigations involving oil palm leaf (Rozali *et al*., 2021; Tahir *et al.*, 2016; Vargas *et al.*, 2016), root (Muhammad *et al.*, 2021; Nurazah *et al*., 2021), seedling (Dzulkafli *et al*., 2019) and

[1] Malaysian Palm Oil Board,
6 Persiaran Institusi, Bandar Baru Bangi,
43000 Kajang, Selangor, Malaysia.

[2] Faculty of Arts and Science,
International University of Malaya-Wales (IUMW),
City Campus, Ground Floor,
Block A, Administration Wing, Jalan Tun Ismail,
50480 Kuala Lumpur, Malaysia.

* *Corresponding author e-mail: umi@mpob.gov.my*

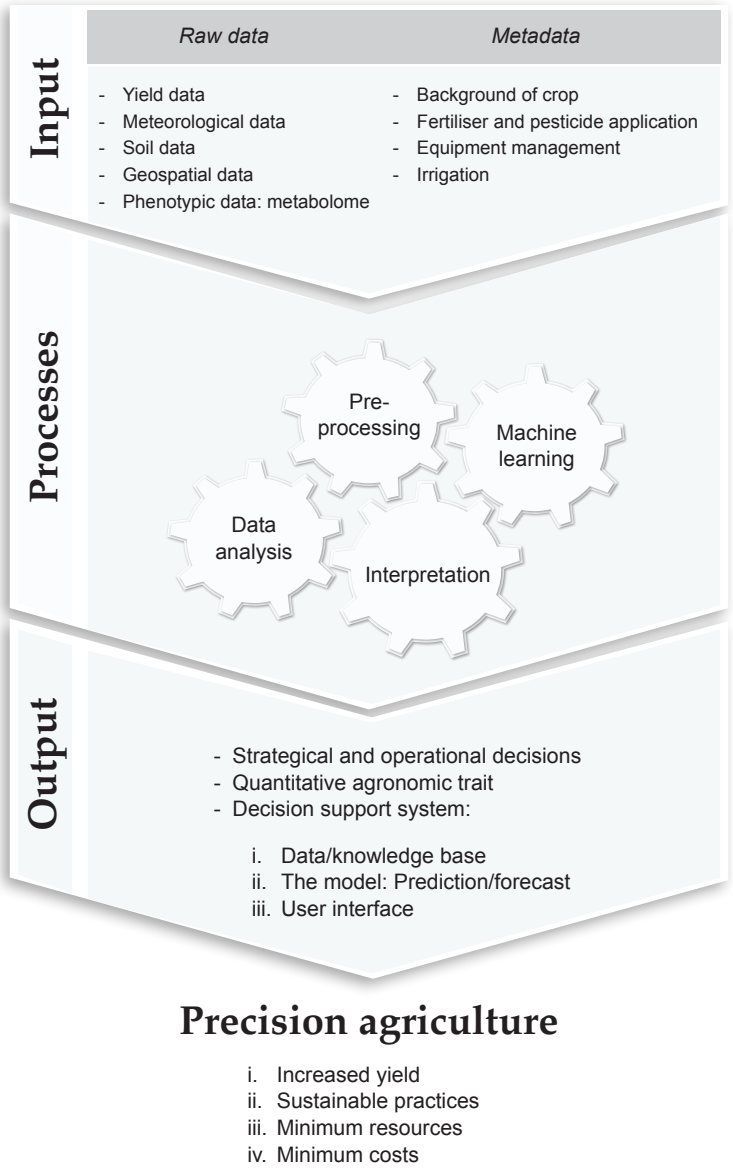


Figure 1. The general data-driven workflow for precision agriculture.

mesocarp (Teh *et al*., 2013) were performed using various analytical approaches to elucidate the crop's biochemical characteristics. Among the metabolomics platforms, liquid chromatography paired with mass spectrometry (LC-MS) is recognised as the most frequently utilised in metabolomics (Sindelar and Patti, 2020; Xiao *et al*., 2012) especially plant ecometabolomics strategy and can cover the separation and detection of diverse and inclusive plant metabolites (Sardans *et al*., 2020). To systematically analyse and interpret a metabolomics dataset, chemometrics is employed (Ishak *et al*., 2021). Chemometrics is an arm of data science for the extraction and evaluation of analytical-chemical data. Within the context of precision agriculture, the machine learning of chemometrics data collected in the field will allow automated extraction of information and further provide a model for characteristic prediction as outlined in *Figure 1.* Statistical techniques and machine learning have only lately gained popularity in oil palm research, for example, in remote sensing (Jia *et al*., 2019), palm oil and fruit quality (Goggin *et al*., 2021; Goh *et al*., 2021). Here, the application of cross-validation (CV) and receiver operating characteristic (ROC) approaches to an oil palm metabolome dataset were evaluated and verified for the first time as figures of merit in the endeavour to develop a screening and predictive workflow for metabolomics-assisted crop phenotyping.

MATERIALS AND METHODS

The raw data from LC-MS of the oil palm spear leaf metabolome from an ecometabolomics study

is similar to the settings demonstrated by Tahir *et al*. (2016) and guided by mass-spectrometry-based metabolomics recommendations (Alseekh *et al*., 2021) was organised into a tabular dataset format with rows of retention times against columns of peak intensities from 1.0-59.5 min analysis time with 'binned' components containing peak intensities from mass-to-charge ratio (*m*/*z*) of 50-1000. A signal-to-noise (S/N) threshold of 5.0 was applied in which a signal must surpass the set value to be used in the peak detection. The metabolome was extracted from oil palm leaves consisting of top, middle and basal leaflets on a selected frond '0' (spear leaf) from one specific clonal oil palm line, sampled from two different planting sites of mineral and peat soil types.

Oil Palm Metabolomics Workflow

The general plant metabolomics workflow from oil palm tissue sampling for chemometrics is described in *Figure 2*, involving sample collection, storage and extraction before the analysis using analytical platforms to detect and measure the small molecules. Consideration for photo-, heat-, and temporal-sensitive specimens must be taken into account to avoid deterioration and to minimise metabolome variations. The inspection of the generated data for inconsistencies and missing values is crucial in data interpretation as it will affect subsequent statistical analysis, and poor data processing may result in or further aggravate unwanted variance (Engel *et al*., 2013). Uni- and multivariate analysis reduce the dimensions of the data and provide visualisation for interpretation. For definitive performance assessment of the statistical classification, the metabolome dataset is further validated for machine learning using CV and ROC approaches.

LC-MS Dataset Validation

CV of the dataset (n=42) was performed according to leave-p-out analyses parameters of leave-one-out, leave-5%-out and leave-10%-out CV. ROC and the confidence intervals for metabolite classifiers were calculated in MetaboAnalyst 5.0 (Pang *et al*., 2021) according to group assigned parameter of soil where the x-axis was referred to as the '1-specificity' in terms of the recorded false positives and the y-axis was referred to the sensitivity in terms of the recorded true positives. Both axes were given values between 0 and 1. A test assumption was made that the first attribute is the mineral soil and the second attribute is the peat soil. Analyses and parameters were set up in ProfileAnalysis 2.1 (Bruker Daltonics, Bremen, Germany). Supervised statistical analysis of an orthogonal partial least square-discriminant analysis (OPLS-DA) predictive model with Pareto scaling and ROC model classification accuracy was performed using SIMCA-P+ 14.1 software (Sartorius Stedim Data Analytics AB, Umeå/Malmö, Sweden).

RESULTS AND DISCUSSION

Cross-validation (CV) of Oil Palm Leaf Metabolome Dataset

The CV method keeps a portion of analyses out of the model calculation and calculates several parallel models from the reduced data before it forecasts the removed data by the different models and compares the predicted values with the actual ones (Schmidt *et al*., 2019). A model is constructed and optimised using the training data while the test set is applied to see how well the model works. The procedure will be repeated in such a way that each sample appears once and only once in the test set, and the prediction error is representative of new samples. A completely independent test set must not be pretreated, preprocessed, or scaled.

The most common types of CV are leave-one-out and k-fold (Xi *et al*., 2014). Considering a case where the sample size is n, in leave-one-out CV, n-1 samples are used as a training set for fitting a classification model, and the remaining sample is used for testing. This process is repeated n times, and each sample

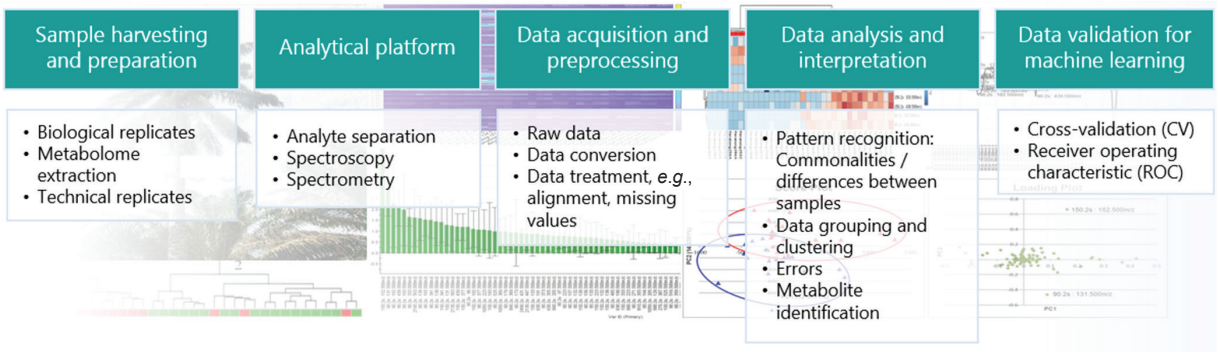


Figure 2. Oil palm metabolomics workflow.

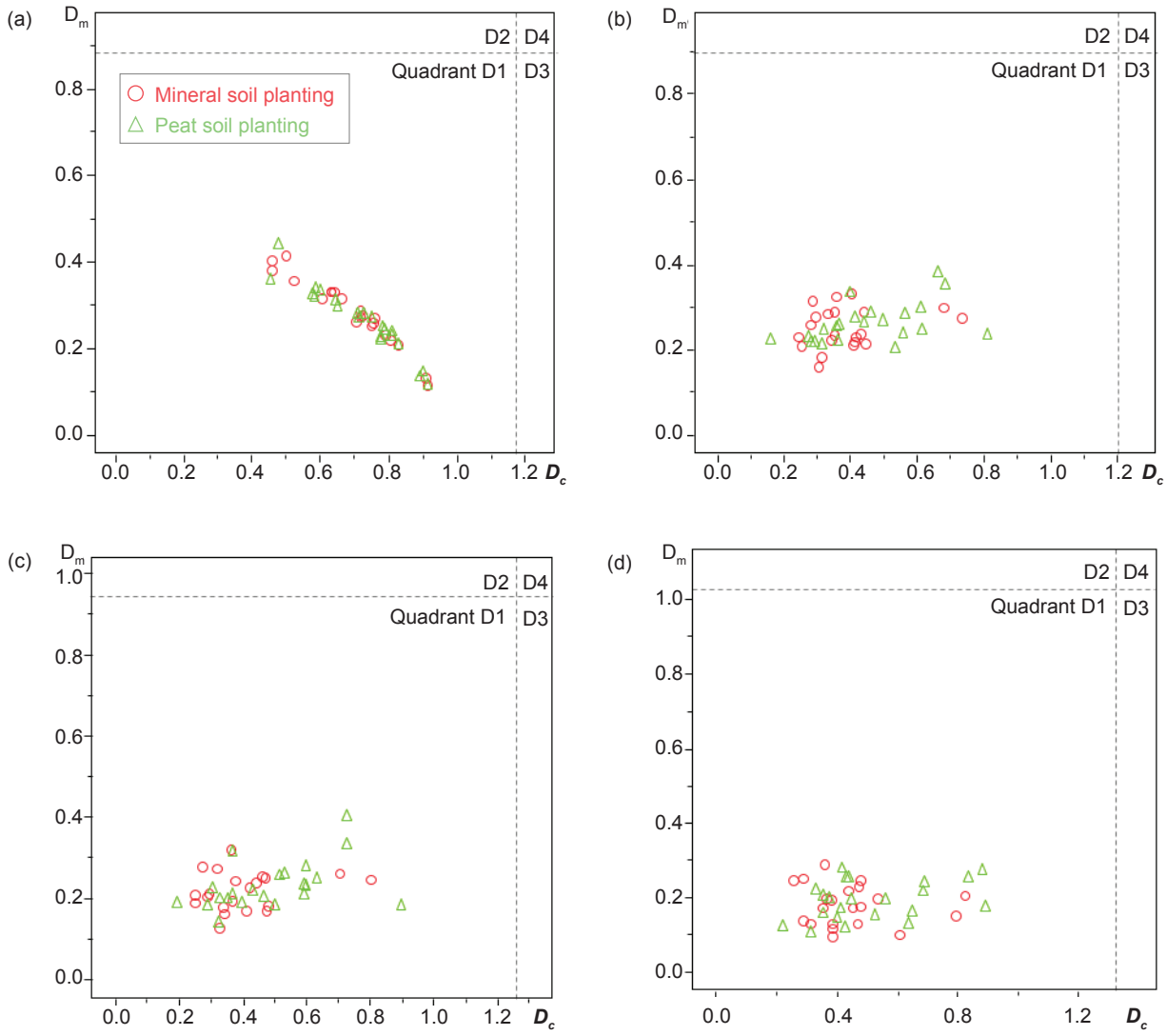
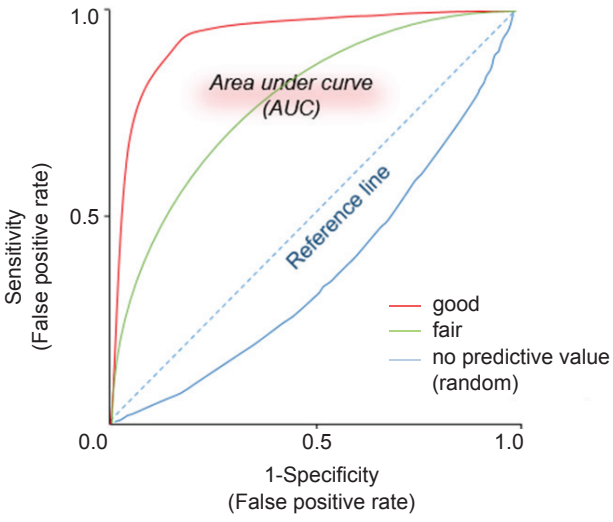


Figure 3. Influence plots of oil palm leaf metabolome dataset; (a) before cross-validation, (b) leave-one-out cross-validation, (c) leave-5%-out cross-validation and (d) leave-10%-out cross-validation (D_m - 'Distance to model' and D_c - 'Distance to centre').

is implemented just once as test data. A model constructed from *n-1* samples is approximately as accurate as one constructed from all *n* samples. The proportion of misclassified test data points is used to calculate the classification error rate. In *k*-fold CV, the entire dataset is partitioned into *k* subsets of similar size (*e.g.*, *k*=5 or *k*=10). *k-1* subsets are combined and used as a training set for each iteration, while the remaining subset is used as a test set. Every sample serves as a test data point only once. *Figure 3a* shows the influence plot of the oil palm leaf metabolome dataset before the application of any validation method while *Figures 3b, 3c* and *3d* are the influence plots after the leave-one-out, leave-5%-out and leave-10%-out CV respectively. All data points were located in the distance 1 (D1) quadrant corresponding to analyses inside the model space after the CV, indicating a good proportion of the model.



Source: Ferraris (2019).

Figure 4. Types of ROC curves for classifier accuracy.

Receiver Operating Characteristic (ROC) Curve for Discrimination Threshold

The ROC curve is an evaluation of the distinctive quality of a classifier (*i.e.*, metabolites or soil type) where the best possible prediction feature yields a curve in the direction of the upper left corner of the plot towards 100% sensitivity and 100% specificity. *Figure 4* summarises the main verdicts that can be drawn from a ROC curve.

In *Figure 5*, the accuracy of dopamine ($C_8H_{11}NO_2$, *m/z* 152.0719 $[M-H]^-$) and asparagine ($C_4H_8N_2O_3$, *m/z* 131.0434 $[M-H]^-$) in discriminating the two planting locations were demonstrated by the ROC curves which were plotted closer to the left and the top border of the ROC space, consistent with previous findings (Tahir *et al*., 2016). The jagged shape of the ROC curves could be improved by adding more measurements to get smoother arcs (Xia *et al*., 2013). According to Bünger and Mallet (2016) and Ferraris (2019), any classifier designated as a test criterion displaying a high area under the ROC curve (AUC) value of close to 1.0 indicates high diagnostic capability in discriminating two populations. As dopamine and asparagine showed high AUC values of 0.852 (0.725-0.955 confidence interval) and 0.781 (0.634-0.911 confidence interval) respectively, these metabolites are excellent classifiers for the different groups of oil palm specimens.

Assessment of Predictive Model from Oil Palm Leaf Metabolome Dataset

An orthogonal partial least square-discriminant analysis (OPLS-DA) model was constructed using the dataset based on its suitability in separating predictive from non-predictive (orthogonal) variation (Bylesjö *et al*., 2006). Ranging from 0-1, a low value of 0.1822 root-mean-square CV error (RMSECV) was obtained for the model indicating a reliable and predictive ability (Lee *et al*., 2018; Liu *et al*., 2020). The statistical model from the training set was found to be significantly robust with a total accuracy of 100% correct classification and a low Fisher value ($p<0.01$) as tabulated in *Table 1* (Tarapoulouzi *et al*., 2020). An external validation using three unknown samples from different planting trials as a test set ($n=3$) which were subjected to similar metabolome extraction, data acquisition and the preprocessing protocol was able to prove that the model can successfully predict the planting soil type of the unknown oil palm samples from three different mineral soil trials. The misclassification table (*Table 1*) of the constructed model indicated that the blind samples were grouped with the mineral group samples.

TABLE 1. OPLS-DA MODEL MISCLASSIFICATION TABLE OF OIL PALM METABOLOME SPECIMENS FROM DIFFERENT PLANTING TRIALS

	No. of specimen	Correct classification (%)	Mineral	Peat
Mineral	21	100	21	0
Peat	21	100	0	21
Unknown specimen	3		3	0
Total specimen	45	100	24	21
Fisher's probability	1.9×10^{-12}			

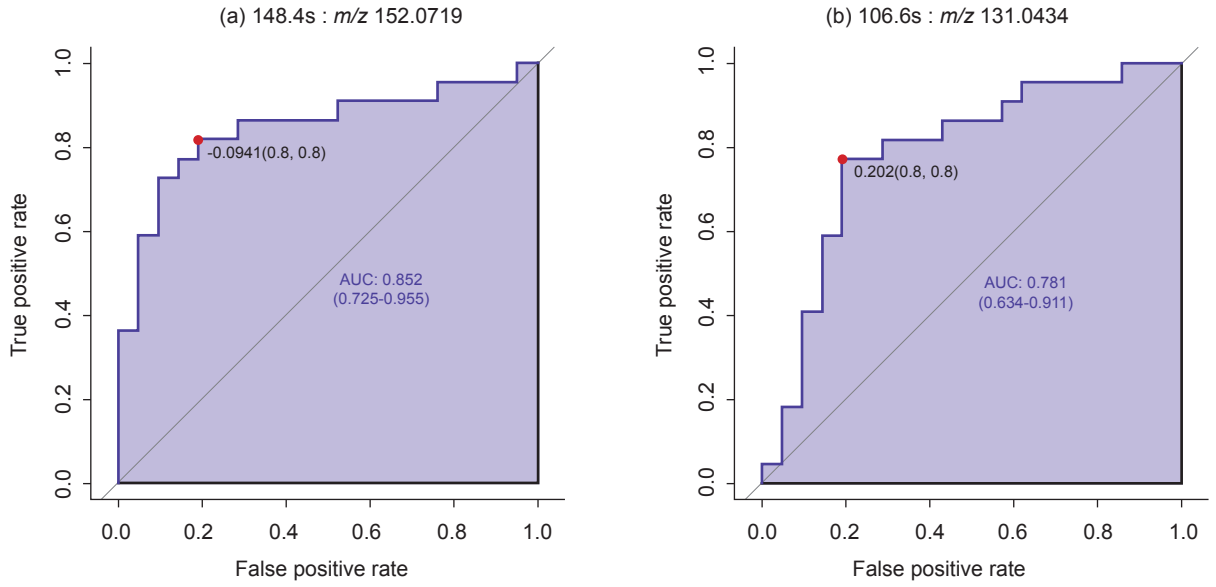


Figure 5. ROC curves with AUC values for (a) dopamine with an AUC value of 0.852 and (b) asparagine with an AUC value of 0.781.

Figure 6 presents the predicted score scatter plot of the test set merged with the training set samples from the mineral and peat soils. From the test set, two unknown samples (SampleX1 and SampleX2) were plotted on the left-hand side of the plot together with the mineral soil cluster while one unknown sample (SampleX3) was found in the outer region of the 95% mineral soil confidence ellipse. The three unknown samples are classified as specimens of mineral soil type, with SampleX3 exhibiting slight variation from the others.

An additional ROC analysis performed to assess the predictive OPLS-DA model's ability to appropriately categorise the oil palm specimens resulted in an AUC value of 1.0 (*Figure 7*), indicating its excellent classification power in separating the oil palm leaf metabolome samples to their corresponding planting soils (Ruisánchez *et al.*, 2021).

CONCLUSION

This work demonstrated the validation and evaluation methods of CV and ROC on an oil palm metabolome dataset in an attempt to obtain a screening and predictive workflow for metabolomics-assisted crop phenotyping. The demarcation of oil palm leaf samples from the peat and mineral soil planting sites by dopamine and asparagine respectively was verified as statistically significant for discriminating and predicting the two classes/groups of samples. The predictive statistical model constructed from the chemometric analysis also demonstrated excellent predictive ability. These findings established the provision of metabolome data exploration for oil palm phenotyping and its potential utilisation for machine learning which is highly prospective for oil palm integrated precision agriculture.

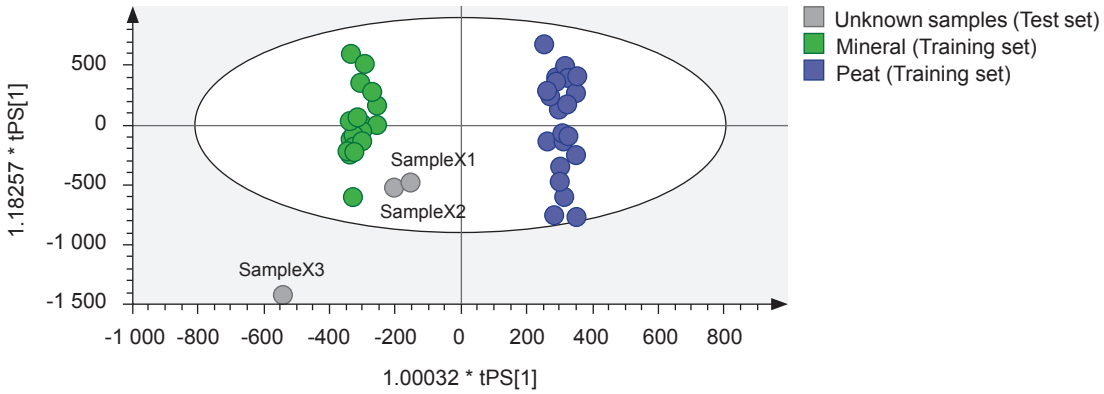


Figure 6. Predicted score plot with training set merged with the test set for oil palm spear leaf samples from different planting sites.

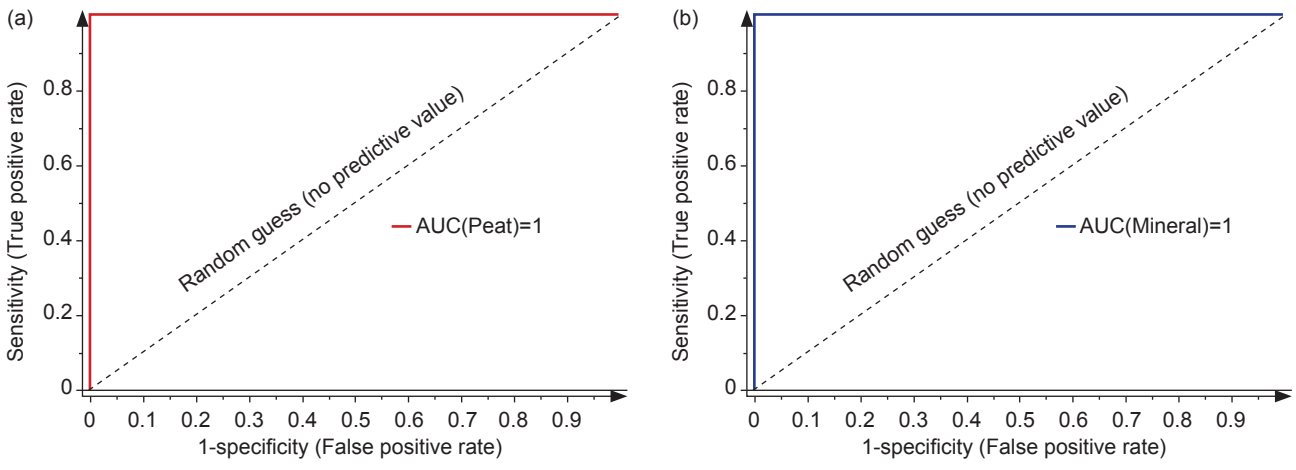


Figure 7. ROC curves for the classification accuracy of the OPLS-DA model with the area under curve (AUC) values of 1.0 for (a) peat soil and (b) mineral soil planting trials.

ACKNOWLEDGEMENT

The authors thank the Director-General of MPOB for permission to publish this article and Dr. Zainab Idris for her technical comments. The authors appreciate Prof. Jianping Yang (Zhejiang Sci-Tech University, China) and Mr. Kathiresan Gopal (Universiti Putra Malaysia) for technical contributions. We are grateful to Dr. Mohamad Arif Abd Manaf for his consistent support and the Proteomics and Metabolomics (PROMET) research team for their invaluable assistance.

REFERENCES

Alseekh, S; Aharoni, A; Brotman, Y; Contrepois, K; D'Auria, J; Ewald J; Ewald, J C; Fraser, P D; Giavalisco, P; Hall, R D; Heinemann, M; Link, H; Luo, J; Neumann, S; Nielsen, J; Perez de Souza, L; Saito, K; Sauer, U; Schroeder, F C; Schuster, S; Siuzdak, G; Skirycz, A; Sumner, L W; Snyder, M P; Tang, H; Tohge, T; Wang, Y; Wen, W; Wu, S; Xu, G; Zamboni, N and Fernie, A R (2021). Mass spectrometry-based metabolomics: A guide for annotation, quantification and best reporting practices. *Nat. Methods, 18(7)*: 747-756.

Bünger, R and Mallet, R T (2016). Metabolomics and receiver operating characteristic analysis: A promising approach for sepsis diagnosis. *Crit. Care Med., 44(9)*: 1784-1785.

Bylesjö, M; Rantalainen, M; Cloarec, O; Nicholson, J K; Holmes, E and Trygg, J (2006). OPLS discriminant analysis: Combining the strengths of PLS-DA and SIMCA classification. *J. Chemom., 20(8-10)*: 341-351.

Chawade, A; van Ham, J; Blomquist, H; Bagge, O; Alexandersson, E and Ortiz, R (2019). High-throughput field-phenotyping tools for plant breeding and precision agriculture. *Agronomy, 9(5)*: 258.

Dzulkafli, S B; Abrizah, O; Syahanim, S; Nurazah, Z; Manaf, M A A; Idris, A S; Amiruddin, M D; Tahir, N I and Ramli, U S (2019). Identification of chelidonic acid and asparagine in *Ganoderma boninense*-inoculated oil palm seedlings. *J. Oil Palm Res., 31*: 53-66.

Engel, J; Gerretzen, J; Szymańska, E; Jansen, J J; Downey, G; Blanchet, L and Buydens, L M C (2013). Breaking with trends in pre-processing? *Trends Analyt. Chem., 50*: 96-106.

Ferraris, V A (2019). Commentary: Should we rely on receiver operating characteristic curves? From submarines to medical tests, the answer is a definite maybe! *J. Thorac. Cardiovasc. Surg., 157(6)*: 2354-2355.

Goggin, K A; Brodrick, E; Wicaksono, A; Covington, J A; Davies, A N and Murphy, D J (2021). A proof-of-concept study: Determining the geographical origin of crude palm oil with the combined use of GC-IMS fingerprinting and chemometrics. *J. Oil Palm Res., 33(2)*: 227-234.

Goh, J Q; Mohamed Shariff, A R and Mat Nawi, N (2021). Application of optical spectrometer to determine maturity level of oil palm fresh fruit bunches based on analysis of the front equatorial, front basil, back equatorial, back basil and apical parts of the oil palm bunches. *Agriculture, 11(12)*: 1179.

Goodacre, R; Vaidyanathan, S; Dunn, W B; Harrigan, G G and Kell, D B (2004). Metabolomics by numbers: Acquiring and understanding global metabolite data. *Trends Biotechnol., 22(5)*: 245-252.

Ishak, N A; Tahir N I; Mohd Sa'id, S N; Kathiresan, G; Abrizah, O and Ramli, U S (2021). Comparative analysis of statistical tools for oil palm phytochemical research. *Heliyon, 7(2)*: e06048.

Jia, X; Khandelwal, A; Carlson, K; Gerber, J S; West, P C and Kumar, V (2019). Plantation mapping in Southeast Asia. *Front. Big Data, 2*: 46.

Lee, B J; Zhou, Y; Lee, J S; Shin, B K; Seo, J A; Lee, D; Kim, Y S and Choi, H K (2018). Discrimination and prediction of the origin of chinese and korean soybeans using fourier transform infrared spectrometry (FT-IR) with multivariate statistical analysis. *PLoS ONE, 13*: e0196315.

Lee, C L; Strong, R and Dooley, K E (2021). Analyzing precision agriculture adoption across the globe: A systematic review of scholarship from 1999-2020. *Sustainability, 13(18)*: 10295.

Li, Q and Yan, J (2020). Sustainable agriculture in the era of omics: Knowledge-driven crop breeding. *Genome Biol., 21*: 154.

Liu, L; Zuo, Z T; Xu, F R and Wand, Y Z (2020). Study on quality response to environmental factors and geographical traceability of wild *Gentiana rigescens* franch. *Front. Plant Sci., 11*: 1128.

Muhammad, I I; Abdullah, S N A; Saud, H M; Shaharuddin, N A and Isa, N M (2021). The dynamic responses of oil palm leaf and root metabolome to phosphorus deficiency. *Metabolites, 11(4)*: 217.

Nurazah, Z; Idris, A S; Amiruddin, M D; Manaf, M A A; Abrizah, O and Ramli, U S (2021). Metabolite fingerprinting of oil palm (*Elaeis guineensis* Jacq.) root for the identification of altered metabolic pathways associated with basal stem rot (BSR) disease. *Physiol. Mol. Plant Pathol., 115*: 101647.

Pang, Z; Chong, J; Zhou, G; de Lima Morais, D A; Chang, L; Barrette, M; Gauthier, C; Jacques, P É; Li, S and Xia, J (2021). MetaboAnalyst 5.0: Narrowing the gap between raw spectra and functional insights. *Nucleic Acids Res., 49(W1)*: W388-W396.

Razzaq, A; Sadia, B; Raza, A; Khalid Hameed, M and Saleem, F (2019). Metabolomics: A way forward for crop improvement. *Metabolites, 9(12)*: 303.

Reinke, S N and Broadhurst, D I (2012). Moving metabolomics from a data-driven science to an integrative systems science. *Genome Med., 4(11)*: 85.

Rozali, N L; Tahir, N I; Hassan, H; Abrizah, O and Ramli, U S (2021). Identification of amines, amino and organic acids in oil palm (*Elaeis guineensis* Jacq.) spear leaf using GC- and LC/Q-TOF MS metabolomics platforms. *Biocatal. Agric. Biotechnol., 37*: 102165.

Ruisánchez, I; Jiménez-Carvelo, A M and Callao, M P (2021). ROC curves for the optimization of one-class model parameters. A case study: Authenticating extra virgin olive oil from a Catalan protected designation of origin. *Talanta, 222*: 121564.

Sardans, J; Gargallo-Garriga, A; Urban, O; Klem, K; Walker, T W N; Holub, P; Janssens, I A and Peñuelas, J (2020). Ecometabolomics for a better understanding of plant responses and acclimation to abiotic factors linked to global change. *Metabolites, 10(6)*: 239.

Schmidt, J; Marques, M R G; Botti, S and Marques, A L (2019). Recent advances and applications of machine learning in solid-state materials science. *NPJ Comput. Mater., 5*: 83.

Sindelar, M and Patti, G J (2020). Chemical discovery in the era of metabolomics. *J. Am. Chem. Soc., 142(20)*: 9097-9105.

Tahir, N I; Shaari, K; Abas, F; Ishak, Z; Tarmizi, A; Amiruddin, M D; Parveez, G K A and Ramli, U S (2016). Metabolome analysis of oil palm clone P325 of different planting trials. *J. Oil Palm Res., 28(4)*: 431-441.

Tarapoulouzi, M; Kokkinofta, R and Theocharis, C R (2020). Chemometric analysis combined with FTIR spectroscopy of milk and Halloumi cheese samples according to species' origin. *Food Sci. Nutr., 8*: 3262-3273.

Teh, H F; Neoh, B K; Hong, M P L; Low, J Y S; Ng, T L M; Ithnin, N; Thang, Y M; Mohamed, M; Chew, F T; Yusof, H M; Kulaveerasingam, H and Appleton, D R (2013). Differential metabolite profiles during fruit development in high-yielding oil palm mesocarp. *PLoS ONE, 8(4)*: e61344.

Vargas, L H G; Neto, J C R; De Aquino Ribeiro, J A; Ricci-Silva, M E; Souza, M T; Rodrigues, C M; De Oliveira, A E and Abdelnur, P V (2016). Metabolomics analysis of oil palm (*Elaeis guineensis*) leaf: Evaluation of sample preparation steps using UHPLC–MS/MS. *Metabolomics, 12(10)*: 153.

Xi, B; Gu, H; Baniasadi, H and Raftery, D (2014). Statistical analysis and modeling of mass spectrometry-based metabolomics data. *Mass Spectrometry in Metabolomics. Methods in Molecular Biology (Methods and Protocols)* (Raftery, D ed.). Vol. 1198. Humana Press, New York, NY. p. 1198:333-353.

Xia, J; Broadhurst, D I; Wilson, M and Wishart, D S (2013). Translational biomarker discovery in clinical metabolomics: An introductory tutorial. *Metabolomics, 9(2)*: 280-299.

Xiao, J F; Zhou, B and Ressom, H W (2012). Metabolite identification and quantitation in LC-MS/MS-based metabolomics. *TrAC - Trends Anal. Chem., 32*: 1-14.



PIPOC 2023

MPOB International Palm Oil Congress and Exhibition

Navigating Uncertainties Building Resilience

7-9 NOVEMBER 2023
Kuala Lumpur Convention Centre

MINISTRY OF PLANTATION AND COMMODITIES

MPOB

Organised by
Malaysian Palm Oil Board
Ministry of Plantation and Commodities, Malaysia

pipoc@mpob.gov.my

pipoc.mpob.gov.my | www.mpob.gov.my

JOURNAL OF OIL PALM RESEARCH

GUIDE FOR AUTHORS

(for more details, kindly surf http://jopr.mpob.gov.my)

Type of Articles

1. **Regular Article**
   Full-length original empirical investigations, consisting of introduction, materials and methods, results and discussion, conclusions. Original work must provide references and an explanation on research findings that contain new and significant findings. Conclusion should be brief and focus on the research output, should not be in point form. These papers should not exceed 6000 words of text (including tables, figures and references) and generally not more than a total of 10 figures and tables. After peer-review, the article word count limit can be extended to a maximum of 8000 words to better address the reviewers' and editors' comments. Any additional figures or tables can be included in the supplementary data. Please note that papers submitted to JOPR will be sent back to authors because of poor figure resolution or exceeding the number of figures permitted.

2. **Short Communication**
   Significant new information to readers of the Journal in a short but complete form. Preferably not exceeding 3000 words (including tables, figures and references), and is intended for rapid publication. They are not intended for publishing preliminary results or to be a reduced version of regular article.

3. **Review Article**
   Critical evaluation of materials about current research that have already been published by organising, integrating, and evaluating previously published materials. Re-analyses as meta-analysis and systemic reviews are encouraged. Review articles provide systemic overview, evaluation and interpretation of research in a given field. They should not exceed 12 000 words (excluding references only) and should contain no more than a total of 20 figures and tables. Any additional figures or tables can be included in the supplementary data. Please note that papers submitted to JOPR will be sent back to authors because of poor figure resolution or exceeding the number of figures permitted. The same information should not be repeated in a figure and a table.

Language

Please write your text in good English (only British English is accepted). We do not accept American English or a mixture of these.

JOPR's Template

JOPR's template, which is a standard format that facilitates the manuscript writing and copyediting process. This template is created to provide a detail and clear house style of JOPR. The template is drafted according to JOPR's house style, but in standard word version format. When writing a paper, authors need to format their papers to fit into the journal's house style. To make this easier, Word templates are available for many of other established journals, ready for them to download and apply to their research paper format. It is crucial for author to write a research paper while considering formatting. Each journal has its own guidelines for formatting; hence, the template defines how an article will look when it is published online or in print.

JOPR's Aims & Scope

This is established to provide a detail and clear aims and scope for author reference. Authors should declare in the cover letter how the research fits the aims and scope of JOPR.

JOPR's House Style

A detail listing of JOPR's house style for authors and a checklist to facilitate the copyediting process and standardise the copyediting process. The JOPR's house style remains the same and is drafted into a detail version for author's reference.

Manuscript Submission

- Manuscripts should be submitted via: https://mc04.manuscriptcentral.com/jopres
- JOPR does not permit dual submission, publication and/or any archive platform (preprint) in violation of journal ethical practices.

For more details and to download the JOPR's House Style and Template, kindly surf http://jopr.mpob.gov.my



Contents of the Coming Issue
Journal of Oil Palm Research
Vol. 35 (3) September 2023*

- Oil Palm Water Requirement and the Need for Irrigation in Dry Malaysian Areas
  Afandi A M; Zulkifli H; Nur Zuhaili H A Z A; Norliyana Z Z; Hisham H; Saharul A M; Dzulhelmi M N and Vu Thanh T A

- Surface Properties and Aggregation Behaviour of Hexadecyltrimethyammonium Bromide-palm-based Caprylic Acid Mixed Surfactant Systems
  Wen Huei Lim and Xiou Shuang Yong

- Antiproliferative Effects of Palm Oil in the Presence of Photobiomodulation against K562 Cancer Cells
  Azadeh Hekmat; Kimia Farokhi Bahar and Zahra Hajebrahimi

- Integrated Microwave-steam Sterilisation of Loose Oil Palm Fruits: Enhanced Heating Uniformity, Crude Palm Oil Quality, and Energy Savings
  Syed Mohammad Ahsan Shah; Arshad Adam Salema; Nik Suhaimi Mat Hassan; Yosri Mohd Siran and Syahril Anuar Md Rejab

- Oil Palm MSP2 Promoter Isolation, *in silico* Analysis and Functional Characterisation
  Nurniwalis Abdul Wahab; Zubaidah Ramli; Mohamad Arif Abd Manaf and Ahmad Parveez Ghulam Kadir

- Bunch Oil and Fatty Acid Profile in *Elaeis oleifera* Taisha - Ecuador, *Elaeis guineensis* Jacq, Interspecific Hybrids and Backcrosses
  Laura Mendoza; Julian Barba and Gustavo Ligarreto

Note: * Subject to change.